University of Huddersfield Repository

Carvalho Couto De Azevedo, Orlando Delfim

Photoswitching of Emission in Naphthopyran Substituted Transition Metal Complexes

Original Citation

Carvalho Couto De Azevedo, Orlando Delfim (2019) Photoswitching of Emission in Naphthopyran Substituted Transition Metal Complexes. Doctoral thesis, University of Huddersfield.

This version is available at http://eprints.hud.ac.uk/id/eprint/35124/

The University Repository is a digital collection of the research output of the University, available on Open Access. Copyright and Moral Rights for the items on this site are retained by the individual author and/or other copyright owners. Users may access full items free of charge; copies of full text items generally can be reproduced, displayed or performed and given to third parties in any format or medium for personal research or study, educational or not-for-profit purposes without prior permission or charge, provided:

- The authors, title and full bibliographic details is credited in any copy;
- A hyperlink and/or URL is included for the original metadata page; and
- The content is not changed in any way.

For more information, including our policy and submission procedure, please contact the Repository Team at: E.mailbox@hud.ac.uk.

http://eprints.hud.ac.uk/

Photoswitching of Emission in Naphthopyran Substituted Transition Metal Complexes

Orlando Delfim Carvalho Couto de Azevedo

A Thesis Submitted to the University of Huddersfield in Partial Fulfilment of the Requirements for the Degree of Doctor of Philosophy

The University of Huddersfield

May 2019

Copyright statement

I. The author of this thesis (including any appendices and/or schedules to this thesis) owns any copyright in it (the "Copyright") and s/he has given The University of Huddersfield the right to use such copyright for any administrative, promotional, educational and/or teaching purposes.

II. Copies of this thesis, either in full or in extracts, may be made only in accordance with the regulations of the University Library. Details of these regulations may be obtained from the Librarian. This page must form part of any such copies made.

III. The ownership of any patents, designs, trademarks and any and all other intellectual property rights except for the Copyright (the "Intellectual Property Rights") and any reproductions of copyright works, for example graphs and tables ("Reproductions"), which may be described in this thesis, may not be owned by the author and may be owned by third parties. Such Intellectual Property Rights and Reproductions cannot and must not be made available for use without the prior written permission of the owner(s) of the relevant Intellectual Property Rights and/or Reproductions.

Acknowledgments

I would like first and foremost thank Professor Mark Heron for his teachings, patience and enlightenment during my PhD and for the essential assistance given during the development of this thesis.

I would like to thank Dr Christopher Gabbutt, Professor Paul Elliott and Dr Paul Scattergood for all the support given during my PhD.

I would also like to thank Dr Stuart Aiken for his teachings and help during my PhD.

I would like to thank everyone from the Department of Applied Sciences, staff and students that I met during the last 3 years, especially Ross Edgar, Tom Broadbent, Oliver Glenister, Dr Lee Brown, Dimitrios Zonidis, Dr Georgina Armitage, Thomas Bousfield, Dr Daniel Crossley, Dylan Wallace, Dr Julien Doulcet, Bimod Thapa, Gabriel Mengheres, Rebecca Wilson, Joseph Mwansa, Dr Hamad Akriem, Dr Robert Faulkner, João Barbosa and Dr James Rooney.

I would like to thank Dr Jack Blackburn and Dr Sean Ward for their mass spectrometry service for IPOS, and Professor Craig Rice for his X-ray crystallography contributions.

Finally, I would like to thank the University of Huddersfield for the funding and providing all the conditions for the development of this project.

Para a Catarina, obrigado pelo teu amor e apoio,

Para a minha mãe, pai e irmão,

Para os meus avós,

Para a Ana e o Miguel

Table of Contents

Abstract ix

List of Abbreviations x

List of Figures xvi

List of Tables xxiii

List of Schemes xxv

1. INTRODUCTION 0

1.1 Concepts of Photochromism 1

1.2 Photochromic Systems 9

1.2.1 Azobenzenes 9

1.2.2 Diarylethenes 11

1.2.2.1 Stilbenes 11

1.2.2.2 Dithienylethenes 14

1.2.3 Spirobenzopyrans and Spirooxazines 17

1.2.4 Naphthopyrans 21

1.3 Synthesis and Photochromism of Naphthopyrans 21

1.3.1 Methods of Synthesis 24

1.3.2 Photochromic Properties of 3*H*-naphtho[2,1-*b*]pyrans 28

1.3.3 Applications of 3*H*-naphtho[2,1-*b*]pyrans 48

1.4 Photochromic Rhenium(I) Complexes 50

1.4.1 Photochrome Coordinated to Rhenium(I) 52

1.4.2 Photochrome Covalently Bonded to Bidentate Ligand 58

1.5 Aims of the Present Study 63

2. DISCUSSION 65

2.1 Synthesis of Pyridyl Substituted 3*H*-Naphtho[2,1-*b*]pyrans 66

2.1.0 Strategic Ideas 66

2.1.0.1 Strategy A – By a Suzuki cross-coupling reaction after chromenization 66

2.1.0.2 Strategy B – By a Heck cross-coupling reaction protocol 67

2.1.0.3 Strategy C – By a Suzuki cross-coupling reaction before chromenization..... 68

2.1.1 Strategy A – By a Suzuki cross-coupling reaction after chromenization 71

2.1.1.1 Synthesis of 10-Pyridyl-3*H*-Naphtho[2,1-*b*]pyrans 71

2.1.1.2 Synthesis of 9-Pyridyl-3*H*-Naphtho[2,1-*b*]pyrans 74

2.1.1.3 Synthesis of 8-Pyridyl-3*H*-Naphtho[2,1-*b*]pyrans 81

2.1.1.4 Synthesis of 7-Pyridyl-3*H*-Naphtho[2,1-*b*]pyrans 92

2.1.1.5 Synthesis of 5-Pyridyl-3*H*-Naphtho[2,1-*b*]pyrans 95

2.1.1.6 Synthesis of a 8-(Pyridyl-triazole)-3*H*-Naphtho[2,1-*b*]pyran 102

2.1.2 Strategy B – By a Heck cross-coupling protocol 107

2.1.2.1 Synthesis of 3-Pyridyl-3*H*-Naphtho[2,1-*b*]pyrans 107

2.1.3 Strategy C – By a Suzuki cross-coupling reaction before chromenization..... 124

2.1.3.1 Attempted Synthesis of 5-Pyridyl-3*H*-Naphtho[2,1-*b*]pyrans 124

2.1.3.2 Synthesis of 6-Pyridyl-Naphtho[2,1-*b*]pyrans 132

2.2 Synthesis of Photochromic Rhenium(I) Complexes 140

2.2.1 Synthesis of *fac*-[Re(N^N)$(CO)_3$Cl]^0 140

2.2.2 Synthesis of *fac*-[Re(BPy)$(CO)_3$NP]$^+$ 143

2.2.3 Synthesis of *fac*-[Re(PyTz)$(CO)_3$NP]$^+$ 147

2.2.4 Synthesis of *fac*-[Re(BTz)$(CO)_3$NP]$^+$ 154

2.2.5 Synthesis of *fac*-[Re(PyTzNP)$(CO)_3$Cl]^0 157

2.2.6 Synthesis of *fac*-[Re(N^N)$(CO)_3$naphthalene]$^+$ 159

2.3 Photophysical Properties 162

2.3.1 Photochromic Properties of the Pyridyl Substituted 3*H*-naphtho[2,1-*b*]pyrans 162

2.3.1.1 10-Pyridyl-3*H*-naphtho[2,1-*b*]pyran 164

2.3.1.2 9-Pyridyl-3*H*-naphtho[2,1-*b*]pyran 165

2.3.1.3 8-Pyridyl-3*H*-naphtho[2,1-*b*]pyran 170

2.3.1.4 8-(Pyridyl-triazole)-3*H*-naphtho[2,1-*b*]pyran 180

2.3.1.5 7-Pyridyl-3*H*-naphtho[2,1-*b*]pyran 182

2.3.1.6 6-Pyridyl-3*H*-naphtho[2,1-*b*]pyran 184

2.3.1.7 3-Pyridyl-3*H*-naphtho[2,1-*b*]pyran 188

2.3.1.8 8-Aryl-3*H*-naphtho[2,1-*b*]pyrans 190

2.3.2 Photochromism and Photoswitching of the Rhenium(I) Complexes 195

2.3.2.1 Photochromism and Photoswitching of *fac*-[Re(BPy)(CO)$_3$NP]PF$_6$, NP = 10-Pyridyl-3*H*-naphtho[2,1-*b*]pyran 199

2.3.2.2 Photochromism and Photoswitching of *fac*-[Re(N^N)(CO)$_3$NP]PF$_6$, NP = 9-Pyridyl-3*H*-naphtho[2,1-*b*]pyran and N^N = BPy, PyTz 202

2.3.2.3 Photochromism and Photoswitching of *fac*-[Re(N^N)(CO)$_3$NP]PF$_6$, NP = 8-Pyridyl-3*H*-naphtho[2,1-*b*]pyran and N^N = BPy, PyTz, BTz 209

2.3.2.4 Photochromism and Photoswitching of *fac*-[Re(N^N)(CO)$_3$NP]PF$_6$, NP = 7-Pyridyl-3*H*-naphtho[2,1-*b*]pyran and N^N = BPy, PyTz 222

2.3.2.5 Photochromism and Photoswitching of *fac*-[Re(PyTz)(CO)$_3$NP]PF$_6$, NP = 6-Pyridyl-3*H*-naphtho[2,1-*b*]pyran 229

2.3.2.7 Photochromism and Photoswitching of *fac*-[Re(PyTzNP)(CO)$_3$Cl]^0, NP = 3*H*-naphtho[2,1-*b*]pyran 236

2.3.2.6 Photochromism and Photoswitching of *fac*-[Re(N^N)(CO)$_3$NP]PF$_6$, NP = 3-Pyridyl-3*H*-naphtho[2,1-*b*]pyran and N^N = BPy, BTz 241

2.4 Ring-contraction of Naphthopyrans 246

2.4.1 Preamble 246

2.4.2 Discussion 251

3. EXPERIMENTAL 267

3.1 Equipment and Reagents 268

3.2 Synthesis of Pyridyl Substituted 3*H*-Naphtho[2,1-*b*]pyrans 269

3.2.1 Strategy A – By a Suzuki cross-coupling reaction after chromenization 269

3.2.1.1 Preparation of 10-Pyridyl-3*H*-Naphtho[2,1-*b*]pyrans 269

3.2.1.2 Preparation of 9-Pyridyl-3*H*-Naphtho[2,1-*b*]pyrans 272

3.2.1.3 Preparation of 8-Pyridyl and 8-Aryl Substituted Naphthopyrans 279

3.2.1.4 Preparation of 7-Pyridyl-3*H*-Naphtho[2,1-*b*]pyrans 293

3.2.1.5 Preparation of 5-Pyridyl-3*H*-Naphtho[2,1-*b*]pyrans 297

3.2.1.6 Preparation of 8-(Pyridyl-triazole)-3*H*-Naphtho[2,1-*b*]pyran 302

3.2.2 Strategy B – By a Heck cross-coupling reaction protocol 306

3.2.2.1 Preparation of 3-Pyridyl-3*H*-Naphtho[2,1-*b*]pyrans 306

3.2.3 Strategy C – By a Suzuki cross-coupling reaction before chromenization 317

3.2.3.1 Preparation of 5-Pyridyl-3*H*-Naphtho[2,1-*b*]pyrans 317

3.2.3.2 Preparation of 6-Pyridyl-3*H*-Naphtho[2,1-*b*]pyrans 327

3.3 Synthesis of Photochromic Rhenium(I) Complexes 339

3.3.1 Synthesis of *fac*-[Re(N^N)(CO)$_3$Cl]^0 Complexes 339

3.3.2 Synthesis of *fac*-[Re(BPy)(CO)$_3$NP]PF$_6$ Complexes 341

3.3.3 Synthesis of *fac*-[Re(PyTz)(CO)$_3$NP]PF$_6$ Complexes 346

3.3.4 Synthesis of *fac*-[Re(BTz)(CO)$_3$NP]PF$_6$ Complexes 353

3.3.5 Synthesis of *fac*-[Re(PyTzNP)(CO)$_3$Cl]^0 355

3.3.6 Synthesis of *fac*-[Re(N^N)(CO)$_3$naphthalene]PF$_6$ 356

3.4 Ring-Contraction of Naphthopyrans 359

3.4.1 Kinetic Study of the Ring-Contraction of 3,3-Bis(4-methoxyphenyl)-3*H*-naphtho[2,1-*b*]pyran (2.147) 359

3.4.2 General Experimental Procedure for the Pyran (Dihydroquinoline) Ring-Contraction 361

3.4.3 General Methods for the Synthesis of 2-(Bis(4-methoxyphenyl)methyl)-5-methoxy-3-(*p*-tolyl)naphtho[1,2-*b*]furan (2.353) 367

4. CONCLUSIONS AND FURTHER WORK 369

5. REFERENCES 373

Abstract

This project explores the synthesis of novel photochromic 3*H*-naphtho[2,1-*b*]pyrans, which have been decorated with pyridine units that serve as ligands in luminescent rhenium(I) complexes. It is envisioned that cycling the naphthopyrans would not only generate the coloured photomerocyanines but would also modulate the luminescence of the derived rhenium(I) complexes. Diverse synthetic strategies were devised to access the rhenium(I) complexes depending on the position and orientation of the pyridyl substituent on the naphthopyran ring. For the majority of the naphthopyrans which bear the pyridyl unit on the naphthalene moiety of the naphthopyran, Suzuki cross-coupling of either a bromo-, iodo- or trifloxy- substituted 3*H*-naphtho[2,1-*b*]pyran proved to be effective for introduction of the pyridyl unit. For the preparation of the 6-(pyridyl) substituted 3*H*-naphtho[2,1-*b*]pyran isomer, construction of a 1-bromo-4-(pyridyl)-2-naphthol was required, which was subjected Heck cross-coupling protocol to create the pyran ring. The 3-(4-pyridyl)-3*H*-naphtho[2,1-*b*]pyran was also obtained by a Heck cross-coupling strategy commencing from 1-phenyl-1-(4-pyridyl)prop-2-en-1-ol.

All of the new pyridyl substituted 3*H*-naphtho[2,1-*b*]pyrans exhibit good photochromic properties with the reversible generation of mostly red hues; the persistence of the photomerocyanines was dependent upon the location and orientation of the pyridyl unit. Spectroscopic measurements have shown that the novel rhenium(I) complexes exhibited both T- and P-type photochromism with an overall increase in colourability and variable half-times depending on both the point of attachment and orientation of the pyridyl unit on the naphthopyran core and also the nature of the bidentate ligands. Furthermore, the novel rhenium(I) complexes exhibited visible light induced photochromism due to a triplet photosensitization mechanism. Additionally, reversible quenching of the ^{3}MLCT excited state emission occurred as a result of the photochromic reaction, which depended on the relative energies of the ^{3}MLCT and ^{3}IL excited states and on the extent of the photochromic reaction.

During the Suzuki cross-coupling of the pyridine unit to the naphthopyran nucleus, a ring contraction of the pyran ‘motif’ was observed. This reaction has been developed into an efficient base-mediated protocol to a diverse series of novel naphthofurans, naphthodifurans and benzo-fused indoles in generally good yields.

List of Abbreviations

AcOH	Acetic acid
ACS	American Chemical Society
An	Anisyl (4-$MeOC_6H_4$)
APCI	Atmospheric Pressure Chemical Ionization
app.	Apparent
aq.	Aqueous
Ar	Aryl
ATR	Attenuated Total Reflection
Bn	Benzyl
B_2Pin_2	Bis(pinacolato)diboron
bpy	2,2'-Bipyridine
btz	1,1'-Dibenzyl-1*H*,1'*H*-4,4'-bi(1,2,3-triazole)
CF	Closed-form
CI	Conical intersection
COSY	Homonuclear Correlation Spectroscopy
CPS	Counts per second
CT	Charge transfer
Cy	Cyclohexyl
δ	Chemical shift (in ppm)
Δ	Heat
d	Doublet
DAC	Donor-acceptor complex

dba	Dibenzylideneacetone
1,2-DCE	1,2-Dichloroethane
DCM	Dichloromethane
dd	Doublet of doublets
DFT	Density functional theory
DIAD	Diisopropyl azodicarboxylate
DMAc	Dimethylacetamide
DMF	Dimethylformamide
DMSO	Dimethylsulfoxide
dppf	1,1′-Bis(diphenylphosphino)ferrocene
dt	Doublet of triplets
DTE	4,4'-Bisdithienylethene
ε	Molar extinction coefficient
ε_{PSS}	Molar extinction coefficient of the photostationary state
e.g.	*Exempli gratia*
ESI	Electrospray ionization
EWG	Electron withdrawing group
Φ	Quantum yield
fac	Facial
FRET	Fluorescence Resonance Energy Transfer
FT-IR	Fourier transform infrared spectroscopy
η	Refractive index
HMBC	Heteronuclear Multiple-Bond Correlation

HMDS	Hexamethyldisilazane
HOMO	Highest occupied molecular orbital
HRMS	High-resolution mass spectrometry
HSQC	Heteronuclear single quantum coherence
HV	High vibrational
ICP-MS	Inductively coupled plasma mass spectrometry
IL	Intra-ligand
^{3}IL	Triplet intra-ligand
IOD	Induced optical density
IPA	Isopropanol
ISC	Inter-system crossing
J	Coupling constant (in Hz)
k	Rate constant
k_{Δ}	Rate constant of thermal bleaching
$k_{\Delta 1}$	Rate constant of thermal bleaching (1st order)
$k_{\Delta 2}$	Rate constant of thermal bleaching (2nd order)
λ_{Abs}	Absorbance maxima (in nm)
λ_{Em}	Emission maxima (in nm)
λ_{exc}	Excitation wavelength (in nm)
λ_{max}	Absorbance maxima (in nm)
LMCT	Ligand-to-metal charge transfer
LUMO	Lowest unoccupied molecular orbital
LV	Low vibrational

m	Multiplet
MeCN	Acetonitrile
mer	Meridional
***m*-CPBA**	*meta*-Chloroperoxybenzoic acid
MLCT	Metal-to-ligand charge transfer
^{1}MLCT	Singlet metal-to-ligand charge transfer
^{3}MLCT	Triplet metal-to-ligand charge transfer
MOM	Methoxymethyl
MOMCl	Chloromethyl methyl ether
m.p.	Melting point
MS	Mass spectrometry
NBS	*N*-Bromosuccinimide
NIR	Near-Infrared
NMP	*N*-Methyl-2-pyrrolidone
NMR	Nuclear magnetic resonance
N^N	Bidentate ligand
NP	Naphthopyran
1PA	One-photon absorption
2PA	Two-photon absorption
Ph	Phenyl
phen	Phenanthroline
PhMe	Toluene
Pin	Pinacol

pKa	Acid dissociation constant
pKb	Base dissociation constant
***p*-MSB**	1,4-Bis(4-methylstyryl)benzene
ppm	Parts per million
PPTS	Pyridinium *p*-toluenesulfonate
PSS	Photostationary state
***p*TSA**	*p*-Toluenesulfonic acid
Py	Pyridyl
pytz	2-(1-Benzyl-1*H*-1,2,3-triazol-4-yl)pyridine
R_f	Retardation factor
RNA	Ribonucleic acid
r.t.	Room temperature
s	Singlet
S_EAr	Electrophilic aromatic substitution
S_N2	Nucleophilic substitution bimolecular
S_NV	Nucleophilic vinylic substitution
SOPY	Spironaphthoxazine-containing pyridine
stpy	Styrylpyridine
τ	Emission lifetime
$t_{½}$	Half-time
t	Triplet
TBAB	Tetrabutylammonium bromide
TBAC	Tetrabutylammonium chloride

TC	*Transoid-cis*
TCI	Tokyo Chemical Industry
Temp.	Temperature
Tf	Triflyl
TFA	Trifluoroacetic acid
tfms	Trifluoromethanesulfonate
THF	Tetrahydrofuran
TLC	Thin-layer chromatography
T.M.	Transition moment
TMS	Trimethylsilyl
TMSOH	Trimethylsilanol
TT	*Transoid-trans*
TTBP	Tri-*tert*-butylphosphonium
Tz	1,2,3-Triazole
UV	Ultraviolet
UV-Vis	Ultraviolet-visible
$\boldsymbol{\nu_{max}}$	Maximum wavenumber (in cm^{-1})

List of Figures

Figure 1.1 Hackmanite, before and after sunlight exposure.....1

Figure 1.2 UV-Vis Spectrum of hypothetical photochrome A and its corresponding coloured state B.....2

Figure 1.3 One-Photon Absorption (1PA) mechanism (by a singlet excited state S_1).....4

Figure 1.4 One-Photon Absorption (1PA) mechanism (by a triplet excited state T_1).....5

Figure 1.5 Simultaneous two-photon absorption (2PA) mechanism.....5

Figure 1.6 Stepwise two-photon absorption (2PA) mechanism via S_1 excited state.....6

Figure 1.7 Stepwise two-photon absorption (2PA) mechanism via T_1 excited state.....6

Figure 1.8 Stepwise two-photon absorption (2PA) mechanism via photoproduct (S'_0).....6

Figure 1.9 Photophysical processes upon photoexcitation of 3*H*-naphtho[2,1-*b*]pyran.....23

Figure 1.10 Photophysical processes that *fac*-[Re(bpy)$(CO)_3$Cl] **1.159** in acetonitrile undergoes after it is excited by light with a wavelength of 365 nm.....52

Figure 1.11 Energy-transfer pathway for *trans*-isomers **1.160** and **1.162**.....54

Figure 1.12 Energy-transfer pathway for *cis*-isomers **1.161** and **1.163**.....54

Figure 1.13 Energy-transfer pathway for both Re(I) complexes **1.164** and **1.165.**.....55

Figure 1.14 Energy-transfer pathway for ring-opened isomer **1.166**.....56

Figure 1.15 Energy-transfer pathway for ring-closed isomer **1.167** after photoisomerization.....56

Figure 1.16 Energy-transfer pathway for Re(I) complex **1.168**.....57

Figure 1.17 Energy-transfer pathway for Re(I) complex **1.170** before and after photoisomerization.....59

Figure 1.18 Energy-transfer pathway for Re(I) complex **1.172** before and after photoisomerization.....59

Figure 1.19 Energy-transfer pathway for Re(I) complex **1.174** before and after photoisomerization.....61

Figure 1.20 Energy-transfer pathway for Re(I) complex **1.176**.....62

Figure 1.21 Energy-transfer pathway for Re(I) complex **1.177**.....63

Figure 2.1 1-Pyridyl-3*H*-naphtho[2,1-*b*]pyrans **2.26** and 2-pyridyl-3*H*-naphtho[2,1-*b*]pyrans **2.27**.....70

Figure 2.2 3-(2,4-Dimethoxyphenyl)-3-(4-methoxyphenyl)-pyridyl-3*H*-naphtho[2,1-*b*]pyran **2.76**.....87

Figure 2.3 8-(4-Pyridyl)-3*H*-naphtho[2,1-*b*]pyran **2.57** and the corresponding naphthofuran **2.58**.....92

Figure 2.4 ^{1}H NMR spectrum of a naphthopyran **2.101**:photomerocyanine **2.103** (85:15) mixture in $CDCl_3$....97
Figure 2.5 COSY NMR of a naphthopyran **2.101**:photomerocyanine **2.103** (85:15) mixture in $CDCl_3$....98
Figure 2.6 Octahedral geometry of *fac* and *mer* $[Re(N^\wedge N)(CO)_3Cl]^0$ complexes....141
Figure 2.7 Crystal structure of rhenium(I) complex **2.232** (R = 0.0957)....143
Figure 2.8 Stereoisomers of rhenium(I) complexes **2.237**....152
Figure 2.9 Stereoisomers of rhenium(I) complex **2.244**....152
Figure 2.10 ^{1}H NMR spectrum in acetone-d_6 of the 1:1 mixture of stereoisomers of rhenium(I) complex **2.244**....153
Figure 2.11 *fac*-$[Re(N^\wedge N)(CO)_3$naphthalene$]^+$ complexes **2.248**–**2.250**....159
Figure 2.12 UV-Vis spectra of 3*H*-naphtho[2,1-*b*]pyran **2.36** (1.1 mM in toluene in the closed form (black) and in the PSS (yellow)....164
Figure 2.13 UV-Vis spectra of the bleaching in the dark of the PSS of **2.36** (0.38 mM in a mixture of PhMe:DCM (1:1), after UV irradiation) with a 120 seconds scan interval....165
Figure 2.14 UV-Vis spectra of 3*H*-naphtho[2,1-*b*]pyran **2.48** (3.0 mM in toluene in the closed form (black) and in the PSS (red)....166
Figure 2.15 UV-Vis spectra of 3*H*-naphtho[2,1-*b*]pyran **2.50** (6.8 mM in toluene in the closed form (black) and in the PSS (red)....167
Figure 2.16 **Figure 2.16** (a) UV-Vis spectra of the bleaching in the dark of the PSS of **2.48** (3.0 mM in toluene, after UV irradiation) with a 40 seconds scan interval; (b) Linear regression (2nd order)....168
Figure 2.17 UV-Vis spectra of the bleaching in the dark of the PSS of **2.50** (6.8 mM in toluene, after UV irradiation) with 120 seconds scan interval....169
Figure 2.18 Minimized energy structure of photomerocyanine **2.255** by using ChemDraw 3D MM2 force field method....169
Figure 2.19 UV-Vis spectra of 3*H*-naphtho[2,1-*b*]pyran **2.57** (6.0 mM in toluene in the closed form (black) and in the PSS (red)....170
Figure 2.20 UV-Vis spectra of the bleaching in the dark of the PSS of **2.57** (6.0 mM in toluene, after UV irradiation) with a 120 seconds scan interval....172
Figure 2.21 UV-Vis spectra of 3*H*-naphtho[2,1-*b*]pyran **2.59** (6.6 mM in toluene) in the closed form (black) and in the PSS (red)....173
Figure 2.22 UV-Vis spectra of the bleaching in the dark of the PSS of **2.59** (6.6 mM in toluene, after UV irradiation) with a 120 seconds scan interval....174

Figure 2.23 UV-Vis spectra of 3*H*-naphtho[2,1-*b*]pyran **2.65** (5.2 mM in toluene) in the closed form (black) and in the PSS (yellow).....175
Figure 2.24 p-Electron donation to the LUMO of naphthalene of **2.263**.....176
Figure 2.25 UV-Vis spectra of 3*H*-naphtho[2,1-*b*]pyran **2.77** (0.033 mM in toluene in the closed form (black) and in the PSS (red).....177
Figure 2.26 UV-Vis spectra of the bleaching in the dark of the PSS of **2.77** (0.033 mM in toluene, after UV irradiation) with a 20 seconds scan interval.....179
Figure 2.27 *Transoid-cis* (TC) of isomer **2.265**.....180
Figure 2.28 UV-Vis spectra of 3*H*-naphtho[2,1-*b*]pyran **2.110** (1.9 mM in toluene in the closed form (black) and in the PSS (red).....181
Figure 2.29 UV-Vis spectra of 3*H*-naphtho[2,1-*b*]pyran **2.98** (6.7 mM in toluene) in the closed form (black) and in the PSS (red).....183
Figure 2.30 UV-Vis spectra of 3*H*-naphtho[2,1-*b*]pyran **2.214** (4.0 mM in toluene) in the closed form (black) and in the PSS (red).....184
Figure 2.31 UV-Vis spectra of 3*H*-naphtho[2,1-*b*]pyran **2.215** (14 mM in toluene) in the closed form (black) and in the PSS (red).....185
Figure 2.32 UV-Vis spectra of the bleaching in the dark of the PSS of **2.114** (4.0 mM in toluene, after UV irradiation) with a 120 seconds scan interval.....188
Figure 2.33 UV-Vis spectra of the bleaching in the dark of the PSS of **2.115** (14 mM in toluene, after UV irradiation) with an 80 seconds scan interval.....188
Figure 2.34 UV-Vis spectra of 3*H*-naphtho[2,1-*b*]pyran **2.170** (0.19 mM in toluene) in the closed form (black) and in the PSS (yellow).....189
Figure 2.35 UV-Vis spectra of the bleaching in the dark of the PSS of **2.170** (0.19 mM in toluene, after UV irradiation) with a 30 seconds scan interval.....190
Figure 2.36 UV-Vis spectra of 3*H*-naphtho[2,1-*b*]pyrans **2.70** (4.4 mM in toluene) in the closed form (black) and in the PSS (red).....191
Figure 2.37 UV-Vis spectra of 3*H*-naphtho[2,1-*b*]pyrans **2.72** (5.4 mM in toluene) in the closed form (black) and in the PSS (red).....192
Figure 2.38 UV-Vis spectra of 3*H*-naphtho[2,1-*b*]pyrans **2.74** (0.048 mM in toluene) in the closed form (black) and in the PSS (red) 192
Figure 2.39 UV-Vis spectra of the bleaching in the dark of the PSS of **2.70** (0.078 mM in toluene, after UV irradiation) with a 240 seconds scan interval.....193
Figure 2.40 UV-Vis spectra of the bleaching in the dark of the PSS of **2.74** (0.048 mM in toluene, after UV irradiation) with a 120 seconds scan interval.....193

Figure 2.41 UV-Vis spectra of the bleaching in the dark of the PSS **2.72** (5.4 mM in toluene, after UV irradiation) with a 120 seconds scan interval.....194
Figure 2.42 Normalized spectra of emission of **2.239** (0.034 mM in degassed toluene, λ_{exc} 388 nm, green), emission of **2.239** (0.016 mM in a degassed mixture of dichloromethane:toluene (1:1), λ_{exc} 394 nm, red) and emission of **2.239** (0.019 mM in degassed acetonitrile, λ_{exc} 392 nm, blue).....197
Figure 2.43 Energy transfer pathway for the *fac*-[Re(N^N)(CO)$_3$NP]PF$_6$ complexes.....198
Figure 2.44 UV-Vis spectra of the Re(I) complex **2.229** (0.014 mM in a mixture of toluene:dichloromethane (1:1)) in the closed form (black) and in the PSS (red).....200
Figure 2.45 Emission spectrum of Re(I) complex **2.229** with λ_{exc} 400 nm (0.024 mM in degassed acetonitrile) in the closed form.....201
Figure 2.46 Normalized spectra of absorbance of the PSS of **2.230** (0.033 mM in a mixture of toluene:dichloromethane (1:1), after UV irradiation, red) and emission of **2.230** (0.017 mM in a degassed mixture of toluene:dichloromethane (1:1), λ_{exc} 360 nm, yellow).....204
Figure 2.47 Normalized spectra of absorbance of the PSS of **2.231** (0.064 mM in toluene, after UV irradiation, blue) and emission of **2.231** (0.034 mM in a degassed mixture of toluene:dichloromethane (1:1), λ_{exc} 384 nm, yellow).....204
Figure 2.48 Energy transfer pathway for *fac*-[Re(BPy)(CO)$_3$NP]PF$_6$ **2.230** and **2.231**, NP = 9-Pyridyl-3*H*-naphtho[2,1-*b*]pyran.....205
Figure 2.49 Normalized spectra of absorbance of the PSS of **2.238** (0.027 mM in toluene, after UV irradiation, red) and emission of complex **2.238** (0.027 mM in degassed toluene, λ_{exc} 384 nm, blue).....205
Figure 2.50 Energy transfer pathway for *fac*-[Re(PyTz)(CO)$_3$NP]PF$_6$ **2.238**, NP = 9-Pyridyl-3*H*-naphtho[2,1-*b*]pyran.....206
Figure 2.51 Emission spectra of rhenium(I) complex **2.230** with λ_{exc} 360 nm (0.017 mM in a degassed mixture of toluene:dichloromethane (1:1)) in the closed form (blue) and in the PSS (red).....207
Figure 2.52 Emission spectra of rhenium(I) complex **2.231** with λ_{exc} 384 nm (0.034 mM in a degassed mixture of toluene:dichloromethane (1:1)) in the closed form (blue) and in the PSS (red).....208
Figure 2.53 Emission spectra of rhenium(I) complex **2.238** with λ_{exc} 384 nm (0.027 mM in degassed toluene) in the closed form (black) and in the PSS (after UV irradiation, red).....208
Figure 2.54 Normalized spectra of absorbance of the PSS of **2.232** (0.039 mM in a mixture of toluene:dichloromethane (1:1), after UV irradiation, red) and emission of **2.232** (0.041 mM in a degassed mixture of toluene:dichloromethane (1:1), λ_{exc} 403 nm, orange).....212

Figure 2.55 Normalized spectra of absorbance of the PSS of **2.239** (0.019 mM in acetonitrile, after UV irradiation, blue) and emission of **2.239** (0.019 mM in degassed acetonitrile, λ_{exc} 392 nm, red)....212
Figure 2.56 Normalized spectra of absorbance of the PSS of **2.245** (0.035 mM in acetonitrile, after UV irradiation, blue) and emission of **2.245** (0.035 mM in degassed acetonitrile, λ_{exc} 387 nm, green)....213
Figure 2.57 Emission spectra of the Re(I) complex **2.232** with λ_{exc} 403 nm (0.041 mM in a degassed mixture of toluene:dichloromethane (1:1)) in the closed form (red) and in the PSS (blue)....214
Figure 2.58 Emission spectra of the Re(I) complex **2.239** with λ_{exc} 392 nm (0.019 mM in degassed acetonitrile) in the closed form (blue) and in the PSS (after UV irradiation, red)....214
Figure 2.59 Emission spectra of the Re(I) complex **2.245** with λ_{exc} 387 nm (0.035 mM in degassed acetonitrile) in the closed form (blue) and in the PSS (red)....215
Figure 2.60 Emission spectra of the Re(I) complex **2.240** with λ_{exc} 382 nm (0.011 mM in degassed acetonitrile) in the closed form (green) and in the PSS (red)....217
Figure 2.61 Normalized spectra of absorbance of the PSS of **2.240** (0.013 mM in degassed acetonitrile, after UV irradiation, red) and emission of **2.240** (0.011 mM in degassed acetonitrile, λ_{exc} 382 nm, green)....218
Figure 2.62 Normalized spectra of absorbance of the PSS of **2.239** (0.016 mM in acetonitrile, after UV irradiation, blue), emission of **2.239** (0.016 mM in degassed acetonitrile, λ_{exc} 392 nm, red) and emission **of 2.239** (0.034 mM in degassed toluene, λ_{exc} 388 nm, green)....219
Figure 2.63 Normalized spectra of absorbance of the PSS of **2.245** (0.035 mM in acetonitrile, after UV irradiation, blue), emission of **2.245** (0.028 mM in degassed toluene, λ_{exc} 346 nm, green) and emission of **2.245** (0.035 mM in degassed acetonitrile, λ_{exc} 387 nm, red)....219
Figure 2.64 Absorbance cycles of the Re(I) complex **2.239** (CF – PSS) after UV irradiation (0.016 mM in degassed acetonitrile)....220
Figure 2.65 Emission cycles of the Re(I) complex **2.239** (CF – PSS) after UV irradiation (0.016 mM in degassed acetonitrile)....220
Figure 2.66 Absorbance cycles of the Re(I) complex **2.240** (CF – PSS) after UV irradiation (0.013 mM in degassed acetonitrile)....221
Figure 2.67 Emission cycles of the Re(I) complex **2.240** (CF – PSS) after UV irradiation (0.013 mM in degassed acetonitrile)....221

Figure 2.68 Normalized spectra of absorbance of the PSS of **2.235** (0.024 mM in a mixture of toluene:dichloromethane (1:1), after UV irradiation, red) and emission of **2.235** (0.024 mM in a degassed mixture of toluene:dichloromethane (1:1), λ_{exc} 397 nm, yellow).....225
Figure 2.69 Normalized spectra of absorbance of the PSS of **2.241** (0.016 mM in degassed acetonitrile, after UV irradiation, red) and emission of **2.241** (0.029 mM in degassed toluene, λ_{exc} 394 nm, blue).....225
Figure 2.70 Emission spectra of rhenium(I) complex **2.235** with λ_{exc} 397 nm (0.024 mM in a degassed mixture of toluene:dichloromethane (1:1)) in the closed form (red) and in the PSS (green).....226
Figure 2.71 Emission spectra of rhenium(I) complex **2.241** with λ_{exc} 394 nm (0.029 mM in degassed toluene) in the closed-form (blue) and in the PSS (red).....227
Figure 2.72 Normalized spectra of absorbance of the PSS of **2.241** (0.016 mM in degassed acetonitrile, after UV irradiation, blue), emission of **2.241** (0.029 mM in degassed toluene, λ_{exc} 394 nm, green) and emission of **2.241** (0.016 mM in degassed acetonitrile, λ_{exc} 382 nm, red).....228
Figure 2.73 Absorbance cycles of rhenium(I) complex **2.241** (CF – PSS) after UV irradiation (0.016 mM in degassed acetonitrile).....228
Figure 2.74 Emission cycles of rhenium(I) complex **2.241** (CF – PSS) after UV irradiation (0.016 mM in degassed acetonitrile).....229
Figure 2.75 Normalized spectra of absorbance of the PSS of **2.242** (0.018 mM in toluene, after UV irradiation, blue) and emission of **2.242** (0.018 mM in degassed toluene, λ_{exc} 402 nm, red).....233
Figure 2.76 Normalized spectra of absorbance of the PSS of **2.243** (0.045 mM in toluene, after UV irradiation, red) and emission of **2.243** (0.020 mM in degassed toluene, λ_{exc} 358 nm, red).....233
Figure 2.77 Emission spectra of rhenium(I) complex **2.242** with λ_{exc} 402 nm (0.018 mM in degassed toluene) in the closed form (blue) and in the PSS (red).....234
Figure 2.78 Emission spectra of rhenium(I) complex **2.243** with λ_{exc} 358 nm (0.020 mM in degassed toluene) in the closed form (blue) and in the PSS (red).....234
Figure 2.79 Normalized spectra of absorbance of the PSS of **2.242** (0.018 mM in toluene, after UV irradiation, blue), emission of **2.242** (0.018 mM in degassed toluene, λ_{exc} 402 nm, green) and emission of **2.242** (0.024 mM in degassed acetonitrile, λ_{exc} 396 nm, red).....235
Figure 2.80 Spectra of emission of **2.247** (0.043 mM in a aerated mixture of toluene:dichloromethane (1:1), λ_{exc} 372 nm, green) and emission of the PSS of **2.247** (0.043 mM in a aerated mixture of toluene:dichloromethane (1:1), λ_{exc} 372 nm, yellow).....238

Figure 2.81 Normalized spectra of emission of **2.247** (0.043 mM in a aerated mixture of toluene:dichloromethane (1:1), λ_{exc} 372 nm, blue) and emission of **2.247** (0.021 mM in a degassed mixture of toluene:dichloromethane (1:1), λ_{exc} 411 nm, red)....239
Figure 2.82 Emission of **2.247** (0.021 mM in a degassed mixture of toluene:dichloromethane (1:1), λ_{exc} 411 nm, green) and emission of the PSS of **2.247** (0.021 mM in a degassed mixture of toluene:dichloromethane (1:1), λ_{exc} 411 nm, yellow)....239
Figure 2.83 Energy-transfer pathway for Re(I) complex **2.247** before and after photoisomerization, under air....240
Figure 2.84 Energy-transfer pathway for Re(I) complex **2.247** before and after photoisomerization, under degassed conditions....241
Figure 2.85 Normalized spectra of absorbance of the PSS of **2.236** (0.034 mM in toluene, after UV irradiation, yellow) and emission of **2.236** (0.017 mM in a degassed mixture of toluene:dichloromethane (1:1), λ_{exc} 381 nm, green)....244
Figure 2.86 Emission spectra of rhenium(I) complex **2.236** with λ_{exc} 381 nm (0.017 mM in a degassed mixture of toluene:dichloromethane (1:1)) in the closed form (blue) and in the PSS (red)....245
Figure 2.87 Emission spectra of rhenium(I) complex **2.246** with λ_{exc} 330, 363 and 400 nm (0.043 mM in degassed acetonitrile)....245
Figure 2.88 Rate plot of the ring-contraction of **2.330** by using K_2CO_3 (1.5 equiv) and $Pd(PPh_3)_4$ (5 mol%) in PhMe:EtOH (1:1) at reflux....253
Figure 2.89 Rate plot of the ring-contraction of the 3*H*-naphtho[2,1-*b*]pyran **2.330** by using K_2CO_3 (1.5 and 3 equiv) in PhMe:EtOH (1:1) at reflux....254
Figure 2.90 Rate plot of the ring-contraction of the 3*H*-naphtho[2,1-*b*]pyran **2.330** by using different carbonate bases (1.5 equiv) in PhMe:EtOH (1:1) at reflux....255
Figure 2.91 Rate plot of the ring-contraction of the 3*H*-naphtho[2,1-*b*]pyran **2.330** by using K_2CO_3 (1.5 equiv) and 18-crown-6 (3 equiv) in toluene at reflux....258
Figure 2.92 Rate plot of the ring-contraction of the 3*H*-naphtho[2,1-*b*]pyran **2.330** by using Na_2CO_3 (1.5 equiv) and 15-crown-5 (3 equiv) in PhMe at reflux, in the presence and in the absence of $Pd(PPh_3)_4$ (5 mol%)....260
Figure 2.93 Rate plot for the ring-contraction of the 3*H*-naphtho[2,1-*b*]pyran **2.330** by using K_2CO_3 (0.1 equiv) and 18-crown-6 (0.2 equiv)....261

List of Tables

Table 1.1 Spectrokinetic data for naphthopyrans **1.94**–**1.96**.....29

Table 1.2 Spectroscopic data for naphthopyrans **1.100**.....30

Table 1.3 Spectrokinetic data for naphthopyrans **1.101**.....31

Table 1.4 Spectrokinetic data for naphthopyrans **1.113**.....34

Table 1.5 Spectroscopic data for naphthopyrans **1.118**.....36

Table 1.6 Spectroscopic data for naphthopyrans **1.122**.....37

Table 1.7 Spectroscopic data for naphthopyrans **1.130**.....40

Table 2.1 Synthesis of 8-aryl-3*H*-naphtho[2,1-*b*]pyran**s** **2.70**, **2.72**, **2.74** and the corresponding naphthofurans **2.71**, **2.73**, **2.75** from 8-bromo-3*H*-naphtho[2,1-*b*]pyran **2.56**.....86

Table 2.2 Suzuki cross-coupling reactions between **2.104** and different boronic acids under multiple conditions.....101

Table 2.3 Attempted Heck reactions between 1-bromo-2-naphthol **2.137** and different Heck partners under various conditions.....110

Table 2.4 Attempted Heck reactions between 1-iodo-2-naphthol **2.143** and different Heck parntners under various conditions.....112

Table 2.5 Attempted Heck reactions between between 2-acetoxy-1-bromonaphthalene **2.149** and different Heck partners under various conditions.....115

Table 2.6 Heck cross-coupling reactions between **2.162** and **2.129** under various conditions.....121

Table 2.7 Summary of the synthesis of the 10-, 9-, 8-, 7-, 6-, 5-, 3-pyridyl substituted 3*H*-naphtho[2,1-*b*]pyrans.....139

Table 2.8 Synthesis of the *fac*-[Re(N^N)$(CO)_3$Cl]^0 complexes.....142

Table 2.9 Synthesis of the *fac*-[Re(BPy)$(CO)_3$NP]$^+$ complexes **2.228**.....144

Table 2.10 Synthesis of the *fac*-[Re(PyTz)$(CO)_3$NP]$^+$ complexes **2.237**.....148

Table 2.11 Tabular summary of the spectroscopic data of the pyridyl substituted 3*H*-naphtho[2,1-*b*]pyrans (in toluene).....163

Table 2.12 Spectroscopic data of *fac*-[Re(BPy)$(CO)_3$NP]PF_6, NP = 10-Pyridyl-3*H*-naphtho[2,1-*b*]pyran in toluene.....200

Table 2.13 Spectroscopic data of *fac*-[Re(N^N)$(CO)_3$NP]PF_6, NP = 9-Pyridyl-3*H*-naphtho[2,1-*b*]pyran and N^N = BPy, PyTz in toluene.....203

Table 2.14 Spectroscopic data of *fac*-[Re(N^N)$(CO)_3$NP]PF_6, NP = 9-Pyridyl-3*H*-naphtho[2,1-*b*]pyran and N^N = BPy, PyTz in toluene.....207

Table 2.15 Spectroscopic data of *fac*-[Re(N^N)(CO)$_3$NP]PF$_6$, NP = 8-Pyridyl-3*H*-naphtho[2,1-*b*]pyran and N^N = BPy, PyTz, BTz in toluene.....210
Table 2.16 Spectroscopic data of *fac*-[Re(N^N)(CO)$_3$NP]PF$_6$, NP = 8-Pyridyl-3*H*-naphtho[2,1-*b*]pyran and N^N = BPy, PyTz, BTz in toluene.....216
Table 2.17 Spectroscopic data of *fac*-[Re(N^N)(CO)$_3$NP]PF$_6$, NP = 7-(4-Pyridyl)-3*H*-naphtho[2,1-*b*]pyran and N^N = BPy, PyTz in toluene.....224
Table 2.18 Spectroscopic data of *fac*-[Re(PyTz)(CO)$_3$NP]PF$_6$, NP = 6-Pyridyl-3*H*-naphtho[2,1-*b*]pyran in toluene.....229
Table 2.19 Spectroscopic data of *fac*-[Re(PyTzNP)(CO)$_3$Cl]^0 with NP = 3*H*-naphtho[2,1-*b*]pyran in toluene.....237
Table 2.20 Spectroscopic data of *fac*-[Re(N^N)(CO)$_3$NP]PF$_6$, NP = 3-Pyridyl-3*H*-naphtho[2,1-*b*]pyran in toluene.....243
Table 2.21 Experimental conditions and rate constant for the ring-contraction of the 3*H*-naphtho[2,1-*b*]pyran **2.330**.....257
Table 2.22 Experimental conditions and rate constant of the ring-contraction of the 3*H*-naphtho[2,1-*b*]pyran **2.330** using different crown ethers.....261
Table 2.23 Synthesis of naphthofurans, naphthodifurans and benzo-fused indoles.....263
Table 2.24 Ring-contraction of the 2*H*-naphtho[1,2-*b*]pyrans **2.350** and **2.352**.....266

List of Schemes

Scheme 1.1 *Trans* (*E*) – *cis* (*Z*) isomerization of azobenzene....9
Scheme 1.2 Azo coupling....10
Scheme 1.3 Mills reaction....10
Scheme 1.4 Wallach transformation....10
Scheme 1.5 *Trans-cis* isomerization of stilbene....12
Scheme 1.6 Photocyclization of stilbene to phenanthrene....12
Scheme 1.7 Perkin condensation....13
Scheme 1.8 Wittig reaction....13
Scheme 1.9 Mizoroki–Heck cross-coupling reaction....14
Scheme 1.10 Photoisomerization of dithienylethene....15
Scheme 1.11 Nucleophilic vinylic substitution (S_NV) of perfluorocyclopentenes with aryllithium....15
Scheme 1.12 Photoisomerization of photochromic hybrid **1.33**....16
Scheme 1.13 Photoisomerization of dithienylethene **1.37**....17
Scheme 1.14 Photoisomerization of spirobenzopyran and spirooxazine....18
Scheme 1.15 Photoisomerization of spirobenzopyran....18
Scheme 1.16 Synthesis of spirobenzopyran **1.45**....18
Scheme 1.17 Photoisomerization of spirooxazine....19
Scheme 1.18 Synthesis of spirooxazine **1.50**....19
Scheme 1.19 Photoisomerization of 3*H*-naphtho[2,1-*b*]pyran....23
Scheme 1.20 Synthesis of naphthopyran **1.58**....24
Scheme 1.21 Synthesis of naphthopyran **1.64**....24
Scheme 1.22 Synthesis of naphthopyrans **1.66** and **1.67**....25
Scheme 1.23 Synthesis of pyran **1.69**....25
Scheme 1.24 Synthesis of bisnaphthopyran **1.73**....25
Scheme 1.25 Synthesis of naphthopyran **1.77**....26
Scheme 1.26 Synthesis of naphthopyran **1.81**....26
Scheme 1.27 Synthesis of naphthopyrans **1.83**–**1.84**....27
Scheme 1.28 Synthesis of naphthopyrans **1.86**....27
Scheme 1.29 Putative mechanism of the acid-catalysed condensation between naphthol **1.74** and propynol **1.85**....28
Scheme 1.30 Absence of photoisomerization of naphthopyran **1.92**....28

Scheme 1.31 Oxidation of naphthopyran **1.104**, followed by UV-promoted ring-contraction to **1.106**.....32
Scheme 1.32 Photoisomerization of naphthopyran **1.114**.....34
Scheme 1.33 Photoisomerization of bisnaphthopyran **1.148**.....46
Scheme 1.34 Photoisomerization of biphotochromic system **1.149**.....47
Scheme 1.35 Photoisomerization of naphthopyran-bridge-benzimidazole dyad **1.153**.....49
Scheme 1.36 Photoisomerization and spectrokinetic data of Re(I) complexes **1.160** and **1.161**.....53
Scheme 1.37 Photoisomerization and spectrokinetic data of Re(I) complexes **1.162** and **1.163**.....53
Scheme 1.38 Photoisomerization and spectrokinetic data of Re(I) complexes **1.164** and **1.165**.....55
Scheme 1.39 Photoisomerization of Re(I) complexes **1.166** and **1.167**.....56
Scheme 1.40 Photoisomerization and spectroscopic data of Re(I) complexes **1.168** and **1.169**.....57
Scheme 1.41 Photoisomerization and spectrokinetic data of Re(I) complexes **1.170** and **1.171**.....58
Scheme 1.42 Photoisomerization and spectrokinetic data of Re(I) complexes **1.172** and **1.173**.....60
Scheme 1.43 Photoisomerization and spectrokinetic data of Re(I) complexes **1.174** and **1.175**.....61
Scheme 1.44 Photoisomerization and spectroscopic data of Re(I) complexes **1.176** and **1.177**.....62
Scheme 2.1 Strategy A – By a Suzuki reaction after chromenization – for the preparation of pyridyl substituted 3*H*-naphtho[2,1-*b*]pyrans **2.1**.....66
Scheme 2.2 Strategy A – By a Suzuki reaction after chromenization – to prepare 8-(pyridyl-triazole)-3*H*-naphtho[2,1-*b*]pyran **2.5**.....67
Scheme 2.3 Naphthopyran **2.12** with electron withdrawing groups at C-3 prepared by the acid-catalysed condensation between 2-naphthol **2.10** and the corresponding propynol **2.11**.....68
Scheme 2.4 Strategy B – By a Heck cross-coupling reaction protocol – for the preparation of 3-pyridyl-3*H*-naphtho[2,1-*b*]pyrans **2.13**.....68
Scheme 2.5 Strategy C – By the direct acid-catalysed condensation – for the preparation of pyridyl substituted 3*H*-naphtho[2,1-*b*]pyrans **2.16**.....69
Scheme 2.6 Strategy C – By protecting the pyridyl substituent – for the preparation of pyridyl substituted 3*H*-naphtho[2,1-*b*]pyrans **2.16**.....69
Scheme 2.7 Strategy C – By the Heck cross-coupling reaction – for the preparation of pyridyl substituted 3*H*-naphtho[2,1-b]pyrans **2.16**.....70
Scheme 2.8 Synthesis of 8-iodo-2-naphthol **2.29**.....71
Scheme 2.9 Mechanism of the synthesis of 8-iodo-2-naphthol **2.29**.....72
Scheme 2.10 Synthesis of 10-iodo-3*H*-naphtho[2,1-*b*]pyran **2.34**.....72
Scheme 2.11 Synthesis of 10-(4-pyridyl)-3*H*-naphtho[2,1-*b*]pyran **2.36**.....73
Scheme 2.12 General mechanism of a Suzuki cross-coupling reaction.....74

Scheme 2.13 Route A to 9-pyridyl-3*H*-naphtho[2,1-*b*]pyran **2.41**.....75
Scheme 2.14 Route B to 9-pyridyl-3*H*-naphtho[2,1-*b*]pyran **2.41**.....75
Scheme 2.15 Synthesis of 7-bromo-2-naphthol **2.38** (Method A) 76
Scheme 2.16 Synthesis of 7-bromo-2-naphthol **2.38** (Method B) 76
Scheme 2.17 Mechanism of the synthesis of 7-bromo-2-naphthol **2.38**.....77
Scheme 2.18 Synthesis of 9-bromo-3*H*-naphtho[2,1-*b*]pyran **2.39**.....77
Scheme 2.19 Synthesis of 9-pyridyl-3*H*-naphtho[2,1-*b*]pyrans and corresponding naphthofurans from 9-bromo-3*H*-naphtho[2,1-*b*]pyran **2.39**.....78
Scheme 2.20 Synthesis of 9-hydroxy-3*H*-naphtho[2,1-*b*]pyran **2.40**.....79
Scheme 2.21 Synthesis of 9-triflyloxy-3*H*-naphtho[2,1-*b*]pyran **2.43**.....79
Scheme 2.22 Mechanism of the synthesis of 9-triflyloxy-3*H*-naphtho[2,1-*b*]pyran **2.43**.....80
Scheme 2.23 Synthesis of 9-pyridyl-3*H*-naphtho[2,1-*b*]pyrans and corresponding naphthofurans from 9-triflyloxy-3*H*-naphtho[2,1-*b*]pyran **2.43**.....80
Scheme 2.24 Synthesis of 8-bromo-3*H*-naphtho[2,1-*b*]pyran **2.56**.....81
Scheme 2.25 Synthesis of 8-pyridyl-3*H*-naphtho[2,1-*b*]pyrans and corresponding naphthofurans from 8-bromo-3*H*-naphtho[2,1-*b*]pyran **2.56**.....82
Scheme 2.26 Synthesis of 8-boronyl-3*H*-naphtho[2,1-*b*]pyran **2.62** via a two-step metalation protocol (Method A).....83
Scheme 2.27 Synthesis of 8-boronyl-3*H*-naphtho[2,1-*b*]pyran **2.62** by a Pd-mediated borylation (Method B) 84
Scheme 2.28 Synthesis of 8-(4-pyridyl)-3*H*-naphtho[2,1-*b*]pyran **2.57** and the corresponding naphthofuran **2.58** from 8-boronyl-3*H*-naphtho[2,1-*b*]pyran **2.62**.....84
Scheme 2.29 Synthesis of 8-(2-pyridyl)-3*H*-naphtho[2,1-*b*]pyran **2.65** and the corresponding naphthofuran **2.66** from 8-boronyl-3*H*-naphtho[2,1-*b*]pyran **2.62**.....85
Scheme 2.30 Synthesis of 8-aryl-3*H*-naphtho[2,1-*b*]pyrans **2.70**, **2.72**, **2.74** and the corresponding naphthofurans **2.71**, **2.73**, **2.75** from 8-bromo-3*H*-naphtho[2,1-*b*]pyran **2.56**.....86
Scheme 2.31 Retrosynthetic route to 8-(4-pyridyl)-3*H*-naphtho[2,1-*b*]pyran **2.77**.....88
Scheme 2.32 Synthesis of benzophenone **2.80**.....88
Scheme 2.33 Mechanism of the synthesis of benzophenone **2.80**.....89
Scheme 2.34 Synthesis of propynol **2.79**.....89
Scheme 2.35 Mechanism of the synthesis of propynol **2.79**.....90
Scheme 2.36 Synthesis of 8-bromo-3*H*-naphtho[2,1-*b*]pyran **2.78**.....90
Scheme 2.37 Synthesis of 8-(4-pyridyl)-3*H*-naphtho[2,1-*b*]pyran **2.77** and the corresponding naphthofuran **2.89**.....91

Scheme 2.38 Synthesis of 5-bromo-2-naphthol **2.93**.....93
Scheme 2.39 Synthesis of 7-bromo-3*H*-naphtho[2,1-*b*]pyran **2.94**.....93
Scheme 2.40 Synthesis of 4-pyridineboronic acid **2.97**.....94
Scheme 2.41 Synthesis of 4-pyridineboronic acid pinacol ester **2.35**.....94
Scheme 2.42 Synthesis of 7-(4-pyridyl)-3*H*-naphtho[2,1-*b*]pyran **2.98**.....95
Scheme 2.43 Synthesis of 5-hydroxy-3*H*-naphtho[2,1-*b*]pyran **2.101**.....96
Scheme 2.44 Synthesis of 5-triflyloxy-3*H*-naphtho[2,1-*b*]pyran **2.104**.....99
Scheme 2.45 Suzuki cross-coupling reactions between 2.104 and different boronic acids under multiple conditions.....101
Scheme 2.46 Synthesis of 5-(4-pyridyl)-3*H*-naphtho[2,1-*b*]pyran **2.106**.....102
Scheme 2.47 Retrosynthesis of 8-(pyridyl-triazole)-3*H*-naphtho[2,1-*b*]pyran **2.110**.....102
Scheme 2.48 Retrosynthesis of bromo substituted pyridyl triazole **2.111**.....103
Scheme 2.49 Synthesis of 4-bromo-2-ethynylpyridine **2.112** by Method A.....103
Scheme 2.50 Synthesis of bromo substituted pyridyl-triazole **2.112** by Method B.....104
Scheme 2.51 General mechanism of a Sonogashira cross-coupling reaction.....104
Scheme 2.52 Synthesis of benzyl azide **2.113**.....105
Scheme 2.53 Mechanism of the synthesis of benzyl azide **2.113**.....105
Scheme 2.54 Synthesis of the pyridyl-triazole **2.111**.....105
Scheme 2.55 Mechanism of the Click-type reaction.....106
Scheme 2.56 Synthesis of 8-(pyridyl-triazole)-3*H*-naphtho[2,1-*b*]pyran **2.110**.....107
Scheme 2.57 Synthesis of propenol **2.126**.....107
Scheme 2.58 Mechanism of the synthesis of propenol **2.126**.....108
Scheme 2.59 Synthesis of propenol **2.129**.....108
Scheme 2.60 General mechanism of a Heck cross-coupling reaction.....109
Scheme 2.61 Heck cross-coupling reactions between 1-bromo-2-naphthol **2.137** and different Heck partners under multiple conditions.....110
Scheme 2.62 Synthesis of 1-iodo-2-naphthol **2.143**.....111
Scheme 2.63 Mechanism of the iodination of 2-naphthol **2.142**.....111
Scheme 2.64 Heck cross-coupling reactions between 1-iodo-2-naphthol **2.143** and different Heck partners under different conditions.....112
Scheme 2.65 Mechanism of the base promoted electrocyclization of **2.146** to **2.147**.....113
Scheme 2.66 Synthesis of 2-acetoxy-1-bromonaphthalene **2.149**.....113
Scheme 2.67 Mechanism of the synthesis of 2-acetoxy-1-bromonaphthalene **2.149**.....114

Scheme 2.68 Heck cross-coupling reactions between 2-acetoxy-1-bromonaphthalene **2.149** and different Heck partners under different conditions.....115
Scheme 2.69 Synthesis of ((1-iodonaphthalen-2-yl)oxy)trimethylsilane **2.155**.....116
Scheme 2.70 Mechanism of the trimethysilylation of 1-iodo-2-naphthol **2.143**.....116
Scheme 2.71 Synthesis of 2-(4-methoxyphenyl)naphtho[2,1-*b*]furan **2.158**.....117
Scheme 2.72 Putative mechanism of the palladium catalysed oxidative cyclization to **2.159**.....118
Scheme 2.73 Synthesis of 1-bromo-2-(methoxymethoxy)naphthalene **2.162**.....118
Scheme 2.74 Mechanism of the synthesis of 1-bromo-2-(methoxymethoxy)naphthalene **2.162**.....119
Scheme 2.75 Synthesis of Heck product **2.165**.....119
Scheme 2.76 Heck cross-coupling reactions between **2.162** and **2.129** under different conditions.....121
Scheme 2.77 Synthesis of Pd(*t*-$Bu_3P)_2$ from the reaction of $Pd(dba)_2$ with P(*t*-Bu)$_3$HBF$_4$.....122
Scheme 2.78 Putative mechanism of the synthesis of 3*H*-naphtho[2,1-*b*]pyran **2.147**.....122
Scheme 2.79 Synthesis of 3-(4-pyridyl)-3*H*-naphtho[2,1-*b*]pyran **2.170**.....122
Scheme 2.80 Putative mechanism of the synthesis of 3-(4-pyridyl)-3*H*-naphtho[2,1-*b*]pyran **2.170**.....123
Scheme 2.81 Synthesis of 3-(4-pyridyl)-2-methoxynaphthalene **2.175**.....124
Scheme 2.82 Synthesis of 3-(3-pyridyl)-2-methoxynaphthalene **2.178**.....125
Scheme 2.83 Mechanism of the synthesis of 3-bromo-2-methoxynapthalene **2.174** from 2-methoxynaphthalene **2.176**.....125
Scheme 2.84 Synthesis of 3-pyridyl-2-naphthols **2.180** and **2.181**.....126
Scheme 2.85 Mechanism of the demethylation of 3-(4-pyridyl)-2-methoxynaphthalene **2.175**.....126
Scheme 2.86 Synthesis of 6-(4-pyridyl)-2-naphthol **2.183**.....127
Scheme 2.87 Failed synthesis of 8-(4-pyridyl)-3*H*-naphtho[2,1-*b*]pyran **2.57**.....127
Scheme 2.88 Failed synthesis of 8-(4-pyridyl)-3*H*-naphtho[2,1-*b*]pyran **2.57**.....128
Scheme 2.89 Synthesis of 1,3-dibromo-6-(4-pyridyl)-2-naphthol **2.185**.....129
Scheme 2.90 Synthesis of 1-bromo-6-(4-pyridyl)-2-naphthol **2.186**.....129
Scheme 2.91 Mechanism for the synthesis of 1-bromo-6-(4-pyridyl)-2-naphthol **2.186**.....129
Scheme 2.92 Synthesis of 1-bromo-6-(4-pyridyl)-2-(methoxymethoxy)naphthalene **2.188**.....130
Scheme 2.93 Synthesis of 1-bromo-3-pyridyl-2-naphthol **2.189** and **2.190**.....130
Scheme 2.94 Synthesis of 1-bromo-3-pyridyl-2-(methoxymethoxy)naphthalene **2.191** and **2.192**.....131
Scheme 2.95 Attempted synthesis of Heck product **2.193**.....131
Scheme 2.96 Synthesis of Heck product **2.194**.....132

Scheme 2.97 Synthesis of 3-methoxy-1-naphthol **2.196**.....133
Scheme 2.98 Mechanism for the synthesis of 3-methoxy-1-naphthol **2.196**.....134
Scheme 2.99 Synthesis of 3-methoxy-1-triflyloxynaphthalene **2.203**.....134
Scheme 2.100 Synthesis of 2-methoxy-4-pyridylnaphthalenes **2.204** and **2.205**.....135
Scheme 2.101 Synthesis of 4-pyridyl-2-naphthols **2.206** and **2.207**.....135
Scheme 2.102 Synthesis of 1-bromo-4-pyridyl-2-naphthols **2.208** and **2.209**.....136
Scheme 2.103 Synthesis of MOM-protected naphthalenes **2.210** and **2.211**.....136
Scheme 2.104 Synthesis of Heck products **2.212** and **2.213**.....137
Scheme 2.105 Electronic conjugation on **2.191**, **2.192**, **2.210** and **2.211**.....138
Scheme 2.106 Synthesis of 6-pyridyl-3*H*-naphtho[2,1-*b*]pyrans **2.214** and **2.215**.....138
Scheme 2.107 Synthesis of the *fac*-[Re(N^N)$(CO)_3$Cl]^0 complexes **2.216**.....140
Scheme 2.108 Synthesis of the *fac*-[Re(BPy)$(CO)_3$NP]$^+$ complexes **2.228**.....143
Scheme 2.109 Synthesis of the *fac*-[Re(PyTz)$(CO)_3$NP]$^+$ complexes **2.237**.....147
Scheme 2.110 Synthesis of Re(I) complex **2.245**.....154
Scheme 2.111 Synthesis of the Re(I) complex **2.246**.....156
Scheme 2.112 Synthesis of the *fac*-[Re(PyTzNP)$(CO)_3$Cl]^0 complex **2.247**.....158
Scheme 2.113 Synthesis of the 6-(4-pyridyl)-2-methoxynaphthalene **2.252**.....160
Scheme 2.114 Synthesis of *fac*-[Re(N^N)$(CO)_3$naphthalene]$^+$ complexes **2.248**–**2.250**.....160
Scheme 2.115 Electrocyclic ring-opening of 3*H*-naphtho[2,1-*b*]pyran **2.36**.....164
Scheme 2.116 Thermal isomerization of TT – TC of photomerocyanine **2.252**.....165
Scheme 2.117 Electrocyclic ring-opening of 3*H*-naphtho[2,1-*b*]pyran **2.48** and **2.50**.....166
Scheme 2.118 Resonance structures of photomerocyanines **2.253** and **2.255**.....168
Scheme 2.119 Electrocyclic ring-opening of 3*H*-naphtho[2,1-*b*]pyran **2.57**.....170
Scheme 2.120 Resonance structures of photomerocyanine **2.257**.....171
Scheme 2.121 Electrocyclic ring-opening of 3*H*-naphtho[2,1-*b*]pyran **2.59**.....172
Scheme 2.122 Resonance structures of photomerocyanine **2.260**.....173
Scheme 2.123 Electrocyclic ring-opening of 3*H*-naphtho[2,1-*b*]pyran **2.65**.....174
Scheme 2.124 Resonance structures of photomerocyanine **2.262**.....176
Scheme 2.125 Electrocyclic ring-opening of 3*H*-naphtho[2,1-*b*]pyran **2.65**.....177
Scheme 2.126 Resonance structures of photomerocyanine **2.265**.....178
Scheme 2.127 Electrocyclic ring-opening of 3*H*-naphtho[2,1-*b*]pyran **2.110**.....180
Scheme 2.128 Resonance structure of photomerocyanine **2.269**.....181
Scheme 2.129 Electrocyclic ring-opening of 3*H*-naphtho[2,1-*b*]pyran **2.98**.....182
Scheme 2.130 Resonance structures of the photomerocyanine **2.272**.....183

Scheme 2.131 Electrocyclic ring-opening of 3*H*-naphtho[2,1-*b*]pyrans **2.214** and **2.215**.....184
Scheme 2.132 Resonance structures of the photomerocyanine **2.274**.....186
Scheme 2.133 Resonance structures of the photomerocyanine **2.275**.....187
Scheme 2.134 Electrocyclic ring-opening of 3*H*-naphtho[2,1-*b*]pyran **2.170**.....189
Scheme 2.135 Electrocyclic ring-opening of 3*H*-naphtho[2,1-*b*]pyrans **2.70**, **2.72** and **2.74**.....191
Scheme 2.136 Resonance structures of the photomerocyanine **2.283**.....195
Scheme 2.137 Electrocyclic ring-opening of *fac*-[Re(N^N)$(CO)_3$NP]PF_6 complexes, with NP = Pyridyl-3*H*-naphtho[2,1-*b*]pyran and N^N = BPy, PyTz or BTz.....196
Scheme 2.138 Electrocyclic ring-opening of Re(I) complex **2.229**.....199
Scheme 2.139 Electrocyclic ring-opening of Re(I) complexes **2.230**, **2.231** and **2.238**.....202
Scheme 2.140 Electrocyclic ring-opening of Re(I) complexes **2.293**.....209
Scheme 2.141 Electrocyclic ring-opening of Re(I) complexes **2.235** and **2.241**.....222
Scheme 2.142 Electrocyclic ring-opening of Re(I) complexes **2.242** and **2.243**.....229
Scheme 2.143 Photoisomerization of Re(I) complex **2.247**.....236
Scheme 2.144 Electrocyclic ring-opening of Re(I) complexes **2.236** and **2.246**.....241
Scheme 2.145 Oxidative ring-contraction of the 1,2-dihydrospiro[benzo[*f*]chromene-3,9'-xanthene] **2.302**.....246
Scheme 2.146 Ring-contraction of the 2*H*-naphtho[1,2-*b*]pyran **2.304**.....246
Scheme 2.147 Mechanism of the ring-contraction of the 2*H*-naphtho[1,2-*b*]pyran **2.304**.....247
Scheme 2.148 Ring-contraction of the spiro(3*H*-naphtho[2,1-*b*]pyran-3,9′-thioxanthene-10,10-dioxide) **2.309**.....248
Scheme 2.149 Ring-contraction of the spiro(2*H*-naphtho[1,2-*b*]pyran-2,9′-thioxanthene-10,10-dioxide) **2.311**.....248
Scheme 2.150 Mechanism of the ring-contraction of the spiro(2*H*-naphtho[1,2-*b*]pyran-2,9′-thioxanthene-10,10-dioxide) **2.311**.....249
Scheme 2.151 Ring-contraction of the bis-sulfone **2.317**.....249
Scheme 2.152 Ring-contraction of the 3*H*-naphtho[2,1-*b*]pyran **2.319**.....250
Scheme 2.153 Synthesis of 2-(diarylmethyl)-5-styrylbenzofuran **2.322**.....250
Scheme 2.154 Mechanism of the synthesis of 2-(diarylmethyl)-5-styrylbenzofuran **2.322**.....251
Scheme 2.155 Generic Suzuki cross-coupling reaction between the halo or pseudo-halo substituted 3*H*-naphtho[2,1-*b*]pyran **2.327** and the pyridine boronic acid pinacol ester **2.40**.....252
Scheme 2.156 Ring-contraction of 3*H*-naphtho[2,1-*b*]pyran **2.330**.....252
Scheme 2.157 Selective coupling of **2.56** and **2.35** to give 3*H*-naphtho[2,1-*b*]pyran **2.57**.....256
Scheme 2.158 Selective synthesis of 10-(4-pyridyl)-3*H*-naphtho[2,1-*b*]pyran **2.36**.....256

Scheme 2.159 Synthesis of the naphthofuran **2.58**.....259
Scheme 2.160 Proposed mechanism for the ring-contraction of the 3*H*-naphtho[2,1-b]pyran **2.330**.....262
Scheme 2.161 Synthesis of naphthofurans, naphthodifurans and benzo-fused indoles.....263
Scheme 2.162 Ring-contraction of the 2*H*-naphtho[1,2-*b*]pyrans **2.350** and **2.352**.....266

1. INTRODUCTION

1.1 Concepts of Photochromism

Photochromism is defined as "the light-induced reversible transformation of a chemical entity into one or more isomeric species that possess different absorption spectra".[1] Simply put, photochromic materials reversibly change colour upon exposure to radiation.[1]

Photochromism was first described by Fritzche in 1866 by reporting the reversible photodimerisation of anthracene.[2] In 1867, Fritzche described the bleaching (color fading) of an orange solution of tetracene when exposed to light and regeneration of the color in the dark.[3] Ter Meer reported the color change of the potassium salt of 1,1-dinitroethane in the solid state, although this apparent photochromic phenomenon has been more recently refuted, as the color generation is due to the formation of the colored potassium salt of ethylnitrolic acid which is a photolytic product.[3, 4] In 1899, Markwald reported the light-induced reversible color change of 2,3,4,4-tetrachloronaphthalen-1-one in the solid state.[3] The word photochromism, etymologically deriving from the Ancient Greek words *phos* (light) and *chroma* (color), was first introduced in 1950 by Hirshberg to describe this photophysical phenomenon.[3] In 1971, Brown released the first major review on photochromism.[5]

Photochromism occurs in both organic and inorganic compounds, as well in biological systems.[6] Among the inorganic compounds exhibiting photochromic behaviour there are examples of oxides of group 5 metals, alkaline earth sulfides, titanates, poly(oxometalates), alkali metal azides, mercury salts and metal halides.[6,7] Hackmanite, $Na_8Al_6Si_6O_{24}Cl_2$, is a naturally occurring mineral that shows photochromism, as its violet color darkens when exposed to visible light, and slowly regains its original color once in the dark (**Figure 1.1**).[6] Organic photochromic families include diarylethenes,[8] naphthopyrans,[9] spiropyrans,[10] spirooxines,[11] benzopyrans,[12] azobenzenes,[13] stilbenes,[14] anils,[15] viologens,[16] fulgides,[17] and flavyliums.[18] Upon irradiation, the most common processes of photochromism for these compounds are *trans*-to-*cis* isomerization and pericyclic reactions.[19]

Figure 1.1 Hackmanite, before and after sunlight exposure (source: http://www.geologyin.com)

Most photochromes have a colourless or very pale yellow state **A**, and become coloured when irradiated with light due to the formation of a state **B** – positive photochromism (**Figure 1.2**).[2, 6]

Another class of photochromes are coloured in the dark, and turn colourless once irradiated by light – negative photochromism. [2, 6]

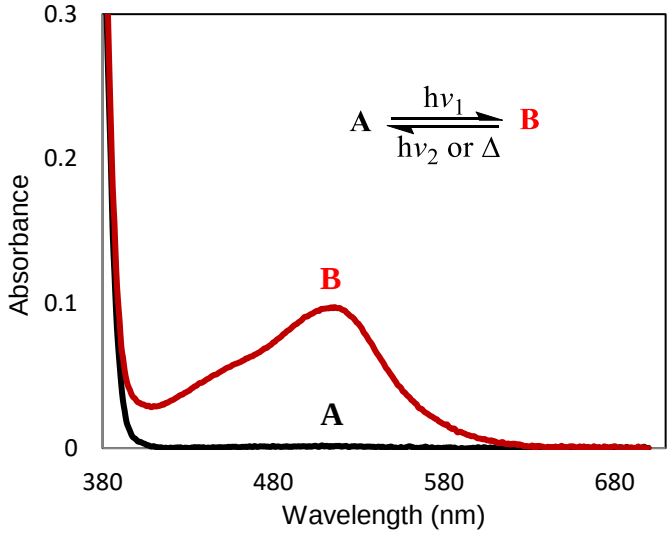

Figure 1.2 UV-Vis Spectrum of hypothetical photochrome **A** and its corresponding coloured state **B**.

When the back reaction is thermally driven the term used is T-type photochromism. [20] Otherwise, when the back reaction is photochemically driven the term used is P-type photochromism.[20] However, nowadays, it is conceived that this convenient conception is to a certain degree ambiguous, as many photochromes described as T-type show some component of P-type behaviour, with the reverse reaction showing dependence not only on temperature but also on radiation.

The absorption of light can be considered as an exercise in time-dependent perturbation theory.[21] A molecule in the stationary state can be described by the wavefunction Ψ_i and the latter is subjected to the Schrödinger equation:

(1) $H_0\Psi_i = E\Psi_i$.

If the system is perturbed by light, the sinusoidal oscillation electric vector of the light waves induces oscillating forces on the charged particles of the molecule. At this point, the Hamiltonian operator H_0 must be replaced by $(H_0 + H')$, where H' is the perturbation operator. The eigenfunctions $(H_0 + H')$ will be different from the initial wavefunction Ψ_i and will also be time-dependent. Therefore:

(2) $(H_0 + H')\Psi(x, t) = E\Psi(x, t)$.

The resulting wavefunctions can be expanded in terms of the wavefunctions of the unperturbed system, so:

(3) $\Psi(x, t) = \sum a_k(t)\Psi_k$, where the coefficient $a_k(t)$ being a function of time.

Therefore, the effect of the perturbation can be considered as a time-dependent mixing of the initial wavefunction with all other possible wavefunctions. The probability of the system to be found in the final state Ψ_f is given by the square of the coefficient $a_f(t)$. By mathematical analysis:

(4) $[a_f(t)]^2 = 8\pi^3/3h^2 <\Psi_i|\mathbf{\mu}|\Psi_f>^2 \rho(\nu_{if})t$, where $\rho(\nu_{if})$ is the radiation density (energy per unit volume) at the frequency ν_{if} corresponding to the transition, t is the time of irradiation and $<\Psi_i|\mathbf{\mu}|\Psi_f>$ (or $\int \Psi_i \,.\, \mathbf{\mu} \,.\, \Psi_f \, d\tau$) is the *transition moment* (T.M.), where $\mathbf{\mu}$ is the dipole moment operator $e \sum \mathbf{r}_j$ (e is the electronic charge and r_j the distance of the jth electron). The former equation shows that the probability of a given electronic transition is proportional to the square of the transition moment. In order to evaluate the T.M. aproximations must be introduced.[21]

The Born-Oppenheimer approximation simply states that the nuclear motion is very slow when compared to electronic motion, so the electrons are thought to be moving in the potential field of a static nuclei.[21] As a consequence, the total wavefunction can be factorized in a nuclear (vibrational) wavefunction θ and an electronic wavefunction ψ, therefore:

(5) $\Psi = \theta \,.\, \psi$

The T.M. is given by:

(6) T.M. $= \int \theta_i\psi_i \,.\, \mathbf{\mu} \,.\, \theta_f\psi_f \, d\tau$.

As the dipole moment operator $\mathbf{\mu}$ only operates on the electrons, the equation can be rewritten as:

(7) T.M. $= \int \theta_i\theta_f \, d\tau_N \,.\, \int \psi_i \,.\, \mathbf{\mu} \,.\, \theta_f\psi_f \, d\tau_e$.

Assuming that ψ (i) can be represented as the product of one-electron wavefunctions (orbitals) ϕ and that the orbitals are the same in both ground and excited states, and (ii) only one electron is promoted during the electronic transition, the equation can be rewritten as:

(8) T.M. $= \int \theta_i\theta_f \, d\tau_N \,.\, \int \phi_i \,.\, \mathbf{\mu} \,.\, \phi_f \, d\tau_e$, where ϕ_i and ϕ_f are the initial and final orbitals of the excited electron.

Finally, assuming that the orbitals can be factorized in both space and spin orbitals, then:

(9) $\phi = \varphi \,.\, S$, T.M. can be written as:

(10) T.M. $= \int \theta_i\theta_f \, d\tau_N \,.\, \int S_iS_f \, d\tau_s \,.\, \int \varphi_i \,.\, \mathbf{\mu} \,.\, \varphi_f \, d\tau_e$. The first term is the overlap integral of the wavefunctions for nuclear vibrations, the second term is the spin overlap integral and its values depends on the initial and final spin states of the promoted electron. The third term refers to the electronic transition moment and its value depends on the symmetries and amount of overlap of the initial and final spatial orbitals. As a result, the Schrödinger equation can be divided in three simpler equations:

(11) $H\theta = E\theta$.

(12) HS = ES.

(13) Hφ = Eφ.

The total molecular energy expressed as the sum of vibration, spin and electronic energies:

(14) $E = E_v + E_S + E_e$.[21]

As previously mentioned, the effect of electron spin upon transition intensities (or T.M.) is given by $\int S_i S_f \, d\tau_s$.[21] In singlet (S) → triplet (T) transitions, as the electron changes its spin state, the spin overlap integral is $\int \alpha\beta \, d\tau_s = \int \beta\alpha \, d\tau_s = 0$, which is a result of the α and β spin wavefunctions being orthogonal. The transition moment is zero and the transition is therefore forbidden in the light of the Born-Oppenheimer approximation. However, singlet (S) → triplet (T) transitions do occur as a consequence of spin-orbit coupling. Changing the electron spin implies changing the direction of its magnetic moment, which can be accomplished by the magnetic field produced by the orbital motion of the charged electron. Once the magnetic moment of the spinning electron becomes coupled to the orbital magnetic field, S → T transitions may occur. The probability of the S → T transition is higher by increasing the atomic number, giving rise to the heavy atom effect. In organic molecules, S → T transitions will be highly dependent on the presence of heavy atoms, either incorporated in the molecule or being present in the surrounding environment.[21] Many photochromic reactions involve a one-photon absorption (1PA) mechanism. Absorption of a photon by matter occurs within approximately 1-2 fs generating an excited state that quickly relaxes to the lowest energy excited state (S_1) via internal conversion within a few femtoseconds to tens of picoseconds. Kasha's rule states that photophysical processes occur from this generated excited state (S_1). A molecule once in the S_1 state can cascade down through the vibrational levels to the S_0 state by internal conversion or it may drop to the S_0 state by emitting light within nanoseconds – fluorescence. Usually, the latter processes are very slow and often unlikely, so faster photochromic processes may arise (e.g. photochemical reactions) (**Figure 1.3**). Otherwise, a photoproduct can arise from a triplet excited state T_1 formed by inter-system crossing (ISC) (**Figure 1.4**). [3, 22] Alternatively, a molecule once in the T_1 state may return to the S_0 by giving up heat or light – phosphorescence (10^{-8} - 10^{1} seconds).

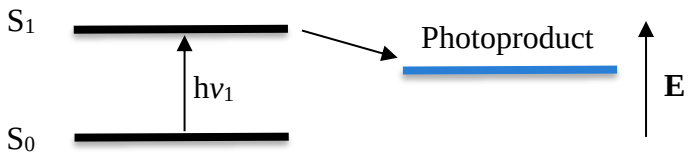

Figure 1.3 One-Photon Absorption (1PA) mechanism (by a singlet excited state S_1).

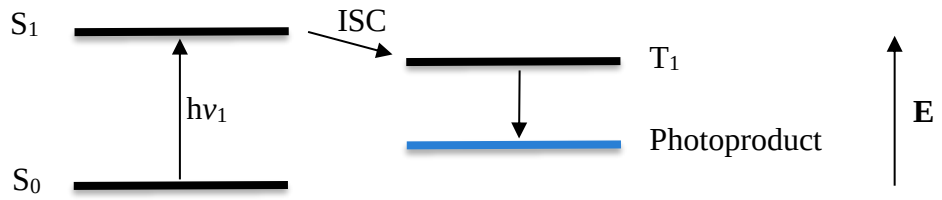

Figure 1.4 One-Photon Absorption (1PA) mechanism (by a triplet excited state T_1).

If an intense light source is used, e.g. laser pulses, a simultaneous or stepwise two-photon absorption process (2PA) can occur. In simultaneous 2PA, two photons are absorbed instantaneously, producing the excited state (S_2) via a virtual state (**Figure 1.5**).[3, 22]

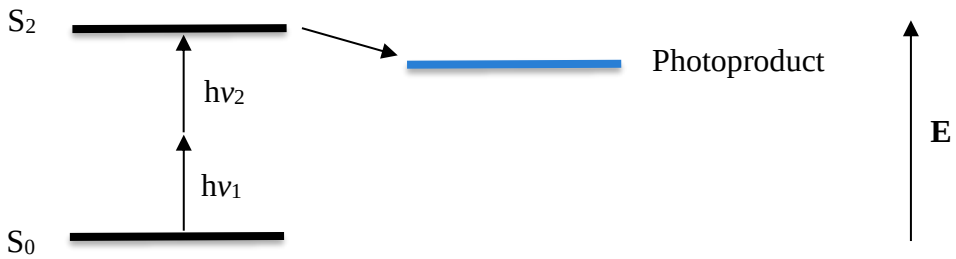

Figure 1.5 Simultaneous two-photon absorption (2PA) mechanism.

In a stepwise 2PA, there is the absorption of a second photon from a real stationary electronic state. The intermediate transient species could be either a singlet excited state (S_1) (**Figure 1.6**), a triplet excited state (T_1) (**Figure 1.7**) or the ground state of a photoproduct (S'_0) (**Figure 1.8**). In the first and second cases, the lifetimes of the S_1 states are in the order of tens of picoseconds to nanoseconds, while for the T_1 states are in the order of tens of nanoseconds to microseconds. For the third case, the stepwise 2PA occurs via the ground state of a photogenerated specie generated by a photochemical reaction, which has a lifetime longer than tens of nanoseconds. By using long-lived transient states, as in the second and third cases, the power threshold of the stepwise 2PA can be significantly decreased.[22]

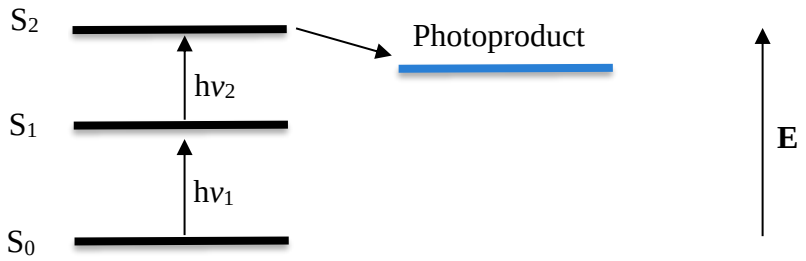

Figure 1.6 Stepwise two-photon absorption (2PA) mechanism via S_1 excited state.

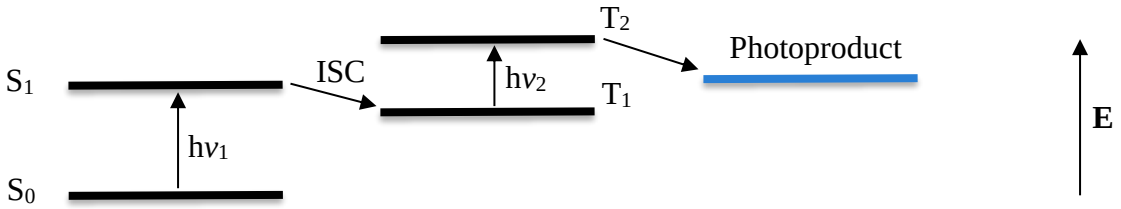

Figure 1.7 Stepwise two-photon absorption (2PA) mechanism via T_1 excited state.

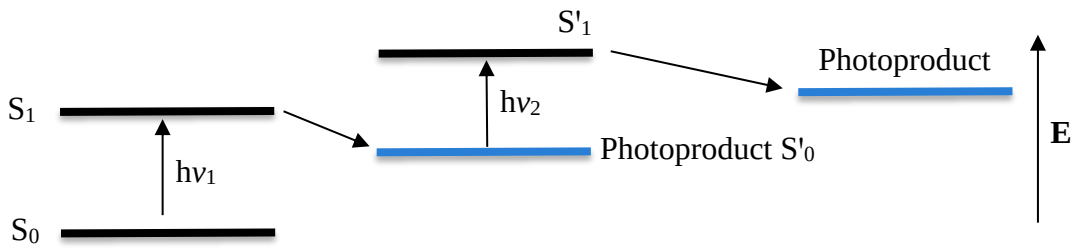

Figure 1.8 Stepwise two-photon absorption (2PA) mechanism via photoproduct (S'_0).

Singlet transitions ($S_0 \rightarrow S_n$) and triplet transitions ($T_1 \rightarrow T_n$) can correspond to electronic transitions of different nature. Thus, the most common transitions include $\sigma \rightarrow \sigma^*$, $\pi \rightarrow \pi^*$, $n \rightarrow \pi^*$, $n \rightarrow \sigma^*$ and charge transfer (CT):[21, 23]

a) $\sigma \rightarrow \sigma^*$ transitions occur in alkanes which have no *n* or π electrons. Light of very high energy (far-UV) is necessary for these types of transitions.

b) Singlet ($\pi \rightarrow \pi^*$) transitions are very common in alkenes, aldehydes, carboxylic esters, while triplet ($\pi \rightarrow \pi^*$) transitions are very weak in most organic molecules. Conjugation shifts the ($\pi \rightarrow \pi^*$) transitions to longer wavelengths – bathochromic shift (or red shift) – because the energy gap between the Highest Ocupied Molecular Orbital (HOMO) and the Lowest Unocuppied Molecular Orbital (LUMO) becomes progressively

smaller as the π conjugation system is extended. The opposite effect is called hypsochromic shift (or blue shift).

c) ($n \rightarrow \pi^*$) transitions are characteristic of molecules containing chromophores containing multiple bonded heteroatoms (e.g. C=O, C=N, N=N, N=O). These type of transitions are caused by UV radiation. Furthermore, molecules containing a carbonyl group can have both ($\pi \rightarrow \pi^*$) and ($n \rightarrow \pi^*$) transitions which would give rise to at least two peaks in the UV.

d) ($n \rightarrow \sigma^*$) transitions occur in compounds with heteroatoms singly bonded to carbon (R-X, R-OH, R-SH, R-NH_2).

e) Charge transfer (CT) transitions occur in mixtures of electron donors and acceptors that are weakly bonded. These exhibit a new broad and structureless absorption band which is shown by neither component separately and is a result of the formation of a donor-acceptor complex (DAC). CT transitions occur in coordination complexes and depending on the direction of the charge transfer they are classified either Metal-to-Ligand-Charge-Transfer (MLCT) or Ligand-to-Metal-Charge-Transfer (LMCT). A molecule in an excited state (S_1 or T_1) may also transfer its excess energy to a nearby molecule, either intra- or inter-molecularly, in a process called photosensitization. Consequently, a molecule can reach an excited state either by photon absorption or by transfer from a previously excited molecule or chromophore. On the other hand, charge transfer between neighouring molecules may result in quenching or deactivation of the excited state of a molecular entity.

Photochromism is usually characterized by the following parameters:

1) λ_{max} of absorbance of the coloured species. A bathochromic shift (or red shift) is a change of the λ_{max} to lower frequency (longer wavelength). On the contrary, an hypsochromic shift (or blue shift) is a change of the λ_{max} to higher frequency (shorter wavelength).
2) Colourability which is the induced optical density (IOD) of the coloured species at its λ_{max} achieved after irradiation to a constant value – photostationary state – at a specified temperature. A hyperchromic shift occurs when there is an increase of the IOD of the coloured species, while a hypochromic shift occurs when there is a decrease of the IOD of the coloured species.
3) Persistence of colour or the speed of the backward reaction is measured by recording the loss of colour with time, reporting the data as $t_{½}$ (s), which is the time in seconds required for the sample to return to half the optical density of the equilibrium value (photostationary state). Alternatively, the loss of colour with time is sometimes recorded as $t_{¾}$ (s), for

ophthalmic lenses comparison, which is the time in seconds required for the sample to return to ¾ of the optical density of the photostationary state. In some instances, the loss of colour with time is presented as the rate constant k_{Δ}.

The ideal combination of photochromic properties for variable optical transmission devices is the rapid (sub-second) intense colour generation (low transmittance (%) in the visible region) from a colourless inactivated state with a reasonably rapid rate of fade (seconds) of the coloured form (bleaching) at ambient temperature or with temperature independence. It is also important that the compound exhibits good fatigue resistance; the ring-opening – ring-closing cycle must be repeatable many times (> 10^6) without loss of performance.

Photochromic isomers obtained from a photochromic reaction can possess different physicochemical properties, such as, colour, luminescence, electron conductivity, refractive index, dielectric constant, oxidation/reduction potential and geometries.[24] As a result, photochromic molecules have been widely employed as switches to modulate various physical properties e.g. conductance, shape, viscosity, fluorescence, in addition to their inherent colour switching.[25] Photochromes have been applied in many fields such as optical information storage media, ophthalmic lenses, chemical sensors and intelligent stimuli-responsive materials.[25, 26, 27]

1.2 Photochromic Systems

A recent (January 2019) Scifinder (ACS, Chemical Abstracts) search on the word photochromism resulted on 26,200 references. Amongst these references, popular photochromes that were applied in transition metal complexes include azobenzenes, diarylethenes (stilbenes and dithienylethenes), spirobenzopyrans and spirooxazines.[28]

1.2.1 Azobenzenes

Azobenzenes, also called diphenyldiazenes, first discovered by Mitscherlich in 1834, are a very popular class of photochromes. Their photochromic behavior is due to the *trans* (*E*) – *cis* (*Z*) isomerization of the azo functional group which is normally achieved by UV irradiation (**Scheme 1.1**).[29] The corresponding back-reaction is usually attained by either visible light irradiation or thermal relaxation.[29]

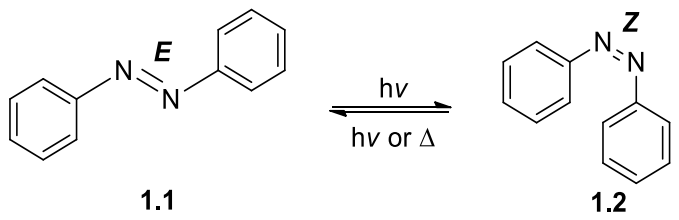

Scheme 1.1 *Trans* (*E*) – *cis* (*Z*) isomerization of azobenzene.

Azobenzenes can be prepared by several methods including most importantly (i) the azo coupling reaction between a diazonium salt **1.3** and an activated arene **1.4** (**Scheme 1.2**), (ii) the Mills reaction or the condensation of a nitroso compound **1.7** with a primary arylamine **1.8** (**Scheme 1.3**), and (iii) the Wallach transformation which involves the rearrangement of an azoxybenzene **1.11** into a hydroxylated azobenzene **1.12** (**Scheme 1.4**).[30]

(i) Azo Coupling[31]

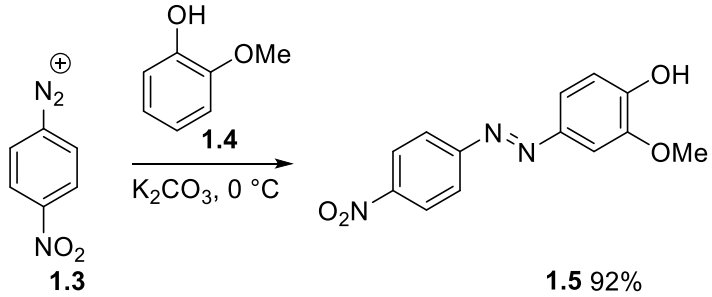

Scheme 1.2 Azo coupling.

(ii) Mills Reaction[32]

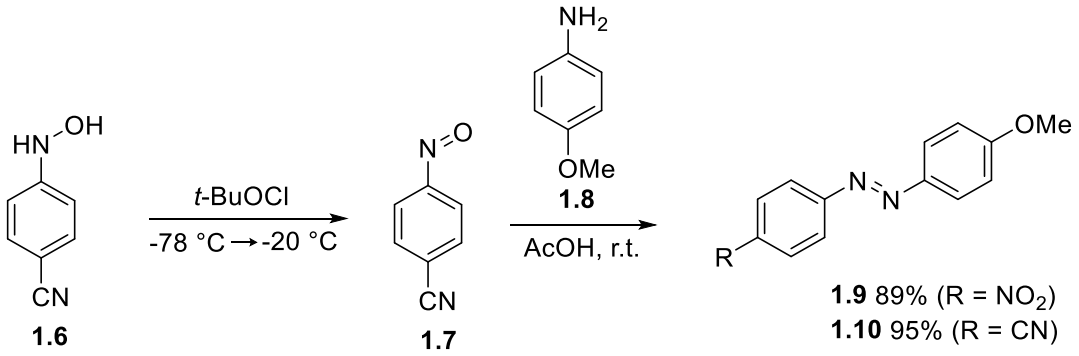

Scheme 1.3 Mills reaction.

(iii) Wallach Transformation[33]

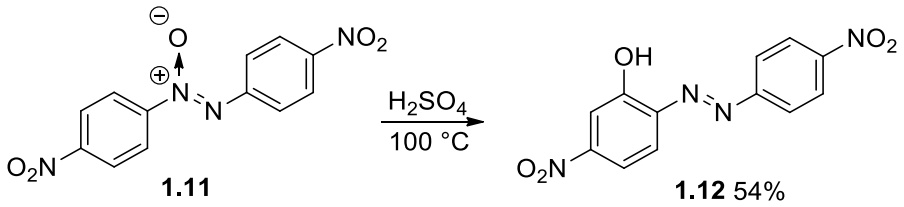

Scheme 1.4 Wallach transformation.

Azobenzenes have wide applications as molecular machines, dyes, pigments, biosensors, pharmaceuticals, food dyes and additives, optical storage media, chemosensors, indicators, and in nonlinear optics.[29, 30]

Photoresponsive polymers undergoing structure and property changes as a response to external stimuli are attracting increasing attention.[34] Gaub *et al.*, have reported the synthesis of a poly(azobenzene) peptides that performs mechanical work.[35] The authors were able to optically lengthen and contract individual polymers by using the light-driven switch. The polymer was found

to contract against an external force acting along the polymer backbone, thus delivering mechanical work. Novak *et al*., have recently reported the synthesis of poly(carbodiimides) which were decorated with azobenzene photochromic groups at the imine positions.[36] As the polymer helicity was governed by the helical backbone, by changing the dynamic isomerization of the azobenzene pendants the helical arrangement was affected. Therefore, upon UV illumination the azobenzene pendants were confined into the *cis* configuration which induced a highly contracted helical arrangement. Removing the UV source allowed the polymer backbone to elongate and become less helical. As a consequence, photoisomerization was effectively changing the thin film surface roughness. Hecht *et al.*, have reported the synthesis of a rigid-rod polymer that included azobenzene in its poly(*para*-phenylene) backbone which showed light-driven reversible and efficient shrinkage with a substantial decrease in its hydrodynamic volume.[37]

Stimuli-responsive drug delivery systems have attracted the interest of the research community in recent years.[38] Croissant *et al.*, reported the synthesis of nanoimpellers funtionalized with a two-photon fluorophore with a high two photon aborption cross-section suitable for *Fluorescence Resonance Energy Transfer* (FRET) in order to photoisomerize azobenzene using deep-penetrating non-harmful NIR light.[39] The nanoimpeller groups pendant in the porous framework physically entrapped the anti-cancer drug camptothecin. The latter was then released by the two-photon-triggered photoisomerization process which ultimately led to *in vitro* killing of the cancer cells.

Azobenzenes have been incorporated into rotaxanes - which are molecular systems in which a macrocycle (e.g. cyclodextrin) threads a linear subunit with two bulky stoppers.[40] The *cis*−*trans* photoisomerization of the azobenzene unit resulted in the motion of the cyclodextrin macrocycle along the track.

Sen *et al.*, have designed light-responsive molecular pumps composed of β-cyclodextrin and water-soluble azobenzene. Under UV irradiation, azobenzene molecules isomerized and left their cyclodextrin hosts, which allowed fluid flow. The pump could also be activated by chemical stimuli and recharged by visible light irradiation.[41]

1.2.2 Diarylethenes

Diarylethenes are a broad class of photochromes that are characterized by possessing two aryl groups connected through an olefin which encompasses stilbenes and dithienylethenes.

1.2.2.1 Stilbenes

Stilbenes or diphenylethenes were first discovered in 1843 by French scientist Auguste Laurent. The more thermodynamically stable *trans* (E) isomer **1.13** photoisomerizes typically under UV

irradiation to the *cis* (Z) isomer **1.14** and then returns to the former either thermally or through irradiation usually with visible light (**Scheme 1.5**).[42]

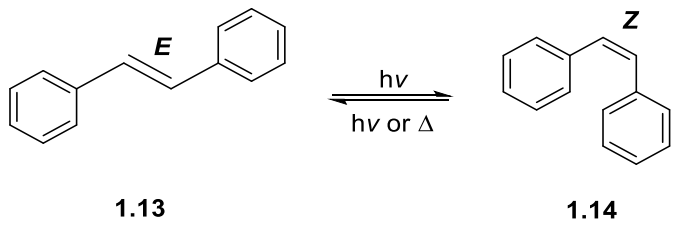

Scheme 1.5 *Trans-cis* isomerization of stilbene.

In contrast to azobenzenes, stilbenes can undergo an oxidative photocyclization to phenanthrene through a 6π–electrocyclization of the *trans* isomer followed by oxidation – Mallory reaction (**Scheme 1.6**).[43] However this side reaction can be prevented by either introducing substituents at the *ortho* position of the aryl rings or by introducing heteroaromatic ring systems.[42]

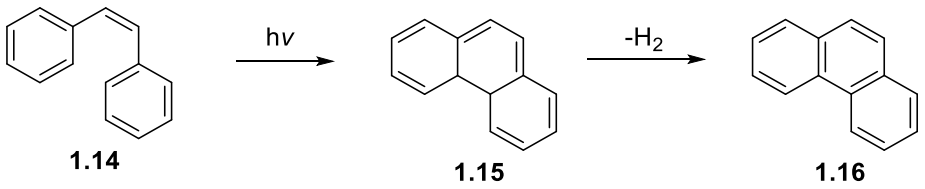

Scheme 1.6 Photocyclization of stilbene to phenanthrene.

There are many different methods employed to synthesize stilbenes.[44] A more traditional approach to synthesize stilbenes is by a Perkin condensation. In this regard, Lima *et al.*, have performed the Perkin condensation between 3,4-dimethoxybenzaldehyde **1.17** with phenylacetic acid **1.18** to give the corresponding cinnamic acid **1.19** in 49% yield.[45] Decarboxylation with copper chromite in quinoline followed by acid-catalysed isomerization gave the corresponding *trans*-stilbene **1.21** (**Scheme 1.7**).

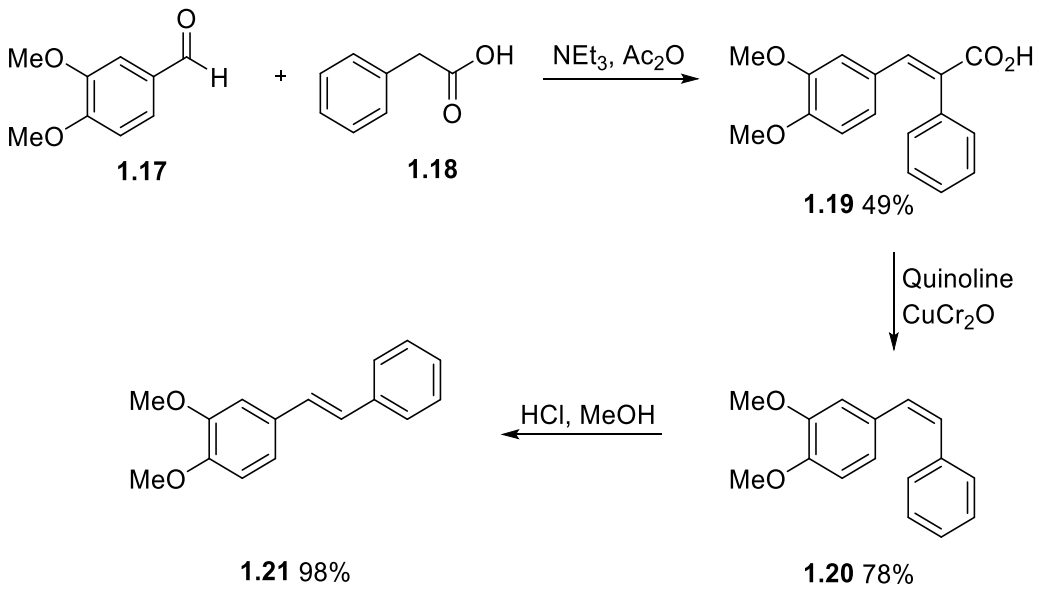

Scheme 1.7 Perkin condensation.

A versatile strategy employed to prepare stilbenes involves a Wittig reaction. For example, Hahm *et al.*, have reported the synthesis of 4,4′-dinitrostilbene **1.25** by a Wittig reaction between the (4-nitrobenzyl)triphenylphosphonium bromide **1.23** and 4-nitrobenzaldehyde **1.24** under basic conditions in 54% yield (**Scheme 1.8**).[46]

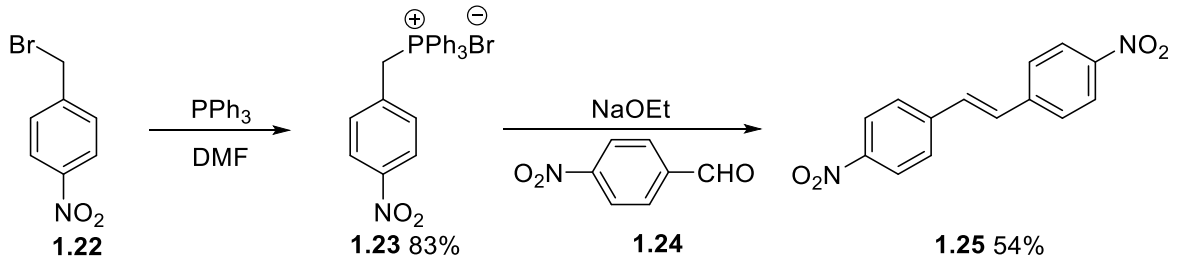

Scheme 1.8 Wittig reaction.

A convenient approach to prepare stilbenes is using a Mizoroki–Heck cross-coupling reaction. For example, Mahdavi *et al.*, have employed a Heck reaction between 2-bromobenzaldehyde **1.26** and styrene **1.27** to synthesize the corresponding stilbene **1.28** in 90% yield (**Scheme 1.9**).[47]

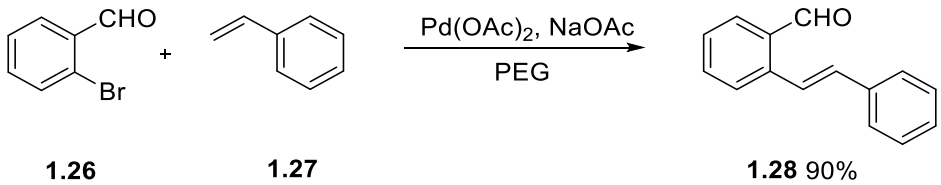

Scheme 1.9 Mizoroki–Heck cross-coupling reaction.

Photochromic stilbenes have been investigated as organic chromophores.[48]

Zhou *et al.*, have recently reported the synthesis of an 'aptasensor' based on a Malachite Green RNAaptamer and a water-soluble stilbene which could selectively and rapidly bind to Malachite Green and tetramethylrosamine allowing ligand quantification by changes in the stilbene fluorescence decay *kinetics* – fluorescence decay was found to be linearly dependent on the ligand concentration.[49]

Takeoka *et al.*, have reported the preparation of a color filter capable of exhibing multiple colours by combining the Christiansen filter effect with the photoisomerization of stilbene. The filter color change was due to the wavelength dependency (dispersion) of the refractive index of stilbene isomerized by UV irradiation.[50]

Wei *et al.*, have reported the preparation of 2D organic semiconductor single crystals of stilbene oligomers 1,4-bis(4-methylstyryl)benzene (*p*-MSB) that were applied as channel layers in organic field-effect transistors (OFETs).[51] *Trans*−*cis* photoisomerization of *p*-MSB was observed in the corresponding transistors, and the drain current was reversibly modulated by alternation of low-intensity irradiation (395 nm).

1.2.2.2 Dithienylethenes

Following Richard Kellogg's seminal work on the photoisomerization of dithienylethenes,[52] Irie and Uchida were the first authors to report the synthesis of dithienylethenes as thermally irreversible and fatigue resistant photochromes.[53] This nowadays popular class of P-type photochromes are characterized by a ring-opened form **1.29** – which is usually colourless – and that reversibly photoisomerizes to a ring-closed form **1.30** – which is usually coloured (**Scheme 1.10**).[53]

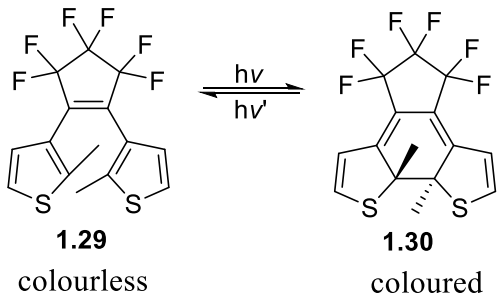

Scheme 1.10 Photoisomerization of dithienylethene.

A diarylethene with five-membered heterocyclic rings has two conformations with the two rings in mirror symmetry (parallel conformation) and in C_2 symmetry (antiparallel conformation). The photocyclization reaction can proceed only from the antiparallel conformation.[54] In the ring-opened form, absorption occurs mainly in the UV region. On the other hand, by ring-closing, π-electrons delocalize throughout the two condensed thiophene rings and further extend to the substituents shifting the absorption maximum to the visible region.[54,55] The absorption spectra of the closed-ring isomers depend on the substituents of the thiophene moieties and on the upper cycloalkene structure.[54]

There are many different synthetic strategies to prepare dithienylethenes reported in the literature.[56] A well-known general approach to the synthesis of dithienylethenes devised by Irie involves the nucleophilic vinylic substitution (S_NV) of perfluorocyclopentenes with an aryllithium. Lithiation of the halogenated thiophene **1.31** derivative in THF at -78 °C, followed by the addition of octafluorocyclopentene, afforded the corresponding dithienylethene **1.32** in 52% yield (**Scheme 1.11**).[53]

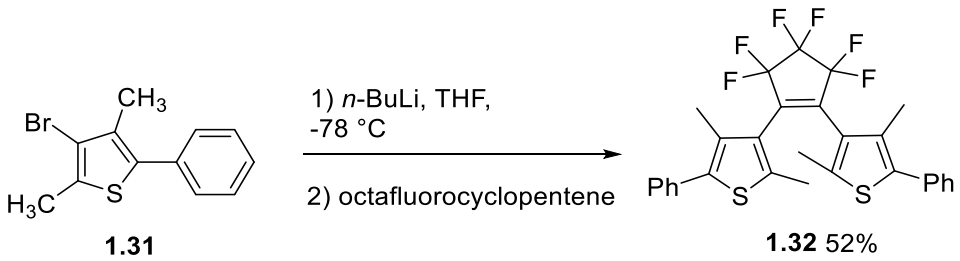

Scheme 1.11 Nucleophilic vinylic substitution (S_NV) of perfluorocyclopentenes with aryllithium.

Dithienylethenes have been successfully applied to the modulation of surface properties, in optical memory media, photoswitching of fluorescent and optical properties, modulation of polymer properties and photomechanical response.[55]

Feringa *et al.*, have recently reported a photochromic hybrid system consisting of an overcrowded alkene-based molecular motor and a dithienylethene (**Scheme 1.12**). Visible-light excitation led to the usual rotary motor behaviour when the dithienylethene was in the open-form. However, when the latter was closed, the rotary motion was inhibited.[57]

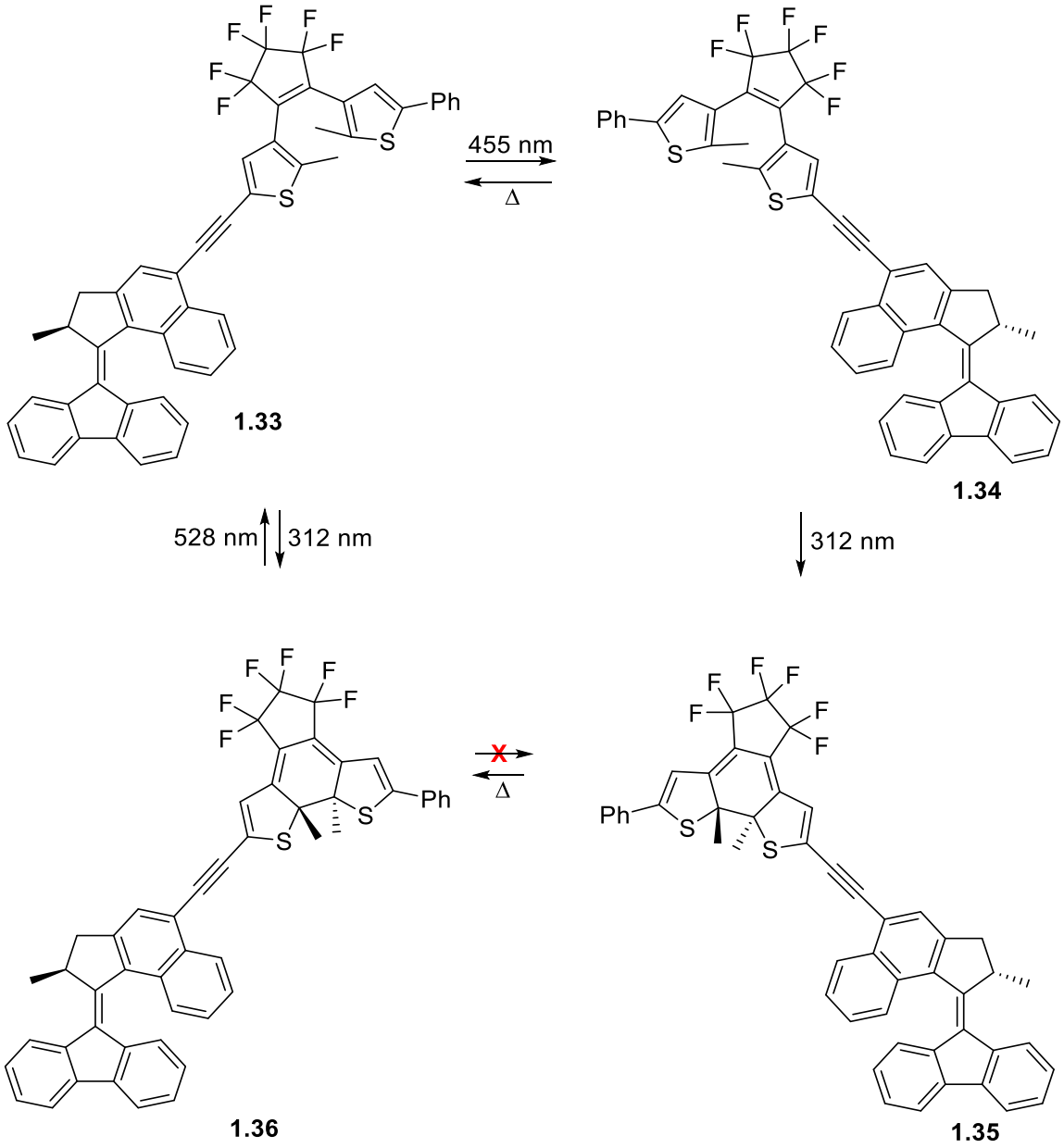

Scheme 1.12 Photoisomerization of photochromic hybrid **1.33**.

Kobatake *et al.*, have recently reported a photochromic dithienylethene crystal that, upon irradiation with ultraviolet light, initially bends away from the incident light and then suddenly

straightens. This unusual bending behaviour was due to both the photochromic reaction and a reversible thermodynamic Single-Crystal-to-Single-Crystal phase transition.[58]

Wöll *et al.*, have reported a few examples of photochromic fluorescent sulfone-based dithienylethenes (**Scheme 1.13**). These were characterized by strong fluorescence in their closed-form (**1.38**) which was switched off once ring-opened (**1.37**) with visible light. These photoswitches are also suitable candidates for super-resolution fluorescence microscopy.[59]

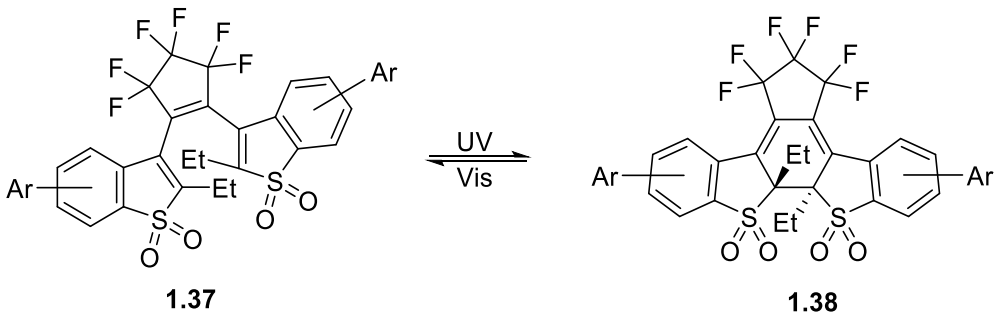

Scheme 1.13 Photoisomerization of dithienylethene **1.37**.

Dithienylethenes have also been successively applied to the development of light-driven chemical sensors. Wang *et al.*, have reported a dithienylethene that selectively formed a 1:1 metal complex with Al^{3+}, resulting in a "turn-on" fluorescence signal.[60] A photoswitchable fluorescein-dithienylethene-based fluorescence probe was developed to detect Cd^{2+} with high sensitivity and selectivity.[61] In a similar work, Tang *et al.*, have developed a photochromic dithienylethene derivative with 2-hydrazinobenzothiazole for colorimetric detection of CN^- and for fluorimetric recognition of I^-.[62]

1.2.3 Spirobenzopyrans and Spirooxazines

Spirobenzopyrans **1.39** (X = CH) and spirooxazines (X = N) are photochromic spirocycles that consist of two disconnected π-electron systems that absorb almost exclusively in the UV region, therefore being colorless or pale yellow (**Scheme 1.14**). By applying an external stimulus, the photomerocyanines **1.40** are formed, containing a single π-system in which the electrons are delocalized across the molecule. The more extended delocalization of the photomerocyanines causes a broad absorption in the visible region. For positive photochromes, UV excitation leads to ring-opening while excitation with visible light leads to ring-closure.[25, 63]

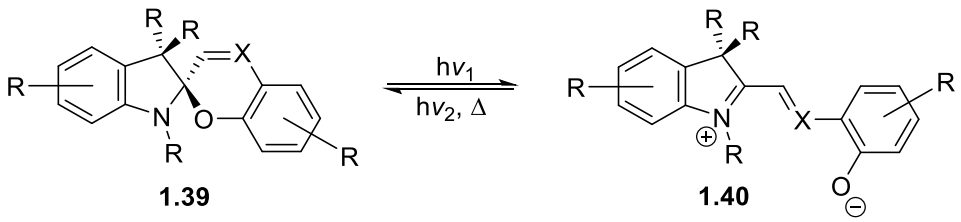

X = CH, CR – Spirobenzopyrans; X = N – Spirooxazines

Scheme 1.14 Photoisomerization of spirobenzopyran and spirooxazine.

Spirobenzopyrans are a class of photochromic spirocycles, first discovered in 1952,[64] that produce strong violet to blue coloured photomerocyanines (**Scheme 1.15**).[65] They are multi-stimuli-responsive molecules as they can change their structure and properties in response to different external stimuli such as light, heat, pH and mechanical force. Additionally, spirobenzopyrans bearing strong electron-withdrawing groups exhibit good negative photochromism.[66]

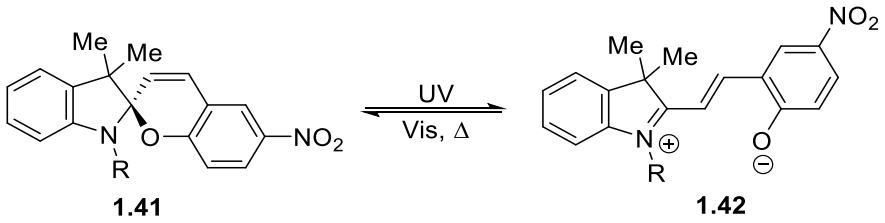

Scheme 1.15 Photoisomerization of spirobenzopyran.

Spirobenzopyrans **1.45** are commonly prepared from the condensation of a Fischer's base **1.43** and a salicylaldehyde **1.44** using either piperidine or Et_3N typically in ethanol or DMF (**Scheme 1.16**).[67, 68]

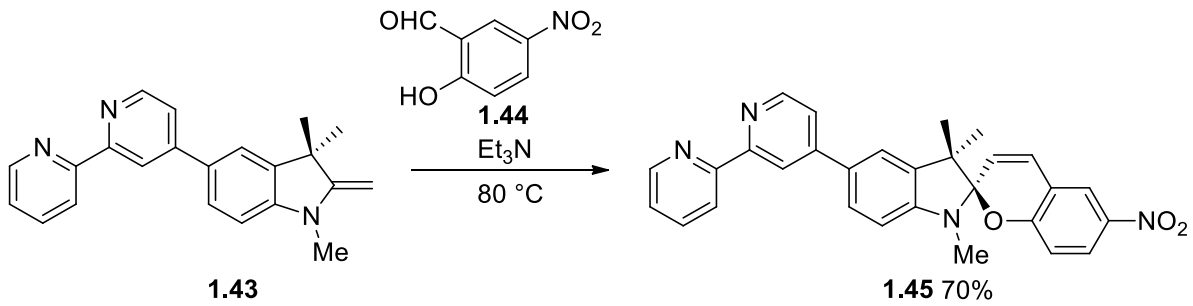

Scheme 1.16 Synthesis of spirobenzopyran **1.45**.

Spirooxazines are a popular class of photochromic spirocycles that are characterized by containing a 1,4-oxazine system (**Scheme 1.17**). Compared to spirobenzopyrans they generally exhibit much better performance in photo-response, environment-stability and fatigue-resistance.[69] Spirooxazines have been applied to the preparation of light sensitive materials that possess high photocoloration quantum yields and robusteness.[70]

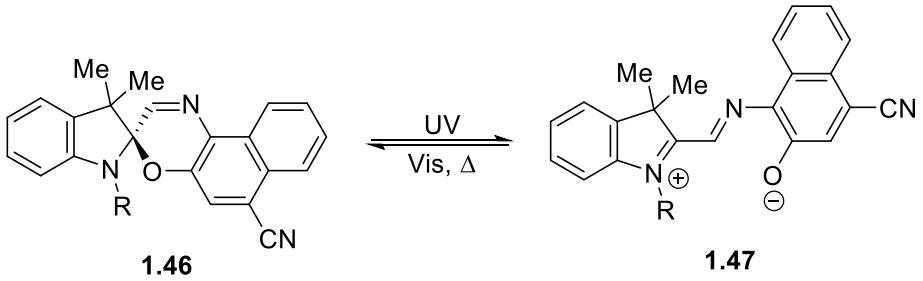

Scheme 1.17 Photoisomerization of spirooxazine.

Spirooxazines **1.50** are usually prepared by condensation between Fischer's base **1.48** and a nitroso-substituted naphthol **1.49** in ethanol or trichloroethylene (**Scheme 1.18**).[71]

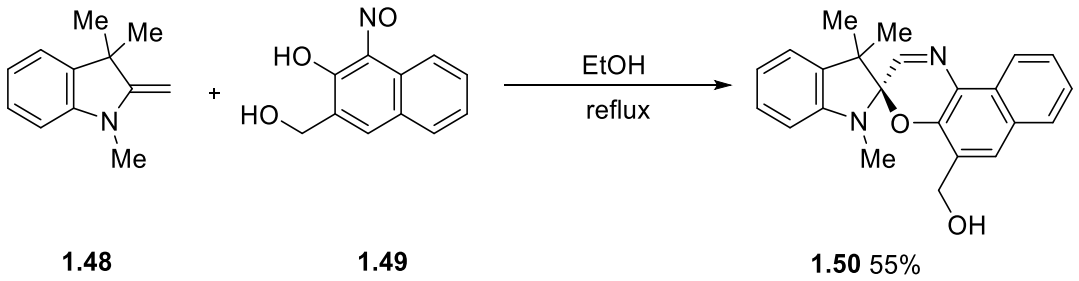

Scheme 1.18 Synthesis of spirooxazine **1.50**.

Spirobenzopyrans and spirooxazines have found many and diverse applications, including in molecular electronics and photonics. Furthermore, these compounds have been applied to the transmission of biochemical information and signals across biological membranes and to photochemically switched enzymatic, bio- and chemosensoric systems.[72]

Mukherjee *et al.*, have recently reported a three-dimensional organic cage decorated with spirobenzopyran moieties with high chemical stability and reversible thermo- and photo-responsive color change with no apparent fatigue.[10]

Heckel *et al.*, have presented the synthesis of a water-soluble pyridine-spirobenzopyran photoswitch that acted as a photoacid − the two isomeric states had different acidic properties. The different pKa of the pyridine nitrogen in the ring-opened and ring-closed isomeric forms led to a reversible proton release in the aqueous phase in the pH range of 3–7.[73]

Wang and Jiang reported the synthesis of photochromic spirobenzopyran-Au nanoparticles. Considering that the corresponding photomerocyanine had a coordination ability with several metal ions such as copper(II) and ferric(III) ions, the photochromic reaction was used as a trigger for the reversible aggregation of Au nanoparticles when the ion metals were present in the medium. These logic gates have potential application in biological and biomedical systems.[74]

In a recent instalment, Genovese *et al.*, have developed photochromic spirobenzopyran-doped silk fibroin nanofibres. By converting the spirobenzopyran molecules into the fluorescent photomerocyanines with UV light, the fibres could respond to the presence of acidic vapors and heavy metal ions dispersed in solution, which were monitored by changes in the UV-Vis and emission spectra.[75]

Haag *et al.*, reported a hyperbranched poly(glycerol) surface coated with spirobenzopyran molecules. The functionalized coated surface exhibited a good photoregulated antifouling behaviour as the photochromic reaction allowed the dynamic control of the interaction with proteins and/or cells. In the closed-form, the surface had a hydrophobic nature therefore presenting a nonspecific protein adsorption and cell adhesion. By ring-opening the spirobenzopyrans with UV radiation, the surface developed a hydrophilic character and consequently highly resisted protein adsorption and cell adhesion.[76]

A spirooxazine has been effectively applied to a wool fabric via thiol-halogen S_N2 reaction. The treated wool fabric showed reversible colour switching between blue and pink, with slow bleaching kinetics ($t_{½}$ = 6 min), however it fatigued over just 20 switching cycles. The photochromic effect of the photochromic wool also decreased over repeated washing cycles.[77]

Kuch *et al.*, have recently reported the highly efficient and bidirectional photochromic behaviour of a spirooxazine molecular switch in direct contact with a Au(111) surface which was found to stabilize the photomerocyanine isomers.[78]

Anderson *et al.*, have recently reported the synthesis of a spirooxazine photochromic switch linked to a fluorophore through a molecular bridge that displayed high photoconversion, broad absorption in the visible region and good fatigue resistance under excitation with 405 nm light. Excellent reversible quenching of fluorescence with the photochromic reaction was observed due to the *Fluorescence Resonance Energy Transfer* (FRET) mechanism of energy transfer and to the appropriate donor-acceptor distance of 15.4 Å.[79]

Spirooxazines have the property of photoinduced merocyanine-aggregation in a polymer matrix, which can be applied to fluorescence emission and stable information storage. Liu *et al.*, have reported the preparation of a spirooxazine-doped polymer on which highly-efficient and stable fluorescent holographic gratings were inscribed by coherent irradiation from a blue-violet laser with irradiation at 403 nm.[80]

1.2.4 Naphthopyrans

Following the seminal works from Iwai and Ide on the synthesis of 3*H*-naphtho[2,1-*b*]pyrans in 1962,[81] Cottam and Livingstone on the synthesis of 2*H*-naphtho[2,3-*b*]pyrans in 1964,[82] and Becker and Michl on the development of photochromic chromenes in 1966,[83] naphthopyrans have acquired great popularity. Indeed, a recent (March 2019) Scifinder search on the word "naphthopyran" resulted in 1100 references.

Naphthopyrans are naturally occurring metabolites − cytotoxic naphthopyrans were isolated from leaves of *Adenaria floribunda*[84] and other naphthopyran derivatives were extracted from the fruits of *Musa* × *paradisiaca* cultivar.[85] Naphthopyrans, although possessing interesting biological activities,[86] are essentially known for their photochromic properties as they are one the most commercially important classes of photochromic molecules.[87] In this regards, naphthopyrans have been applied to commercially available ophthalmic photochromic sun and contact lenses.[88] Other commercial applications of naphthopyrans include fuel and security markers,[89] UV light intensity indicators[90] and hair dyes.[91] The commercial success of naphthopyrans can be attributed to the fact that functional groups can be introduced in a cost-effective way allowing a wide range of colours that span across the visible spectrum from yellows to blues.[87] Furthermore, commercial naphthopyrans are regarded as being very stable and less sensitive towards temperature than other photochromes.[87]

1.3 Synthesis and Photochromism of Naphthopyrans

Of the three isomeric *geminal* diaryl substituted naphthopyrans, the linear isomer 2*H*-naphtho[2,3-*b*]pyran **1.51** displays no significant photochromic response at ambient temperature.[20] On the other hand, 2*H*-naphtho[1,2-*b*]pyran **1.52** and 3*H*-naphtho[2,1-*b*]pyran **1.53** have received much attention since they display good photochromic properties in solution and in polymers under ambient conditions.[92]

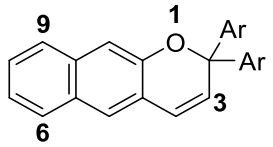

1.51

2*H*-naphtho[2,3-*b*]pyran

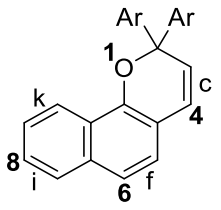

1.52

2*H*-naphtho[1,2-*b*]pyran

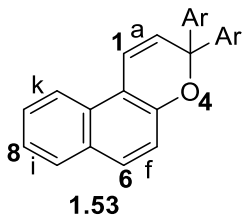

1.53

3*H*-naphtho[2,1-*b*]pyran

Naphthopyrans are the stable colourless ground state heterocycles that undergo a photoinduced electrocyclic ring-opening to the corresponding open-forms, the photomerocyanines, which due to the extended delocalization absorb at a longer wavelength, typically in the visible region.[93,94] The photoinduced pyran ring-opening process caused by the C_3–O_4 bond cleavage leads to the formation of two isomeric photoproducts: *transoid-cis* (TC) and *transoid-trans* (TT).[95] On cessation of irradiation, the unstable photomerocyanines thermally revert over time to their original state. Alternatively, the back-reaction can, in some instances, be driven by excitation with visible light. Furthermore, the TC and TT isomers possess similar absorption bands and are energetically close to each other but differ in thermal stability. The bleaching caused by the TC thermal depopulation occurs within tens of seconds in solution at room temperature, while TT depopulation decays over a much longer time-scale (hours) in the dark.[95] Nowadays, there is still quite a considerable amount of debate concerning the photochromic reaction mechanism,[96,97,98] especially regarding the TT formation. Herzog *et al.*, propose that upon photoexcitation of the closed-form (CF) with 320 nm light, the first or second excited singlet states, S_1 or S_2, were populated in the Franck-Condon region (**Figure 1.9**).[96] Fast vibrational relaxation led to the lowest vibrational ground state of S_1 with a lifetime τ_1 in the picosecond timescale. The latter excited state minimum had a similar structure to the original CF, with only slightly attenuated bond lengths accompanying the electronic excitation. The transition through a conical intersection (CI) with a lifetime τ_2 – picosecond timescale – led to the breaking of the C(sp^3)-O bond for the majority of the population forming the ring-opened isomers while a minority of the population relaxed to the ground state S_0. The authors were not conclusive if after τ_2, one or both ring-opened isomers were initially formed, but they propose that there was an overlaying population transfer between the two product isomers with a lifetime τ_3.

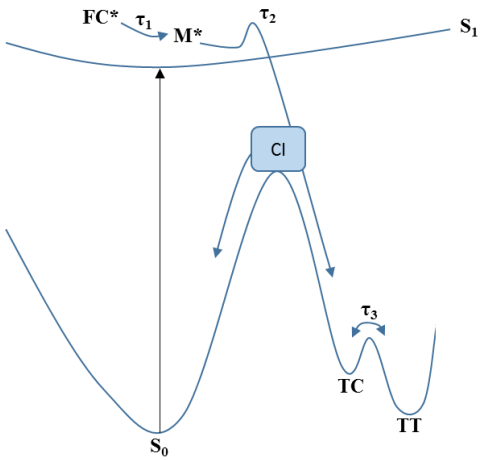

Figure 1.9 Photophysical processes upon photoexcitation of 3*H*-naphtho[2,1-*b*]pyran.[96]

In a recent account, Burdzinski *et al.*, propose that the initially photoexcited Franck-Condon CF relaxes in the S_1 ($\pi \rightarrow \pi^*$) toward the conical intersection region, CI (S_1/S_0) in a barrierless manner.[97] Most of the population then relaxes to the lowest energy conformer of TC. The authors propose that the TT is formed through isomerization of the TC by absorption of second photon in a stepwise fashion (**Scheme 1.19**). According to the authors, the thermal back reaction from the TT isomer to the CF is slow since the energy barrier for the twist about the C_1=C_{10b} double bond was substantial (~ 1.2 eV).[99] A convenient way to overcome this hindrance is through photoexcitation of the TT form, which allows photorelaxation to the TC geometry in the closed-shell electronic ground state after the UV-induced rotation about the C_1=C_{10a} double bond.

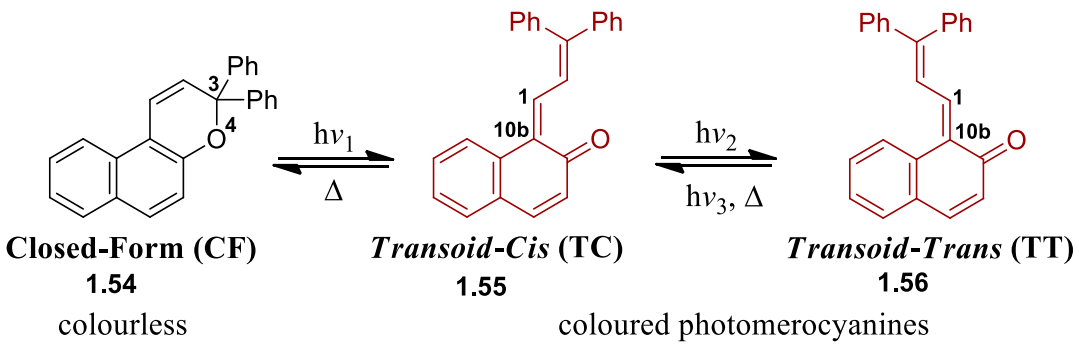

Scheme 1.19 Photoisomerization of 3*H*-naphtho[2,1-*b*]pyran.

1.3.1 Methods of Synthesis

There are several routes for the synthesis of naphthopyrans reported in the literature.[20,100]

In 1964, Livingstone *et al.*, prepared the 3,3-diphenyl-3*H*-naphtho[2,1-*b*]pyran **1.58** by the nucleophilic addition of a phenylmagnesium bromide to the lactone function of benzocoumarin **1.57** in poor yield (16%) (**Scheme 1.20**).[82a,101]

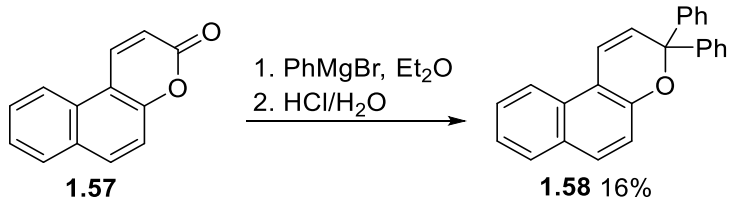

Scheme 1.20 Synthesis of naphthopyran **1.58**.

In 1983, Talley performed the 1,2-addition of a dilithiated *o*-bromonaphthol **1.60** to an α,β-unsaturated aldehyde **1.61** which rearranged and cyclised to the 2*H*-naphtho[2,3-*b*]pyran **1.64** in 90% yield (**Scheme 1.21**).[102]

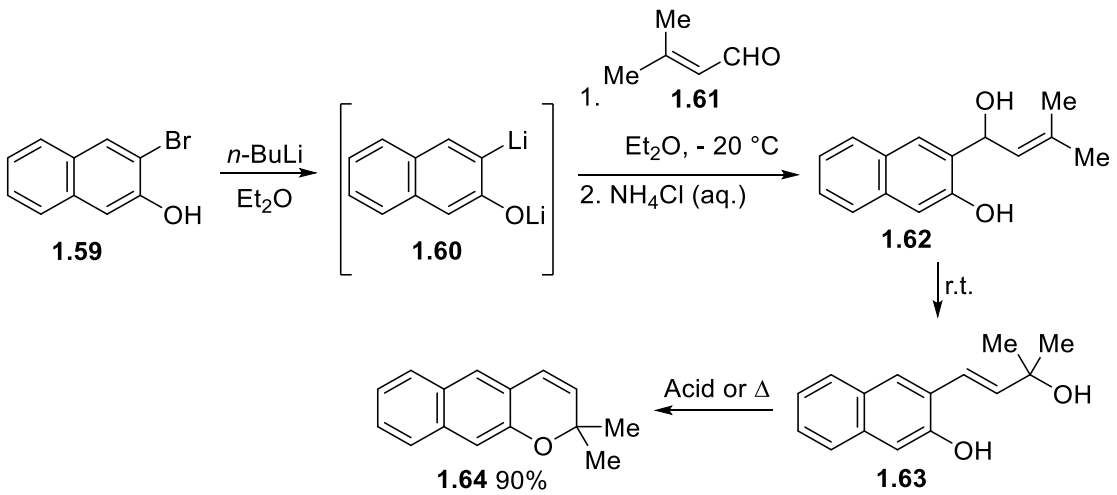

Scheme 1.21 Synthesis of naphthopyran **1.64**.

Gabbutt *et al.*, have prepared 1-bromo-3*H*-naphtho[2,1-*b*]pyrans **1.66** (28%) and **1.67** (33%) by refluxing the corresponding chromanones **1.65** with PBr_3 (28–33%) (**Scheme 1.22**).[103] The 1-bromo-substituted naphthopyrans could serve as useful precursors of alkenyl lithium reagents by metal-halogen exchange reaction with *n*-BuLi which allows the introduction of a wide range of electrophiles at the C-1 position.

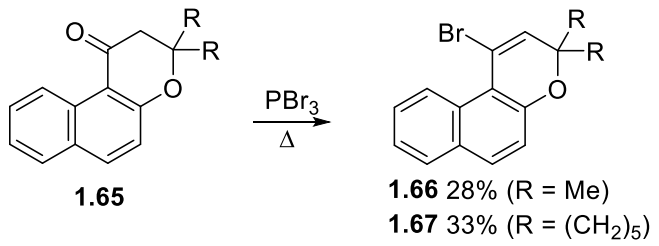

Scheme 1.22 Synthesis of naphthopyrans **1.66** and **1.67**.

Another route to prepare naphthopyrans – although not a very practical one – is by the reaction between titanium(IV) phenolates derived from 'hydroxy heterocycles' e.g. **1.68** and β-phenylcinnamaldehydes (**Scheme 1.23**).[104]

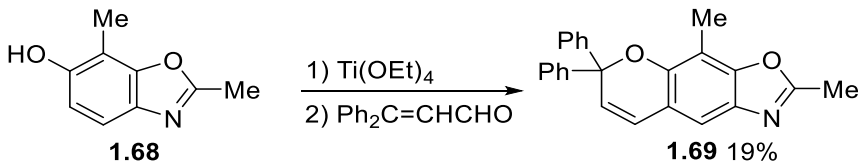

Scheme 1.23 Synthesis of pyran **1.69**.

Putala *et al.*, have prepared a bisnaphthopyran through a key Heck reaction between an iodonaphthol **1.70** and an allylic alcohol **1.71** followed by acid-catalysed cyclization (**Scheme 1.24**).[105]

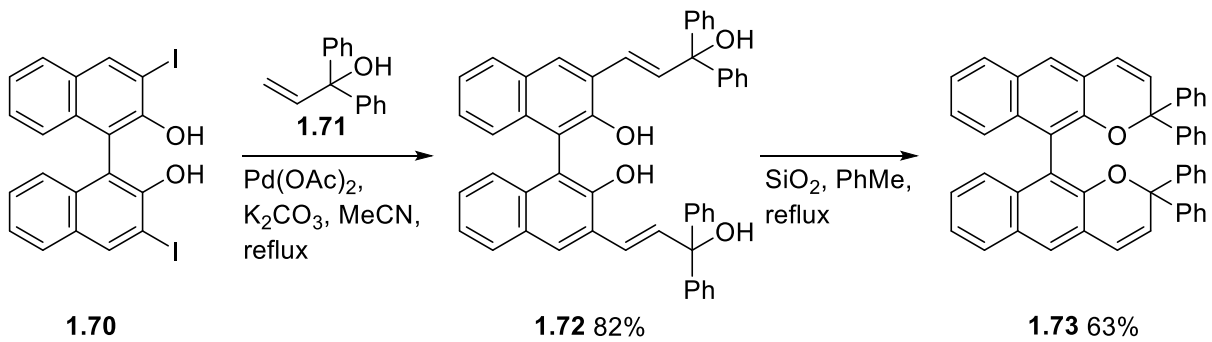

Scheme 1.24 Synthesis of bisnaphthopyran **1.73**.

The synthetic pathway devised by Iwai and Ide involving the alkylation of a naphthol **1.74** with a haloalkyne **1.75** is the most expeditious route to naphthopyrans **1.77**, although originally lacking generality and providing the target products in poor yield (**Scheme 1.25**).[81]

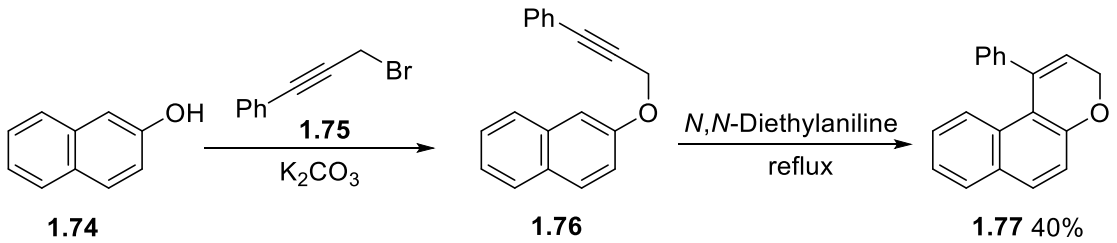

Scheme 1.25 Synthesis of naphthopyran **1.77**.

A modified and successful version of this strategy involves the Claisen rearrangement of propargyl ethers **1.80** obtained *in situ* from the reaction of a α,α-disubstituted propargyl alcohol **1.79** with the 2-naphthol **1.78** under acidic conditions.[106] One variation of this strategy involves using as catalyst *p*-toluenesulfonic acid (*p*TSA) in anhydrous DCM (**Scheme 1.26**)[107] or in toluene.[108]

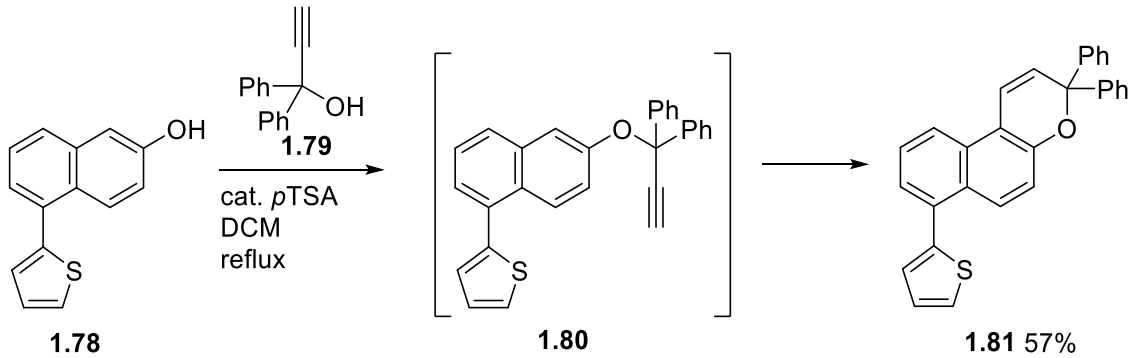

Scheme 1.26 Synthesis of naphthopyran **1.81**.[107]

Another variation of this method involves using the acidic Al_2O_3 catalyst in toluene under reflux.[109, 110, 111] In this regard, Aiken *et al.*, have performed the acid-catalysed condensation of 2-naphthol **1.74** with the respective propynols **1.82** to afford the corresponding photochromic naphthopyrans **1.83**–**1.84** in moderate yield (**Scheme 1.27**).[112]

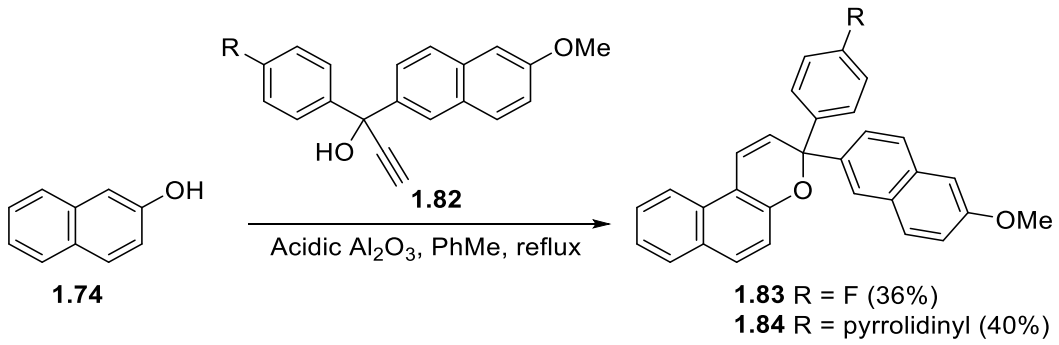

Scheme 1.27 Synthesis of naphthopyrans **1.83**–**1.84**.

A further variation of this strategy involves reacting propargyl alcohols with naphthol derivatives in the presence of a catalytic amount of pyridinium *p*-toluenesulfonate (PPTS).[113, 114, 115] In this regard, Carreira *et al*., have reported a facile one-pot synthesis of naphthopyrans **1.86** in excellent yield (92–99%) by reacting propargyl alcohols **1.85** with 2-naphthol **1.74** in the presence of 5 mol% of PPTS and 2 equiv of $(MeOH)_3CH$ in 1,2-dichloroethane (1,2-DCE) (**Scheme 1.28**).[116]

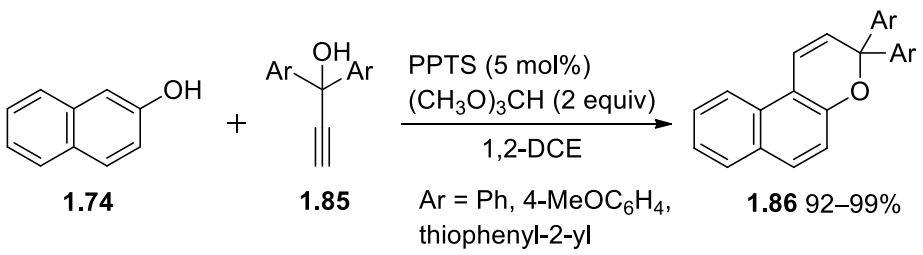

Scheme 1.28 Synthesis of naphthopyrans **1.86**.

The reaction between a propynol and a naphthol reportedly involves the thermal [3,3]-sigmatropic reaarangement (Claisen rearrangement) of naphthyl propargyl ether **1.88** formed *in situ* from the acid-catalysed etherification of naphthol **1.74** with the carbocation **1.87**. Alternatively, and possibly in a competitive way, the allene intermediate **1.89** can also be formed by electrophilic aromatic substitution directly from the naphthol **1.74**. A subsequent [1,5]-sigmatropic rearrangement followed by a 6π-electrocyclization gives the corresponding naphthopyran **1.86** (**Scheme 1.29**).[111]

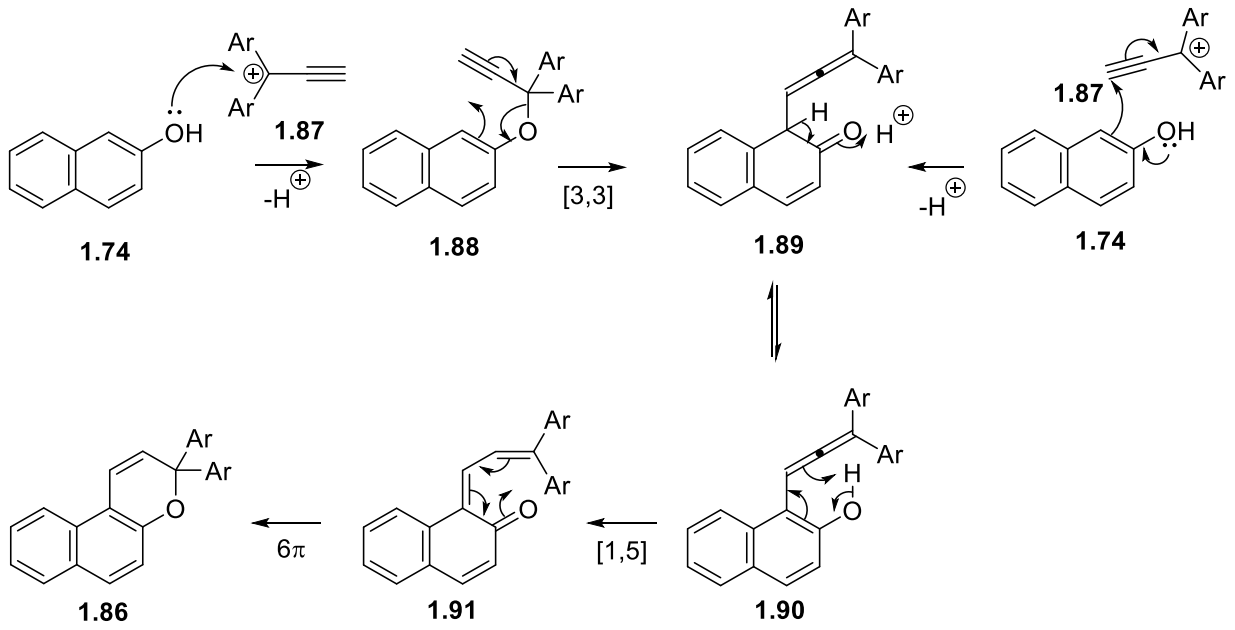

Scheme 1.29 Putative mechanism of the acid-catalysed condensation between naphthol **1.74** and propynol **1.85**.

1.3.2 Photochromic Properties of 3*H*-naphtho[2,1-*b*]pyrans

Naphthopyrans possessing an aryl substituent at the C-1 of the naphthopyran scaffold **1.92** have no reported photochromism at room-temperature (**Scheme 1.30**).[117]

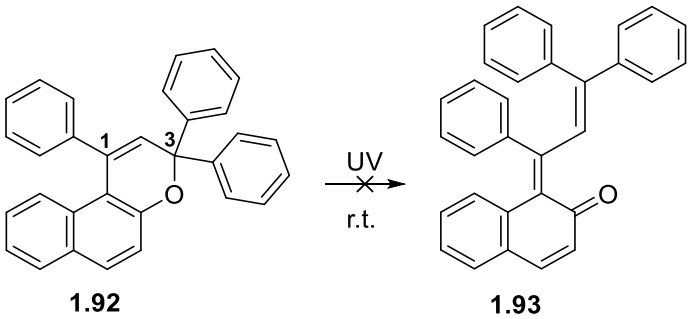

Scheme 1.30 Absence of photoisomerization of naphthopyran **1.92**.

As stated before, naphthopyrans generate the *transoid-cis* (TC) and *transoid-trans* (TT) isomers upon UV irradiation. While the thermal back reaction of the TC isomer takes from several seconds to minutes, for the TT isomer is considerably longer (several minutes/ hours). One strategy to develop very fast photochromic naphthopyrans for application in photochromic lenses is by introducing a bulky substituent at the C-2 which effectively surpresses the generation of the TT isomer.[118] Abe *et al.*, have found that by introducing a bromine at C-2 the thermal back reaction of

2-bromonaphthopyran **1.95** (**entry 2**, **Table 1.1**) ($t_{½}$ = 2.5 ms) was dramatically accelerated when compared to naphthopyran **1.94** (**entry 1**, **Table 1.1**) ($t_{½}$ = 34 min).[119] According to the authors, substitution at the C-2 was found to be important to accelerate the thermal back reaction from the TC isomer to the CF due to the large steric and electrostatic repulsions between the bromine at C-2 and the carbonyl group of the photomerocyanine. The authors moved on to replace bromine for the more photostable prenyl substituent producing an even faster photochrome **1.96** (**entry 3**, **Table 1.1**) ($t_{½}$ = 46 µs) due to the large steric and electrostatic repulsions of the prenyl group when compared to bromine. However, the authors do not report any data about the colourability (IOD) of the given naphthopyrans. One potential problem with these very fast photochromic naphthopyrans is the poor colourability in solution.

Table 1.1 Spectrokinetic data for naphthopyrans **1.94**–**1.96**.

Entry	Naphthopyran	λ_{max}/ nm (benzene)	$t_{½}$
1	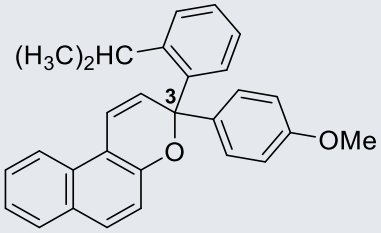 **1.94**	465	34 min
2	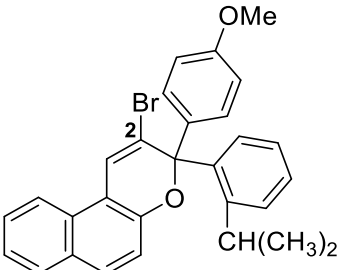 **1.95**	415	2.5 ms
3	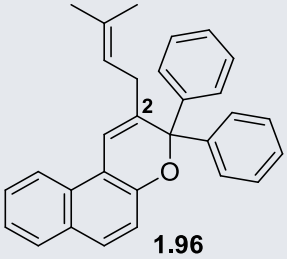 **1.96**	452	46 µs

According to Van Gemert *et al.*, incorporating electron-donating groups such as methoxy in the *para* position of the phenyl at C-3 resulted in a bathochromic shift of the λ_{max}: one methoxy group (**1.98**) increased the λ_{max} by 36 nm relative to **1.97**, while an additional methoxy group on the

second aryl group (**1.99**) provided only an additional 12 nm bathochromic shift. A secondary effect of the addition of electron donating groups was the loss in colourability (smaller IOD).[120]

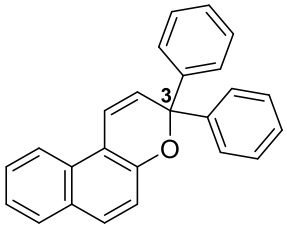

1.97 λ_{max} 432 nm
$t_{½}$ 45 s
IOD 0.36

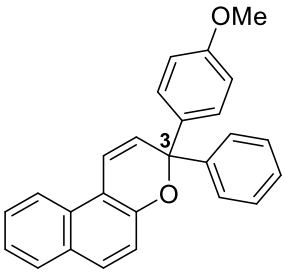

1.98 λ_{max} 468 nm
$t_{½}$ 35 s
IOD 0.25

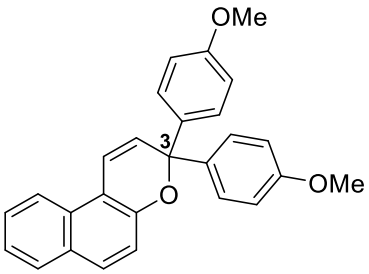

1.99 λ_{max} 480 nm
$t_{½}$ 40 s
IOD 0.15

Introducing different nitrogen-based electron-donating groups at the *para* position of the C-3 phenyl group results in a bathocromic shift, the magnitude of which was related to the donating ability of the terminal amino group and the solvent chosen. According to Gabbutt *et al.*, for all the solvents used, the pyrrolidino and diethylamino derivatives were the most bathochromic dyes while the morpholino analogue absorbed at the shortest wavelength (**Table 1.2**).[121] The behaviour of the dyes in solvents of different dielectric constant suggested that solvent interaction changed the polarity of the dyes, which were relatively weakly polar in a non-polar solvent but became significantly polar through stabilisation of the charge with solvents of higher dielectric constants.

Table 1.2 Spectroscopic data for naphthopyrans **1.100**.

Aryl Substituent (X)	λ_{max} (*n*-hexane)/ nm	λ_{max} (DMSO)/ nm	λ_{max} (EtOH)/ nm
N-Me_2	487	550	568
N-Et_2	497	570	579
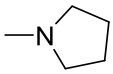	498	567	579
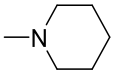	479	529	548
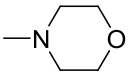	461	505	506

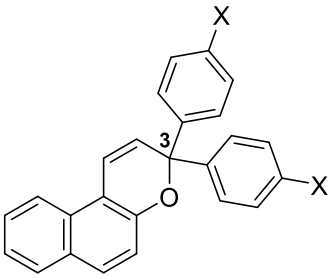

1.100

Heron *et al.*, have prepared multiple *ortho*-substituted naphthopyrans at C-3 with a strongly electron donating *para* pyrrolidine ring that induced a significant bathochromic shift in λ_{max} up to 108 nm when compared to 3,3-diphenyl-3*H*-naphtho[2,1-*b*]-pyran (λ_{max} 430 nm).[122] The authors noted that increasing the size of the *ortho* substituent was accompanied by an increase of $t_{½}$, which was attributed to the large steric encumberment to ring-closure imposed by the *ortho*-substituents, leading to an observed increase in color intensity, with virtually no change in λ_{max} (**Table 1.3**). In a following work, the authors noted that the visible spectrum of the photomerocyanine from **1.102** and **1.103** contained two bands of approximately equal intensity because the *ortho* groups were spatially demanding (X = Cl, Me) leading to organic photochromes that appeared as dull shades of brown.

Table 1.3 Spectrokinetic data for naphthopyrans **1.101**.

Aryl Substituent (X)	λ_{max} (PhMe)/ nm	$t_{½}$/ s
F	554	40
Cl	554	741
Br	554	1024
I	553	1167
MeO	555	351
Me	555	639
H	538	5

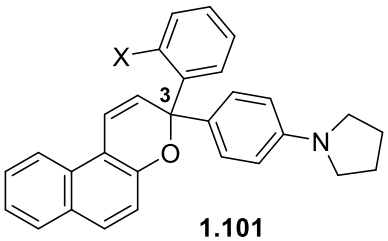

1.101

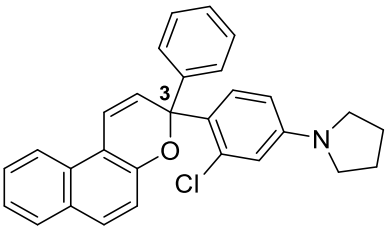

1.102 λ_{max} 403, 480 nm
$t_{½}$ 44 s

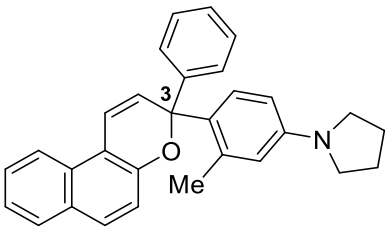

1.103 λ_{max} 410, 507 nm
$t_{½}$ 104 s

It is generally accepted that introducing electron-withdrawing substituted aryl groups at C-3 causes an hypsochromic shift and slows down the rate of fade.[123] Heron *et al.*, have prepared a 3,3-bis(4-methylthiophenyl)-3*H*-naphtho[2,1-*b*]pyran **1.104** which λ_{max} (478 nm) was similar to 3,3-

bis(4-methoxyphenyl)-3*H*-naphtho[2,1-*b*]pyran (λ_{max} 480 nm) (**Scheme 1.31**).[124] The authors moved on to oxidize **1.104** to the sulfone **1.105** which electron-withdrawing groups at the *para* position resulted in a substantial hypsochromic shift of 63 nm on the λ_{max}. The authors have also found that sulfone **1.105** fatigued after a few irradiation cycles, generating the naphthofuran **1.106**.

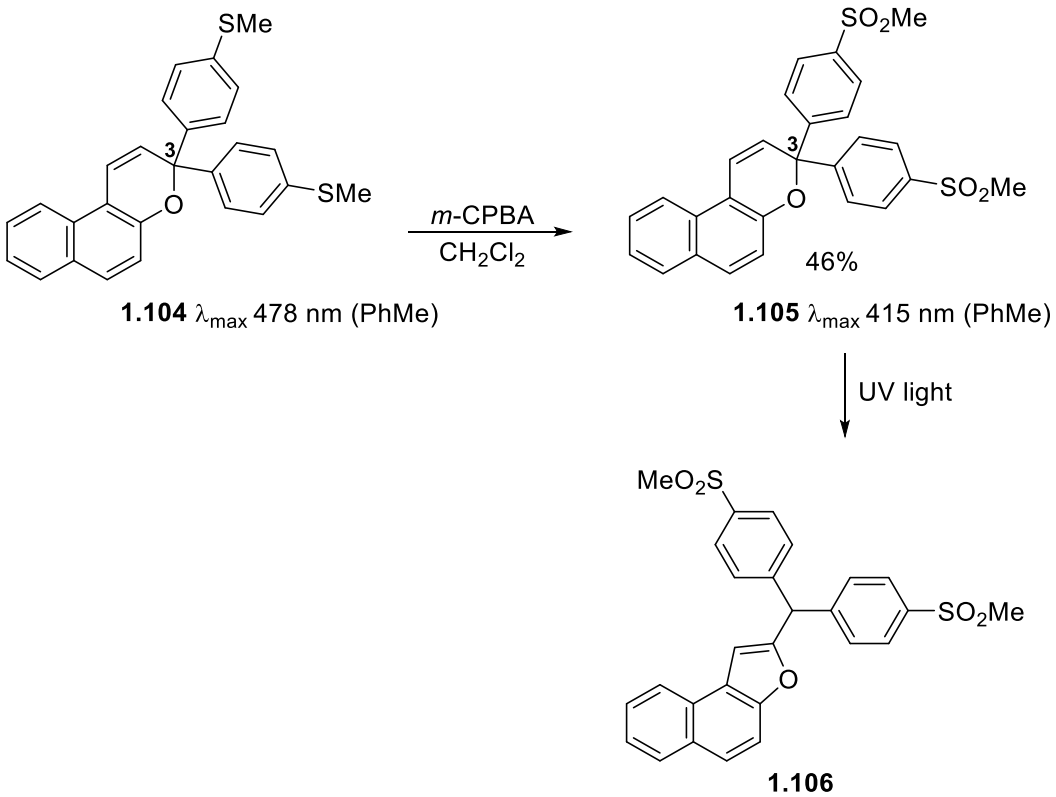

Scheme 1.31 Oxidation of naphthopyran **1.104**, followed by UV-promoted ring-contraction to **1.106**.

According to Alberti *et al.*, the presence of fluorine and bromine atoms at the *para* position of the aryl groups at C-3 did not produce a significant shift on the λ_{max} when compared to 3*H*-naphtho[2,1-*b*]pyran **1.97**.[125]

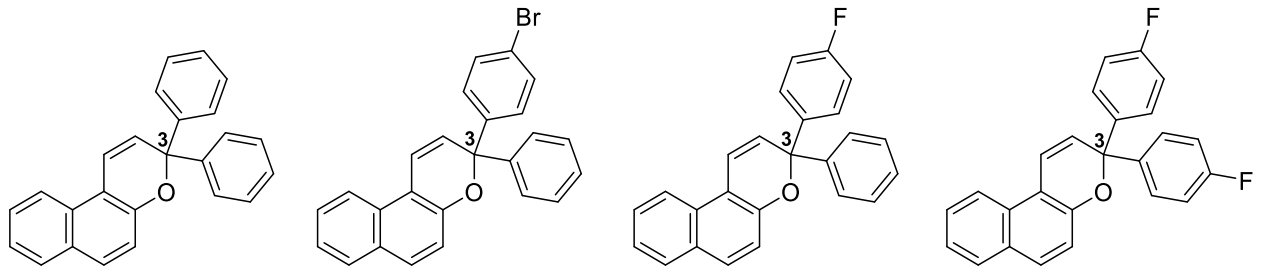

1.97 λ_{max} 432 nm (PhMe) IOD 0.17 | **1.107** λ_{max} 432 nm (PhMe) IOD 0.13 | **1.108** λ_{max} 431 nm (PhMe) IOD 0.14 | **1.109** λ_{max} 430 nm (PhMe) IOD 0.16

According to the same study, the presense of an electron-withdrawing trifluoromethyl group in the aryl at C-3 of the naphthopyran core induced an hypsochromic shift independently of its position in the ring – similar to having an *ortho*-F in the aryl at C-3.[125]

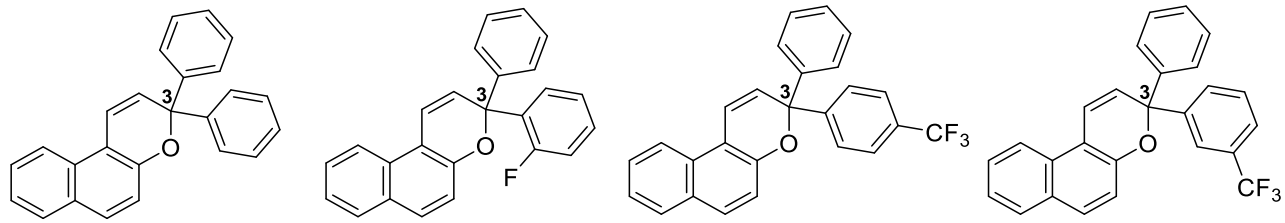

1.97 λ_{max} 432 nm (PhMe) IOD 0.17 | **1.110** λ_{max} 421 nm (PhMe) IOD 0.22 | **1.111** λ_{max} 421 nm (PhMe) IOD 0.21 | **1.112** λ_{max} 420 nm (PhMe) IOD 0.15

Gabbutt *et al.*, have prepared multiple *meta*-substituted naphthopyrans at C-3 with a strongly electron donating *para*-pyrrolidine ring (**Table 1.4**).[126] According to the authors, the colour of the photomerocyanine was manipulated through the control of the steric interaction between the *para* pyrrolidine group and the *meta* substituents. Increasing the steric clash between both groups resulted in an hypsochromic shift of the $\lambda_{max,}$ the only exception being OMe potentially because of its electron-donating nature despite being in a non-conjugated position. The rate of fade was virtually unaffected by the *meta*-substitution in contrast to what was observed at the *ortho* position.[120, 122]

Table 1.4 Spectrokinetic data for naphthopyrans **1.113**.

Aryl Substituent (X)	λ_{max} (PhMe)/ nm	$t_{½}$/ s
I	494	5
Br	493	4
Cl	513	4
F	529	4
Me	517	3
OMe	557	5
H	538	5

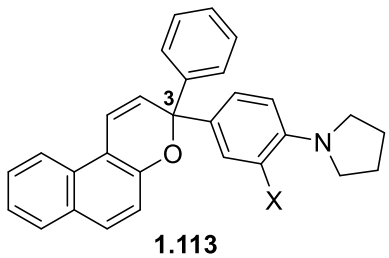

1.113

According to Gabbutt *et al.*, the introduction of diaryl-substituted vinyl units at C-3 induced a bathochromic shift of the λ_{max} (*ca.* 25–40 nm) when compared to the non-vinyl substituted analogues, which can be attributed to the more extended π conjugated system (**Scheme 1.32**).[127] For example, by comparing 3-(4-methoxyphenyl)-3-phenyl-3*H*-naphtho[2,1-*b*]pyran **1.98** to 3-[2,2-bis-(4-methoxyphenyl)vinyl]-3-phenyl-3*H*-naphtho[2,1-*b*]pyran **1.114**, the λ_{max} in toluene of the corresponding photomerocyanines red-shifted from 465 nm to 502 nm, respectively.

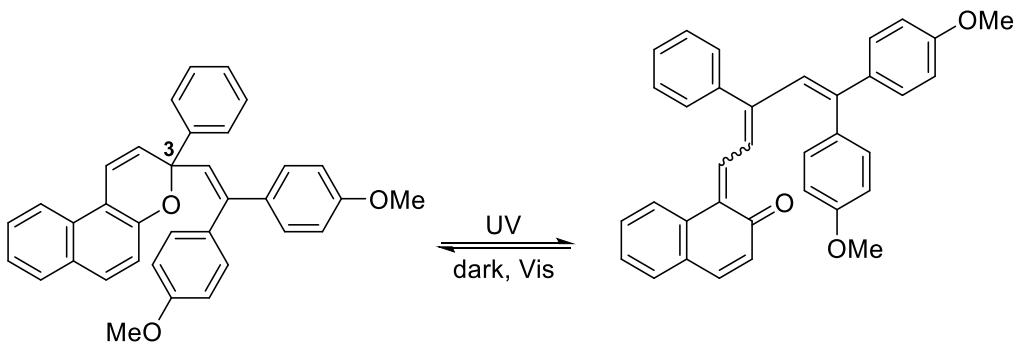

1.114 **1.115**

Scheme 1.32 Photoisomerization of naphthopyran **1.114**.

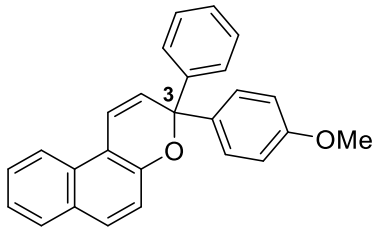

1.98 λ_{max} 465 nm (PhMe)

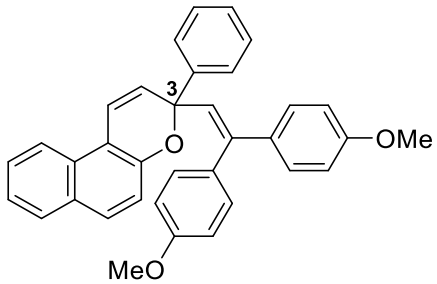

1.114 λ_{max} 502 nm (PhMe)

Rebiere *et al.*, have reported a study on the photochromic properties of a large set of thienyl-substituted naphthopyrans.[128] A naphthopyran containing two thiophene substituents at C-3 **1.116** was characterized by a bathochromic shift of 40 nm on its λ_{max}, weaker colourability and faster fading rate when compared to 3,3-diphenyl-3*H*-naphtho[2,1-*b*]pyran **1.97**. The authors have also reported a bathochromic shift of 72 nm on the λ_{max} of the dithienyl naphthopyran **1.117** with an increase on the colourability and in the fading rate when compared to 3,3-diphenyl-3*H*-naphtho[2,1-*b*]pyran **1.97**.

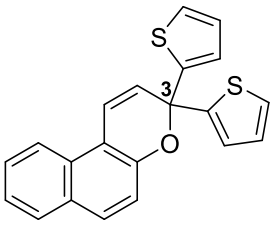

1.116 λ_{max} 472 nm (PhMe)
IOD 0.60
$k_{\Delta 1}$ 0.42 s^{-1} (29%)
$k_{\Delta 2}$ 0.16 s^{-1} (71%)

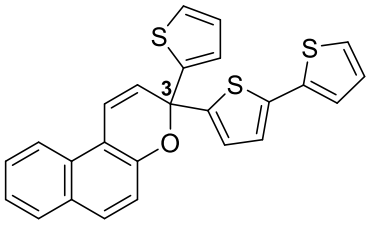

1.117 λ_{max} 510 nm (PhMe)
IOD 1.92
$k_{\Delta 1}$ 0.49 s^{-1} (25%)
$k_{\Delta 2}$ 0.22 s^{-1} (75%)

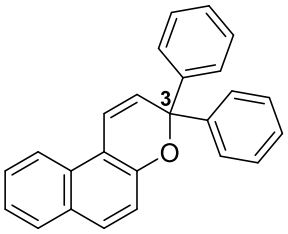

1.97 λ_{max} 432 nm (PhMe)
IOD 0.84
$k_{\Delta 1}$ 0.09 s^{-1} (100%)

The presense of electron-donating methoxy groups at positions C-5, C-7 and C-9 have barely no effect on the λ_{max} of the photomerocyanine (**Table 1.5**).[129] The presence of an electron-donor methoxy group at C-6 hypsochromically shifted λ_{max} by 13 nm when compared to 3,3-diphenyl-3*H*-naphtho[2,1-*b*]pyran, and increased colourability by slowing down the speed of fade. On the other hand, a methoxy group at C-8 bathochromically shifted λ_{max} by 41 nm with increased colourability.[20]

Table 1.5 Spectroscopic data for naphthopyrans **1.118**.

Aryl Substituent (R)	λ_{max} (**acrylate polymer**)/ nm
5-MeO	435
6-MeO	423
7-MeO	435
8-MeO	477
9-MeO	432
H	436

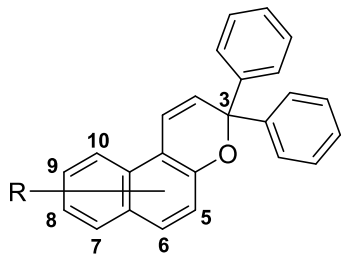

1.118

Pozzo *et al.*,[130] have prepared the 5-amino-substituted naphthopyran **1.119** which electron-donating amino group blue-shifted the λ_{max} by only 8 nm, with a decrease in the speed of fade when compared to 3,3-diphenyl-3*H*-naphtho[2,1-*b*]pyran **1.97**.[131]

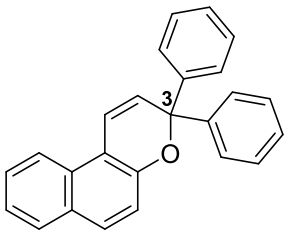

1.97 λ_{max} 432 nm (PhMe)
IOD 0.84
$k_{\Delta 1}$ 0.09 s^{-1}

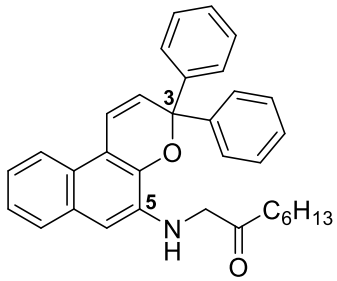

1.119 λ_{max} 425 nm (PhMe)
IOD 0.77
$k_{\Delta 1}$ 0.021 s^{-1}

Zhang *et al.*, have reported the synthesis of naphthopyran **1.121** which electron-withdrawing *N*-phenylamido group caused a substantial bathochromic shift in the λ_{max} (60 nm) accompanied by a faster rate of fade with no change in its already weak colourabity when compared to 3,3-bis(4-diethylaminophenyl)-3*H*-naphtho[2,1-*b*]pyran **1.120**.[132]

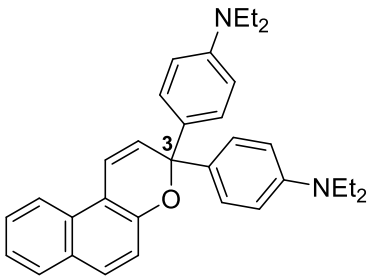

1.120 λ_{max} 580 nm
IOD 0.01
$t_{½}$ 6 s

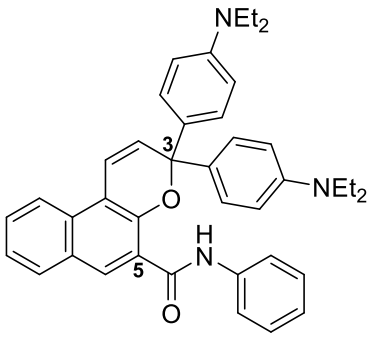

1.121 λ_{max} 640 nm
IOD 0.01
$t_{½}$ < 1s

The presence of the electron-donating morpholino group at C-6 (**entry 4**, **Table 1.6**) hypsochromically shifted λ_{max} by 38 nm when compared to 3,3-bis(4-methoxyphenyl)-3*H*-naphtho[2,1-*b*]pyran (**entry 1**, **Table 1.6**) with a substantial increase in colourability.[133] Substituting one *para*-methoxy for a trifluoromethyl group at C-3 (**entry 5**, **Table 1.6**) resulted in an even more pronounced hypsochromic shift in the λ_{max} (58 nm) with increased colourability.

Table 1.6 Spectroscopic data for naphthopyrans **1.122**.

Entry	X	Y	Z	λ_{max}/ nm	IOD
1	OMe	H	H	490	0.12
2	CF_3	H	H	450	0.15
3	OMe	OMe	H	488	0.69
4	OMe	H	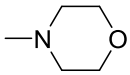	452	1.57
5	CF_3	H	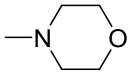	432	1.72
6	OMe	OMe	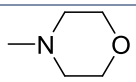	432	2.39

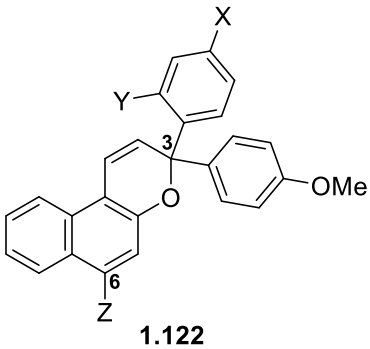

1.122

There are just a few reported examples of naphthopyrans with electron-withdrawing groups at C-6. Samat *et al.*, have reported the the crystal structure of 6-cyano-3,3-bis(4-methoxyphenyl)-3*H*-naphtho[2,1-*b*]pyran **1.123** but no photophysical analysis was presented.[134] Furthermore, a few examples of 6-halo-3*H*-naphtho[2,1-*b*]pyrans **1.124** were published in a Japanese patent.[135]

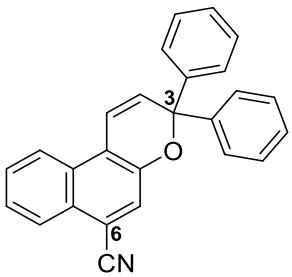

1.123

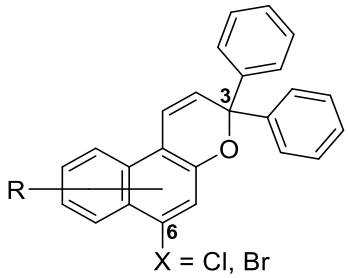

1.124

Rebiere *et al.*, have prepared the 7-(2-thienyl)naphthopyran **1.125** which thiophene group at C-7 induced a bathochromic shift of 10 nm potentially because it gives a photomerocyanine with a more extended π-conjugated system with increased colourability and faster rate of fade when compared to 3,3-diphenyl-3*H*-naphtho[2,1-*b*]pyran **1.97**.[128]

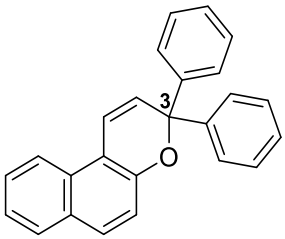

1.97 λ_{max} 432 nm (PhMe)
IOD 0.84
$k_{\Delta 1}$ 0.09 s^{-1} (100%)

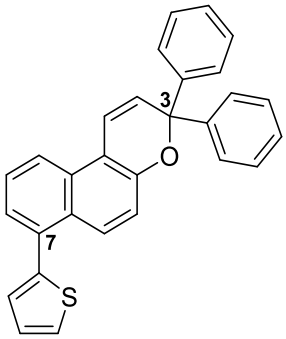

1.125 λ_{max} 442 nm (PhMe)
IOD 1.60
$k_{\Delta 1}$ 0.25 s^{-1} (91%)
$k_{\Delta 2}$ 0.03 s^{-1} (9%)

The same authors have also reported the synthesis of a dithienyl naphthopyran **1.126** in which an extra dithienyl at C-7 resulted in a bathochromic shift of only 10 nm in the λ_{max}, however it increased substantially the fading rate and colourability when compared to dithienyl naphthopyran **1.117**.[128]

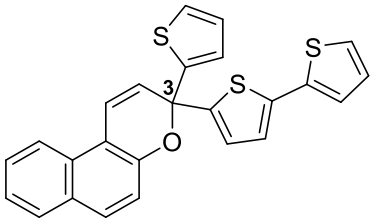

1.117 λ_{max} 510 nm (PhMe)
IOD 1.92
$k_{\Delta 1}$ 0.49 s^{-1} (25%)
$k_{\Delta 2}$ 0.22 s^{-1} (75%)

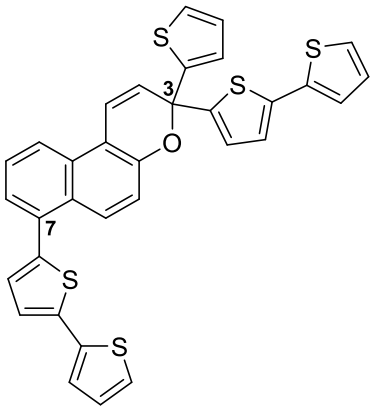

1.126 λ_{max} 520 nm (PhMe)
IOD 3.90
$k_{\Delta 1}$ 0.67 s^{-1} (98%)
$k_{\Delta 2}$ 0.08 s^{-1} (2%)

There are just a handful of reported examples of naphthopyrans with electron-withdrawing groups at C-7. Katritzsky *et al.*, have prepared 7-carboxamido naphthopyrans **1.139** but no photophysical analysis was presented.[136]

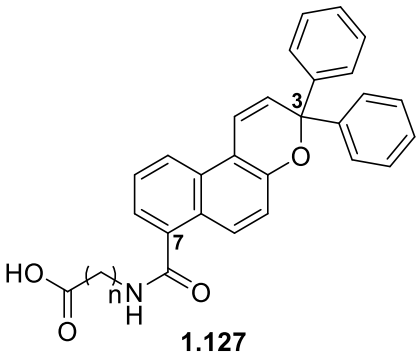

1.127

Introducing the strong electron-withdrawing diethoxyphosphoryl group at C-8 (**1.129**) produced an hypsochromic shift of only 8 nm, while introducing a weak electron-withdrawing bromine atom at C-8 (**1.128**) induced a 25 nm bathochromic shift on the λ_{max} when compared to 3,3-bis(4-fluorophenyl)-3*H*-naphtho[2,1-*b*]pyran **1.109**.[125]

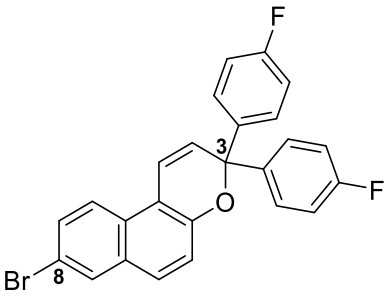

1.128 λ_{max} 455 nm (PhMe)

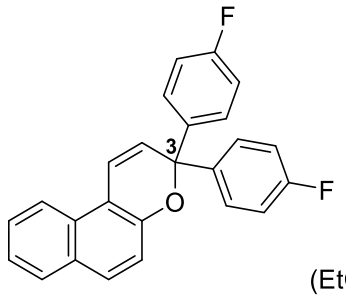

1.109 λ_{max} 430 nm (PhMe)

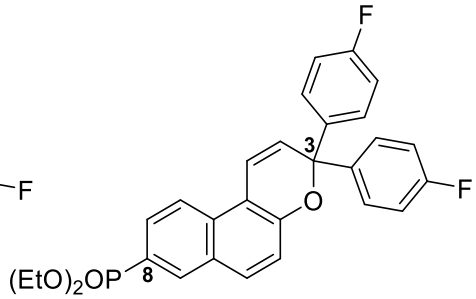

1.129 λ_{max} 422 nm (PhMe)

According to Shilova *et al.*, strong electron-donating *N*-containing heterocycles at C-8 led to an overall bathochromic shift in the λ_{max} up to 120 nm in the case of pyrrolidine when compared to 3,3-phenyl-3*H*-naphtho[2,1-*b*]pyran (**Entry 1**, **Table 1.7**).[137]

Table 1.7 Spectroscopic data for naphthopyrans **1.130**.

Entry	Aryl Substituent (X)	λ_{max} (MeCN)/ nm
1	H	432
2	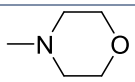	503
3	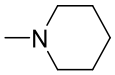	524
4	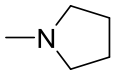	552
5	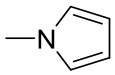	462

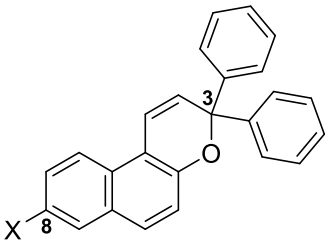

1.130

Coen *et al.*, have prepared naphthopyrans with vinylthiophene substituents at C-9 **1.131**–**1.132** that showed a bathochromic shift in the λ_{max} due to the more extended π conjugated system when compared to 3,3-diphenyl-3*H*-naphtho[2,1-*b*]pyran (λ_{max} 432 nm in toluene).[138]

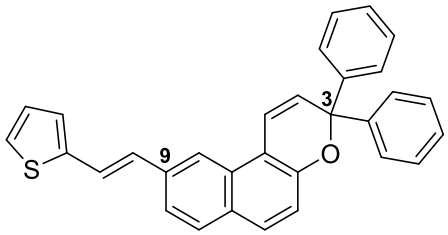

1.131 λ_{max} 485 nm (PhMe)

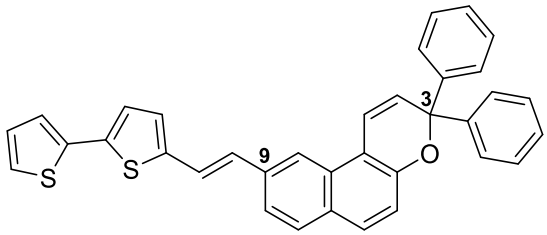

1.132 λ_{max} 499 nm (PhMe)

There are relatively few reported examples of naphthopyrans with electron-withdrawing groups at C-9 (**1.133**). All the examples possess complicated structures making it very hard to access the overall effect of the substituent on their photochromic properties.[139]

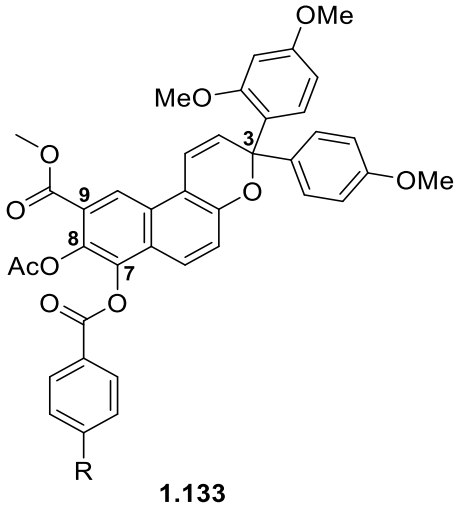

1.133

There are just a handful of reported examples of naphthopyrans with electron-donating groups at C-10 (**1.134**); the complicated structures make it very difficult to access the overall effect of the substituent on their photochromic properties.[140]

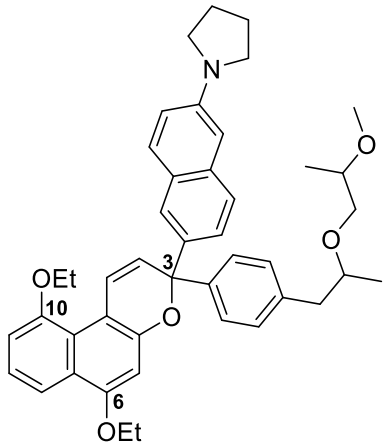

1.134

There are just a few reported examples of naphthopyrans with electron-withdrawing groups at C-10 (**1.135**). The intricate structures reported in a Japanese patent render it very difficult to discern the overall effect of the electron-withdrawing substituents on their photochromic properties.[140]

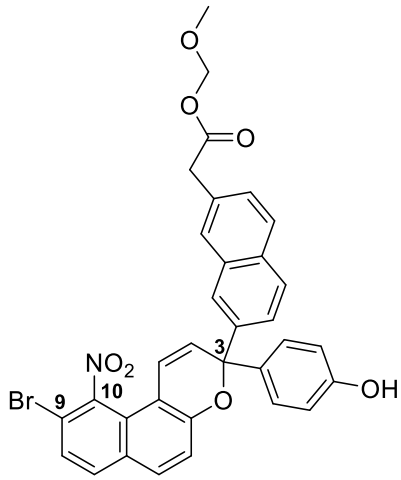

1.135

An exception was the work from Abe *et al.*, who, as stated before, have reported the synthesis of the 10-bromo-substituted naphthopyran **1.136**, in which the weakly electron-withdrawing bromine at C-10 induced an hypsochromic shift of only 10 nm in benzene solution with a substantial decrease of $t_{½}$ when compared to naphthopyran **1.94**. [119] Abe *et al.*, have found that by introducing a bromine at C-10 the thermal back reaction from the TC isomer to the CF was more than 20 times faster than for naphthopyran **1.94**. On the other hand, the decay of the TT isomer of **1.136** was extremely decelerated and most of the TT isomer remained even after 45h. The slow thermal isomerization reaction from the TT isomer to the TC isomer of **1.136** compared to **1.94** was

attributed to the high activation energy barrier towards the formation of the TC isomer from the TT isomer of **1.136**.

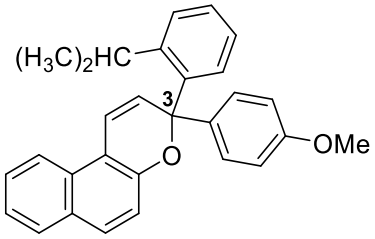

1.94 λ_{max} 465 nm (benzene)
$t_{½}$ 34 min

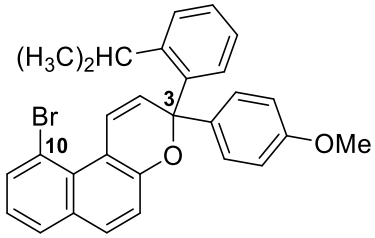

1.136 λ_{max} 455 nm (benzene)
$t_{½}$ 1 min

Guglielmetti *et al*., have reported the synthesis of 10-formyl-3,3-diphenyl-3*H*-naphtho[2,1-*b*]pyran **1.137** but the authors did not present photophysical data for the given compound.[141]

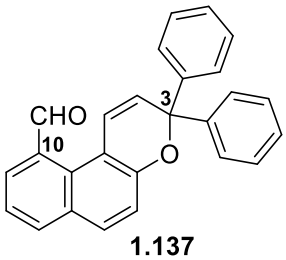

1.137

Besides inductive, resonance, steric and heterocycle substitution effects, there are other effects employed to modulate the photochromic properties of pyran containing photochromes. These effects are beyond the scope of this thesis so they will only be mentioned briefly:

1. *Heterocycle annulation*. Annulation of diarylbenzopyrans with different heterocycles has been shown to modulate the absorption properties, fade rate constants and fatigue resistance. In this regard, benzopyrans have been annulated with a variety of 5- and 6- membered heterocyclic rings, such as, pyrrole,[142] oxazole,[142] indole,[142] benzofuran,[142] thiophene,[143] pyrimidine.[144]

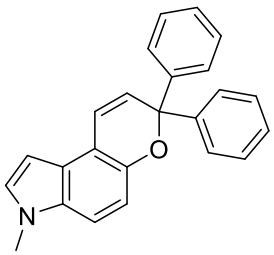

1.138 λ_{max} 437, 531 nm (PhMe)
$k_{\Delta 1}$ < 10^{-4} s^{-1}

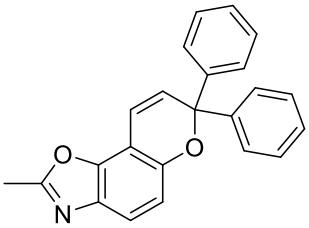

1.139 λ_{max} 423, 513 nm (PhMe)
$k_{\Delta 1}$ 0.25 s^{-1}

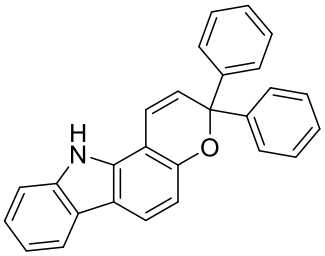

1.140 λ_{max} 436, 560 nm (PhMe)
$k_{\Delta 1}$ 0.15 s^{-1}

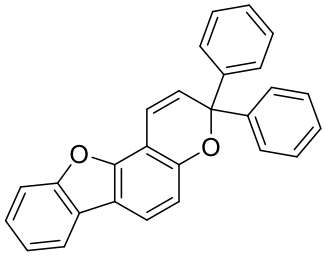

1.141 λ_{max} 424, 518 nm (PhMe)
$k_{\Delta 1}$ 0.21 s^{-1}

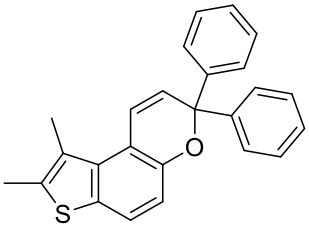

1.142 λ_{max} 452, 542 nm (PhMe)
$k_{\Delta 1}$ 0.17 s^{-1}

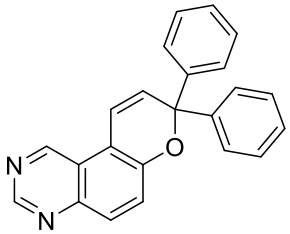

1.143 λ_{max} 442 nm (PhMe)
$t_{1/2}$ 1000 min
IOD 0.37

2. *Stereoelectronic effects*. In a 2016 review, Moorthy and Mukhopadhyay discussed toroidal conjugation, through-space electronic effect, phane effect along with nucleophile-electrophile interaction, helicity as a steric force and intramolecular hydrogen bonding, as subtle strategies to modulate the spectrokinetics of the photomerocyanines derived from diarylbenzopyrans.[145]

3. *Union of photochromic systems*. 3*H*-Naphtho[2,1-*b*]pyrans have been integrated in biphotocromic systems. Photochromic units can be independently linked together, being possible to excite them simultaneously. Such systems are considered multi-mode photoswitching systems.[145] Amongst these there are systems in which two 3*H*-naphtho[2,1-*b*]pyran units are linked together through one of the C-3 substituents by a flexible ethylene bridge.[146] According to Gabbutt *et al.*, the symmetrical bisnaphthopyran **1.144** may be thought as two units of individual naphthopyrans isolated from each other as the absorption bands of the bisnaphthopyran and the individual naphthopyran were virtually coincidental.

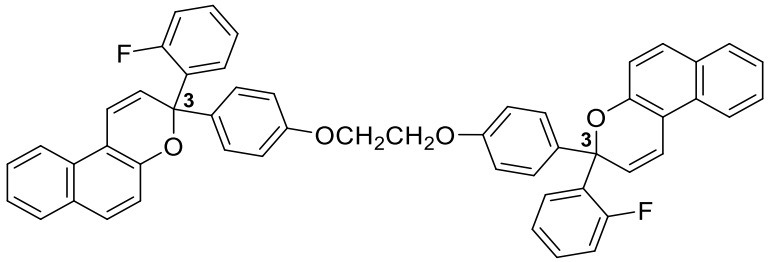

1.144 λ_{max} 450 nm (PhMe)

Favaro *et al.*, have reported the synthesis of a symmetrical bisnaphthopyran where the individual naphthopyrans were connected through the C-8 by a rigid acetylene bridge.[147] The bisnaphthopyran **1.145** behaved like a classical thermoreversible photochromic system. However, the same authors have shown that the unsymmetrical bisnaphthopyran **1.146**, connected through an ester unit, and bisnaphthopyran **1.147**, connected through an ethylene bridge, exhibit unusual thermal and photochemical reversibility which was attributed to the formation of multiple photoproducts with different thermo- and photo-reversibilities.

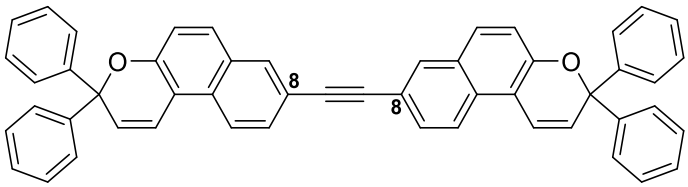

1.145 λ_{max} 485 nm (PhMe)

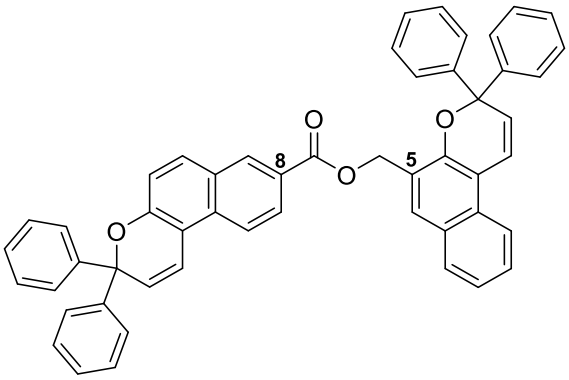

1.146 λ_{max} 443 nm (PhMe)

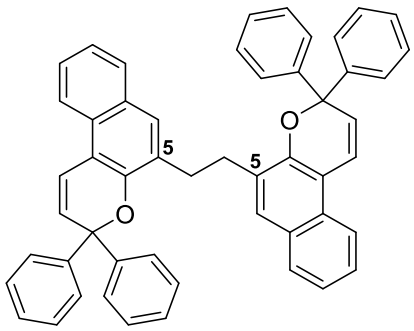

1.147 λ_{max} 431 nm (PhMe)

Another possible design of biphotochromic systems involves connecting the two photochromic units while maintaining some degree of communication between them, which leads to unusual spectrokinetic properties of the photomerocyanines.[145] Such systems can divided into two different

classes: one in which both photochromic units are naphthopyrans[112] and another in which the naphthopyran is linked to a different photochrome.[148]

Carreira *et al.*, have prepared oligothiophene linked bisnaphthopyrans which photochromic properties were dependent on the length of the oligothiophene linker.[149] For example, the presence of a bisthiophene linker leads to high colourability and unusual photochromic behaviour. The authors have shown that by irradiating **1.148** at 366 nm for 5 s the near colourless solution rapidly underwent coloration to orange-red. Further irradiation resulted in a change to red-purple after 30 s and to purple-blue after 4 min. Removal of the irradiation source resulted the thermal bleach in the reverse order. The dramatic change of color of upon continuous irradiation with UV light suggested that a sequential photochromic process had taken place, namely ring-opening and coloration of the second naphthopyran unit happened after the opening of the first naphthopyran unit (**Scheme 1.33**).

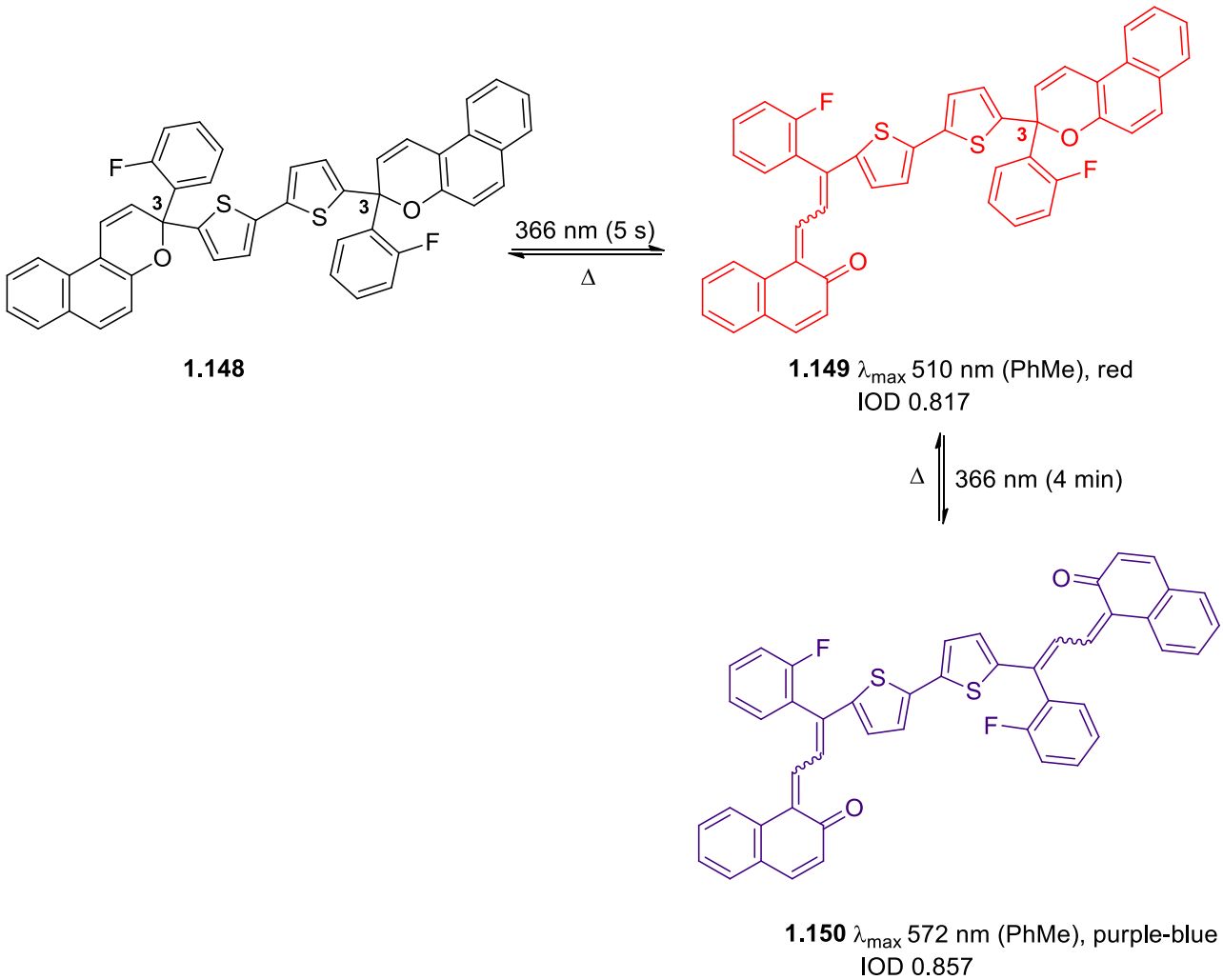

Scheme 1.33 Photoisomerization of bisnaphthopyran **1.148**.

Frigoli *et al.*, have reported the synthesis of a combined system consisting of a naphthopyran unit and a dithienylethene which were connected by the sp^3 C-3 of the naphthopyran scaffold, meaning that both photochromic units were electronically decoupled.[150] An important feature of this design was the different absorption behaviour of the naphthopyran and the dithienylethene as the system had a read-out window between 350 and 380 nm where the naphthopyran group could be switched selectively without affecting the dithienylethene unit. Irradiation of **1.149** with wavelength above 350 nm ring-opened the naphthopyran without ring-closing the dithienylethene generating **1.150** which had an orange colour in solution (λ_{max} 456 nm in toluene) (**Scheme 1.34**). On the other hand, continuous irradiation of **1.149** with wavelength of 313 nm triggered both the ring-opening reaction of the naphthopyran and the ring-closing of the dithienylethene generating **1.152** which had a brown colour in solution (absorption up to 800 nm with three absorption maxima at 434, 539 and 618 nm). Thermal ring-closing of the ring-opened isomer of the naphthopyran gave rise to **1.151** which had a pink colour in solution (the maxima at 434 and 618 nm disappeared and a new absorption maximum at 516 nm emerged).

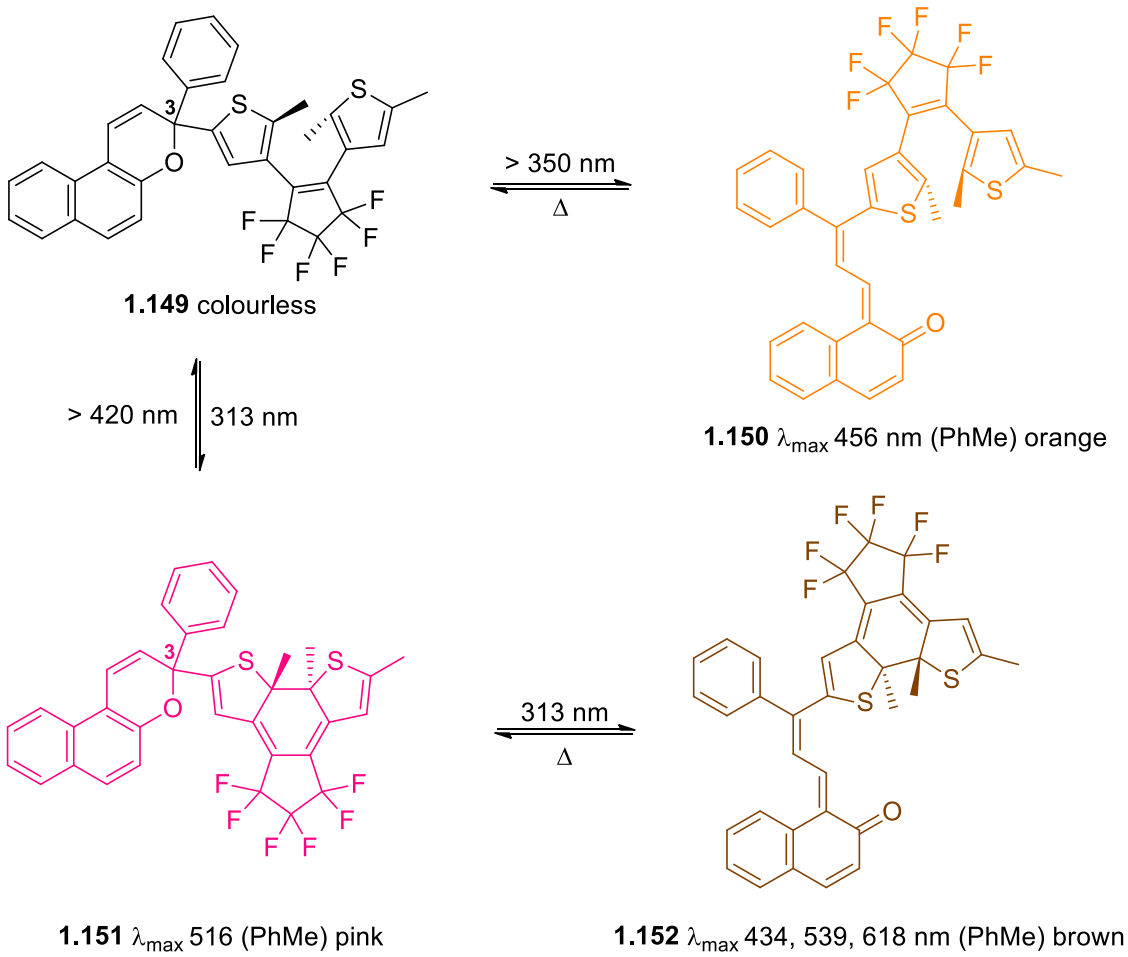

Scheme 1.34 Photoisomerization of biphotochromic system **1.149**.

1.3.3 Applications of 3*H*-naphtho[2,1-*b*]pyrans

Naphthopyrans have a wide range of applications: in the development of ophthalmic lenses, photochromic switches, molecular electronic devices, photoswitchable molecular receptors, photoresponsive polymers, photochromic thin films, photoresponsive gels, photoactive ormosil materials, photoresponsive nanomaterials, photochromic liquid crystalline materials and smart and functional optical materials.[145] Indeed a recent (January 2019) Scifinder search revealed 255 patents which contained the 3,3-diaryl-3*H*-naphtho[2,1-*b*]pyran unit with applications in variable transmission devices.

As mentioned previously, the major application of 3*H*-naphtho[2,1-*b*]pyrans concerns the development of ophthalmic lenses.[88, 151] The utility of naphthopyrans for constructing photochromic plastic lenses continues to drive much interest of the research community into this class of dyes. Although numerous molecules have been patented in the last few decades, of which only a very small amount have been commercialised, improvement on the design of naphthopyrans is still desirable. [87] Improvements on the design are usually accomplished through a combination of different structural changes in order to generate photochromes with higher colourability, faster bleaching kinetics, less fatigue and better thermal stability.[145]

Naphthopyrans have been integrated into fluorescent photoswitching systems.[152] Wang *et al*., have reported the synthesis of a naphthopyran-bridge-benzimidazole dyad which exhibited both fluorescence and photochromism. [153] The authors have found that photoisomerization of the naphthopyran **1.153** to the merocyanine **1.154** quenched the emission of the benzimidazole by up to 93% by an intramolecular energy-transfer process, although the authors were not able to restore the initial fluorescence after the first irradiation cycle (**Scheme 1.35**). According to the authors, the high-contrast fluorescence photoswitching characteristics and the capacity of non-destructive readout of information makes this type of dyads promising candidates in erasable optical information technology.[154]

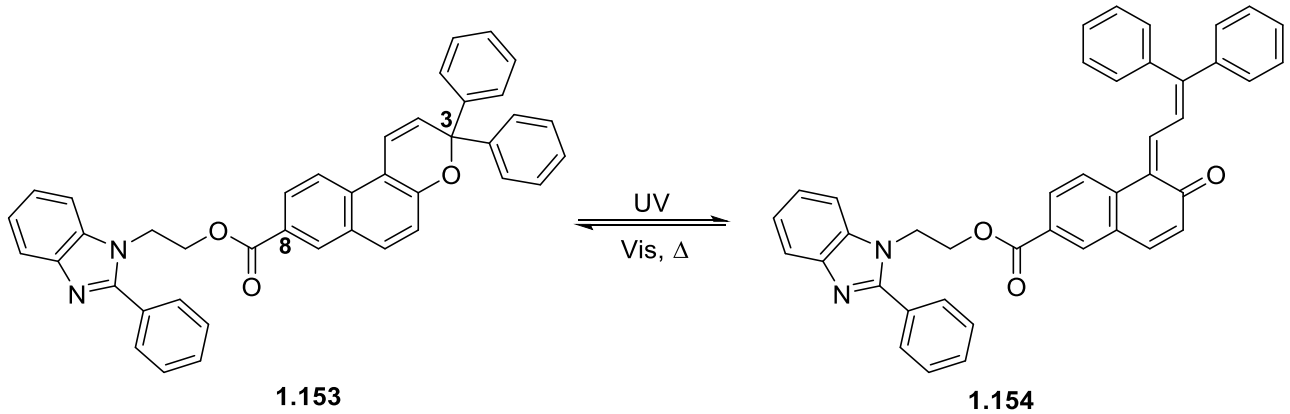

Scheme 1.35 Photoisomerization of naphthopyran-bridge-benzimidazole dyad **1.153**.

Naphthopyrans have been widely applied in photoswitchable molecular receptors.[155] For example, Kumar and Sahoo have reported the synthesis of a naphthopyran with a salicylaldimine moiety at C-5 (**1.155**) that functions as a selective chelator for Cu^{2+}, allowing its detection with excellent photoreversibility.[156] Other designs involve binding a crown ether to the C-5 of the naphthopyran scaffold (**1.156**)[157] or to the aryl at C-3 (**1.157**).[158] For instance, after irradiation of **1.156**, in the presence of metal ions, the band of the photomerocyanine was usually bathochromic shifted (up to 80 nm). The red-shift depended on the coordinated metal which allowed the selective detection of metal ions in solution.

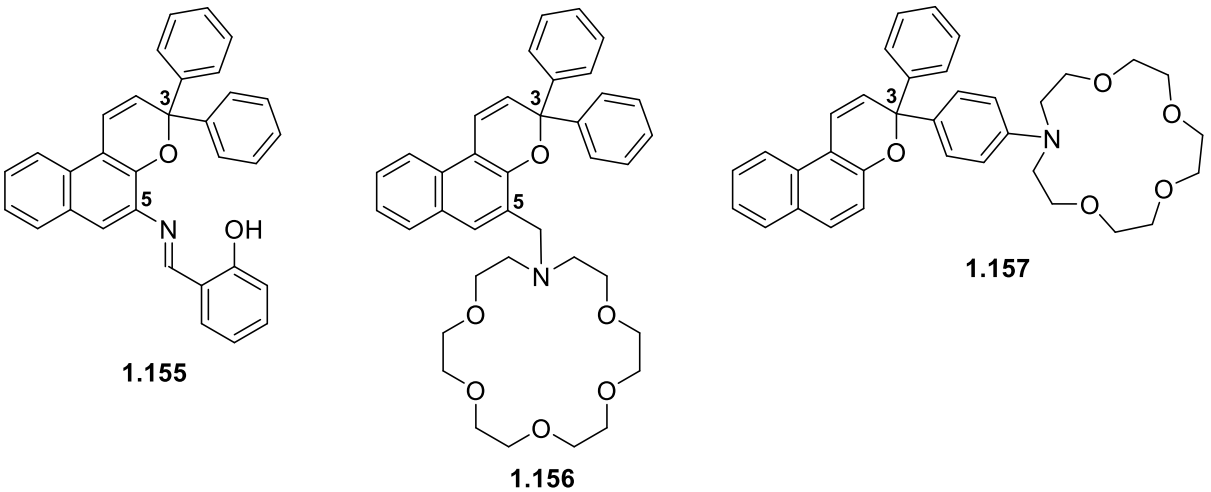

Naphthopyrans have also been applied to the development of molecular electronic devices.[159] Guglielmetti and co-workers have developed a series of oligothiophene bridged biphotochromic systems.[160] The oligothienyl-substituted naphthopyrans **1.158** when optically excited underwent a structural change passing from a neutral closed-state to the strongly polarized opened-form, accompanied by a large increase in the electrical conductivity – the conductivity increased by a

factor of about 100. The resulting photoinduced dipole moment determined the current flow direction and diode characteristic. The authors expected that the switch performance would improve by using longer bridging units that would provide longer conjugation lengths.

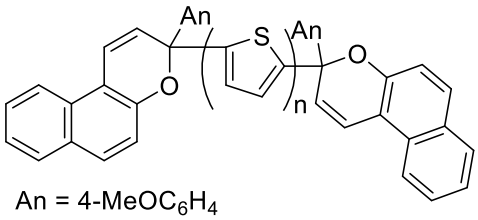

An = 4-MeOC$_6$H$_4$
n = 1, 2, 3 **1.158**

Naphthopyrans have also been applied to the development of photoresponsive polymers. Jiang et al.,[161] have reported the preparation of a compound micelle based on the self-assembly of a naphthopyran-containing block copolymer and a fluorophore-containing block copolymer. According to the authors, the fluorescence intensity of the micelles could be switched by light due to a photo-induced energy transfer process between the fluorophore and the naphthopyran in the micelle cores. The micelle could be used for encapsulation of guest molecules which could be released in a light-controlled way.

1.4 Photochromic Rhenium(I) Complexes

Transition metal complexes display interesting properties such as luminescence from triplet excited states,[162] reversible redox switching[163] and magnetism[164] which are rarely present in organic molecules. These properties arise from the d-orbitals at the metal centres, π-orbitals on the ligands that are electronically perturbed and coupled with the metal centres and the heavy atom effect of the metal centres. Heavy metal-induced triplet states display properties that differ from the single excited states from organic molecules.[165]

Transition metal complexes offer several advantages over organic molecules – complexes containing metal ions such as Ru(II) and Re(I) display: 1) absorption and emission behavior in the visible region due to the MLCT excited states; 2) various redox states, and 3) moderate excited state lifetimes. Additionally, the optical properties of these complexes can be tuned by the careful choice of ligands and by introducing suitable substituents.[166]

Rhenium(I) tricarbonyl complexes of the type *fac*-[Re(N^N)(CO)$_3$(X)]$^{0/+}$, where the bidentate ligand N^N is commonly either 2,2-bipyridine, 1,10-phenanthroline or substituted derivatives, and the axial ligand X is either a halide or a neutral N-donor, are a particular example of metal complexes that are emissive in aerated solution.[167] These typically exhibit a HOMO dominated by a

Re 5d-orbital − with additional carbonyl π* contributions as well as p-orbital contributions of the axial group − and a bidentate π*-based LUMO. Photoemission, energy transfer processes and electron transfer processes of *fac*-rhenium(I) tricarbonyl complexes occur either from the lowest vibrational level of the ^{3}MLCT excited state or in some cases from the triplet intra-ligand (^{3}IL) excited state.

Exciting *fac*-[Re(bpy)(CO)$_3$Cl] **1.159** in acetonitrile by irradiation at 365 nm or 400 nm first gives rise to the ^{1}MLCT excited state, which has an λ_{abs} of 405 nm and decays to the highest vibrational level of the ^{3}MLCT excited state after approximately 70 fs.[168] The latter releases energy in approximately 5–15 ps giving the lowest vibrational level of the ^{3}MLCT excited state which emits light with a lifetime of about 25 ns (**Figure 1.10**). The photophysical properties of rhenium(I) tricarbonyl complexes can be significantly modulated by modification of the structure of the bidentate ligand and therefore changing the energy of the LUMO. On the other hand, by changing the axially coordinated ligand the energy of the HOMO varies.[167]

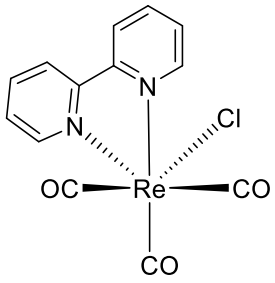

1.159

The development of transition metal complexes, including rhenium(I) tricarbonyl complexes, that contain photochromic ligands has received increasing attention in the last two decades. Incorporation of the photochromic moiety either by coordination to the metal centre or by covalently binding it to a coordinated ligand has shown to perturb and vary the photochromic properties. The heavy atom effect induces triplet states in the organic photochromes by photosensitization. On the other hand, the photochromic reaction has been shown to photomodulate and/or photoswitch the luminescence of the transition metal complexes.[169]

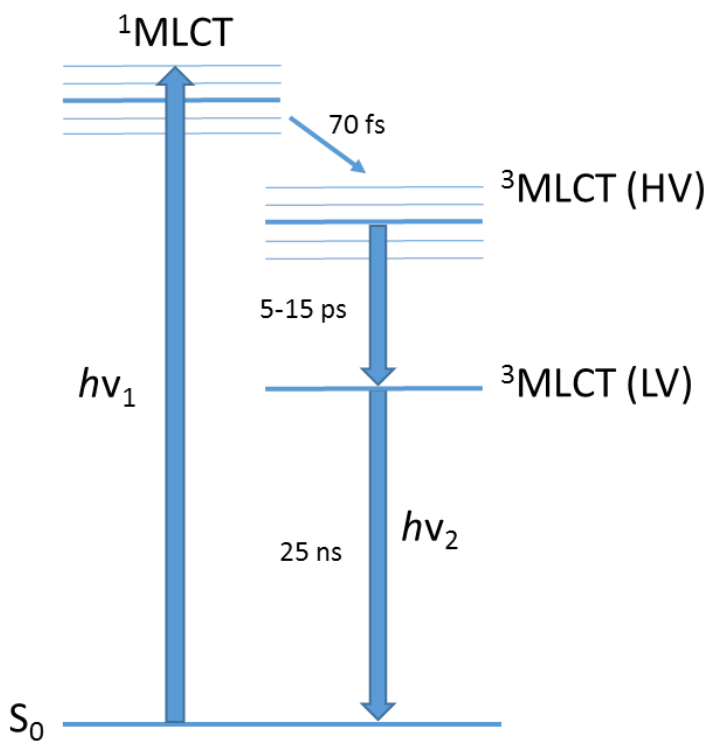

Figure 1.10 Photophysical processes that *fac*-[Re(bpy)(CO)$_3$Cl] **1.159** in acetonitrile undergoes after it is excited by light with a wavelength of 365 nm.

1.4.1 Photochrome Coordinated to Rhenium(I)

Yam *et al.*, were the first authors to report in 1998 the synthesis of photochromic rhenium(I) bidentate complexes by coordination of stilbene- and azo-containing pyridine ligands with tricarbonylrhenium(I) bipyridine complexes (**Schemes 1.36** and **1.37**, respectively).[170] The authors prepared the complexes by refluxing [Re(CO)$_3$(N^N)(MeCN)]OTf and the corresponding ligand in THF under an inert atmosphere of nitrogen.

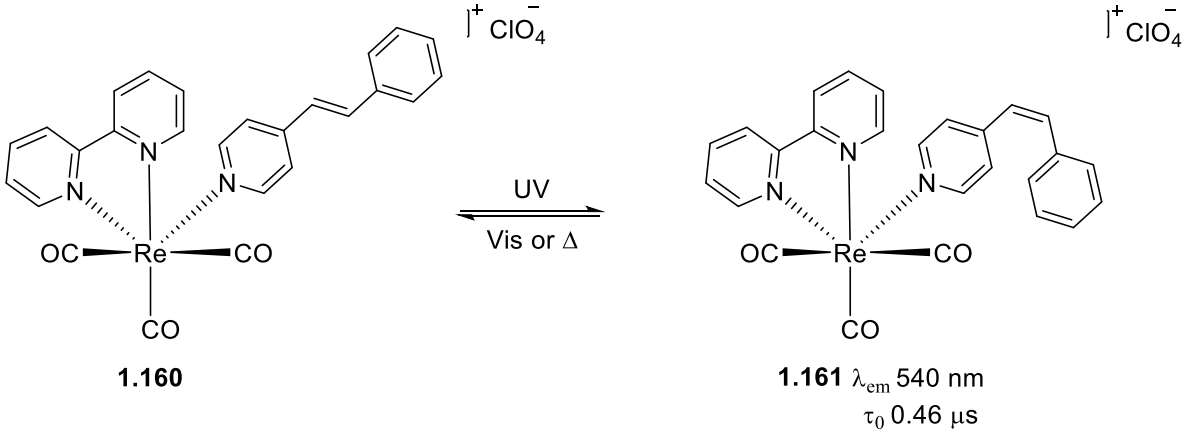

Scheme 1.36 Photoisomerization and spectrokinetic data of Re(I) complexes **1.160** and **1.161**.

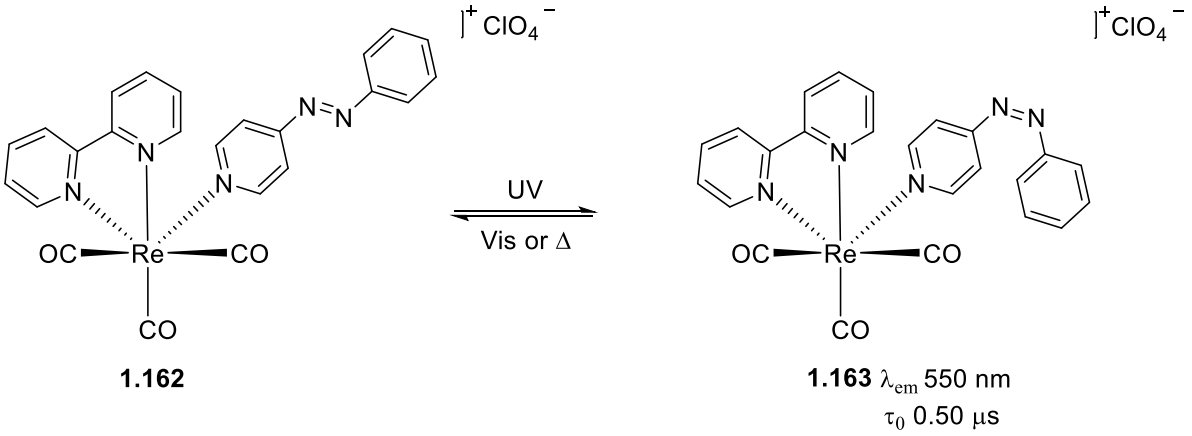

Scheme 1.37 Photoisomerization and spectrokinetic data of Re(I) complexes **1.162** and **1.163**.

Reversible *trans*-to-*cis* isomerization could be induced by excitation into the MLCT transition. The authors suggested a triplet photoisomerization mechanism which involved an intramolecular energy transfer from the ^{3}MLCT excited state to a non-emissive triplet intraligand (^{3}IL) excited state of the *trans*-isomers **1.160** and **1.162** (**Figure 1.11**).[171] Furthermore, the authors noticed that by *trans*-to-*cis* isomerization, a ^{3}MLCT emission band at *ca.* 510-580 nm typical of the tricarbonylrhenium(I) bipyridine complexes appeared. Increased steric congestion in the *cis*-isomers **1.161** and **1.163** resulted in less orbital overlap due to the twisting of the phenyl/pyridyl rings which led to a higher-lying ^{3}IL excited state. As a result, the triplet intramolecular energy transfer pathway was blocked, and the yellowish-green phosphorescence was restored (**Figure 1.12**).

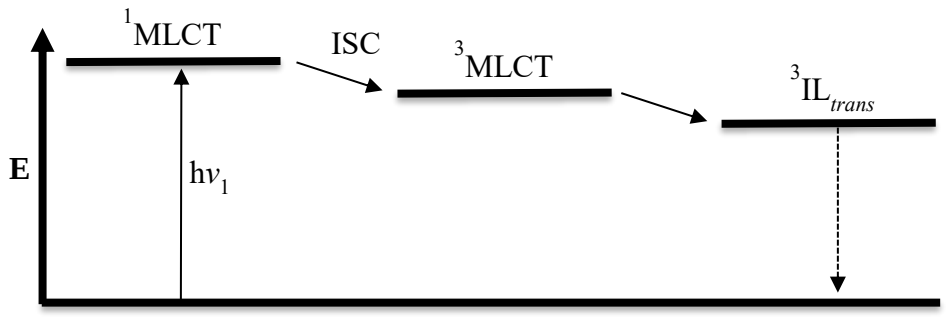

Figure 1.11 Energy-transfer pathway for *trans*-isomers **1.160** and **1.162**.

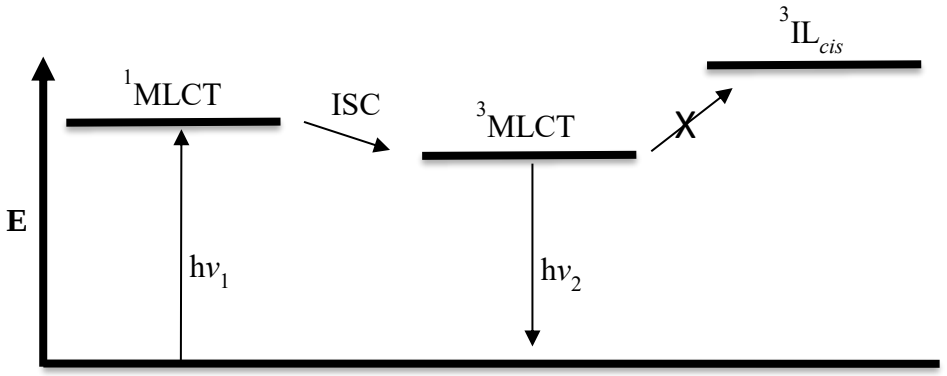

Figure 1.12 Energy-transfer pathway for *cis*-isomers **1.161** and **1.163**.

In a similar fashion, other subsequently reported *fac*-[Re(CO)$_3$(N^N)-(t*rans*-L)]$^+$ complexes, L = 1,2-bis(4-pyridyl)ethylene or styrylpyridine (stpy), were practically non-emissive when compared to their emissive *cis*-isomers.[172] In contrast, Amaral *et al.*, have recently reported the synthesis of *fac*-[Re(CO)$_3$(N^N)(stpyCN)]$^+$ that exhibited emission from both *trans* **1.164** and *cis* **1.165** isomers (**Scheme 1.38**).[173] The authors prepared complex **1.164** by refluxing the *fac*-[Re(CO)$_3$(bpy)(tfms)] precursor with the *trans*-stpyCN in methanol and, after cooling, by adding NH_4PF_6 which precipitated the product as a yellow solid. The emission from both *trans* **1.164** and *cis* **1.165** isomers presented remarkable resemblances in spectral profile, emission quantum yields (ϕ_{em}) and emission lifetimes (τ_0). According to the authors, the lack of a "rigidochromic effect", insensitivity to substituents in the bidentate ligand and resemblance to the emission of the axial ligand, demonstrated that the emission from both *trans* **1.164** and *cis* **1.165** isomers arised from an emissive ^{3}ILstpyCN, and not from a ^{3}MLCT excited state (**Figure 1.13**).

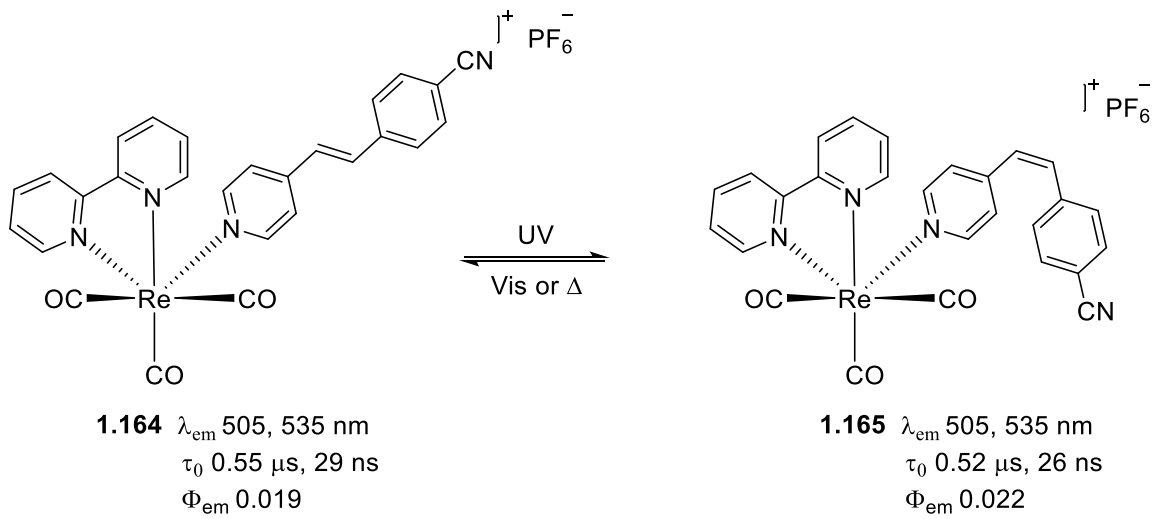

Scheme 1.38 Photoisomerization and spectrokinetic data of Re(I) complexes **1.164** and **1.165**.

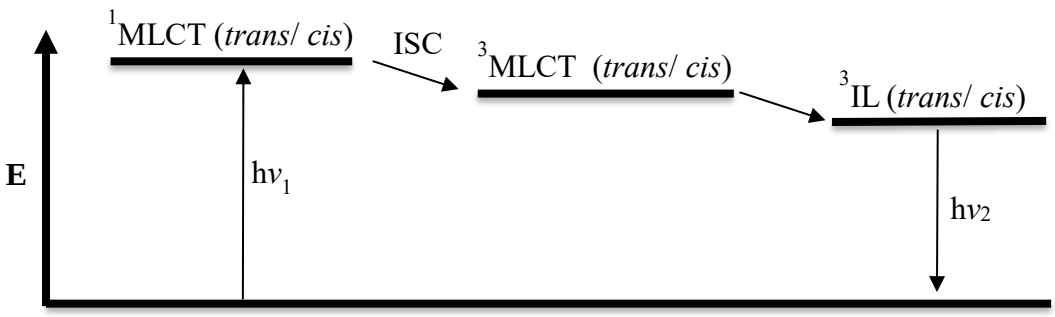

Figure 1.13 Energy-transfer pathway for both Re(I) complexes **1.164** and **1.165**.

Wenger *et al.*, have reported the synthesis of a rhenium(I) tricarbonyl complex coordinated to a pyridyl substituted dithienylethene (**1.166**) that in the opened-form exhibited yellow Re(I)-phen ^{3}MLCT excited state phosphorescence. Upon 350 nm irradiation, the dithienylethene photoisomerized to the ring-closed form (**1.167**) (**Scheme 1.39**). As a result, up to 83% of the intensity of the phosphorescence was quenched by energy transfer from the ^{3}MLCT excited state to the lower-lying non-emissive ^{3}IL excited state of the more π-extended ring-closed form (**Figures 1.14** and **1.15**).[174]

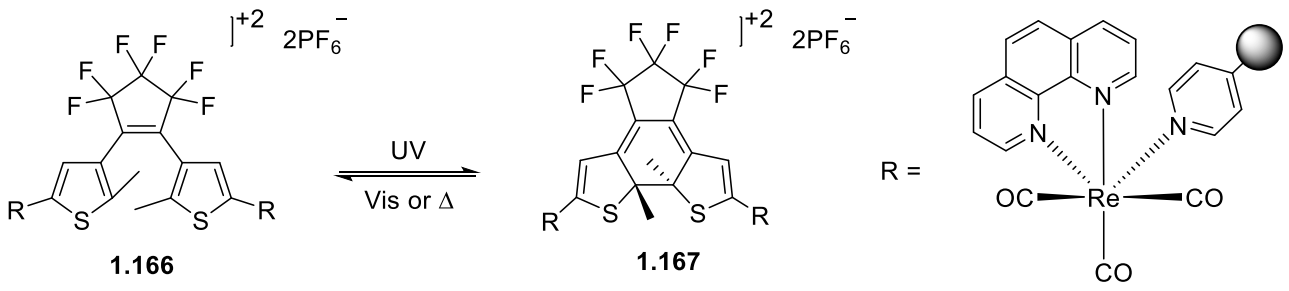

Scheme 1.39 Photoisomerization of Re(I) complexes **1.166** and **1.167**.

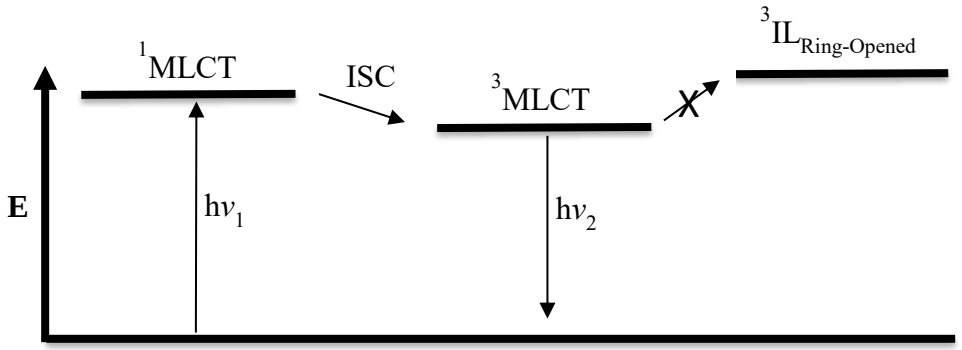

Figure 1.14 Energy-transfer pathway for ring-opened isomer **1.166**.

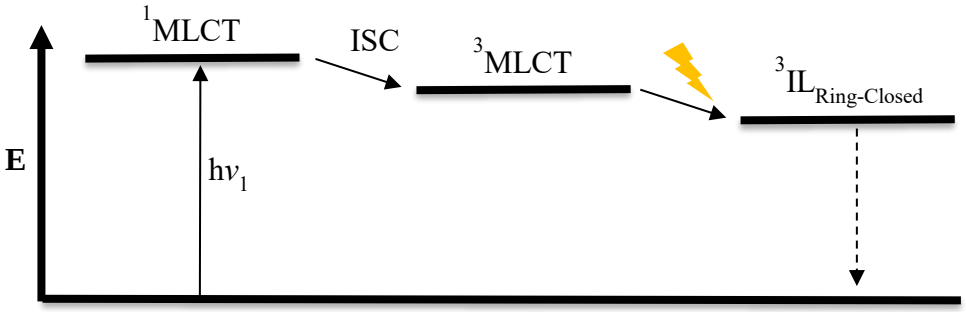

Figure 1.15 Energy-transfer pathway for ring-closed isomer **1.167** after photoisomerization.

Yam *et al.*, have reported the synthesis of a spironaphthoxazine-containing pyridine (SOPY) that was coordinated to a series of rhenium(I) tricarbonyl complexes with variable bidentate ligands (*t*-Bu$_2$bpy, Me$_2$bpy, phen).[175] Upon irradiation at 366 nm, the complexes **1.168** showed photochromism, with the formation of an absorption band peaking at *ca.* 604 nm corresponding to the generation of the photomerocyanines **1.169** (**Scheme 1.40**). After the irradiation ceased, the absorbance at 604 nm returned thermally to the original value, with a smaller fading rate when

compared to the free ligand. Like previous examples, excitation into the MLCT band at 420 nm also gave rise to the photochromic reaction by a triplet photosensitization process. Complexes **1.168** have also been shown to exhibit strong luminescence, while the free ligand SOPY showed only very weak luminescence upon 355 nm excitation. The close resemblance between the emission spectrum of the free ligand and those of the rhenium(I) complexes **1.168**, and very importantly that the emission energies of the latter were insensitive to the nature of the bidentate ligands, were indicative that the complexes **1.168** displayed ^{3}IL phosphorescence instead of the typical ^{3}MLCT phosphorescence. According to the authors, an intramolecular energy transfer from the ^{3}MLCT excited state to the SOPY moiety occurred, populating the ^{3}IL state, which would either return to the ground state by emission of light or, upon prolonged irradiation, would undergo ring-opening to give the photomerocyanine **1.169** (**Figure 1.16**).

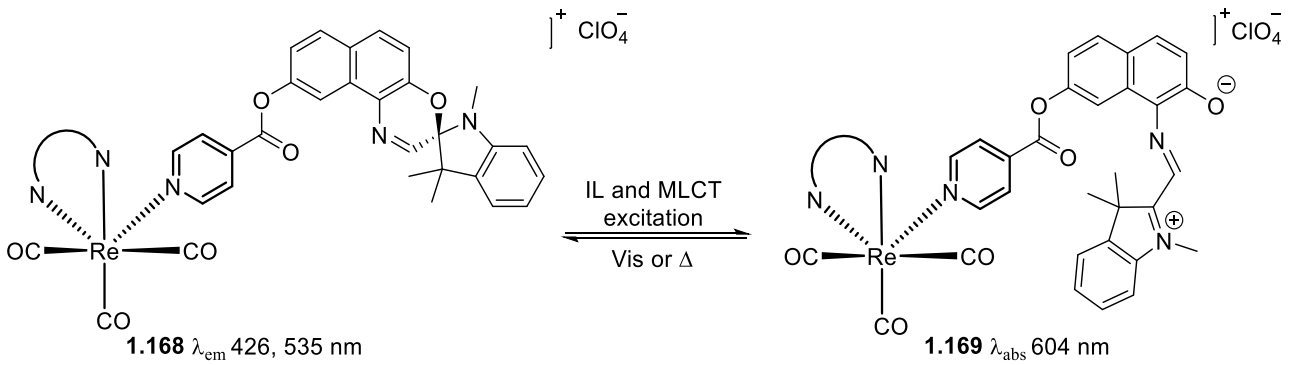

Scheme 1.40 Photoisomerization and spectroscopic data of Re(I) complexes **1.168** and **1.169**.

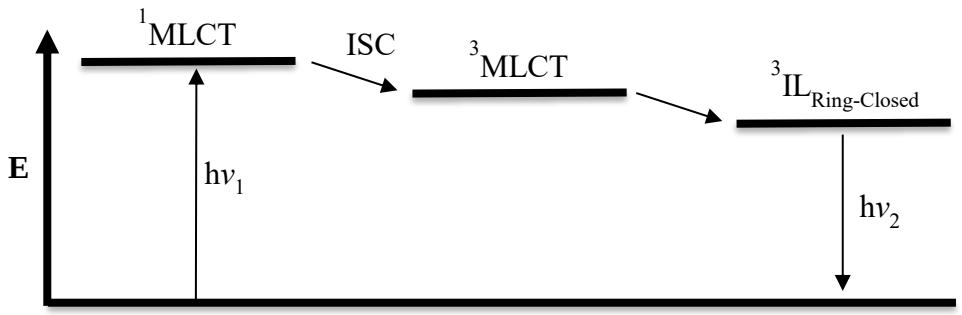

Figure 1.16 Energy-transfer pathway for Re(I) complex **1.168**.

1.4.2 Photochrome Covalently Bonded to Bidentate Ligand

Yam *et al.*, have prepared a series of spirooxazine-containing 2,2'-bipyridine ligands which were coordinated to rhenium(I) complexes.[176] The authors mixed $[Re(CO)_5Cl]$ and the corresponding bidentate ligands in anhydrous benzene at 50 °C giving the corresponding products as yellow or red solids. Excitation of rhenium(I) complex **1.170** in dichloromethane with λ > 400 nm at room temperature resulted in strong luminescence, with an emission maximum at 695 nm. This emission band derived from a ^{3}MLCT excited state probably mixed with some ^{3}IL character. Upon irradiation at 365 nm, both the free ligand and the complex **1.170** exhibited photochromism, with a growth in intensity of the absorption band at 604 nm, corresponding to the generation of the photomerocyanine **1.171** (**Scheme 1.41**). It is noteworthy that the complex **1.170** did not show photochromism with MLCT (400–440 nm) excitation, because the energy of the ^{3}MLCT excited state of the complex **1.170** was smaller than of the ^{3}IL excited state of the spirooxazine. Rhenium(I) complex **1.170** also displayed photolumicescence in $EtOH/MeOH/CH_2Cl_2$ (4:1:1, v/v/v) at 77 K with λ > 400 nm with an emission maximum at 600 nm. Upon irradiation at 365 nm the original emission band disappeared with the evolution of a new emission band peaking at 710 nm corresponding to the formation of photomerocyanine **1.171**. According to the authors, the close resemblance of the emission band of the ring-opened isomer to that of the free ligand, and the insensitivity of the emission energy to the nature of the bipyridine ligand, was indicative that the emission derived from a ^{3}IL excited state rather than a ^{3}MLCT excited state (**Figure 1.17**).

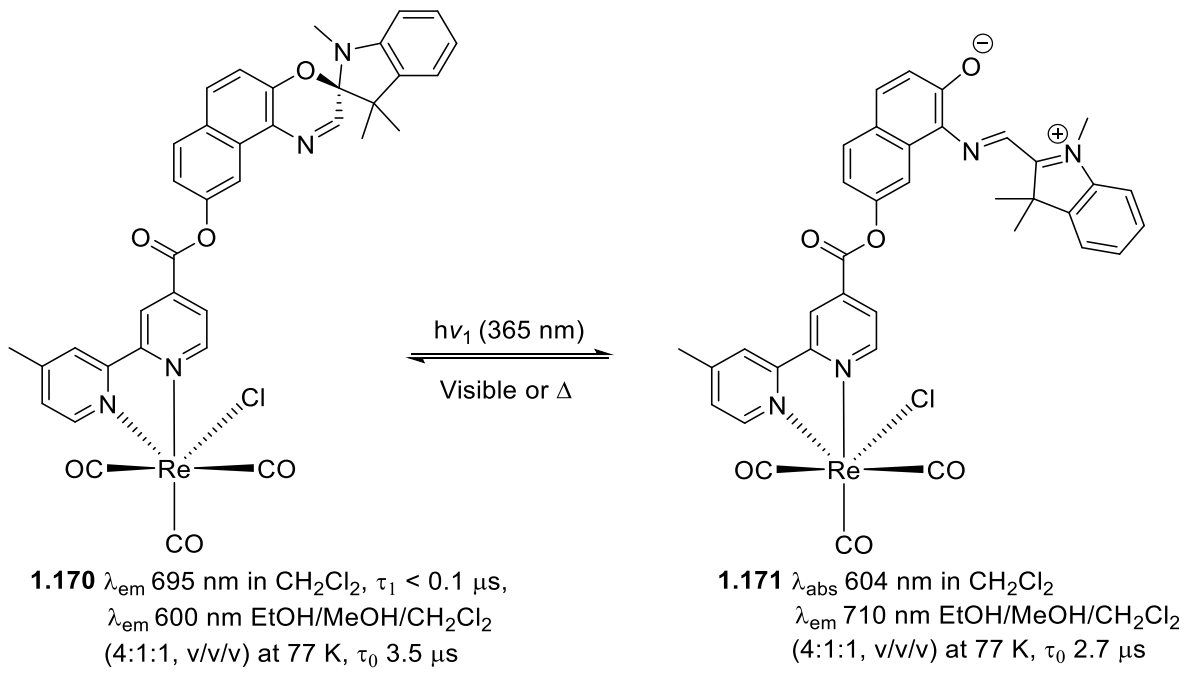

Scheme 1.41 Photoisomerization and spectrokinetic data of Re(I) complexes **1.170** and **1.171**.

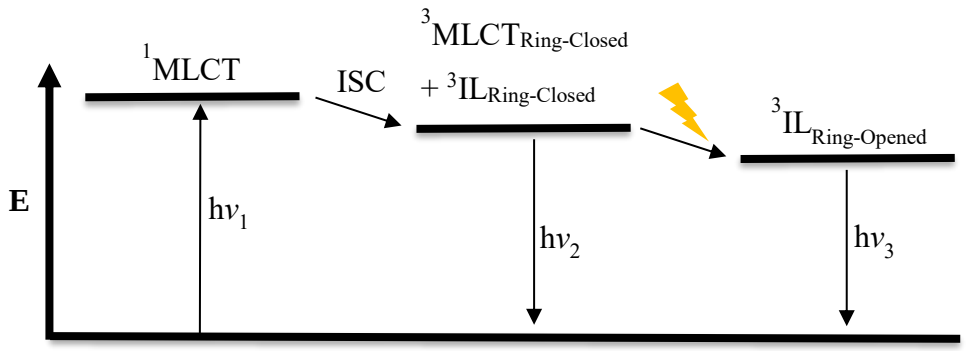

Figure 1.17 Energy-transfer pathway for Re(I) complex **1.170** before and after photoisomerization.

Bozec *et al.*, have designed photochromic metal complexes combining 4,4'-bisdithienylethene (DTE) vinyl-substituted bipyridines with different metallic fragments, among them rhenium(I) tricarbonyl bromide.[177] According to the authors, the long lifetimes (μs), low energy and structured spectra of the resulting metal complex **1.172** was indicative of emission from a ^{3}IL excited state predominantly localized on the bpy-C=C-Ar moiety rather from a ^{3}MLCT excited state (**Scheme 1.42**). Upon ring-closing to **1.173** at room temperature and re-freezing to 77K, a substantial quench (80−90%) of the 77K luminescence was observed. Quenching of emission was attributed to intramolecular energy transfer from the emissive ^{3}IL excited state to the non-emissive lower-lying ^{3}IL excited state of the closed-ring of the DTE part of the molecule (**Figure 1.18**). In all examples described extensive overlap of the emission bands of the Re chromophore with the low-energy absorption band of the acceptor photochromic unit in its closed form was observed.

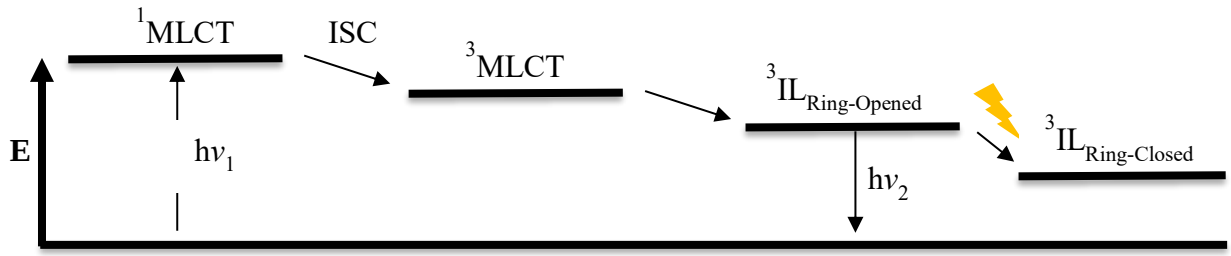

Figure 1.18 Energy-transfer pathway for Re(I) complex **1.172** before and after photoisomerization.

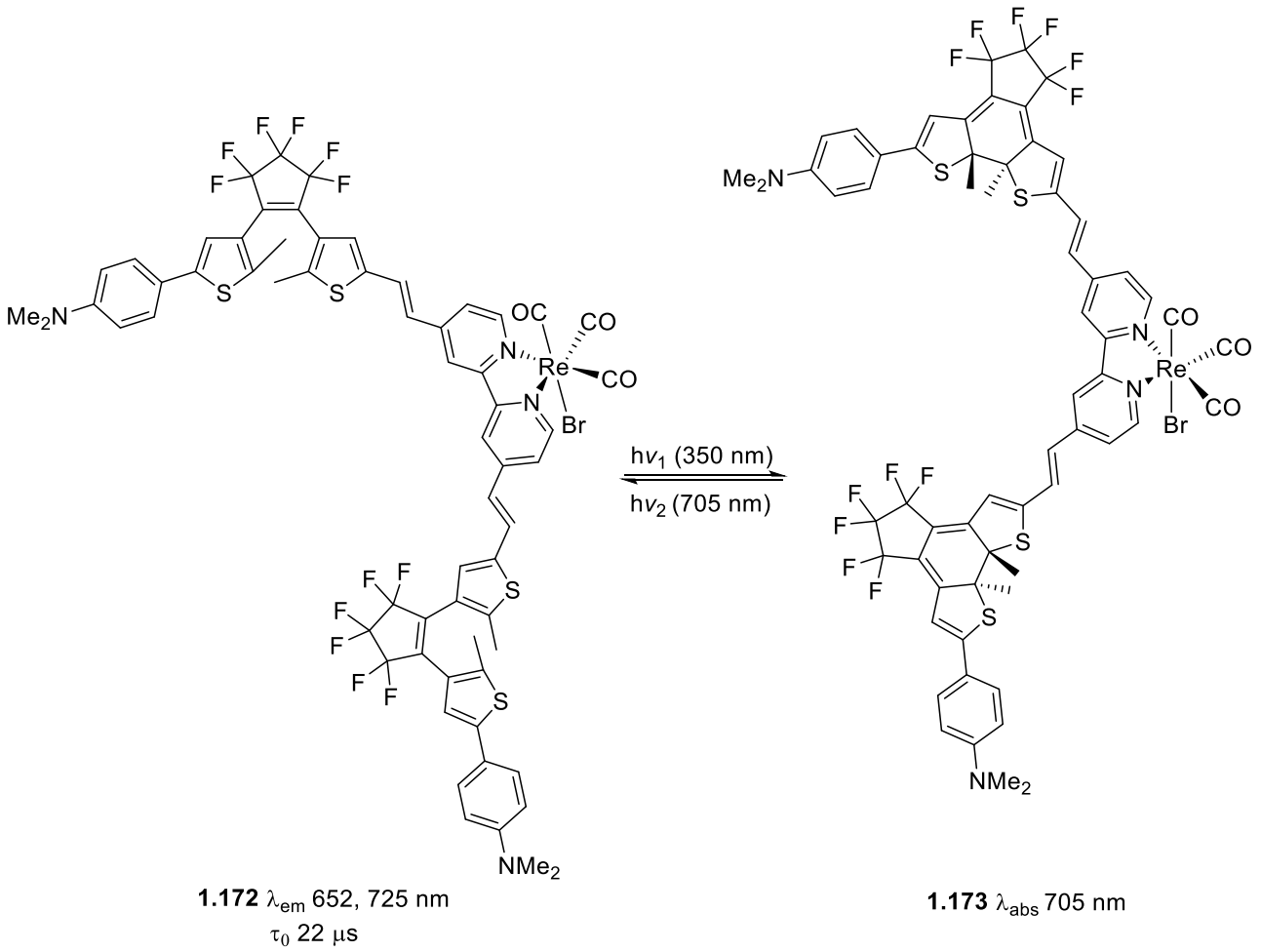

Scheme 1.42 Photoisomerization and spectrokinetic data of Re(I) complexes **1.172** and **1.173**.

Yam *et al.*, have prepared a dithienylethene containing 1,10-phenanthroline ligand that was coordinated to a rhenium(I) complex.[178] Upon UV irradiation (310 nm) absorption bands at 546 nm and 580 nm appeared corresponding to the generation of the photomerocyanine **1.175** from rhenium(I) complex **1.174** (**Scheme 1.43**). On the other hand, irradiation with visible light (580 nm) restored the ring-opened isomer **1.174**. The ring-closed isomer **1.175** also underwent slow thermal back reaction, with the complex ($t_{½}$ 78 h) bleaching faster than the free ligand ($t_{½}$ 143 h). Excitation into the MLCT absorption bands also led to the photochromic reaction as part of a triplet photoisomerization mechanism. The ring-opened isomer **1.174** in benzene solution produced luminescence at 595 nm [τ_0 0.26 μs, Φ_{em} (λ_{ex} 470 nm) 0.02] which was attributed to the ^{3}MLCT excited state phosphorescence with additional mixture of ^{3}IL character.[179] Upon conversion to the closed form **1.175** in the photostationary state, the emission band changed. The ring-closed isomer **1.175** in benzene solution displayed red photoluminescence, with an emission maximum at 644 nm [τ_0 < 0.1 μs, Φ_{em} (λ_{ex} 470 nm) 0.003]. The bathochromic shift (49 nm) in the emission energy of the

ring-closed isomer **1.175** was due to the more extended π-conjugated system upon photoinduced ring-closing reaction. According to the authors, the different emission band structure and the shorter emission lifetime of the ring-closed isomer **1.175** compared to its ring-opened isomer **1.174** in solution was suggestive of a different emission origin. Considering the close resemblance of the emission energies and the vibronic structures of free ligand and the corresponding rhenium complex in their closed forms, an emission origin of metal-perturbed IL character was proposed. It was suggested that upon photoinduced ring-closing the ^{3}IL excited state became lower-lying in energy than the ^{3}MLCT excited state, giving the ^{3}IL excited state as the predominant emissive state (**Figure 1.19**).

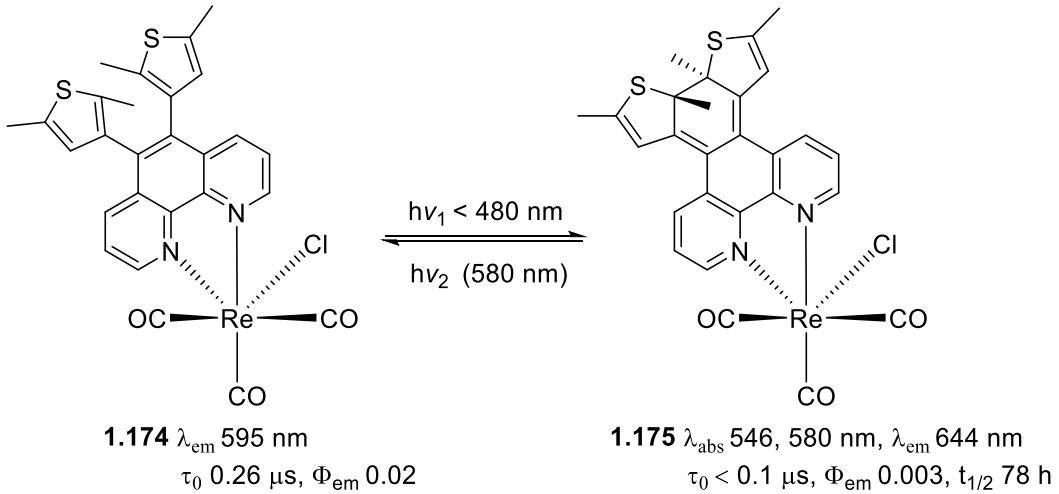

Scheme 1.43 Photoisomerization and spectrokinetic data of Re(I) complexes **1.174** and **1.175**.

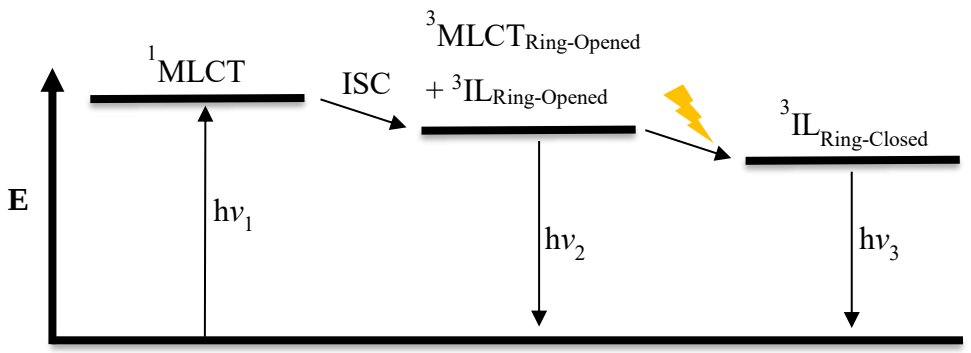

Figure 1.19 Energy-transfer pathway for Re(I) complex **1.174** before and after photoisomerization.

The same authors have also reported the synthesis of a diarylethene containing 1-aryl-substituted 2-(2-pyridyl)imidazole ligand which was coordinated to a rhenium(I) complex.[180] Upon

irradiation of the rhenium(I) complex **1.176** with λ < 450 nm into either the IL or MLCT transitions, three absorption bands were generated at *ca.* 288, 480 and 713 nm due to the formation of the photomerocyanine **1.177** (**Scheme 1.44**). Excitation into either the IL or MLCT bands of rhenium(I) complex **1.176** in chloroform resulted in an emission band centered at 570 nm. This emission was assigned as ^{3}MLCT excited state phosphorescence (**Figure 1.20**). Upon prolonged irradiation at 352 nm, photocyclization occurred, and the emission intensity at 570 nm decreased by energy-transfer from the ^{3}MLCT excited state to the lower-lying non-emissive ^{3}IL excited state of the photomerocyanine **1.177** (**Figure 1.21**).

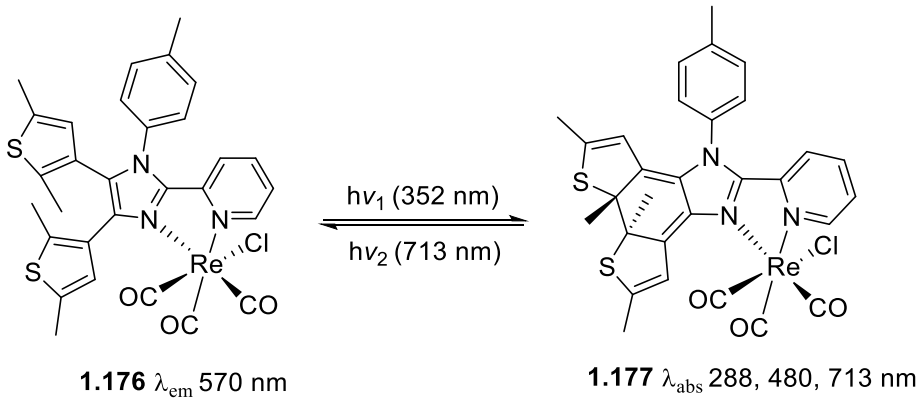

Scheme 1.44 Photoisomerization and spectroscopic data of Re(I) complexes **1.176** and **1.177**.

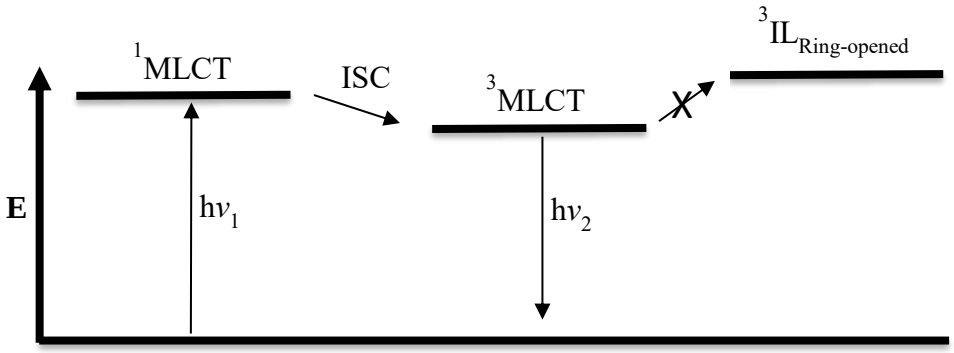

Figure 1.20 Energy-transfer pathway for Re(I) complex **1.176**.

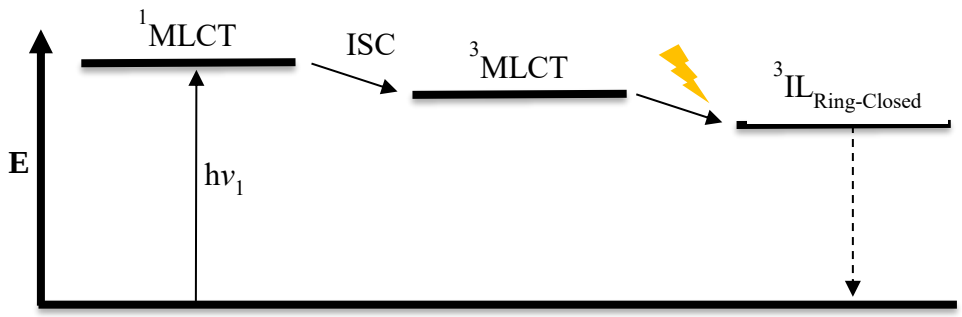

Figure 1.21 Energy-transfer pathway for Re(I) complex **1.177**.

1.5 Aims of the Present Study

Simply stated the aims of this investigation are:

1) to devise and implement synthetic strategies to obtain pyridyl substituted photochromic 3*H*-naphtho[2,1-*b*]pyrans of the general structures **1.178**, **1.179** and **1.180**, and to characterize their photochromic response.

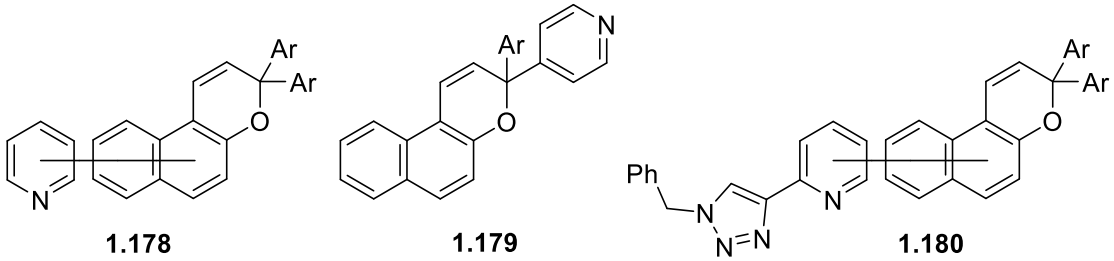

2) to employ the foregoing pyridyl naphthopyrans as 'dynamic' ligands to obtain new emissive Re(I) complexes of the type **1.181** and **1.182**.

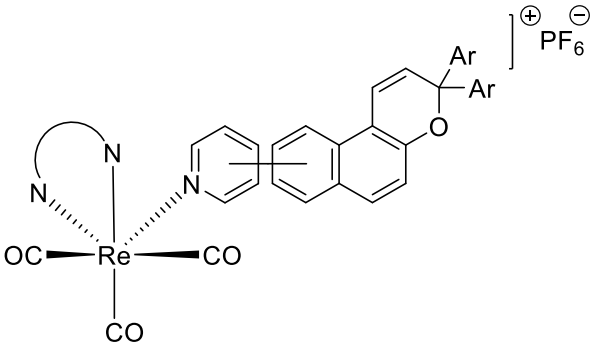

1.181

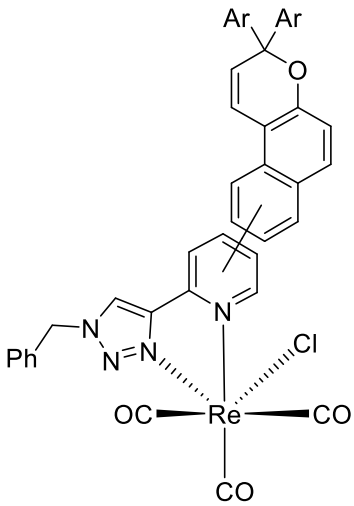

1.182

3) to explore the influence of cycling the photochromic naphthopyran upon the photophysical (absorption and emission) properties of the foregoing Re(I) complexes. It was predicted that the photochromic reaction could be used as a trigger to switch ON/OFF the ^{3}MLCT – ^{3}IL energy transfer pathway, allowing reversible photoswitching of the Re(I) complexes ^{3}MLCT phosphorescence.

2. DISCUSSION

2.1 Synthesis of Pyridyl Substituted 3*H*-Naphtho[2,1-*b*]pyrans

2.1.0 Strategic Ideas

2.1.0.1 Strategy A – By a Suzuki cross-coupling reaction after chromenization

When conceiving strategies for the preparation of the pyridyl substituted 3*H*-naphtho[2,1-*b*]pyrans different factors were considered, for example, the starting material availability and price, the estimated overall yield, and the number of steps for a given pathway.

A straighforward strategy envisioned for the preparation of the pyridyl substituted 3*H*-naphtho[2,1-*b*]pyrans (or, benzochromenes) **2.1** involves performing Suzuki cross-coupling reactions, after chromenization,[114] between the halo or pseudo-halo substituted naphthopyran **2.2** with the appropriate pyridyl boronic acids – **Strategy A** (**Scheme 2.1**). Furthermore, the naphthopyrans would be prepared by the established acid-catalysed condensation of the corresponding 2-naphthols **2.3** with the appropriate propynols. Additionally, this strategy also requires the preparation of halo or pseudo-halo substituted 2-naphthols **2.3**, when these were not commercially available or overly expensive, from commercially obtainable and relatively cheap 2-naphthols **2.4**. **Strategy A** was employed for the preparation of the 10-, 9-, 8-, 7- and 5-pyridyl substituted 3*H*-naphtho[2,1-*b*]pyrans.

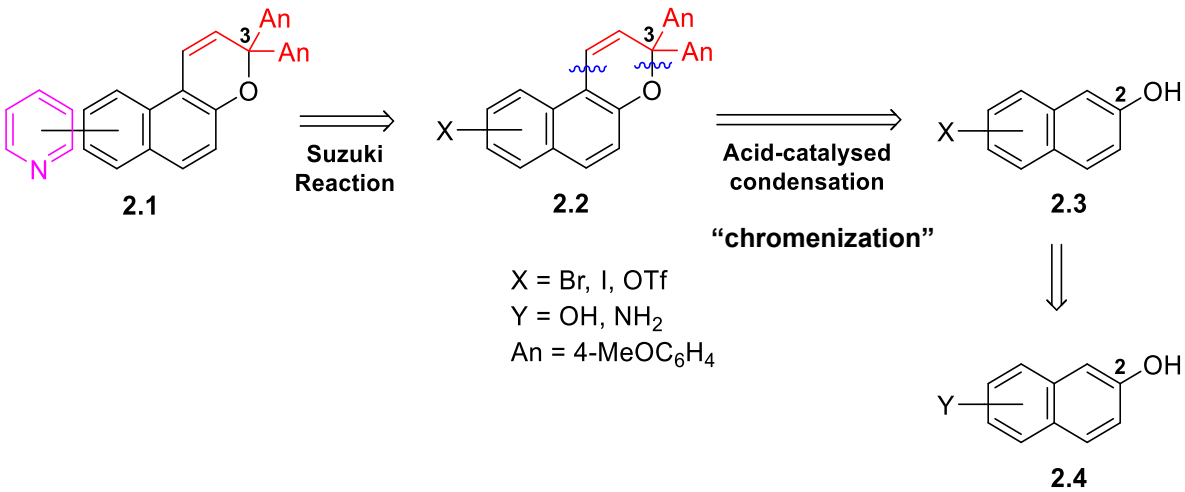

Scheme 2.1 Strategy A – By a Suzuki reaction after chromenization – for the preparation of pyridyl substituted 3*H*-naphtho[2,1-*b*]pyrans **2.1**.

For the synthesis of the 8-(pyridyl-triazole)-3*H*-naphtho[2,1-*b*]pyran **2.5**, it was predicted that **Strategy A** could also be employed (**Scheme 2.2**). Thus, the 8-(pyridyl-triazole)-3*H*-naphtho[2,1-

b]pyran **2.5** would be prepared by the Suzuki cross-coupling reaction between a halo substituted pyridyl triazole **2.6** and a boronyl substituted 3*H*-naphtho[2,1-*b*]pyran **2.7** – which could be prepared from the borylation of an 8-bromo-3*H*-naphtho[2,1-*b*]pyran. Furthermore, the bromo-substituted pyridyl-triazole **2.6** could be synthesized from 4-halo-2-ethynylpyridine **2.8** and benzyl azide *via* a 1,3-dipolar cycloaddition (Click Reaction). The 4-halo-2-ethynylpyridine **2.8** required preparation by a regioselective Sonogashira coupling between TMS acetylene and 2,4-dihalopyridine **2.9**.

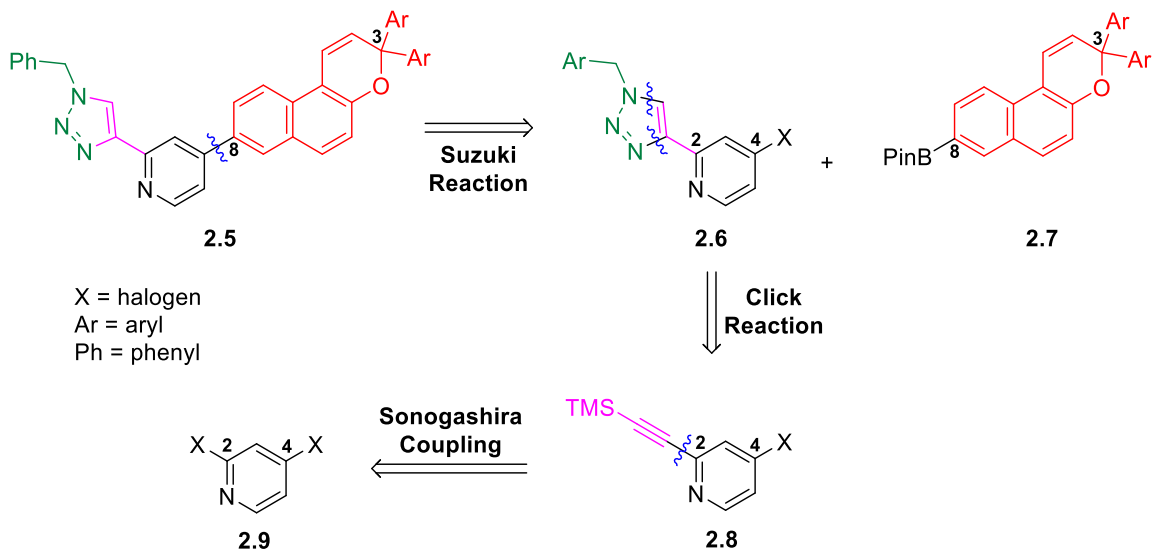

Scheme 2.2 Strategy A – By a Suzuki reaction after chromenization – to prepare 8-(pyridyl-triazole)-3*H*-naphtho[2,1-*b*]pyran **2.5**.

2.1.0.2 Strategy B – By a Heck cross-coupling reaction protocol

Incorporation of either basic or electron-withdrawing groups at C-3 of the naphthopyrans by acid-catalysed condensation between 2-naphthol **2.10** and propynol **2.11** has been previously accomplished only in very poor yields (**Scheme 2.3**).[124, 146]

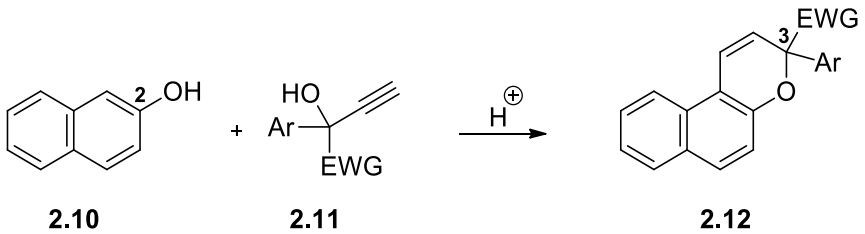

EWG = electron withdrawing group
Ar = aryl

Scheme 2.3 Naphthopyran **2.12** with electron withdrawing groups at C-3 prepared by the acid-catalysed condensation between 2-naphthol **2.10** and the corresponding propynol **2.11**.

Inspired by the work of Putala *et al.*, it was envisioned that a Heck cross-coupling reaction protocol could be employed to prepare 3-pyridyl-3*H*-naphtho[2,1-*b*]pyrans **2.13** from commercially available and easily prepared 1-halo-2-naphthols **2.15** (**Scheme 2.4**).[105]

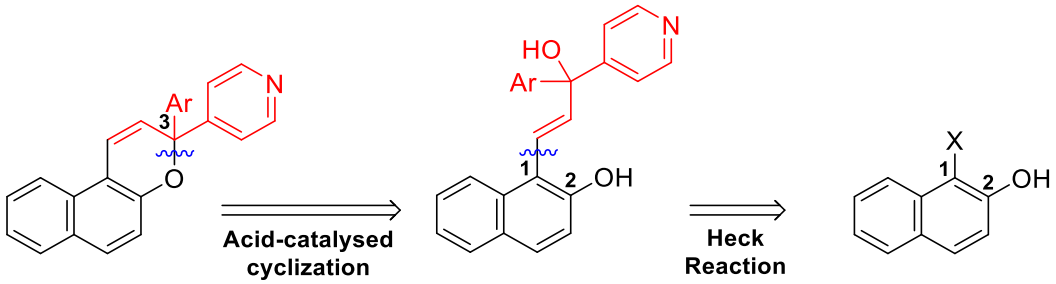

Ph = phenyl
Ar = aryl
X = halide

Scheme 2.4 Strategy B – By a Heck cross-coupling reaction protocol – for the preparation of 3-pyridyl-3*H*-naphtho[2,1-*b*]pyrans **2.13**.

2.1.0.3 Strategy C – By a Suzuki cross-coupling reaction before chromenization

It was rationalized that the preparation of 6-pyridyl-3*H*-naphtho[2,1-*b*]pyrans by employing **Strategy A** could be problematic because neither 4-bromo-2-naphthol nor 4-amino-2-naphthol were commercially available. As an alternative, it was envisioned that a different strategy – **Strategy C** – in which the pyridyl substituents would be incorporated by Suzuki cross-coupling reactions before chromenization (**Scheme 2.5**). A straightforward approach would be to prepare the pyridyl substituted 3*H*-naphtho[2,1-*b*]pyrans **2.16** by the direct acid-catalysed condensation between the pyridyl-2-naphthol **2.17** with the appropriate propynol. Thus, the pyridyl-2-naphthol **2.17** would be prepared from **2.18** by a deprotection step. Hence, the latter would be prepared from **2.19** by a

Suzuki cross-coupling reaction with the appropriate pyridylboronic acid. For the 6-pyridyl-3*H*-naphtho[2,1-*b*]pyran route, in the absence of the 4-halo-2-naphthols, the coupling partner would necessarily be 4-trifloxy-2-methoxynaphthalene **2.20**, that would be derived from the commercially available 1,3-dihydroxynaphthaplene **2.21** in two steps.

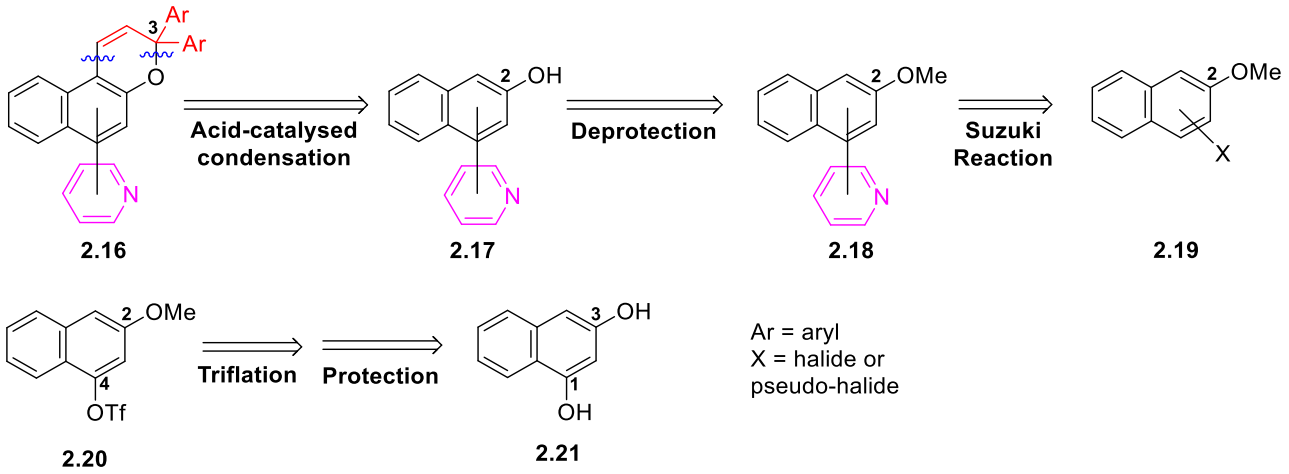

Scheme 2.5 Strategy C – By the direct acid-catalysed condensation – for the preparation of pyridyl substituted 3*H*-naphtho[2,1-*b*]pyrans **2.16**.

A potential problem with the foregoing route would be the basicity of the pyridyl substituent, which may hinder the acid-catalysed condensation of pyridyl-2-naphthol **2.17** with the appropriate propynol, as it was not completely clear of how reactive the pyridinium-2-naphthol would be. An alternative variation would include the protection of the pyridyl substituent of pyridyl-2-naphthol **2.17** as the *N*-oxide **2.23**, therefore not allowing its protonation during the acid-catalysed condensation step (**Scheme 2.6**).

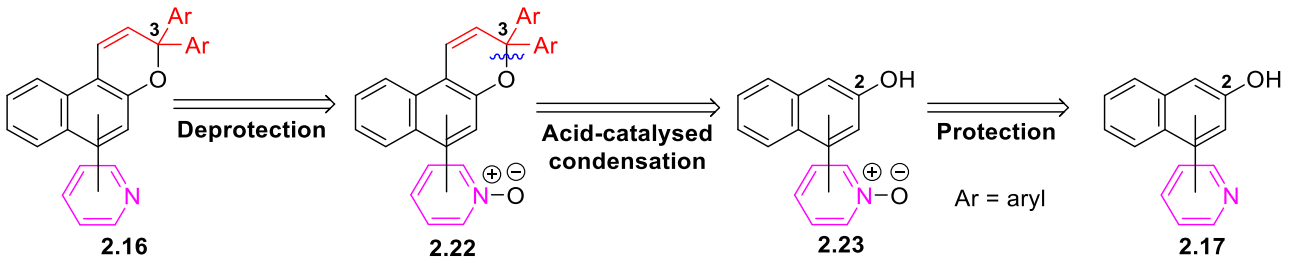

Scheme 2.6 Strategy C – By protecting the pyridyl substituent – for the preparation of pyridyl substituted 3*H*-naphtho[2,1-*b*]pyrans **2.16**.

A more elegant variation of **Strategy C** involves the synthesis of pyridyl substituted 3*H*-naphtho[2,1-*b*]pyrans **2.16** by the acid-catalysed cyclization of alkene **2.24**, prepared by the Heck cross-coupling reaction between 1-halo-pyridyl-2-naphthol **2.25** with the appropriate propenol (**Scheme 2.7**). This route would require the preparation of the Heck coupling partner **2.25** by the regioselective halogenation of pyridyl-2-naphthol **2.17**.

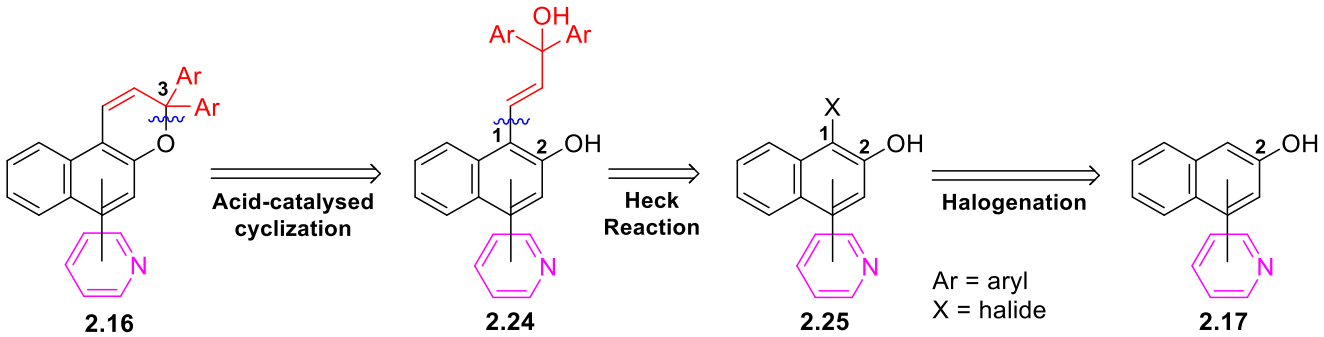

Scheme 2.7 Strategy C – By the Heck cross-coupling reaction – for the preparation of pyridyl substituted 3*H*-naphtho[2,1-*b*]pyrans **2.16**.

Naphthopyrans possessing an aryl substituent at the C-1 of the naphthopyran scaffold have no reported photochromism at room-temperature,[117] therefore the synthesis of 1-pyridyl-3*H*-naphtho[2,1-*b*]pyrans **2.26** (**Figure 2.1**) was not explored. Furthermore, 2-pyridyl-3*H*-naphtho[2,1-*b*]pyrans **2.27** (**Figure 2.1**) were predicted to be very fast photochromes[119] with suspected poor colourability – the latter being of great importance for the photoswitching of the luminescence of the rhenium(I) complexes. Therefore, this design was most probably flawed and was not investigated.

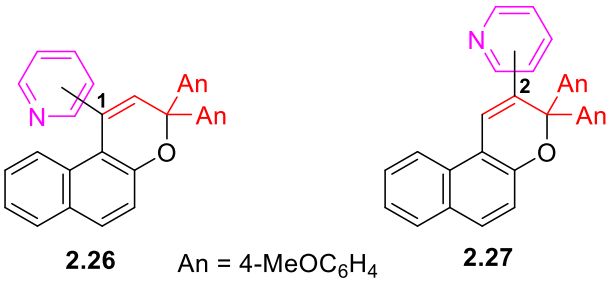

Figure 2.1 1-Pyridyl-3*H*-naphtho[2,1-*b*]pyrans **2.26** and 2-pyridyl-3*H*-naphtho[2,1-*b*]pyrans **2.27**.

2.1.1 Strategy A – By a Suzuki cross-coupling reaction after chromenization

2.1.1.1 Synthesis of 10-Pyridyl-3*H*-Naphtho[2,1-*b*]pyrans

To prepare 10-pyridyl-3*H*-naphtho[2,1-*b*]pyrans according to **Strategy A**, it was first necessary to synthesize an 8-halo-2-naphthol, as neither 8-iodo-2-naphthol nor 8-bromo-2-naphthol were readily accessible. For this reason, 8-iodo-2-naphthol **2.29** was prepared in good yield (73%) from the commercially available 8-amino-2-naphthol **2.28** by a Sandemeyer-type reaction, which involves the diazotization of 8-amino-2-naphthol **2.28**, followed by treatment with potassium iodide (**Scheme 2.8**).[181]

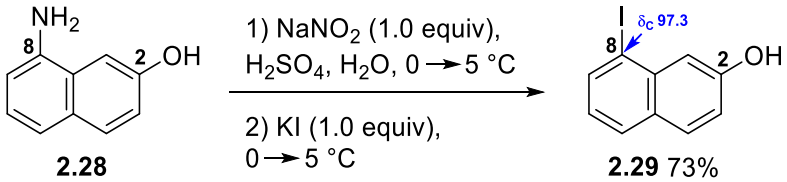

Scheme 2.8 Synthesis of 8-iodo-2-naphthol **2.29**.

In the reaction mechanism, the nucleophilic attack of the amino group from **2.28** on the nitrosonium ion, formed *in situ* from the reaction of sodium nitrite with H_2SO_4, resulted in the formation of intermediate **2.31** that by dehydration generated the diazonium ion **2.32** (**Scheme 2.9**). *Ipso* nucleophilic attack of the iodide to **2.32** caused the displacement of nitrogen, resulting in the formation of 8-iodo-2-naphthol **2.29**.

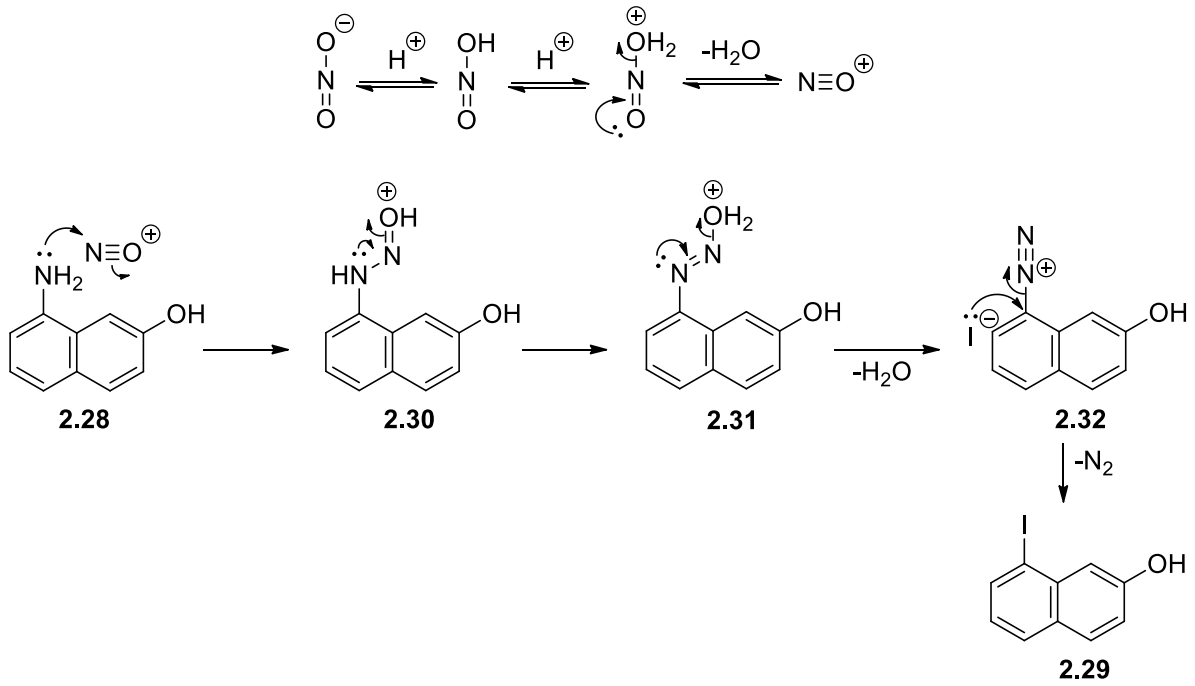

Scheme 2.9 Mechanism of the synthesis of 8-iodo-2-naphthol **2.29**.

To access 10-(4-pyridyl)-3*H*-naphtho[2,1-*b*]pyran **2.36**, the precursor 10-iodo-3*H*-naphtho[2,1-*b*]pyran **2.34** was first prepared by the acid-catalysed condensation reaction between 8-iodo-2-naphthol **2.29** and the readily available propynol **2.33**, following a modification of a procedure from Carreira *et al*. (**Scheme 2.10**).[116] The poor yield (39%) was attributed to decomposition of the naphthopyran **2.34** during the column chromatography separation. Although it was isolated with only approximately 83% purity, due its proclivity to decomposition, it was used in the next step without further purification. The mechanism for the pyran ring formation from a naphthol and a propynol has been described in **Scheme 1.29**.

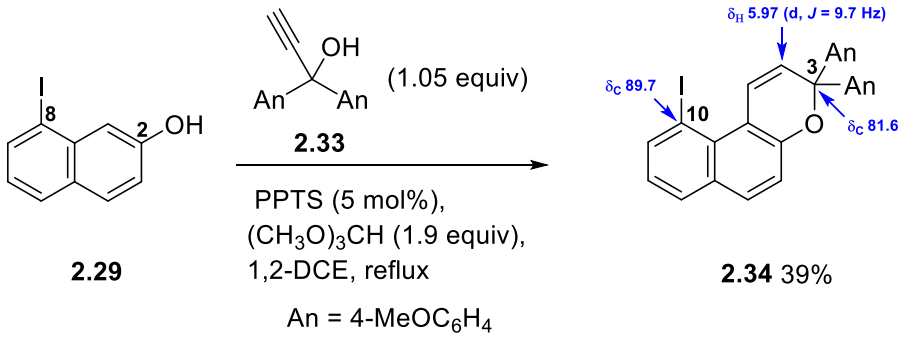

Scheme 2.10 Synthesis of 10-iodo-3H-naphtho[2,1-b]pyran **2.34**.

Suzuki cross-coupling reaction between **2.34** and 4-pyridineboronic acid pinacol ester **2.35** afforded 10-(4-pyridyl)-3*H*-naphtho[2,1-*b*]pyran **2.36** in good yield (66%) after 5 days of reflux (**Scheme 2.11**), following a variation of literature protocol which involved using KF instead of K_2CO_3.[182] An interesting observation was the 1-H, that usually resonates at *ca.* 7.3 ppm, appeared upfield on **2.34** at 6.01 ppm as it was shielded by the induced anisotropic field.

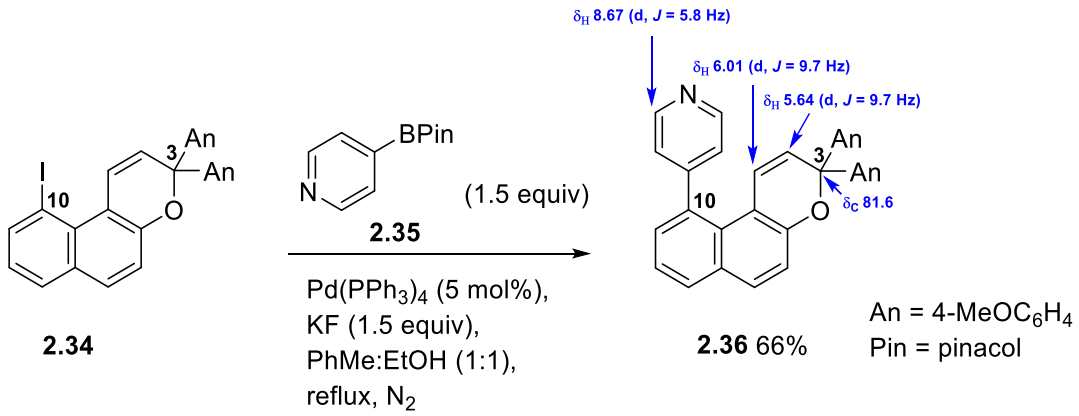

Scheme 2.11 Synthesis of 10-(4-pyridyl)-3*H*-naphtho[2,1-*b*]pyran **2.36**.

The choice of the base for this Suzuki cross-coupling reaction is one of the major subjects of **Chapter 2.4**. According to Le Duc *et al.*,[183] in the fluoride-mediated Suzuki reaction, fluoride plays three roles: two are antagonistic in the rate-determining transmetallation: 1) formation of the reactive *trans*-[$ArPdL_2F$] (L = PPh_3), which reacts with $Ar'B(OR)_2$ and 2) formation of the unreactive $Ar'B(OR)_{3-n}F_n$. A positive third role is the fast promotion of the reductive elimination from the *trans*-[$ArPdAr'L_2$] intermediate. It is worth mentioning at this point that one implication of the mechanism of the Suzuki cross-coupling reaction is that at least 2 equiv of a monobasic base like KF would be required for a fully successful catalytic cycle (**Scheme 2.12**). However, only 1.5 equiv of KF were used in this reaction which could help to explain the yield of only 66%. On the other hand, the big steric encumberment of C-10 due to its proximity to the pyran ring could have contributed to the slow reaction rate and lower yield.

Overall, 10-(4-pyridyl)-3*H*-naphtho[2,1-*b*]pyran **2.36** was synthesized from 8-amino-2-naphthol **2.28** in a three step linear route in 19% yield.

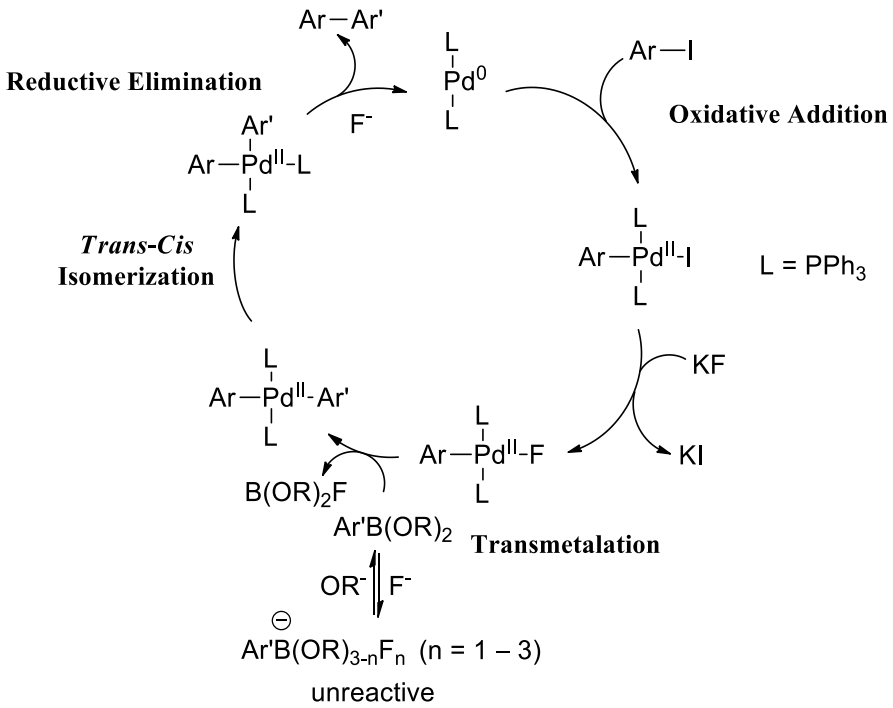

Scheme 2.12 General mechanism of a Suzuki cross-coupling reaction.

2.1.1.2 Synthesis of 9-Pyridyl-3*H*-Naphtho[2,1-*b*]pyrans

The synthesis of 9-pyridyl-3*H*-naphtho[2,1-*b*]pyrans was accomplished according to **Strategy A**. The commercially available 7-bromo-2-naphthol **2.38** could have been used as the starting material, however 2,7-dihydroxynaphthalene **2.37** was substantially cheaper and therefore was chosen as starting material. As a result, two routes to **2.41** were undertaken:

1. Route A – Involves the transformation of 2,7-dihydroxynaphthalene **2.37** into 7-bromo-2-naphthol **2.38**, followed by the acid-catalysed condensation of the latter with the appropriate propynol **2.33**, leading to 9-bromo-3*H*-naphtho[2,1-*b*]pyran **2.39** (**Scheme 2.13**). It also includes the Suzuki cross-coupling reaction between **2.39** and the appropriate pyridyl boronic acid pinacol ester **2.40** affording the 9-pyridyl-3*H*-naphtho[2,1-*b*]pyran **2.41**.

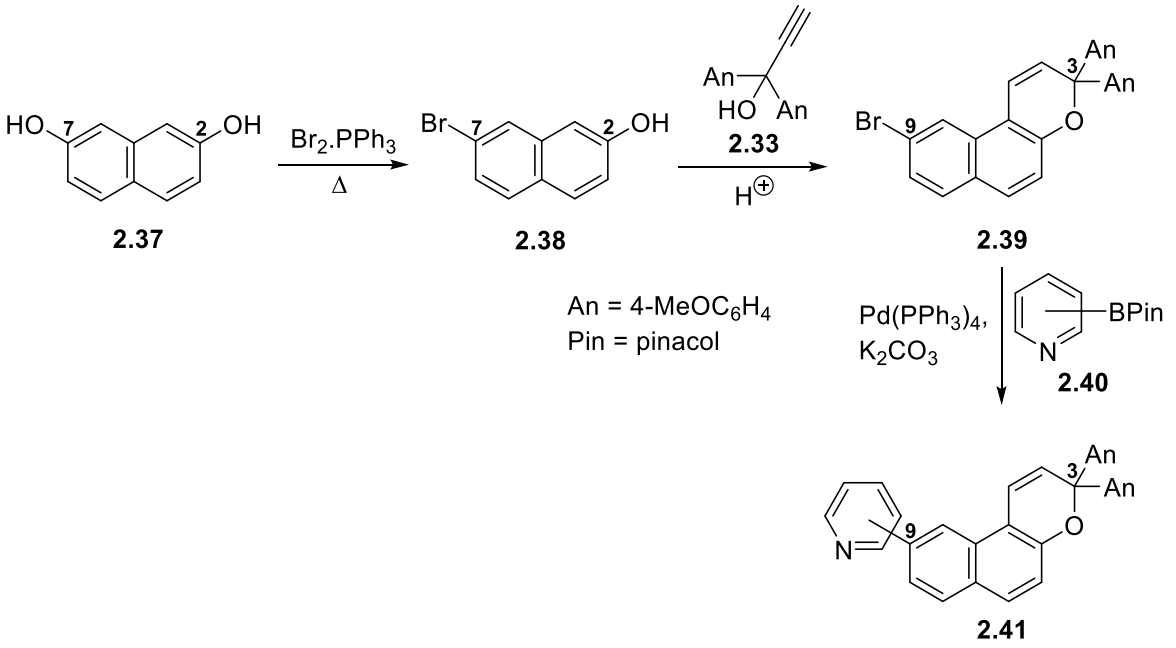

Scheme 2.13 Route A to 9-pyridyl-3*H*-naphtho[2,1-*b*]pyran **2.41**.

2. Route B – Includes the direct acid-catalysed condensation of 2,7-dihydroxynaphthalene **2.37** with the appropriate propynol **2.33**, and subsequent triflation, leading to 9-trifloxy-3*H*-naphtho[2,1-*b*]pyran **2.43** (**Scheme 2.14**). It also includes the Suzuki cross-coupling reaction between **2.43** and the appropriate pyridyl boronic acid pinacol ester **2.40** affording the 9-pyridyl-3*H*-naphtho[2,1-*b*]pyran **2.41**.

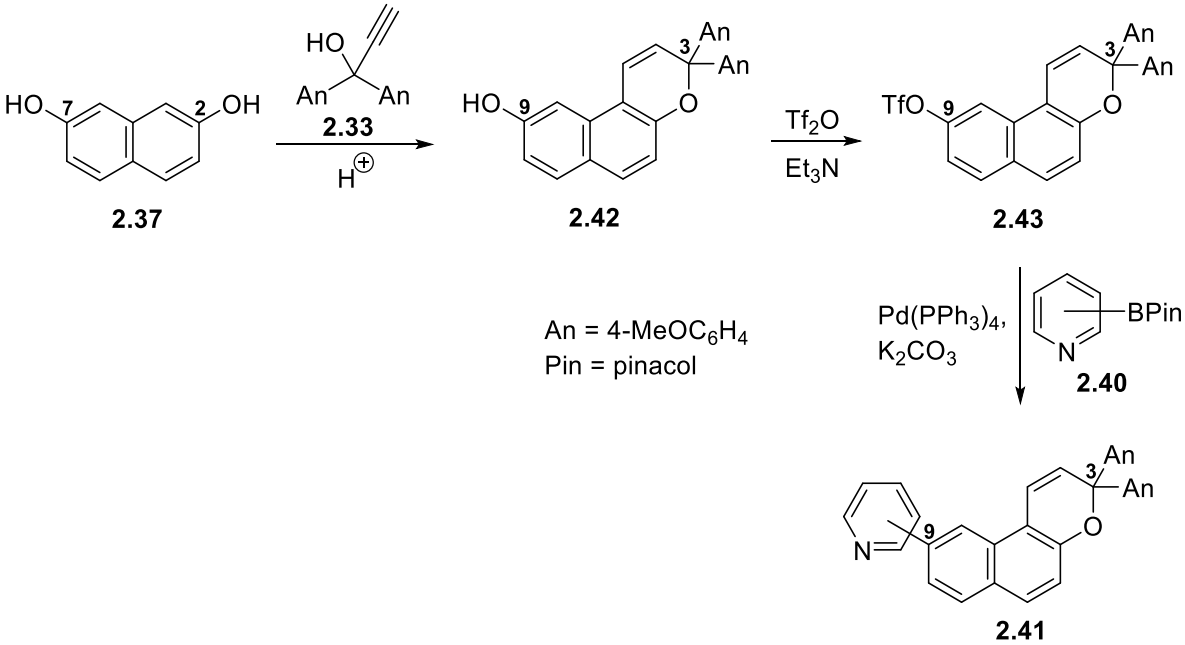

Scheme 2.14 Route B to 9-pyridyl-3*H*-naphtho[2,1-*b*]pyran **2.41**.

1. Route A

The transformation of 2,7-dihydroxynaphthalene **2.37** into 7-bromo-2-naphthol **2.38** was accomplished by reacting 2,7-dihydroxynaphthalene **2.37** with a triphenyldibromophosphorane intermediate formed *in situ* by mixing Br_2 and triphenylphosphine in acetonitrile, followed by heating.[184] In a first attempt to synthesize 7-bromo-2-naphthol **2.38** from 2,7-dihydroxynaphthalene **2.37**, following a literature procedure by Zou *et al.* (Method A),[185] the desired product **2.38** was isolated in very poor yield (0.4%) (**Scheme 2.15**). Many brominated products were formed during this attempt, including 3,7-dibromo-2-naphthol **2.44** (18%) and 3,6-dibromo-2,7-dihydroxynaphthalene **2.45** (0.6%). It is noteworthy that there are discrepancies in the literature melting points of 3,6-dibromo-2,7-dihydronaphthalene **2.45**, possibly due to polymorphic effects.

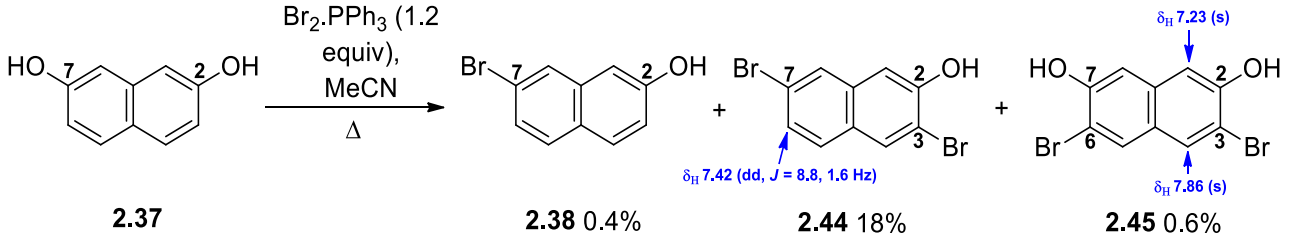

Scheme 2.15 Synthesis of 7-bromo-2-naphthol **2.38** (Method A).

In a second attempt to prepare 7-bromo-2-naphthol **2.38** from 2,7-dihydroxynaphthalene **2.37**, using a literature procedure by Bandin *et al*. (Method B),[186] the desired product **2.38** was isolated in much improved yield (48%) (**Scheme 2.16**).

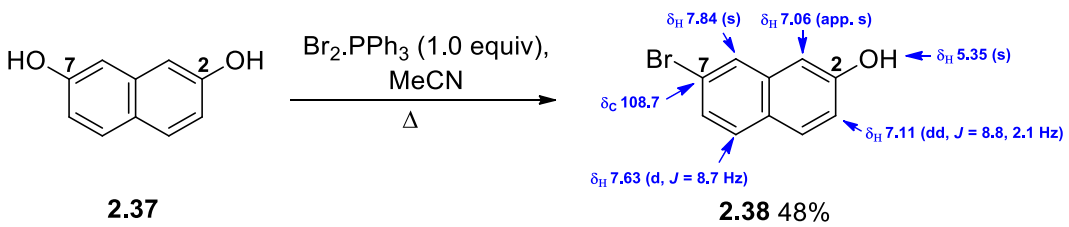

Scheme 2.16 Synthesis of 7-bromo-2-naphthol **2.38** (Method B).

Although there are just a few differences between the two methods, e.g. the volume of acetonitrile (Method A: 14.0 mL; Method B: 3.0 mL), the biggest difference was that, in Method B, the suspension of triphenylphosphine and Br_2 in acetonitrile was stirred much more vigorously when compared to Method A, which allowed the more efficient formation *in situ* of the

triphenyldibromophosphorane intermediate that could then react with the 2,7-dihydroxynaphthalene **2.37**. Besides the higher yield, further evidence of the enhanced formation of the triphenyldibromophosphorane intermediate, in Method B, was the virtual absence of polybrominated products.

In the reaction mechanism,[187] the nucleophilic attack of the hydroxyl group from naphthol **2.37** on the phosphorous atom of the $Br_2.PPh_3$ **2.46** resulted in the formation of the intermediate **2.47**. By thermal treatment, the latter cleaved forming 7-bromo-2-naphthol **2.38** and triphenylphosphine oxide (**Scheme 2.17**).

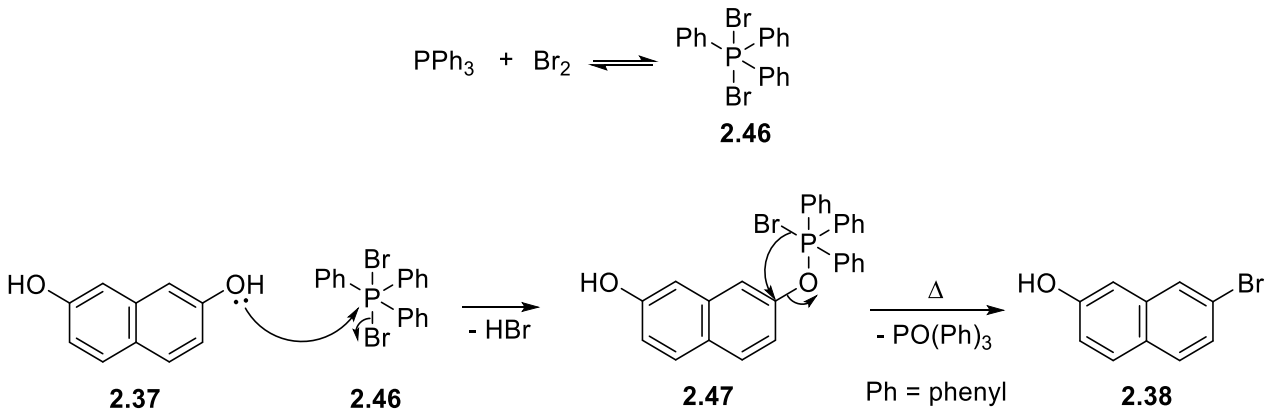

Scheme 2.17 Mechanism of the synthesis of 7-bromo-2-naphthol **2.38**.

The acid-catalysed condensation between 7-bromo-2-naphthol **2.38** and the appropriate propynol **2.33** afforded the 9-bromo-3*H*-naphtho[2,1-*b*]pyran **2.39** in very good yield (86%) (**Scheme 2.18**).

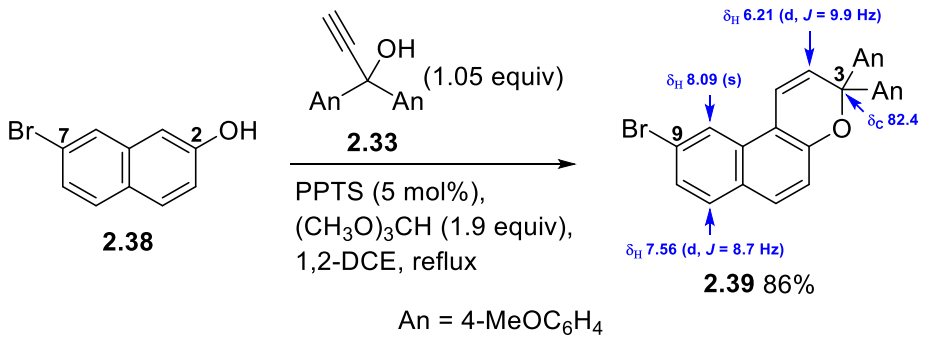

Scheme 2.18 Synthesis of 9-bromo-3*H*-naphtho[2,1-*b*]pyran **2.39**.

Suzuki cross-coupling reactions between either the 4- or 3-pyridineboronic acid pinacol esters with 9-bromo-3*H*-naphtho[2,1-*b*]pyran **2.39** afforded the corresponding 9-pyridyl substituted 3*H*-naphtho[2,1-*b*]pyrans in fair to good yields: 9-(4-pyridyl)-3*H*-naphtho[2,1-*b*]pyran **2.48** (57%) and 9-(3-pyridyl)-3*H*-naphtho[2,1-*b*]pyran **2.50** (70%) (**Scheme 2.19**). Besides the desired targets, minor amounts of naphthofurans **2.49** (4-pyridyl, 10%) and **2.51** (3-pyridyl, 11%) were isolated as by-products of the Suzuki cross-coupling reactions, being the result of the ring-contraction of the 9-pyridyl-3*H*-naphtho[2,1-*b*]pyrans. The slightly fluorescent non-photochromic naphthofurans are structural isomers of the corresponding 9-pyridyl-3*H*-naphtho[2,1-*b*]pyrans, and their formation, during the Suzuki cross-coupling reactions, made it extremely complicated to purify each of the 9-pyridyl-3*H*-naphtho[2,1-*b*]pyrans and the corresponding naphthofurans by flash column chromatography as a consequence of their similar R_f values on a variety of TLC plates and in a variety of solvent systems.

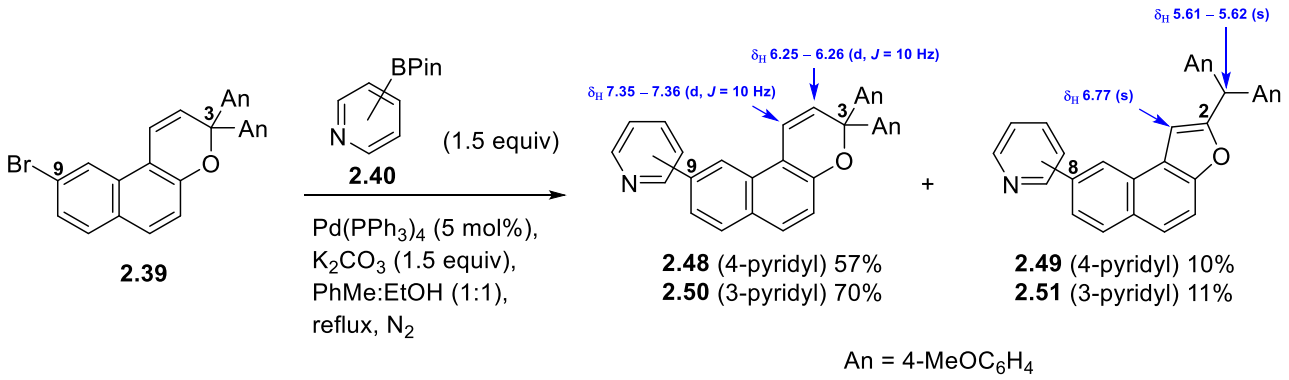

Scheme 2.19 Synthesis of 9-pyridyl-3*H*-naphtho[2,1-*b*]pyrans and corresponding naphthofurans from 9-bromo-3*H*-naphtho[2,1-*b*]pyran **2.39**.

Route B

The acid-catalysed condensation between 2,7-dihydroxynaphthalene **2.37** and the appropriate propynol **2.33** afforded the target 9-hydroxy-3*H*-naphtho[2,1-*b*]pyran **2.40** in poor yield (28%), similar to what had been described in the literature,[188] due to the low regioselectivity of the reaction (**Scheme 2.20**). Additionally, 3,3,10,10-tetrakis(4-methoxyphenyl)-3,10*H*-naphtho[2,1-*b*]pyran **2.52** was isolated as a by-product (17%) from this reaction.

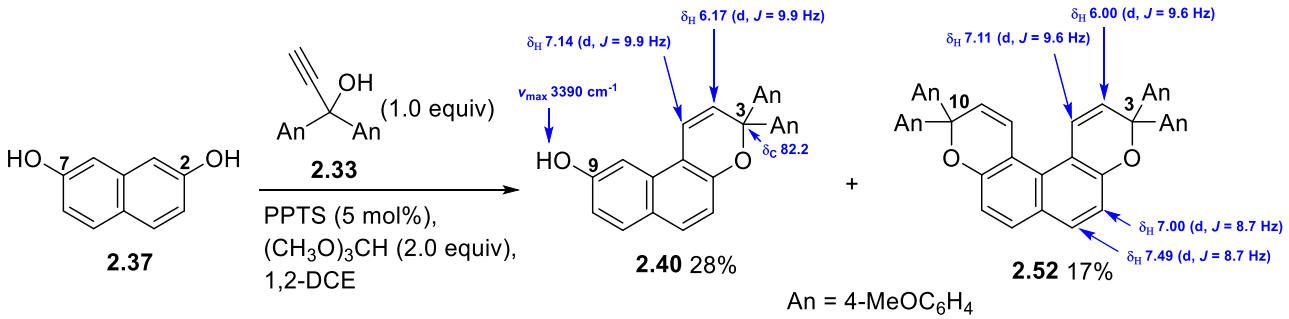

Scheme 2.20 Synthesis of 9-hydroxy-3*H*-naphtho[2,1-*b*]pyran **2.40**.

Aryl triflates can be prepared by base-catalysed reaction of phenols with triflic anhydride.[189] Treatment of 9-hydroxy-3*H*-naphtho[2,1-*b*]pyran **2.40** with triflic anhydride in the presence of triethylamine generated the 9-triflyloxy-3*H*-naphtho[2,1-*b*]pyran **2.43** in very good yield (87%) (**Scheme 2.21**).

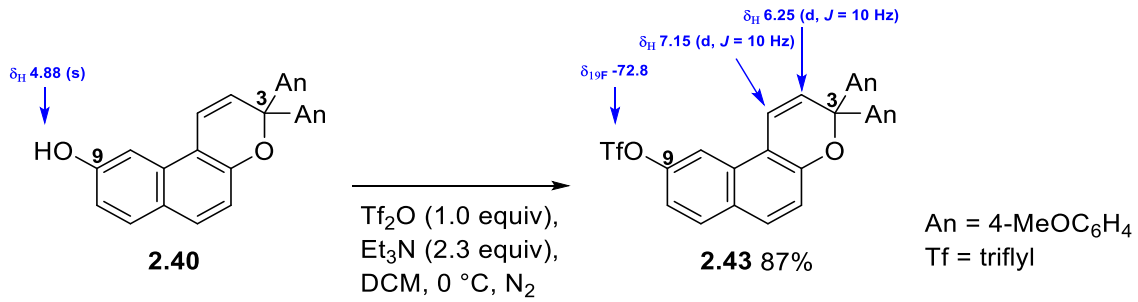

Scheme 2.21 Synthesis of 9-triflyloxy-3*H*-naphtho[2,1-*b*]pyran **2.43**.

In the reaction mechanism, the nucleophilic attack of **2.53**, formed by base-promoted deprotonation of 9-hydroxy-3*H*-naphtho[2,1-*b*]pyran **2.40** upon the triflic anhydride led to intermediate **2.54** (**Scheme 2.22**). Elimination of the triflate ion resulted in the formation of the corresponding aryl triflate **2.43**.

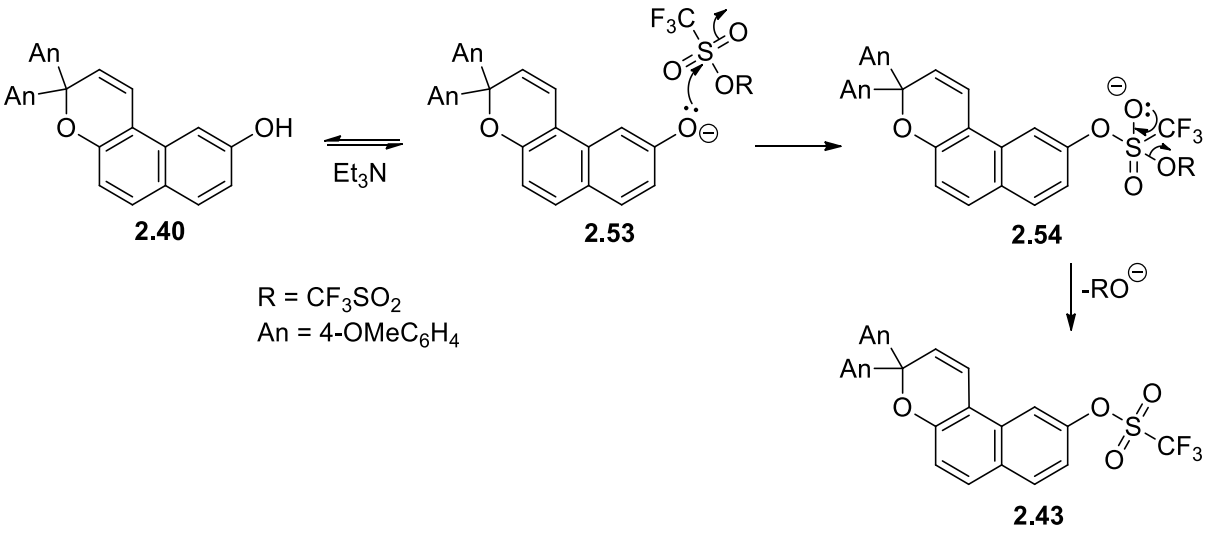

Scheme 2.22 Mechanism of the synthesis of 9-triflyloxy-3*H*-naphtho[2,1-*b*]pyran **2.43**.

Suzuki cross-coupling reactions between either the 4- or 3-pyridineboronic acid pinacol esters with 9-triflyloxy-3*H*-naphtho[2,1-*b*]pyran **2.43** afforded the corresponding 9-pyridyl substituted 3*H*-naphtho[2,1-*b*]pyrans in poor to fair yields: 9-(4-pyridyl)-3*H*-naphtho[2,1-*b*]pyran **2.48** (21%) and 9-(3-pyridyl)-3*H*-naphtho[2,1-*b*]pyran **2.50** (56%) (**Scheme 2.23**). Besides the desired targets, the naphthofurans **2.49** (4-pyridyl, 31%) and **2.51** (3-pyridyl, 9%) were again isolated from the Suzuki cross-coupling reactions, being the result of the ring-contraction of the 9-pyridyl-3*H*-naphtho[2,1-*b*]pyrans.

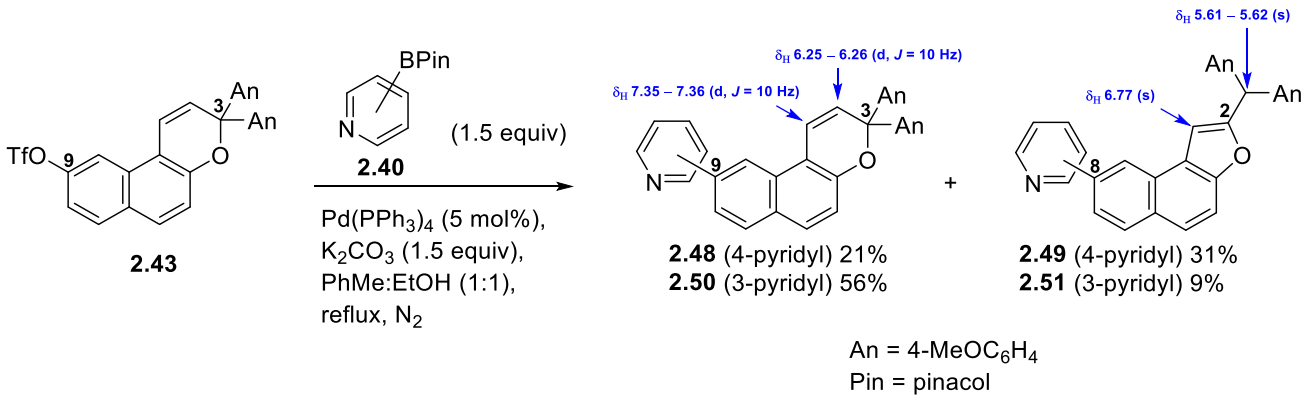

Scheme 2.23 Synthesis of 9-pyridyl-3*H*-naphtho[2,1-*b*]pyrans and corresponding naphthofurans from 9-triflyloxy-3*H*-naphtho[2,1-*b*]pyran **2.43**.

Route A (via Method A) afforded the 9-(4-pyridyl)-3*H*-naphtho[2,1-*b*]pyran **2.48** and the 9-(3-pyridyl)-3*H*-naphtho[2,1-*b*]pyran **2.50** in a three step linear route with an overall yield of 24% and

29%, respectively. On the other hand, Route B afforded the 9-(4-pyridyl)-3*H*-naphtho[2,1-*b*]pyran **2.48** and the 9-(3-pyridyl)-3*H*-naphtho[2,1-*b*]pyran **2.50** in a three step linear route with an overall yield of 5% and 14%, respectively. As a result, Route A provided the desired targets with a higher overall yield in the same number of steps when compared to Route B. Furthermore, 9-triflyloxy-3*H*-naphtho[2,1-*b*]pyran **2.43** has proven to be a less effective coupling partner than 9-bromo-3*H*-naphtho[2,1-*b*]pyran **2.39**, since the yield of the Suzuki cross-coupling reaction of the former (21–56%) was lower compared to the latter (57–70%).

2.1.1.3 Synthesis of 8-Pyridyl-3*H*-Naphtho[2,1-*b*]pyrans

The synthesis of 8-pyridyl-3*H*-naphtho[2,1-*b*]pyrans was accomplished according to **Strategy A**. The inexpensive commercially available 6-bromo-2-naphthol **2.55** was the ideal starting material for this route.

The acid-catalysed condensation between 6-bromo-2-naphthol **2.55** and propynol **2.33** afforded the 8-bromo-3*H*-naphtho[2,1-*b*]pyran **2.56** in excellent yield (97%) (**Scheme 2.24**). It is noteworthy that triethyl orthoformate was used as dehydrating agent in this reaction, instead of trimethyl orthoformate. It is possible that triethyl orthoformate is more effective that trimethyl orthoformate, as the yield for this reaction (96%) was considerably higher than any other acid-catalysed condensations in which trimethyl orthoformate was used.

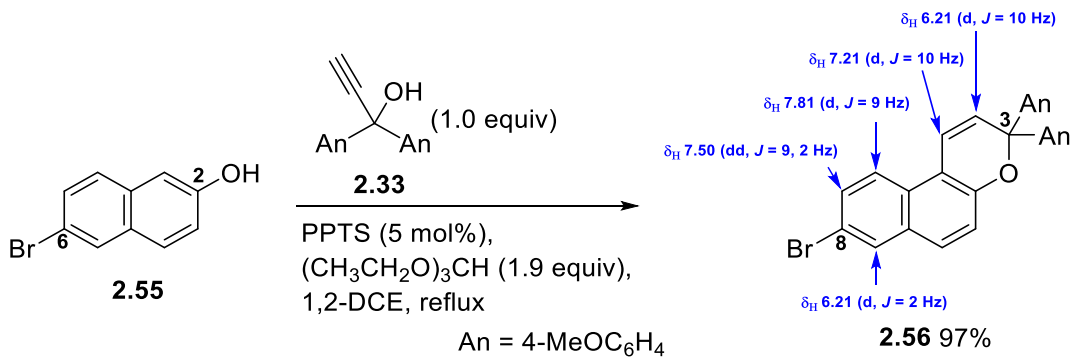

Scheme 2.24 Synthesis of 8-bromo-3*H*-naphtho[2,1-*b*]pyran **2.56**.

Suzuki cross-coupling reactions between either the 4- or 3-pyridineboronic acid pinacol esters with 8-bromo-3*H*-naphtho[2,1-*b*]pyran **2.56** led to the corresponding 8-pyridyl substituted 3*H*-naphtho[2,1-*b*]pyrans in fair to good yields: 8-(4-pyridyl)-3*H*-naphtho[2,1-*b*]pyran **2.57** (63%) and 8-(3-pyridyl)-3*H*-naphtho[2,1-*b*]pyran **2.59** (70%) (**Scheme 2.25**). Besides the desired targets, the naphthofurans **2.58** (4-pyridyl, 3%) and **2.60** (3-pyridyl, 6%) were again isolated, after extensive

flash column chromatography purifications, being the result of the ring-contraction of the 8-pyridyl-3*H*-naphtho[2,1-*b*]pyrans.

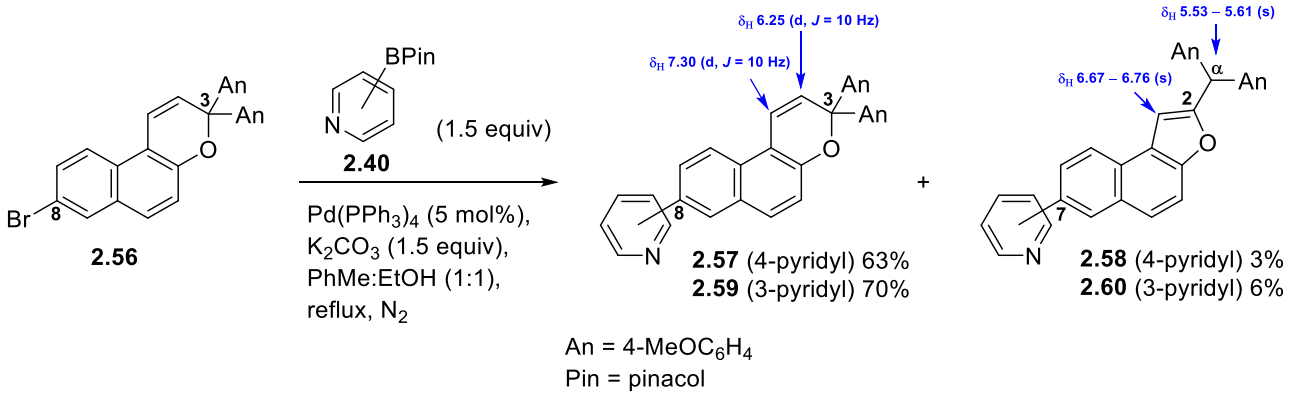

Scheme 2.25 Synthesis of 8-pyridyl-3*H*-naphtho[2,1-*b*]pyrans and corresponding naphthofurans from 8-bromo-3*H*-naphtho[2,1-*b*]pyran **2.56**.

In conclusion, 8-(4-pyridyl)-3*H*-naphtho[2,1-*b*]pyran **2.57** and 8-(3-pyridyl)-3*H*-naphtho[2,1-*b*]pyran **2.59** were prepared in a two steps linear route from 6-bromo-2-naphthol **2.55** in 61% and 68% yield, respectively.

The frailty of pyridine-2-boronic acids under Suzuki cross-coupling conditions is known.[190] Given the foregoing fact, it was envisioned that 8-(2-pyridyl)-3*H*-naphtho[2,1-*b*]pyran **2.65** could be prepared by the Suzuki cross-coupling reaction between the inverted coupling partners 8-boronyl-3*H*-naphtho[2,1-*b*]pyran **2.62** – prepared from the borylation of 8-bromo-3*H*-naphtho[2,1-*b*]pyran **2.56** – and the stable 2-bromopyridine **2.64**. The borylation of 8-bromo-3*H*-naphtho[2,1-*b*]pyran **2.56** was accomplished by two different methods:

1. Method A – By a two-step metalation.
2. Method B – By a Pd-mediated borylation.

Method A – By a two-step metalation

The boronic acid **2.61** was first prepared from 8-bromo-3*H*-naphtho[2,1-*b*]pyran **2.56** by a two-step metalation protocol, and then esterified with pinacol affording the 8-boronyl-3*H*-naphtho[2,1-*b*]pyran **2.62** in 49% yield (from **2.56**) (**Scheme 2.26**).

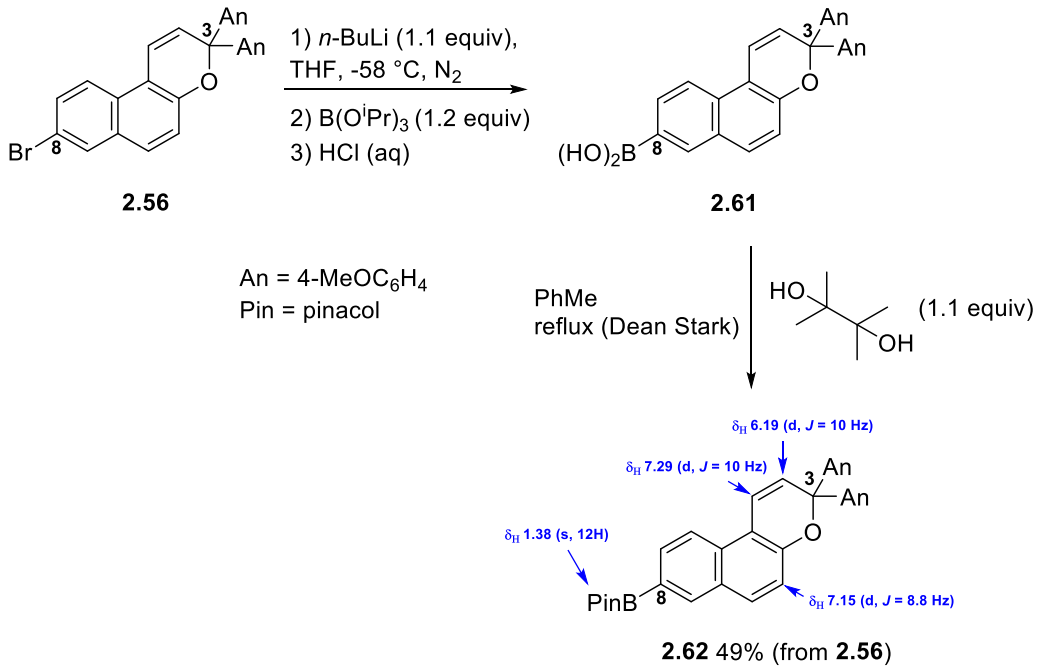

Scheme 2.26 Synthesis of 8-boronyl-3*H*-naphtho[2,1-*b*]pyran **2.62** via a two-step metalation protocol (Method A).

Method B – By a Pd-mediated borylation

The Suzuki-type cross-coupling between halopyridines and tetralkoxydiboron (e.g. B_2Pin_2) or dialkoxydiboron[191] (e.g. HBPin) is a widely applied approach for the preparation of the majority of pyridyl boronic esters, having a broad substrate scope and good tolerance for most functional groups. The most commonly used tetraalkoxydiboron is bis(pinacolato)diboron (B_2Pin_2).[192] In an attempt to synthesize 8-boronyl-3*H*-naphtho[2,1-*b*]pyran **2.62** by a coupling reaction between the 8-bromo-3*H*-naphtho[2,1-*b*]pyran **2.56** and bis(pinacolato)diboron (B_2Pin_2) using bis(triphenylphosphine)palladium dichloride ($Pd(PPh_3)_2Cl_2$) in DMF,[193] the desired product **2.62** was isolated in very poor yield (2%) (**Scheme 2.27**). Additionally, the corresponding naphthofuran **2.63** was also isolated in very poor yield (3%). It is noteworthy that the TLC of the crude contained multiple spots but barely no starting material. This could be an indication of decomposition under the reaction conditions.

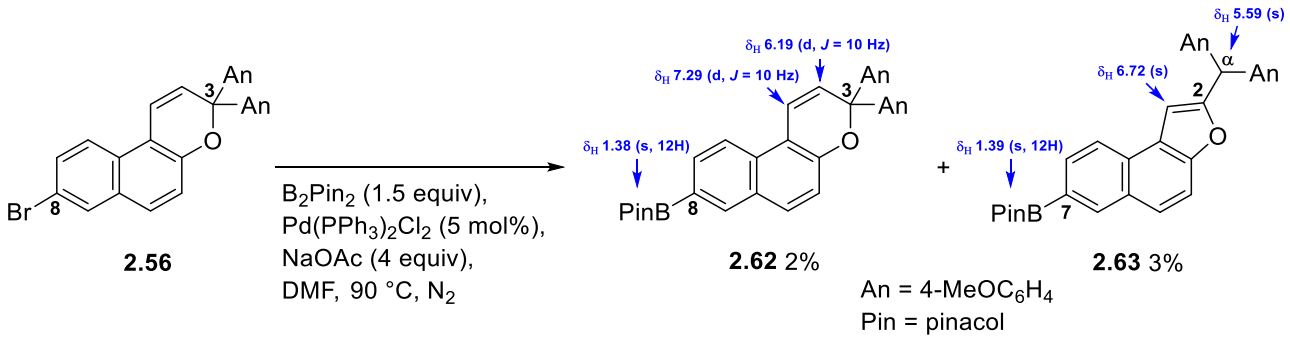

Scheme 2.27 Synthesis of 8-boronyl-3*H*-naphtho[2,1-*b*]pyran **2.62** by a Pd-mediated borylation (Method B).

As a test reaction, the 8-boronyl-3*H*-naphtho[2,1-*b*]pyran **2.62** was successfully coupled to 4-bromopyridine hydrochloride **2.63**, under Suzuki-Miyaura conditions, affording the 8-(4-pyridyl)-3*H*-naphtho[2,1-*b*]pyran **2.57** in 67% yield (**Scheme 2.28**). A small remark about this test reaction was the use of an extra amount of K_2CO_3 (2.3 equiv instead of just 1.5 equiv), in order to release *in situ* the 4-bromopyridine from the hydrochloride salt. The corresponding naphthofuran **2.58** was formed during the reaction but it was not quantitatively isolated in this instance. Moreover, the yield of the synthesis of the 8-(4-pyridyl)-3*H*-naphtho[2,1-*b*]pyran **2.57** (67%) from 8-boronyl-3*H*-naphtho[2,1-*b*]pyran **2.62** is similar to the yield of the reversed synthesis of 8-(4-pyridyl)-3*H*-naphtho[2,1-*b*]pyran **2.57** (63%) from 8-bromo-3*H*-naphtho[2,1-*b*]pyran **2.56**.

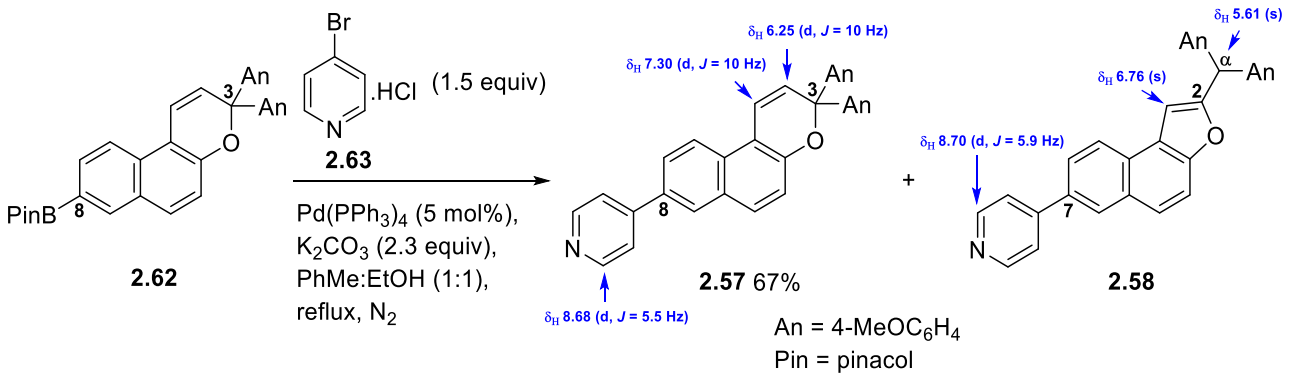

Scheme 2.28 Synthesis of 8-(4-pyridyl)-3*H*-naphtho[2,1-*b*]pyran **2.57** and the corresponding naphthofuran **2.58** from 8-boronyl-3*H*-naphtho[2,1-*b*]pyran **2.62**.

In a similar fashion, the 8-(2-pyridyl)-3*H*-naphtho[2,1-*b*]pyran **2.65** was accessed by the Suzuki cross-coupling reaction between 8-boronyl-3*H*-naphtho[2,1-*b*]pyran **2.62** and 2-bromopyridine **2.64**

in very good yield (84%) (**Scheme 2.29**). Once again, the corresponding naphthofuran **2.66** was isolated as a by-product (4%).

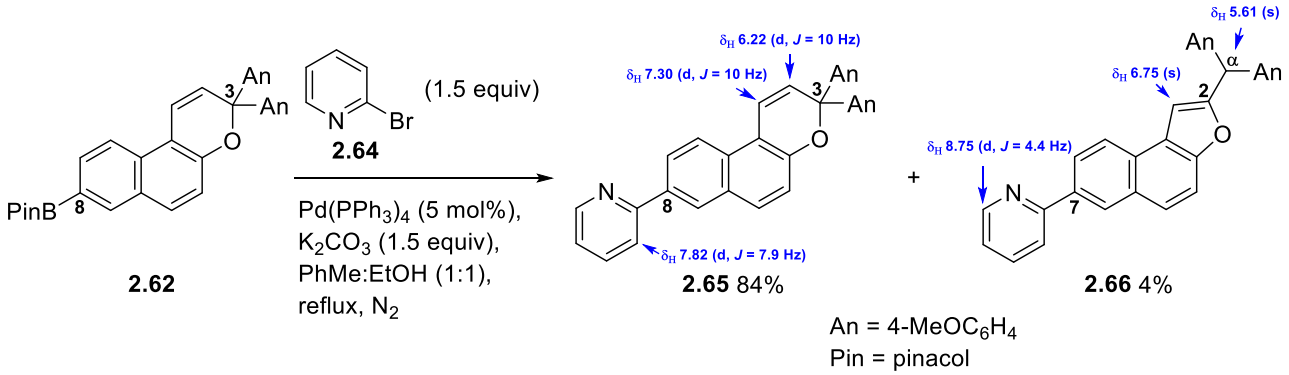

Scheme 2.29 Synthesis of 8-(2-pyridyl)-3*H*-naphtho[2,1-*b*]pyran **2.65** and the corresponding naphthofuran **2.66** from 8-boronyl-3*H*-naphtho[2,1-*b*]pyran **2.62**.

In conclusion, 8-(2-pyridyl)-3*H*-naphtho[2,1-*b*]pyran **2.65** was prepared from 6-bromo-2-naphthol **2.55**:

1. Via Method A in a four steps linear route in 40% overall yield;
2. Via Method B in a three steps linear route in 1.6% overall yield.

On the other hand, 8-(4-pyridyl)-3*H*-naphtho[2,1-*b*]pyran **2.57** was prepared from 6-bromo-2-naphthol **2.55**:

1. Via Method A in a four steps linear route in 32% overall yield;
2. Via Method B in a three steps linear route in 1.3% overall yield.

In order to understand the effect of the electronic nature of substituents at C-8 on the spectrokinetic properties of the 3*H*-naphtho[2,1-*b*]pyrans, different 8-aryl-3*H*-naphtho[2,1-*b*]pyrans **2.70**, **2.72**, **2.74** were succefully prepared by the Suzuki cross-coupling reaction between 8-bromo-3*H*-naphtho[2,1-*b*]pyran **2.56** and the corresponding aryl boronic acids **2.67** – **2.69** (**Scheme 2.30** and **Table 2.1**). Again, the corresponding naphthofurans **2.71**, **2.73** and **2.75** were formed but not isolated in this instance.

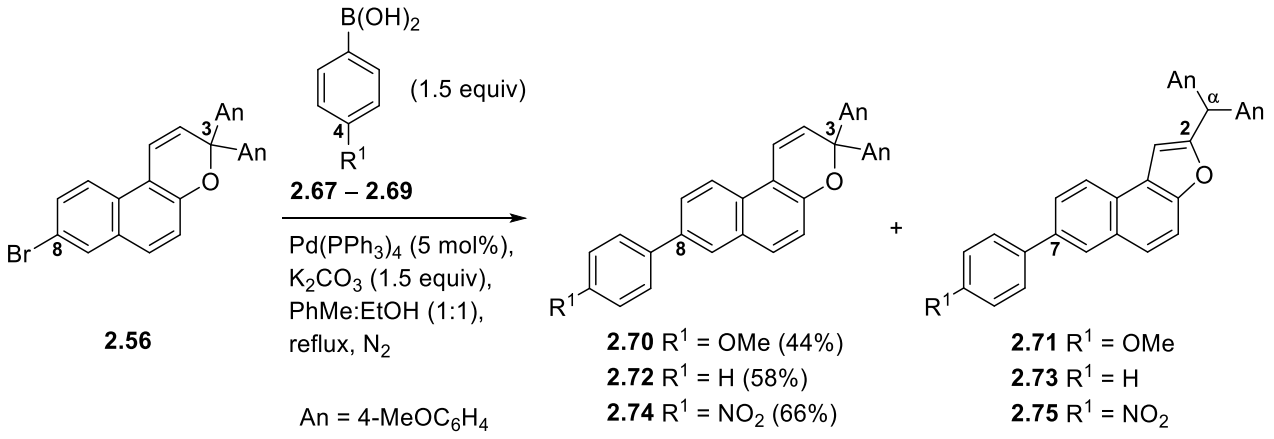

Scheme 2.30 Synthesis of 8-aryl-3*H*-naphtho[2,1-*b*]pyrans **2.70**, **2.72**, **2.74** and the corresponding naphthofurans **2.71**, **2.73**, **2.75** from 8-bromo-3*H*-naphtho[2,1-*b*]pyran **2.56**.

Table 2.1 Synthesis of 8-aryl-3*H*-naphtho[2,1-*b*]pyran**s 2.70**, **2.72**, **2.74** and the corresponding naphthofurans **2.71**, **2.73**, **2.75** from 8-bromo-3*H*-naphtho[2,1-*b*]pyran **2.56**.

Entry	Naphthopyran	Boronic acid	Product (%)	By-product (%)
1	**2.56**	**2.67** R^1 = OMe	**2.70** R^1 = OMe (44%)	**2.71** (not isolated)
2	**2.56**	**2.68** R^1 = H	**2.72** R^1 = H (58%)	**2.73** (not isolated)
3	**2.56**	**2.69** R^1 = NO_2	**2.74** R^1 = NO_2 (66%)	**2.75** (not isolated)

It was rationalized that the quench of the luminescence from the photochromic rhenium(I) complexes would depend on the amount of photomerocyanine at the photostationary state (PSS). Therefore, it was predicted that better photochromic colourability, which is a consequence of having more photomerocyanine at the steady state, would lead to a better quench of the luminescence from the photochromic rhenium(I) complexes. A design explored in this project involved preparing 3*H*-naphtho[2,1-*b*]pyrans **2.76** (**Figure 2.2**) that contained an extra methoxyl group at C-2 of one of the anisyl substituents, which has been reported to increase the colourability of 3*H*-naphtho[2,1-*b*]pyrans by sterically hindering the ring-closure of the photomerocyanine.[122]

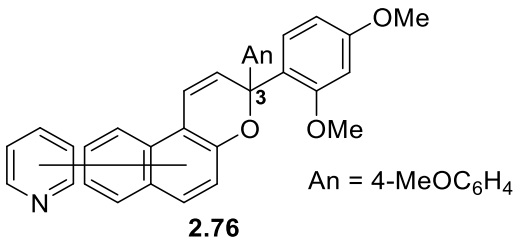

Figure 2.2 3-(2,4-Dimethoxyphenyl)-3-(4-methoxyphenyl)-pyridyl-3*H*-naphtho[2,1-*b*]pyran **2.76**.

It was envisioned that 8-(4-pyridyl)-3*H*-naphtho[2,1-*b*]pyran **2.77**, that contains an extra methoxyl at C-2 of one of the anisyl substituents, could be prepared by the Suzuki cross-coupling reaction between the corresponding 8-bromo-3*H*-naphtho[2,1-*b*]pyran **2.78** and 4-pyridineboronic acid pinacol ester **2.35** (**Scheme 2.31**). Additionally, 8-bromo-3*H*-naphtho[2,1-*b*]pyran **2.78** could be prepared by the acid-catalysed condensation between propynol **2.79** and 6-bromo-2-naphthol **2.55**. Furthermore, propynol **2.79**, which in contrast to propynol **2.33** was not readily to hand, could be prepared by the nucleophilic addition of a lithium acetylide to benzophenone **2.80**. The latter could be prepared by the acid-catalysed S_EAr between 1,3-dimethoxybenzene **2.81** and *p*-anisic acid **2.82**.

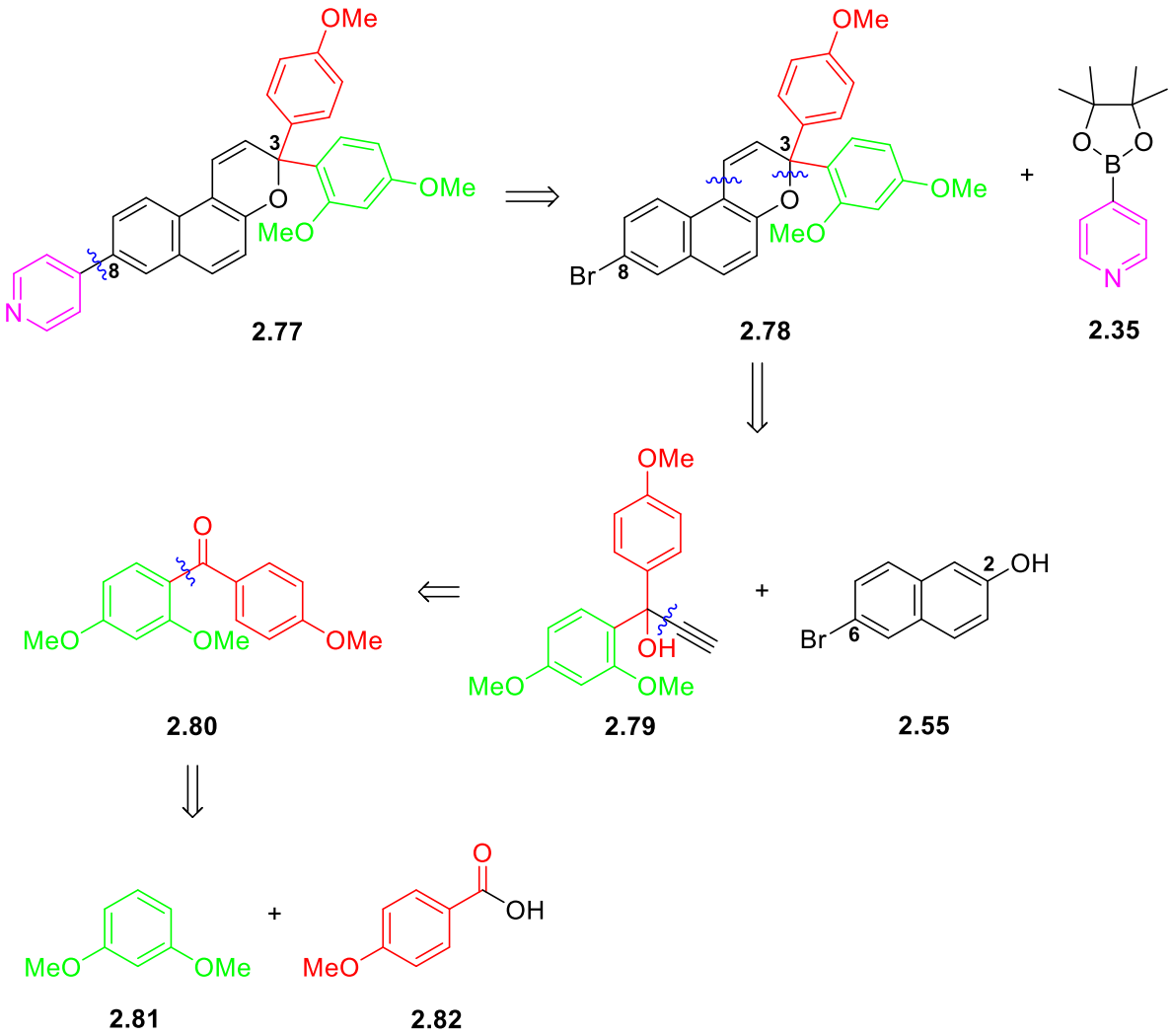

Scheme 2.31 Retrosynthetic route to 8-(4-pyridyl)-3*H*-naphtho[2,1-*b*]pyran **2.77**.

Acid-catalysed S_EAr between 1,3-dimethoxybenzene **2.81** and *p*-anisic acid **2.82** afforded benzophenone **2.80** in 57% yield (**Schemes 2.32** and **2.33**).

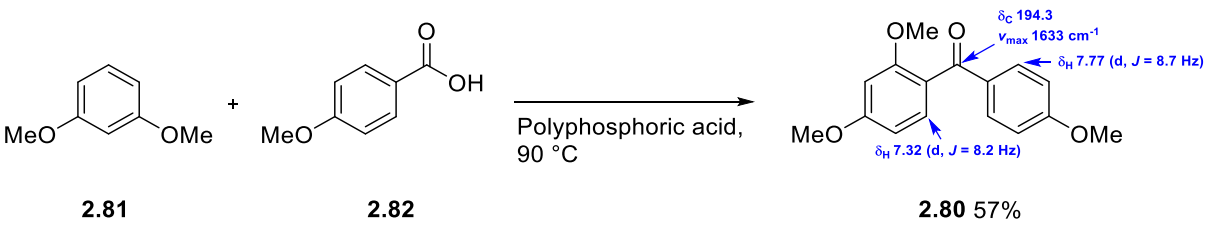

Scheme 2.32 Synthesis of benzophenone **2.80**.

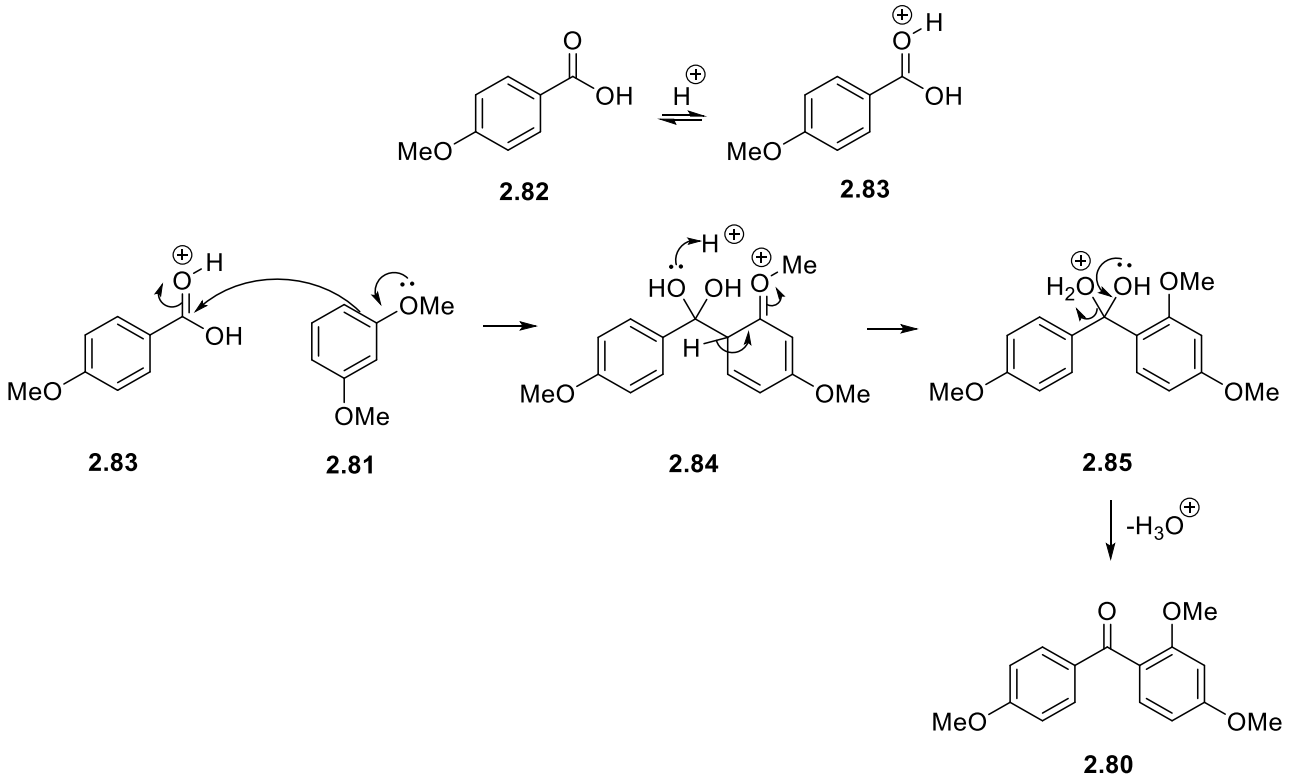

Scheme 2.33 Mechanism of the synthesis of benzophenone **2.80**.

The nucleophilic addition of lithium trimethylsilyl acetylide **2.87**, formed *in situ* by the addition of *n*-BuLi to trimethylsilyl acetylene in THF at -5 °C, to **2.80**, followed by treatment with a methanolic solution of KOH, afforded propynol **2.79** in quantitative yield (**Schemes 2.34** and **2.35**).

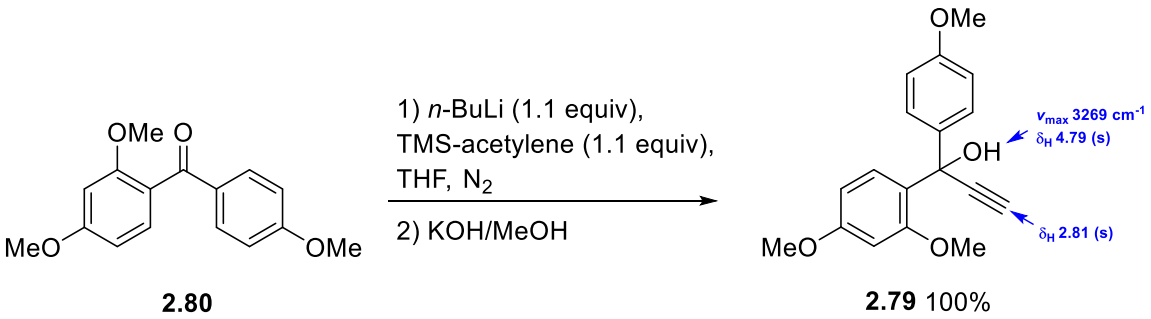

Scheme 2.34 Synthesis of propynol **2.79**.

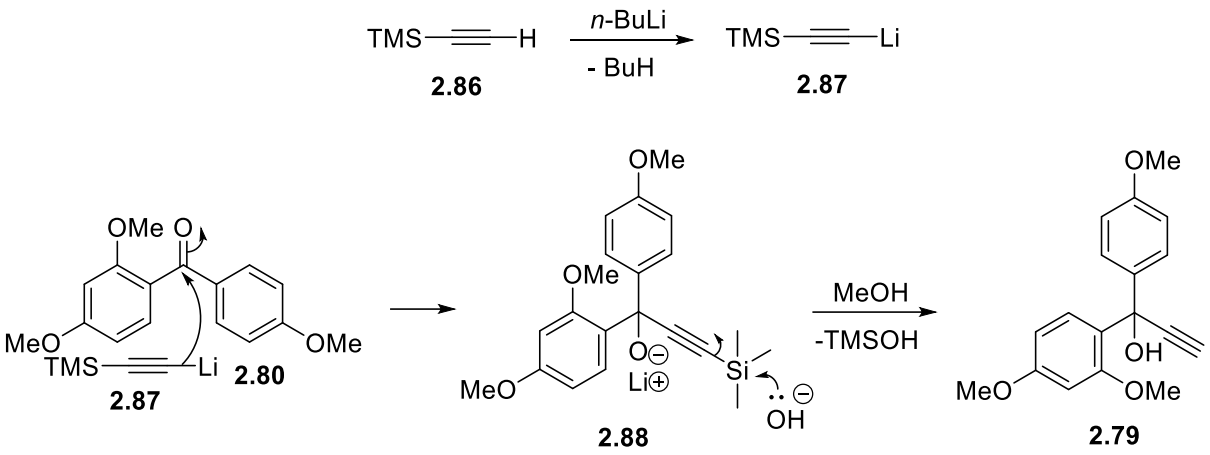

Scheme 2.35 Mechanism of the synthesis of propynol **2.79**.

Subsequently, the acid-catalysed condensation reaction between propynol **2.79** and 6-bromo-2-naphthol **2.55** afforded the coupling partner 8-bromo-3*H*-naphtho[2,1-*b*]pyran **2.78** in very good yield (88%) (**Scheme 2.36**).

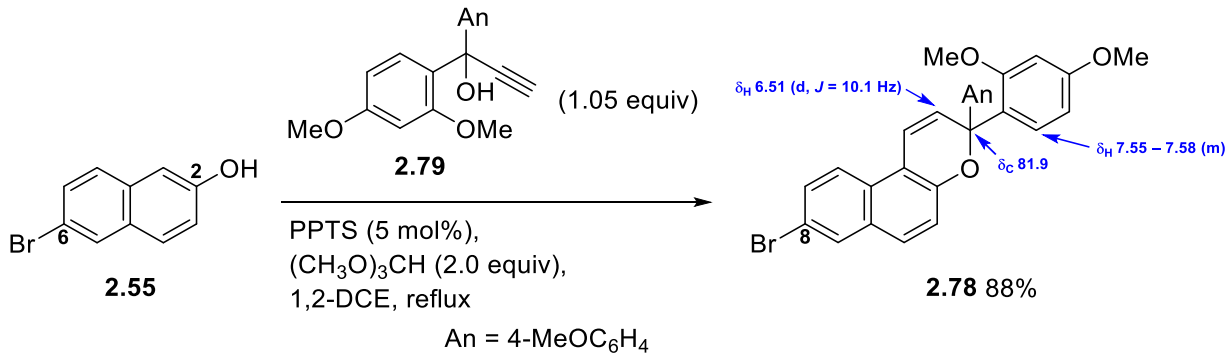

Scheme 2.36 Synthesis of 8-bromo-3*H*-naphtho[2,1-*b*]pyran **2.78**.

Suzuki cross-coupling reaction between 8-bromo-3*H*-naphtho[2,1-*b*]pyran **2.78** and 4-pyridineboronic acid pinacol ester **2.35** led to 8-(4-pyridyl)-3*H*-naphtho[2,1-*b*]pyran **2.77** in fair yield (60%) (**Scheme 2.37**). Once again the corresponding naphthofuran **2.89**, formed by ring-contraction of **2.77**, was isolated as a by-product in 11% yield.

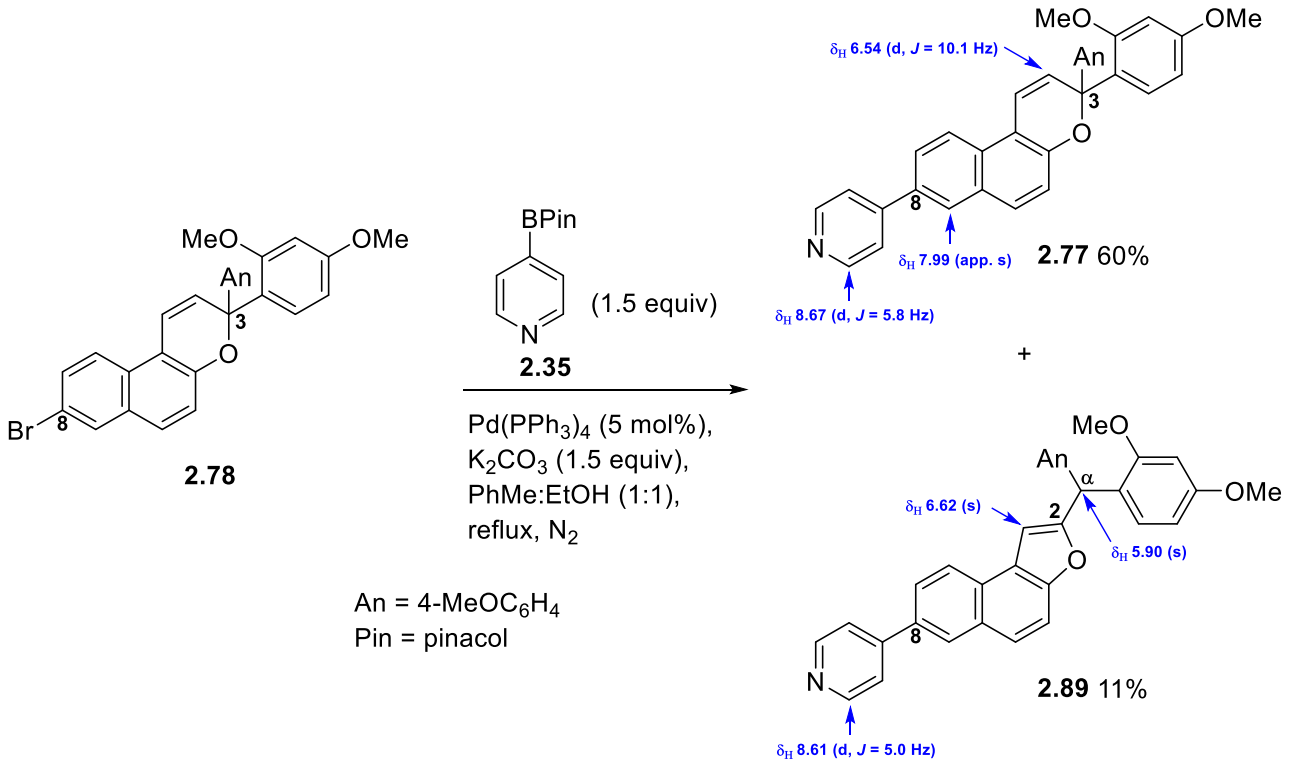

Scheme 2.37 Synthesis of 8-(4-pyridyl)-3*H*-naphtho[2,1-*b*]pyran **2.77** and the corresponding naphthofuran **2.89**.

In conclusion, 8-(4-pyridyl)-3*H*-naphtho[2,1-*b*]pyran **2.77** was prepared from 1,3-dimethoxybenzene **2.81** and *p*-anisic acid **2.82** in a four step convergent route in 30% overall yield. From another perspective, 8-(4-pyridyl)-3*H*-naphtho[2,1-*b*]pyran **2.77** was prepared from 6-bromo-2-naphthol **2.55** in a two step linear route in 53% yield.

In summary, the formation of the target naphthopyrans and naphthofurans by-products was established by ^{1}H NMR spectroscopy. The ^{1}H NMR spectra of all the target naphthopyrans were characterized by: 1) a singlet appearing at 3.77 – 3.78 ppm corresponding to the resonance of 4′- and 4″-OCH_3; 2) a doublet at 6.22 – 6.26 ppm with a coupling constant of ~10 Hz corresponding to the resonance of H-2; 3) an apparent doublet appearing at 6.84 – 6.85 ppm with a coupling constant of ~8.8 Hz corresponding to the resonance of H-3′, 5′ and H-3″, 5″ and 4) doublet appearing at 7.29 – 7.36 ppm with a coupling constant of ~10 Hz corresponding to the resonance of H-1 indicative of a *cis* configuration (**Figure 2.3**). The ^{13}C NMR spectra of all target naphthopyrans is characterized by one or more peaks at *ca.* 55.4 ppm corresponding to the resonance of the methoxyl carbons and a peak at *ca.* 82.5 ppm corresponding to the resonance of C-3. On the other hand, the ^{1}H NMR spectra of all the target naphthofurans were characterized by: 1) a singlet appearing at 3.73 – 3.82

ppm corresponding to the resonance of 4′- and 4″-OCH_3; 2) a singlet at 5.53 – 5.62 ppm corresponding to the resonance of H-α; 3) a singlet appearing at 6.67 – 6.77 ppm corresponding to the resonance of H-1; 4) an apparent doublet at 6.81 – 6.90 ppm with a coupling constant of 8.7 Hz corresponding to the resonance of H-3′, 5′ and H-3″, 5″ and 5) an apparent doublet at 7.10 – 7.19 ppm with a coupling constant of 8.7 Hz corresponding to the resonance of H-2′, 6′ and H-2″, 6″ (**Figure 2.3**).

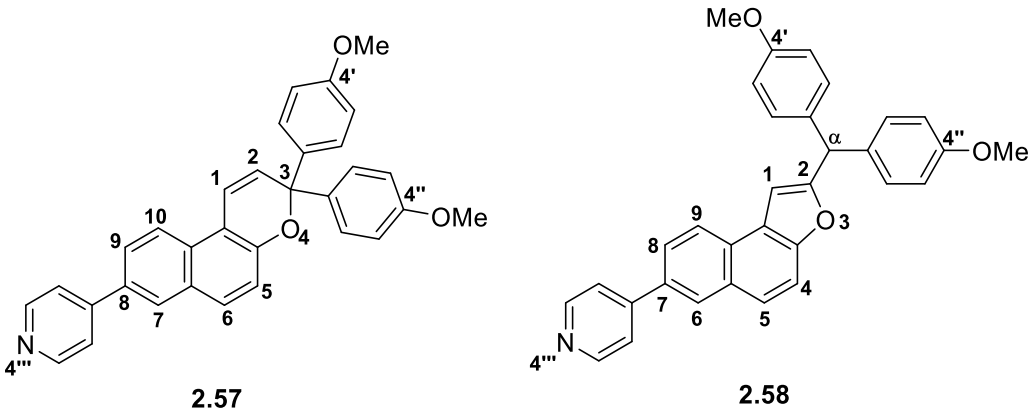

Figure 2.3 8-(4-Pyridyl)-3*H*-naphtho[2,1-*b*]pyran **2.57** and the corresponding naphthofuran **2.58**.

2.1.1.4 Synthesis of 7-Pyridyl-3*H*-Naphtho[2,1-*b*]pyrans

It was rationalized that 7-pyridyl-3*H*-naphtho[2,1-*b*]pyrans could be prepared according to **Strategy A**. However, it was required first to synthesize a 5-halo-2-naphthol, as neither 5-iodo-2-naphthol nor 5-bromo-2-naphthol were readily available.

5-Bromo-2-naphthol **2.93** was prepared in three steps from 5-amino-2-naphthol **2.90** in 25% overall yield following a literature procedure described by Everett *et al*. (**Scheme 2.38**).[194] First, the sulfonation of 5-amino-2-naphthol **2.90**, by treatment with H_2SO_4, generated 1-sulfonyl-5-amino-2-naphthol **2.91**. The sulfonyl group at C-1 was intended to favour the Sandmeyer reaction and to block this activated position from potential azo-coupling. The Sandmeyer reaction of aminonaphthol sulfonic acid **2.91** generated bromonaphthol **2.92**, which was immediately hydrolyzed to 5-bromo-2-naphthol **2.93** by treatment with an aqueous solution of H_2SO_4.

Thus, the formation of the target 5-bromo-2-naphthol **2.93** was determined by HRMS analysis, as the mass spectrum of **2.93** revealed an ion corresponding to the $[M+H]^+$ adduct with M = $C_{10}H_7{}^{79}BrO$. Furthermore, in the ^{13}C NMR spectrum of **2.93**, the peak at 110.9 ppm was assigned to the resonance of C-5 due to the moderate heavy atom effect.

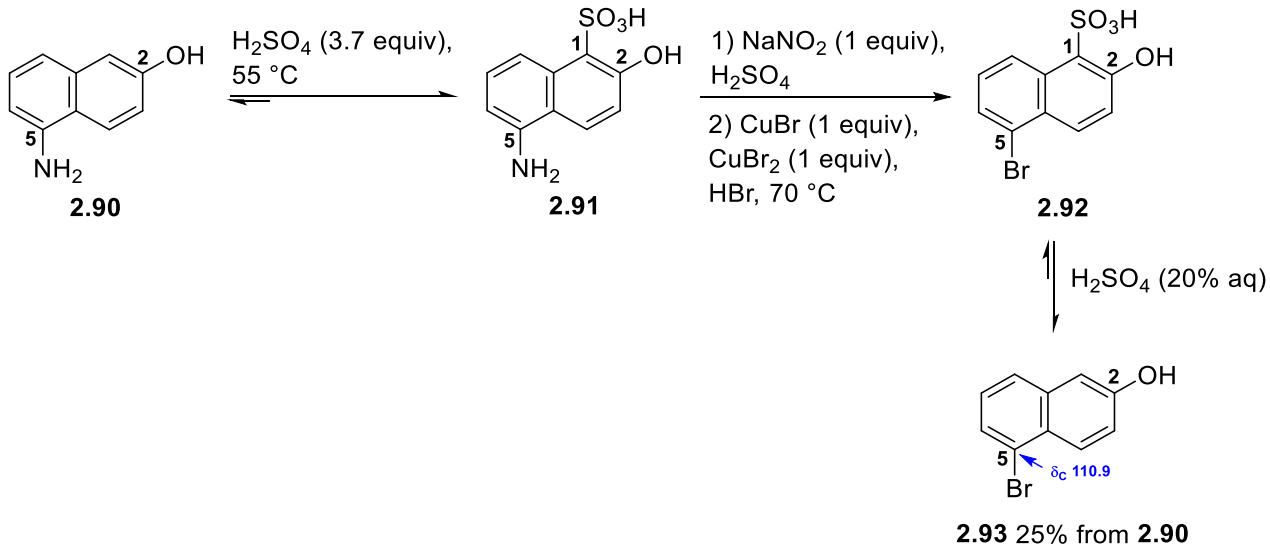

Scheme 2.38 Synthesis of 5-bromo-2-naphthol **2.93**.

The acid-catalysed condensation between 5-bromo-2-naphthol **2.93** and propynol **2.33** afforded the 7-bromo-3*H*-naphtho[2,1-*b*]pyran **2.94** in 62% yield (**Scheme 2.39**). Losses during the recrystallization step help to explain the moderate yield.

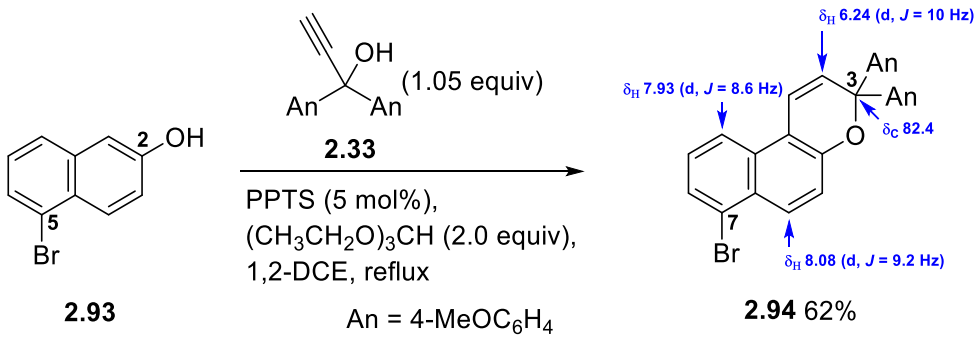

Scheme 2.39 Synthesis of 7-bromo-3*H*-naphtho[2,1-*b*]pyran **2.94**.

It was envisioned that a Suzuki cross-coupling reaction between 7-bromo-3*H*-naphtho[2,1-*b*]pyran **2.94** and 4-pyridineboronic acid pinacol ester **2.35** would lead to the corresponding 7-(4-pyridyl)-3*H*-naphtho[2,1-*b*]pyran **2.98**. Even though 4-pyridineboronic acid pinacol ester is commercially available, it is also relatively easy to prepare from 4-bromopyridine hydrochloride **2.63**. Therefore, 4-pyridineboronic acid **2.97** was first prepared in three consecutive steps from 4-bromopyridine hydrochloride **2.63** in 55% overall yield, following an *in situ* quenching approach described by Li and co-workers (**Scheme 2.40**).[195] This method takes advantage of the faster Li – Br exchange when compared to the *n*-BuLi and $B(O^iPr)_3$ reaction. It is noteworthy that, after releasing

the 4-bromopyridine **2.95** from the hydrochloride salt **2.63**, the Et_2O layer had to be evaporated at a low temperature, because there was a potential risk of polymerization decomposition.

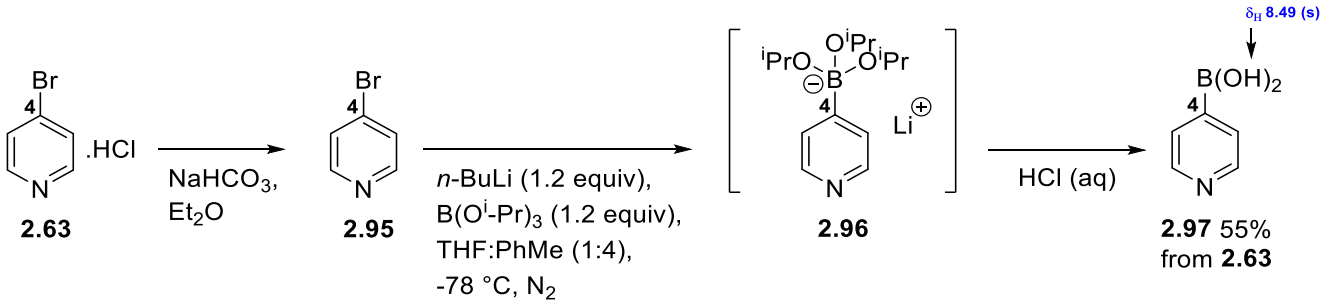

Scheme 2.40 Synthesis of 4-pyridineboronic acid **2.97**.

Subsequently, 4-pyridineboronic acid pinacol ester **2.35** was prepared by the esterification of 4-pyridineboronic acid **2.97** with pinacol in excellent yield (92%) (**Scheme 2.41**).

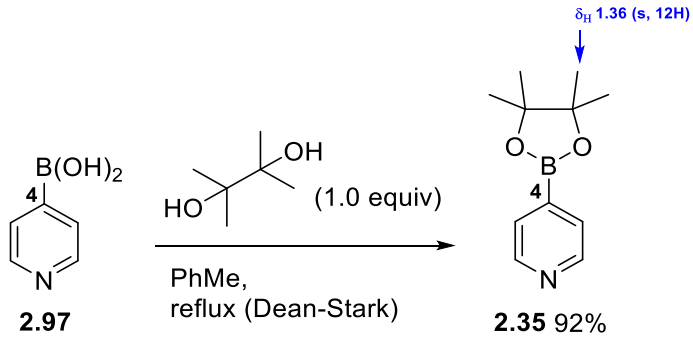

Scheme 2.41 Synthesis of 4-pyridineboronic acid pinacol ester **2.35**.

Suzuki cross-coupling reaction between 7-bromo-3*H*-naphtho[2,1-*b*]pyran **2.94** and 4-pyridineboronic acid pinacol ester **2.35** afforded 7-(4-pyridyl)-3*H*-naphtho[2,1-*b*]pyran **2.98** in fair yield (66%) (**Scheme 2.42**). Similar to previous Suzuki reactions, the corresponding naphthofuran **2.99** was formed as a by-product of the reaction, but it was not isolated in this instance.

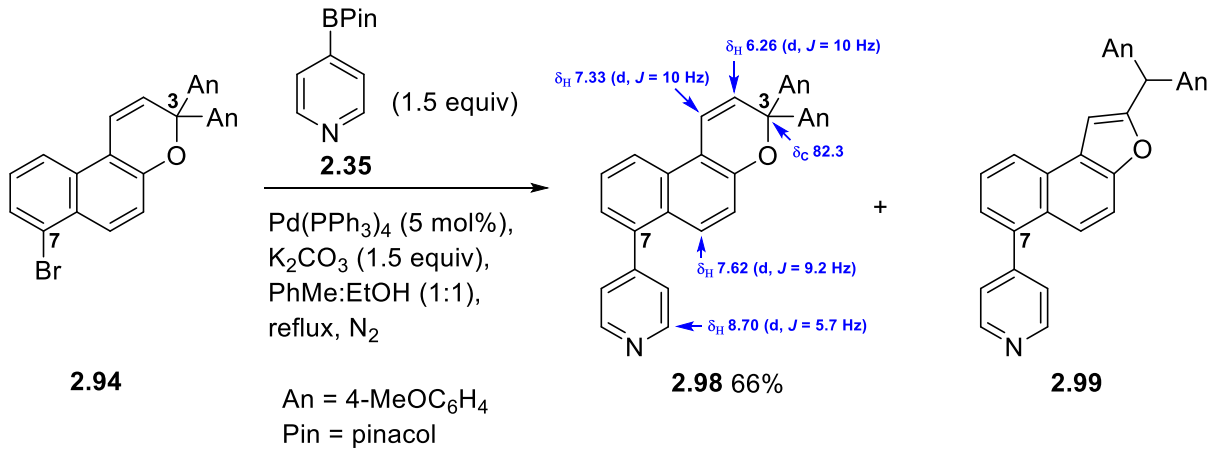

Scheme 2.42 Synthesis of 7-(4-pyridyl)-3*H*-naphtho[2,1-*b*]pyran **2.98**.

Overall, 7-(4-pyridyl)-3*H*-naphtho[2,1-*b*]pyran **2.98** was prepared from 5-amino-2-naphthol **2.90** in a five step linear route in 10% yield.

2.1.1.5 Synthesis of 5-Pyridyl-3*H*-Naphtho[2,1-*b*]pyrans

It was envisioned that 5-pyridyl-3*H*-naphtho[2,1-*b*]pyrans could be prepared according to **Strategy A**. The relatively cheap (£22 per 25 g/TCI) and readily accessible 2,3-dihydroxynaphthalene **2.100** was used as the starting material for this route.

The acid-catalysed condensation between 2,3-dihydroxynaphthalene **2.100** and propynol **2.79** – prepared previously – afforded 5-hydroxy-3*H*-naphtho[2,1-*b*]pyran **2.101** in 36% yield (**Scheme 2.43**). The poor yield was attributed in part to the low regioselectivity of the reaction – bisnaphthopyran **2.102** was also formed but not isolated. Decomposition during flash column chromatography purification also contributed to the poor overall yield.

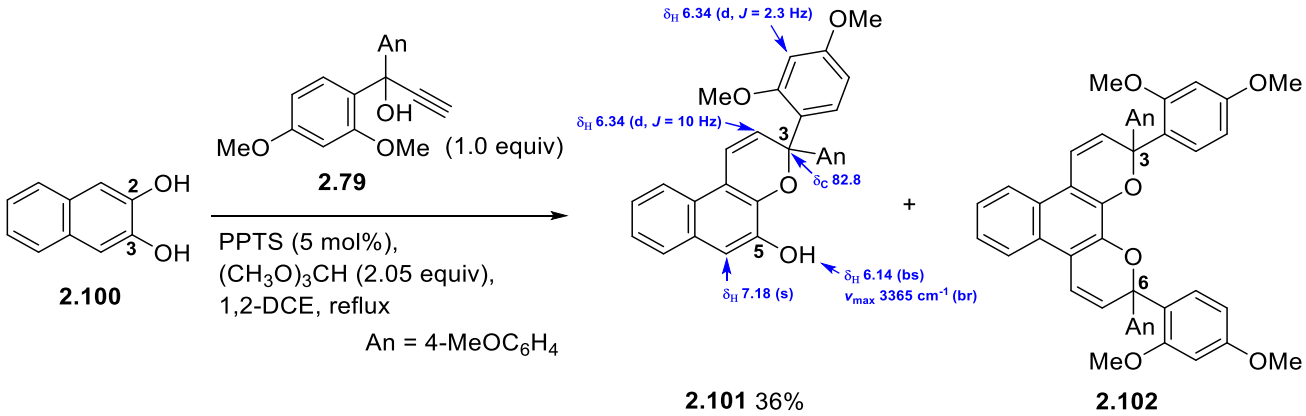

Scheme 2.43 Synthesis of 5-hydroxy-3*H*-naphtho[2,1-*b*]pyran **2.101**.

It is noteworthy that the 5-hydroxy-3*H*-naphtho[2,1-*b*]pyran **2.101** most probably forms a naphthopyran **2.101**:photomerocyanine **2.103** (85:15) mixture in $CDCl_3$, due to the particular stabilizing hydrogen-bond formation in the photomerocyanine **2.103**. This hyphothesis is supported by the ^{1}H NMR spectrum of the mixture that clearly shows a doublet at 8.95 ppm (J = 12 Hz) corresponding to the resonance of 2-H of the *transoid-cis* (TC), a doublet at 6.87 ppm (J = 8.9 Hz) corresponding to the resonance of 3′, 5′-H protons (anisyl) and three singlets at 3.65, 3.85 and 3.93 corresponding to the resonance of the methoxyl hydrogens (TC) (**Figure 2.4**). The doublet (J = 12 Hz) corresponding to the resonance of 1-H (TC) is underneath a multiplet at 7.85 ppm, and it was identified by COSY NMR as it correlates with 2-H (TC) (**Figure 2.5**). The chemical shifts and coupling constants of the signals identified in **Figure 2.4** are identical to the signals from ^{1}H NMR spectra of analogous photomerocyanines reported in the literature.[196]

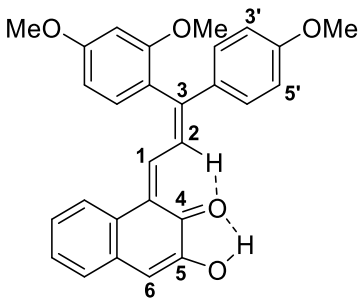

2.103

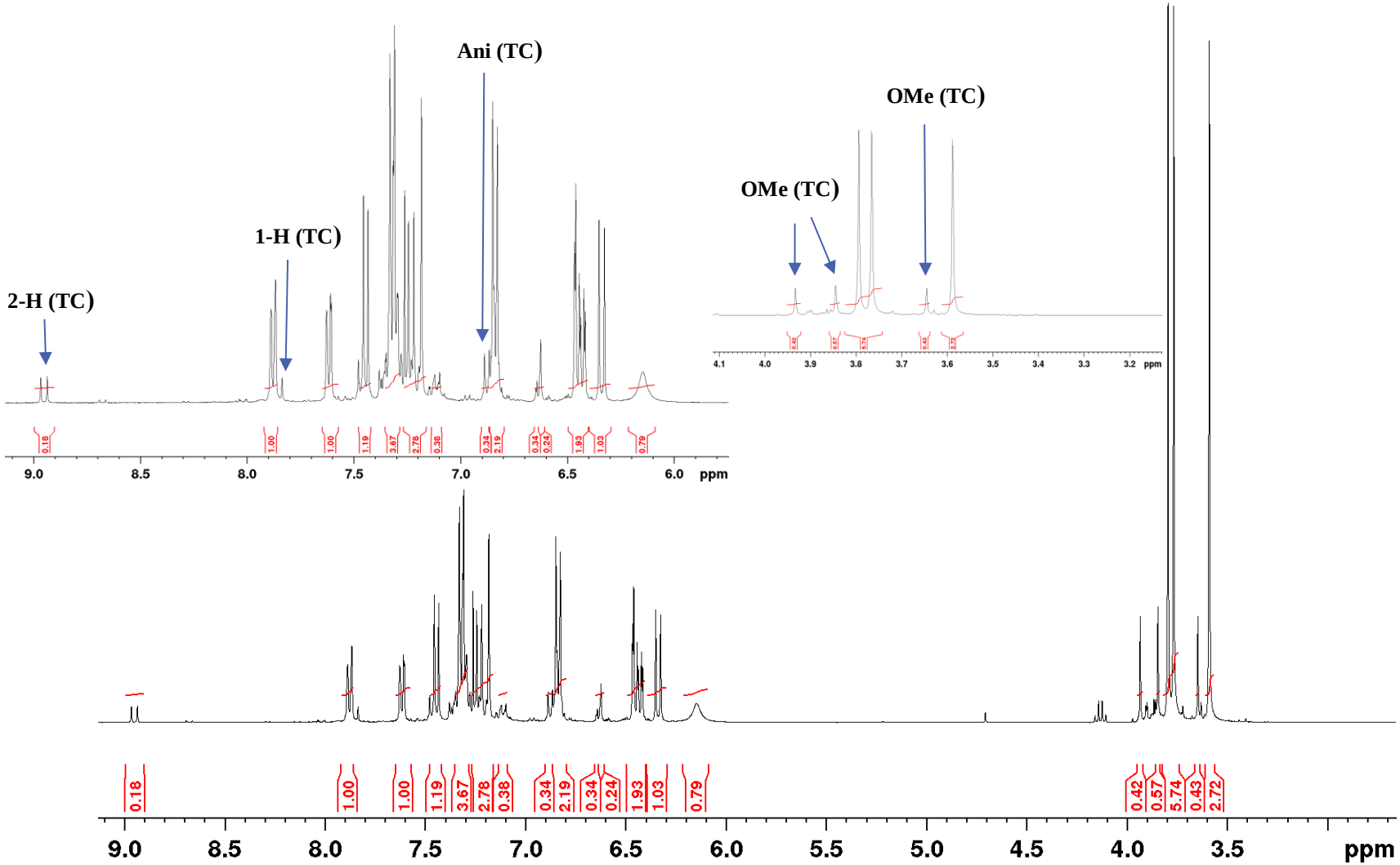

Figure 2.4 ^{1}H NMR spectrum of a naphthopyran **2.101**:photomerocyanine **2.103** (85:15) mixture in $CDCl_3$.

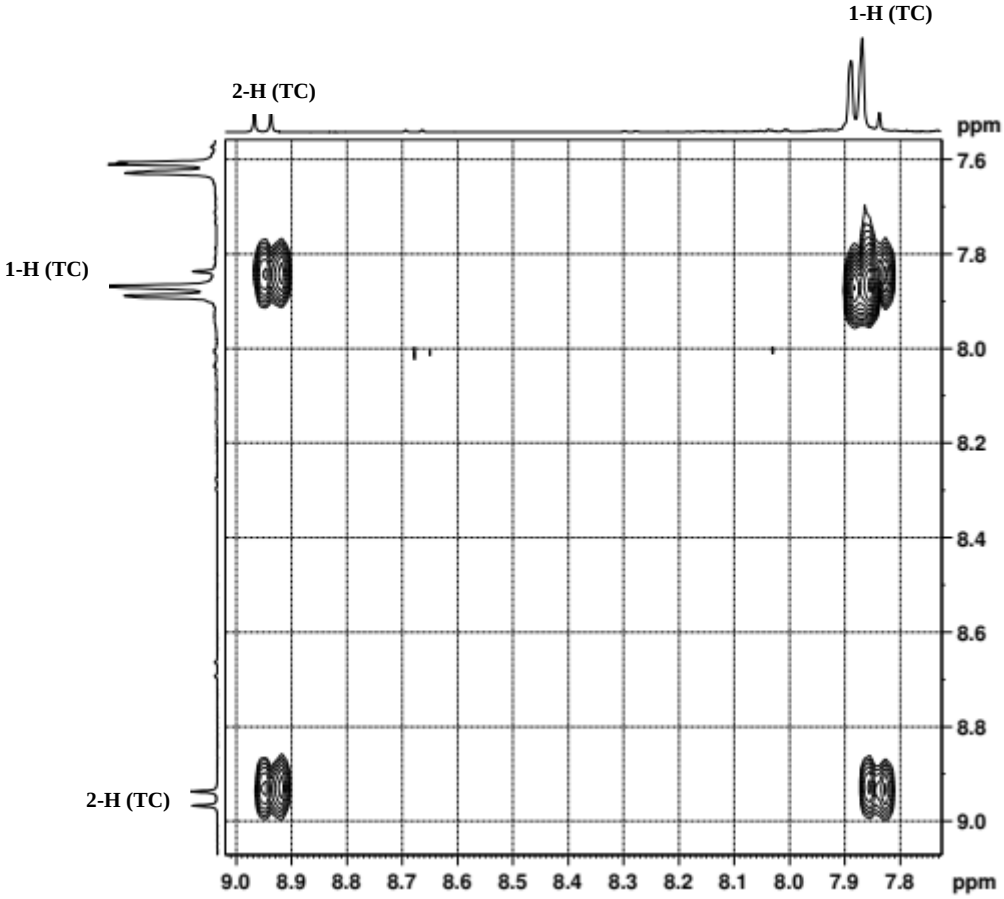

Figure 2.5 COSY NMR spectrum of a naphthopyran **2.101**:photomerocyanine **2.103** (85:15) mixture in $CDCl_3$.

Subsequently, triflation of 5-hydroxy-3*H*-naphtho[2,1-*b*]pyran **2.101** led to 5-triflyloxy-3*H*-naphtho[2,1-*b*]pyran **2.104** in excellent yield (95%) (**Scheme 2.44**). It is interesting to note that, by triflating the hydroxyl group, the hydrogen bond in the photomerocyanine **2.103** was broken and, as a result, the photomerocyanine was no longer visible in the ^{1}H NMR spectrum.

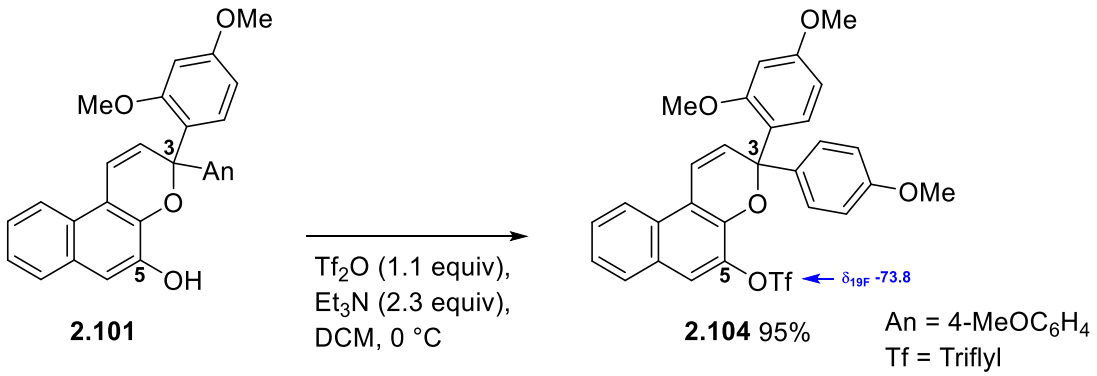

Scheme 2.44 Synthesis of 5-triflyloxy-3*H*-naphtho[2,1-*b*]pyran **2.104**.

Suzuki cross-coupling reaction between 5-triflyloxy-3*H*-naphtho[2,1-*b*]pyran **2.104** and 4-pyridineboronic acid pinacol ester **2.35** by using $Pd(PPh_3)_4$ (5 mol%), KF (3.3 equiv) in EtOH/PhMe (1:1) at reflux for 23h, afforded a mixture of 5-(4-pyridyl)-3*H*-naphtho[2,1-*b*]pyran **2.106**: naphthofuran **2.107** (90:10) (**Entry 1**, **Table 2.2**). This proved to be problematic as this mixture was extremely difficult to purify by either flash column chromatography or crystallization.

The ring-contraction to the naphthofurans is a temperature dependent reaction (this was further analysed in **Chapter 2.4**). Therefore if the Suzuki cross-coupling reaction is performed at room-temperature, ring-contraction to the naphthofurans might be avoided. Inspired by the work from Fu *et al.*,[197] an attempt to perform the Suzuki cross-coupling reaction at room temperature between **2.104** and **2.35** was tried by using $Pd(OAc)_2$ (5 mol%), PCy_3 (6 mol%), KF (3.3 equiv) in THF for 4h (**Entry 2**, **Table 2.2**). However, no reaction was observed.

Most probably, the Suzuki cross-coupling reaction requires heating in order to overcome the activation energy barrier. As a result, an attempt to perform the Suzuki cross-coupling reaction at 38 °C between **2.104** and phenylboronic acid **2.105** was tried by using $PdCl_2$ (7 mol%), PCy_3 (15 mol%), KF (3.3 equiv) in DMAc for 2 days (**Entry 3**, **Table 2.2**). The naphthopyran **2.108** was isolated in 25% yield but most importantly no ring-contraction was observed. The same conditions were applied to the Suzuki cross-coupling reaction between **2.104** and 4-pyridineboronic acid pinacol ester **2.35** but no reaction was observed after 16h (**Entry 4**, **Table 2.2**). No reaction happened after 23h even when 4-pyridineboronic acid **2.97** was used (**Entry 5**, **Table 2.2**). Furthermore, once the crude was heated to 50 °C both the Suzuki cross-coupling and ring-contraction reactions were observed.

Additionally, a Suzuki cross-coupling reaction between **2.104** and **2.35** was performed by using $Pd(PPh_3)_4$ (5 mol%), K_3PO_4 (1.7 equiv) in DMF at 110 °C for 3h which afforded a mixture of **2.106**:**2.107** (11:89) (**Entry 6**, **Table 2.2**). Further studies shown in **Chapter 2.4** are indicative that

the ring-contraction occurs much slower than the Suzuki cross-coupling reaction for a model system. Those studies also show that the ring-contraction kinetics are dependent on the nature of the base and, very importantly, on the base stoichiometry: when only a catalytic amount of base is used, the ring-contraction is decelerated substantially. It was rationalized that by reducing the stoichiometry of K_3PO_4 to 1.1 equiv, the ring-contraction would occur slower and yet providing enough base for a successful Suzuki catalytic cycle. Furthermore, as the kinetics of both Suzuki cross-coupling reaction and ring-contraction are different, it was envisioned stopping the reaction at a point where the Suzuki cross-coupling reaction was finished with no significant ring-contraction. Consequently, a Suzuki cross-coupling reaction between **2.104** and **2.35** was performed by using $Pd(PPh_3)_4$ (5 mol%), K_3PO_4 (1.1 equiv) in DMF at 110 °C (**Entry 7**, **Table 2.2**). After 20 min, the reaction was stopped as virtually all of the starting material was consumed. By ^{1}H NMR analysis it was determined that the amount of naphthofuran **2.107** in the mixture was less than 2% relative to the naphthopyran **2.106**. Flash column chromatography afforded the desired 5-(4-pyridyl)-3*H*-naphtho[2,1-*b*]pyran **2.106** in 51% yield (Purity > 98%) (**Scheme 2.46**).

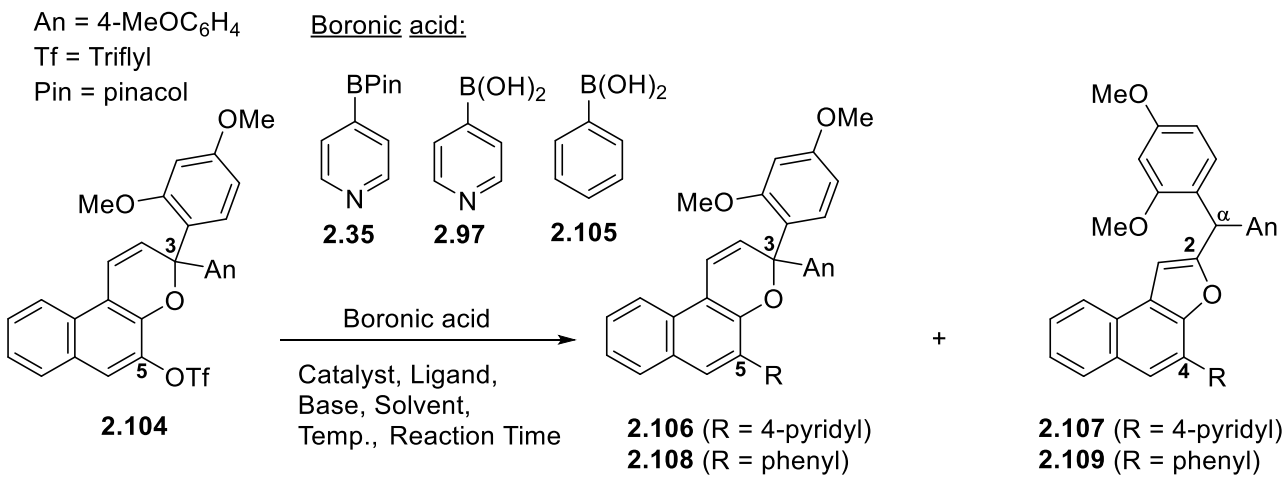

Scheme 2.45 Suzuki cross-coupling reactions between **2.104** and different boronic acids under multiple conditions.

Table 2.2 Suzuki cross-coupling reactions between **2.104** and different boronic acids under multiple conditions.

Entry	Boronic Acid	Catalyst	Ligand	Base	Solvent	Temp.	Time	Ratio*	Yield (%)
1	**2.35** (1.5 equiv)	$Pd(PPh_3)_4$ (5 mol%)	No	KF (3.3 equiv)	EtOH:PhMe (52.0:52.0 mL)	Reflux	23h	**2.106**:**2.107** (90:10)	N/A
2	**2.35** (1.5 equiv)	$Pd(OAc)_2$ (5 mol%)	PCy_3 (6 mol%)	KF (3.3 equiv)	THF (9 mL)	Room-temperature	4h	No reaction	N/A
3	**2.105** (1.5 equiv)	$PdCl_2$ (7 mol%)	PCy_3 (15 mol%)	KF (3.3 equiv)	DMAc (8.0 mL)	38 °C	5 days	**2.108**:**2.109** (100:0)	25
4	**2.35** (1.5 equiv)	$PdCl_2$ (8 mol%)	PCy_3 (15 mol%)	KF (3.4 equiv)	DMAc (8.0 mL)	38 °C	16h	No reaction	N/A
5	**2.97** (1.5 equiv)	$PdCl_2$ (7 mol%)	PCy_3 (15 mol%)	KF (3.3 equiv)	DMAc (10.0 mL)	38 °C	23h	No reaction	N/A
6	**2.35** (1.2 equiv)	$Pd(PPh_3)_4$ (5 mol%)	No	K_3PO_4 (1.7 equiv)	DMF (3.0 mL)	110 °C	3h	**2.106**:**2.107** (9:89)	N/A
7	**2.35** (1.1 equiv)	$Pd(PPh_3)_4$ (5 mol%)	No	K_3PO_4 (1.1 equiv)	DMAc (7.5 mL)	110 °C	20 min	**2.106**:**2.107** (99:1)	51

* Relative proportion of naphthopyran : naphthofuran was calculated based on the integral of the ^{1}H NMR spectrum of the reaction mixture.

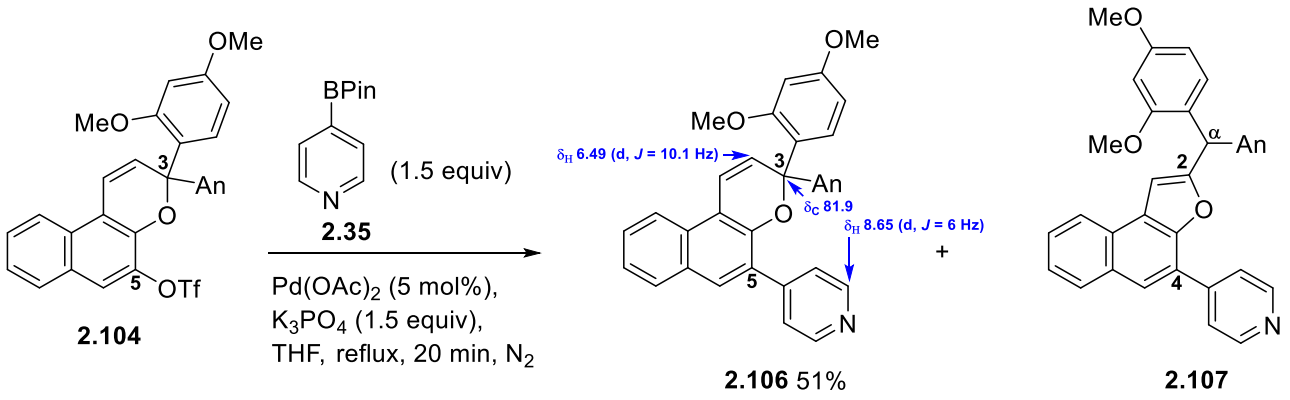

An = 4-MeOC$_6$H$_4$, Tf = triflyl, Pin = pinacol

Scheme 2.46 Synthesis of 5-(4-pyridyl)-3*H*-naphtho[2,1-*b*]pyran **2.106**.

Overall, 5-(4-pyridyl)-3*H*-naphtho[2,1-*b*]pyran **2.106** was prepared from 2,3-dihydroxynaphthalene **2.100** in a three step linear route in 17% yield.

2.1.1.6 Synthesis of a 8-(Pyridyl-triazole)-3*H*-Naphtho[2,1-*b*]pyran

It was rationalized that 8-(pyridyl-triazole)-3*H*-naphtho[2,1-*b*]pyran **2.110** could be prepared according to **Strategy A** which relies on a key Suzuki cross-coupling reaction between 8-boronyl-3*H*-naphtho[2,1-*b*]pyran **2.62**, prepared previously from the borylation of a 8-bromo-3*H*-naphtho[2,1-*b*]pyran **2.56**, and the bromo substituted pyridyl-triazole **2.111** (**Scheme 2.47**).

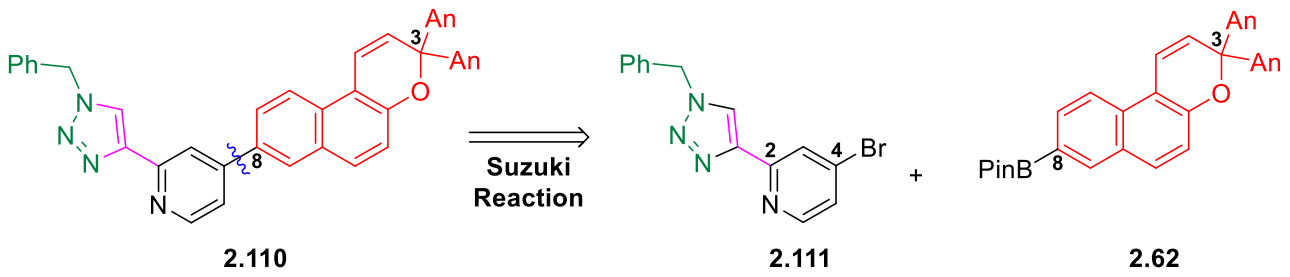

An = 4-MeOC$_6$H$_4$
Ph = phenyl

Scheme 2.47 Retrosynthesis of 8-(pyridyl-triazole)-3*H*-naphtho[2,1-*b*]pyran **2.110**.

The bromo substituted pyridyl-triazole **2.111** could be prepared from 4-bromo-2-ethynylpyridine **2.112** and benzyl azide **2.113** via a 1,3-dipolar cycloaddition (Click Reaction).

Furthermore, 4-bromo-2-ethynylpyridine **2.112** could be prepared by a Sonogashira cross-coupling reaction between TMS- acetylene and 2,4-dibromopyridine **2.114** (**Scheme 2.48**).

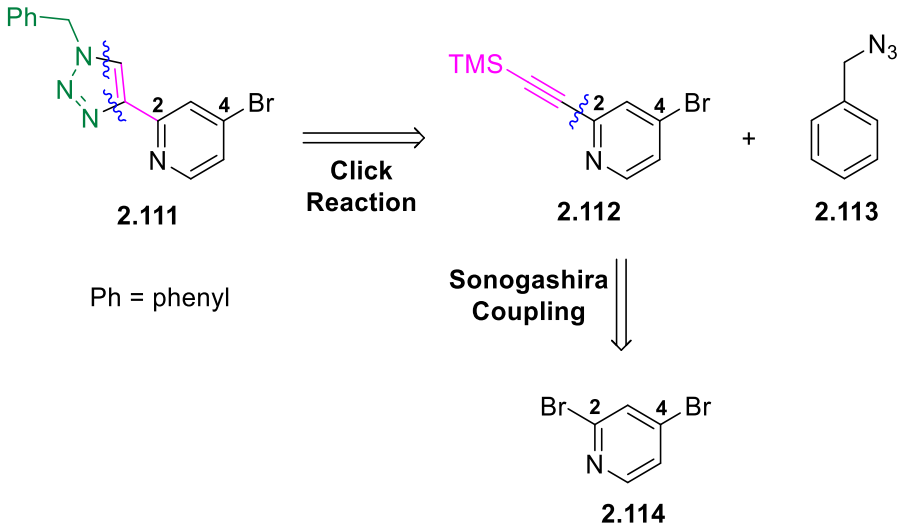

Scheme 2.48 Retrosynthesis of bromo substituted pyridyl-triazole **2.111**.

The 4-bromo-2-ethynylpyridine **2.112** was synthesized by the regioselective Sonogashira cross-coupling between TMS acetylene and 2,4-dibromopyridine **2.114**. Two different sets of conditions were employed:

1. Method A – Using TMS acetylene (1.5 equiv), $Pd(OAc)_2$ (5 mol%), *i*-Pr_2NH (1 equiv), PPh_3 (10 mol%), CuI (5 mol%) in anhydrous MeCN at reflux **2.112** in poor yield (23%) (**Scheme 2.49**).[198] 2,4-Bis((trimethylsilyl)ethynyl)pyridine **2.115** was also formed as a by-product but it was not isolated pure. The obtained yield is smaller to the one reported in the literature (43%), potentially because the reaction conditions were not anhydrous as *i*-Pr_2NH was not dried prior to the reaction.

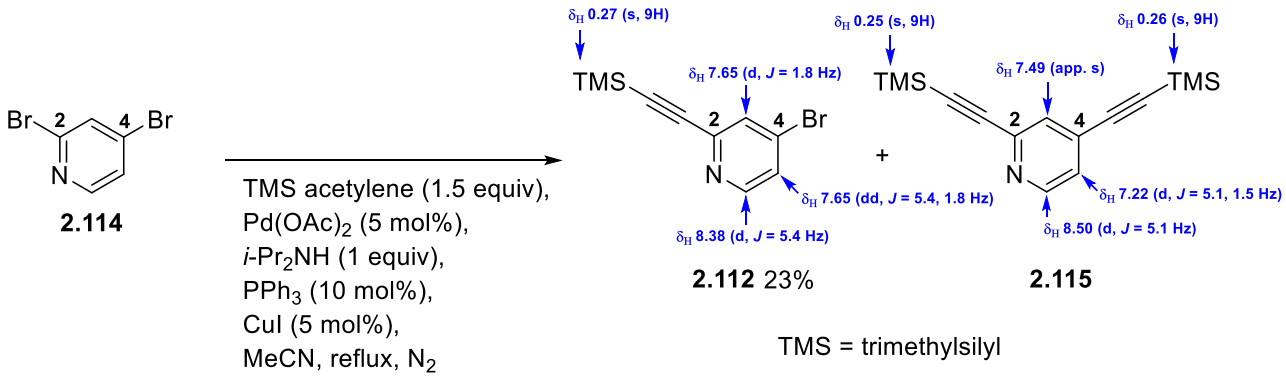

Scheme 2.49 Synthesis of 4-bromo-2-ethynylpyridine **2.112** by Method A.

2. Method B – Using TMS acetylene (2.05 equiv), $Pd(PPh_3)_2Cl_2$ (1 mol%), anhydrous NEt_3 (1 equiv), PPh_3 (15 mol%), CuI (8 mol%) at reflux afforded the corresponding **2.112** in poor yield (45%) (**Scheme 2.50**). 2,4-Bis((trimethylsilyl)ethynyl)pyridine **2.115** was also formed as a by-product (6%).[199]

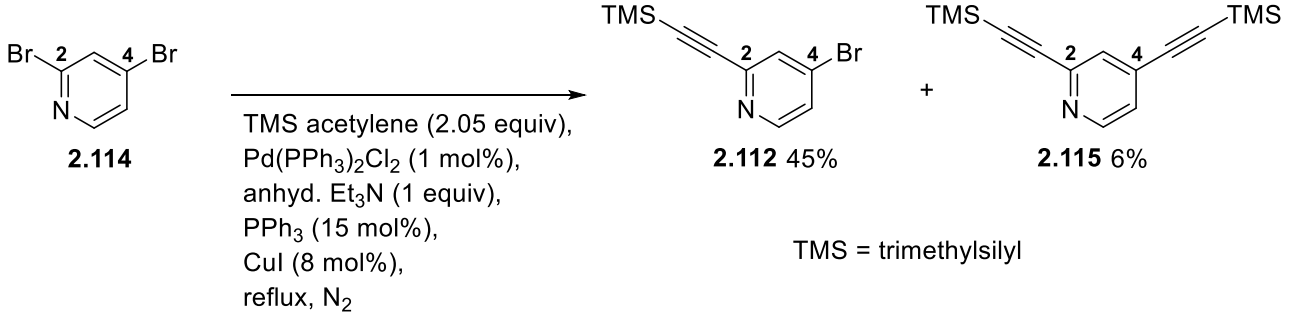

Scheme 2.50 Synthesis of bromo substituted pyridyl-triazole **2.112** by Method B.

The Sonogashira cross-coupling reaction undergoes a palladium cycle similar to the Suzuki cross-coupling reaction (**Scheme 2.12**), however there are a few differences: a transmetalation step occurs between the palladate **2.116**, generated from the oxidative addition step, and the copper salt **2.117**, formed by the reaction involving the base, Cu^IX and TMS acetylene, which leads to the palladate **2.118** (**Scheme 2.51**). Furthermore, there is a *trans* / *cis* isomerization step, that preceeds the reductive elimination step, in which the palladate **2.118** isomerizes to **2.119**.

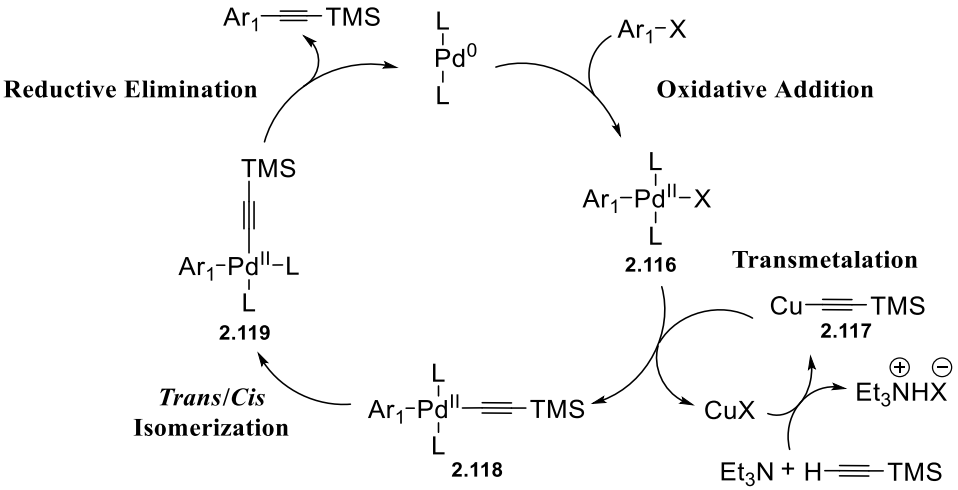

Scheme 2.51 General mechanism of a Sonogashira cross-coupling reaction.

Even though benzyl azide **2.113** is commercially available, it was synthesized from benzyl bromide **2.120** in a S_N2 reaction with NaN_3 in excellent yield (90%) (**Schemes 2.52** and **2.53**), by following a variation of a literature procedure.[200]

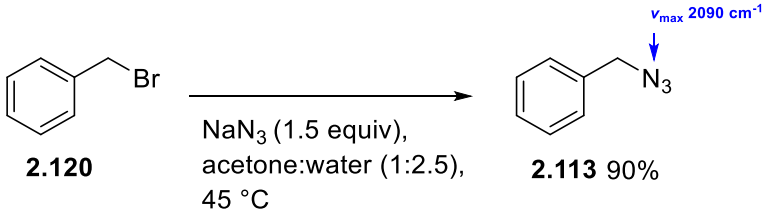

Scheme 2.52 Synthesis of benzyl azide **2.113**.

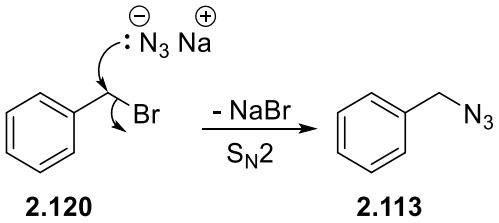

Scheme 2.53 Mechanism of the synthesis of benzyl azide **2.113**.

The bromo substituted pyridyl-triazole **2.111** was synthesized from 4-bromo-2-ethynylpyridine **2.112** and benzyl azide **2.113** by a Click-type reaction in very good yield (81%), following a variation of a literature protocol (**Scheme 2.54**).[201]

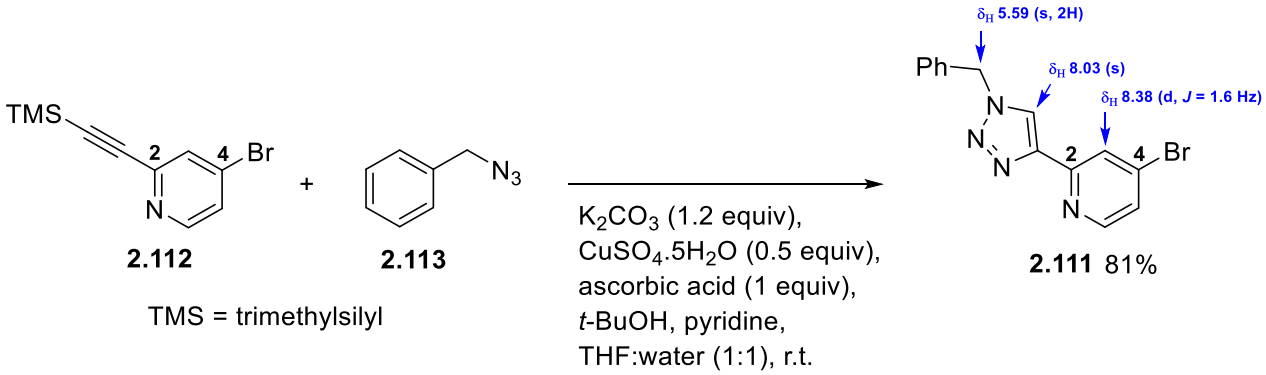

Scheme 2.54 Synthesis of the pyridyl-triazole **2.111**.

The addition of K_2CO_3 to the reaction mixture allowed the *in situ* alkyne deprotection. The active Cu(I) catalyst is probably generated by reduction of the Cu(II) salt ($CuSO_4.5H_2O$) by using ascorbic acid as the reducing agent. According to Fokin *et al.*, the 1,3-dipolar cycloaddition occurs by the coordination of the azide **2.113** with a σ-bound copper acetylide bearing a π-bound copper **2.121**, generating a six-membered copper metallacycle **2.122** (**Scheme 2.55**).[202] Ring contraction to a triazolyl-copper derivative **2.123** is followed by protonolysis that delivers the triazole product **2.111** and regenerates the Cu(I) catalyst.

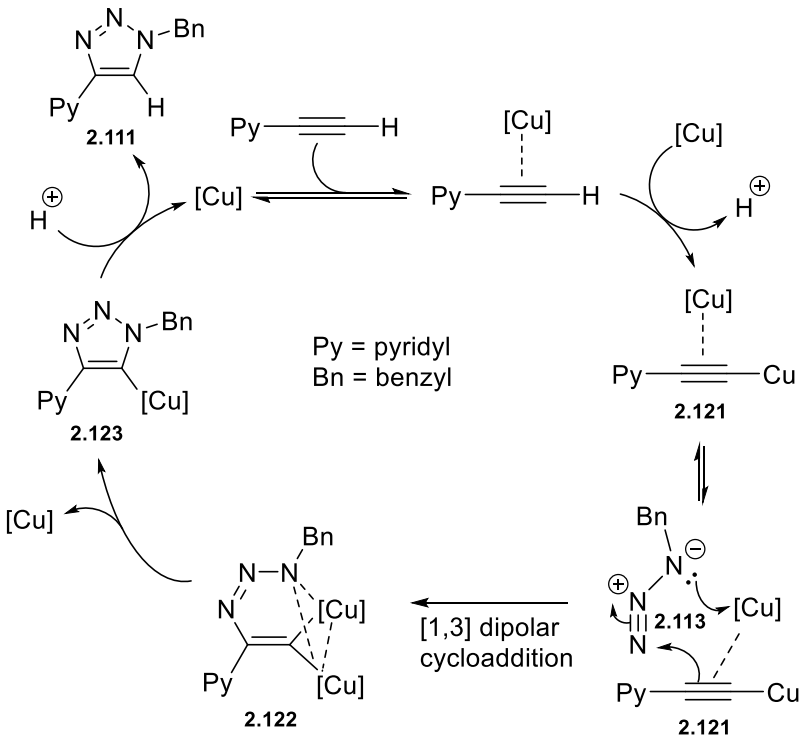

Scheme 2.55 Mechanism of the Click-type reaction.

Suzuki cross-coupling reaction between the 8-boronyl-3*H*-naphtho[2,1-*b*]pyran **2.62** and the bromo substituted pyridyl triazole **2.111** afforded the desired 8-(pyridyl-triazole)-3*H*-naphtho[2,1-*b*]pyran **2.110** in 31% yield (**Scheme 2.56**). The poor yield was attributed partly to a significant ring-contraction of **2.110** to the corresponding naphthofuran **2.124** – which was not isolated pure. On the other hand, there were complications during flash column chromatography as both structural isomers had very similar retention times.

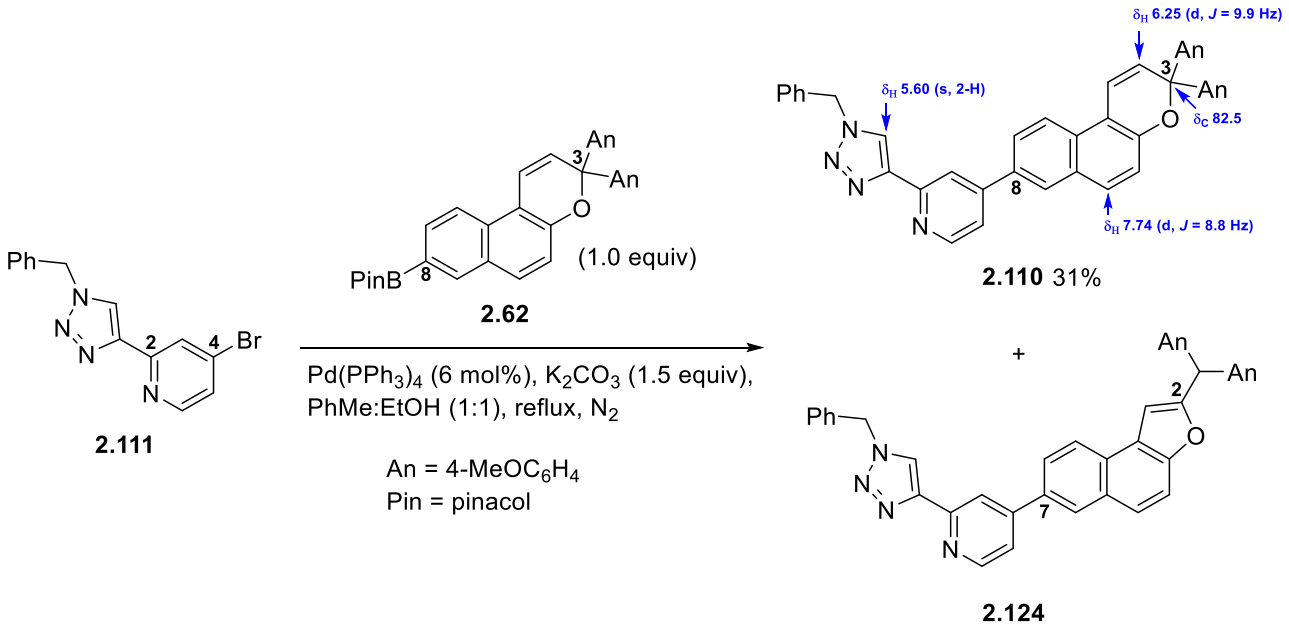

Scheme 2.56 Synthesis of 8-(pyridyl-triazole)-3*H*-naphtho[2,1-*b*]pyran **2.110**.

In conclusion, 8-(pyridyl-triazole)-3*H*-naphtho[2,1-*b*]pyran **2.110** was prepared from 2,4-dibromopyridine **2.114** in a three step linear route (via Method B) in 11% overall yield.

2.1.2 Strategy B – By a Heck cross-coupling protocol

2.1.2.1 Synthesis of 3-Pyridyl-3*H*-Naphtho[2,1-*b*]pyrans

In order to synthesize 3-(4-pyridyl)-3*H*-naphtho[2,1-*b*]pyran **2.170** according to **Strategy B**, it was first necessary to prepare the Heck coupling partner **2.126**. This was accomplished by the nucleophilic addition of vinylmagnesium chloride to the commercially available 4-benzoylpyridine **2.125** affording the corresponding product **2.126** in very good yield (86%) (**Schemes 2.57** and **2.58**).[203]

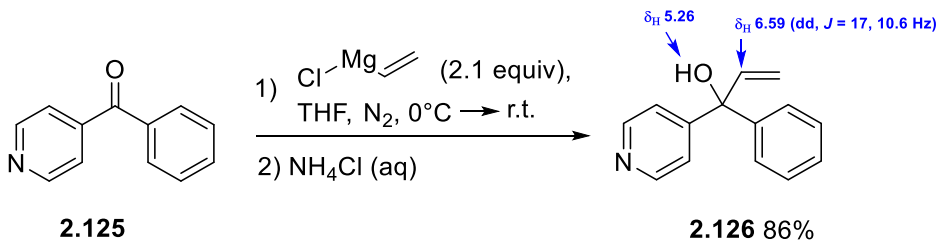

Scheme 2.57 Synthesis of propenol **2.126**.

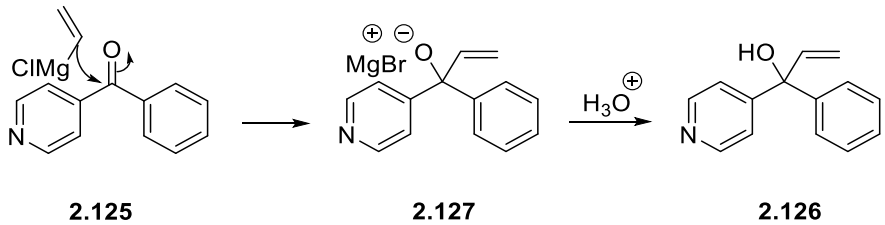

Scheme 2.58 Mechanism of the synthesis of propenol **2.126**.

Furthermore, the same protocol was employed to synthesize propenol **2.129** in excellent yield (99%) from benzophenone **2.128** (**Scheme 2.59**).

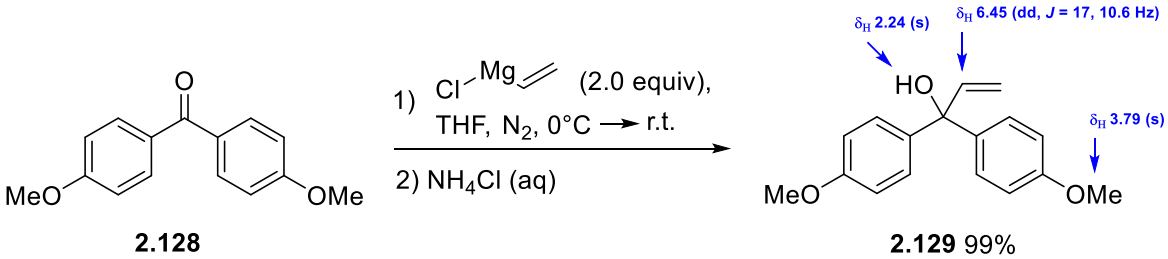

Scheme 2.59 Synthesis of propenol **2.129**.

Simply put, the Heck cross-coupling reaction involves a palladium catalytic cycle that includes four major steps (**Scheme 2.60**):

1. Oxidative addition – the palladate **2.130** is formed by the oxidative addition of Ar-X to PdL_2;
2. Insertion – the alkene **2.131** inserts into the palladium – carbon bond in a *syn* addition step, immediately after the formation a π complex **2.132**;
3. β-Hydride elimination – the elimination of a β-hydride in **2.133** generates the π complex **2.134**, that subsequently breaks down liberating the alkene product **2.135** and the palladate **2.136**;
4. Reductive elimination – the palladate **2.136** is reduced by the action of the base to restore PdL_2.

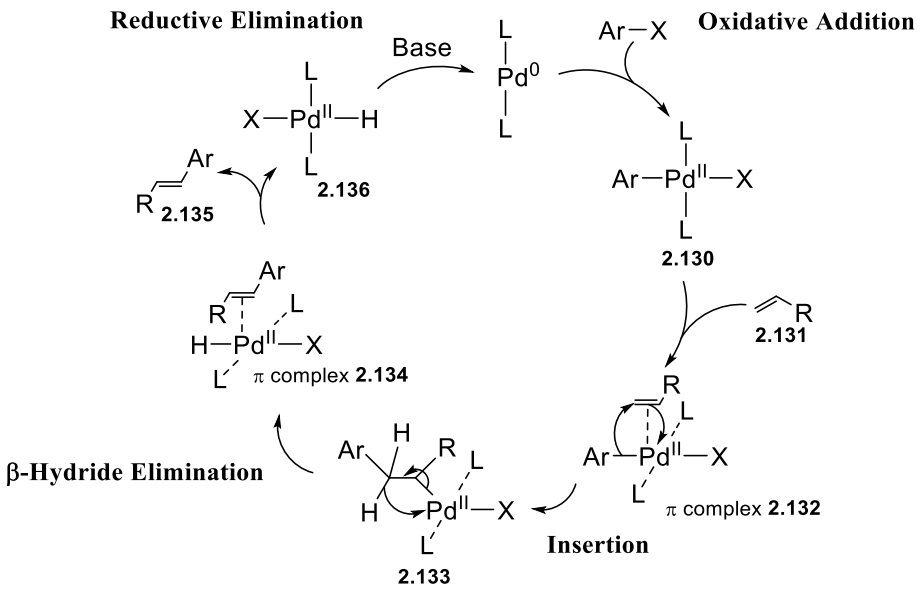

Scheme 2.60 General mechanism of a Heck cross-coupling reaction.

The Heck cross-coupling between propenol **2.126** and the commercially available 1-bromo-2-naphthol **2.137** proved to be problematic as multiple conditions – both phosphine and phosphine free conditions – failed to achieve any degree of reaction (**Entries 1** – **3**, **Table 2.3**). Moreover, no reaction was observed between 1-bromo-2-naphthol **2.137** and propenol **2.129** (**Entry 4**, **Table 2.3**). It was rationalized that the palladium catalytic cycle might not be occurring due to the bulkiness of the propenol **2.126**, which would result in too large of a steric clash for its insertion into the palladium – carbon bond in the insertion step. To test this hypothesis, the Heck cross-coupling reaction between **2.137** and the less sterically hindered 4-methoxystyrene **2.138** was tried without success (**Entry 5**, **Table 2.3**). The latter result showed that the bulkiness of the alkene was most probably not responsible for the failed catalytic cycle.

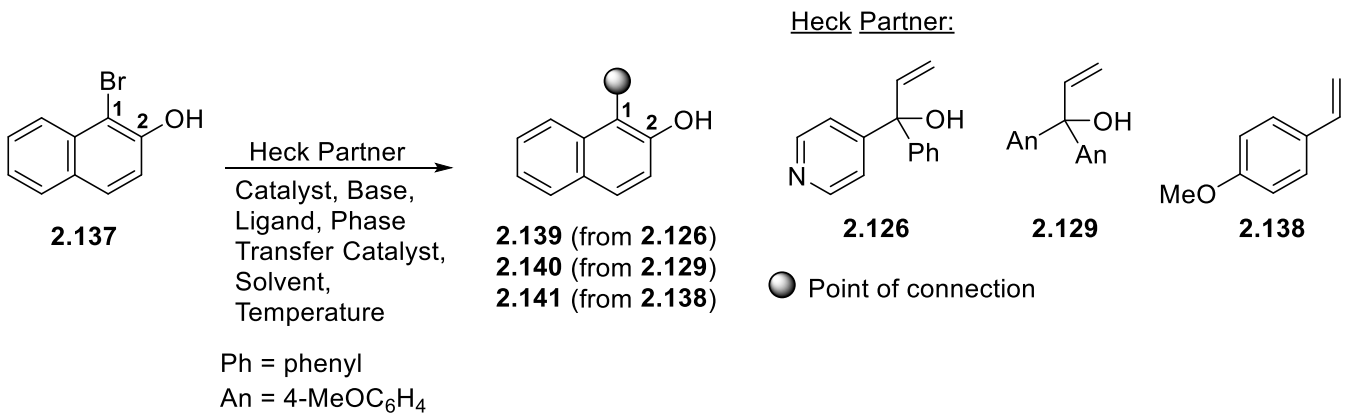

Scheme 2.61 Heck cross-coupling reactions between 1-bromo-2-naphthol **2.137** and different Heck partners under multiple conditions.

Table 2.3 Attempted Heck reactions between 1-bromo-2-naphthol **2.137** and different Heck partners under various conditions.

Entry	Heck Partner	Catalyst	Base	Ligand	Phase Transfer Catalyst	Solvent	Temp.	Result
1	**2.126** (2.2 equiv)	$Pd(OAc)_2$ (8 mol%)	$NaHCO_3$ (3.5 equiv)	No	TBAB (3.5 equiv)	DMF	90 °C	No reaction
2	**2.126** (1.3 equiv)	$Pd(OAc)_2$ (3 mol%)	NEt_3 (2.3 equiv)	PPh_3 (3 mol%)	No	MeCN	Reflux	No reaction
3	**2.126** (1.3 equiv)	$Pd(OAc)_2$ (8 mol%)	Cs_2CO_3 (1 equiv)	No	No	MeCN	Reflux	No reaction
4	**2.129** (1.4 equiv)	$Pd(OAc)_2$ (3 mol%)	NEt_3 (2.3 equiv)	PPh_3 (4 mol%)	No	MeCN	Reflux	No reaction
5	**2.138** (1.3 equiv)	$Pd(OAc)_2$ (3 mol%)	NEt_3 (2.3 equiv)	PPh_3 (4 mol%)	No	MeCN	Reflux	No reaction

It was envisioned that 1-iodo-2-naphthol **2.143** would serve as a better Heck coupling partner than 1-bromo-2-naphthol **2.142** as iodine is a better leaving group. Consequently, the former was prepared by the regioselective iodination of 2-naphthol in excellent yield (92%), by following a literature protocol (**Scheme 2.62**).[204]

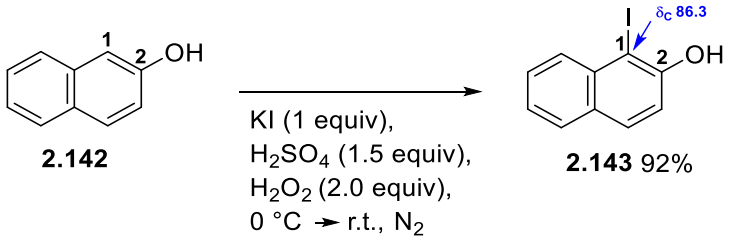

Scheme 2.62 Synthesis of 1-iodo-2-naphthol **2.143**.

The 1-iodo-2-naphthol **2.143** was formed by a S_EAr reaction between 2-naphthol **2.142** and molecular iodine formed *in situ* from the oxidation of the readily accessible KI in the presence of hydrogen peroxide and H_2SO_4 (**Scheme 2.63**).

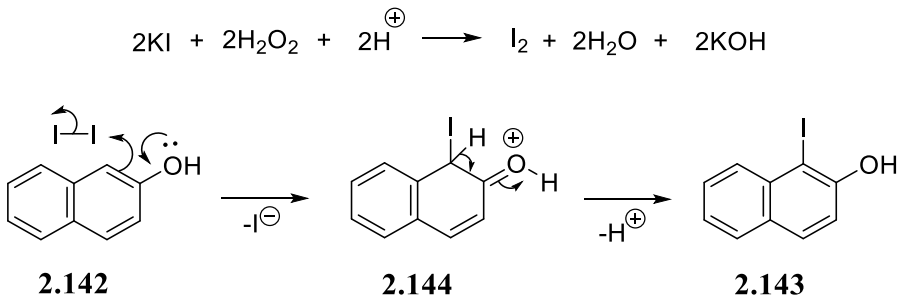

Scheme 2.63 Mechanism of the iodination of 2-naphthol **2.142**.

A few experiments were undertaken to couple 1-iodo-2-naphthol **2.143** with different Heck partners (**Table 2.4**). When reacting **2.143** with propenol **2.126** under Heck conditions – only phosphine free conditions were employed – no reaction was observed (**Entries 1 – 2**, **Table 2.4**). It would have been interesting to run a test reaction under phosphine conditions as triphenylphosphine could have facilitated the pre-activation of $Pd(OAc)_2$ – Pd(II) is reduced to Pd(0) as triphenylphosphine is oxidized to triphenylphosphine oxide. On the other hand, the 3*H*-naphtho[2,1-*b*]pyran **2.147** was isolated in very poor yield (3%) when reacting 1-iodo-2-naphthol **2.143** with propenol **2.129** (**Entry 3**, **Table 2.4**). The 3*H*-naphtho[2,1-*b*]pyran **2.147** was probably formed by the base-catalysed electrocyclization of the alkene product **2.146** (**Scheme 2.65**).

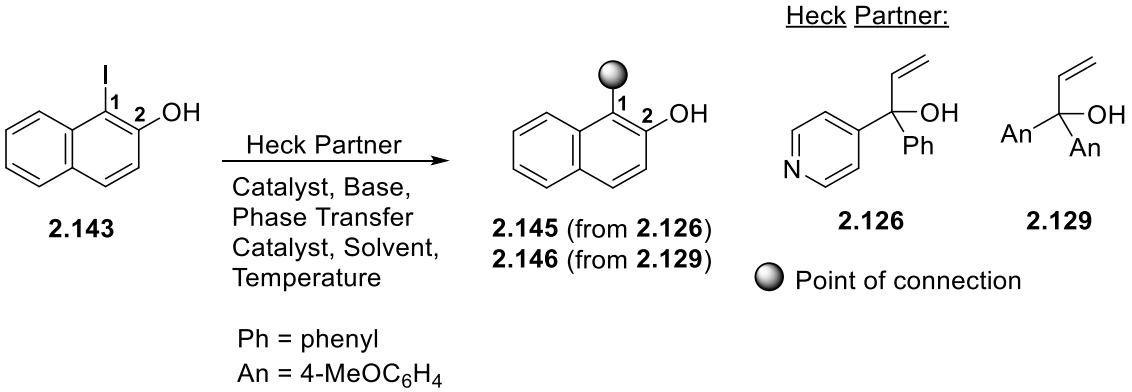

Scheme 2.64 Heck cross-coupling reactions between 1-iodo-2-naphthol **2.143** and different Heck partners under different conditions.

Table 2.4 Attempted Heck reactions between 1-iodo-2-naphthol **2.143** and different Heck parntners under various conditions.

Entry	Heck Partner	Catalyst	Base	Phase Transfer Catalyst	Solvent	Temp.	Yield (%)
1	**2.126** (1.3 equiv)	$Pd(OAc)_2$ (8 mol%)	Cs_2CO_3 (1.0 equiv)	No	MeCN	Reflux	No reaction
2	**2.126** (1.3 equiv)	$Pd(OAc)_2$ (8 mol%)	Cs_2CO_3 (1.0 equiv)	TBAB (1.0 equiv)	MeCN	Reflux	No reaction
3	**2.129** (1.4 equiv)	$Pd(OAc)_2$ (8 mol%)	Cs_2CO_3 (1.0 equiv)	No	MeCN	Reflux	**2.147** (3%); Formed from **2.146**

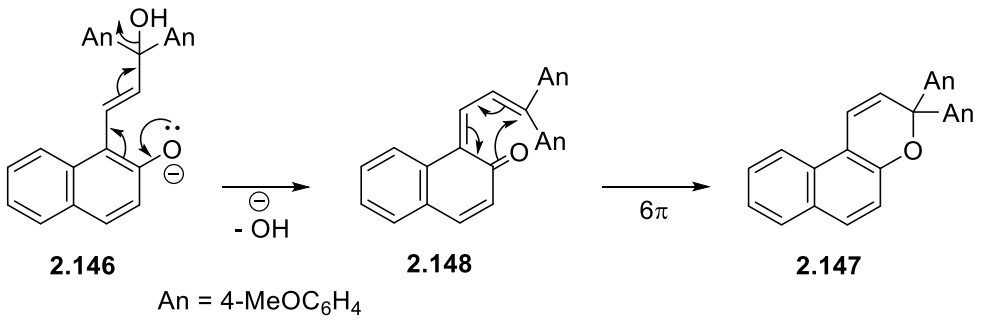

Scheme 2.65 Mechanism of the base promoted electrocyclization of **2.146** to **2.147**.

Following the unsatisfactory experiments performed up to this point, it was rationalized that possibly the hydroxyl group of the naphthol **2.137** required protection in order to allow a successful oxidative addition to the active palladium catalyst. Protecting groups chosen needed to be stable under basic conditions, relatively easy to remove and small enough not to further sterically hinder C-1 of the naphthalene scaffold.[205] First choice was an acetoxyl group: 2-acetoxy-1-bromonaphthalene **2.149** was prepared by the base-promoted acetylation of 1-bromo-2-naphthol **2.137** giving the former product in very good yield (81%) (**Scheme 2.66**).[206] The reaction mechanism includes the nucleophilic addition of **2.150** to **2.151** which generates the tetrahedral intermediate **2.152**, followed by elimination of an acetoxyl group, leading to the product **2.149** (**Scheme 2.67**).

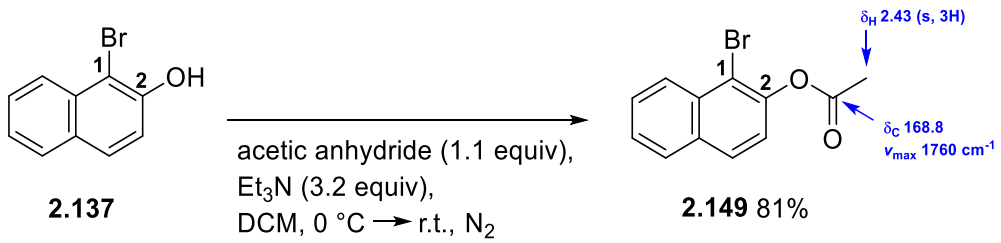

Scheme 2.66 Synthesis of 2-acetoxy-1-bromonaphthalene **2.149**.

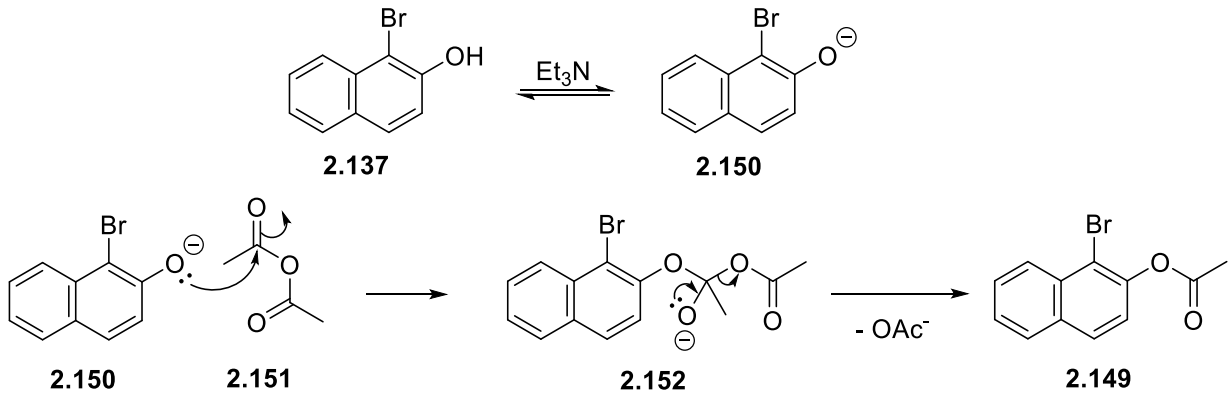

Scheme 2.67 Mechanism of the synthesis of 2-acetoxy-1-bromonaphthalene **2.149**.

The Heck cross-coupling reactions between 2-acetoxy-1-bromonaphthalene **2.149** and different Heck partners, under both phosphine and phosphine free conditions, were not successful as the *O*-acetyl protecting group proved to be too labile (**Table 2.5**).

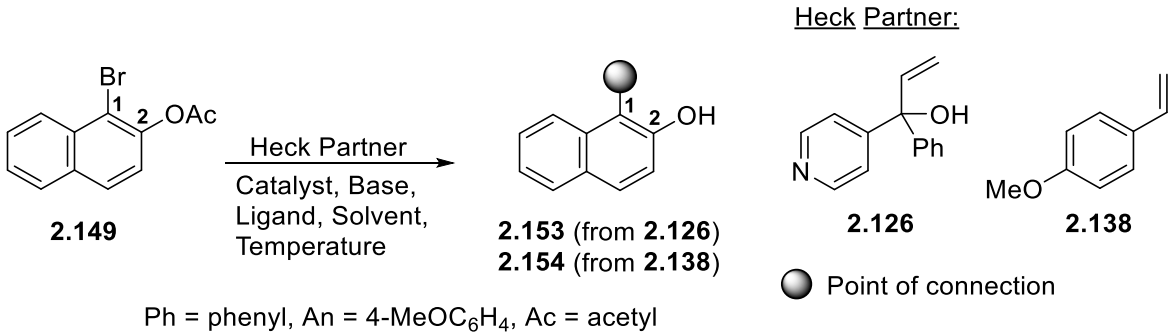

Scheme 2.68 Heck cross-coupling reactions between 2-acetoxy-1-bromonaphthalene **2.149** and different Heck partners under different conditions.

Table 2.5 Attempted Heck reactions between between 2-acetoxy-1-bromonaphthalene **2.149** and different Heck partners under various conditions.

Entry	Heck Partner	Catalyst	Base	Ligand	Solvent	Temp.	Result
1	**2.126** (1.3 equiv)	$Pd(PPh_3)_4$ (5 mol%)	NEt_3 (2.4 equiv)	No	MeCN	Reflux	No reaction
2	**2.126** (1.3 equiv)	$PdCl_2$ (5 mol%)	NEt_3 (2.4 equiv)	No	MeCN	Reflux	No reaction
3	**2.138** (1.4 equiv)	$Pd(OAc)_2$ (3 mol%)	NEt_3 (2.4 equiv)	PPh_3 (4 mol%)	MeCN	Reflux	No reaction

A second choice for protecting the hydroxyl group of the naphthol was as a trimethylsilyl ether. Trimethylsilylation of 1-iodo-2-naphthol **2.143** using hexamethyldisilazane (HMDS) in THF gave ((1-iodonaphthalen-2-yl)oxy)trimethylsilane **2.155** in 31% yield (**Scheme 2.69**).[207] The latter appeared to have a very short-life at room temperature as it decomposed rapidly to **2.143**. In the reaction mechanism, HMDS, besides acting as a reactant, it probably also acts as a base abstracting a proton from **2.143** leading to **2.156** (**Scheme 2.70**). A S_N2 reaction between **2.156** and **2.157** afforded the product **2.155**. Trimethylsilylation of 1-bromo-2-naphthol **2.137** was not successful as the product decomposed to the starting material during the work-up.

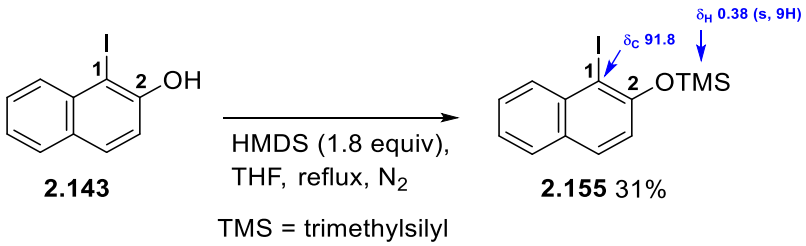

Scheme 2.69 Synthesis of ((1-iodonaphthalen-2-yl)oxy)trimethylsilane **2.155**.

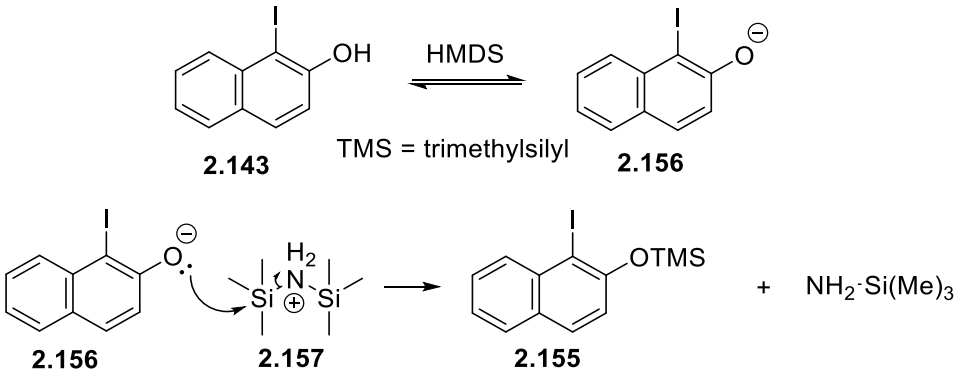

Scheme 2.70 Mechanism of the trimethysilylation of 1-iodo-2-naphthol **2.143**.

Even though TMS had shown to be a very labile protecting group, **2.155** was successfully coupled to 4-methoxystyrene **2.138** giving 2-(4-methoxyphenyl)naphtho[2,1-*b*]furan **2.159** in 13% yield, after the oxidative cyclization of the Heck product **2.158** (**Scheme 2.71**). Based on the previous results, it was rationalized that the Heck cross-coupling reaction occurred while the hydroxyl group was protected and then stopped as soon as the TMS ether was cleaved, which helps to rationalise the poor yield. This reaction represents a unoptimized one step method for the preparation of 2-arylnaphthofurans via a Heck cross-coupling protocol without the deliberate use of oxidants e.g. (diacetoxyiodo)benzene.[208] Probably the palladium catalyst might have acted as an

oxidant similarly to hypervalent iodine. Thus, the oxidative addition of Pd^0L_2 to the oxygen – hydrogen bond of **2.158** afforded the palladate **2.160** (**Scheme 2.72**). Then, the double bond inserted itself in the palladium – oxygen bond in a *syn* addition to form **2.161**. The latter was converted into **2.159** by a β-hydride elimination liberating $Pd^{II}L_2H_2$. Lastly, the base-promoted reduction of $Pd^{II}L_2H_2$ regenerated Pd^0L_2. It is noteworthy that it has been reported the involvement of amorphous palladium in an analogous cyclization reaction with no need of base to regenerate the active nanoparticulate Pd(0). [209]

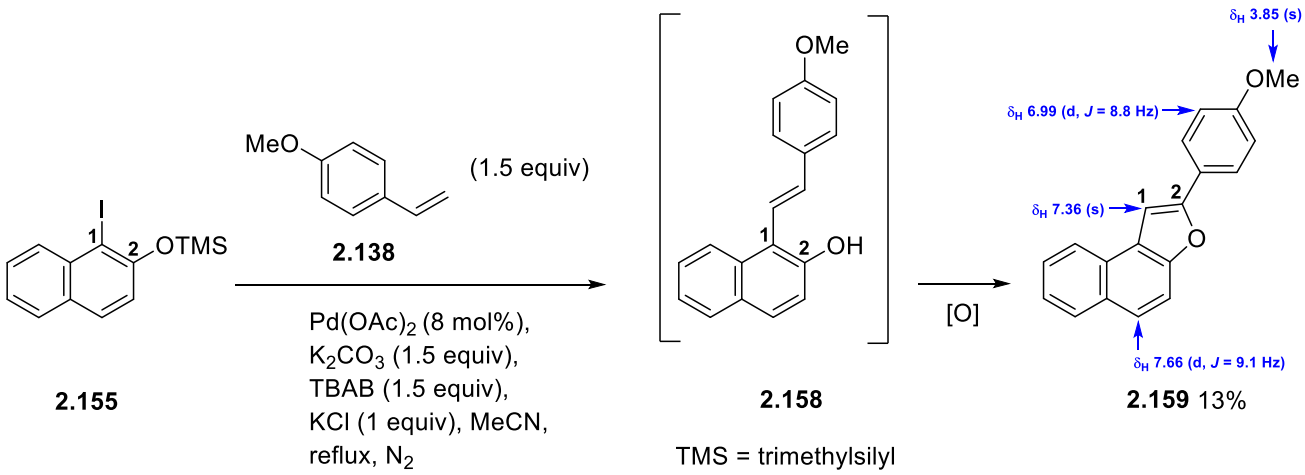

Scheme 2.71 Synthesis of 2-(4-methoxyphenyl)naphtho[2,1-*b*]furan **2.158**.

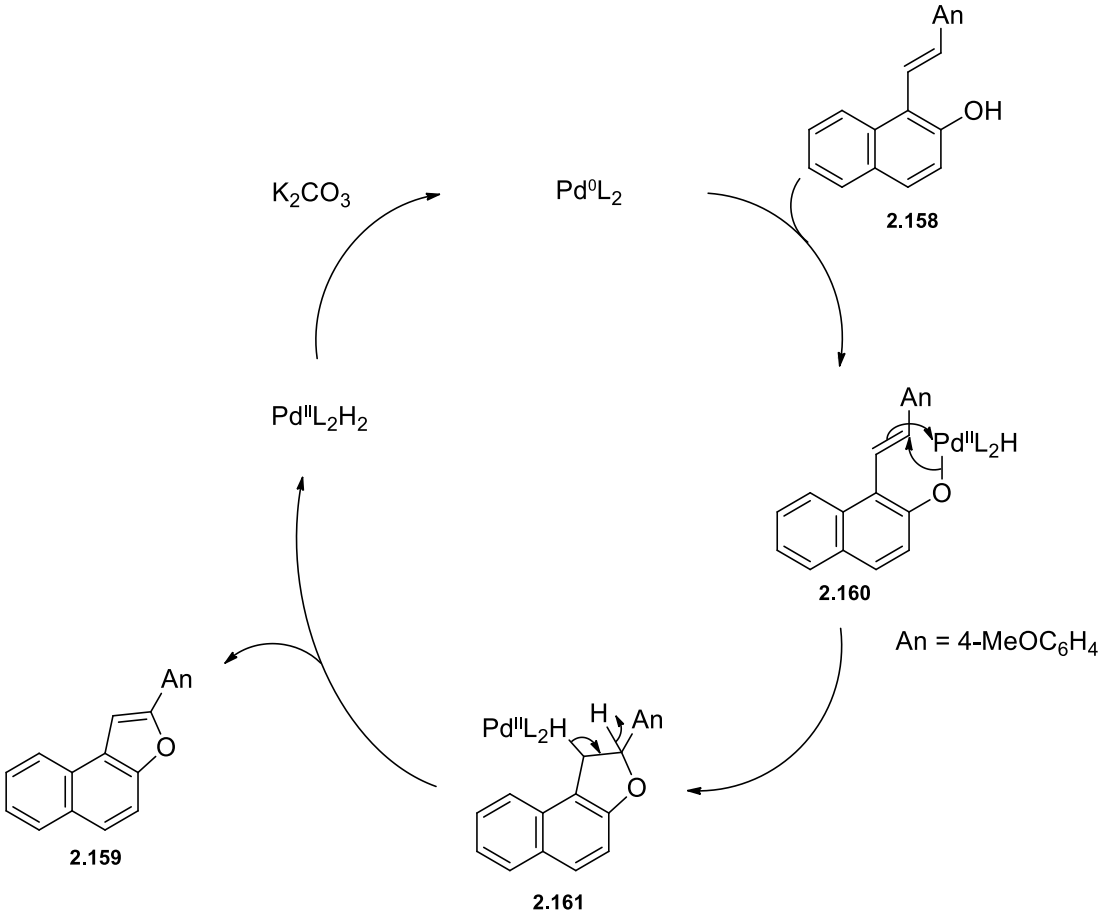

Scheme 2.72 Putative mechanism of the palladium catalysed oxidative cyclization to **2.159**.

A third choice for protecting the hydroxyl group of the naphthalene derivative was as a methoxymethyl ether: 1-bromo-2-(methoxymethoxy)naphthalene **2.162** was prepared from the base-catalysed S_N2 reaction between 1-bromo-2-naphthol **2.137** and the relatively expensive chloromethyl methyl ether (MOMCl) in excellent yield (99%) (**Schemes 2.73** and **2.74**).[210]

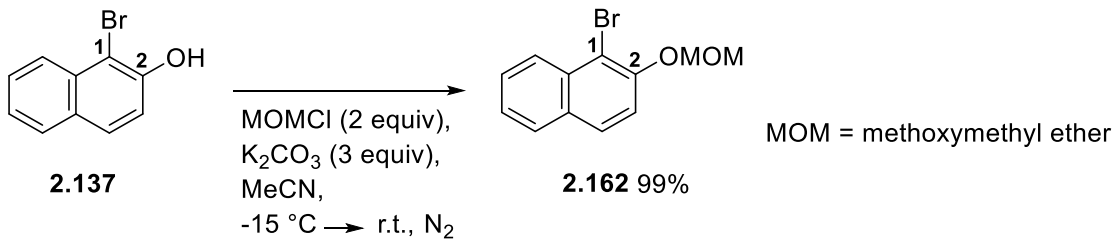

Scheme 2.73 Synthesis of 1-bromo-2-(methoxymethoxy)naphthalene **2.162**.

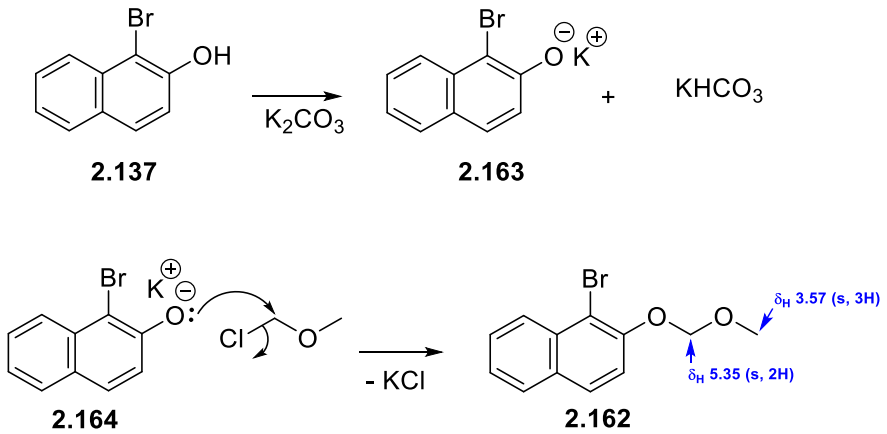

Scheme 2.74 Mechanism of the synthesis of 1-bromo-2-(methoxymethoxy)naphthalene **2.162**.

A successful Heck cross-coupling reaction between **2.162** and propenol **2.126** resulted in the formation of the Heck product (*E*)-3-(2-(methoxymethoxy)naphthalen-1-yl)-1-phenyl-1-(pyridin-4-yl)prop-2-en-1-ol **2.165** in 41% yield (**Scheme 2.75**).[211] This result seems to be indicative that the previous failed Heck cross-coupling reactions were a consequence of the unsuccessful oxidative addition of the PdL_2 to the C – Br bond of the unprotected 1-bromo-2-naphthol **2.137**. The *E* configuration of the alkene was determined by ^{1}H NMR analysis: the doublets, corresponding to the resonance of the alkene hydrogens, had a coupling constant of 16 Hz.

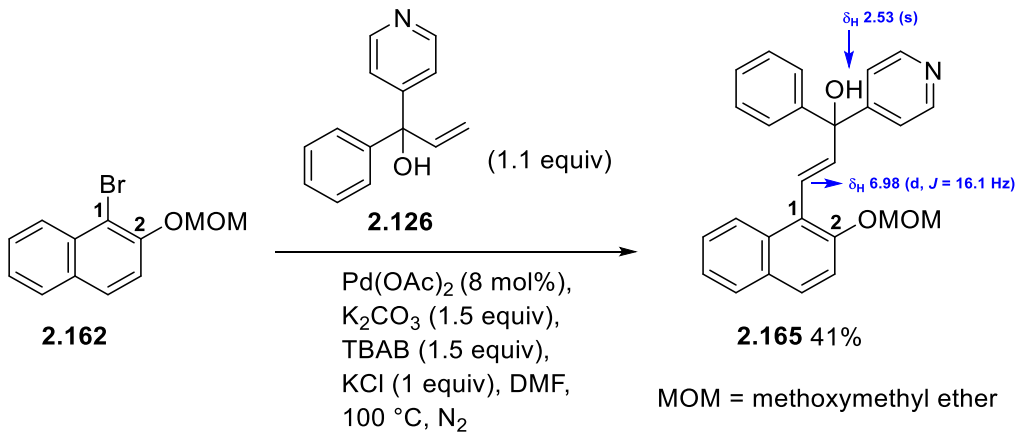

Scheme 2.75 Synthesis of Heck product **2.165**.

The Heck conditions used to prepare the Heck product **2.165** proved to be less effective when **2.162** was coupled to propenol **2.129**, as the Heck product **2.166** was isolated in very poor yield (9%) (**Entry 1**, **Table 2.6**). When using $Pd(OAc)_2$ (5 mol%), *N*-methyldicyclohexylamine [Cy_2NMe] (1.5 equiv), PPh_3 (10 mol%), TBAC (11 mol%) in DMAc at 100 °C, the Heck product

2.166 was again isolated in very poor yield (8%) (**Entry 2**, **Table 2.6**). It was rationalized that by mixing $Pd(dba)_2$ (2 mol%) with tri-*tert*-butylphosphonium tetrafluoroborate [TTBP · HBF_4] (4 mol%), the very active bis(tri-*tert*-butylphosphine)palladium(0) ($Pd(t\text{-}Bu_3P)_2$) would be formed *in situ* (**Scheme 2.77**). The *t*-BuP ligands are strong electron rich phosphine ligands that stabilise proficiently the palladium(II) salt obtained from the oxidative addition step. [212] On the other hand, the bulkiness of the $t\text{-}Bu_3P$ ligands favours the reductive elimination step. Thus, when using $Pd(dba)_2$ (2 mol%), $P(t\text{-}Bu)_3HBF_4$ (4 mol%), *N*-methyldicyclohexylamine (Cy_2NMe) (1.5 equiv), TBAC (10 mol%) in DMAc at 100 °C, the Heck product **2.166** was isolated in higher yield (35%) (**Entry 3**, **Table 2.6**).[213] Besides **2.166**, the 3*H*-naphtho[2,1-*b*]pyran **2.147** was also isolated as a by-product (10%). It is possible either the strong acid HBF_4 or the conjugated acid of Cy_2NMe, formed during the reaction, promoted the acid-catalysed dehydration of **2.166** affording oxonium **2.168** (**Scheme 2.78**). Subsequently, the latter was converted to **2.169** by losing a methyl(methylene)oxonium group. The 6π-electrocyclization of **2.169** afforded 3*H*-naphtho[2,1-*b*]pyran **2.143**.

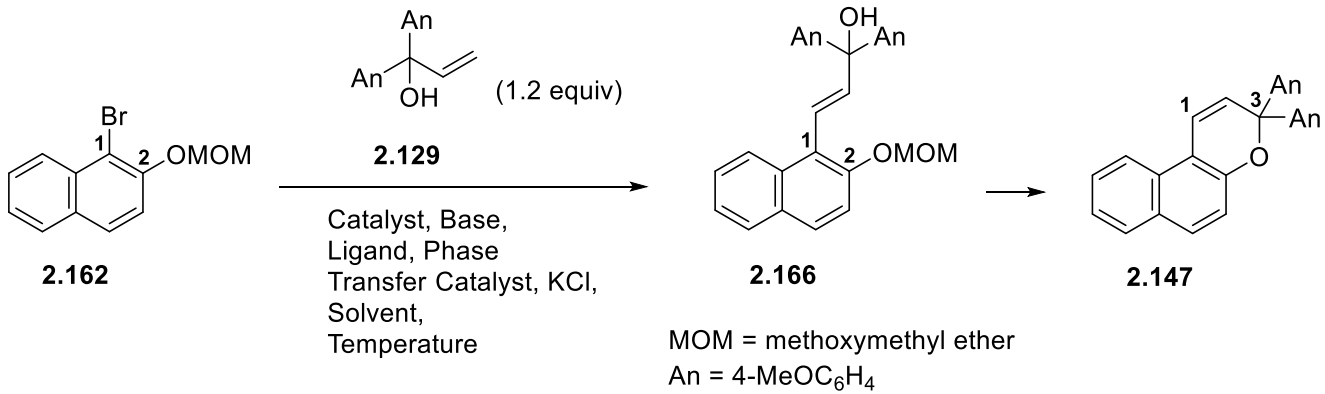

Scheme 2.76 Heck cross-coupling reactions between **2.162** and **2.129** under different conditions.

Table 2.6 Heck cross-coupling reactions between **2.162** and **2.129** under various conditions.

Entry	Catalyst	Base	Ligand	Phase Transfer Catalyst	KCl	Solvent	Temp.	Yield (%)
1	$Pd(OAc)_2$ (9 mol%)	K_2CO_3 (1.5 equiv)	No	TBAB (1.5 equiv)	1.1 equiv	DMAc	100 °C	**2.166** (9%)
2	$Pd(OAc)_2$ (5 mol%)	Cy_2NMe (1.5 equiv)	PPh_3 (10 mol%)	TBAC (11 mol%)	No	DMAc	80 °C	**2.166** (8%)
3	$Pd(dba)_2$ (2 mol%)	Cy_2NMe (1.5 equiv)	$P(t\text{-}Bu)_3HBF_4$ (4 mol%)	TBAC (10 mol%)	No	DMAc	80 °C	**2.166** (35%) **2.147** (10%)

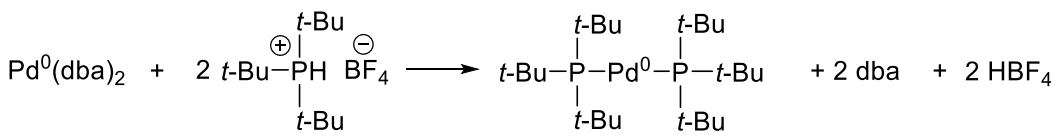

Scheme 2.77 Synthesis of Pd(*t*-Bu$_3$P)$_2$ from the reaction of Pd(dba)$_2$ with P(*t*-Bu)$_3$HBF$_4$.

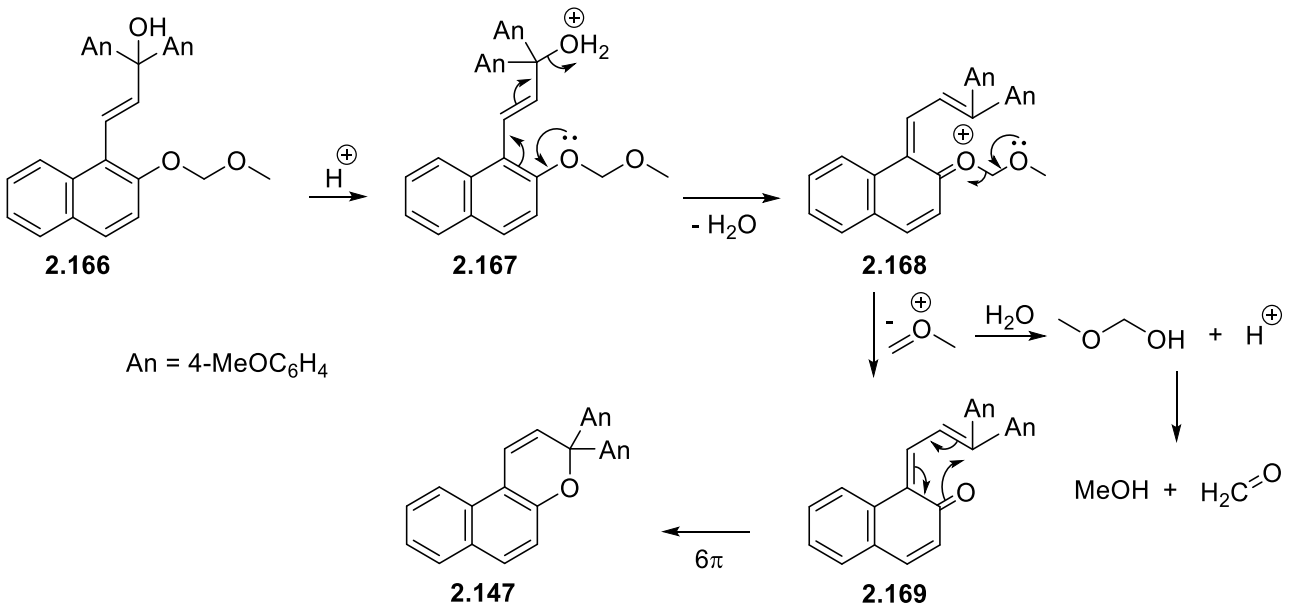

Scheme 2.78 Putative mechanism of the synthesis of 3*H*-naphtho[2,1-*b*]pyran **2.147**.

The 3-(4-pyridyl)-3*H*-naphtho[2,1-*b*]pyran **2.170** was synthesized in an one-pot protocol from the Heck product **2.166** in 61% yield by treatment with TFA in DCM at room temperature (**Scheme 2.79**).[214]

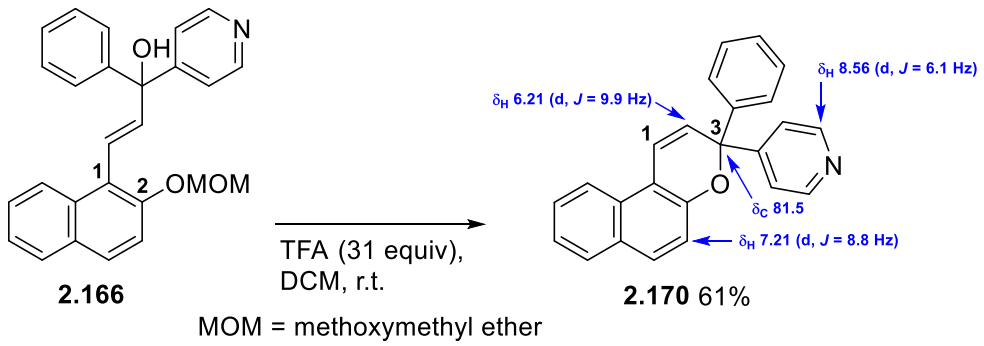

Scheme 2.79 Synthesis of 3-(4-pyridyl)-3*H*-naphtho[2,1-*b*]pyran **2.170**.

The proposed reaction mechanism is identical to the mechanism of the synthesis of 3*H*-naphtho[2,1-*b*]pyran **2.147** described on **Scheme 2.78**: the acid-catalysed dehydration of **2.166** afforded oxonium **2.172**, which was converted to **2.173** by loss of a methyl(methylene)oxonium group. The 6π-electrocyclization of **2.173** afforded 3-(4-pyridyl)-3*H*-naphtho[2,1-*b*]pyran **2.170** (**Scheme 2.80**).

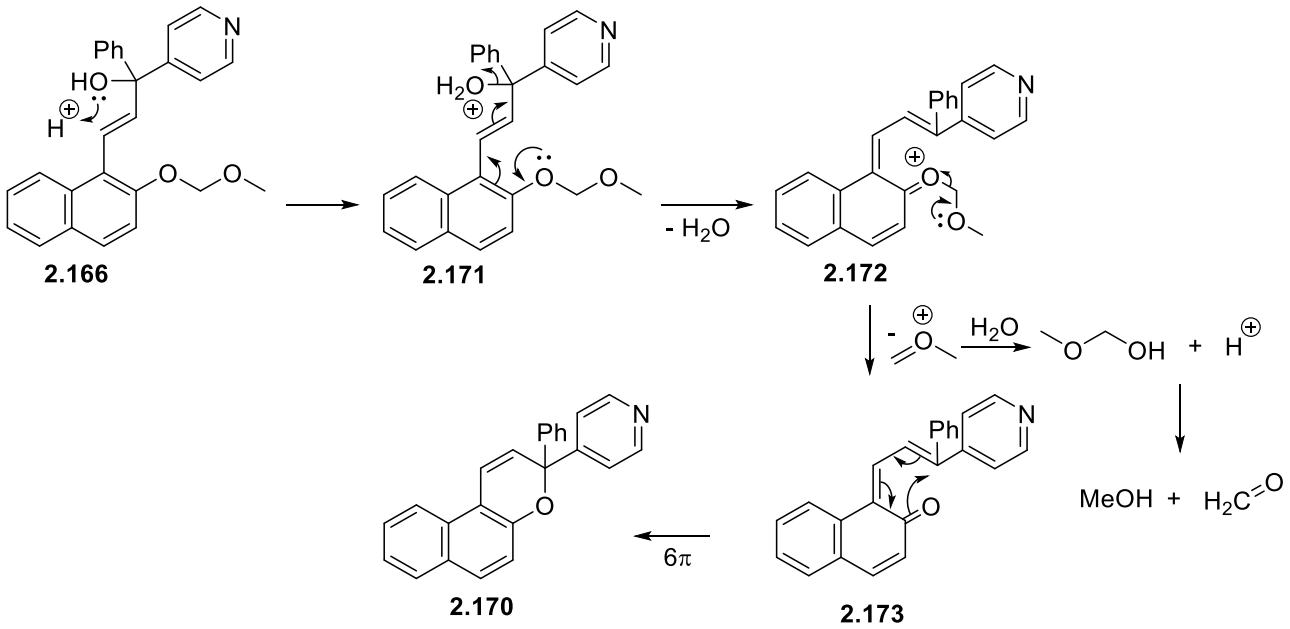

Scheme 2.80 Putative mechanism of the synthesis of 3-(4-pyridyl)-3*H*-naphtho[2,1-*b*]pyran **2.170**.

Overall, 3-(4-pyridyl)-3*H*-naphtho[2,1-*b*]pyran **2.170** was prepared from 1-bromo-2-naphthol **2.137** in a three step linear route in 25% yield.

2.1.3 Strategy C – By a Suzuki cross-coupling reaction before chromenization

2.1.3.1 Attempted Synthesis of 5-Pyridyl-3*H*-Naphtho[2,1-*b*]pyrans

Even though 5-(4-pyridyl)-3*H*-naphtho[2,1-*b*]pyran **2.106** was prepared according to **Strategy A**, it was envisioned that it could also be synthesized according to **Strategy C**. By doing so, it would provide an interesting comparative study in terms of the efficiency of both strategies. Hence, the commercially available 2-methoxynaphthalene **2.176** (£25.90 per 250 g / Alfa Aesar) and the readily to hand 3-bromo-2-methoxynaphthalene **2.174** were used as starting materials for this route.

The Suzuki cross-coupling reaction between 3-bromo-2-methoxynaphthalene **2.174** and 4-pyridineboronic acid pinacol ester **2.35** afforded 3-(4-pyridyl)-2-methoxynaphthalene **2.175** in fair to good yield (60 – 70%) (**Scheme 2.81**).

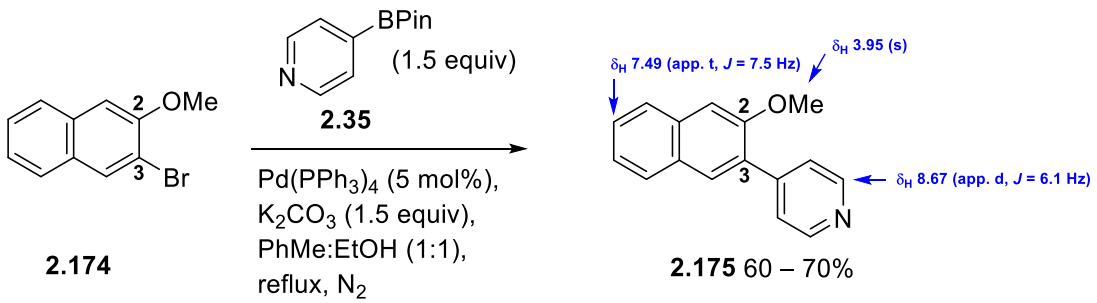

Scheme 2.81 Synthesis of 3-(4-pyridyl)-2-methoxynaphthalene **2.175**.

Furthermore, 3-(3-pyridyl)-2-methoxynaphthalene **2.178** was prepared from the very cheap 2-methoxynaphthalene **2.176** in 27% yield in over two steps (**Scheme 2.82**). First, *n*-BuLi was employed to *ortho*-lithiate 2-methoxynaphthalene **2.176** at C-3 giving **2.179**, which was later treated with 1,2-dibromoethane affording 3-bromo-2-methoxynaphthalene **2.174** (**Scheme 2.83**).[215] The latter was then coupled with 3-pyridineboronic acid pinacol ester **2.177** to give the desired product **2.178**.

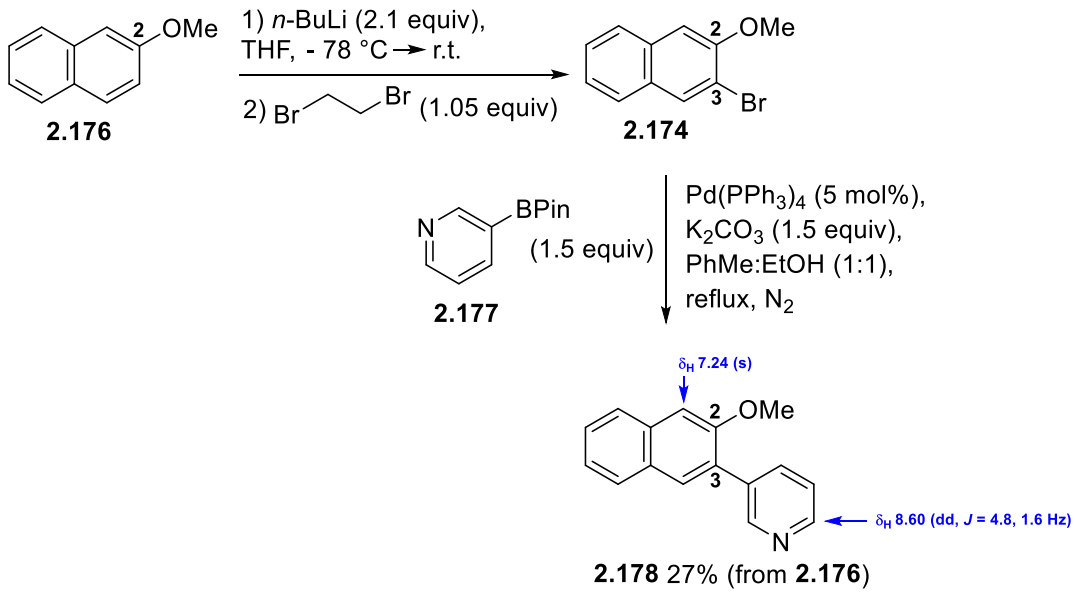

Scheme 2.82 Synthesis of 3-(3-pyridyl)-2-methoxynaphthalene **2.178**.

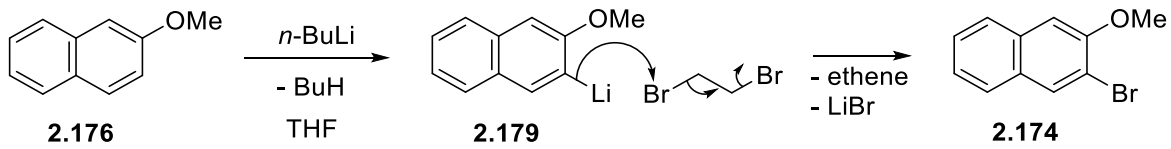

Scheme 2.83 Mechanism of the synthesis of 3-bromo-2-methoxynapthalene **2.174** from 2-methoxynaphthalene **2.176**.

By using HBr (45% w/v) in acetic acid/water at reflux, the 3-pyridyl-2-methoxynaphthalenes **2.175** and **2.178** were demethylated to afford the corresponding 3-pyridyl-2-naphthols **2.180** and **2.181** in 90% and 63% yield, respectively (**Scheme 2.84**). The demethylation of **2.178** to access **2.181** required two extra days of reflux, when compared to the demethylation of **2.175**, which led to more decomposition in the reaction mixture due to the longer exposure to the very harsh reaction conditions. Consequently, the isomer **2.181** was isolated in lower yield when compared to **2.180**.

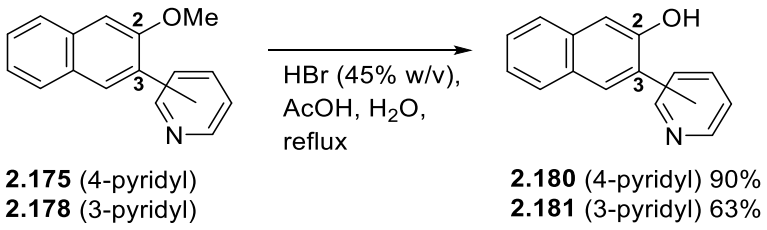

Scheme 2.84 Synthesis of 3-pyridyl-2-naphthols **2.180** and **2.181**.

As an example, the mechanism of demethylation of 3-(4-pyridyl)-2-methoxynaphthalene **2.175** comprises the protonation of the methoxyl group leading to the oxonium **2.182** (**Scheme 2.85**). The nucleophilic attack of the bromide ion to the methyl of **2.182** cleaved the ether bond in a S_N2 displacement reaction leading to desired **2.180** and bromobutane.

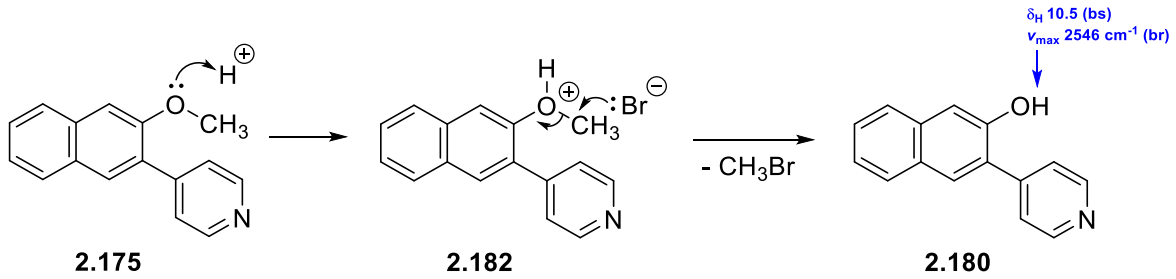

Scheme 2.85 Mechanism of the demethylation of 3-(4-pyridyl)-2-methoxynaphthalene **2.175**.

Since there was only a limited amount of 3-pyridyl-2-naphthols **2.180** and **2.181** for the following steps, a few test reactions were performed on the more readily available isomer 6-(4-pyridyl)-2-naphthol **2.183**, which was prepared from the Suzuki cross-coupling reaction between 6-bromo-2-naphthol **2.55** with 4-pyridineboronic acid pinacol ester **2.35** in fair yield (52 – 61%) (**Scheme 2.86**).

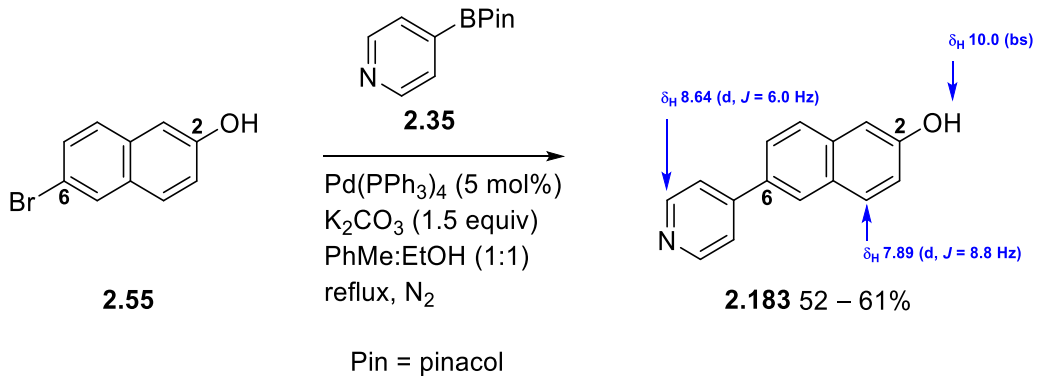

Scheme 2.86 Synthesis of 6-(4-pyridyl)-2-naphthol **2.183**.

The reaction between **2.183** and propynol **2.33** by using PPTS (5 mol%) and trimethylorthoformate (4.0 equiv) in 1,2-DCE at reflux led to no change in the reaction mixture (**Scheme 2.87**). It was rationalized that, under the reaction conditions, the PPTS was being consumed by protonating the basic pyridyl subtituent of **2.183**.

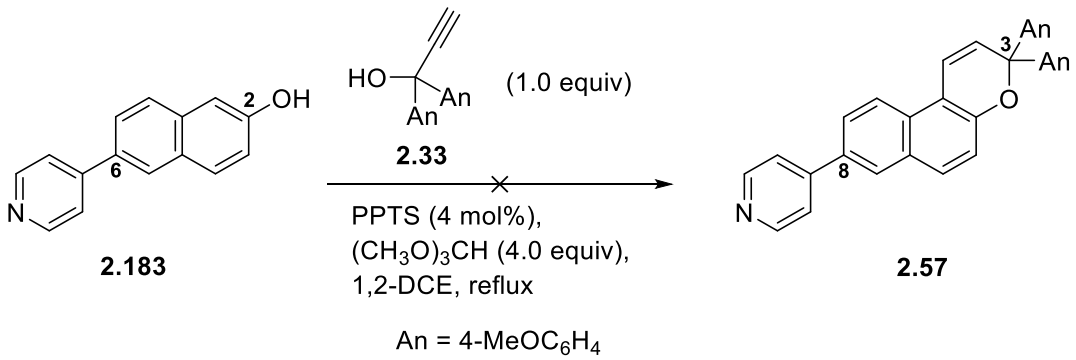

Scheme 2.87 Failed synthesis of 8-(4-pyridyl)-3*H*-naphtho[2,1-*b*]pyran **2.57**.

In addition, the reaction between **2.183** and propynol **2.33** by using PPTS (1.1 equiv) and trimethylorthoformate (2.0 equiv) in 1,2-DCE at reflux generated a very complex mixture from which the desired product **2.57** was not isolated (**Scheme 2.88**).

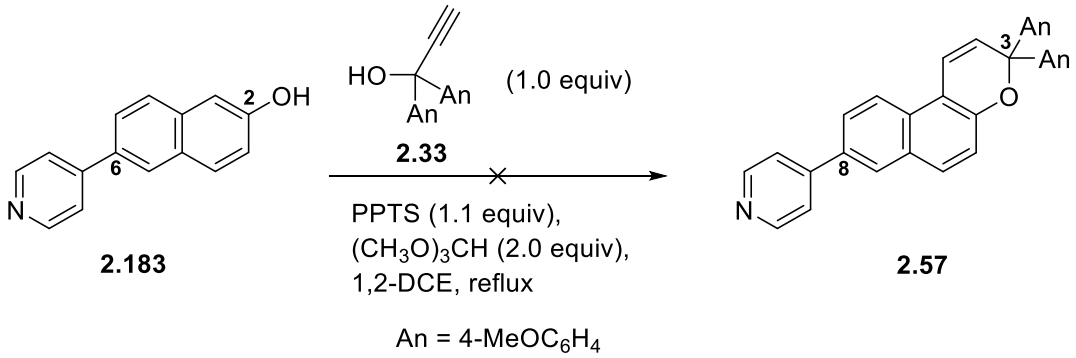

Scheme 2.88 Failed synthesis of 8-(4-pyridyl)-3*H*-naphtho[2,1-*b*]pyran **2.57**.

It was rationalized that the 6-(4-pyridinium)-2-naphthol *p*-toluenesulfonate salt **2.184**, formed in the reaction mixture, was too deactivated to undergo an acid-catalysed condensation reaction with propynol **2.33**. As a result, the route for the preparation of pyridyl substituted 3*H*-naphtho[2,1-*b*]pyrans by following **Strategy C** – By the direct acid-catalysed condensation – was abandoned.

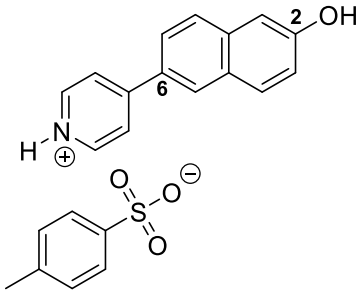

2.184

As an alternative, and considering the success of the Heck protocol to access 3-(4-pyridyl)-3*H*-naphtho[2,1-*b*]pyran **2.170**, **Strategy C** – By the Heck cross-coupling reaction – seemed to be a worthwhile strategy to prepare the 5-pyridyl-3*H*-naphtho[2,1-*b*]pyrans.

In a test reaction, by using molecular bromine (1.1 equiv) in an acetic acid/water mixture at room temperature, bromination of 6-(4-pyridyl)-2-naphthol **2.183** occurred at both C-1 and C-3, giving 1,3-dibromo-6-(4-pyridyl)-2-naphthol **2.185** in very poor yield (18%) (**Scheme 2.89**).[216] Thus, the formation of **2.185** was determined by HRMS analysis, as the mass spectrum revealed an ion corresponding to the $[M+H]^+$ adduct with M = $C_{15}H_9{}^{81}Br_2NO$. In retrospect, using only 0.5 equiv of Br_2 might have been a better choice to synthesize the target 1-bromo-6-(4-pyridyl)-2-naphthol **2.186**, considering the lack of regioselectivity.

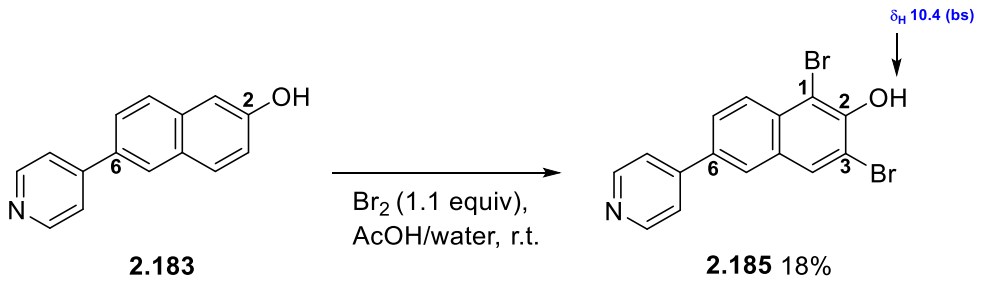

Scheme 2.89 Synthesis of 1,3-dibromo-6-(4-pyridyl)-2-naphthol **2.185**.

By employing *N*-bromosuccinimide (NBS) in DMF at room temperature, bromination occurred regioselectively at C-1 affording 1-bromo-6-(4-pyridyl)-2-naphthol **2.186** (**Scheme 2.90**).[217] It is noteworthy that the bromination happened spontaneously as soon as NBS was added. Unnecessary prolonging of the reaction led to a substantial drop in the yield – 56% after 30 min and 11% after 100 min – due to decomposition. In the reaction mechanism, NBS served as the bromide source for the S_EAr reaction at C-1 (**Scheme 2.91**).

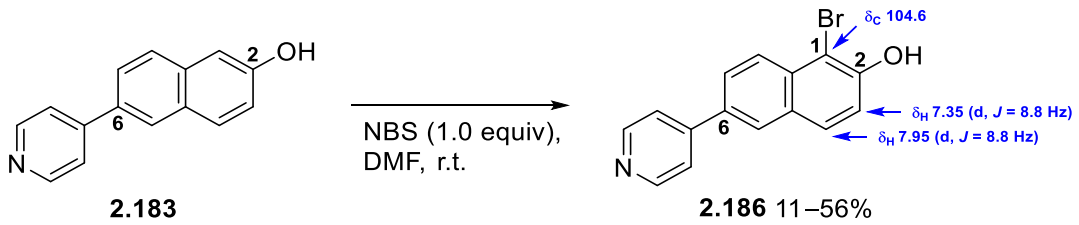

Scheme 2.90 Synthesis of 1-bromo-6-(4-pyridyl)-2-naphthol **2.186**.

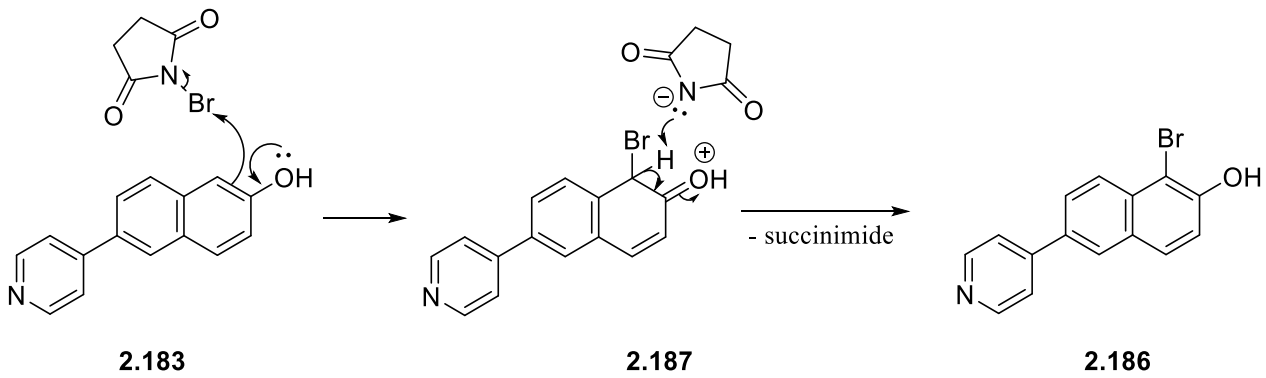

Scheme 2.91 Mechanism for the synthesis of 1-bromo-6-(4-pyridyl)-2-naphthol **2.186**.

In a test reaction, 1-bromo-6-(4-pyridyl)-2-(methoxymethoxy)naphthalene **2.188** was prepared from the base-catalysed S_N2 reaction between 1-bromo-6-(4-pyridyl)-2-naphthol **2.186** and MOMCl in fair yield (63%).

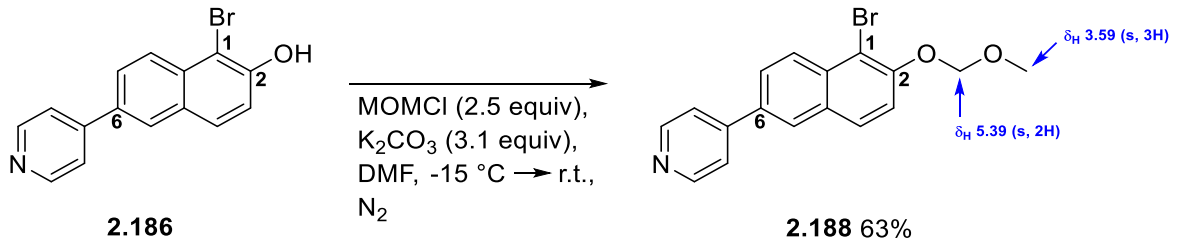

Scheme 2.92 Synthesis of 1-bromo-6-(4-pyridyl)-2-(methoxymethoxy)naphthalene **2.188**.

At this point the focus was shifted towards the bromination of 3-pyridyl-2-naphthols **2.180** and **2.181**. Hence, 1-bromo-3-pyridyl-2-naphthols **2.189** and **2.190** were prepared by the regioselective bromination of 3-pyridyl-2-naphthols **2.180** and **2.181** in 73% and 35% yield, respectively, by using NBS in DMF. The disparity in the yields of the brominations was due to differences in the reaction times – 35 min for isomer **2.189** and 166 min for isomer **2.190**. Thus, the prolonged reaction time in the synthesis of isomer **2.190** led to a substantial amount of decomposition in the crude mixture and ultimately to a poor yield.

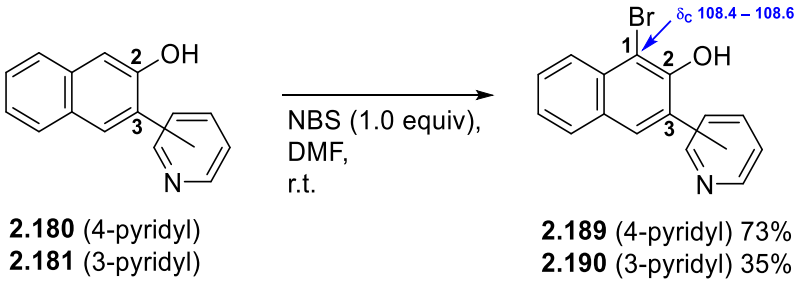

Scheme 2.93 Synthesis of 1-bromo-3-pyridyl-2-naphthol **2.189** and **2.190**.

Protection of the hydroxyl group of the 1-bromo-3-pyridyl-2-naphthols **2.189** and **2.190** as methoxymethyl ethers was accomplished by reaction with MOMCl, in the presence of K_2CO_3 in DMF (**Scheme 2.94**). The corresponding 1-bromo-3-pyridyl-2-(methoxymethoxy)naphthalenes **2.191** and **2.192** were isolated in 33% and 25% yield, respectively. It was rationalized that the poor yields attained were a consequence of the very sterically hindered hydroxyl groups by both the

ortho bromine and pyridyl substituents. In retrospect, these reactions could have been prolonged for longer than just 2h and/or performed at a higher temperature.

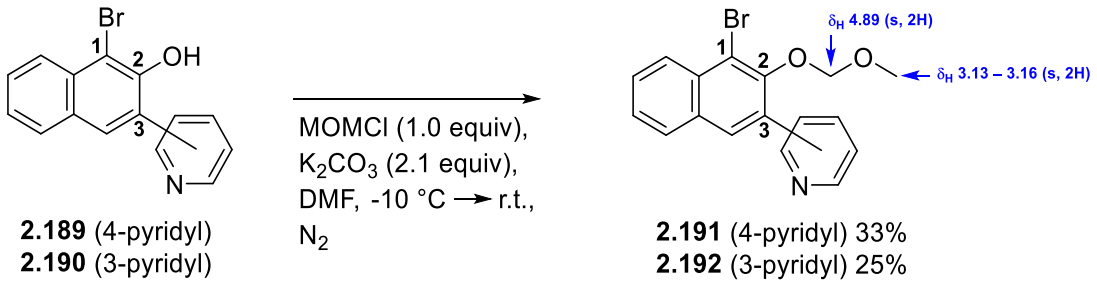

Scheme 2.94 Synthesis of 1-bromo-3-pyridyl-2-(methoxymethoxy)naphthalene **2.191** and **2.192**.

The Heck cross-coupling reaction between 1-bromo-3-(4-pyridyl)-2-(methoxymethoxy)naphthalene **2.191** and Heck partner **2.129** by using $Pd(OAc)_2$ (7 mol%), K_2CO_3 (1.5 equiv), TBAB (1.5 equiv), KCl (1 equiv) in DMF at 100 °C under N_2 led to the formation of the desired Heck product **2.193**. However, the latter was not isolated after flash column chromatography purification.

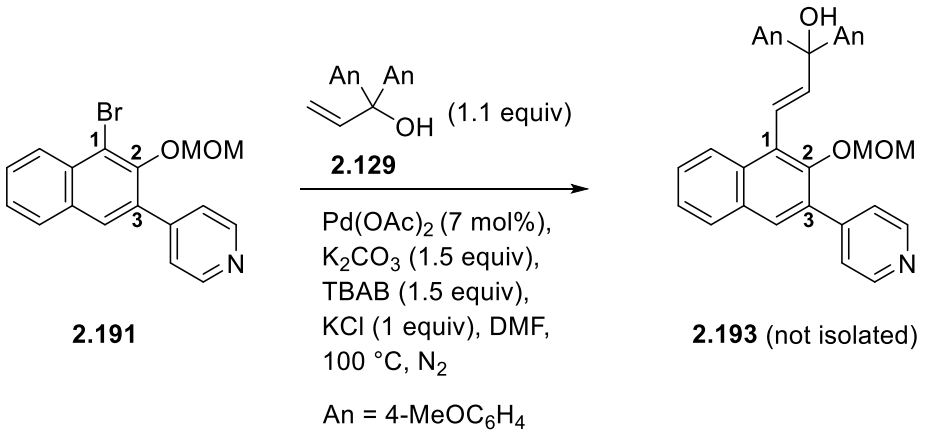

Scheme 2.95 Attempted synthesis of Heck product **2.193**.

The same conditions were employed to synthesize the Heck product **2.194** from the Heck cross-coupling reaction between 1-bromo-3-(3-pyridyl)-2-(methoxymethoxy)naphthalene **2.192** and the Heck partner **2.129** (**Scheme 2.96**). The desired product was isolated as a mixture in very poor yield (< 11%) after flash column chromatography purification. Considering the very small amount of product attained (0.04 g), this mixture was not purified again.

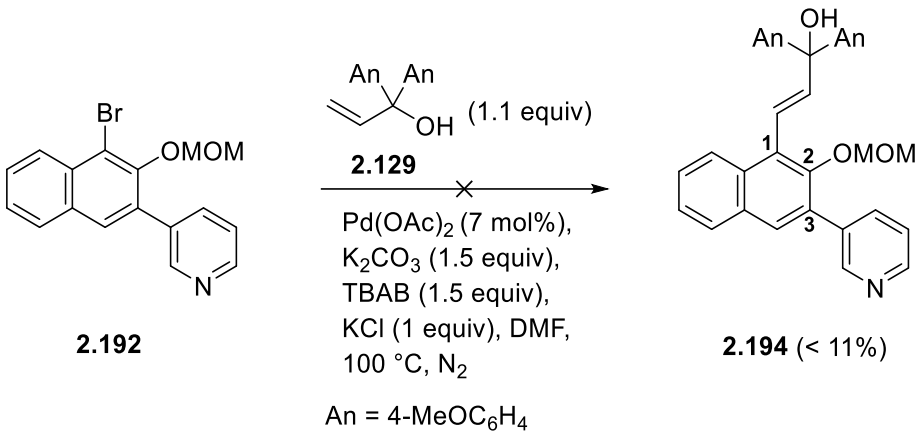

Scheme 2.96 Synthesis of Heck product **2.194**.

TLC analysis of the reaction mixture indicated that the Heck-cross couplings reactions were taking place at a very slow rate as both the Heck products and the corresponding starting materials were present in the crude mixture even after several days of reaction. This observation clearly indicated that the Heck conditions employed were far from ideal. It could be argued if by using $Pd(dba)_2$ (2 mol%), $P(t\text{-}Bu)_3HBF_4$ (4 mol%), *N*-methyldicyclohexylamine (Cy_2NMe) (1.5 equiv), TBAC (10 mol%) in DMAc at 100 °C the outcome of the Heck couplings would have been different, as the latter conditions led to a substantial improvement in the yield of the Heck cross-coupling reaction between **2.162** and **2.129** (**Entry 3**, **Table 2.6**). However, considering the different nature of the substrates this argument is difficult to support. Furthermore, there was clear decomposition during the flash column chromatography purifications as multiples fractions, that there were not present before in the TLC of the crude mixtures, appeared during the separations.

As a result of the unsucessful Heck cross-coupling reactions, there were no more 1-bromo-3-pyridyl-2-(methoxymethoxy)naphthalenes **2.191** and **2.192** available for further experiments. Consequently, the route according to **Strategy C** – By the Heck cross-coupling reaction – for the preparation of 5-pyridyl-3*H*-naphtho[2,1-*b*]pyrans was abandoned.

2.1.3.2 Synthesis of 6-Pyridyl-Naphtho[2,1-*b*]pyrans

It was envisioned that 6-pyridyl-3*H*-naphtho[2,1-*b*]pyrans could be prepared according to **Strategy C** – By the Heck cross-coupling reaction. Despite the failure of this strategy to access the 5-pyridyl-3*H*-naphtho[2,1-*b*]pyrans, it was predicted that, by overcoming the Heck cross-coupling reaction problem, the desired 6-pyridyl-3*H*-naphtho[2,1-*b*]pyrans would be attained. Thus, the commercially available but expensive 1,3-dihydroxynaphthalene **2.195** (£96.60 per 5g / Alfa Aesar) was used as the starting material for this route.

Initially, 3-methoxy-1-naphthol **2.196** was synthesized in 86% yield by the regioselective *O*-methylation of 1,3-dihydroxynaphthalene **2.195** at C-3 by treatment with dry methanolic HCl from acetyl chloride – previously prepared in 63% yield from the reaction between acetic acid and thionyl chloride – and methanol (**Scheme 2.97**).[218] Additionally, 1,3-dimethoxynaphthalene **2.197** was isolated as a by-product in 14% yield. In the reaction mechanism, the dry HCl produced *in situ* from the reaction between methanol and acetyl chloride protonates regioselectively the hydroxyl group at C-3 (**Scheme 2.98**). The regioselectivity derives from the extra resonance structure in the resonance hybrid that is generated when the hydroxyl group at C-3 is protonated, which leads to an additional stabilization of oxonium **2.198** when compared to oxonium **2.201**. Thus, the nucleophilic attack of methanol to **2.198** displaces a water molecule in S_NAr type reaction affording 3-methoxy-1-naphthol **2.196**.

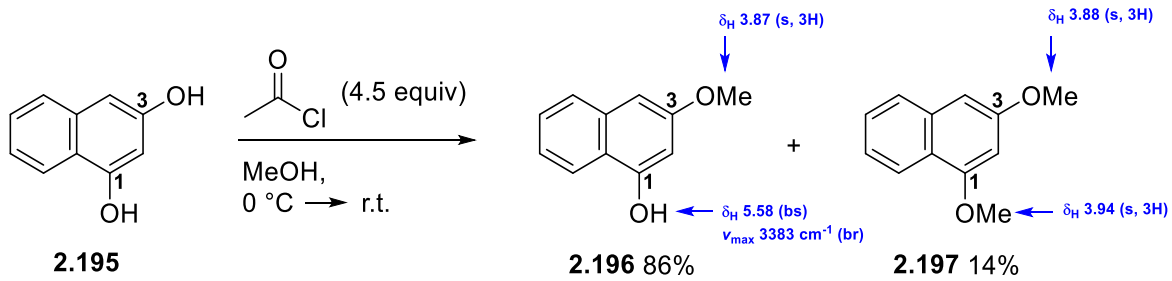

Scheme 2.97 Synthesis of 3-methoxy-1-naphthol **2.196**.

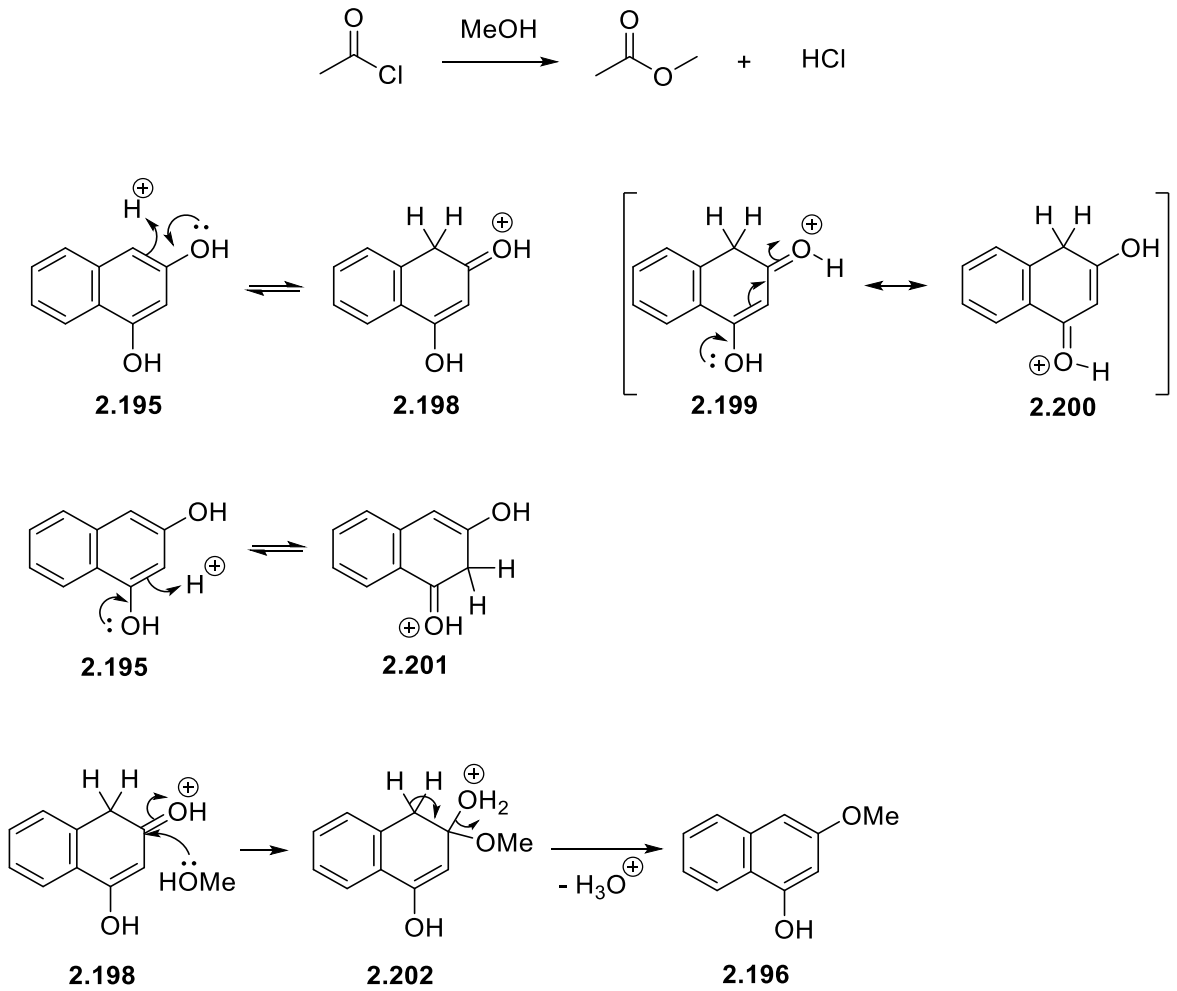

Scheme 2.98 Mechanism for the synthesis of 3-methoxy-1-naphthol **2.196**.

Afterwards, triflation of 3-methoxy-1-naphthol **2.196** by treatment with triflic anhydride and Et_3N in DCM afforded the desired 3-methoxy-1-triflyloxynaphthalene **2.203** in very good yield (81%) (**Scheme 2.99**).

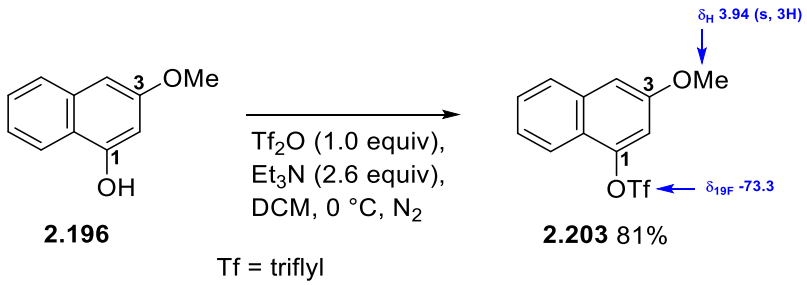

Scheme 2.99 Synthesis of 3-methoxy-1-triflyloxynaphthalene **2.203**.

Subsequently, 3-methoxy-1-triflyloxynaphthalene **2.203** was successfully coupled with 4-pyridine- and with 3-pyridine-boronic acid pinacol ester giving the corresponding 2-methoxy-4-pyridylnaphthalenes **2.204** and **2.205** in good (72 – 79%) to excellent (91%) yield, respectively (**Scheme 2.100**).

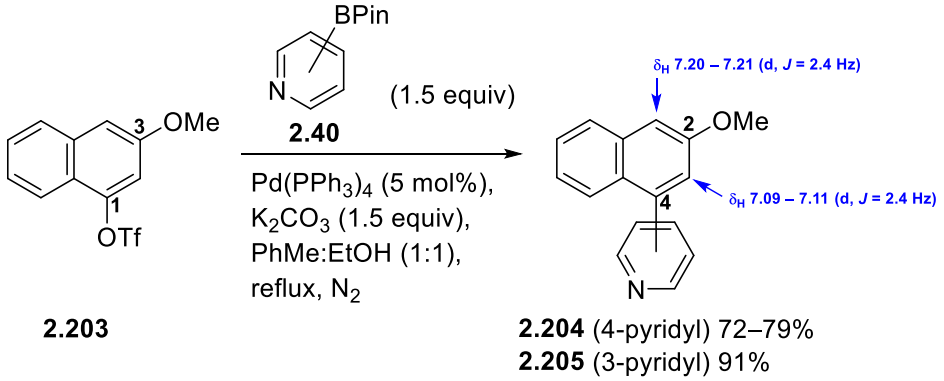

Scheme 2.100 Synthesis of 2-methoxy-4-pyridylnaphthalenes **2.204** and **2.205**.

Afterwards, the 2-methoxy-4-pyridylnaphthalenes **2.204** and **2.205** were both demethylated by the action of hydrobromic acid (45% w/v) in acetic acid:H_2O at reflux giving the corresponding 4-pyridyl-2-naphthols **2.206** and **2.207** in 78 – 93% and 75% yield, respectively (**Scheme 2.101**).

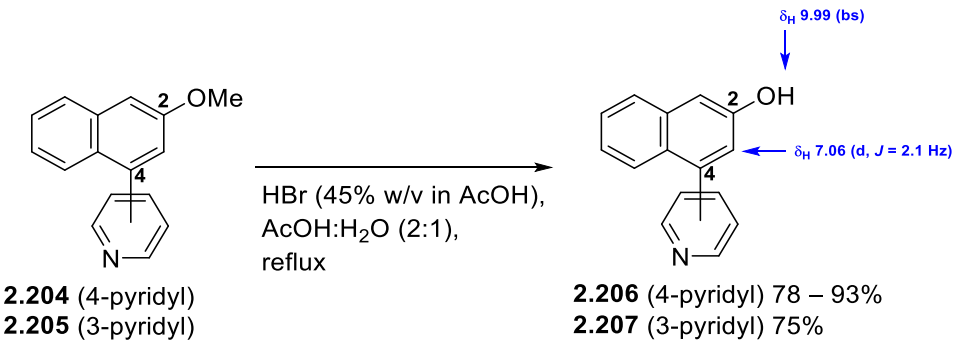

Scheme 2.101 Synthesis of 4-pyridyl-2-naphthols **2.206** and **2.207**.

By employing *N*-bromosuccinimide (NBS) in DMF at 52 °C, bromination occurred regioselectively at the C-1 of the 4-pyridyl-2-naphthols **2.206** and **2.207** affording 1-bromo-4-pyridyl-2-naphthols **2.208** and **2.209** in 54 and 57% yield, respectively (**Scheme 2.102**).

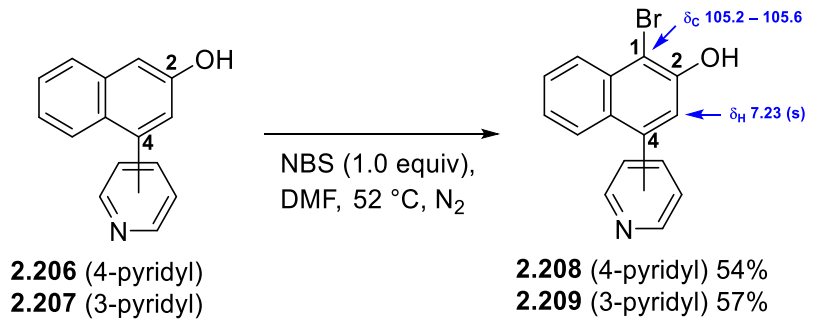

Scheme 2.102 Synthesis of 1-bromo-4-pyridyl-2-naphthols **2.208** and **2.209**.

Protection of the hydroxyl groups of 1-bromo-4-pyridyl-2-naphthols **2.208** and **2.209** as methoxymethyl ethers was achieved by reaction with MOMCl in the presence of K_2CO_3 in DMF, leading to the corresponding 1-bromo-4-pyridyl-2-(methoxymethoxy)naphthalenes **2.210** and **2.211** in 78% and 74% yield, respectively **(Scheme 2.103**). The yields obtained for the MOM protection of 1-bromo-4-pyridyl-2-naphthols **2.208** and **2.209** were noticeably higher than for the MOM protection of 1-bromo-3-pyridyl-2-naphthols **2.191** and **2.192**, because for the formers the hydroxyl groups were much less sterically hindered by comparison.

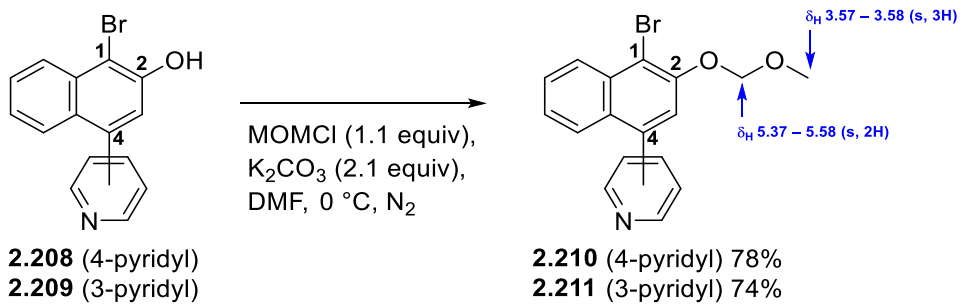

Scheme 2.103 Synthesis of MOM-protected naphthalenes **2.210** and **2.211**.

Previously, the Heck cross-coupling reactions between 1-bromo-3-pyridyl-2-(methoxymethoxy)naphthalenes **2.191** and **2.192** and the Heck partner **2.129** by using $Pd(OAc)_2$ (7 mol%), K_2CO_3 (1.5 equiv), TBAB (1.5 equiv), KCl (1 equiv) in DMF at 100 °C under N_2 led to unsatisfactory outcomes (**Schemes 2.95** and **2.96**). Nevertheless, for comparison, the same conditions were applied for the Heck cross-coupling reactions between 1-bromo-4-pyridyl-2-(methoxymethoxy)naphthalenes **2.210** and **2.211** and the Heck partner **2.129** (**Scheme 2.104**). TLC analysis indicated that the cross-coupling reactions occurred at a faster rate as there were just minor amounts of the starting materials **2.210** and **2.211** after two days of reaction. Thus, flash column

chromatography purification afforded the Heck products **2.212** and **2.213** in 29% and 55% yield, respectively. Furthermore, besides the desired products, other non-identified fractions were also isolated. These fractions were probably the result of decomposition during the chromatography separation as they were not seen in the TLC of the crude mixtures.

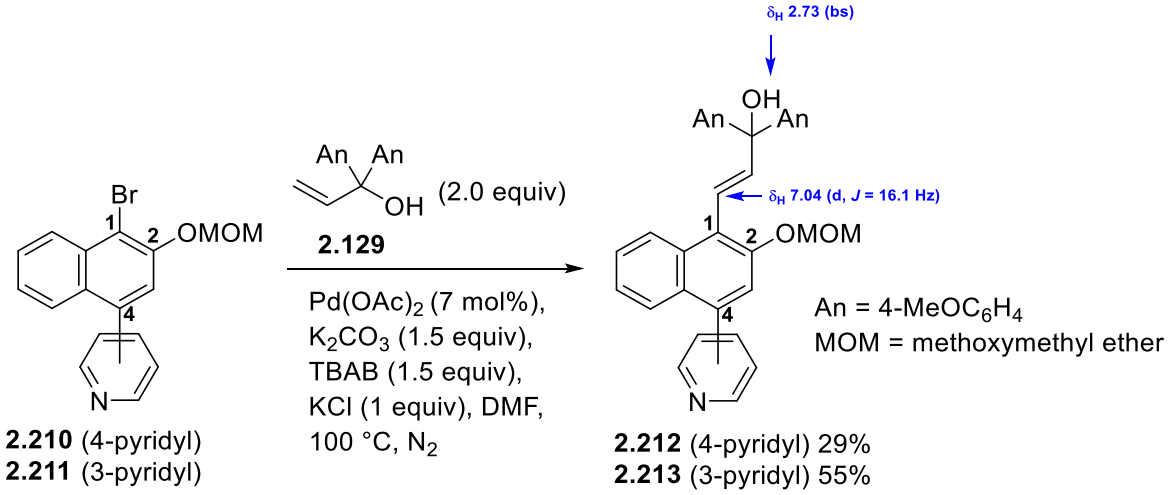

Scheme 2.104 Synthesis of Heck products **2.212** and **2.213**.

A possible explanation for the improvement in the yield of the Heck cross-coupling reactions may be related with the electronic conjugation of the pyridyl substituent at C-4 with the C-1 in the 1-bromo-4-pyridyl-2-(methoxymethoxy)naphthalenes **2.210** and **2.211** (**Scheme 2.105**). In contrast, the pyridyl substituent at C-3 and the C-1 in the 1-bromo-3-pyridyl-2-(methoxymethoxy)naphthalenes **2.191** and **2.192** are electronically decoupled. Consequently, the oxidative addition of PdL_2 to the C – Br bond may be favoured in **2.210** and **2.211** when compared to the **2.191** and **2.192**.

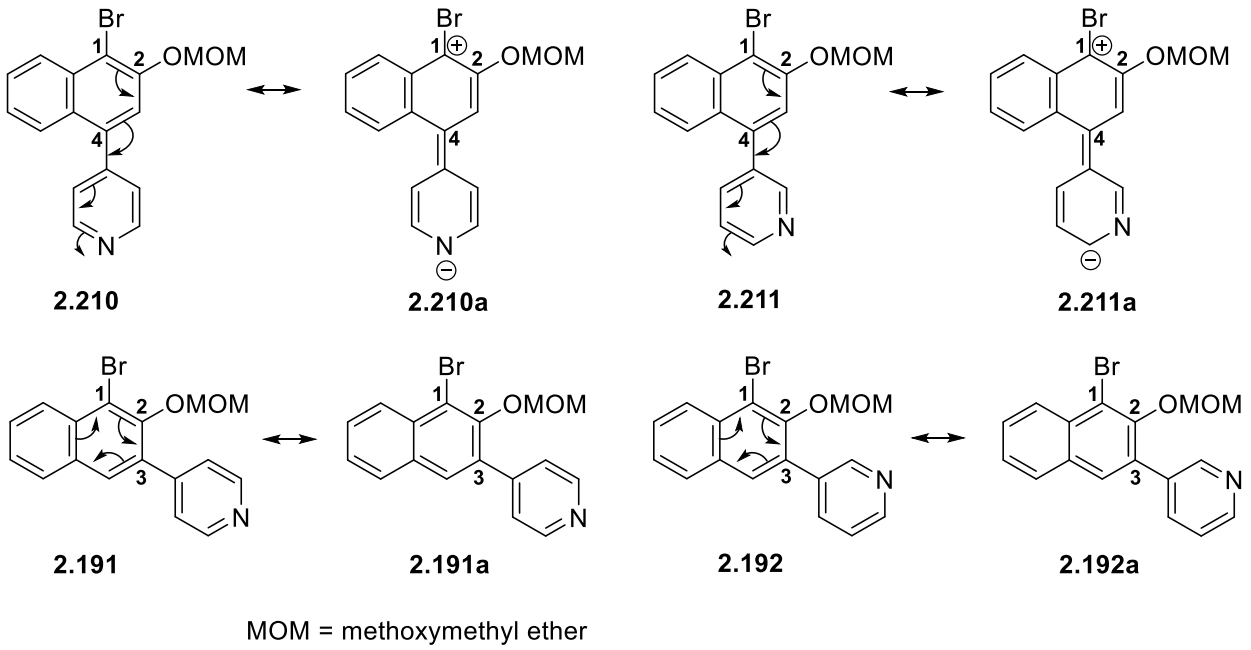

Scheme 2.105 Electronic conjugation on **2.191**, **2.192**, **2.210** and **2.211**.

In a final step, the acid-catalysed unmasking of the OH group of the Heck products **2.212** and **2.213** with concomitant cyclization afforded the corresponding 6-pyridyl-3*H*-naphtho[2,1-*b*]pyrans **2.214** and **2.215** in 61% and 69% yield, respectively (**Scheme 2.106**).

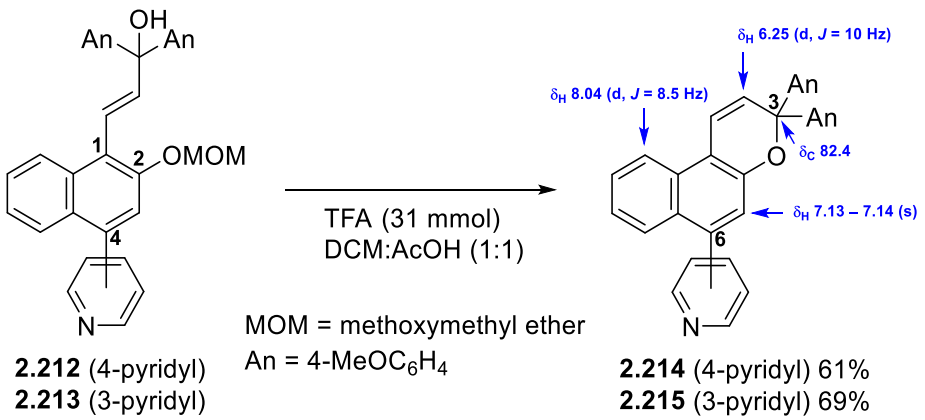

Scheme 2.106 Synthesis of 6-pyridyl-3*H*-naphtho[2,1-*b*]pyrans **2.214** and **2.215**.

Overall, the 6-pyridyl-3*H*-naphtho[2,1-*b*]pyrans **2.214** and **2.215** were prepared from 1,3-dihydroxynaphthalene **2.195** in 8 steps in 4% and 8%, respectively.

In summary, 10, 9, 8, 7, 6, 5, 3-pyridyl substituted 3*H*-naphtho[2,1-*b*]pyrans were prepared by following different strategies (**A**, **B** and **C**) as outlined in **Table 2.7**.

Table 2.7 Summary of the synthesis of the 10-, 9-, 8-, 7-, 6-, 5-, 3-pyridyl substituted 3*H*-naphtho[2,1-*b*]pyrans.

Product	Starting Material	Strategy	Number of Steps	Yield (%)
10-(4-pyridyl)-3*H*-naphtho[2,1-*b*]pyran **2.36**	8-amino-2-naphthol **2.28**	A	3	19
9-(4-pyridyl)-3*H*-naphtho[2,1-*b*]pyran **2.48**	7-bromo-2-naphthol **2.38**	A (Route A)	3	24
	2,7-dihydroxynaphthalene **2.37**	A (Route B)	3	5
9-(3-pyridyl)-3*H*-naphtho[2,1-*b*]pyran **2.50**	7-bromo-2-naphthol **2.38**	A (Route A)	3	29
	2,7-dihydroxynaphthalene **2.37**	A (Route B)	3	14
8-(4-pyridyl)-3*H*-naphtho[2,1-*b*]pyran **2.57**	6-bromo-2-naphthol **2.55**	A	2	61
	6-bromo-2-naphthol **2.55**	A (Method A)	4	32
	6-bromo-2-naphthol **2.55**	A (Method B)	3	1.3
8-(3-pyridyl)-3*H*-naphtho[2,1-*b*]pyran **2.59**	6-bromo-2-naphthol **2.55**	A	2	68
8-(2-pyridyl)-3*H*-naphtho[2,1-*b*]pyran **2.65**	6-bromo-2-naphthol **2.55**	A (Method A)	4	40
	6-bromo-2-naphthol **2.55**	A (Method B)	3	2
8-(4-pyridyl)-3*H*-naphtho[2,1-*b*]pyran **2.77**	6-bromo-2-naphthol **2.55**	A	2	53
8-(pyridyl-triazole)-3*H*-naphtho[2,1-*b*]pyran **2.110**	2,4-dibromopyridine **2.114**	A	3	11
7-(4-pyridyl)-3*H*-naphtho[2,1-*b*]pyran **2.98**	5-amino-2-naphthol **2.90**	A	5	10
6-(4-pyridyl)-3*H*-naphtho[2,1-*b*]pyran **2.214**	1,3-dihydroxynaphthalene **2.195**	C	8	4
6-(3-pyridyl)-3*H*-naphtho[2,1-*b*]pyran **2.215**	1,3-dihydroxynaphthalene **2.195**	C	8	8
5-(4-pyridyl)-3*H*-naphtho[2,1-*b*]pyran **2.106**	2,3-dihydroxynaphthalene **2.100**	A	3	17
3-(4-pyridyl)-3*H*-naphtho[2,1-*b*]pyran **2.170**	1-bromo-2-naphthol **2.137**	B	3	25

2.2 Synthesis of Photochromic Rhenium(I) Complexes

2.2.1 Synthesis of *fac*-[Re(N^N)(CO)$_3$Cl]^0

The synthesis of the *fac*-[Re(N^N)(CO)$_3$Cl]^0 complexes **2.216** was performed based on the high-yielding and wide-ranging methodology described by Stoeffler *et al.* (**Scheme 2.107**). [219] Thus, by mixing rhenium pentacarbonyl chloride with an equimolar amount of the readily accessible within the department bidentate ligand (N^N) in PhMe at reflux the *fac*-[Re(N^N)(CO)$_3$Cl]^0 complexes **2.218**, **2.220**, **2.222**, **2.224** and **2.226** were prepared in fair to excellent yield (62–96%) (**Table 2.8**).

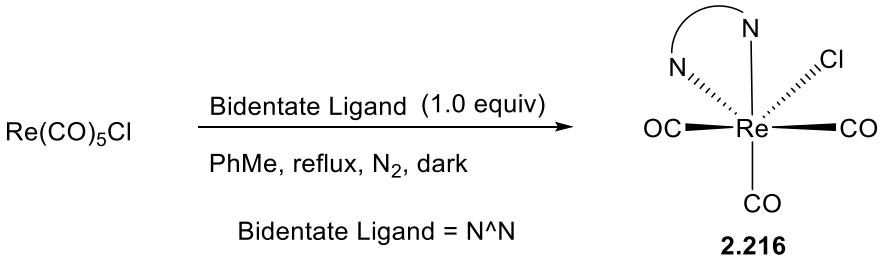

Scheme 2.107 Synthesis of the *fac*-[Re(N^N)(CO)$_3$Cl]^0 complexes **2.216**.

Incorporation of bidentate ligands (N^N) by substitution of two carbon monoxide ligands of rhenium pentacarbonyl chloride occurred in a highly stereoselective fashion. The stereoselectivity of these reactions derived from the *trans* kinetic effect. Consequently, the addition of the bidentate ligands resulted in the formation of only the facial (*fac*) stereoisomers in which the three remaining carbon monoxide ligands occupy the same face of an octahedron (**Figure 2.6**). The [Re(N^N)(CO)$_3$Cl]^0 complexes **2.216** facial stereochemistry was determined by FT-IR spectroscopy. The FT-IR spectra contained one strong band at *ca.* 2027 cm^{-1} and two overlapping bands at 1927–1908 cm^{-1}, corresponding to the frequencies of the carbon monoxide stretches, which is a signature mark of the *fac* stereochemistry of tricarbonyl rhenium(I) complexes. [220]

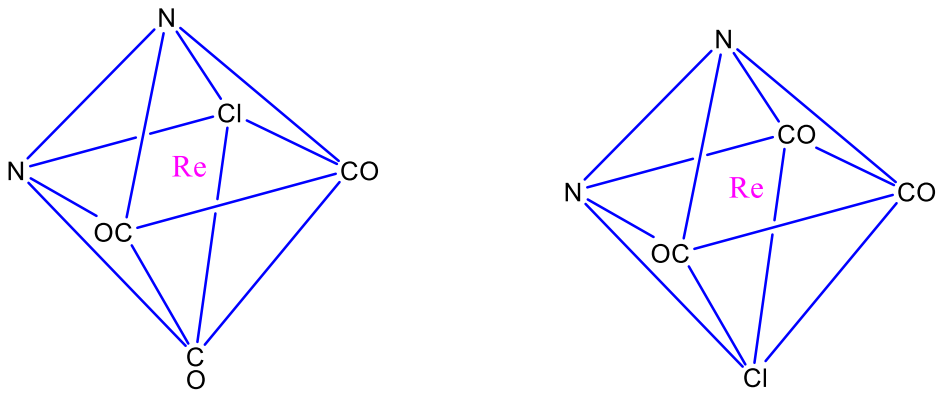

facial (*fac*) *meridional* (*mer*)

Figure 2.6 Octahedral geometry of *fac* and *mer* $[Re(N^{\wedge}N)(CO)_3Cl]^0$ complexes.

It is noteworthy that the ^{13}C NMR spectra of the *fac*-$[Re(N^{\wedge}N)(CO)_3Cl]^0$ complexes **2.216** usually contained two or three very weak signals, appearing in the range 190–196 ppm, corresponding to the resonance of the carbon monoxide carbon atoms.

Table 2.8 Synthesis of the *fac*-[Re(N^N)(CO)$_3$Cl]^0 complexes.

Entry	Bidentate Ligand (N^N)	Product	Yield (%)
1	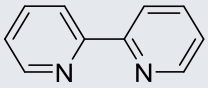 **2.217**	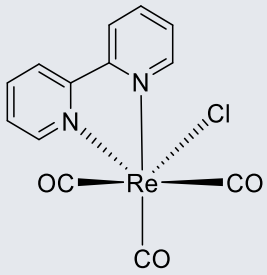 **2.218**	96
2	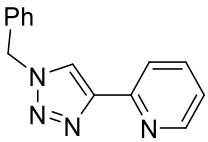 **2.219**	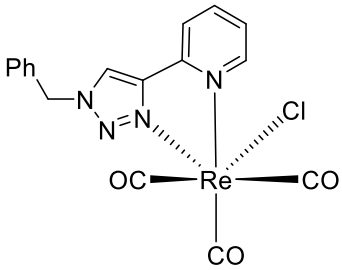 **2.220**	94
3	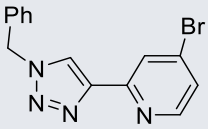 **2.221**	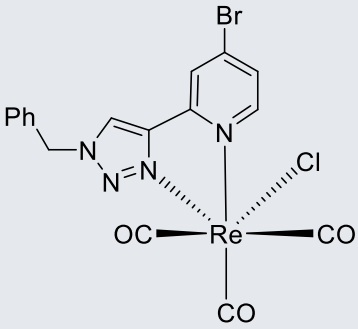 **2.222**	62
4	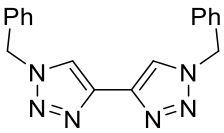 **2.223**	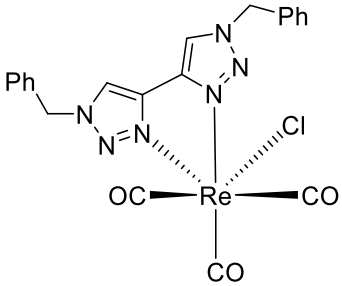 **2.224**	91
5	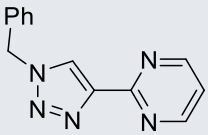 **2.225**	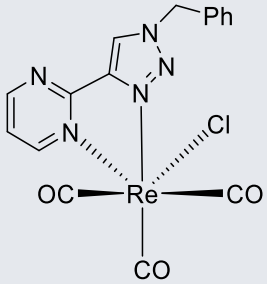 **2.226**	70

2.2.2 Synthesis of *fac*-[Re(BPy)(CO)$_3$NP]$^+$

By taking advantage of the *trans* influence, the chloride ligand of the *fac*-[Re(BPy)(CO)$_3$Cl]^0 complexes **2.218** was thermally substituted by the pyridyl substituted 3*H*-naphtho[2,1-*b*]pyrans **2.227** (**Scheme 2.108**). As a result, the corresponding *fac*-[Re(BPy)(CO)$_3$NP]$^+$ complexes **2.228** (BPy = 2,2'-bipyridine, NP = Pyridyl substituted 3*H*-naphtho[2,1-*b*]pyran) were prepared in variable yield (14–74%) (**Table 2.9**).[168] By using $AgPF_6$, the resulting *fac*-[Re(BPy)(CO)$_3$NP]$^+$ complexes **2.228** were isolated as hexafluorophosphate salts that were readily soluble in organic solvents (e.g. DCM). Additionally, the production of the virtually insoluble AgCl as a by-product worked as a thermodynamic driving force for the completion of the reactions.

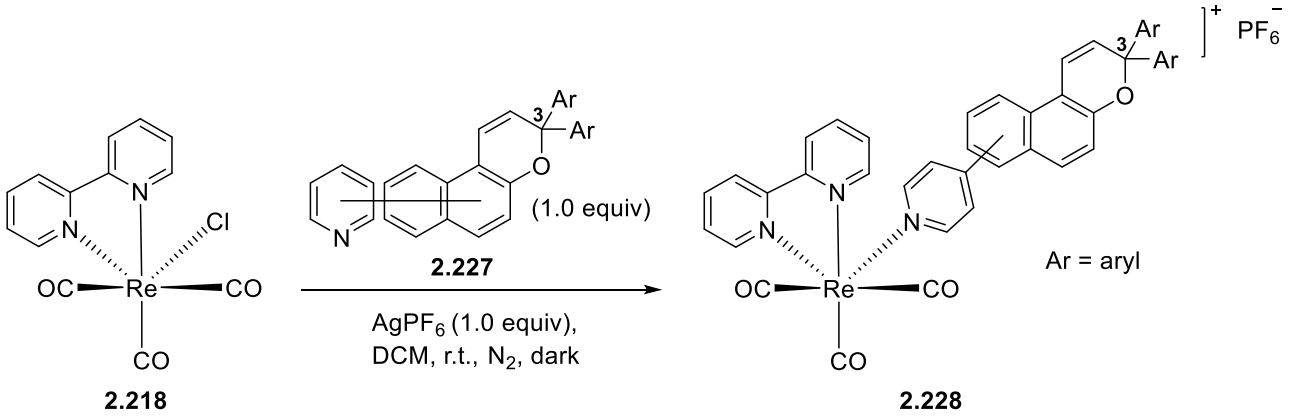

Scheme 2.108 Synthesis of the *fac*-[Re(BPy)(CO)$_3$NP]$^+$ complexes **2.228**.

HRMS data of the *fac*-[Re(BPy)(CO)$_3$NP]$^+$ complexes **2.228** was collected, all of the mass spectra contained a peak which was assigned to the ion [M-PF_6]$^+$, with M corresponding to the hexafluorophosphate salt. A crystal structure of Re(I) complex **2.232** was obtained with a R factor equal to 0.0957, indicating a good fitting between the crystallographic model and the experimental data (**Figure 2.7**). Both crystallographic and FT-IR spectroscopy data revealed that the rhenium(I) complex **2.232** had a *fac* configuration.

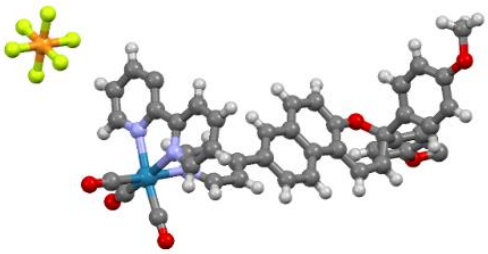

Figure 2.7 Crystal structure of rhenium(I) complex **2.232** (R = 0.0957).

Table 2.9 Synthesis of the *fac*-[Re(BPy)(CO)$_3$NP]$^+$ complexes **2.228**.

Entry	3*H*-Naphtho[2,1-*b*]pyrans	*fac*-[Re(BPy)(CO)$_3$NP]$^+$ complexes 2.228	Yield (%)
1	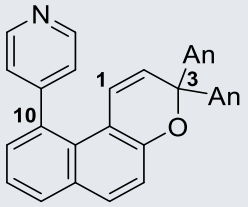 **2.36** An = 4-MeOC$_6$H$_4$	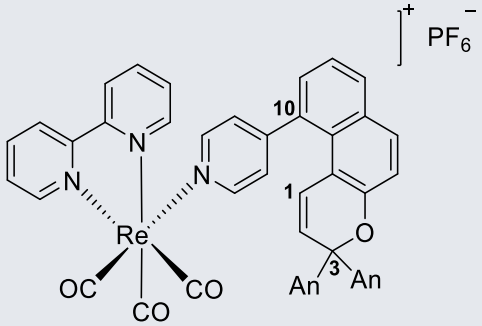 **2.229** An = 4-MeOC$_6$H$_4$	45
2	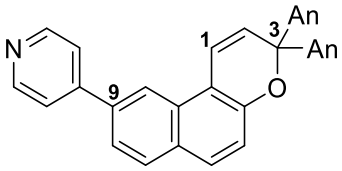 **2.48** An = 4-MeOC$_6$H$_4$	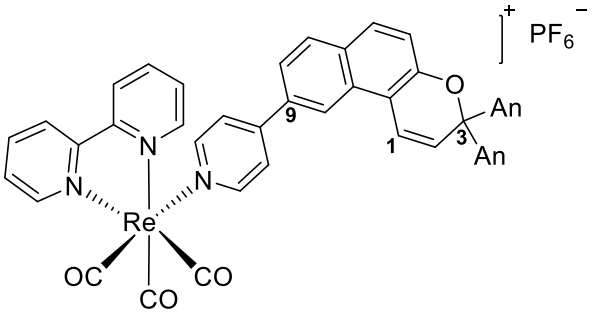 **2.230** An = 4-MeOC$_6$H$_4$	14
3	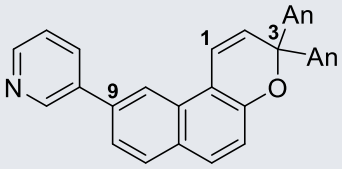 **2.50** An = 4-MeOC$_6$H$_4$	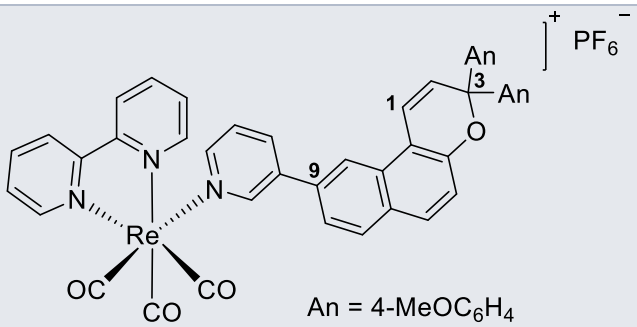 **2.231** An = 4-MeOC$_6$H$_4$	67
4	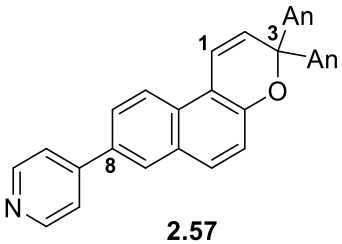 **2.57** An = 4-MeOC$_6$H$_4$	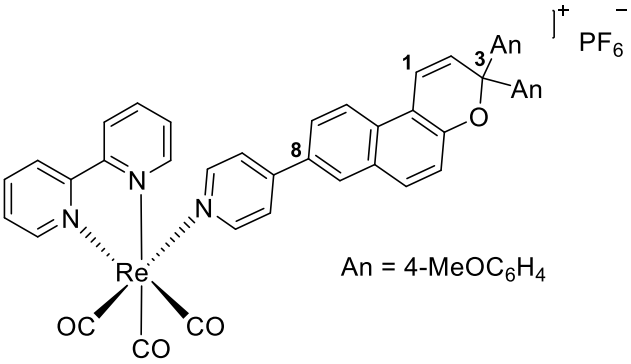 **2.232** An = 4-MeOC$_6$H$_4$	69

Table 2.9 Synthesis of the *fac*-[Re(BPy)(CO)$_3$NP]$^+$ complexes **2.228** (continuation).

Entry	3*H*-Naphtho[2,1-*b*]pyrans	*fac*-[Re(BPy)(CO)$_3$NP]$^+$ complexes 2.228	Yield (%)
5	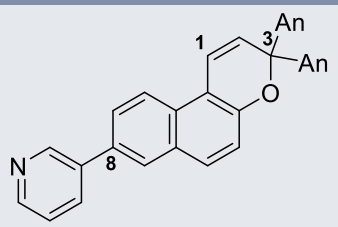 **2.59** An = 4-MeOC$_6$H$_4$	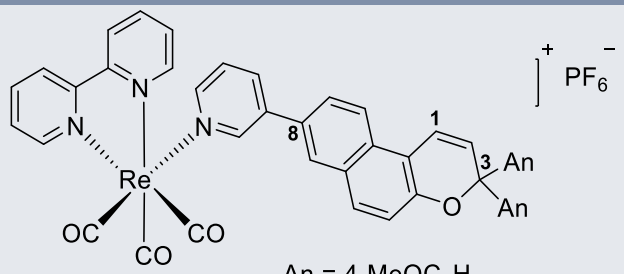 **2.233** An = 4-MeOC$_6$H$_4$	38
6	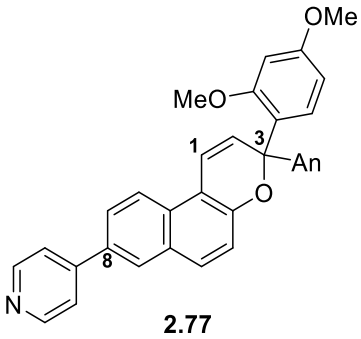 **2.77** An = 4-MeOC$_6$H$_4$	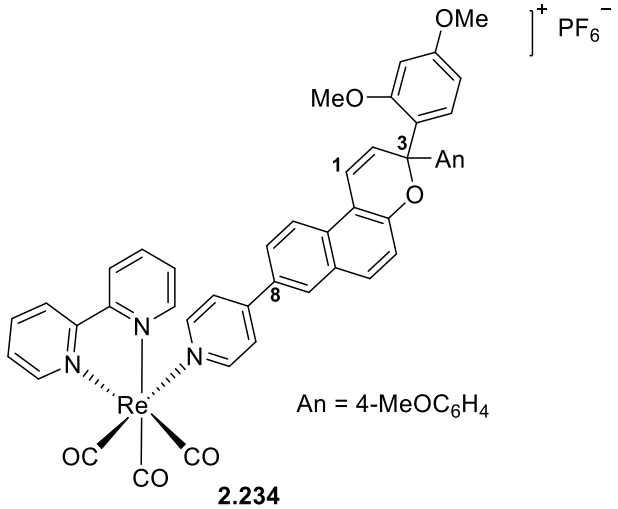 **2.234** An = 4-MeOC$_6$H$_4$	74
7	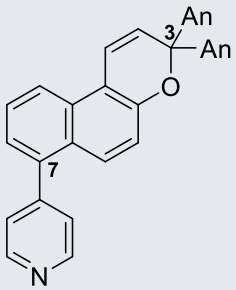 **2.98** An = 4-MeOC$_6$H$_4$	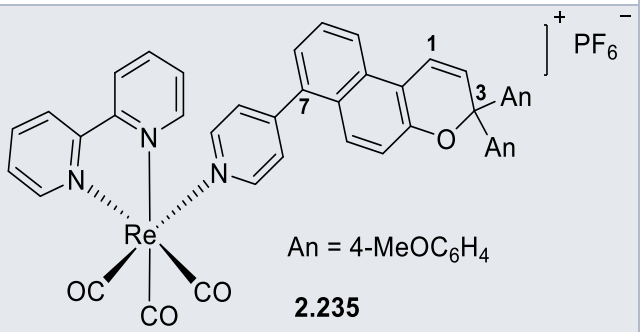 **2.235** An = 4-MeOC$_6$H$_4$	52
8	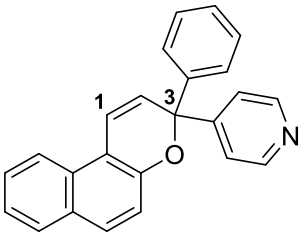 **2.170**	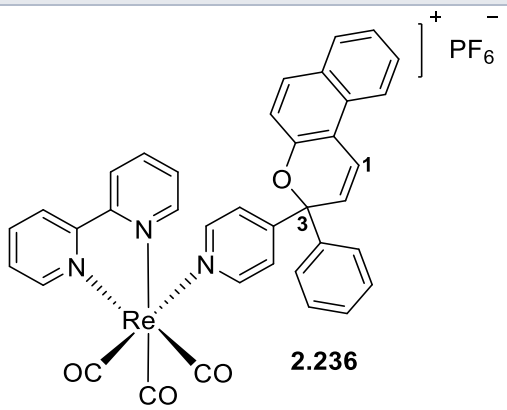 **2.236**	71

Formation of the target *fac*-[Re(BPy)(CO)$_3$NP]$^+$ complexes **2.228** was also established by NMR spectroscopy. As an example, the ^{1}H NMR spectrum of rhenium(I) complex **2.232** in DMSO-d$_6$ contained a singlet at 3.70 ppm corresponding to the resonance of 4′- and 4″-OMe, a doublet at 6.52 ppm with a coupling constant of 10.1 Hz (*cis* configuration) corresponding to the resonance of H-2, an apparent doublet at 6.89 ppm with a coupling constant of 8.8 Hz corresponding to the resonance of H-3′, H-5′, H-3″ and H-5″, a multiplet at 7.31–7.35 ppm corresponding to the resonance of H-5, H-2′, H-6′, H-2″ and H-6″, a doublet appearing at 7.46 ppm with a coupling constant of 10.1 Hz (*cis* configuration) corresponding to the resonance of H-1, a multiplet at 7.84–7.88 ppm corresponding to the resonance of H-6, H-9, H-2‴ and H-6‴, a triplet appearing at 7.95 ppm with a coupling constant of 6.5 Hz corresponding to the resonance of H-5⁗ and H-5′⁗, a doublet at 8.20 ppm with a coupling constant of 9.0 Hz corresponding to the resonance of H-10, a singlet appearing at 8.34 ppm corresponding to the resonance of H-7, a multiplet at 8.40–8.45 ppm corresponding to the resonance of H-3‴, H-5‴, H-4⁗ and H-4′⁗, a doublet appearing at 8.75 ppm with a coupling constant of 8.2 Hz corresponding to the resonance of H-3⁗ and H-3′⁗ and a doublet at 9.40 ppm with a coupling constant of 5.2 Hz corresponding to the resonance of H-6⁗ and H-6′⁗. The ^{13}C NMR spectrum of rhenium(I) complex **2.232** included a signal appearing at 55.5 ppm corresponding to the resonance of the 4′- and 4″-OMe, a signal at 82.3 ppm corresponding to the resonance of C-3, a signal appearing at 113.9 ppm corresponding to the resonance of C-3′, C-5′, C-3″ and C-5″, a signal at 128.2 ppm corresponding to the resonance of C-2′, C-6′, C-2″ and C-6″, a signal appearing at 151.9 ppm corresponding to the resonance of C-4a and two signals appearing at 192.7 ppm and 196.0 ppm corresponding to the resonance of the three carbon monoxide carbons two of which being equivalent.

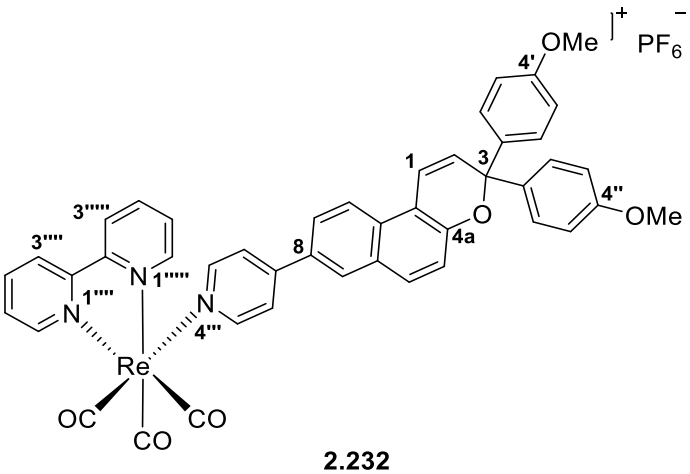

2.232

2.2.3 Synthesis of *fac*-[Re(PyTz)(CO)$_3$NP]$^+$

The *fac*-[Re(PyTz)(CO)$_3$NP]$^+$ complexes **2.237** (PyTz = 2-(1-benzyl-1*H*-1,2,3-triazol-4-yl)pyridyl 2,2′-bipyridine, NP = Pyridyl substituted 3*H*-naphtho[2,1-*b*]pyrans) were prepared by mixing the *fac*-[Re(PyTz)(CO)$_3$Cl]^0 complex **2.220** with an equimolar amount of the pyridyl substituted 3*H*-naphtho[2,1-*b*]pyrans **2.227** in DCM in the presence of an equimolar amount $AgPF_6$ (**Scheme 2.109**). The *fac*-[Re(PyTz)(CO)$_3$NP]$^+$ complexes **2.239**, **2.241**, **2.242**, **2.243**, **2.244** were isolated in good to very good yield (71–83%) (**Table 2.10**). On the other hand, the *fac*-[Re(PyTz)(CO)$_3$NP]$^+$ complexes **2.238** and **2.240** were unexplainably isolated in only 17% and 27% yield, respectively.

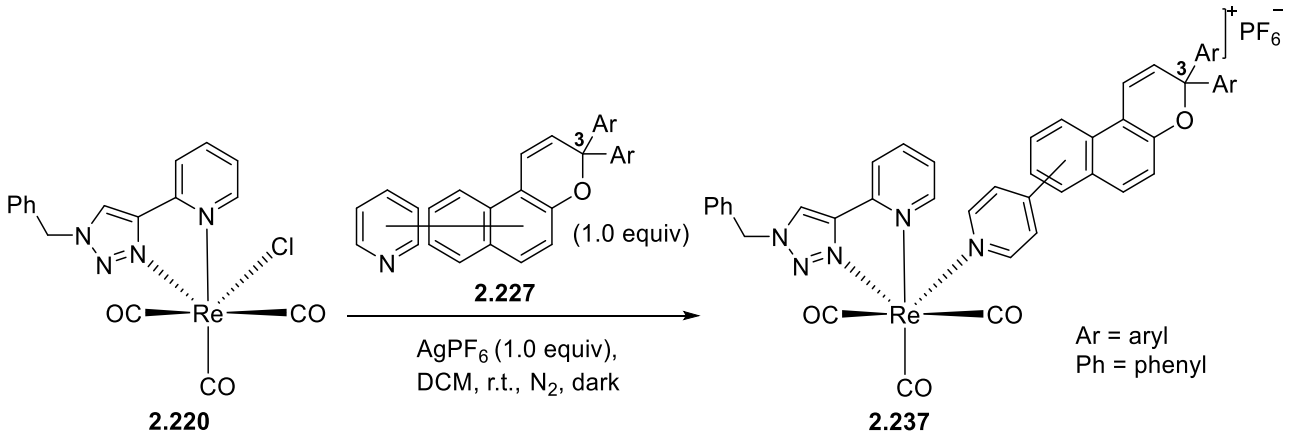

Scheme 2.109 Synthesis of the *fac*-[Re(PyTz)(CO)$_3$NP]$^+$ complexes **2.237**.

Accurate high-resolution mass spectrometry data of the *fac*-[Re(PyTz)(CO)$_3$NP]$^+$ complexes **2.237** was collected, all spectra contained a peak assigned to the ion [M-PF$_6$]$^+$, with M corresponding to the hexafluorophosphate salt. FT-IR spectroscopy data revealed that the rhenium(I) complexes **2.237** had a *fac* configuration.

Table 2.10 Synthesis of the *fac*-[Re(PyTz)(CO)$_3$NP]$^+$ complexes **2.237**.

Entry	3*H*-Naphtho[2,1-*b*]pyrans	*fac*-[Re(PyTz)(CO)$_3$NP]$^+$ complexes	Yield (%)
1	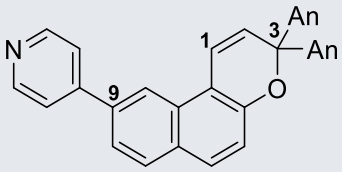 **2.48** An = 4-MeOC$_6$H$_4$	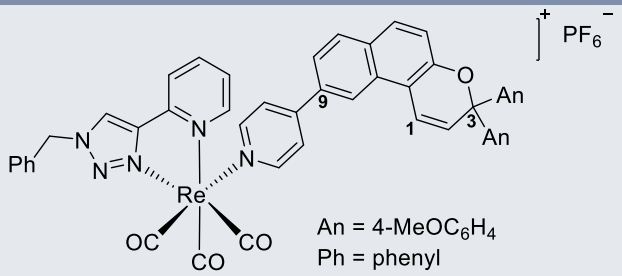 An = 4-MeOC$_6$H$_4$ Ph = phenyl **2.238**	17
2	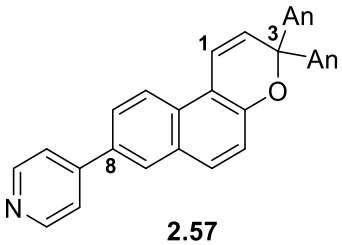 **2.57** An = 4-MeOC$_6$H$_4$	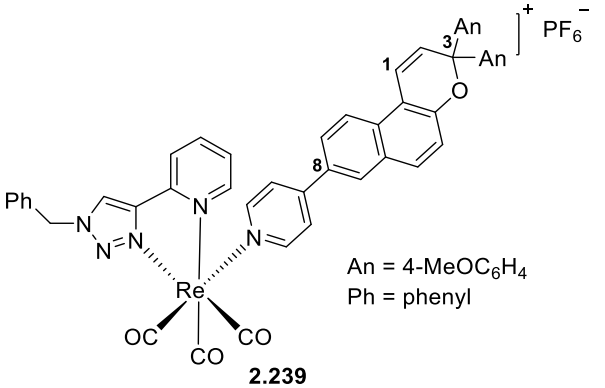 An = 4-MeOC$_6$H$_4$ Ph = phenyl **2.239**	75
3	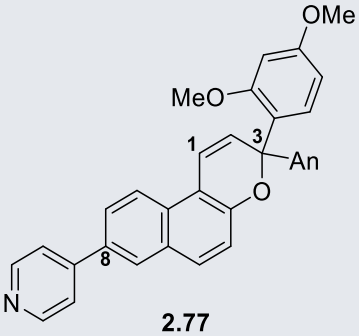 **2.77** An = 4-MeOC$_6$H$_4$	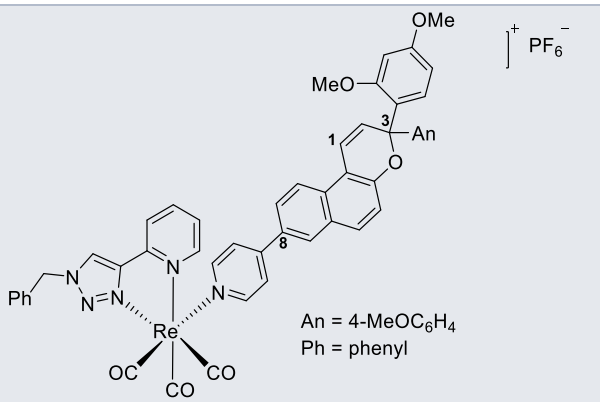 An = 4-MeOC$_6$H$_4$ Ph = phenyl **2.240**	27
4	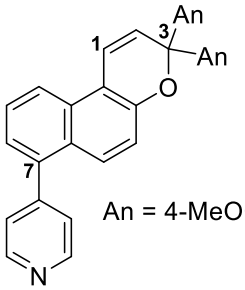 An = 4-MeOC$_6$H$_4$ **2.98**	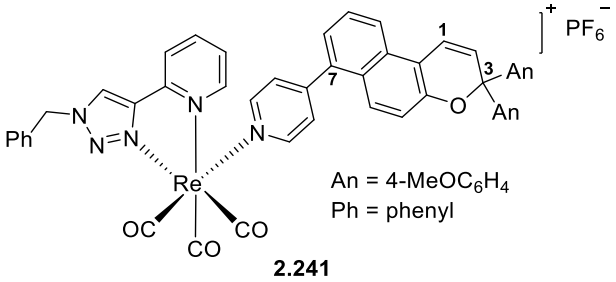 An = 4-MeOC$_6$H$_4$ Ph = phenyl **2.241**	79

Table 2.10 Synthesis of the *fac*-[Re(PyTz)(CO)$_3$NP]$^+$ complexes **2.237** (continuation).

Entry	3*H*-Naphtho[2,1-*b*]pyrans	*fac*-[Re(PyTz)(CO)$_3$NP]$^+$ complexes	Yield (%)
5	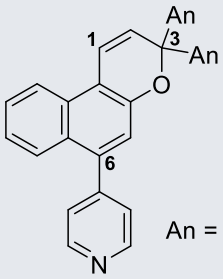 An = 4-MeOC$_6$H$_4$ **2.213**	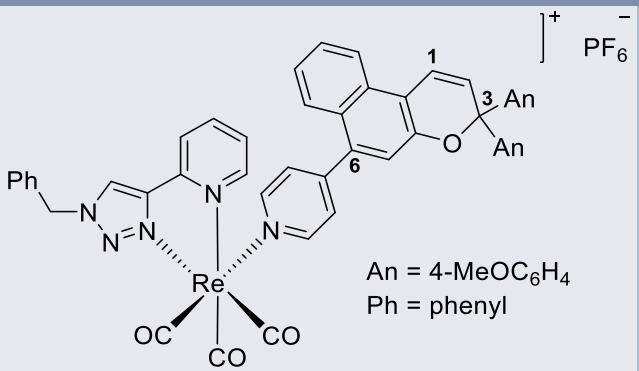 An = 4-MeOC$_6$H$_4$ Ph = phenyl **2.242**	71
6	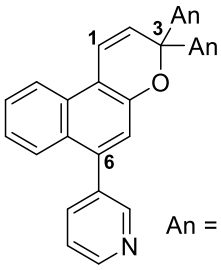 An = 4-MeOC$_6$H$_4$ **2.214**	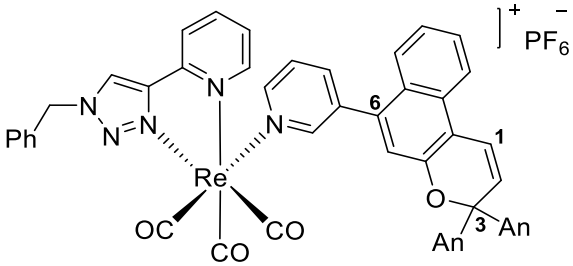 An = 4-OMeC$_6$H$_4$ Ph = phenyl **2.243**	83
7	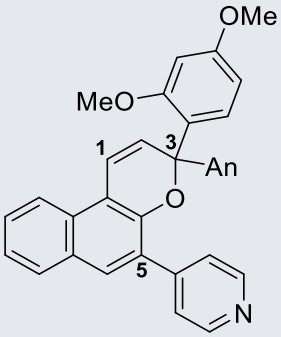 **2.106** An = 4-MeOC$_6$H$_4$	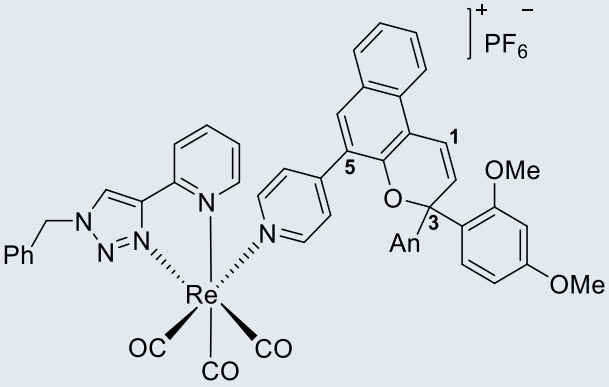 An = 4-OMeC$_6$H$_4$ Ph = phenyl **2.244**	72

Formation of the target the *fac*-[Re(PyTz)(CO)$_3$NP]$^+$ complexes **2.237** was further established by NMR spectroscopy. As an example, the ^{1}H NMR spectrum of rhenium(I) complex **2.239** in $CDCl_3$ contained a singlet at 3.71 ppm corresponding to the resonance of the equivalent 4′- and 4″-OMe, a doublet in a AB spin system at 5.96 ppm with a *geminal* coupling constant of 15.1 Hz corresponding to the resonance of one of the hydrogens of the benzyl C$\underline{H}_2$ (diastereotopic), a doublet in a AB spin system at 6.00 ppm with a *geminal* coupling constant of 15.1 Hz corresponding to the resonance of the other hydrogen of the benzyl C$\underline{H}_2$ (diastereotopic), a doublet at 6.53 ppm with a coupling constant of 10.0 Hz corresponding to the resonance of H-2, an apparent doublet at 6.90 ppm with a coupling constant of 8.5 Hz corresponding to the resonance of H-3′, H-5′, H-3″ and H-5″, a multiplet at 7.34–7.36 ppm corresponding to the resonance of the H-5, H-2′, H-2″, H-6′ and H-6″, a multiplet at 7.47–7.50 ppm corresponding to the resonance of the Ph-H and H-1, a singlet at 9.30 ppm corresponding to the resonance of H-4′′′′ and a doublet at 9.36 ppm with a coupling constant of 5.2 Hz corresponding to the resonance of H-6′′′′′. The ^{13}C NMR spectrum of rhenium(I) complex **2.239** in $CDCl_3$ included a signal at 55.5 ppm corresponding to the resonance of the 4′-, 4″-OMe, a signal at 55.8 ppm corresponding to the resonance of the benzyl $\underline{C}H_2$, a signal at 82.3 ppm corresponding to the resonance of C-3, a signal appearing at 114.0 ppm corresponding to the resonance of C-3′, C-5′, C-3″ and C-5″, a signal at 128.2 ppm corresponding to the resonance of C-2′, C-6′, C-2″ and C-6″ and a signal appearing at 152.0 ppm corresponding to the resonance of C-4a. The signals corresponding to the carbons of the carbon monoxide ligands were too weak to be detected. To this end, using a more concentrated sample or increasing the number of scans would be necessary. However, limited sample availability and restricted time for NMR usage precluded the acquisition of ^{13}C NMR data with better sensitivity. Furthermore, for the PF_6^- ion the ^{19}F NMR spectrum in $CDCl_3$ contained a doublet at -70.1 ppm with a coupling constant of 711 Hz, while the ^{31}P NMR spectrum in $CDCl_3$ contained a septet at -144.2 ppm with a coupling constant of 711 Hz. The multiplicity of the signals in the ^{19}F and ^{31}P NMR spectra were a consequence of the coupling between the fluorine and the phosphorus atoms from the hexafluorophosphate anion.

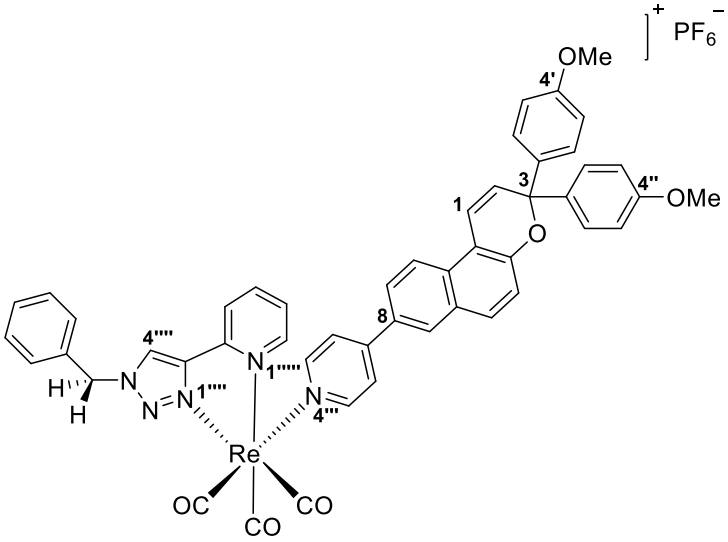

2.239

It is relevant to mention that the *fac*-[Re(PyTz)(CO)$_3$NP]$^+$ complexes **2.237** were obtained as a 1:1 mixture of two diastereomers (α and β) in which both protons and carbons were chemically equivalent (**Figure 2.8**). The only exception was for rhenium(I) complex **2.244**, in which the two stereo configurations α and β had protons and carbons that were not chemically equivalent (**Figure 2.9**). Consequently, the diastereomers produced two sets of signals in the ^{1}H and ^{13}C NMR spectra (**Figure 2.10**). This was possibly due to the spatial proximity of the aryl groups at C-3 and the PyTz ligand, which resulted in differences in the steric hindrance between both diastereomers. It was rationalized that the steric hindrance was greater for diastereomer β as the aryl groups at C-3 and the PyTz ligand were closer in space. Thus, considering that steric hindrance generally results in upfield shifts,[221] the ^{1}H NMR signals of diastereomer β should be slightly more upfield when compared to diastereomer α. It is noteworthy that further experiments (e.g. crystallographic data and/or DFT calculations) would be required to further support this hypothesis. However, despite repeated crystalisations, X-ray quality crystals could not be secured.

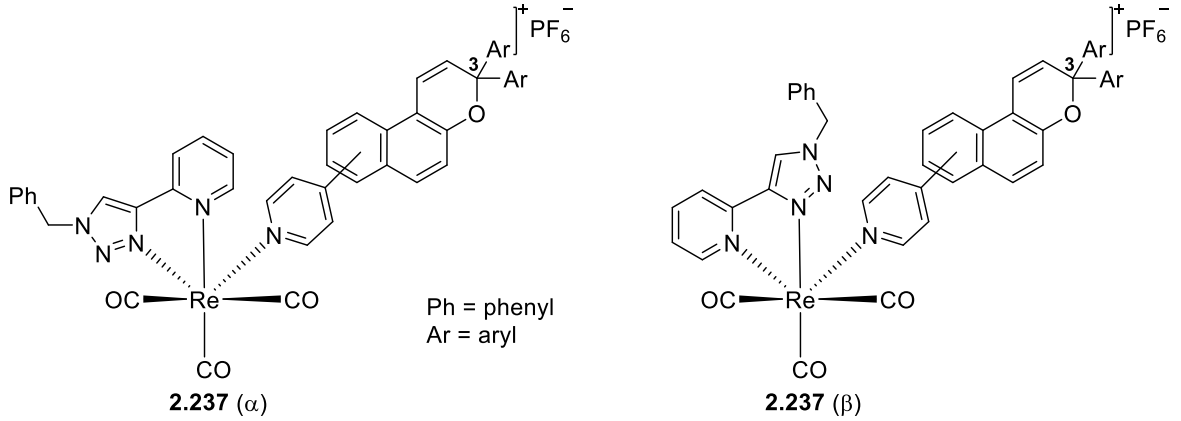

Figure 2.14 Stereoisomers of rhenium(I) complexes **2.237**.

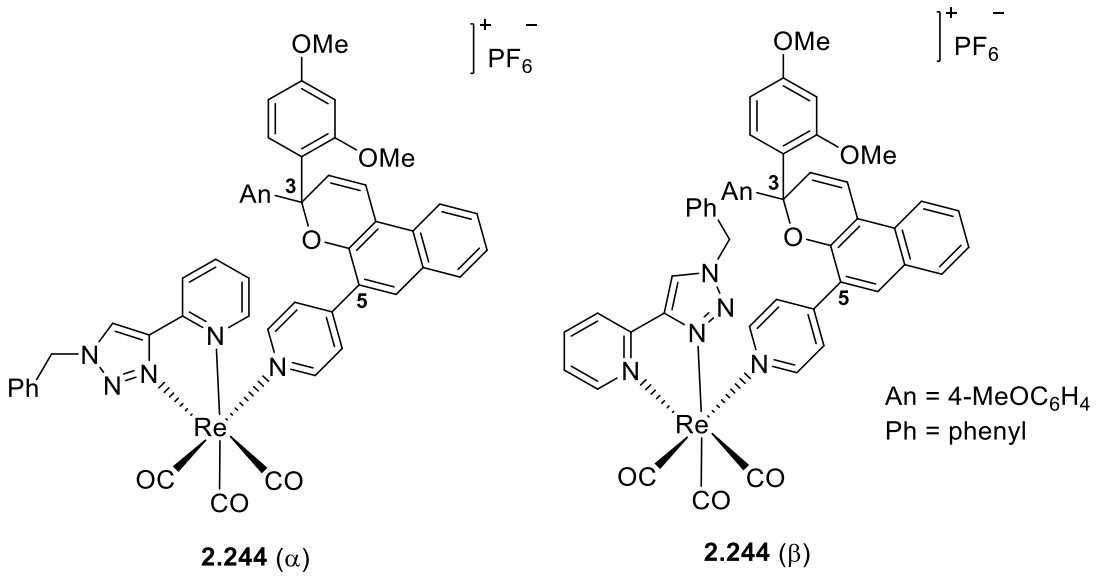

Figure 2.9 Diastereomers of rhenium(I) complex **2.244**.

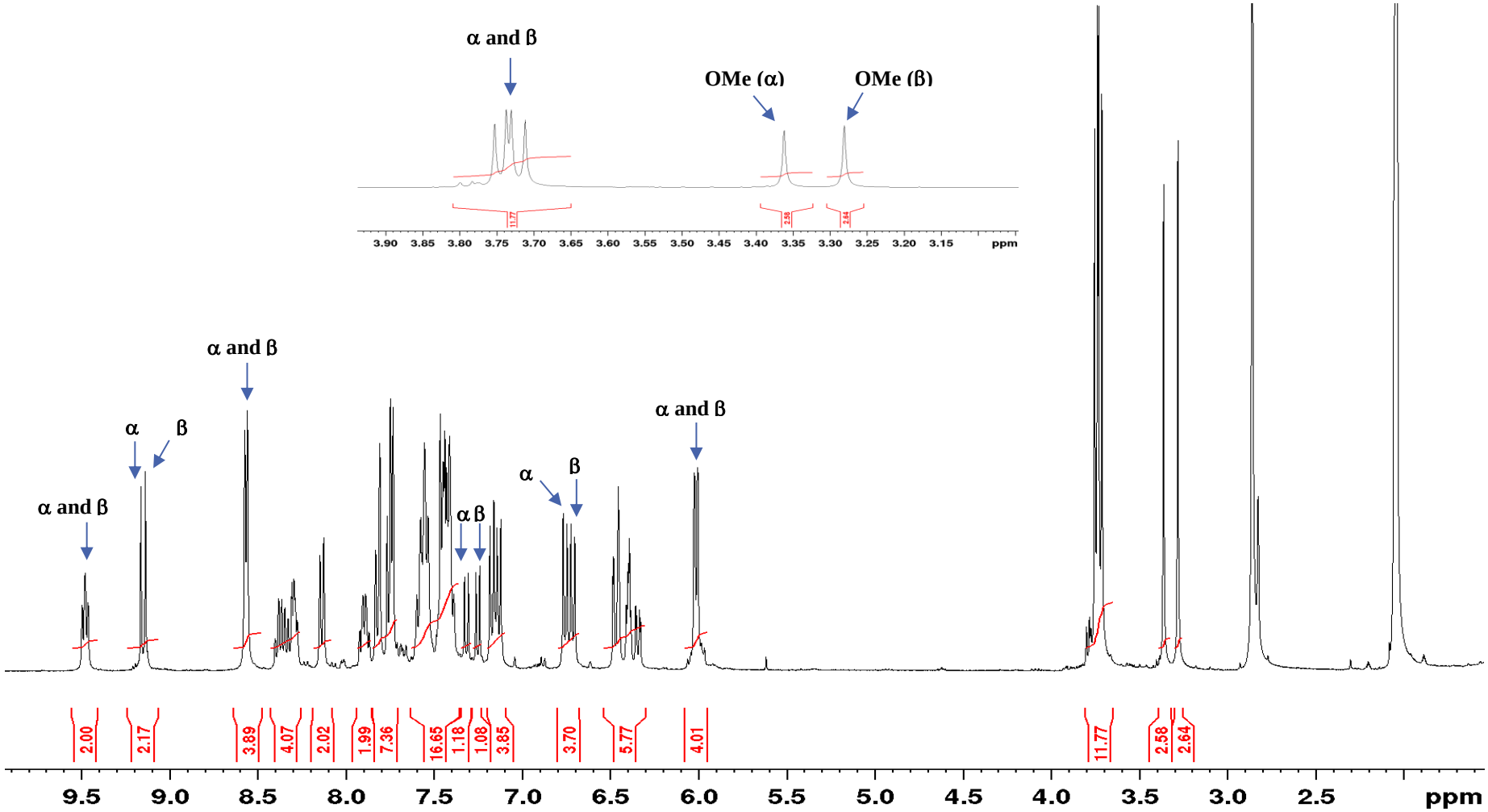

Figure 2.10 ^{1}H NMR spectrum in acetone-d_6 of the 1:1 mixture of stereoisomers of rhenium(I) complex **2.244**.

2.2.4 Synthesis of *fac*-[Re(BTz)(CO)$_3$NP]$^+$

The reaction between *fac*-[Re(BTz)(CO)$_3$Cl]^0 complex **2.224** and 8-pyridyl-3*H*-naphtho[2,1-*b*]pyran **2.57** in the presence of $AgPF_6$ in DCM afforded the Re(I) complex **2.245** in low yield (36%) (**Scheme 2.110**).

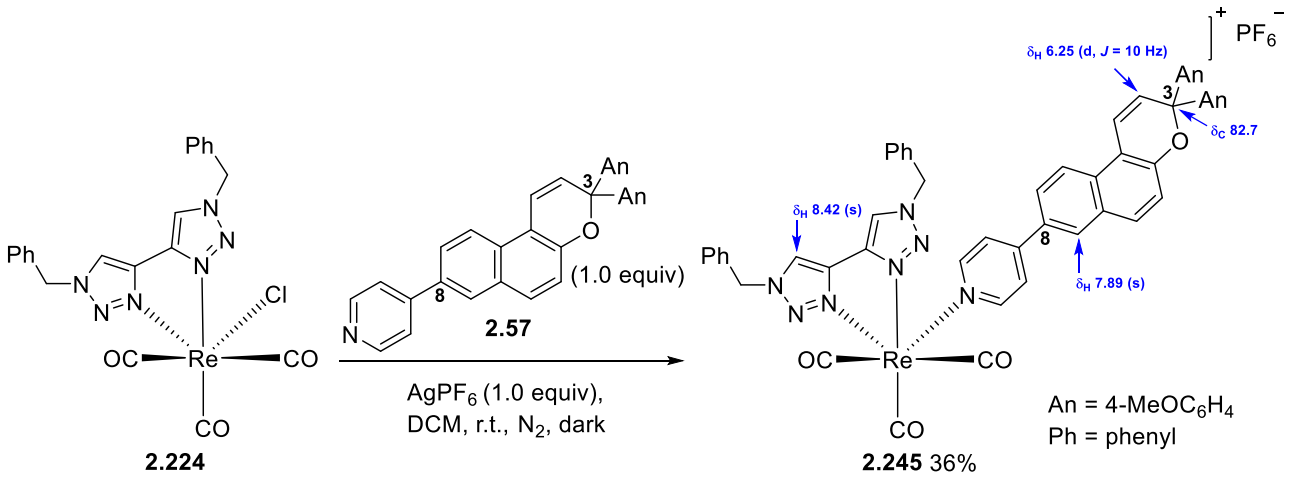

Scheme 2.110 Synthesis of Re(I) complex **2.245**.

Formation of the target Re(I) complex **2.245** was established by NMR spectroscopy. The ^{1}H NMR spectrum of rhenium(I) complex **2.245** in $CDCl_3$ contained a singlet at 3.78 ppm corresponding to the resonance of 4′- and 4″-OMe, a doublet in a AB spin system at 5.60 ppm with a *geminal* coupling constant of 14.4 Hz corresponding to the resonance of the benzyl C$\underline{H}_2$, a doublet in a AB spin system at 5.69 ppm with a *geminal* coupling constant of 14.4 Hz corresponding to the resonance of the benzyl C$\underline{H}_2$, a doublet at 6.25 ppm with a coupling constant of 10.0 Hz corresponding to the resonance of H-2, a multiplet at 6.83–6.86 ppm corresponding to the resonance of H-3′, H-3″, H-5′ and H-5″, a doublet of doublets at 7.57 ppm with coupling constants of 8.9 and 1.8 Hz corresponding to the resonance of H-9, a doublet at 7.89 ppm with a coupling constant of 1.8 Hz corresponding to the resonance of H-7, an apparent doublet at 8.14 ppm with a coupling constant of 6.7 Hz corresponding to the resonance of H-3‴ and H-5‴ and a singlet at 8.42 ppm corresponding to the resonance of H-4⁗ and H-4′′′′′. The ^{13}C NMR spectrum of rhenium(I) complex **2.245** in $CDCl_3$ included a signal at 55.3 ppm corresponding to the resonance of the 4′- and 4″-OMe, a signal at 56.4 ppm corresponding to the resonance of the benzyl $\underline{C}H_2$, a signal at 82.7 ppm corresponding to the resonance of C-3, a signal appearing at 113.9 ppm corresponding to the resonance of C-3′, C-5′, C-3″ and C-5″, a signal at 128.3 ppm corresponding to the resonance of C-

2′, C-6′, C-2″ and C-6″ and a signal appearing at 152.1 ppm corresponding to the resonance of C-4a.

The high-resolution mass spectrum of rhenium(I) complex **2.245** contained a peak assigned to the ion $[M\text{-}PF_6]^+$, with M corresponding to $C_{53}H_{41}N_7O_6{}^{187}RePF_6$.

The FT-IR spectrum contained one strong band at 2034 cm^{-1} and two overlapping bands at 1910 cm^{-1} for the carbon monoxide stretches indicating that the rhenium(I) complex **2.245** had a *fac* configuration.

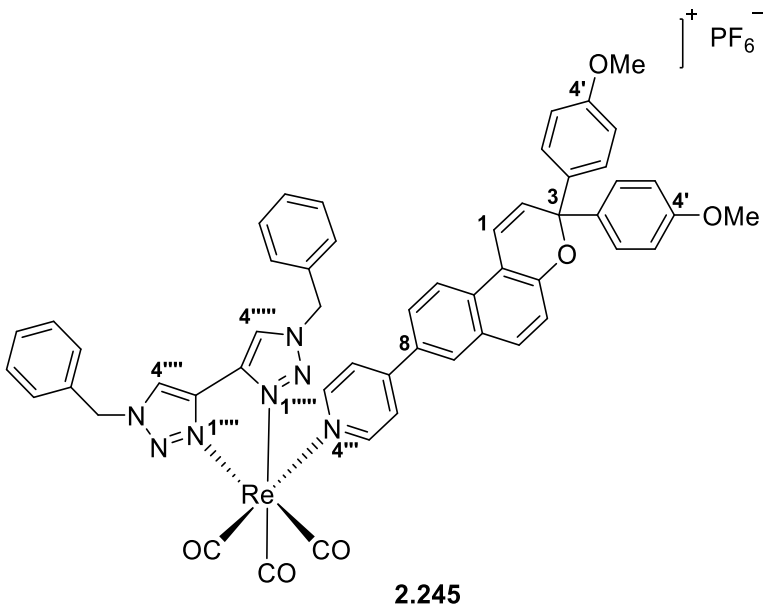

2.245

The Re(I) complex **2.246** was prepared from the Heck product **2.166** in two steps in 39% yield by first treating the latter with TFA in DCM at room temperature and later by reaction with *fac*-$[Re(BTz)(CO)_3Cl]^0$ complex **2.224** in the presence of $AgPF_6$ in DCM (**Scheme 2.111**).[222]

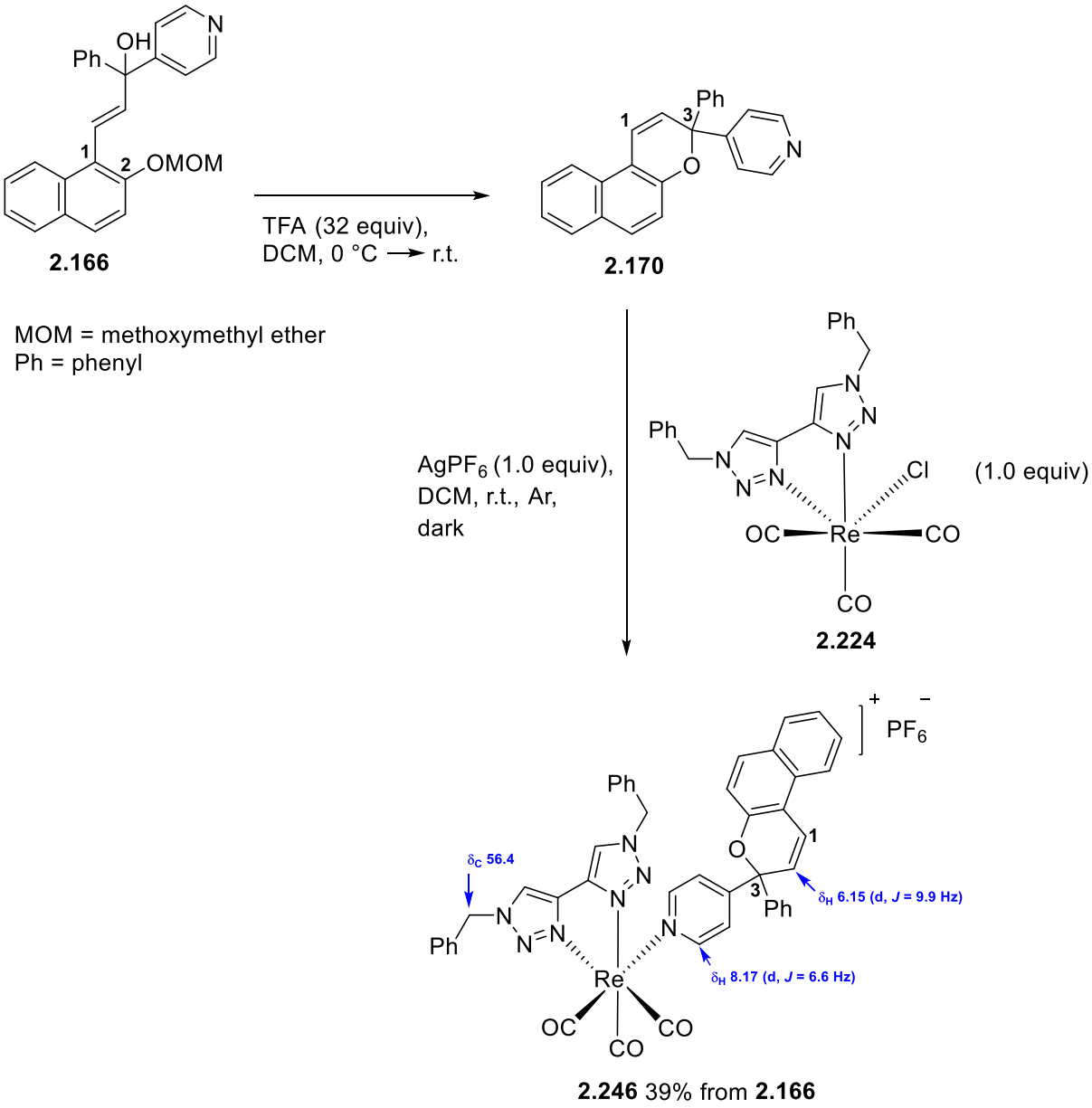

Scheme 2.111 Synthesis of the Re(I) complex **2.246**.

Formation of the target Re(I) complex **2.246** was established by NMR spectroscopy. The ^{1}H NMR spectrum of rhenium(I) complex **2.246** in acetone-d_6 contained a multiplet at 5.60–5.74 ppm corresponding to the resonance of hydrogens of the benzyl C<u>H</u>$_2$, a doublet at 6.15 ppm with a coupling constant of 9.9 Hz corresponding to the resonance of H-2, a doublet appearing at 7.21 ppm with a coupling constant of 8.8 Hz corresponding to the resonance of H-5, a triplet at 7.53 ppm with a coupling constant of 7.3 Hz corresponding to the resonance of H-9, a multiplet at 7.74–7.79 ppm corresponding to the resonance of H-6 and H-7, a multiplet appearing at 7.96–7.98 ppm corresponding to the resonance of H-10, a doublet at 8.17 ppm with a coupling constant of 6.6 Hz corresponding to the resonance of H-3′ and H-5′ and a multiplet appearing at 8.35–8.37

corresponding to the resonance of H-4′′′′ and H-4′′′′′. The ^{13}C NMR spectrum of rhenium(I) complex **2.246** in acetone-d_6 included a signal at 56.4 ppm corresponding to the resonance of the benzyl $\underline{C}H_2$, a signal at 81.1 ppm corresponding to the resonance of C-3, a signal appearing at 151.8 ppm corresponding to the resonance of C-4a and a very weak signal at 194.5 ppm corresponding to the resonance of one of the carbons of the carbon monoxide ligands. The ^{19}F NMR spectrum of rhenium(I) complex **2.246** in acetone-d_6 contained a doublet at -72.2 ppm with a coupling constant of 714 Hz; the multiplicity was a consequence of the coupling between the fluorine and the phosphorus atoms from the hexafluorophosphate anion.

The high-resolution mass spectrum of rhenium(I) complex **2.246** contained a peak assigned to the ion $[M\text{-}PF_6]^+$, with M corresponding to $C_{45}H_{33}N_7O_4{}^{187}RePF_6$.

The FT-IR spectrum contained one strong band at 2036 cm^{-1} and two overlapping bands at 1911 cm^{-1} indicating that the rhenium(I) complex **2.246** had a *fac* configuration.

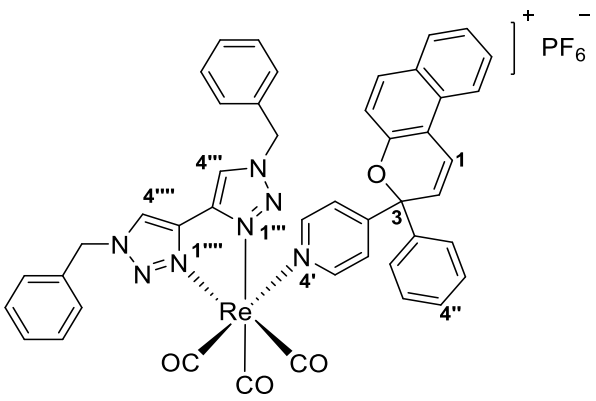

2.246

2.2.5 Synthesis of *fac*-[Re(PyTzNP)(CO)$_3$Cl]^0

The *fac*-[Re(PyTzNP)(CO)$_3$Cl]^0 complex **2.247** was prepared in 78% yield by mixing the 8-(4-pyridyl-triazole)-3*H*-naphtho[2,1-*b*]pyran **2.110** with an equimolar amount of Re(CO)$_5$Cl in PhMe at reflux (**Scheme 2.112**).

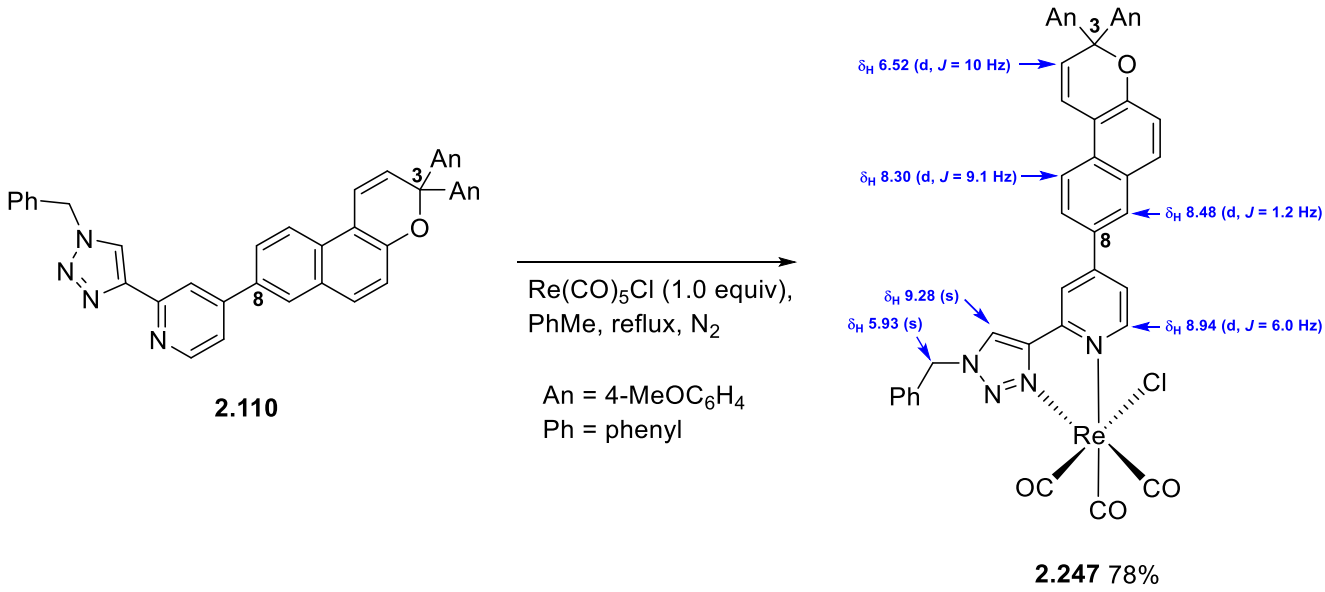

Scheme 2.112 Synthesis of the *fac*-[Re(PyTzNP)(CO)$_3$Cl]^0 complex **2.247**.

Formation of the target *fac*-[Re(PyTzNP)(CO)$_3$Cl]^0 complex **2.247** was established by NMR spectroscopy. The ^{1}H NMR spectrum of rhenium(I) complex **2.247** in DMSO-d$_6$ included a singlet at 3.69 ppm corresponding to the resonance of the equivalent 4′- and 4″-OMe groups, a singlet at 5.93 ppm corresponding to the resonance of the hydrogens of the benzyl C<u>H</u>$_2$, a doublet at 6.52 ppm with a coupling constant of 10.0 Hz (*cis* configuration) corresponding to the resonance of H-2, an apparent doublet at 6.89 ppm with a coupling constant of 8.8 Hz corresponding to the resonance of H-3′, H-5′, H-3″ and H-5″, a doublet at 7.91 ppm with a coupling constant of 9.0 Hz corresponding to the resonance of H-6, a multiplet appearing at 8.04–8.06 ppm corresponding to the resonance of H-9 and H-6‴, a doublet at 8.30 ppm with a coupling constant of 9.1 Hz corresponding to the resonance of H-10, a doublet appearing at 8.48 ppm with a coupling constant of 1.2 Hz corresponding to the resonance of H-7, a doublet at 8.83 ppm with a coupling constant of 1.3 Hz corresponding to the resonance of H-2‴, a doublet appearing at 8.94 ppm with a coupling constant of 6.0 Hz corresponding to the resonance of H-5‴ and a singlet at 9.28 ppm corresponding to the resonance of H-5⁗. The ^{13}C NMR spectrum of rhenium(I) complex **2.247** in DMSO-d$_6$ included a signal appearing at 55.3 ppm corresponding to the resonance of the 4′- and 4″-OMe, a signal at 82.4 ppm corresponding to the resonance of C-3, a signal appearing at 114.0 ppm corresponding to the resonance of C-3′, C-5′, C-3″ and C-5″, a signal at 128.2 ppm corresponding to the resonance of C-2′, C-6′, C-2″ and C-6″, a signal appearing at 151.9 ppm corresponding to the resonance of C-4a

and two very weak signals appearing at 190.1 ppm and 197.3 ppm corresponding to the resonance of the carbon monoxide carbons.

High-resolution mass spectrometry spectrum of rhenium(I) complex **2.247** contained a peak assigned to the ion $[M\text{-}Cl+MeCN]^+$, with M corresponding to $C_{44}H_{32}N_4O_6{}^{187}Re^{35}Cl$.

The FT-IR spectrum contained one strong band at 2021 cm^{-1} and two overlapping bands at 1930 cm^{-1} and 1895 cm^{-1} indicating that the rhenium(I) complex **2.247** had a *fac* configuration.

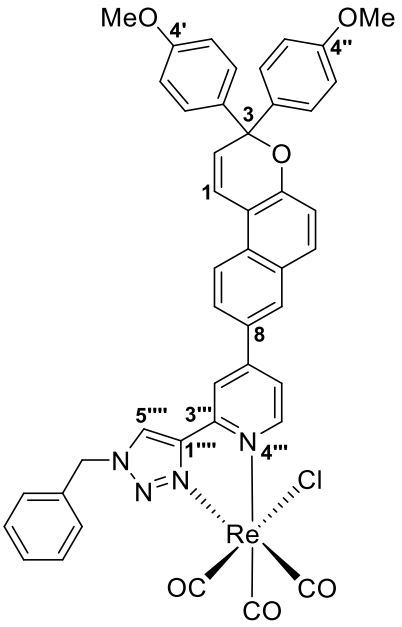

2.247

2.2.6 Synthesis of *fac*-[Re(N^N)(CO)$_3$naphthalene]$^+$

A series of non-photochromic *fac*-[Re(N^N)(CO)$_3$naphthalene]$^+$ complexes (N^N = BPy **2.248**, PyTz **2.249**, BTz **2.250**) were prepared for comparative purposes (**Figure 2.11**).

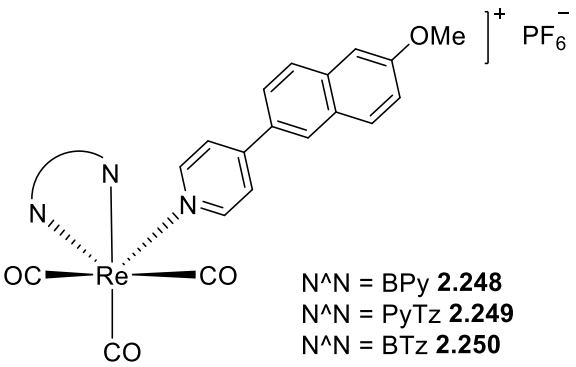

Figure 2.11 *fac*-[Re(N^N)(CO)$_3$naphthalene]$^+$ complexes **2.248**–**2.250**.

Initially, 6-(4-pyridyl)-2-methoxynaphthalene **2.252** was prepared in 68% yield from the Suzuki cross-coupling reaction between 6-bromo-2-methoxynaphthalene **2.251** and 4-pyridineboronic acid pinacol ester **2.35** (**Scheme 2.113**).

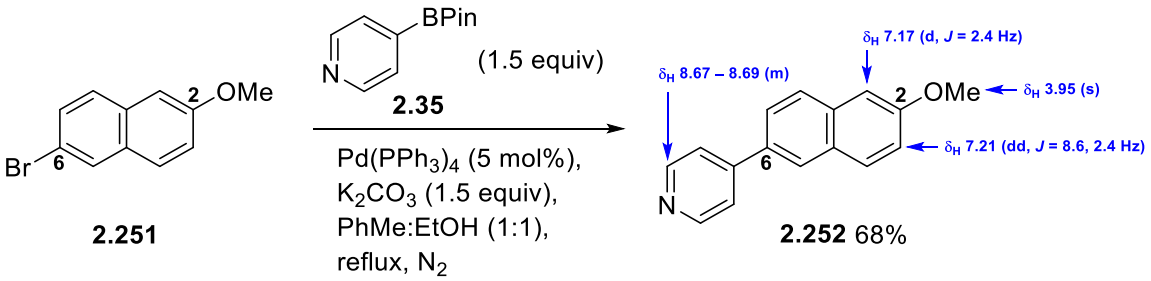

Scheme 2.113 Synthesis of the 6-(4-pyridyl)-2-methoxynaphthalene **2.252**.

Subsequently, the *fac*-[Re(N^N)(CO)$_3$methoxynaphthalene]$^+$ complexes (N^N = BPy **2.248**, PyTz **2.249**, BTz **2.250**) were prepared in very good to excellent yield (87–92%) from the reaction between 6-(4-pyridyl)-2-methoxynaphthalene **2.252** and an equimolar amount of the appropriate *fac*-[Re(N^N)(CO)$_3$Cl]^0 complexes **2.216** in DCM in the presence of $AgPF_6$ (1.0 equiv) at room temperature in the dark (**Scheme 2.114**).

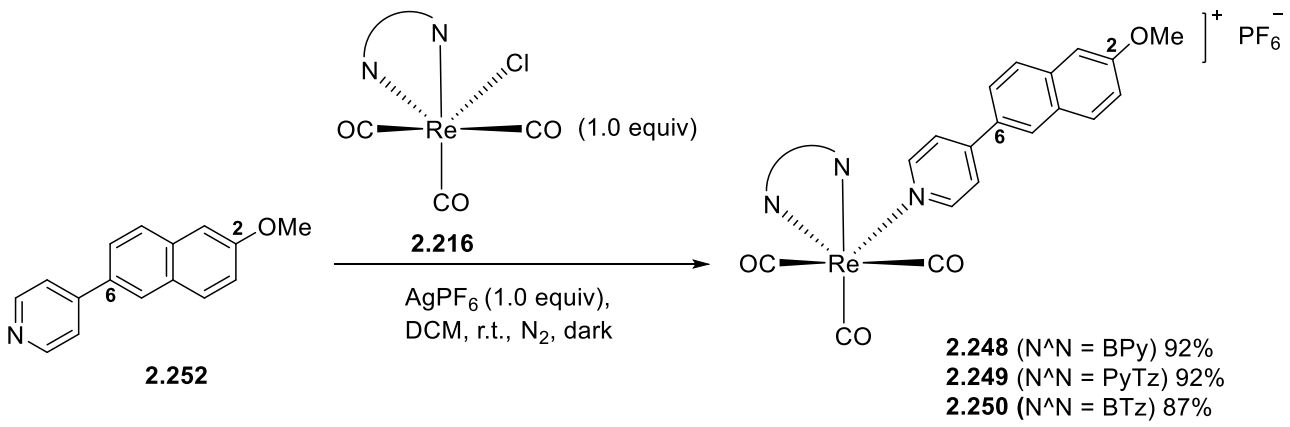

Scheme 2.114 Synthesis of *fac*-[Re(N^N)(CO)$_3$naphthalene]$^+$ complexes **2.248**–**2.250**.

Formation of the target *fac*-[Re(N^N)(CO)$_3$naphthalene]$^+$ complexes **2.248**–**2.250** was established by NMR spectroscopy. The ^{1}H NMR spectra of all of the rhenium(I) complexes **2.248**–**2.250** in $CDCl_3$ contained a singlet at 3.89–3.93 ppm corresponding to the resonance of the 2-OMe, an apparent singlet or a doublet appearing at 7.07–7.12 ppm with a coupling constant of 2 Hz corresponding to resonance of H-1, a doublet of doublets at 7.10–7.15 ppm with coupling constants

of 9 and 2 Hz corresponding to resonance of H-3 and a multiplet or an apparent doublet appearing at 8.12–8.15 ppm with a coupling constant of 6.5 Hz corresponding to the resonance of H-3′ and H-5′. The ^{1}H NMR spectra of the rhenium(I) complexes **2.248**–**2.250** also contained singular signals. For example, in the ^{1}H NMR spectrum of rhenium(I) complex **2.248** there was a doublet at 8.42 ppm with a coupling constant of 8.1 Hz corresponding to the resonance of H-3″ and H-3‴. In the ^{1}H NMR spectrum of rhenium(I) complex **2.249** there was a singlet appearing at 8.75 ppm corresponding to the resonance of H-4‴ and a doublet at 9.03 ppm with a coupling constant of 5.5 Hz corresponding to the resonance of H-6″. In the ^{1}H NMR spectrum of rhenium(I) complex **2.250** there were two doublets (AB spin system) at 5.58 and 5.68 ppm with a geminal coupling constant of 14.5 Hz (*trans*) corresponding to the resonance of the four benzyl hydrogens C$\underline{H}_2$ (diastereotopic) and a singlet appearing at 8.38 ppm corresponding to the resonance of H-4″ and H-4‴. It is noteworthy that in the ^{13}C NMR spectra of the *fac*-[Re(N^N)(CO)$_3$naphthalene]$^+$ complexes **2.248**–**2.250** in $CDCl_3$ the signals corresponding to the resonance of the carbons of the carbon monoxide ligands appeared at 190.6–196.0 ppm.

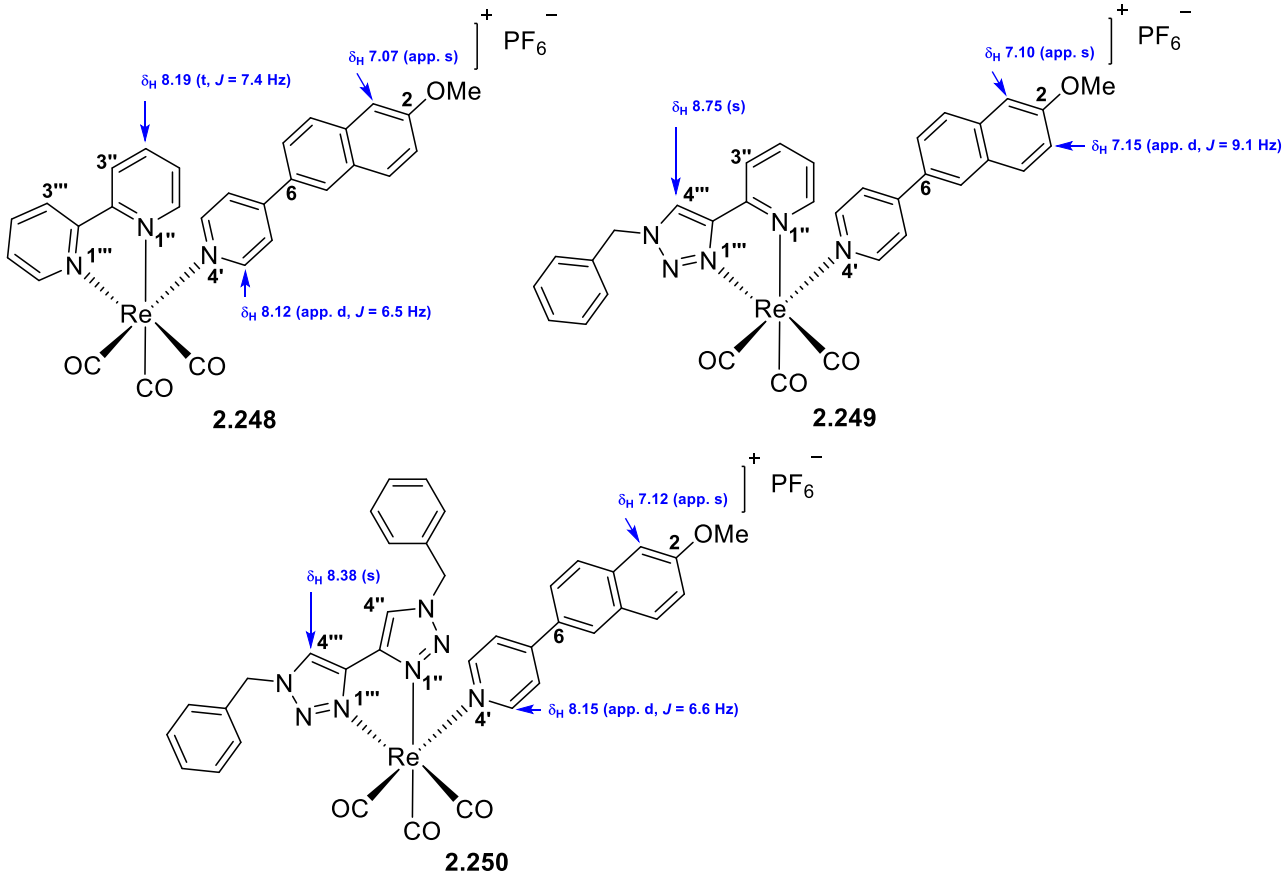

Accurate high-resolution mass spectrometry data of the *fac*-[Re(N^N)(CO)$_3$naphthalene]$^+$ complexes **2.248**–**2.250** was collected, all spectra containing a peak assigned to the ion [M-PF$_6$]$^+$, with M corresponding to the hexafluorophosphate salt.

The FT-IR spectra of the *fac*-[Re(N^N)(CO)$_3$naphthalene]$^+$ complexes **2.248**–**2.250** contained one strong band at *ca.* 2031 cm^{-1} and two overlapping bands at *ca.* 1907 cm^{-1} indicating that the rhenium(I) complexes **2.248**–**2.250** had a *fac* configuration.

2.3 Photophysical Properties

2.3.1 Photochromic Properties of the Pyridyl Substituted 3*H*-naphtho[2,1-*b*]pyrans

Spectroscopic data was obtained for the novel pyridyl substituted 3*H*-naphtho[2,1-*b*]pyrans, including:

1. λ_{max} of absorbance of the photomerocyanines after irradiating with UV light (10 min) the toluene solutions of the 3*H*-naphtho[2,1-*b*]pyrans to a photostationary state (PSS). A Xe-Arc lamp (in Current Mode l_{set} 8.5 A/l_{max} 10.5A 149–150 W) was employed to photoexcite the samples, coupled with a Newport UG-11 filter.
2. Colourability was determined by calculation of the molar extinction coefficients (ε_{max}).
3. Bleaching kinetics which was recorded as $t_{½}$ (s) and k_{Δ}.

The spectroscopic data is summarized in **Table 2.11**.

Table 2.11 Tabular summary of the spectroscopic data of the pyridyl substituted 3*H*-naphtho[2,1-*b*]pyrans (in toluene).

Compounds	R^1	R^2	R^3	R^4	λ_{max} (nm)	$t_{½}$ (s)	k_{Δ} ($M^{-1}.s^{-1}$)	ε_{PSS} ($M^{-1}.cm^{-1}$)
2.36	10-(4-Py)	4-$MeOC_6H_4$	OMe	H	458 464*	7149*	1.43×10^{-3}*	206 261*
2.48	9-(4-Py)	4-$MeOC_6H_4$	OMe	H	472	125	4.69×10^{-2}	70
2.50	9-(3-Py)	4-$MeOC_6H_4$	OMe	H	472	10932	1.71×10^{-4}	78
2.57	8-(4-Py)	4-$MeOC_6H_4$	OMe	H	482 486*	57740 25227*	2.31×10^{-5} 1.08×10^{-4}*	120 170*
2.59	8-(3-Py)	4-$MeOC_6H_4$	OMe	H	476	6643	3.53×10^{-4}	65
2.65	8-(2-Py)	4-$MeOC_6H_4$	OMe	H	No	N/A	N/A	N/A
2.77	8-(4-Py)	4-$MeOC_6H_4$	OMe	OMe	490	94	2.08×10^{-2}	18000
2.110	8-(PyTz)	4-$MeOC_6H_4$	OMe	H	480 486*	5826 1204*	3.63×10^{-4} 2.25×10^{-3}*	141 190*
2.98	7-(4-Py)	4-$MeOC_6H_4$	OMe	H	468	87220	N/A	140
2.214	6-(4-Py)	4-$MeOC_6H_4$	OMe	H	472	3468	1.09×10^{-3}	67
2.215	6-(3-Py)	4-$MeOC_6H_4$	OMe	H	474	1206	2.12×10^{-3}	29
2.170	H	4-Py	H	H	414	< 60	N/A	3400
2.70	8-(4-$MeOC_6H_4$)	4-$MeOC_6H_4$	OMe	H	490	24643	1.38×10^{-4}	296
2.72	8-Ph	4-$MeOC_6H_4$	OMe	H	480	3157	3.29×10^{-4}	120
2.74	8-(4-$NO_2C_6H_4$)	4-$MeOC_6H_4$	OMe	H	488	28064	4.66×10^{-5}	12303

*In a solution of PhMe:DCM (1:1).

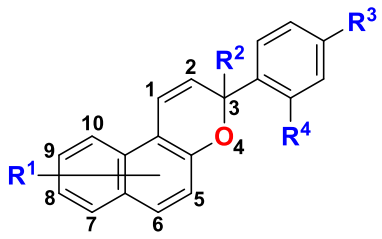

2.251

2.3.1.1 10-Pyridyl-3*H*-naphtho[2,1-*b*]pyran

By UV irradiation of the 10-pyridyl-3*H*-naphtho[2,1-*b*]pyran **2.36** in solution the photomerocyanine **2.252** was formed (**Scheme 2.115**).

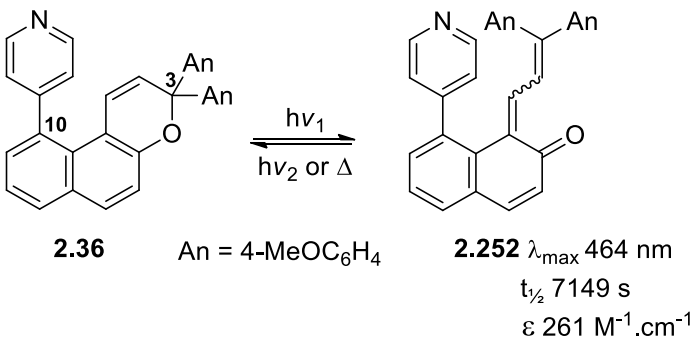

Scheme 2.115 Electrocyclic ring-opening of 3*H*-naphtho[2,1-*b*]pyran **2.36**.

The introduction of a 4-pyridyl substituent at C-10 (λ_{max} 458 nm in toluene) caused an hypsochromic shift of 17 nm when compared to the simple 3,3-bis(4-methoxyphenyl) substituted 3*H*-naphtho[2,1-*b*]pyran (λ_{max} 475 nm in toluene) (**Figure 2.12**). It was rationalized that the blue shift was a result of the steric clash between the bulky 4-pyridyl group at C-10 and the hydrogens of the diene **2.252**, which led to a more twisted conformation and consequently to a less efficient conjugation.

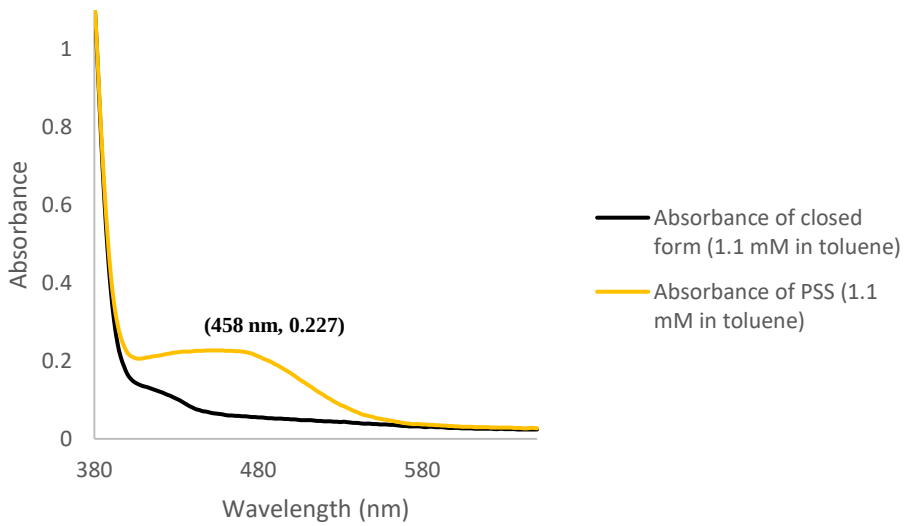

Figure 2.12 UV-Vis spectra of 3*H*-naphtho[2,1-*b*]pyran **2.36** (1.1 mM in toluene in the closed form (black) and in the PSS (yellow).

The introduction of the 4-pyridyl substituent at C-10 accelerated TC – CF isomerization but decelerated the TT – TC isomerization drastically ($t_{½}$ = 7149 s in a mixture PhMe:DCM (1:1)) (**Figure 2.13**). Thus, the very slow thermal isomerization reaction from the TT isomer to the TC isomer was a consequence of the large activation energy barrier towards the formation of the TC isomer from the TT isomer (**Scheme 2.116**).[119]

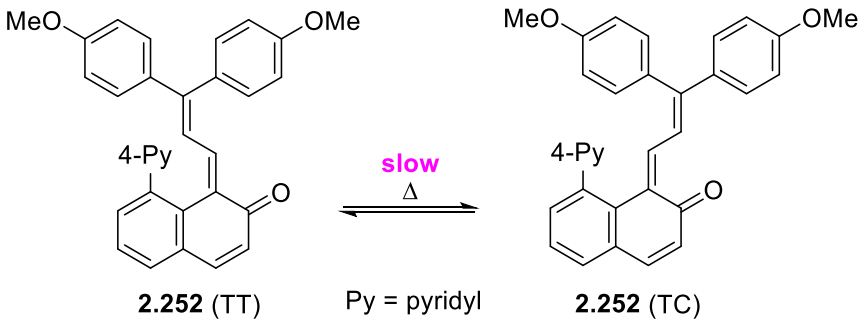

Scheme 2.116 Thermal isomerization of TT – TC of photomerocyanine **2.252**.

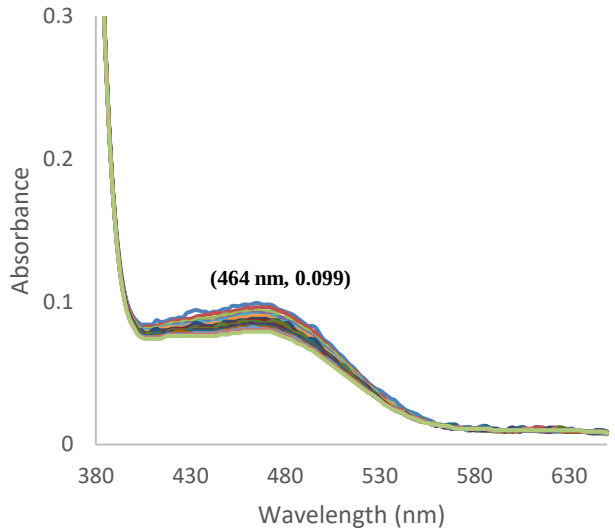

Figure 2.13 UV-Vis spectra of the bleaching in the dark of the PSS of **2.36** (0.38 mM in a mixture of PhMe:DCM (1:1), after UV irradiation) with a 120 seconds scan interval.

2.3.1.2 9-Pyridyl-3*H*-naphtho[2,1-*b*]pyran

By UV irradiation of the 9-pyridyl-3*H*-naphtho[2,1-*b*]pyrans **2.48** and **2.50** in toluene the corresponding photomerocyanines **2.253** and **2.255** were formed (**Scheme 2.117**).

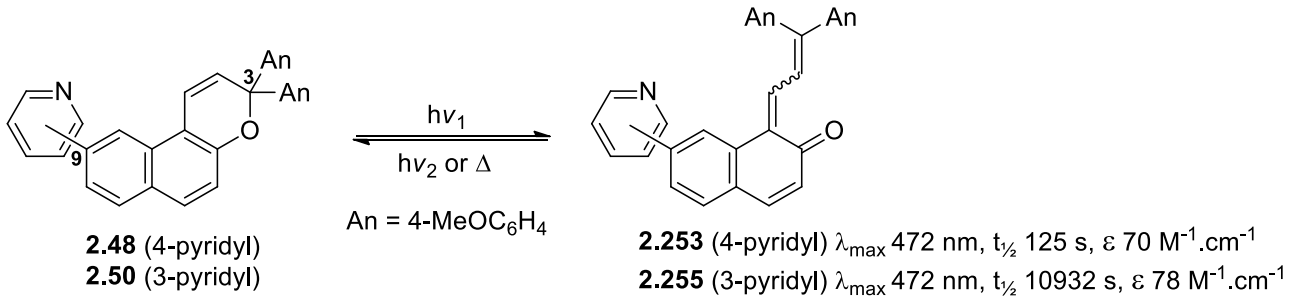

Scheme 2.117 Electrocyclic ring-opening of 3*H*-naphtho[2,1-*b*]pyran **2.48** and **2.50**.

The incorporation of both a 4- and 3-pyridyl substituent at the C-9 (λ_{max} 472 nm in toluene) caused a small hypsochromic shift (3 nm) (**Figures 2.14** and **2.15**) when compared to the simple 3,3-bis(4-methoxyphenyl) substituted 3*H*-naphtho[2,1-*b*]pyran **2.147** (λ_{max} 475 nm in toluene).

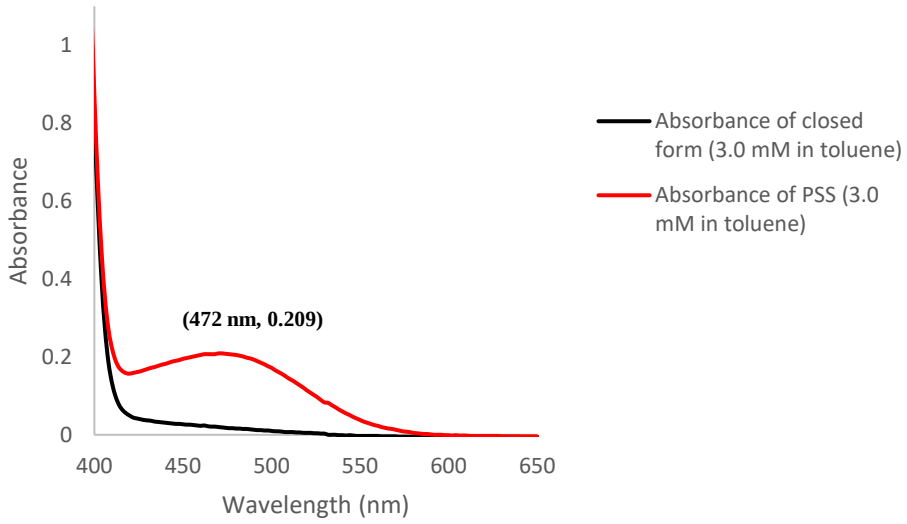

Figure 2.14 UV-Vis spectra of 3*H*-naphtho[2,1-*b*]pyran **2.48** (3.0 mM in toluene) in the closed form (black) and in the PSS (red).

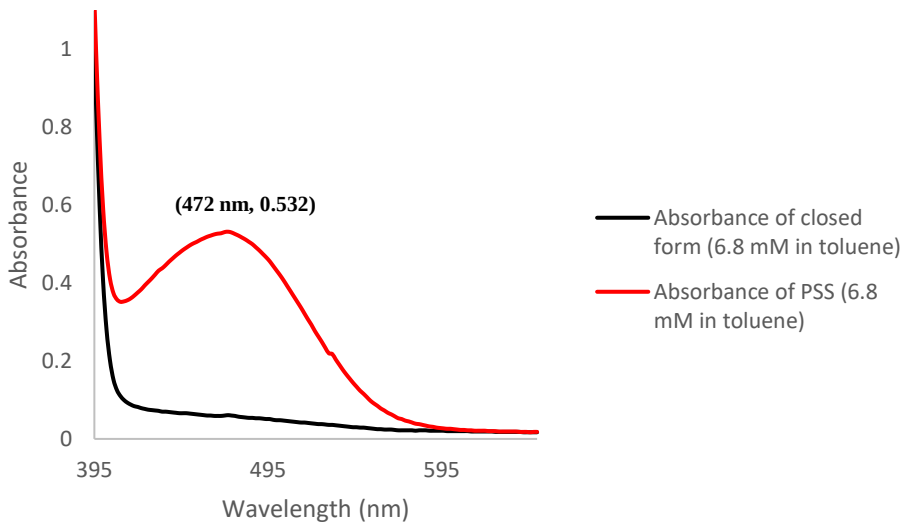

Figure 2.15 UV-Vis spectra of 3*H*-naphtho[2,1-*b*]pyran **2.50** (6.8 mM in toluene) in the closed form (black) and in the PSS (red).

The absence of a bathochromic shift was a consequence of the poor electronic conjugation of the pyridyl groups with the photo-generated π system (**Scheme 2.118**). On the other hand, the observed small hypsochromic shifts may have been a result of a small negative inductive effect that pulls electron density towards the pyridyl unit, as the nitrogen atom is relatively electronegative. Furthermore, both 3*H*-naphtho[2,1-*b*]pyrans **2.48** and **2.50** produced similar colour in toluene solution under UV irradiation (ε = 70 and 78 $M^{-1}.cm^{-1}$, respectively).

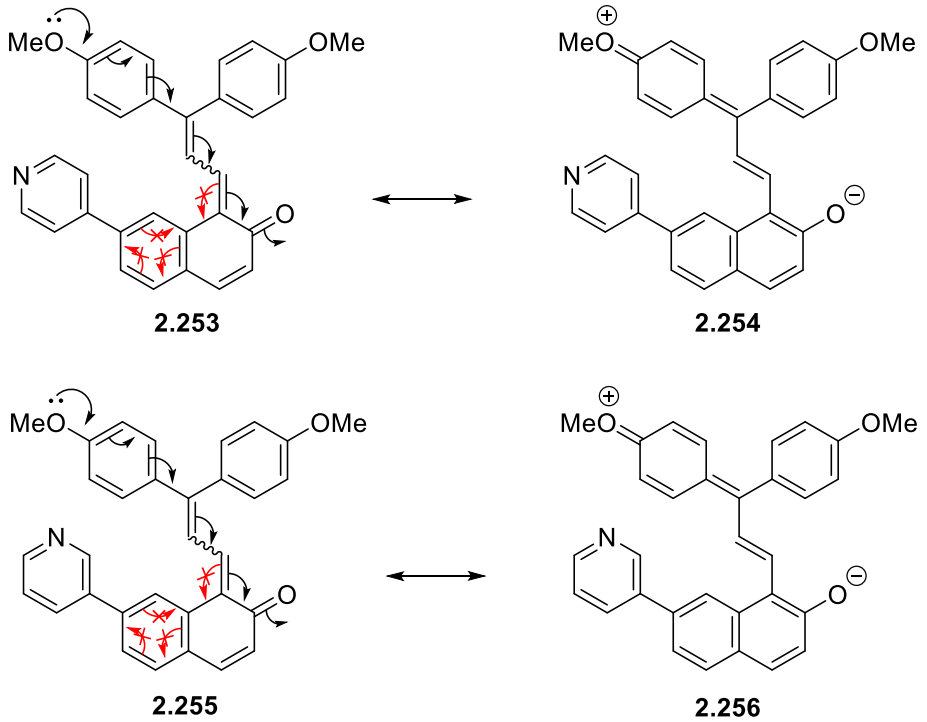

Scheme 2.118 Resonance structures of photomerocyanines **2.253** and **2.255**.

It is noteworthy that the bleaching kinetics of the PSS of 9-pyridyl-3*H*-naphtho[2,1-*b*]pyrans **2.48** and **2.50** were strikingly different ($t_{½}$ = 125 s and 10932 s, respectively) (**Figure 2.16** and **2.17**).

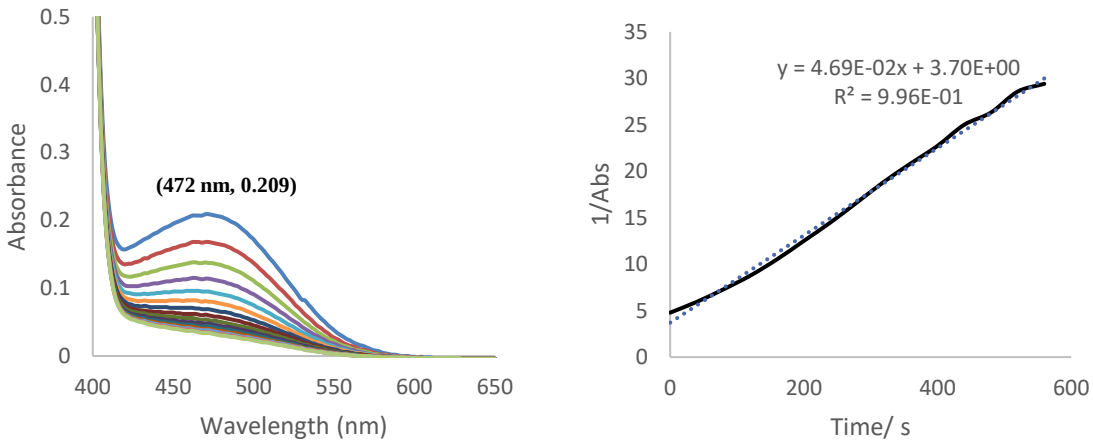

Figure 2.16 (a) UV-Vis spectra of the bleaching in the dark of the PSS of **2.48** (3.0 mM in toluene, after UV irradiation) with a 40 seconds scan interval; (b) Linear regression (2nd order).

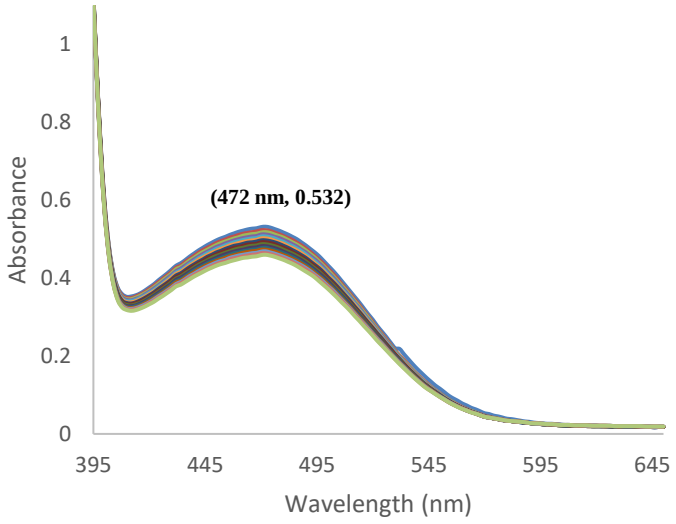

Figure 2.17 UV-Vis spectra of the bleaching in the dark of the PSS of **2.50** (6.8 mM in toluene, after UV irradiation) with 120 seconds scan interval.

It was rationalized that a hydrogen bond between the 3-pyridyl nitrogen and the hydrogen of one of the OCH_3 groups of the photomerocyanine **2.255** (TC isomer) could be established.[223] This hypothesis was supported by energy minimization by using ChemDraw 3D MM2 force field method (**Figure 2.18**). After energy minimization, the distance between the hydrogen and the nitrogen atom was equal to 2.5 Å which is within the region of length for a H-bond. As a consequence of the H-bond formation, the photomerocyanine **2.255** (from 9-(3-pyridyl)-3*H*-naphtho[2,1-*b*]pyran **2.50**) was more efficiently stabilized in comparison with the photomerocyanine **2.253** (from 9-(4-pyridyl)-3*H*-naphtho[2,1-*b*]pyran **2.48**) which led to slower bleaching kinetics.

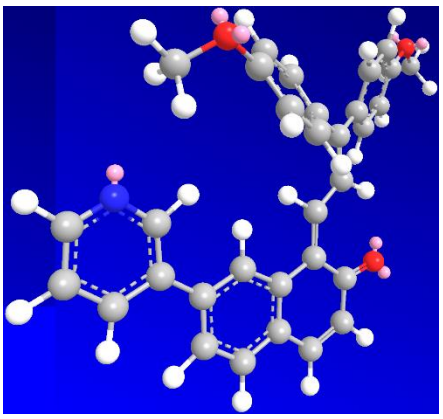

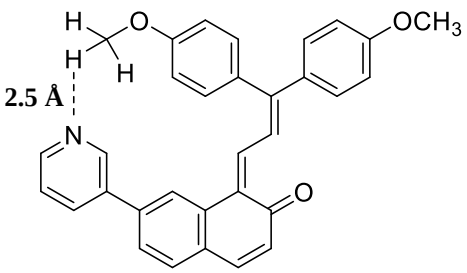

2.255

Figure 2.18 Minimized energy structure of photomerocyanine **2.255** by using ChemDraw 3D MM2 force field method.

2.3.1.3 8-Pyridyl-3*H*-naphtho[2,1-*b*]pyran

By UV irradiation of the 8-(4-pyridyl)-3*H*-naphtho[2,1-*b*]pyran **2.57** in toluene the photomerocyanine **2.257** was formed (**Scheme 2.119**).

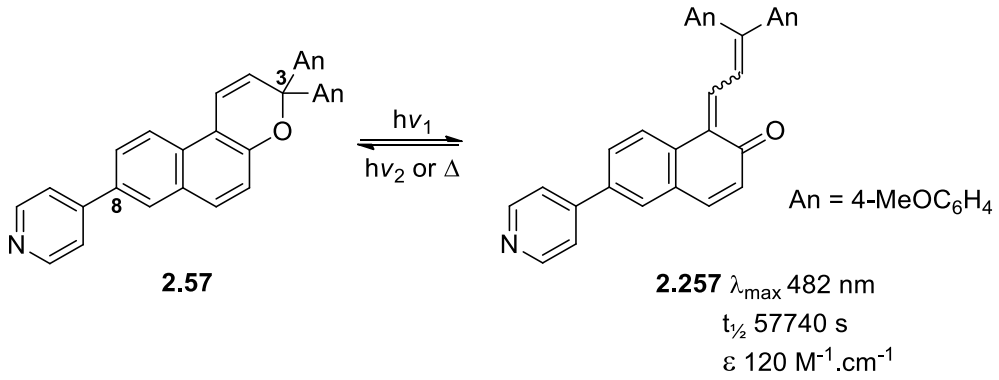

Scheme 2.119 Electrocyclic ring-opening of 3*H*-naphtho[2,1-*b*]pyran **2.57**.

In the 3*H*-naphtho[2,1-*b*]pyran **2.57**, the introduction of a 4-pyridyl substituent at C-8 (λ_{max} 482 nm in toluene) induced a small bathochromic shift (7 nm) when compared to the simple 3,3-bis(4-methoxyphenyl) substituted 3*H*-naphtho[2,1-*b*]pyran (λ_{max} 475 nm in toluene) (**Figure 2.19**).

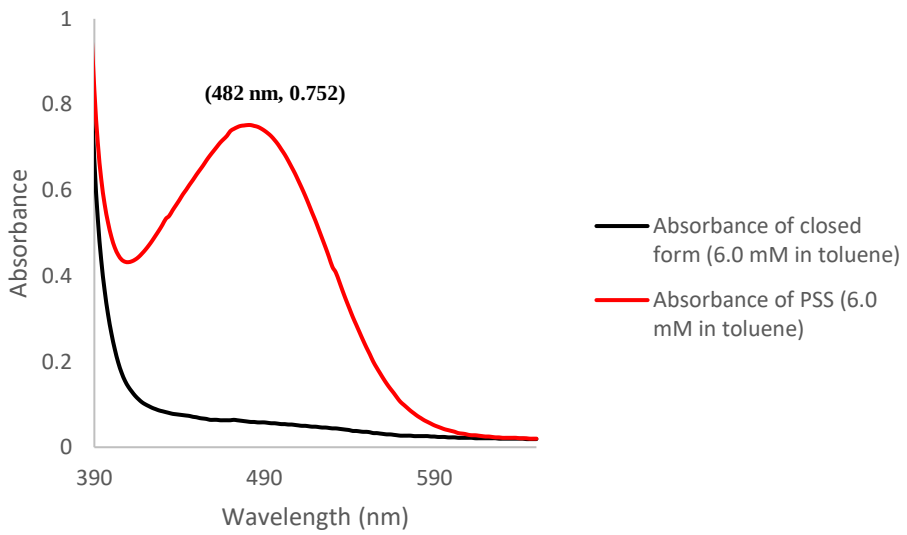

Figure 2.19 UV-Vis spectra of 3*H*-naphtho[2,1-*b*]pyran **2.57** (6.0 mM in toluene in the closed form (black) and in the PSS (red).

The observed red shift was due to the more extended π conjugated system of the photomerocyanine **2.257** (**Scheme 2.120**).

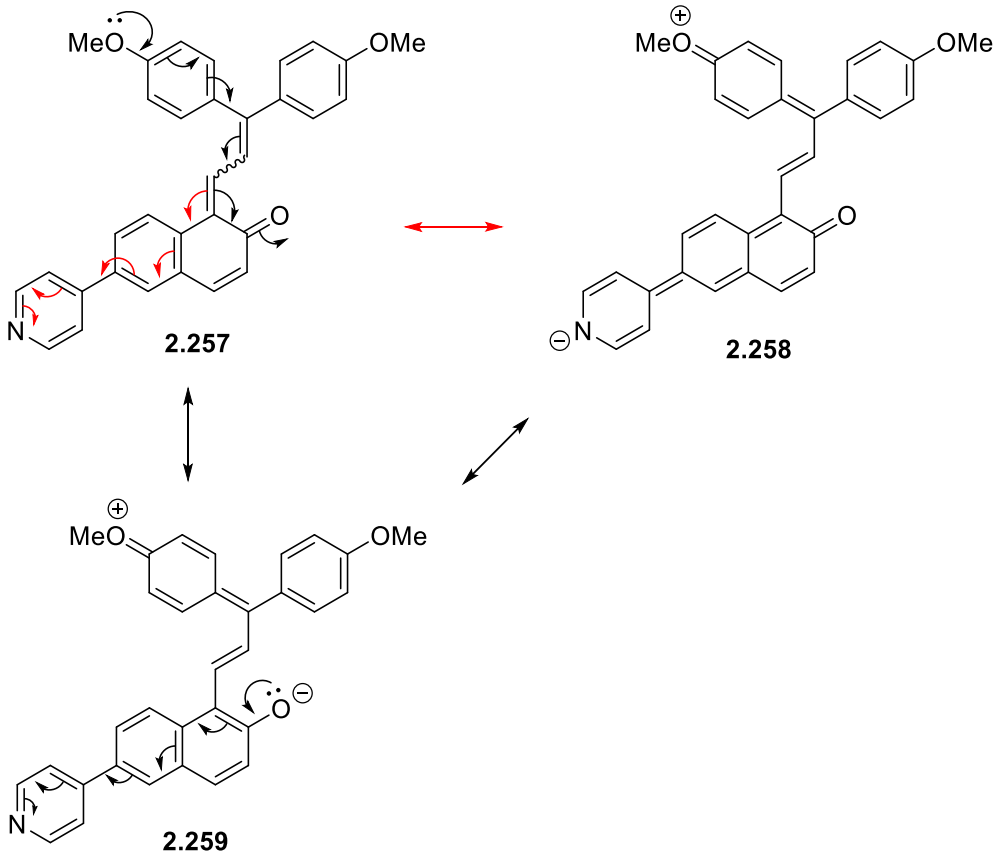

Scheme 2.120 Resonance structures of photomerocyanine **2.257**.

Furthermore, the red colour attributed to the PSS of 3*H*-naphtho[2,1-*b*]pyran **2.57** persisted for a very long period of time ($t_{½}$ = 57740 s in toluene) (**Figure 2.20)**. The slow kinetics was attributed to the stabilization of the photomerocyanine by the delocalized π system. As a result, the colour produced in toluene under UV irradiation (ε = 120 $M^{-1}.cm^{-1}$) was approximately two times more intense than for the 9-pyridyl-3*H*-naphtho[2,1-*b*]pyrans **2.48** and **2.50**.

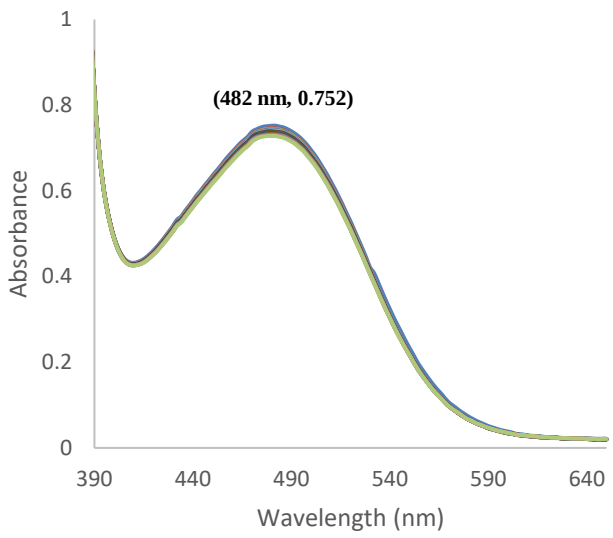

Figure 2.20 UV-Vis spectra of the bleaching in the dark of the PSS of **2.57** (6.0 mM in toluene, after UV irradiation) with a 120 seconds scan interval.

By UV irradiation of the 8-(3-pyridyl)-3*H*-naphtho[2,1-*b*]pyran **2.59** in toluene the photomerocyanine **2.260** was formed (**Scheme 2.121**).

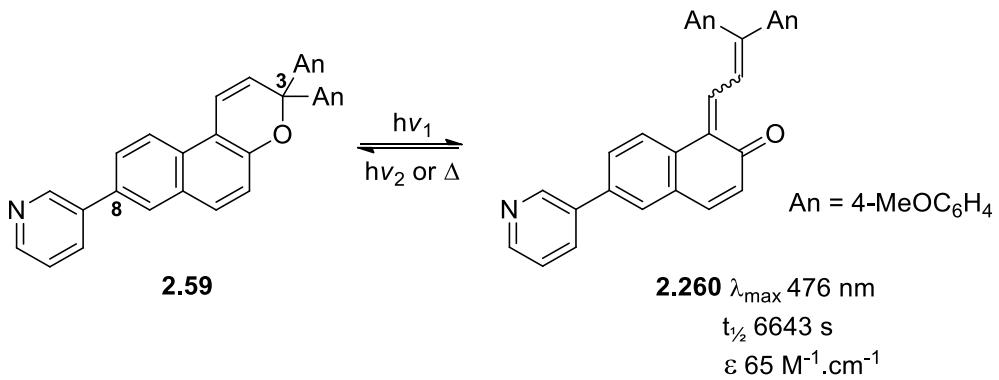

Scheme 2.121 Electrocyclic ring-opening of 3*H*-naphtho[2,1-*b*]pyran **2.59**.

In the 3*H*-naphtho[2,1-*b*]pyran **2.59**, the introduction of a 3-pyridyl substituent at C-8 (λ_{max} 476 nm in toluene) induced a very small bathochromic shift (1 nm) when compared to the simple 3,3-bis(4-methoxyphenyl) substituted 3*H*-naphtho[2,1-*b*]pyran (λ_{max} 475 nm in toluene) (**Figure 2.21**). The negligible red shift was due to the poor electronic conjugation between the 8-(3-pyridyl) substituent with the π system of the photomerocyanine **2.260** (**Scheme 2.122**).

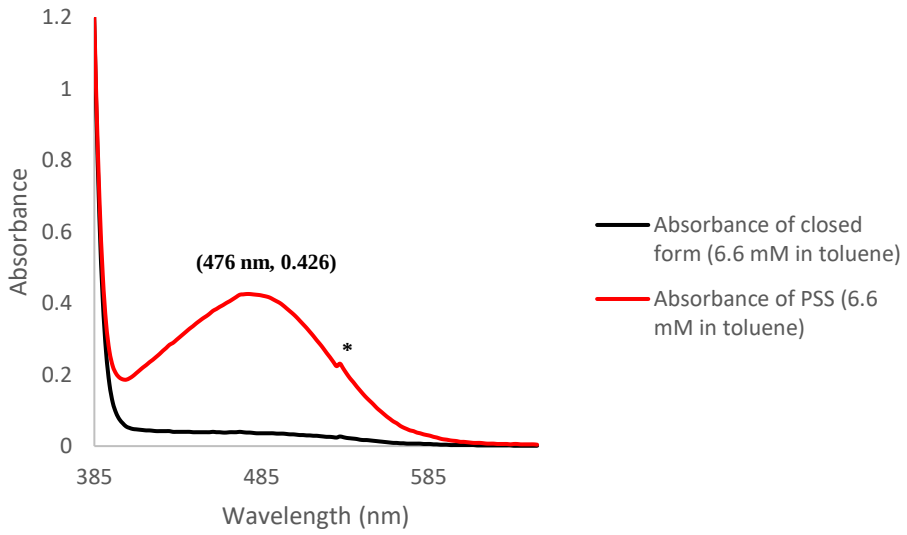

Figure 2.21 UV-Vis spectra of 3*H*-naphtho[2,1-*b*]pyran **2.59** (6.6 mM in toluene) in the closed form (black) and in the PSS (red).

***** Artefact due to a diffraction grating change for long λ region detection.

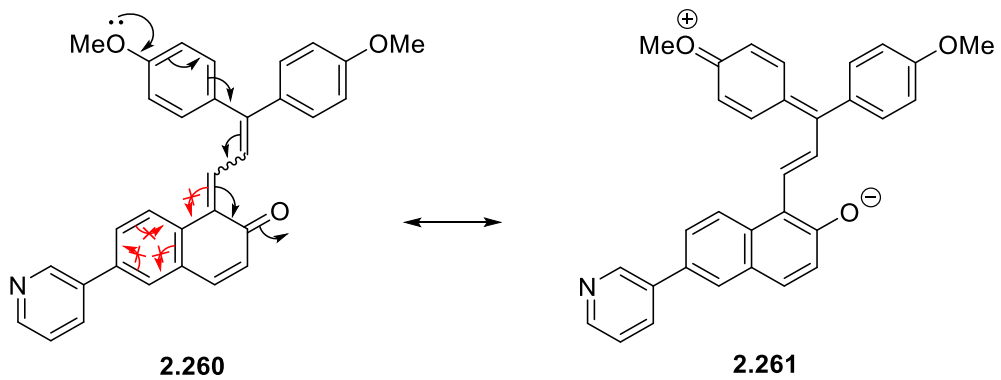

Scheme 2.122 Resonance structures of photomerocyanine **2.260**.

Due to the poor electronic conjugation between the 3-pyridyl N-atom at C-8 and the π system, the bleaching of the PSS of 3*H*-naphtho[2,1-*b*]pyran **2.59** ($t_{½}$ = 6643 s) was much faster when compared to the 3*H*-naphtho[2,1-*b*]pyran **2.57** ($t_{½}$ = 57740 s) (**Figure 2.22**). Thus, the red colour generated in toluene solution (ε = 65 $M^{-1}.cm^{-1}$) was weaker and similar to the one produced by the 9-pyridyl-3*H*-naphtho[2,1-*b*]pyrans **2.48** and **2.50**.

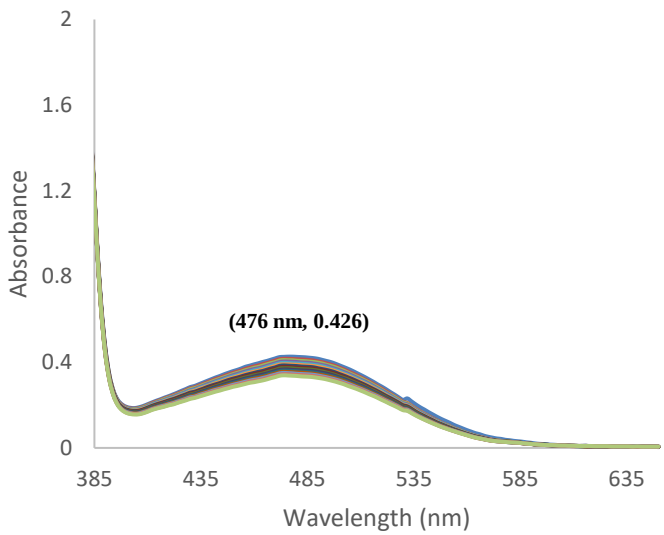

Figure 2.22 UV-Vis spectra of the bleaching in the dark of the PSS of **2.59** (6.6 mM in toluene, after UV irradiation) with a 120 seconds scan interval.

By UV irradiation of the 8-(2-pyridyl)-3*H*-naphtho[2,1-*b*]pyran **2.65** in solution the photomerocyanine **2.262** was formed (**Scheme 2.123**).

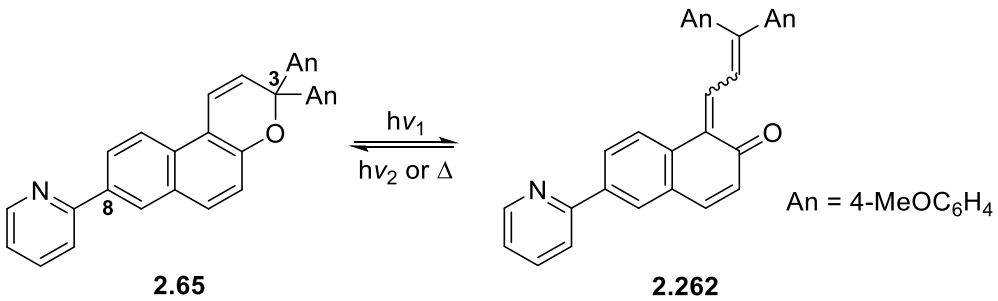

Scheme 2.123 Electrocyclic ring-opening of 3*H*-naphtho[2,1-*b*]pyran **2.65**.

In the 3*H*-naphtho[2,1-*b*]pyran **2.65**, the introduction of a 2-pyridyl substituent at C-8 produced a very weak photochrome as not even a distinct λ_{max} was detected, even though a broad weak absorption band was noted in the range (400 – 600 nm) (**Figure 2.23**).

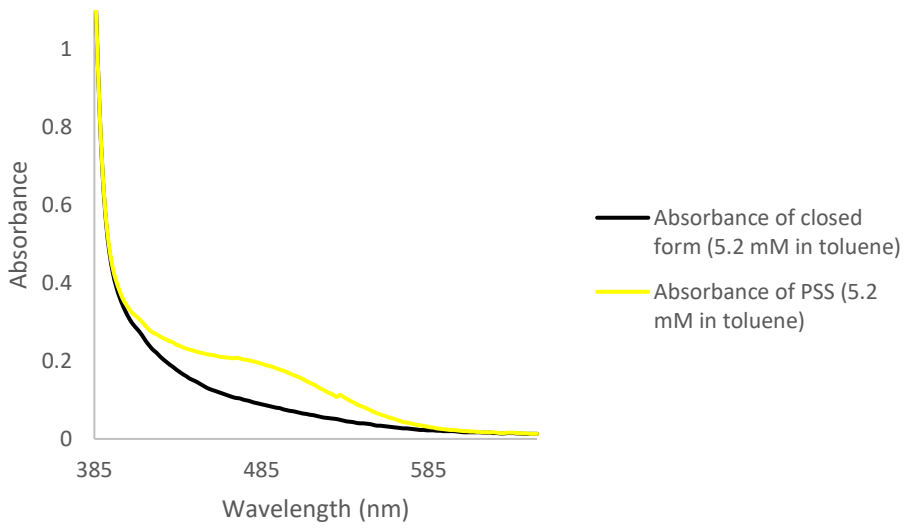

Figure 2.23 UV-Vis spectra of 3*H*-naphtho[2,1-*b*]pyran **2.65** (5.2 mM in toluene) in the closed form (black) and in the PSS (yellow).

In the photomerocyanine **2.262**, the 2-pyridyl at C-8 is electronically conjugated with the π system, therefore it can be envisioned that a resonance structure **2.263** in which the nitrogen has a negative charge and therefore contains two filled 2p orbitals can be presented (**Scheme 2.124**). Considering the proximity of the nitrogen to the naphthalene ring, it was rationalized that the two filled nitrogen 2p orbitals could donate electron density to the LUMO (of antibonding nature) of the naphthalene ring and consequently would destabilize the photomerocyanine formation (**Figure 2.24**).

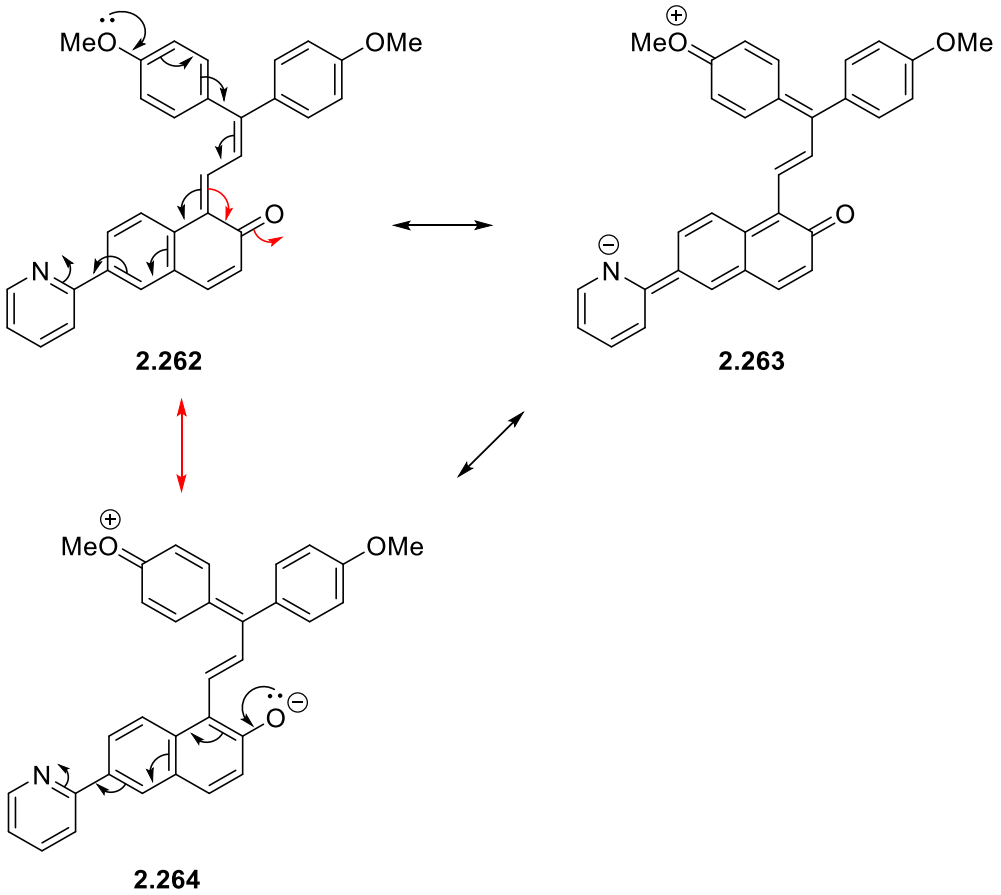

Scheme 2.124 Resonance structures of photomerocyanine **2.262**.

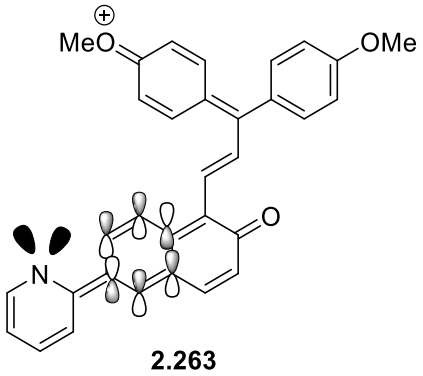

Figure 2.24 p-Electron donation to the LUMO of naphthalene of **2.263**.

By UV irradiation of the trimethoxy substituted 8-(4-pyridyl)-3*H*-naphtho[2,1-*b*]pyran **2.77** in toluene the photomerocyanine **2.265** was generated (**Scheme 2.125**).

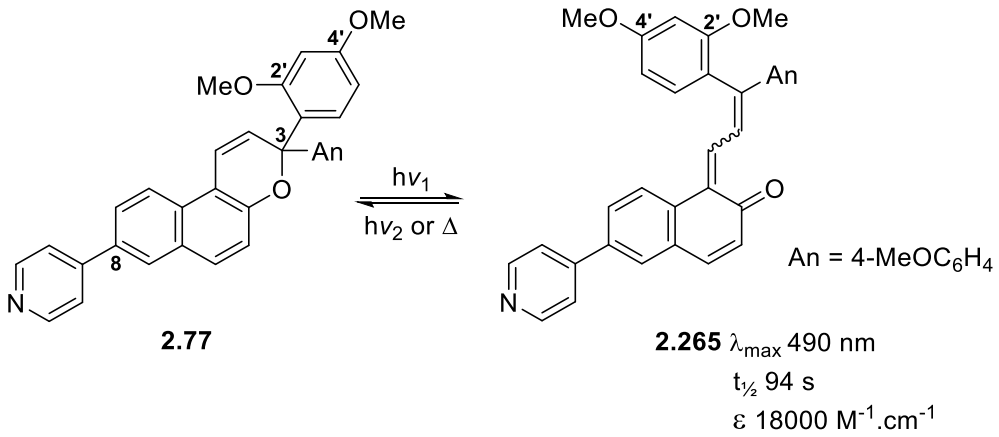

Scheme 2.125 Electrocyclic ring-opening of 3*H*-naphtho[2,1-*b*]pyran **2.65**.

In the 3*H*-naphtho[2,1-*b*]pyran **2.77**, the incorporation of a 4-pyridyl at C-8 (λ_{max} 490 nm in toluene) produced a bathochromic shift of 14 nm when compared to 3*H*-naphtho[2,1-*b*]pyran **2.266** (λ_{max} 476 nm in toluene) (**Figure 2.25**).

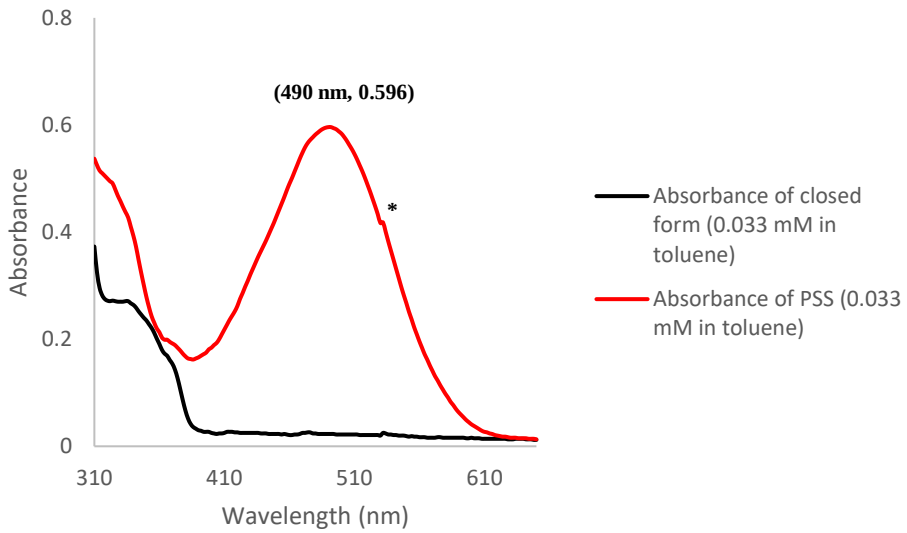

Figure 2.25 UV-Vis spectra of 3*H*-naphtho[2,1-*b*]pyran **2.77** (0.033 mM in toluene in the closed form (black) and in the PSS (red).

***** Artefact due to a diffraction grating change for long λ region detection.

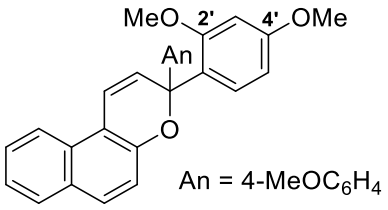

2.266 λ_{max} 476 nm (PhMe)

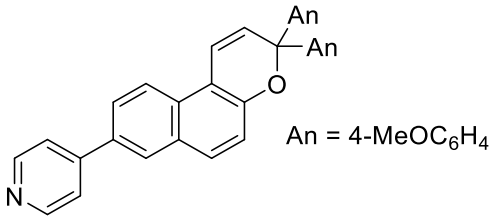

2.57 λ_{max} 482 nm (PhMe)
$t_{½}$ 32261 s

The observed red shift was due to the more extended π conjugated system of the photomerocyanine **2.265** (**Scheme 2.126**).

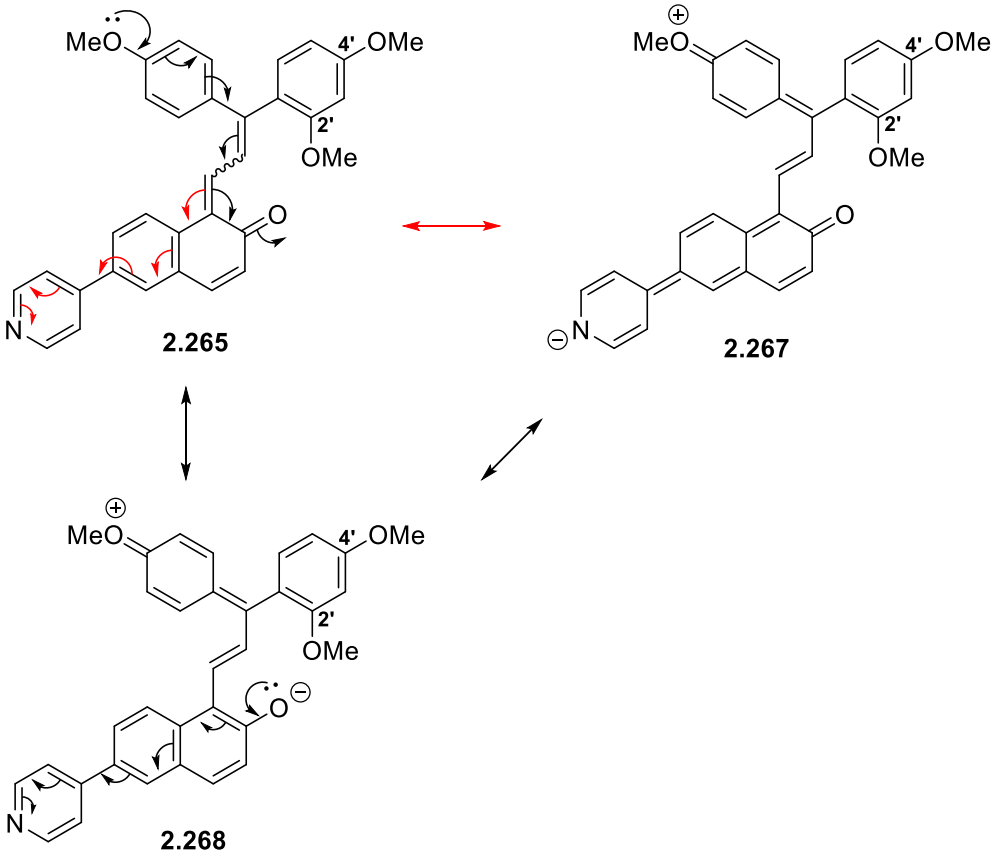

Scheme 2.126 Resonance structures of photomerocyanine **2.265**.

As a result of the extra methoxy group at C-2′ of **2.77**, the colour produced in toluene under UV irradiation (ε = 18000 $M^{-1}.cm^{-1}$) was 150 times more intense than for the 8-(4-pyridyl)-3*H*-naphtho[2,1-*b*]pyran **2.57**. On the other hand, the bleaching in the dark of the PSS of 8-(4-pyridyl)-3*H*-naphtho[2,1-*b*]pyran **2.77** ($t_{½}$ = 94 s) was 343 times faster than the PSS of 8-(4-pyridyl)-3*H*-

naphtho[2,1-*b*]pyran **2.57** ($t_{½}$ = 32260 s) (**Figure 2.26**). It has been reported that by increasing the steric demand made by a substituent at C-2′ the thermal ring closure of the photo-generated coloured species to the colourless pyran slows down (longer $t_{½}$).[122] Considering that the methoxy group at C-2′ is bulkier than hydrogen, it was rationalized, that for this example, the combined effect of the electronic conjugation on the photomerocyanine **2.265** coupled with the effect of the extra methoxy group at C-2′ might have constrained the isomerization of the TC isomer to the TT isomer. By doing so, and considering that the thermal ring closure of the TC isomer is much faster than the thermal isomerization of the TT to the TC, the $t_{½}$ would be substantially smaller.

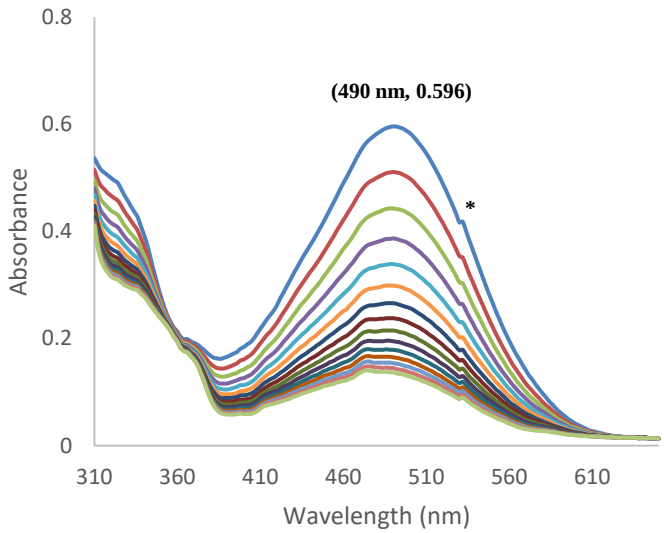

Figure 2.26 UV-Vis spectra of the bleaching in the dark of the PSS of **2.77** (0.033 mM in toluene, after UV irradiation) with a 20 seconds scan interval.

***** Artefact due to a diffraction grating change for long λ region detection.

Furthermore, the λ_{max} for **2.77** was bathochromic shifted by 8 nm relative to that for **2.57**. This must have been a result of the extra electronic donation. It was rationalized that the aryl group could adopt a more planar orientation due to the twist of the $(MeO)_2C_6H_3$ unit due to the steric clash between the *ortho* OMe and the hydrogen of the diene (**Figure 2.27**). Consequently, the aryl group would be a slightly better electron donor resulting in an 8 nm red shift of the λ_{max}.

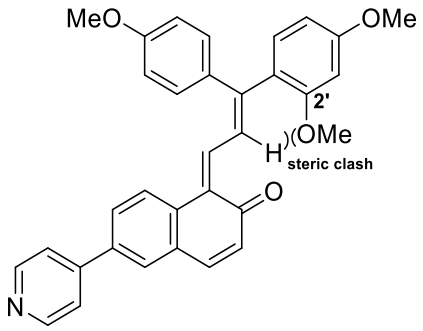

2.265 (TC)

Figure 2.27 *Transoid-cis* (TC) of isomer **2.265**.

2.3.1.4 8-(Pyridyl-triazole)-3*H*-naphtho[2,1-*b*]pyran

By UV irradiation of the 8-(pyridyl-triazole)-3*H*-naphtho[2,1-*b*]pyran **2.110** in toluene the photomerocyanine **2.269** was formed (**Scheme 2.127**).

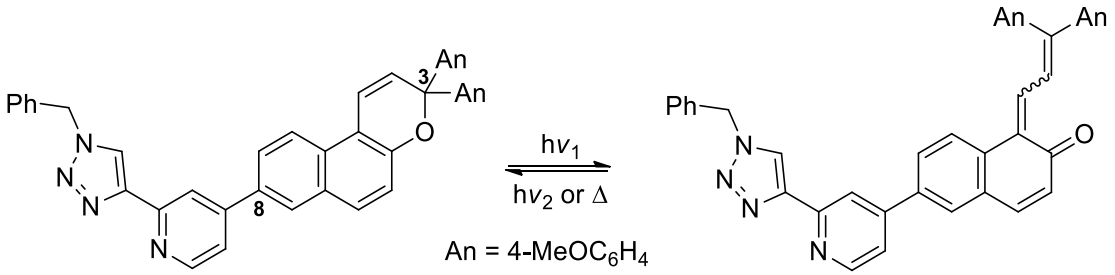

2.110

2.269 λ_{max} 480 nm
$t_{½}$ 5826 s
ε 141 $M^{-1}.cm^{-1}$

Scheme 2.127 Electrocyclic ring-opening of 3*H*-naphtho[2,1-*b*]pyran **2.110**.

In the 3*H*-naphtho[2,1-*b*]pyran **2.110**, the incorporation of a pyridyl-triazole substituent at C-8 (λ_{max} 480 nm in toluene) induced a small bathochromic shift (5 nm) when compared to the simple 3,3-bis(4-methoxyphenyl) substituted 3*H*-naphtho[2,1-*b*]pyran (λ_{max} 475 nm in toluene) (**Figure 2.28**).

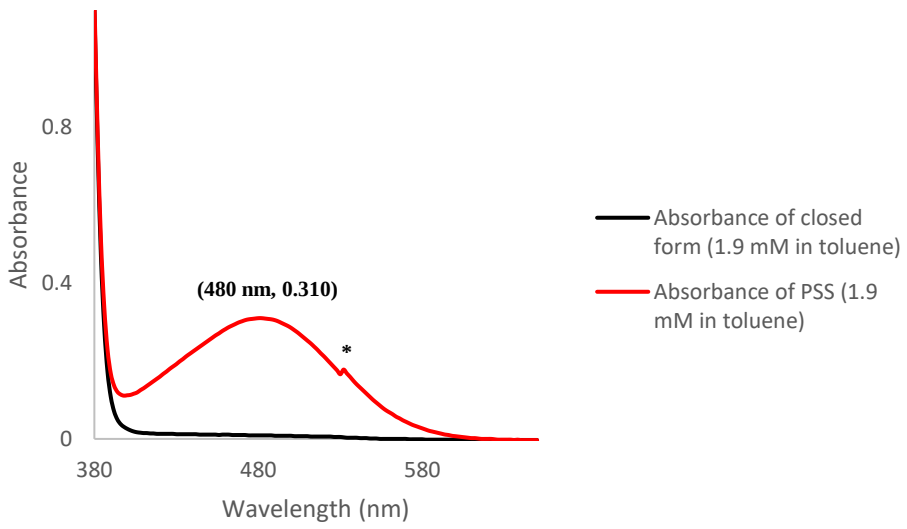

Figure 2.28 UV-Vis spectra of 3*H*-naphtho[2,1-*b*]pyran **2.110** (1.9 mM in toluene) in the closed form (black) and in the PSS (red).

***** Artefact due to a diffraction grating change for long λ region detection.

The observed red shift was due to the more extended π conjugated system of the photomerocyanine **2.269** (**Scheme 2.128**).

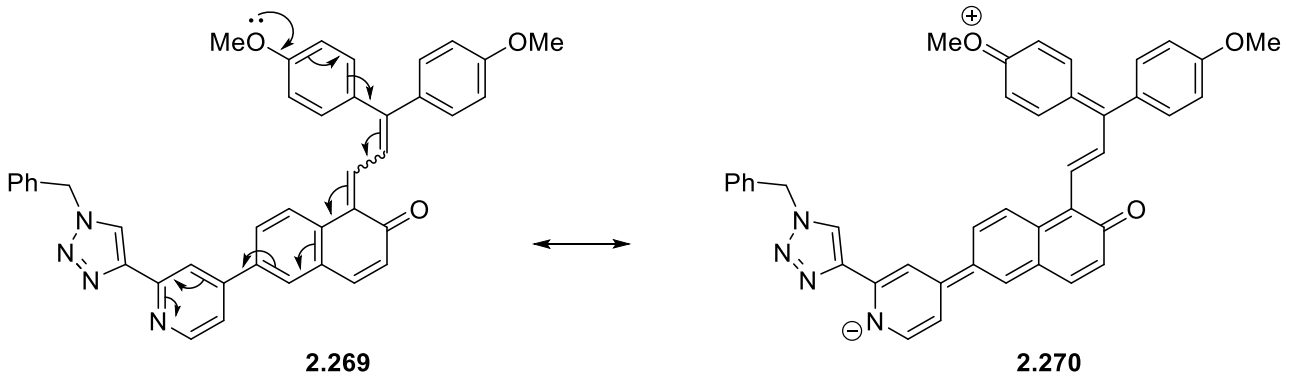

Scheme 2.128 Resonance structure of photomerocyanine **2.269**.

Thus, the generated red colour attributed to the PSS of 3*H*-naphtho[2,1-*b*]pyran **2.110** persisted for a shorter period of time ($t_{½}$ = 5826 s in toluene) when compared to the 8-(4-pyridyl)-3*H*-naphtho[2,1-*b*]pyran **2.57** ($t_{½}$ = 57740 s in toluene). The faster bleaching kinetics was a direct consequence of the presence of the triazole substituent on **2.110**. Potentially, the resonance structure **2.271** could act as a disrupting force of the stabilizing electronic conjugation described on **Scheme 2.128**, leading to a more unstable PSS. Furthermore, the colour produced in toluene under UV

irradiation (ε = 141 $M^{-1}.cm^{-1}$) was of similar intensity when compared to 8-(4-pyridyl)-3*H*-naphtho[2,1-*b*]pyran **2.57** (ε = 120 $M^{-1}.cm^{-1}$).

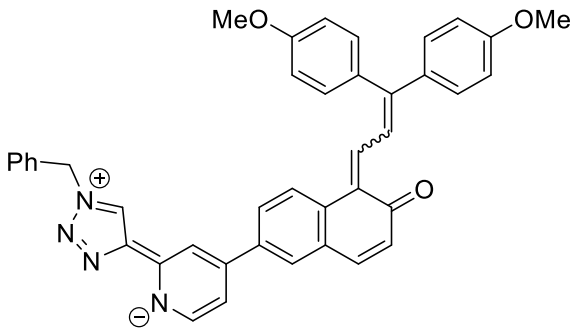

2.271

2.3.1.5 7-Pyridyl-3*H*-naphtho[2,1-*b*]pyran

By UV irradiation of the 7-(4-pyridyl)-3*H*-naphtho[2,1-*b*]pyran **2.98** in toluene the corresponding photomerocyanine **2.272** was formed (**Scheme 2.129**).

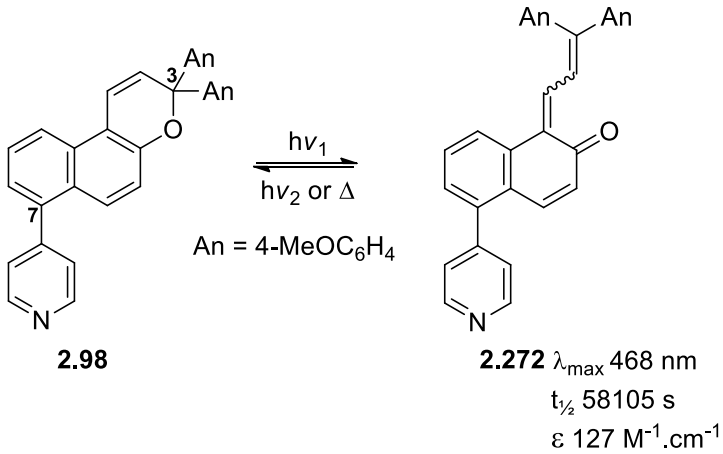

Scheme 2.129 Electrocyclic ring-opening of 3*H*-naphtho[2,1-*b*]pyran **2.98**.

The incorporation of a 4-pyridyl substituent at the C-7 (λ_{max} 468 nm in toluene) caused a small hypsochromic shift (7 nm) when compared to the simple 3,3-bis(4-methoxyphenyl) substituted 3*H*-naphtho[2,1-*b*]pyran (λ_{max} 475 nm in toluene) (**Figure 2.29**).

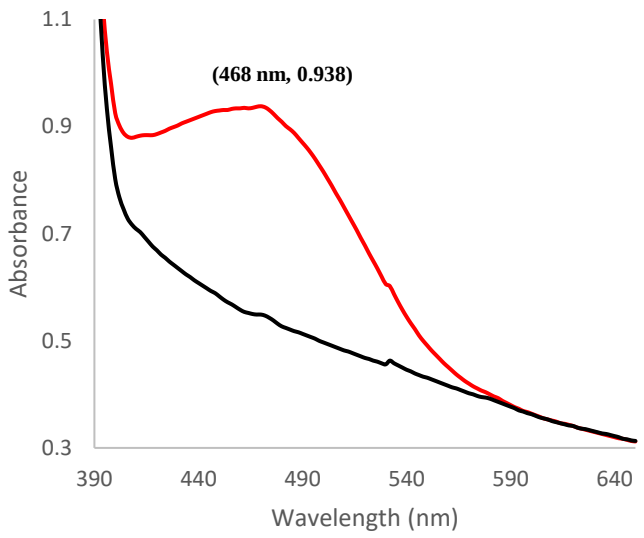

Figure 2.29 UV-Vis spectra of 3*H*-naphtho[2,1-*b*]pyran **2.98** (6.7 mM in toluene) in the closed form (black) and in the PSS (red).

The N-atom of the 4-pyridyl substituent at the C-7 of the photomerocyanine **2.272** is poorly electronically conjugated with the photo-generated π system (**Scheme 2.130**). However, there could be a small negative inductive effect that pulls electron density towards the pyridyl, as the nitrogen atom is relatively electronegative, which could explain the small blue shift in the 7-pyridyl substituted 3*H*-naphtho[2,1-*b*]pyran **2.98**.

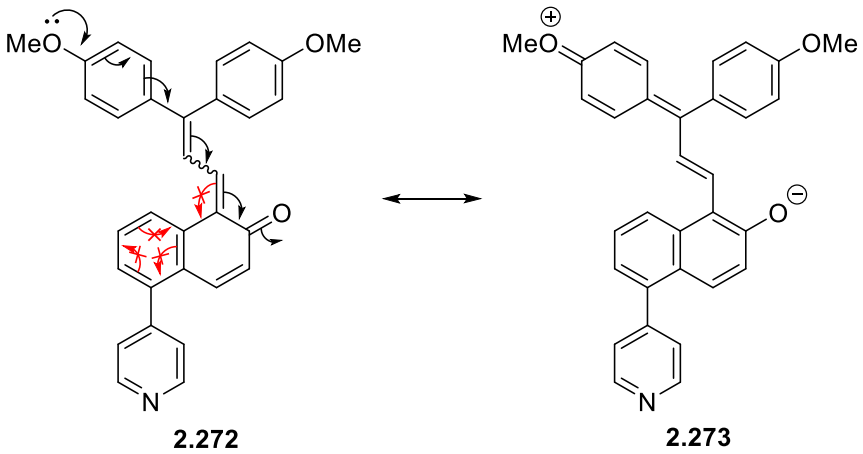

Scheme 2.130 Resonance structures of the photomerocyanine **2.272**.

2.3.1.6 6-Pyridyl-3*H*-naphtho[2,1-*b*]pyran

By UV irradiation of the 6-pyridyl-3*H*-naphtho[2,1-*b*]pyrans **2.214** and **2.215** in toluene the corresponding photomerocyanines **2.274** and **2.275** were formed (**Scheme 2.131**).

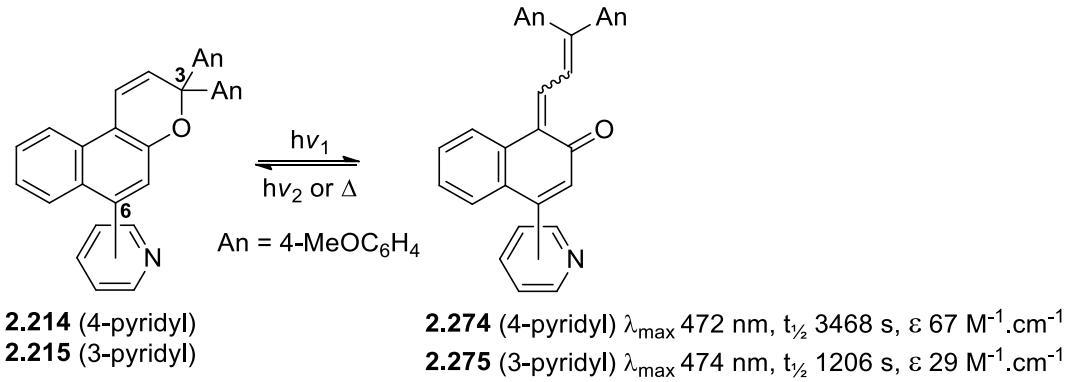

Scheme 2.131 Electrocyclic ring-opening of 3*H*-naphtho[2,1-*b*]pyrans **2.214** and **2.215**.

The incorporation of a 4-pyridyl (λ_{max} 472 nm in toluene) or a 3-pyridyl (λ_{max} 474 nm in toluene) at the C-6 caused a small hypsochromic shift of 3 and 1 nm, respectively, when compared to the simple 3,3-bis(4-methoxyphenyl) substituted 3*H*-naphtho[2,1-*b*]pyran (λ_{max} 475 nm in toluene) (**Figures 2.30** and **2.31**).

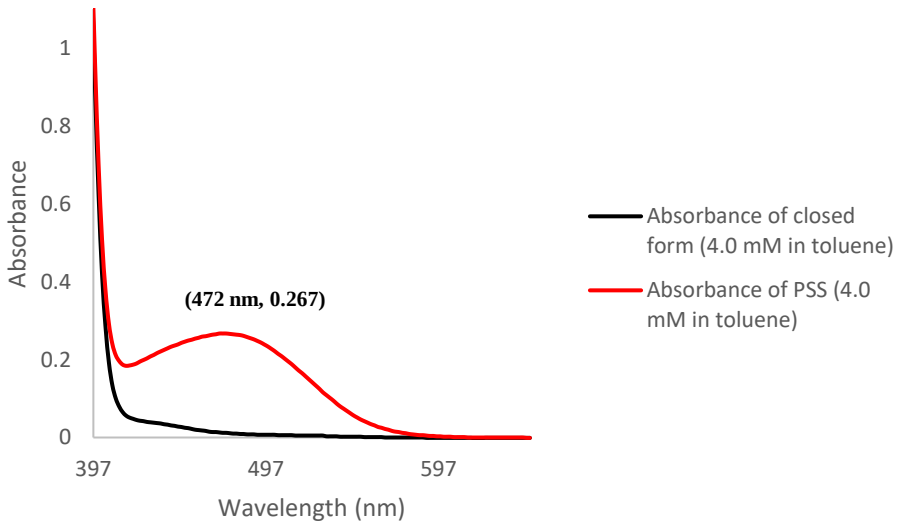

Figure 2.30 UV-Vis spectra of 3*H*-naphtho[2,1-*b*]pyran **2.214** (4.0 mM in toluene) in the closed form (black) and in the PSS (red).

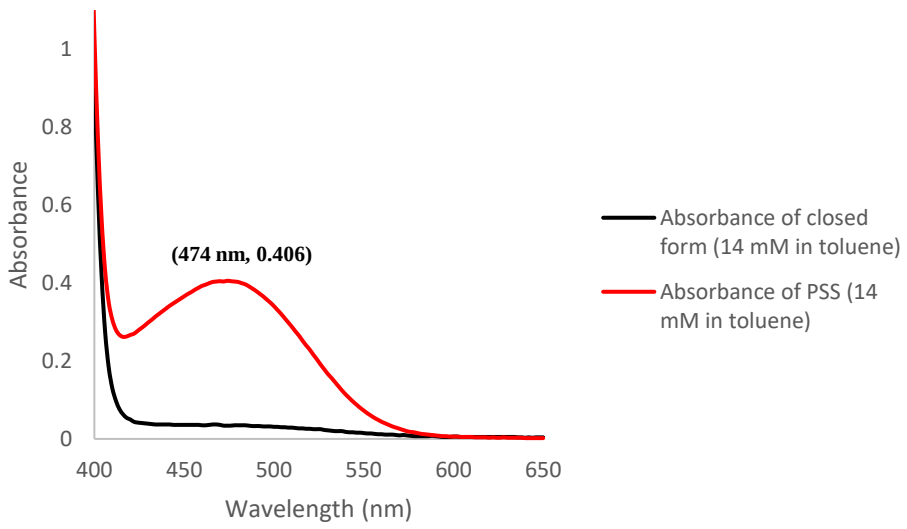

Figure 2.31 UV-Vis spectra of 3*H*-naphtho[2,1-*b*]pyran **2.215** (14 mM in toluene) in the closed form (black) and in the PSS (red).

The 4- and 3-pyridyl substituents at C-6 are poorly electronically conjugated with the photo-generated π system (**Schemes 2.132** and **2.133**). The small blue shift in the λ_{max} was probably a consequence of a small negative inductive effect that pulls electron density towards the pyridyl, as the nitrogen atom is relatively electronegative. Interestingly, the presence of strong electron-donating groups (e.g. MeO and morpholino) at C-6 also leads to an hypsochromic shift of the λ_{max} coupled with increased colourability.[133]

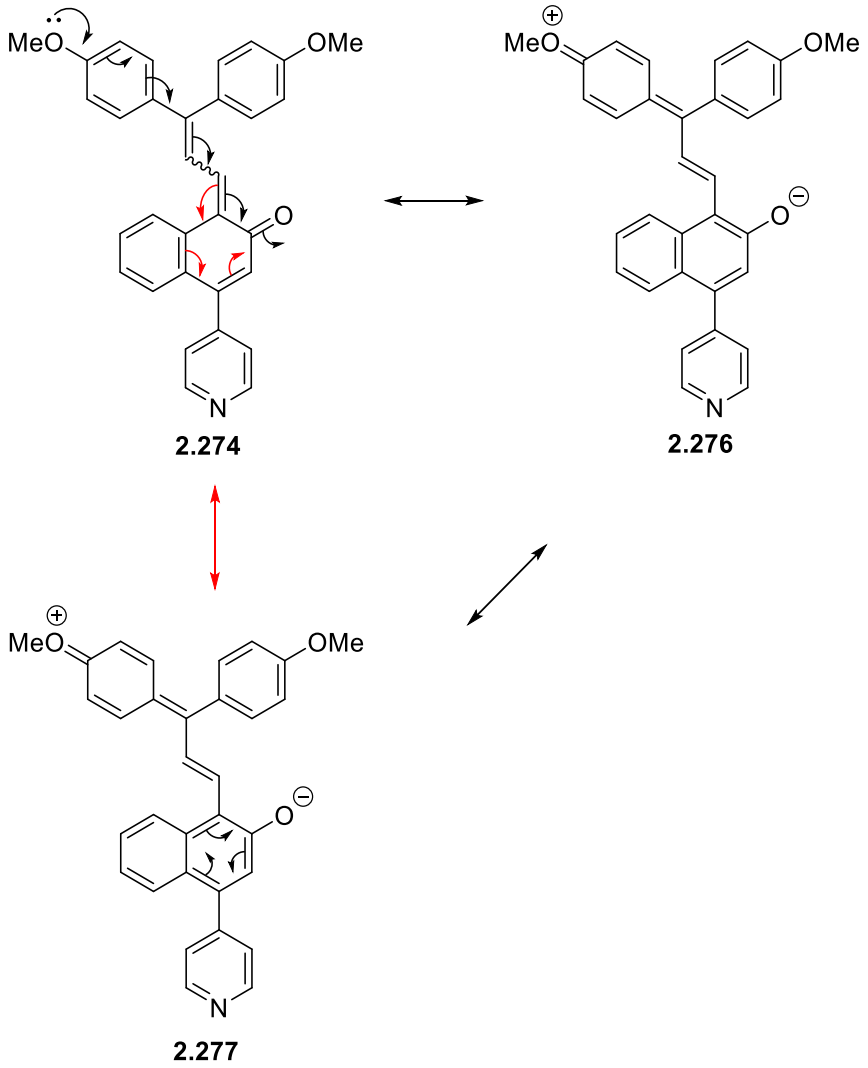

Scheme 2.132 Resonance structures of the photomerocyanine **2.274**.

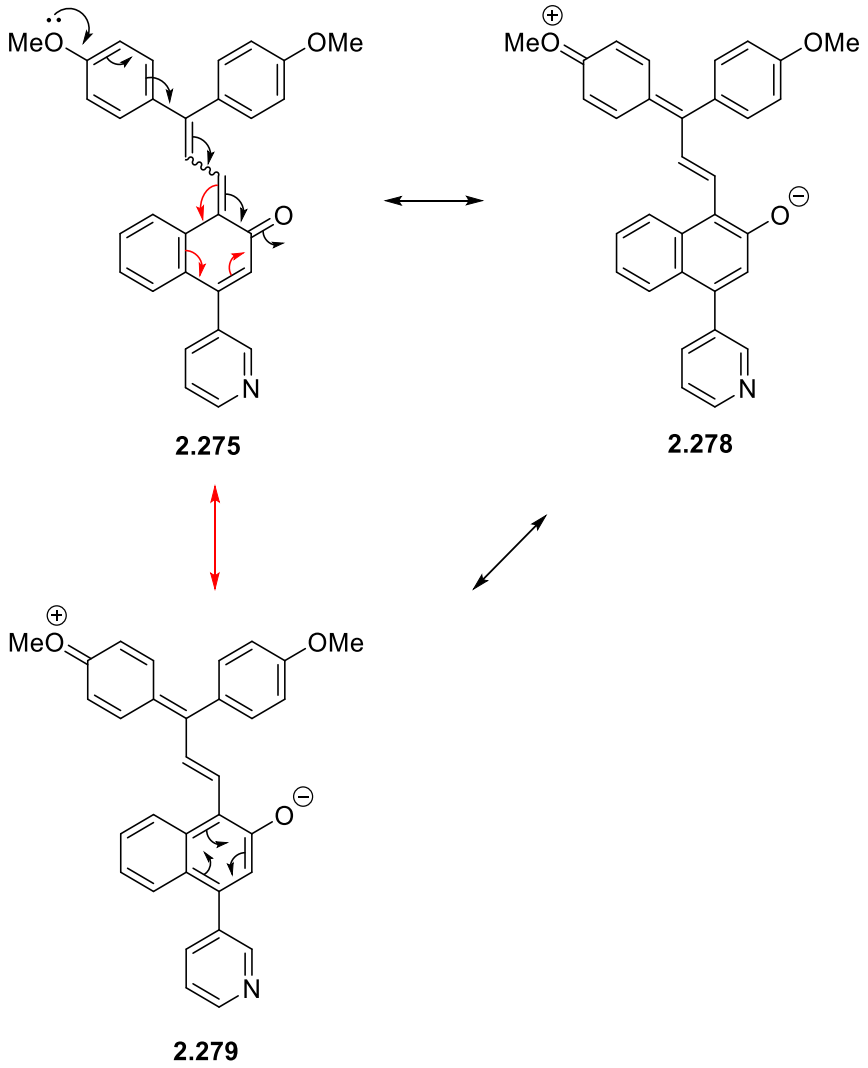

Scheme 2.133 Resonance structures of the photomerocyanine **2.275**.

Furthermore, the orientation of the pyridyl moiety at C-6 had a small yet relevant effect in both the bleaching kinetics and the colourability of the PSS. Hence, the PSS of the 6-(4-pyridyl)-3*H*-naphtho[2,1-*b*]pyran **2.113** was slower to bleach ($t_{½}$ = 3468 s) and produced stronger coloration (ε = 67 $M^{-1}.cm^{-1}$) when compared to the PSS of the 6-(3-pyridyl)-3*H*-naphtho[2,1-*b*]pyran **2.114** ($t_{½}$ = 1206 s; ε = 29 $M^{-1}.cm^{-1}$) (**Figures 2.32** and **2.33**).

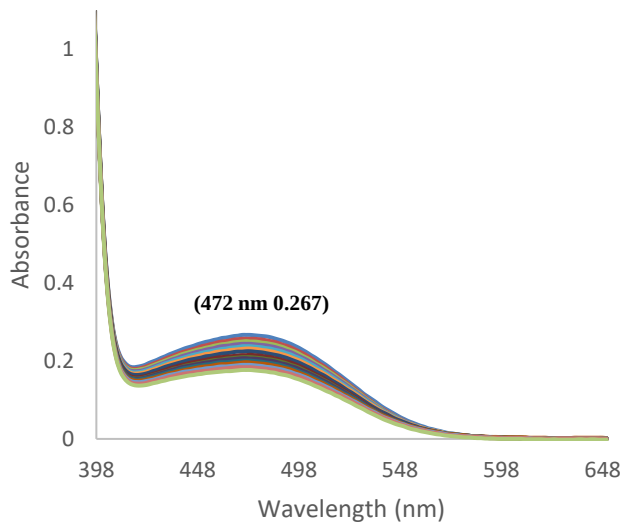

Figure 2.32 UV-Vis spectra of the bleaching in the dark of the PSS of **2.114** (4.0 mM in toluene, after UV irradiation) with a 120 seconds scan interval.

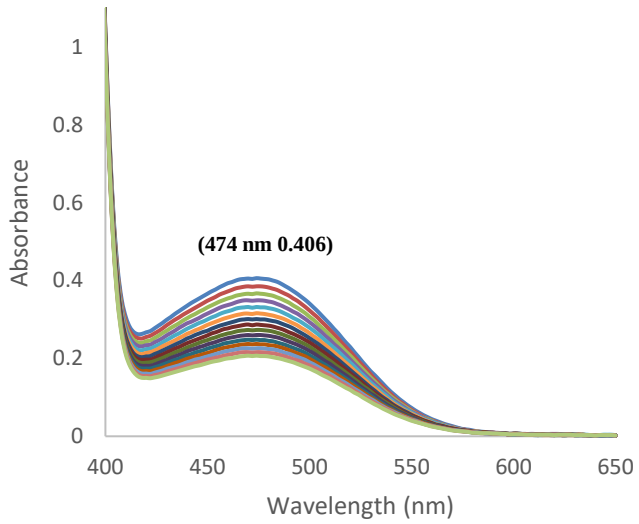

Figure 2.33 UV-Vis spectra of the bleaching in the dark of the PSS of **2.115** (14 mM in toluene, after UV irradiation) with an 80 seconds scan interval.

2.3.1.7 3-Pyridyl-3*H*-naphtho[2,1-*b*]pyran

By UV irradiation of the 3-(4-pyridyl)-3*H*-naphtho[2,1-*b*]pyran **2.170** in toluene the corresponding photomerocyanine **2.280** was formed (**Scheme 2.134**).

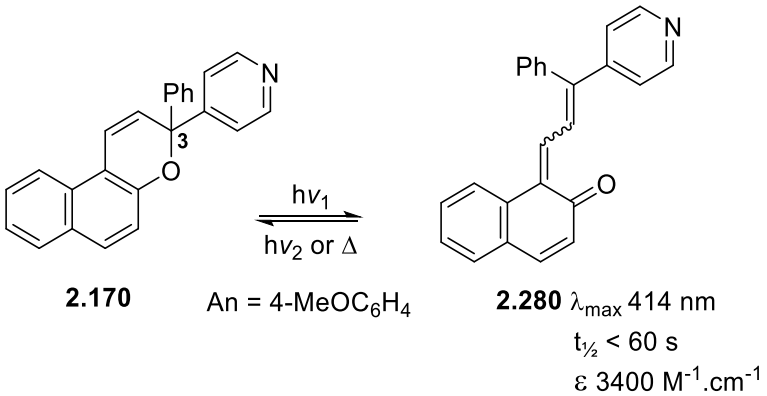

Scheme 2.134 Electrocyclic ring-opening of 3*H*-naphtho[2,1-*b*]pyran **2.170**.

It is well documented that electron-withdrawing groups at C-3 cause an hypsochromic shift in the λ_{max} of the photomerocyanine.[123] Thus, the substitution of a phenyl group for an electron-withdrawing 4-pyridyl group at C-3 caused an hypsochromic shift of 18 nm when compared to the simple 3,3-diphenyl substituted 3*H*-naphtho[2,1-*b*]pyran (λ_{max} 432 nm in toluene) (**Figure 2.34**).

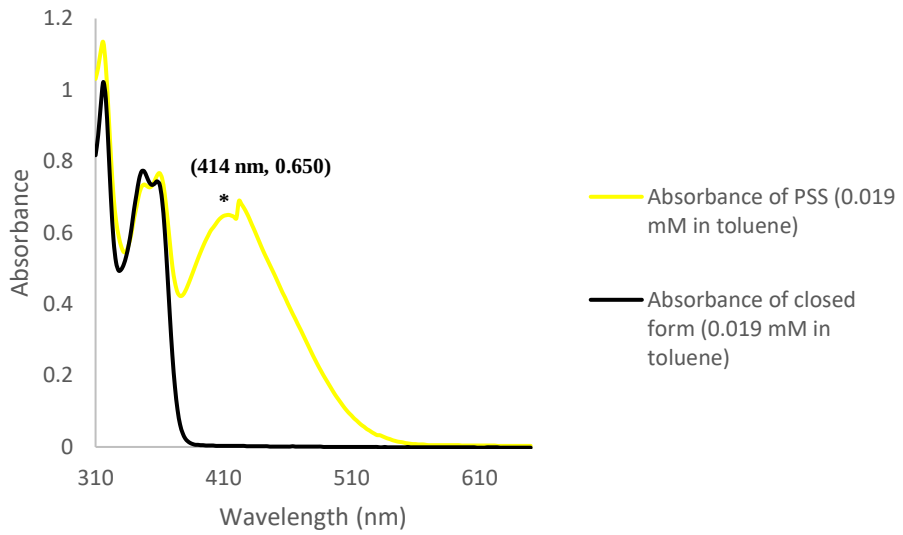

Figure 2.34 UV-Vis spectra of 3*H*-naphtho[2,1-*b*]pyran **2.170** (0.19 mM in toluene) in the closed form (black) and in the PSS (yellow).

*Artefact due to a diffraction grating change for long λ region detection.

Furthermore, the pale yellow colour attributed to the PSS of the 3*H*-naphtho[2,1-*b*]pyran **2.170** persisted for a shorter period time ($t_{½}$ < 60 s in toluene) with a stronger intensity (ε = 3400 $M^{-1}.cm^{-1}$) when compared to other pyridyl substituted 3*H*-naphtho[2,1-*b*]pyrans (**Figure 2.35**). However, the

lack of a *para* methoxy group in the other phenyl at C-3 makes this comparison somehow biased, as its absence on **2.170** was critically important for the faster bleaching kinetics and increased colourability.

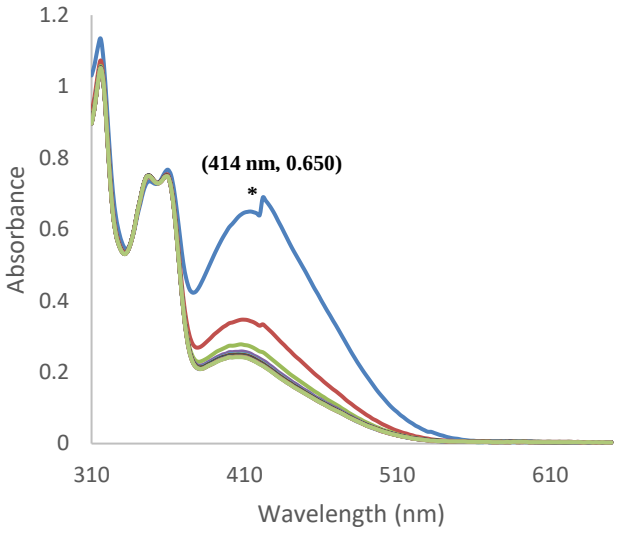

Figure 2.35 UV-Vis spectra of the bleaching in the dark of the PSS of **2.170** (0.19 mM in toluene, after UV irradiation) with a 30 seconds scan interval.

***** Artefact due to a diffraction grating change for long λ region detection.

2.3.1.8 8-Aryl-3*H*-naphtho[2,1-*b*]pyrans

In addition to the pyridyl substituted 3*H*-naphtho[2,1-*b*]pyrans, all containing the electron-withdrawing pyridyl group in different positions of the naphthopyran scaffold, a small series of 8-aryl substituted 3*H*-naphtho[2,1-*b*]pyrans was studied. Thus, three targets were analysed: 1) 3*H*-naphtho[2,1-*b*]pyran **2.70** containing an electron-donating 4-$MeOC_6H_4$ group; 2) 3*H*-naphtho[2,1-*b*]pyran **2.72** containing the electronically neutral phenyl group and 3) 3*H*-naphtho[2,1-*b*]pyran **2.74** containing the electron-withdrawing 4-$NO_2C_6H_4$ group. All target molecules produced the corresponding photomerocyanines under UV irradiation (**Scheme 2.135**).

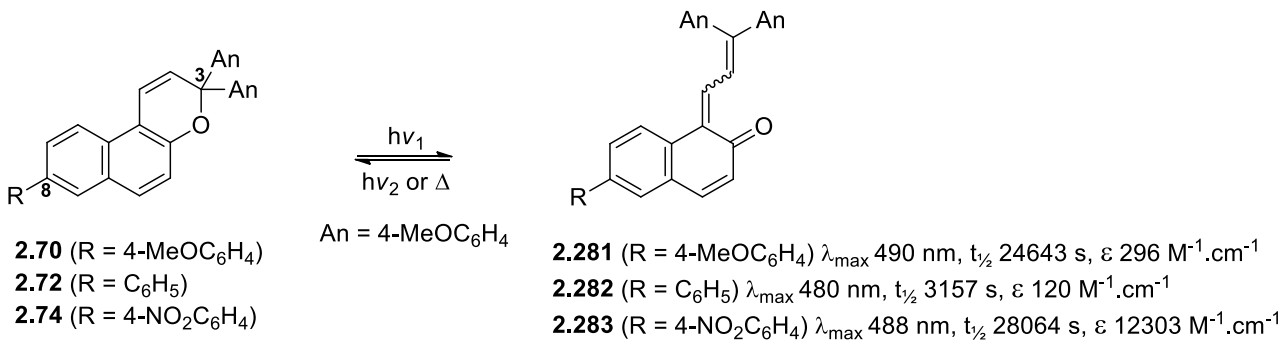

Scheme 2.135 Electrocyclic ring-opening of 3*H*-naphtho[2,1-*b*]pyrans **2.70**, **2.72** and **2.74**.

The PSS of the 3*H*-naphtho[2,1-*b*]pyrans **2.70**, **2.72** and **2.74** had λ_{max} values of 490 nm, 482 nm and 488 nm, respectively. These correspond to a bathochromic shift of 15 nm, 7 nm and 13 nm, respectively, when compared to the simple 3,3-bis(4-methoxyphenyl) substituted 3*H*-naphtho[2,1-*b*]pyran (λ_{max} 475 nm in toluene). The resulting red shift was a consequence of the more extended π system of the corresponding photomerocyanines **2.281**, **2.282** and **2.283**, irrespective of the electronic nature of the terminal group at C-8.

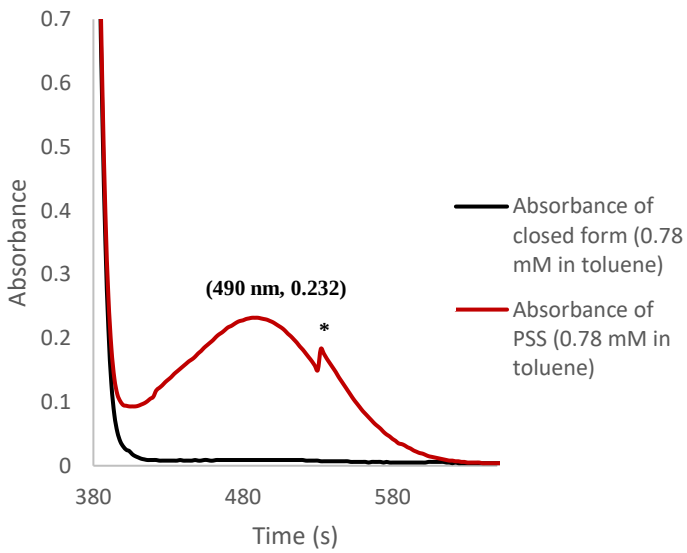

Figure 2.36 UV-Vis spectra of 3*H*-naphtho[2,1-*b*]pyran **2.70** (0.78 mM in toluene) in the closed form (black) and in the PSS (red).

* Artefact due to a diffraction grating change for long λ region detection.

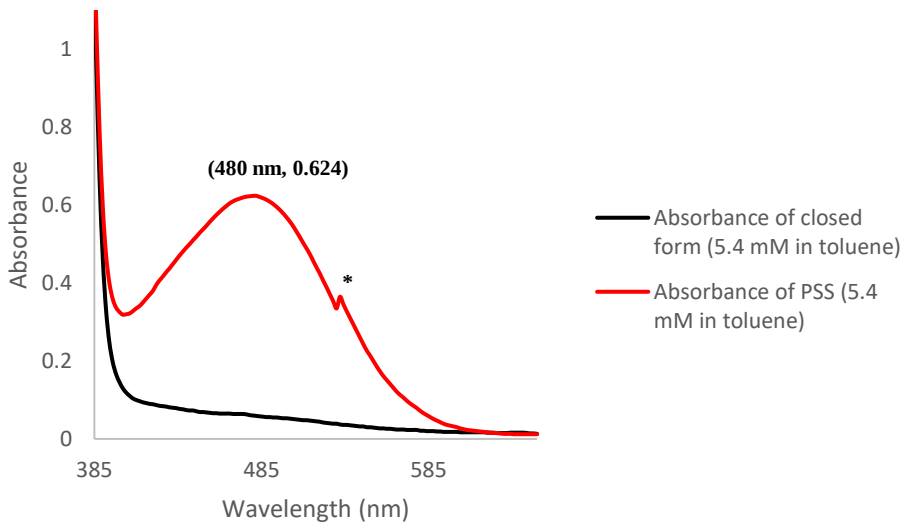

Figure 2.37 UV-Vis spectra of 3*H*-naphtho[2,1-*b*]pyrans **2.72** (5.4 mM in toluene) in the closed form (black) and in the PSS (red).

***** Artefact due to a diffraction grating change for long λ region detection.

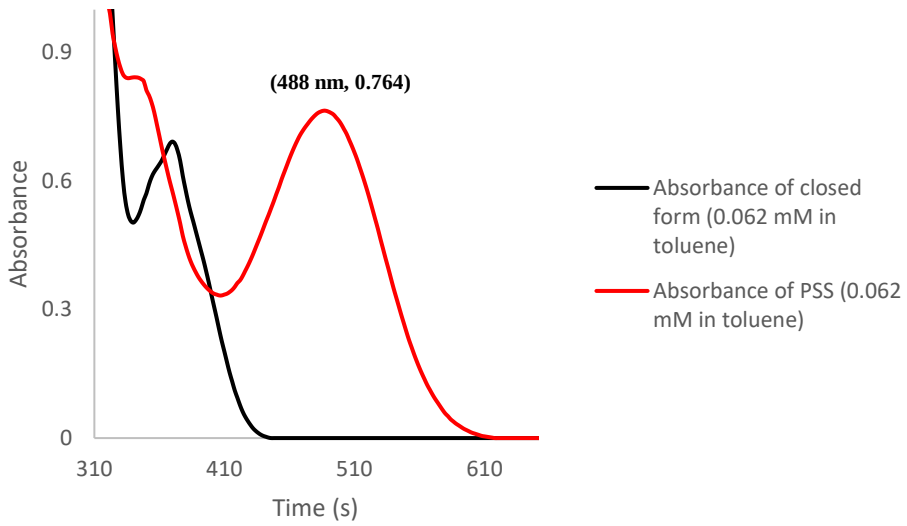

Figure 2.38 UV-Vis spectra of 3*H*-naphtho[2,1-*b*]pyrans **2.74** (0.062 mM in toluene) in the closed form (black) and in the PSS (red).

The red colour attributed to the PSS of the 3*H*-naphtho[2,1-*b*]pyrans **2.70** and **2.74** persisted for a long period of time (**Figures 2.39** and **2.40**). On the other hand, the PSS of the 8-phenyl-3*H*-naphtho[2,1-*b*]pyran **2.72** faded much faster in comparison ($t_{½}$ = 3157 s) (**Figure 2.41**).

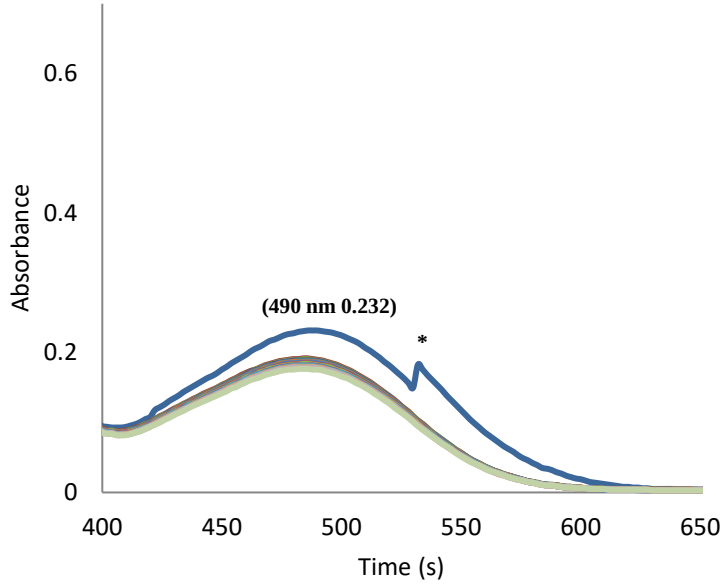

* Artefact due to a diffraction grating change for long λ region detection.

Figure 2.39 UV-Vis spectra of the bleaching in the dark of the PSS of **2.70** (0.078 mM in toluene, after UV irradiation) with a 240 seconds scan interval.

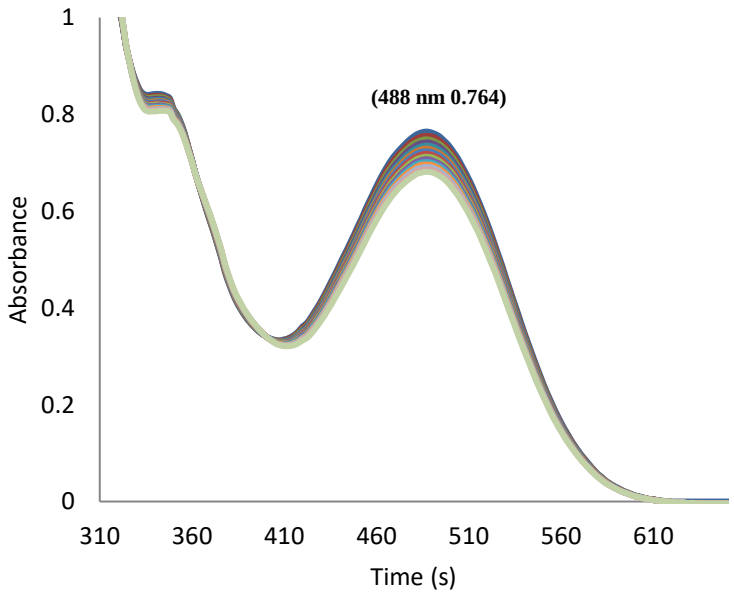

Figure 2.40 UV-Vis spectra of the bleaching in the dark of the PSS of **2.74** (0.062 mM in toluene, after UV irradiation) with a 240 seconds scan interval.

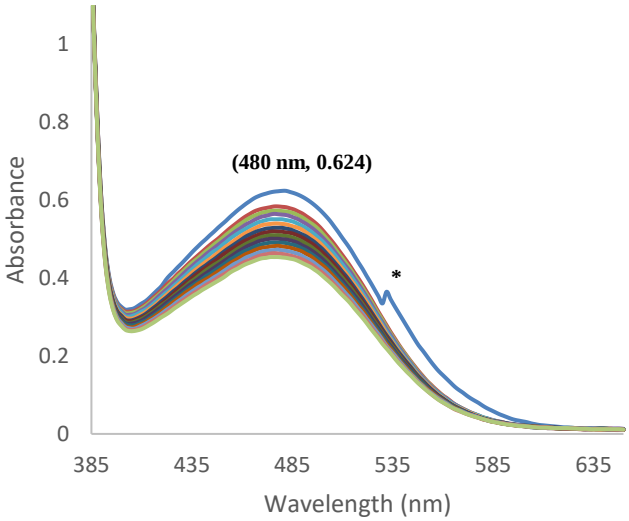

Figure 2.41 UV-Vis spectra of the bleaching in the dark of the PSS **2.72** (5.4 mM in toluene, after UV irradiation) with a 120 seconds scan interval.

***** Artefact due to a diffraction grating change for long λ region detection.

It is noteworthy that the colour produced by the 3*H*-naphtho[2,1-*b*]pyran **2.74** (ε = 12303 $M^{-1}.cm^{-1}$) was several times more intense than the one produced by the 3*H*-naphtho[2,1-*b*]pyran **2.70** (ε = 296 $M^{-1}.cm^{-1}$) and the 3*H*-naphtho[2,1-*b*]pyran **2.72** (ε = 120 $M^{-1}.cm^{-1}$). The strong colourability of the 3*H*-naphtho[2,1-*b*]pyran **2.74** was attributed to the stabilization of the photomerocyanine **2.283** by the delocalized π system (**Scheme 2.136**).

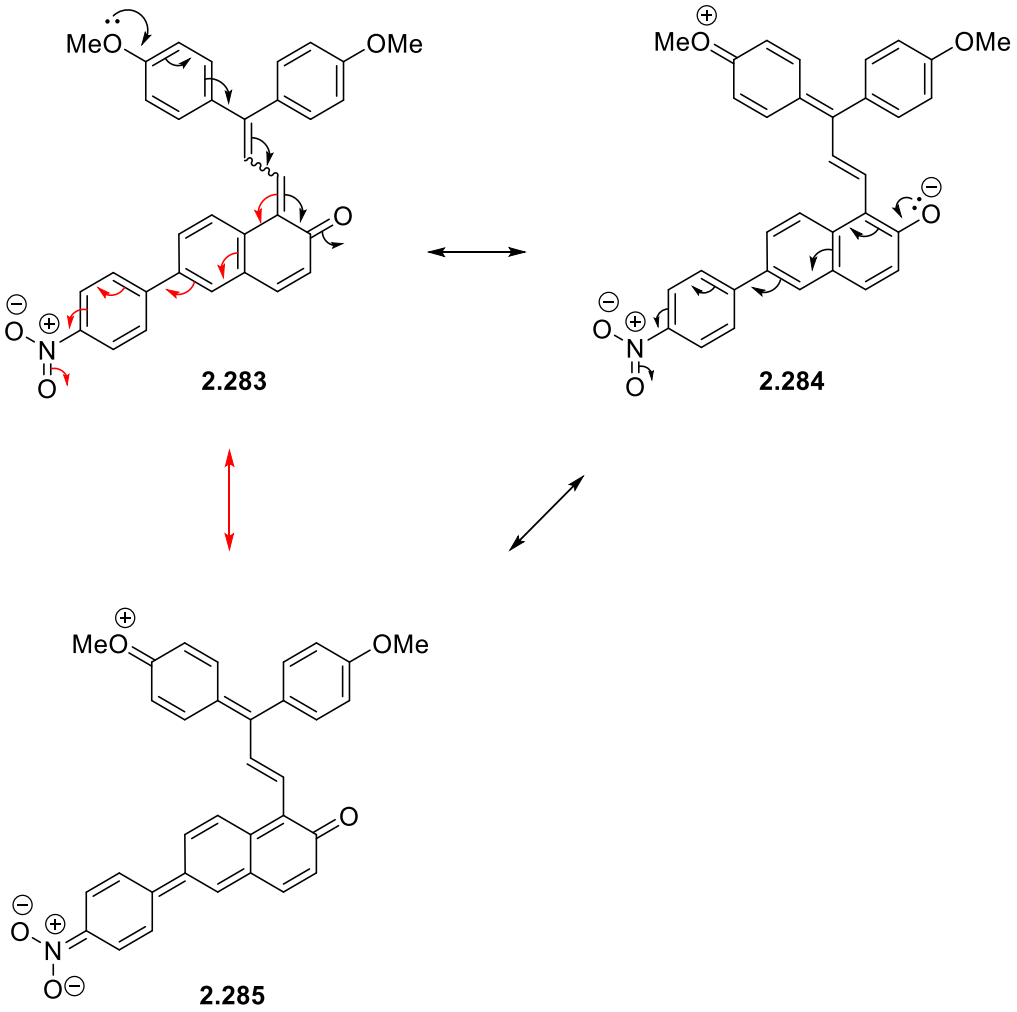

Scheme 2.136 Resonance structures of the photomerocyanine **2.283**.

2.3.2 Photochromism and Photoswitching of the Rhenium(I) Complexes

The *fac*-[Re(N^N)(CO)$_3$NP]PF$_6$ complexes, with NP = Pyridyl-3*H*-naphtho[2,1-*b*]pyran and N^N = BPy, PyTz or BTz, all exhibited photochromism at room temperature by generating coloured solutions after UV irradiation. Thus, the generated colour was attributed to the formation of the corresponding photomerocyanines (**Scheme 2.137**). Furthermore, by either irradiating the photomerocyanines at their λ_{max} or by thermal bleaching, the colourless closed forms were restored, which showed that the rhenium(I) complexes exhibited both P- and T-type photochromism.

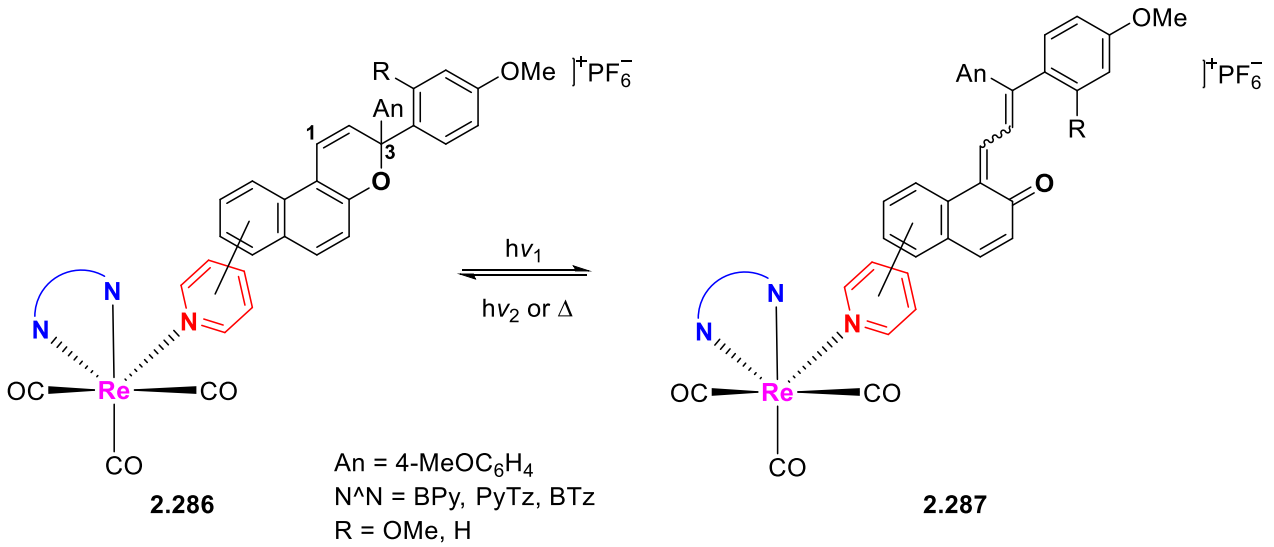

Scheme 2.137 Electrocyclic ring-opening of *fac*-[Re(N^N)(CO)$_3$NP]PF$_6$ complexes, with NP = Pyridyl-3*H*-naphtho[2,1-*b*]pyran and N^N = BPy, PyTz or BTz.

Furthermore, most of the *fac*-[Re(N^N)(CO)$_3$NP]PF$_6$ complexes exhibited bidentate-ligand sensitive ^{3}MLCT phosphorescence. By changing the bidentate ligand, the energy of the LUMO for the ^{1}MLCT transition was modified. Logically, the HOMO – LUMO energy gap for the ^{1}MLCT transition also changed, which consequently affected the emission energy maxima (λ_{Em}) of the ^{3}MLCT phosphorescence. Hence, the E_{LUMO} (BTz) > E_{LUMO} (PyTz) >> E_{LUMO} (BPy) and therefore λ_{Em} (BTz) < λ_{Em} (PyTz) << λ_{Em} (BPy). For example, when comparing the *fac*-[Re(N^N)(CO)$_3$NP]PF$_6$ complexes **2.232**, **2.239** and **2.245**, where only the bidentate ligand was changed, there was a large shift (132 nm) in the λ_{Em} when comparing **2.232** (BPy, λ_{Em} 594 nm) and **2.239** (PyTz, λ_{Em} 462 nm). Moreover, there was only small shift (3 nm) between **2.239** (PyTz, λ_{Em} 462 nm) and **2.245** (BTz, λ_{Em} 459 nm) as the LUMO (BTz) and LUMO (PyTz) were much closer in energy.

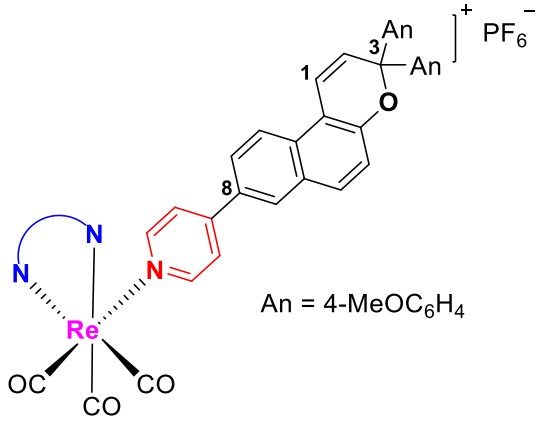

2.232 (N^N = BPy) λ_{Em} 594 nm
2.239 (N^N = PyTz) λ_{Em} 462 nm
2.245 (N^N = BTz) λ_{Em} 459 nm

The ^{3}MLCT emission of all Re(I) complexes showed a typical blue shift in emission energy with decreasing solvent dielectric constant (**Figure 2.42**). The foregoing solvent dependence was due to the increase in the dipole moment of the excited state, which is more stabilized by a polar solvent medium in comparison to its ground state.[224]

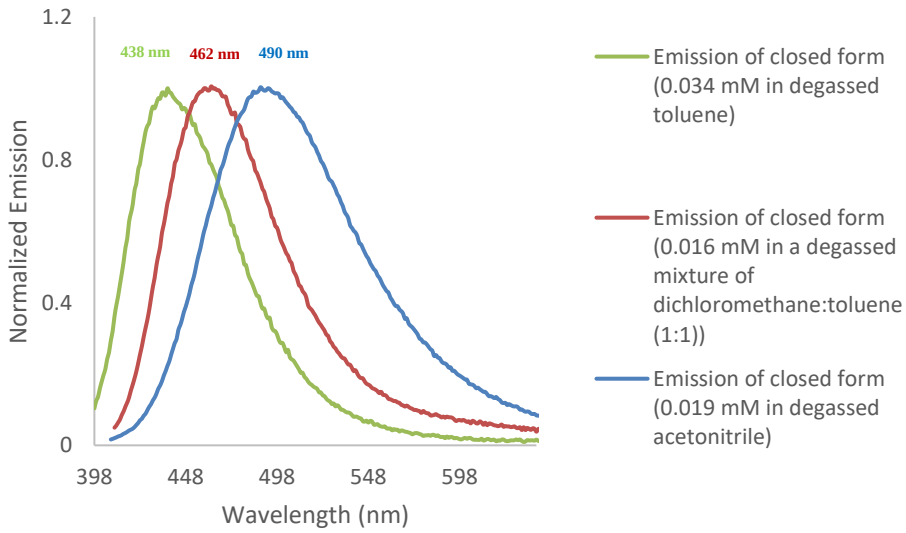

Figure 2.42 Normalized spectra of emission of **2.239** (0.034 mM in degassed toluene, λ_{exc} 388 nm, green), emission of **2.239** (0.016 mM in a degassed mixture of dichloromethane:toluene (1:1), λ_{exc} 394 nm, red) and emission of **2.239** (0.019 mM in degassed acetonitrile, λ_{exc} 392 nm, blue).

The emission of the *fac*-[Re(N^N)(CO)$_3$NP]PF$_6$ complexes had a lifetime of 50 – 171 ns which is similar to the experimentally measured phosphorescence lifetime of the *fac*-[Re(N^N)(CO)$_3$Pyridine]PF$_6$ (129 ns).

As stated before in **Section 1.1**, the photochromic reaction involving 3*H*-naphtho[2,1-*b*]pyrans follows a one-photon absorption (1PA) mechanism. The absorption of an UV photon generates the first or second singlet excited states (S_1 and S_2) which rapidly relax to the lowest energy excited state (S_1). By following Kasha's rule, it is from this generated singlet excited state S_1 that the photochromic reaction occurs. Remarkably, when irradiating the photochromic Re(I) complexes with violet light (450 nm > λ > 400 nm) a PSS was generated which corresponded to 36 – 44% of the PSS reached with UV irradiation at 365 nm. Considering that the pyridyl-3*H*-naphtho[2,1-*b*]pyrans themselves do not absorb in the visible region, it was assumed that the photochromic reaction was occurring due to a triplet photosensitization mechanism. It was envisioned that after exciting in the ^{1}MLCT absorption band, intersystem crossing would populate the ^{3}MLCT excited state. Hence, there would be an intramolecular energy transfer from the ^{3}MLCT excited state to a ^{3}IL excited state localized in the naphthopyran scaffold. Consequently, the photochromic ring-opening reaction would be triggered from this ^{3}IL excited state (**Figure 2.43**). Another important observation was that the PSS was reached much faster under UV irradiation (1 min) when compared to the simple 8-pyridyl-3*H*-naphtho[2,1-*b*]pyrans (10 min) which indicate that possibly two synergic mechanisms were triggering the photochromic reaction under UV irradiation: one from a singlet excited singlet state (S_1) and a second from a ^{3}IL excited state.

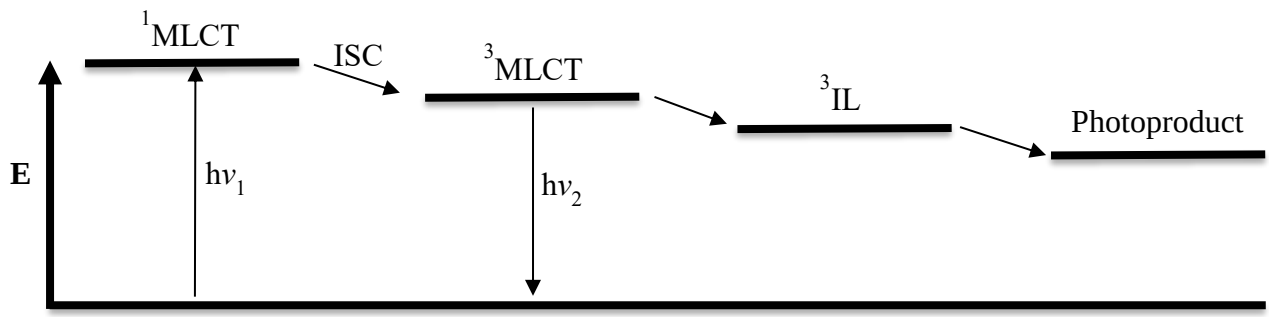

Figure 2.43 Energy transfer pathway for the *fac*-[Re(N^N)(CO)$_3$NP]PF$_6$ complexes.

Thus, the photochromic properties of the *fac*-[Re(N^N)(CO)$_3$NP]PF$_6$ complexes, besides depending on typical effects like inductive, resonance and steric effects, would also depend on the nature of the bidentate ligand and how efficiently the energy transfer from the ^{3}MLCT excited state to the ^{3}IL excited state would occur.

2.3.2.1 Photochromism and Photoswitching of *fac*-[Re(BPy)(CO)$_3$NP]PF$_6$, NP = 10-Pyridyl-3*H*-naphtho[2,1-*b*]pyran

Upon UV irradiation, the Re(I) complex **2.229** generated the photomerocyanines **2.288** in a solution of DCM:PhMe (1:1) (**Scheme 2.138**).

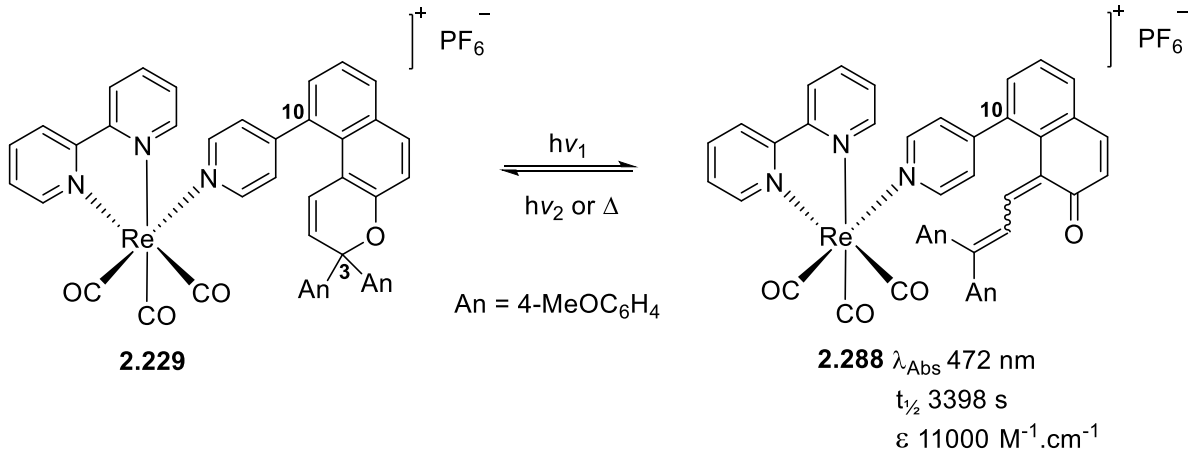

Scheme 2.138 Electrocyclic ring-opening of Re(I) complex **2.229**.

The resulting PSS was characterized by a λ_{Abs} of 472 nm (**Figure 2.44**). When compared to the 10-(4-pyridyl)-3*H*-naphtho[2,1-*b*]pyran **2.36**, there was a small bathochromic shift of 8 nm and faster bleaching kinetics ($t_{½}$ = 3398 s) (**Table 2.12**). Strikingly, the colourability increased by a factor of 42 (ε = 11000 M^{-1}.cm^{-1}). Possibly, the increase in colourability was due to energy transfer from the ^{3}MLCT excited state to the ^{3}IL excited state from which the photochromic reaction was driven. Considering the bulky coordinating 4-pyridyl group at C-10, the slow bleaching kinetics reflected the slow thermal isomerization TT – TC which was a consequence of the large activation energy barrier towards the formation of the TC isomer from the TT isomer.[119]

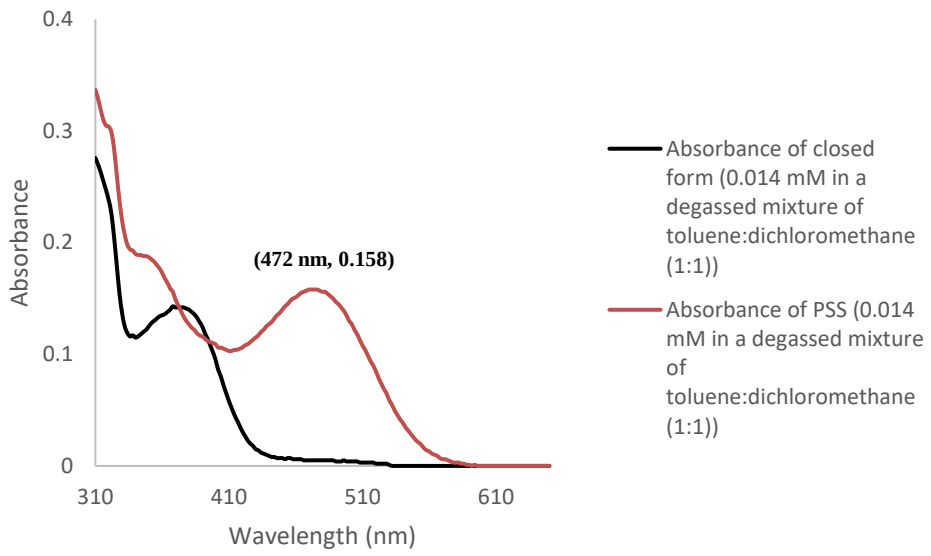

Figure 2.44 UV-Vis spectra of the Re(I) complex **2.229** (0.014 mM in a mixture of toluene:dichloromethane (1:1)) in the closed form (black) and in the PSS (red).

Table 2.12 Spectroscopic data of *fac*-[Re(BPy)(CO)$_3$NP]PF$_6$, NP = 10-Pyridyl-3*H*-naphtho[2,1-*b*]pyran in toluene.

Entry	Compounds	λ_{Abs} (nm)	$t_{½}$ (s)	k_{Δ}	ε_{PSS} ($M^{-1}.cm^{-1}$)	λ_{Em} (nm)	τ_{Em} (ns)
1	**2.36**	458 464*	7149*	1.43×10^{-3} $M^{-1}.s^{-1}$	206 261*	N/A	N/A
2	**2.229**	472*	3398*	1.67×10^{-4} s^{-1}*	11000*	N/A	N/A

* In PhMe:DCM (1:1).

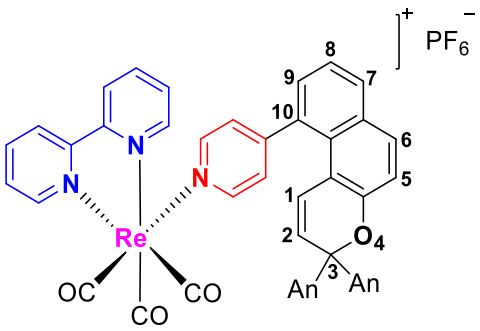

2.229 An = 4-MeOC$_6$H$_4$

Another important observation was that the Re(I) complex **2.229** was not emissive in acetonitrile at room temperature (**Figure 2.45**). This was possibly due to the steric clash between the luminescent unit and the naphthopyran moiety which could have disturbed the ^{3}MLCT emissive excited state. Considering the increase in the photochromic colourability, possibly the energy from

the perturbed ^{3}MLCT excited state was quickly lost by energy transfer to the ^{3}IL excited state and by internal conversion.

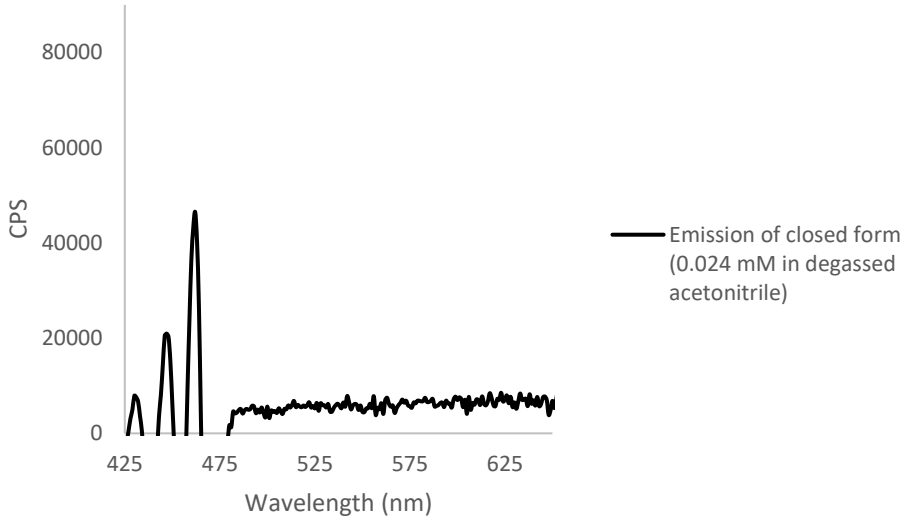

Figure 2.45 Emission spectrum of Re(I) complex **2.229** with λ_{exc} 400 nm (0.024 mM in degassed acetonitrile) in the closed form.

2.3.2.2 Photochromism and Photoswitching of *fac*-[Re(N^N)(CO)$_3$NP]PF$_6$, NP = 9-Pyridyl-3*H*-naphtho[2,1-*b*]pyran and N^N = BPy, PyTz

Upon UV irradiation, the *fac*-[Re(N^N)(CO)$_3$NP]PF$_6$, NP = 9-Pyridyl-3*H*-naphtho[2,1-*b*]pyran and N^N = BPy, PyTz, generated the corresponding photomerocyanines in solution (**Scheme 2.139**).

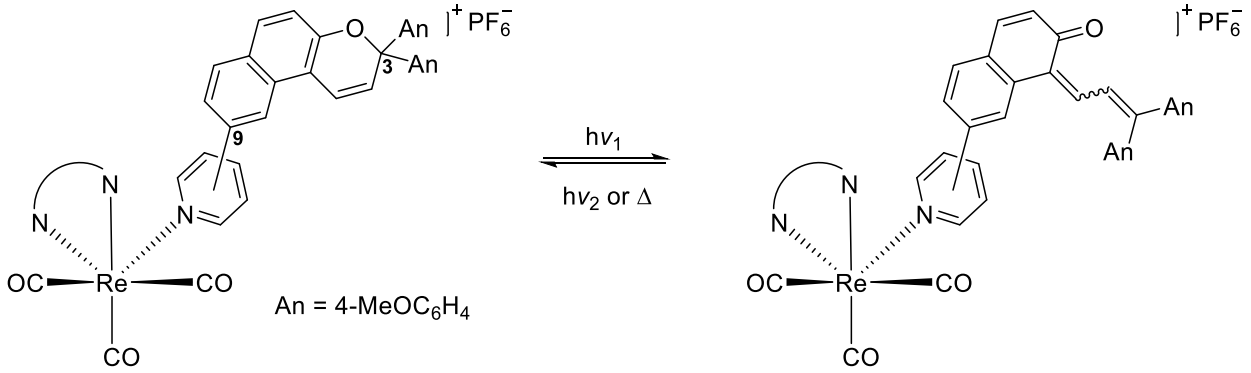

2.230 (N^N = BPy, Py = 4-Py) λ_{Em} 571 nm
2.231 (N^N = BPy, Py = 3-Py) λ_{Em} 577 nm
2.238 (N^N = PyTz, Py = 4-Py) λ_{Em} 491 nm

2.289 (N^N = BPy, Py = 4-Py) λ_{Abs} 474 nm, $t_{½}$ 200 s, ε 4300 $M^{-1}.cm^{-1}$
2.290 (N^N = BPy, Py = 3-Py) λ_{Abs} 480 nm, $t_{½}$ 122 s, ε 4200 $M^{-1}.cm^{-1}$
2.291 (N^N = PyTz, Py = 4-Py) λ_{Abs} 475 nm, $t_{½}$ 15324 s, ε 5952 $M^{-1}.cm^{-1}$

Scheme 2.139 Electrocyclic ring-opening of Re(I) complexes **2.230**, **2.231** and **2.238**.

By comparing to the simple 9-pyridyl-3*H*-naphtho[2,1-*b*]pyrans **2.48** and **2.50**, the *fac*-[Re(N^N)(CO)$_3$NP]PF$_6$ (N^N = BPy, PyTz) generated photostationary states that were slightly bathochromic shifted (2 – 8 nm) (**Table 2.13**). Furthermore, the colourability increased by a factor of 64 – 85 which was a consequence of the triplet photosensitization mechanism. It is worth mentioning that the bleaching of the PSS of Re(I) complex **2.231** (**Entry 4**, **Table 2.13**) was 90 times faster than the 9-(3-pyridyl)-3*H*-naphtho[2,1-*b*]pyran **2.50** (**Entry 2**, **Table 2.13**) partly because the coordination of the rhenium atom prevented the formation of the hypothesized H-bond between the 3-pyridyl nitrogen and the hydrogen of one of the OCH_3 groups of the corresponding photomerocyanine (TC).

Table 2.13 Spectroscopic data of *fac*-[Re(N^N)(CO)$_3$NP]PF$_6$, NP = 9-Pyridyl-3*H*-naphtho[2,1-*b*]pyran and N^N = BPy, PyTz in toluene.

Entry	Compounds	N^N	Py	λ_{Abs} (nm)	$t_{½}$ (s)	k_A	ε_{PSS} ($M^{-1}.cm^{-1}$)	λ_{Em} (nm)
1	**2.48**	No	4-Py	472	125	4.69×10^{-2} $M^{-1}.s^{-1}$	70	N/A
2	**2.50**	No	3-Py	472	10932	1.71×10^{-4} $M^{-1}.s^{-1}$	78	N/A
3	**2.230**	BPy	4-Py	474 480*	200	3.24×10^{-3} s^{-1}	4300 5000*	571*
4	**2.231**	BPy	3-Py	480	122	4.57×10^{-3} s^{-1}	4200	577*
5	**2.238**	PyTz	4-Py	475	15324	1.64×10^{-4} $M^{-1}.s^{-1}$	5952	486 491*

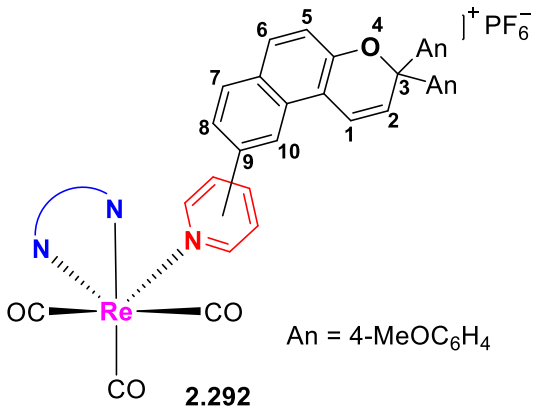

* In PhMe:DCM (1:1).

It is noteworthy that changing the bidentate ligand not only affected the colourability but also the bleaching kinetics. Thus, the Re(I) complexes **2.230** and **2.231** that contained a BPy ligand produced less intense coloured solutions that bleached faster when compared to Re(I) complex **2.238** that contained a PyTz ligand. As stated before, by changing the bidentate ligand the energy of the phosphorescence from the ^{3}MLCT excited state shifts. When the BPy ligand was incorporated, the emission of the Re(I) complexes was much lower in energy than the absorbance of the PSS – the overlap of the emission spectra of the Re(I) complexes and the absorbance of the PSS was very limited (**Figures 2.46** and **2.47**). Assuming that the ^{3}IL excited state, from which the photochromic reaction was driven, was higher in energy than the energy of the absorbance of the PSS, it was rationalized that, when the BPy ligand was employed, the ^{3}MLCT excited state was too low in energy, therefore the energy transfer to the higher-lying ^{3}IL excited state, although still occurring, it was not favoured (**Figure 2.48**).

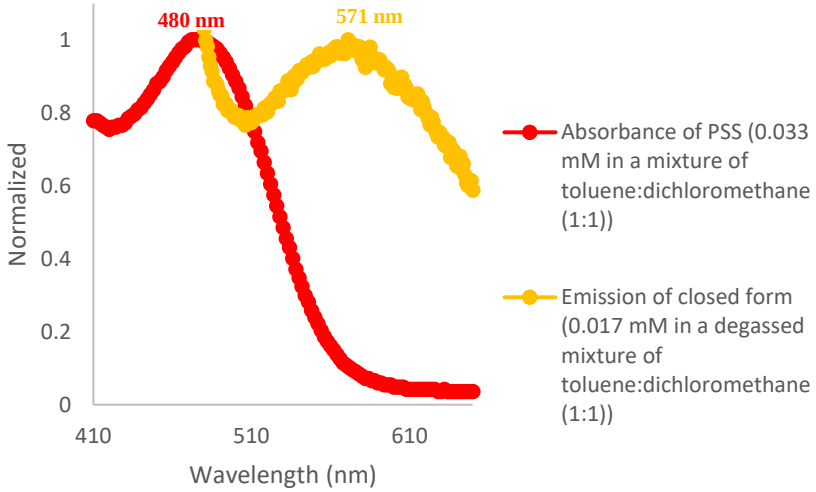

Figure 2.46 Normalized spectra of absorbance of the PSS of **2.230** (0.033 mM in a mixture of toluene:dichloromethane (1:1), after UV irradiation, red) and emission of **2.230** (0.017 mM in a degassed mixture of toluene:dichloromethane (1:1), λ_{exc} 360 nm, yellow).

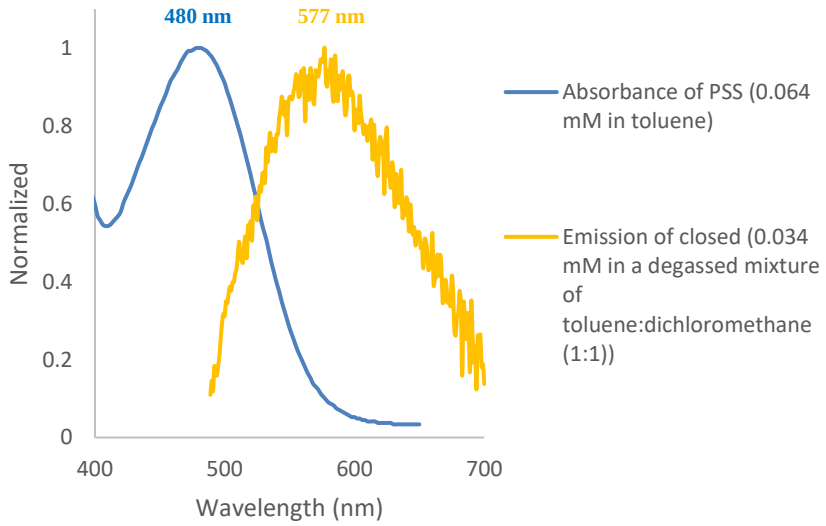

Figure 2.47 Normalized spectra of absorbance of the PSS of **2.231** (0.064 mM in toluene, after UV irradiation, blue) and emission of **2.231** (0.034 mM in a degassed mixture of toluene:dichloromethane (1:1), λ_{exc} 384 nm, yellow).

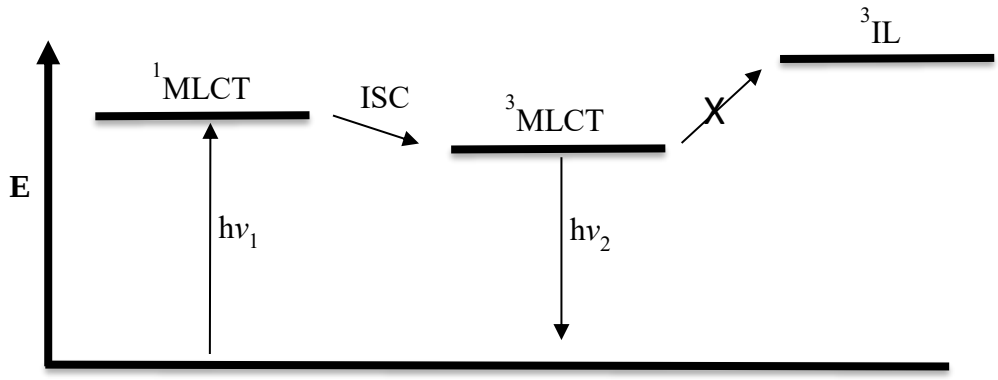

Figure 2.48 Energy transfer pathway for *fac*-[Re(BPy)(CO)$_3$NP]PF$_6$ **2.230** and **2.231**, NP = 9-Pyridyl-3*H*-naphtho[2,1-*b*]pyran.

In contrast, for the Re(I) complex **2.238** that contained a PyTz ligand the overlap of the emission spectrum and the absorbance spectrum of the PSS in toluene was almost complete (**Figure 2.49**). As a result, the ^{3}IL and ^{3}MLCT excited states were much closer in energy which consequently led to an improved energy transfer from the ^{3}MLCT to the ^{3}IL excited state (**Figure 2.50**).

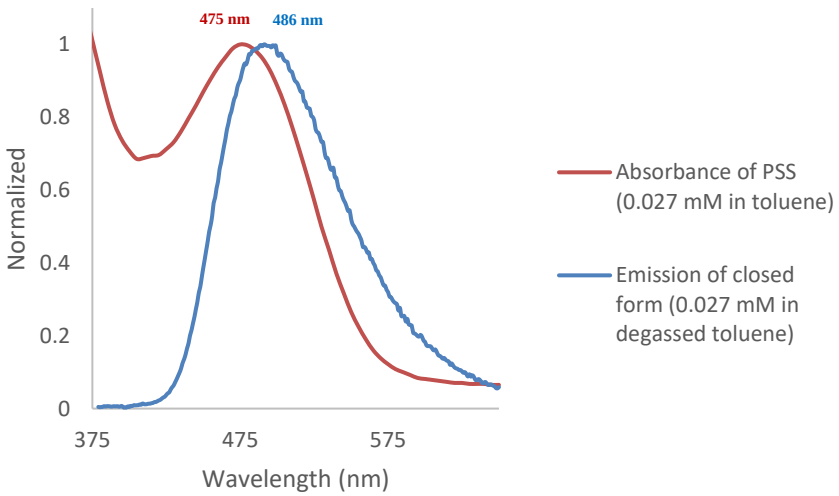

Figure 2.49 Normalized spectra of absorbance of the PSS of **2.238** (0.027 mM in toluene, after UV irradiation, red) and emission of complex **2.238** (0.027 mM in degassed toluene, λ_{exc} 384 nm, blue).

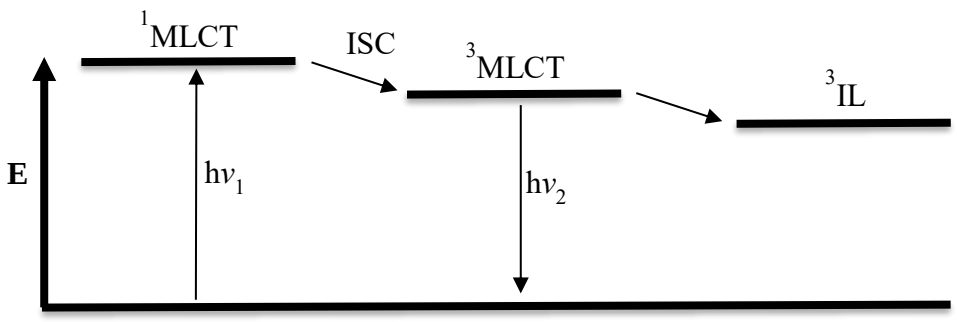

Figure 2.50 Energy transfer pathway for *fac*-[Re(PyTz)(CO)$_3$NP]PF$_6$ **2.238**, NP = 9-Pyridyl-3*H*-naphtho[2,1-*b*]pyran.

As a result of the more efficient triplet – triplet energy transfer pathway, the *fac*-[Re(PyTz)(CO)$_3$NP]PF$_6$ **2.238** produced a more intense coloured solution that persisted for a longer period of time when compared to [Re(BPy)(CO)$_3$NP]PF$_6$ **2.230** and **2.231**.

It is worth mentioning that the quantum yield (ϕ_{CF}) of the ^{3}MLCT phosphorescence of the PyTz ligand containing Re(I) complex **2.238** (**Entry 3**, **Table 2.14**) was higher than the ϕ_{CF} of the BPy ligand containing Re(I) complexes **2.230** (**Entry 1**, **Table 2.14**) and **2.231** (**Entry 2**, **Table 2.14**).

Another very important implication of the triplet – triplet energy transfer pathway is that it effectively depopulates the emissive ^{3}MLCT excited state and populates the non-emissive ^{3}IL excited state. Consequently, the photochromic reaction leads to the reversible photoswitching of the ^{3}MLCT phosphorescence. It was rationalized that the effectiveness of the photoswitching depends on how efficient the triplet – triplet energy transfer pathway is and on the amount of photomerocyanine in the photostationary state (colourability). Understandably, by UV irradiating a solution of the *fac*-[Re(PyTz)(CO)$_3$NP]PF$_6$ **2.238** the phosphorescence quench (68%) was 3 – 6 times higher than the *fac*-[Re(BPy)(CO)$_3$NP]PF$_6$ **2.230** and **2.231** (12% and 24%, respectively) (**Table 2.14**). The emission bands of the PSS and of the closed-forms had the same wavelength maxima which showed that the phosphorescence derived from the same ^{3}MLCT excited state (**Figures 2.51** – **2.53**).

Table 2.14 Spectroscopic data of *fac*-[Re(N^N)(CO)$_3$NP]PF$_6$, NP = 9-Pyridyl-3*H*-naphtho[2,1-*b*]pyran and N^N = BPy, PyTz in toluene.

Entry	Compounds	N^N	Py	λ_{Abs} (nm)	λ_{Em} (nm)	ϕ_{CF} (%)	ϕ_{PSS} (nm)	Quench (%)**
1	**2.230**	BPy	4-Py	474 480*	571*	0.068*	0.039*	12*
2	**2.231**	BPy	3-Py	480	577*	0.032*	0.023*	24*
3	**2.238**	PyTz	4-Py	475	486 491*	13	2.2	68

*In PhMe:DCM (1:1). **Quench (%) was calculated by the ratio between the emission intensity of the closed form and PSS at the maxima of emission.

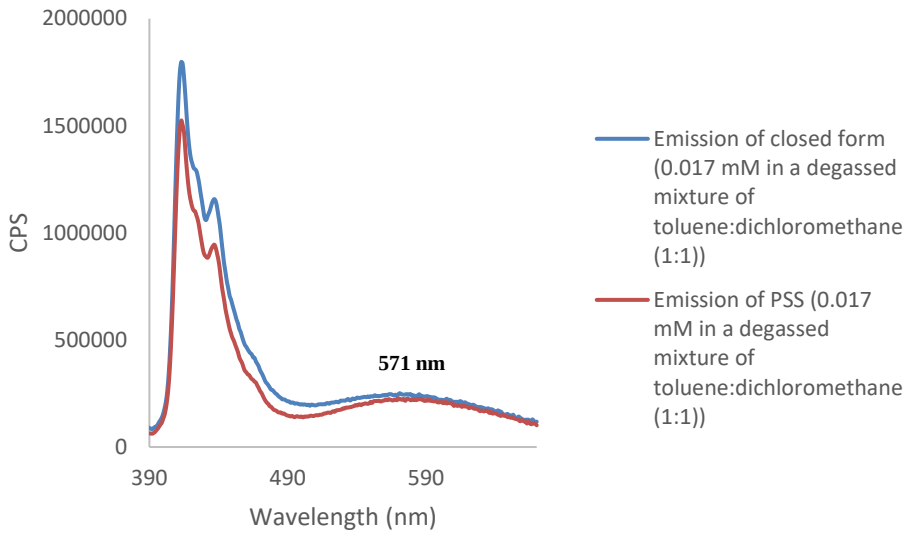

Figure 2.51 Emission spectra of rhenium(I) complex **2.230** with λ_{exc} 360 nm (0.017 mM in a degassed mixture of toluene:dichloromethane (1:1)) in the closed form (blue) and in the PSS (red).

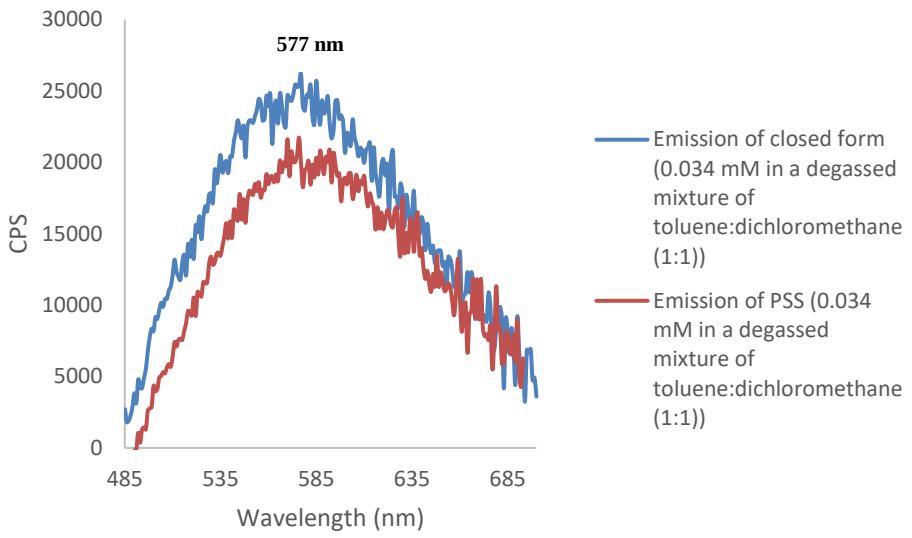

Figure 2.52 Emission spectra of rhenium(I) complex **2.231** with λ_{exc} 384 nm (0.034 mM in a degassed mixture of toluene:dichloromethane (1:1)) in the closed form (blue) and in the PSS (red).

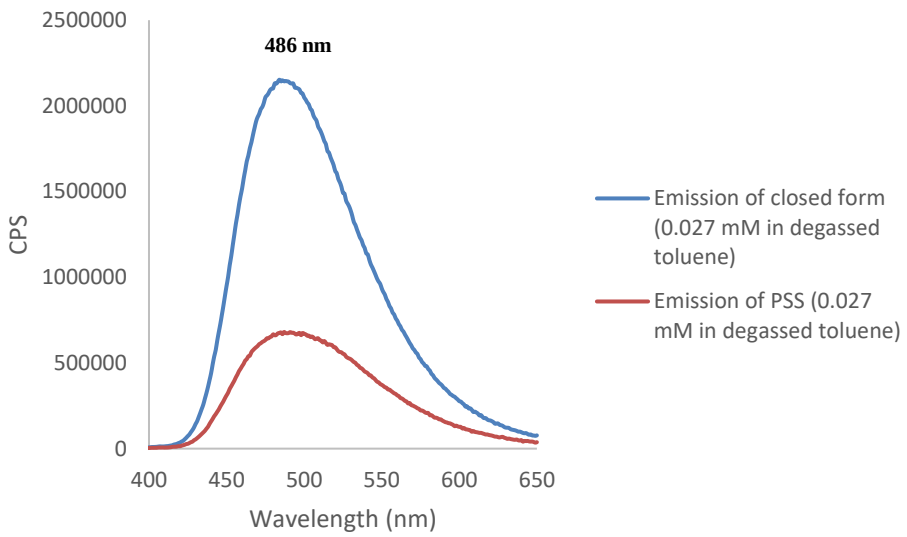

Figure 2.53 Emission spectra of rhenium(I) complex **2.238** with λ_{exc} 384 nm (0.027 mM in degassed toluene) in the closed form (blue) and in the PSS (after UV irradiation, red).

2.3.2.3 Photochromism and Photoswitching of *fac*-[Re(N^N)(CO)$_3$NP]PF$_6$, NP = 8-Pyridyl-3*H*-naphtho[2,1-*b*]pyran and N^N = BPy, PyTz, BTz

Upon UV irradiation, the *fac*-[Re(N^N)(CO)$_3$NP]PF$_6$, NP = 8-Pyridyl-3*H*-naphtho[2,1-*b*]pyran and N^N = BPy, PyTz, BTz, generated the corresponding photomerocyanines in solution (**Scheme 2.140**).

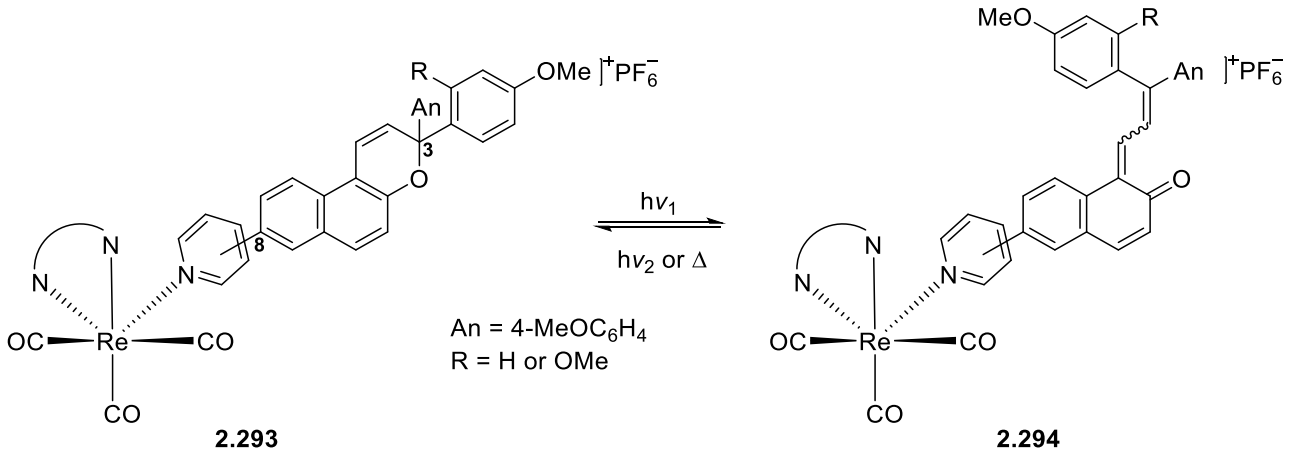

Scheme 2.140 Electrocyclic ring-opening of Re(I) complexes **2.293**.

By comparing to the simple 8-pyridyl-3*H*-naphtho[2,1-*b*]pyrans **2.57**, **2.59** and **2.77**, the *fac*-[Re(N^N)(CO)$_3$NP]PF$_6$ (N^N = BPy, PyTz, BTz) generated photostationary states that were slightly bathochromically shifted (10–14 nm) with better colourability in solution. Remarkably, for the BPy ligand containing rhenium(I) complexes **2.232** and **2.233** there was a simultaneous increase in the colourability and the rate of bleaching. For example, on UV irradiation of a PhMe:DCM (1:1) solution of the rhenium(I) complex **2.232** (**Entry 4**, **Table 2.15**), a photostationary state was generated that was 31 times more coloured and 1682 times faster to bleach ($t_{½}$ = 15 s) than the corresponding 8-(4-pyridyl)-3*H*-naphtho[2,1-*b*]pyran **2.57** (**Entry 1**, **Table 2.15**). The increase in colourability was attributed to the triplet photosensitization mechanism. Moreover, the faster bleaching kinetics was ascribed to the disturbance of the electronic conjugation of the delocalized π system of the photomerocyanine, upon coordination to the rhenium atom, which destabilized the photomerocyanine. Hence, triplet photosensitized naphthopyrans that generate photomerocyanines, upon UV irradiation, that are destabilized by electronic and/or steric effects may prove to be a promising design for very fast photochromes with good colourability in solution.

Table 2.15 Spectroscopic data of *fac*-[Re(N^N)(CO)$_3$NP]PF$_6$, NP = 8-Pyridyl-3*H*-naphtho[2,1-*b*]pyran and N^N = BPy, PyTz, BTz in toluene.

Entry	Compounds	N^N	Py	R	λ_{Abs} (nm)	$t_{½}$ (s)	k_{Δ}	ε_{PSS} ($M^{-1}.cm^{-1}$)	λ_{Em} (nm)
1	**2.57**	No	4-Py	H	482 486*	57740 25227*	2.31×10^{-5} $M^{-1}.s^{-1}$ 1.08×10^{-4}* $M^{-1}.s^{-1}$	120 170*	N/A
2	**2.59**	No	3-Py	H	476	6643	3.53×10^{-4} $M^{-1}.s^{-1}$	65	N/A
3	**2.77**	No	4-Py	OMe	490	94	2.08×10^{-2} $M^{-1}.s^{-1}$	18000	N/A
4	**2.232**	BPy	4-Py	H	500*	15*	N/A	5200*	602* 599**
5	**2.233**	BPy	3-Py	H	486*	84*	7.36×10^{-3} s^{-1}	4000*	583*
6	**2.234**	BPy	4-Py	OMe	496 496*	790	N/A	16000 14000*	603*
7	**2.239**	PyTz	4-Py	H	492 492**	3747**	5.67×10^{-4} $M^{-1}.s^{-1}$**	24000** 8700***	444 462* 490**
8	**2.240**	PyTz	4-Py	OMe	490**	1399**	N/A	32000** 14000***	500**
9	**2.245**	BTz	4-Py	H	492 490**	4058	N/A	5900 8700**	444 459* 490**

* In PhMe:DCM (1:1). ** In MeCN. *** In MeCN (λ_{exc} > 400 nm).

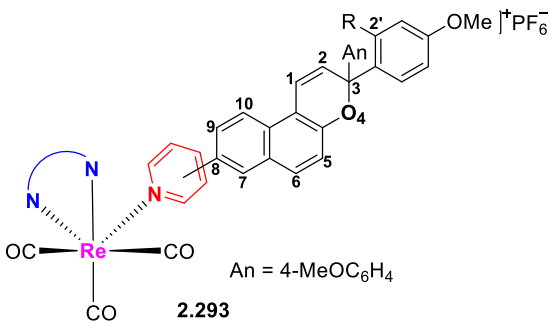

2.293

In contrast to the other BPy ligand containing rhenium(I) complexes, the PSS of **2.234** (**Entry 6**, **Table 2.15**) showed slower bleaching kinetics when compared to the corresponding 8-pyridyl-3*H*-naphtho[2,1-*b*]pyran **2.77**. It was hypothesized that the effect of the electronic conjugation on the photomerocyanine **2.265** (from 8-(4-pyridyl)-3*H*-naphtho[2,1-*b*]pyran **2.77**) in addition to the effect of having an extra methoxy group at C-2′ might have constrained the TC isomerization to the TT isomer, leading to relative fast bleaching kinetics, as the thermal ring closure of the TC isomer is much faster than the isomerization of the TT to the TC isomer. Thus, upon coordination to the rhenium atom, the electronic conjugation of the delocalized π system was disturbed, allowing a more extended isomerization of the TC to the TT isomer. Considering that the steric demand imposed by the methoxy group at C-2′ slows down significantly the thermal isomerization of the TT to the TC isomer, the $t_{½}$ (s) had necessarily to increase.

Upon UV irradiation to a photostationary state, the Re(I) complexes **2.239** (PyTz) (**Entry 7**, **Table 2.15**) and **2.245** (BTz) (**Entry 9**, **Table 2.15**) showed better colourability and slower bleaching kinetics in solution than the Re(I) complex **2.232** (BPy). Thus, the Re(I) complex **2.239** (PyTz) produced a red colour in acetonitrile that was 5 times stronger and 250 times slower to bleach when compared to the BPy containing Re(I) complex **2.232** in PhMe:DCM (1:1). As discussed before, the difference in spectrokinetics between the BPy and PyTz/BTz containing Re(I) complexes was attributed to a difference in the efficiency of the triplet – triplet energy transfer pathway. For the Re(I) complex **2.232** (BPy) there was only a small overlap between the absorbance band of the PSS and the emission band of the closed-form (**Figure 2.54**). Therefore, the ^{3}MLCT excited state was lower in energy than the ^{3}IL excited state which restricted the energy transfer from the former to the latter. On the other hand, for the Re(I) complexes **2.239** (PyTz) and **2.245** (BTz) the overlap between the absorbance band of the PSS and the emission band of the closed-form in acetonitrile was almost complete (**Figures 2.55** and **2.56**). Therefore, the ^{3}MLCT and the ^{3}IL excited states were much closer in energy which led to a more efficient energy transfer from the former to the latter. It was hypothesized that the effect of having a very efficient triplet – triplet energy pathway for the Re(I) complexes **2.239** (PyTz) and **2.245** (BTz) overpowered the destabilizating effect of the disruption of the electronic conjugation of the delocalized π system of the photomerocyanine, ultimately leading to longer $t_{½}$ (s).

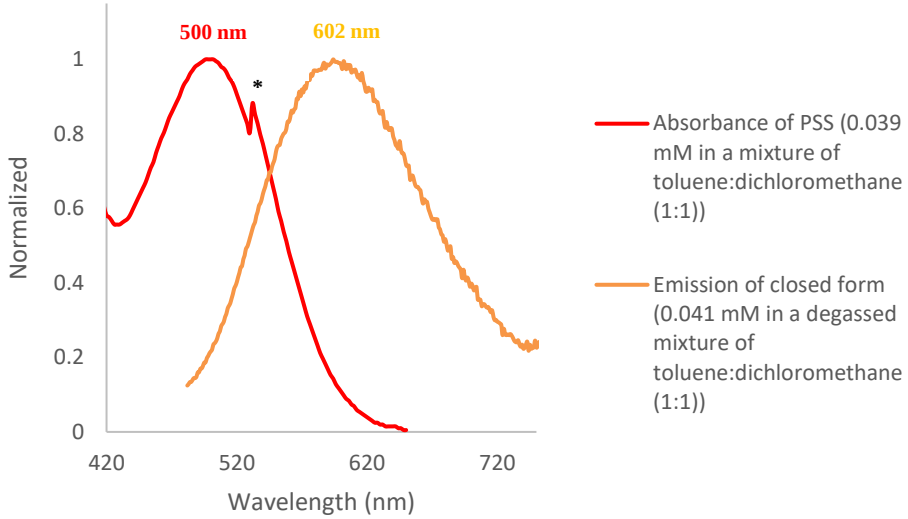

Figure 2.54 Normalized spectra of absorbance of the PSS of **2.232** (0.039 mM in a mixture of toluene:dichloromethane (1:1), after UV irradiation, red) and emission of **2.232** (0.041 mM in a degassed mixture of toluene:dichloromethane (1:1), λ_{exc} 403 nm, orange).

***** Artefact due to a diffraction grating change for long λ region detection.

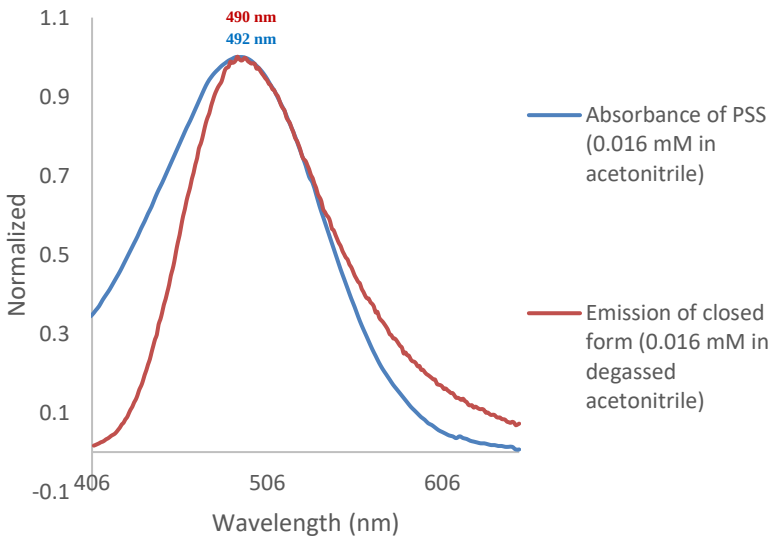

Figure 2.55 Normalized spectra of absorbance of the PSS of **2.239** (0.016 mM in acetonitrile, after UV irradiation, blue) and emission of **2.239** (0.016 mM in degassed acetonitrile, λ_{exc} 392 nm, red).

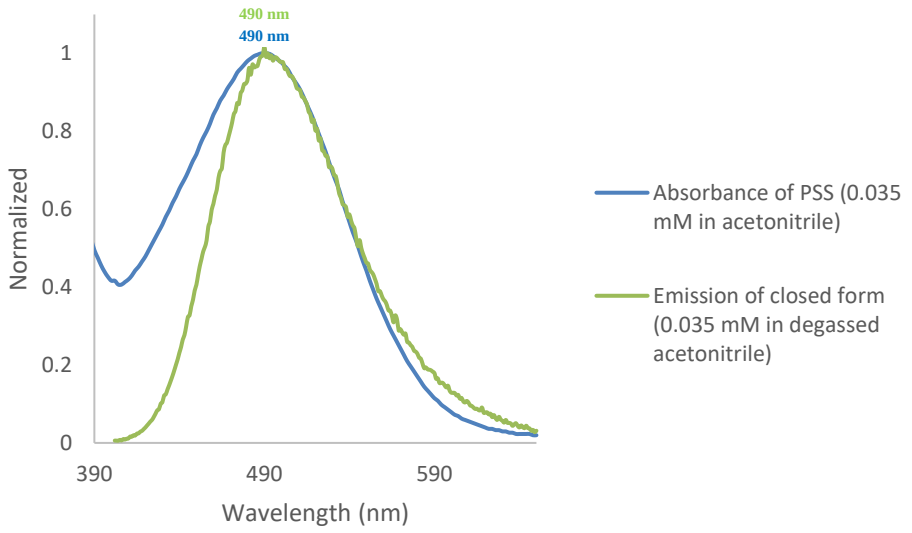

Figure 2.56 Normalized spectra of absorbance of the PSS of **2.245** (0.035 mM in acetonitrile, after UV irradiation, blue) and emission of **2.245** (0.035 mM in degassed acetonitrile, λ_{exc} 387 nm, green).

It is worth mentioning that the quantum yield (ϕ_{CF}) of the ^{3}MLCT phosphorescence of the Re(I) complexes varied with the nature of the bidentate ligand: $\phi_{BTz} > \phi_{PyTz} > \phi_{BPy}$ (**Table 2.16**).

The triplet – triplet energy transfer pathway effectively depleted to a variable degree the emissive ^{3}MLCT excited state and populated the non-emissive ^{3}IL excited state. Consequently, the photochromic reaction led to the reversible photoswitching of the ^{3}MLCT phosphorescence. It was rationalized that the percentage of luminescence quench would be higher if the triplet – triplet energy pathway was more efficient. For example, upon UV irradiation of a PhMe:DCM (1:1) solution of the BPy ligand containing Re(I) complex **2.232** to a photostationary state, only 13% of the ^{3}MLCT phosphorescence was quenched, as the triplet – triplet energy pathway was very ineffective (**Figure 2.57**). On the other hand, for acetonitrile solutions of the Re(I) complexes **2.239** (PyTz) and **2.245** (BTz), 80% and 75% of the ^{3}MLCT phosphorescence was quenched, respectively, upon UV irradiation to a photostationary state (**Figures 2.58** and **2.59**). The improvement of the percentage of luminescence quenched reflected the better energy transfer from the ^{3}MLCT excited state to the ^{3}IL excited state as these were much closer in energy. Overall, for the Re(I) complexes containing PyTz and BTz ligands, the reversible photoswitching of the phosphorescence was substantially higher (57 – 80%) than the Re(I) complexes containing BPy ligands (11 – 19%) (**Table 2.16**).

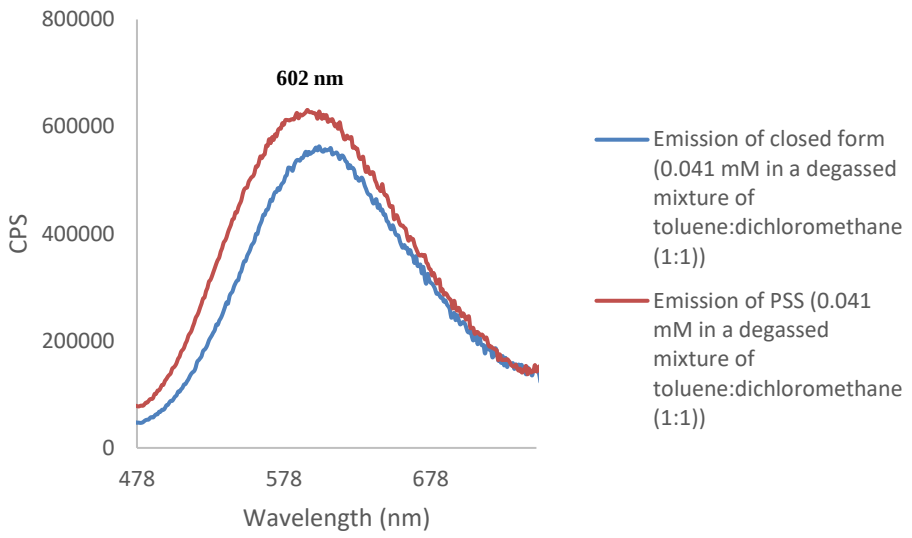

Figure 2.57 Emission spectra of the Re(I) complex **2.232** with λ_{exc} 403 nm (0.041 mM in a degassed mixture of toluene:dichloromethane (1:1)) in the closed form (red) and in the PSS (blue).

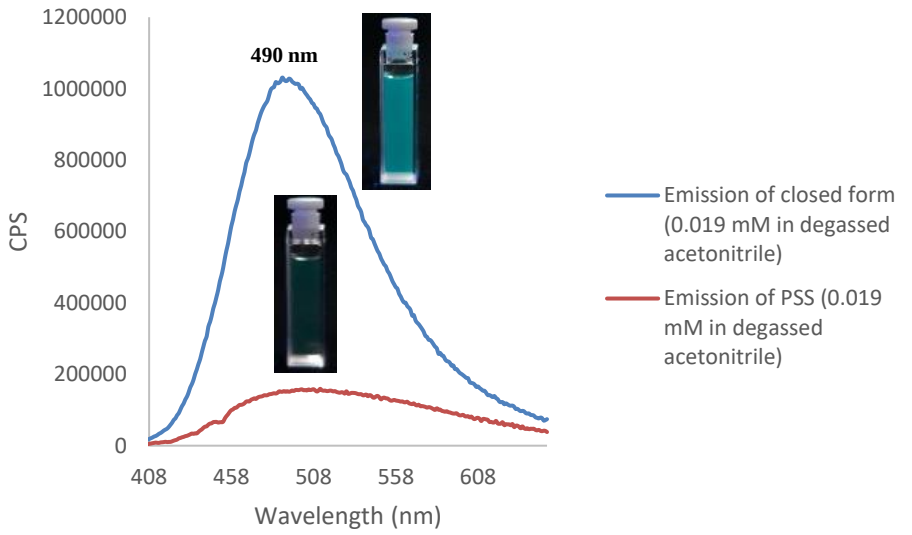

Figure 2.58 Emission spectra of the Re(I) complex **2.239** with λ_{exc} 392 nm (0.019 mM in degassed acetonitrile) in the closed form (blue) and in the PSS (after UV irradiation, red).

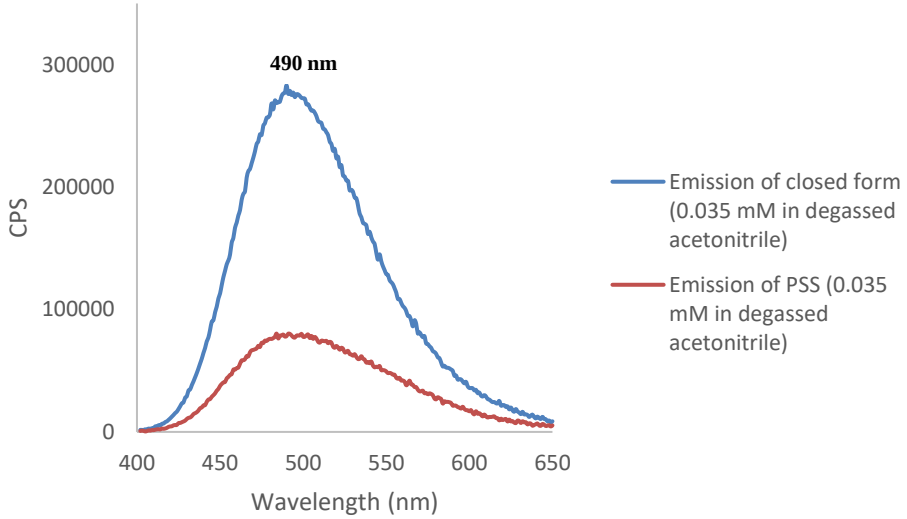

Figure 2.59 Emission spectra of the Re(I) complex **2.245** with λ_{exc} 387 nm (0.035 mM in degassed acetonitrile) in the closed-form (blue) and in the PSS (red).

Table 2.16 Spectroscopic data of *fac*-[Re(N^N)(CO)$_3$NP]PF$_6$, NP = 8-Pyridyl-3*H*-naphtho[2,1-*b*]pyran and N^N = BPy, PyTz, BTz in toluene.

Entry	Compounds	N^N	Py	R	λ_{Abs} (nm)	ε_{PSS} ($M^{-1}.cm^{-1}$)	λ_{Em} (nm)	τ_{Em} (ns)	ϕ_{CF} (%)	ϕ_{PSS} (nm)	Quench (%)****
1	**2.232**	BPy	4-Py	H	500* 599**	5200*	602* 599**	-	0.091* 0.22**	0.073*	13*
2	**2.233**	BPy	3-Py	H	486*	4000*	583*	110, 12, 3 (1.044)*	0.091*	0.046*	19*
3	**2.234**	BPy	4-Py	OMe	496 496*	16000 14000*	603*	-	0.030	0.024	11*
4	**2.239**	PyTz	4-Py	H	492 492**	24000** 8700***	444 462* 490**	4, 27, 55 (1.303)	1.5 0.83**	0.38 0.13**	75 80**
5	**2.240**	PyTz	4-Py	OMe	490**	32000** 14000***	500**	-	0.57**	0.26**	72**
6	**2.245**	BTz	4-Py	H	492 490**	5900 8700**	444 459* 490**	6, 8, 68 (1.270)	24**	7.9**	57 71**

* In PhMe:DCM (1:1). ** In MeCN. *** In MeCN (λ_{exc} > 400 nm). **** Quench (%) was calculated by the ratio between the emission intensity of the closed form and PSS at the maxima of emission.

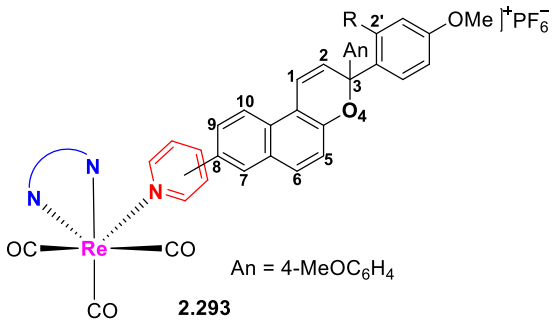

2.293

It was rationalized that the design of photochromic Re(I) complexes with efficient triplet – triplet energy pathways and good colourability would lead to an improved photoswitching of the ^{3}MLCT phosphorescence. Thus, the PyTz ligand containing Re(I) complex **2.240** that had an extra methoxy group at C-2′ was prepared and effectively produced the strongest colour in acetonitrile after UV irradiation (**Entry 5**, **Table 2.16**). Upon reaching a photostationary state, the ^{3}MLCT phosphorescence quench was 'just' 72%, yet practically all the initial green phosphorescence disappeared (**Figure 2.60**). Considering that the emission band was slightly red-shifted (10 nm) when compared to the absorbance band of the PSS in acetonitrile, the ^{3}MLCT excited state might have been slightly low in energy for an ideal energy transfer to the ^{3}IL excited state (**Figure 2.61**).

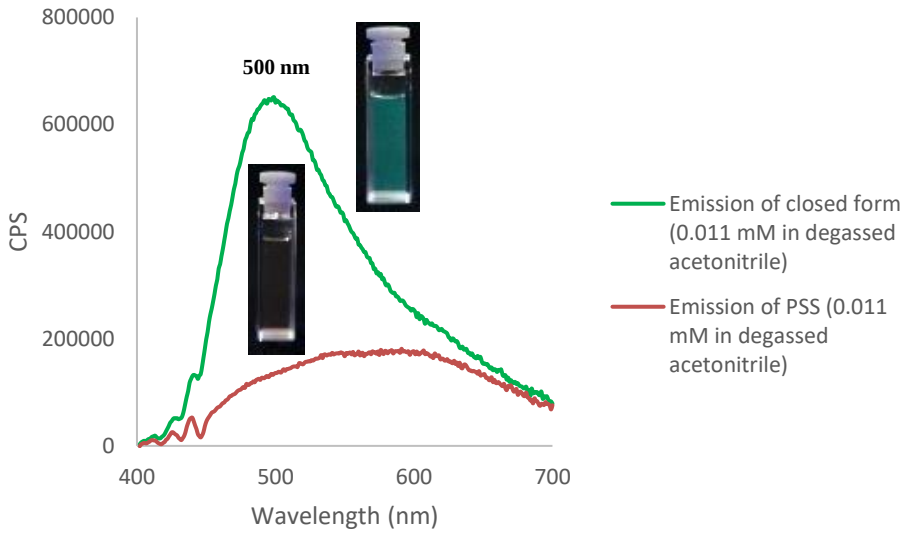

Figure 2.60 Emission spectra of the Re(I) complex **2.240** with λ_{exc} 382 nm (0.011 mM in degassed acetonitrile) in the closed form (green) and in the PSS (red).

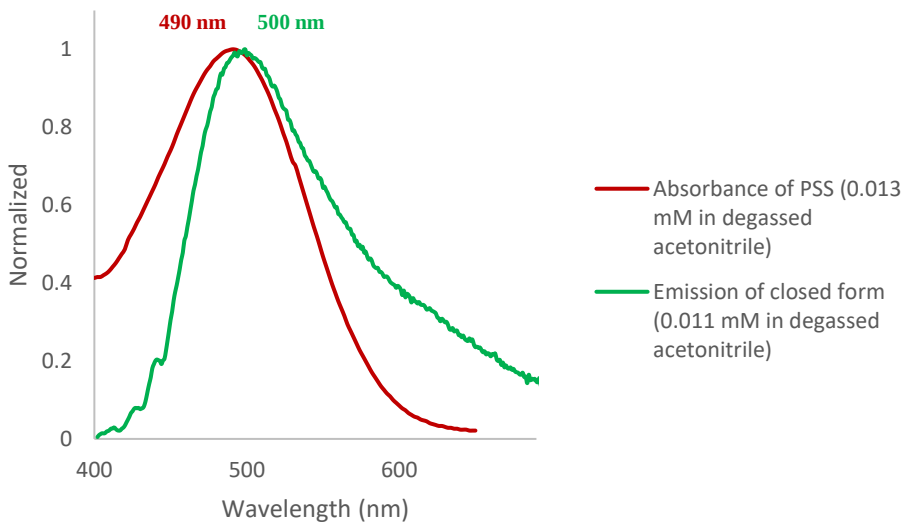

Figure 2.61 Normalized spectra of absorbance of the PSS of **2.240** (0.013 mM in degassed acetonitrile, after UV irradiation, red) and emission of **2.240** (0.011 mM in degassed acetonitrile, λ_{exc} 382 nm, green).

As stated before, the ^{3}MLCT emission of the Re(I) complexes showed a typical red shift in the emission energy by increasing the solvent dielectric constant. Thus, the energy of the ^{3}MLCT emission of the Re(I) complexes can be modulated by simply changing the solvent. Interestingly, an improved luminescence quench was attained when the solvent selected allowed a better overlap between the absorbance band of the PSS and the emission band of the rhenium(I) complex. For example, for the PyTz ligand containing Re(I) complex **2.239** there was a small increase of the luminescence quench from toluene (75%) to acetonitrile (80%) (**Figure 2.62**). A larger increase of the luminescence quench was attained for the BTz ligand containing Re(I) complex **2.245** from toluene (57%) to acetonitrile (71%) (**Figure 2.63**).

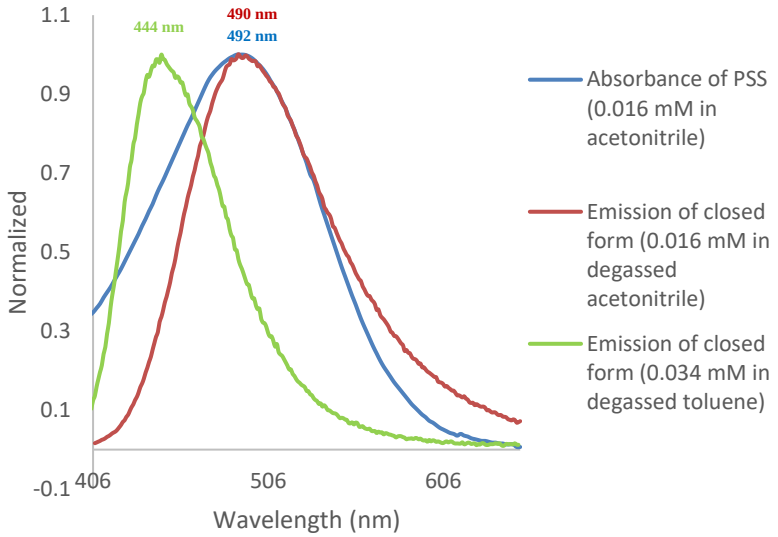

Figure 2.62 Normalized spectra of absorbance of the PSS of **2.239** (0.016 mM in acetonitrile, after UV irradiation, blue), emission of **2.239** (0.016 mM in degassed acetonitrile, λ_{exc} 392 nm, red) and emission **of 2.239** (0.034 mM in degassed toluene, λ_{exc} 388 nm, green).

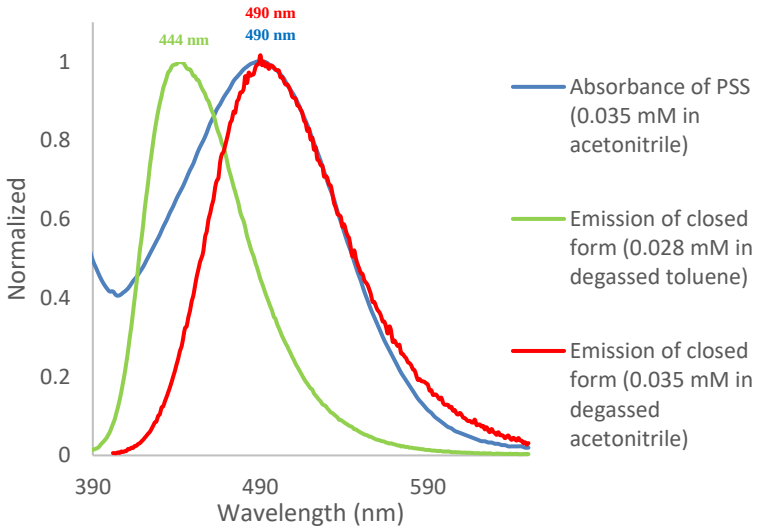

Figure 2.63 Normalized spectra of absorbance of the PSS of **2.245** (0.035 mM in acetonitrile, after UV irradiation, blue), emission of **2.245** (0.028 mM in degassed toluene, λ_{exc} 346 nm, green) and emission of **2.245** (0.035 mM in degassed acetonitrile, λ_{exc} 387 nm, red).

Notably, the PyTz ligand containing Re(I) complexes **2.239** and **2.240**, that displayed very good photoswitching ability, showed no fatigue after ten absorbance and emission cycles in acetonitrile at room temperature (**Figures 2.64** – **2.67**). Each cycle involved generating the PSS upon UV irradiation (365 nm, 20 sec) followed by forced restoration of the closed-form upon irradiation with visible light (λ > 450 nm).

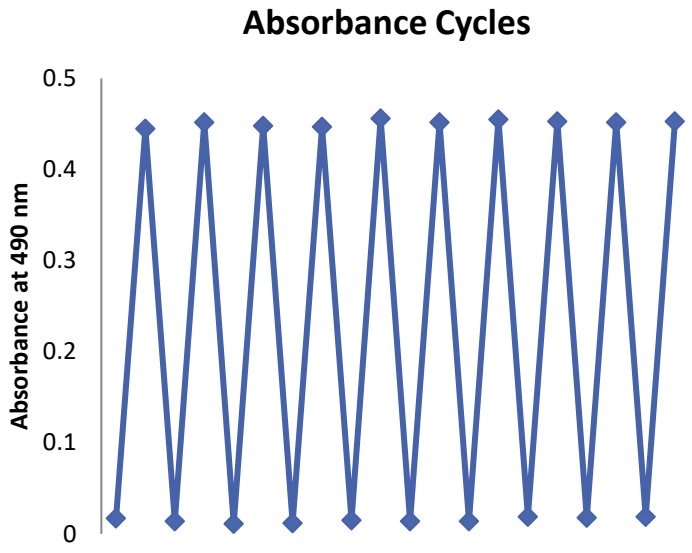

Figure 2.64 Absorbance cycles of the Re(I) complex **2.239** (CF – PSS) after UV irradiation (0.016 mM in degassed acetonitrile).

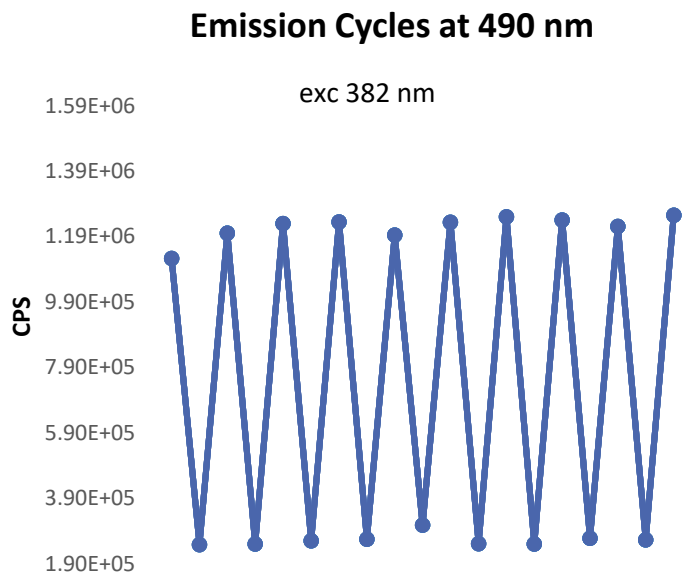

Figure 2.65 Emission cycles of the Re(I) complex **2.239** (CF – PSS) after UV irradiation (0.016 mM in degassed acetonitrile).

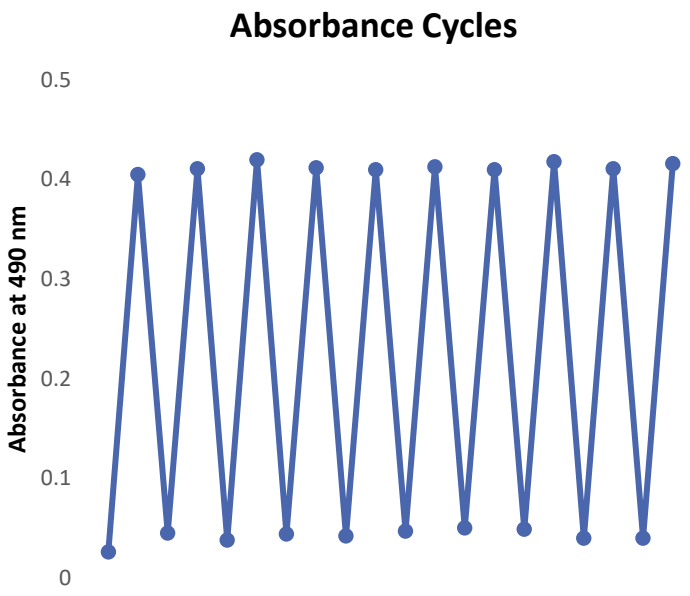

Figure 2.66 Absorbance cycles of the Re(I) complex **2.240** (CF – PSS) after UV irradiation (0.013 mM in degassed acetonitrile).

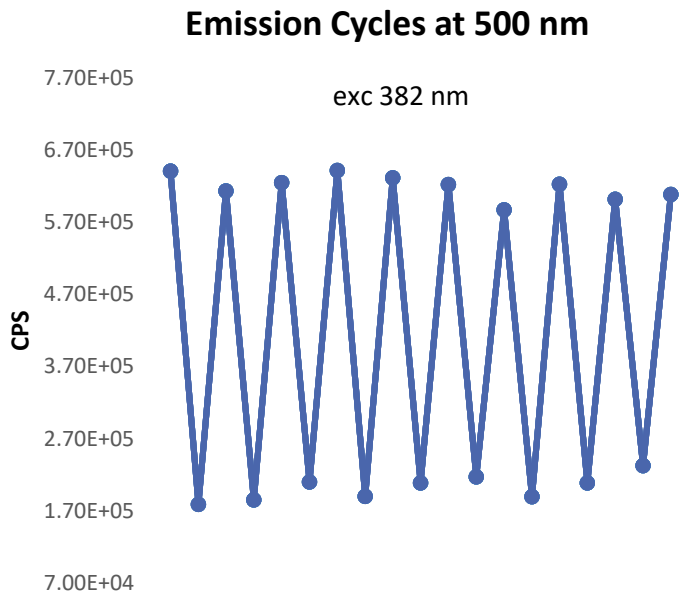

Figure 2.67 Emission cycles of the Re(I) complex **2.240** (CF – PSS) after UV irradiation (0.013 mM in degassed acetonitrile).

2.3.2.4 Photochromism and Photoswitching of *fac*-[Re(N^N)(CO)$_3$NP]PF$_6$, NP = 7-Pyridyl-3*H*-naphtho[2,1-*b*]pyran and N^N = BPy, PyTz

Upon UV irradiation, the *fac*-[Re(N^N)(CO)$_3$NP]PF$_6$, NP = 7-Pyridyl-3*H*-naphtho[2,1-*b*]pyran and N^N = BPy, PyTz, generated the corresponding photomerocyanines in solution (**Scheme 2.141**).

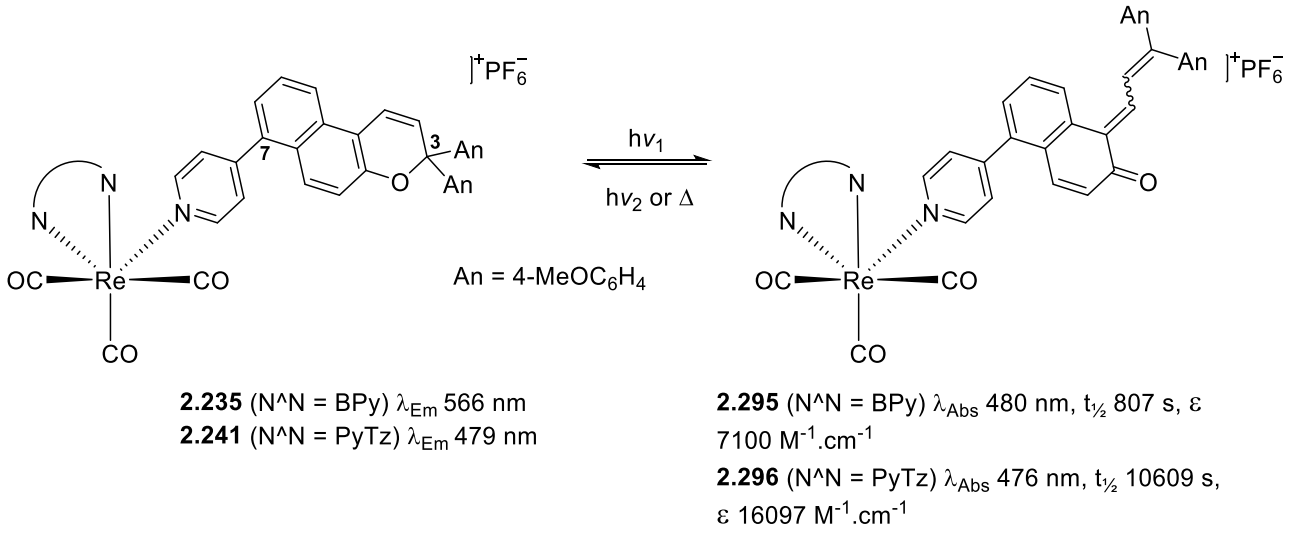

Scheme 2.141 Electrocyclic ring-opening of Re(I) complexes **2.235** and **2.241**.

In comparison to the photochromic performance of the simple 7-(4-pyridyl)-3*H*-naphtho[2,1-*b*]pyran **2.98** (**Entry 1**, **Table 2.17**), the Re(I) complexes **2.235** (BPy) and **2.241** (PyTz) produced slightly bathochromic shifted (8 – 14 nm) photostationary states in solution under UV irradiation. Furthermore, the spectrokinetic properties of the Re(I) complexes were modified by changing the bidentate ligand. Hence, upon UV irradiation of an acetonitrile solution of the PyTz containing Re(I) complex **2.241** (**Entry 3**, **Table 2.17**), a photostationary state was generated that was 2 times more coloured and 13 times slower to bleach than the photostationary state from the BPy containing Re(I) complex **2.235** in toluene (**Entry 2**, **Table 2.17**). It is relevant to mention that for a more accurate comparison of the spectrokinetics properties of the Re(I) complexes **2.235** and **2.241**, it would have been necessary to perform the analysis in the same solvent. Nevertheless, the variation in the spectrokinetics properties of the BPy and PyTz containing Re(I) complexes were attributed to a good degree to differences in the efficiency of the triplet – triplet energy transfer pathway. Thus, for the Re(I) complex **2.235** (BPy) there was only a small overlap between the absorbance band of the PSS and the emission band of the closed-form (**Figure 2.68**). Therefore, the ^{3}MLCT excited state was lower in energy than the ^{3}IL excited state which restricted the energy transfer from the

former to the latter. On the other hand, for the Re(I) complex **2.241** (PyTz) the overlap between the absorbance band of the PSS and the emission band of the closed form in toluene was almost complete (**Figure 2.69**). Therefore, the ^{3}MLCT and the ^{3}IL excited states were much closer in energy which led to a more efficient energy transfer pathway and ultimately to an increase in colourability and $t_{½}$ (s).

Table 2.17 Spectroscopic data of *fac*-[Re(N^N)(CO)$_3$NP]PF$_6$, NP = 7-(4-Pyridyl)-3*H*-naphtho[2,1-*b*]pyran and N^N = BPy, PyTz in toluene.

Entry	Compounds	N^N	λ_{Abs} (nm)	$t_{½}$ (s)	k_{Λ}	ε_{PSS} ($M^{-1}.cm^{-1}$)	λ_{Em} (nm)	τ_{Em} (ns)	ϕ_{CF} (%)	ϕ_{PSS} (nm)	Quench (%)***
1	**2.98**	No	468	87220	N/A	140	N/A	N/A	N/A	N/A	N/A
2	**2.235**	BPy	480 482*	807	7.71×10^{-4} s^{-1}	7100	566*	171, 16, 4 (1.248)*	0.027*	0.015*	37*
3	**2.241**	PyTz	476**	10609**	3.48×10^{-4} $M^{-1}.s^{-1}$**	16097**	475 479* 509**	4, 20, 59 (1.137)	2.3 0.48**	0.16 0.13**	81 71**

* In PhMe:DCM (1:1). ** In MeCN. *** Quench (%) was calculated by the ratio between the emission intensity of the closed form and PSS at the maxima of emission.

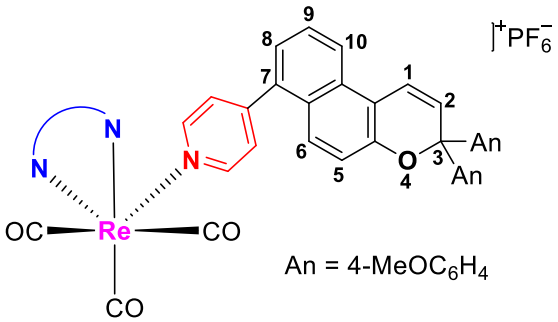

2.235 (N^N = BPy)
2.241 (N^N = PyTz)

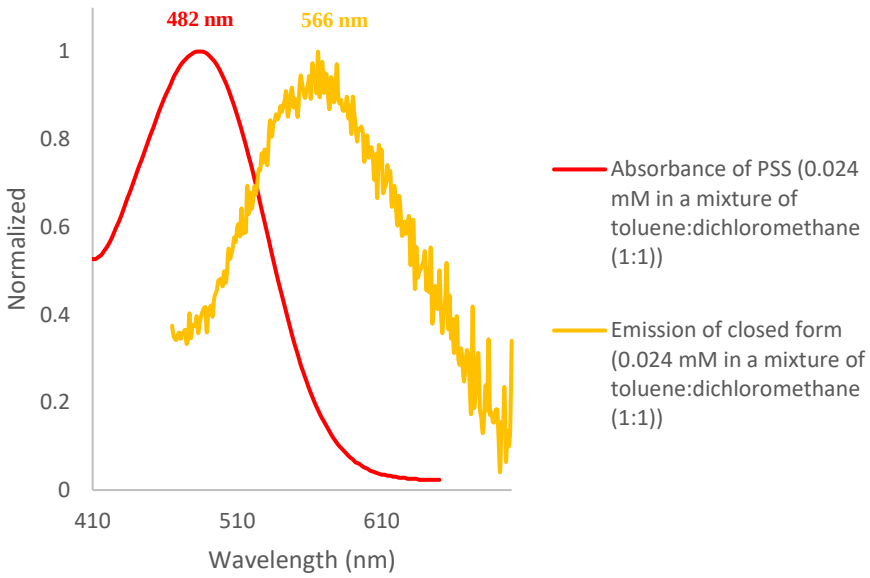

Figure 2.68 Normalized spectra of absorbance of the PSS of **2.235** (0.024 mM in a mixture of toluene:dichloromethane (1:1), after UV irradiation, red) and emission of **2.235** (0.024 mM in a degassed mixture of toluene:dichloromethane (1:1), λ_{exc} 397 nm, yellow).

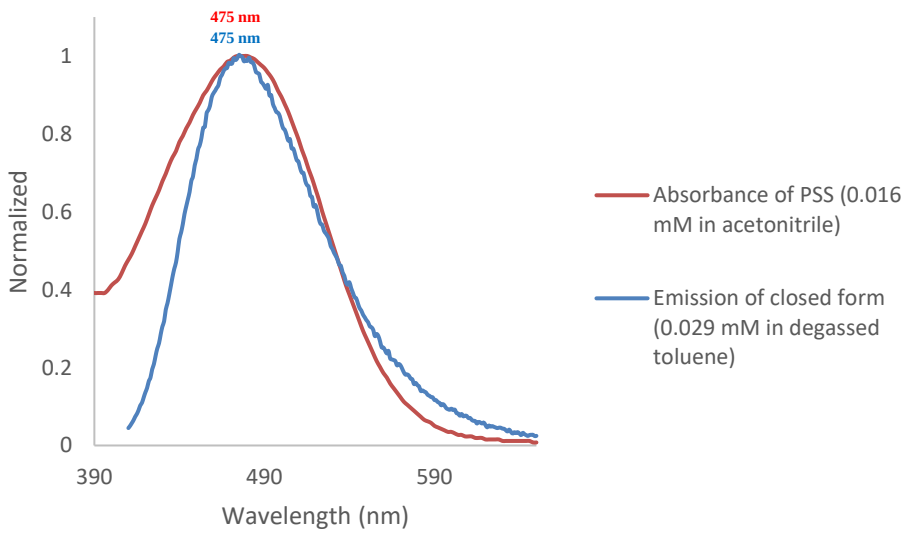

Figure 2.69 Normalized spectra of absorbance of the PSS of **2.241** (0.016 mM in degassed acetonitrile, after UV irradiation, red) and emission of **2.241** (0.029 mM in degassed toluene, λ_{exc} 394 nm, blue).

It is worth mentioning that the quantum yield (ϕ_{CF}) of the ^{3}MLCT phosphorescence of the PyTz ligand containing Re(I) complex **2.241** was higher than the ϕ_{CF} of the corresponding BPy ligand containing Re(I) complex **2.235**.

Upon UV irradiation of solutions of the Re(I) complexes **2.235** and **2.241**, the corresponding photostationary states were generated. As a consequence of the photochromic reaction, the ^{3}MLCT phosphorescence was quenched to a variable degree, because the ^{3}MLCT excited state was partially depleted by energy transfer to the ^{3}IL excited state. The amount of luminescence quenching depended on the efficiency of the triplet – triplet energy transfer pathway. Thus, for the Re(I) complex **2.235** the luminescence quench was only equal to 37% in a PhMe:DCM (1:1) solution (**Figure 2.70**). Hitherto, for the Re(I) complex **2.241** the luminescence quench in solution was much higher and equal to 71 – 81%, reflecting the more proficient triplet – triplet energy transfer process (**Figure 2.71**).

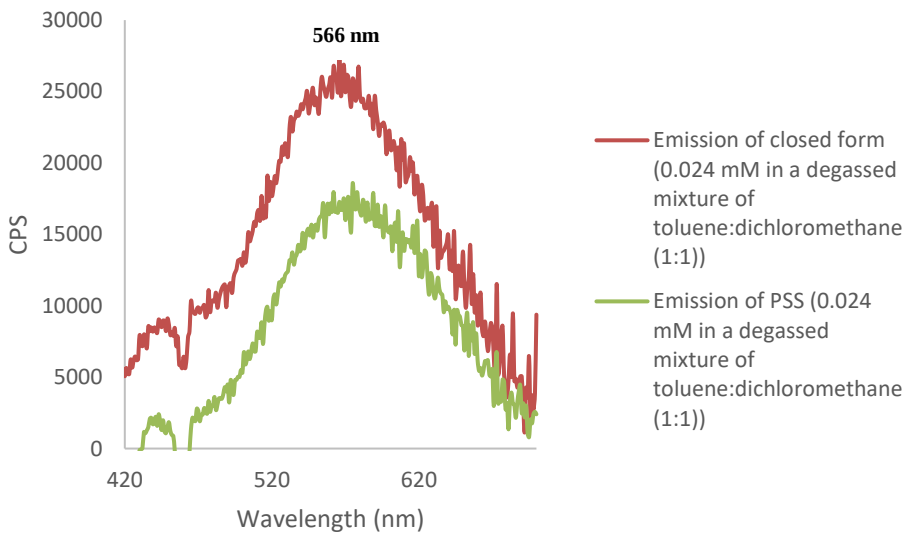

Figure 2.70 Emission spectra of rhenium(I) complex **2.235** with λ_{exc} 397 nm (0.024 mM in a degassed mixture of toluene:dichloromethane (1:1)) in the closed form (red) and in the PSS (green).

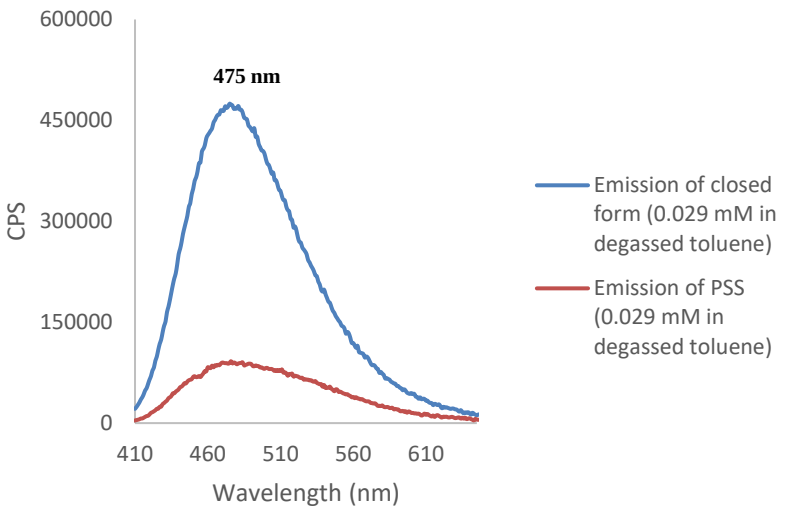

Figure 2.71 Emission spectra of rhenium(I) complex **2.241** with λ_{exc} 394 nm (0.029 mM in degassed toluene) in the closed-form (blue) and in the PSS (red).

The ^{3}MLCT emission of the Re(I) complex **2.241** showed a typical bathochromic shift in the emission energy by increasing the solvent dielectric constant. An improved luminescence quench was attained when toluene was used as solvent as it allowed a better overlap between the absorbance band of the PSS and the emission band of the rhenium(I) complex **2.241** (**Figure 2.72**). Thus, there was a small increase of the luminescence quench from acetonitrile (71%) to toluene (81%).

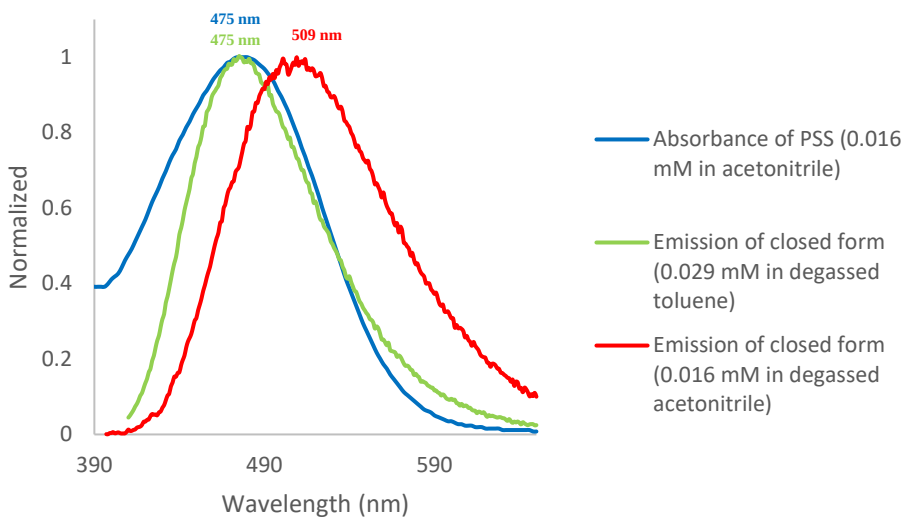

Figure 2.72 Normalized spectra of absorbance of the PSS of **2.241** (0.016 mM in degassed acetonitrile, after UV irradiation, blue), emission of **2.241** (0.029 mM in degassed toluene, λ_{exc} 394 nm, green) and emission of **2.241** (0.016 mM in degassed acetonitrile, λ_{exc} 382 nm, red).

Notably, the PyTz ligand containing Re(I) complex **2.241**, that displayed very good photoswitching ability, showed no fatigue after ten absorbance and emission cycles in acetonitrile at room temperature (**Figures 2.73** and **2.74**). Each cycle involved generating the PSS upon UV irradiation (365 nm, 20 sec) followed by restoration of the closed-form upon irradiation with visible light (λ > 450 nm).

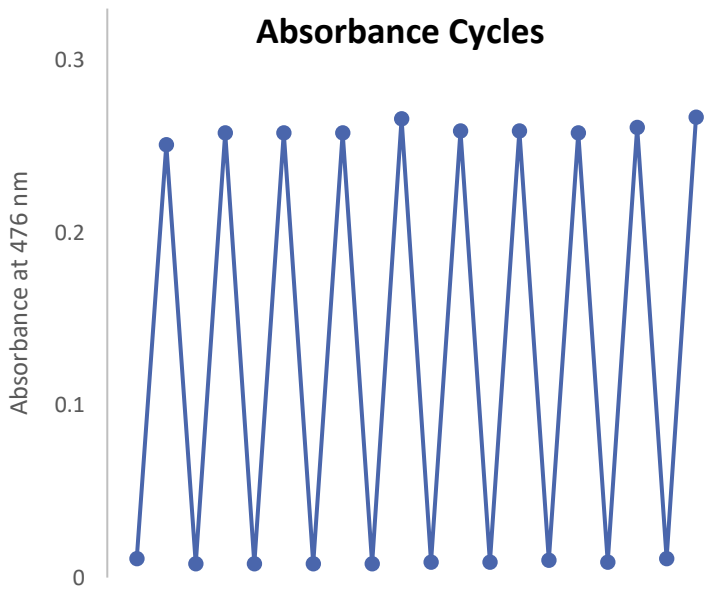

Figure 2.73 Absorbance cycles of rhenium(I) complex **2.241** (CF – PSS) after UV irradiation (0.016 mM in degassed acetonitrile).

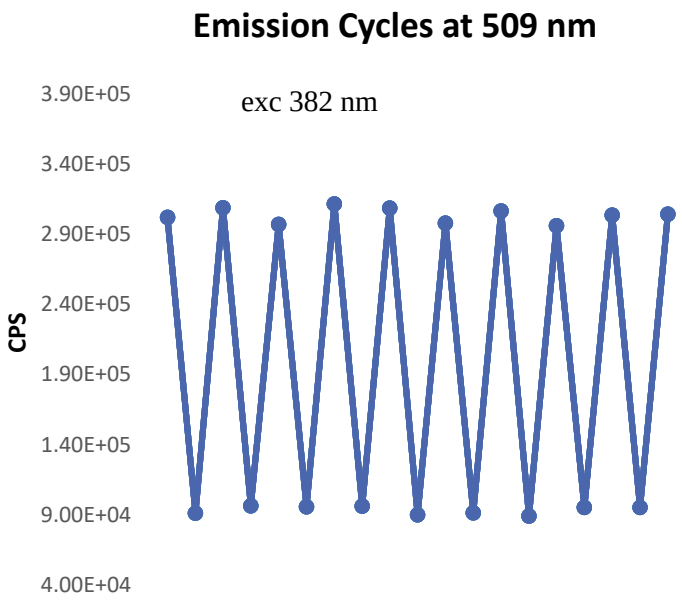

Figure 2.74 Emission cycles of rhenium(I) complex **2.241** (CF – PSS) after UV irradiation (0.016 mM in degassed acetonitrile).

2.3.2.5 Photochromism and Photoswitching of *fac*-[Re(PyTz)(CO)$_3$NP]PF$_6$, NP = 6-Pyridyl-3*H*-naphtho[2,1-*b*]pyran

The UV irradiation of the *fac*-[Re(PyTz)(CO)$_3$NP]PF$_6$, NP = 6-Pyridyl-3*H*-naphtho[2,1-*b*]pyran, generated the corresponding photomerocyanines in solution (**Scheme 2.142**).

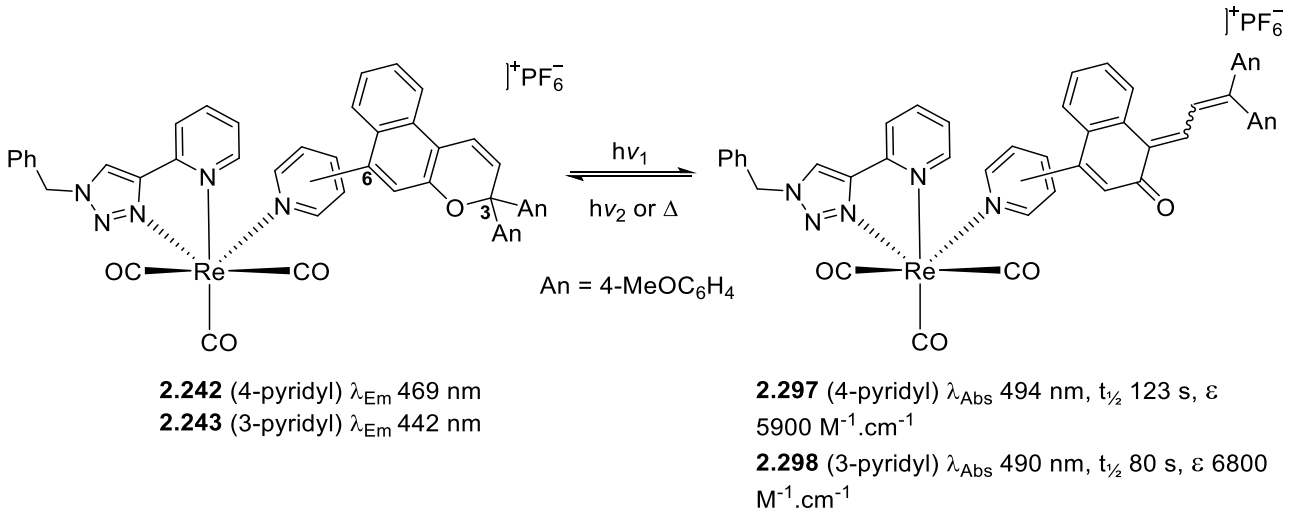

Scheme 2.142 Electrocyclic ring-opening of Re(I) complexes **2.242** and **2.243**.

Upon UV irradiation in toluene, the PyTz ligand containing Re(I) complexes **2.242** and **2.243** generated bathochromic shifted (16 – 24 nm) photostationary states when compared to the simple 6-pyridyl-3*H*-naphtho[2,1-*b*]pyrans **2.214** and **2.215** (**Table 2.18**). Furthermore, the colourability of the Re(I) complexes **2.242** and **2.243** increased by a factor of 88 – 234 which was a consequence of the triplet photosensitization mechanism.

Table 2.18 Spectroscopic data of *fac*-[Re(PyTz)(CO)$_3$NP]PF$_6$, NP = 6-Pyridyl-3*H*-naphtho[2,1-*b*]pyran in toluene.

Entry	Compounds	Py	λ_{Abs} (nm)	$t_{½}$ (s)	k_A	ε_{PSS} ($M^{-1}.cm^{-1}$)	λ_{Em} (nm)	τ_{Em} (ns)	ϕ_{CF} (%)	ϕ_{PSS} (nm)	Quench (%)***
1	**2.214**	4-Py	470	3468	N/A	67	N/A	N/A	N/A	N/A	N/A
2	**2.215**	3-Py	474	1206	2.12×10^{-3} $M^{-1}.s^{-1}$	29	N/A	N/A	N/A	N/A	N/A
3	**2.242**	4-Py	494 490**	123	5.58×10^{-3} s^{-1}	5900	469 470* 477**	10, 50 (1.165)	2.5 1.4**	1.7 0.47**	33 69**
4	**2.243**	3-Py	490	80	7.92×10^{-3} s^{-1}	6800	442 444*	N/A	0.25	0.13	47

* In PhMe:DCM (1:1). ** In MeCN. *** Quench (%) was calculated by the ratio between the emission intensity of the closed form and PSS at the maxima of emission.

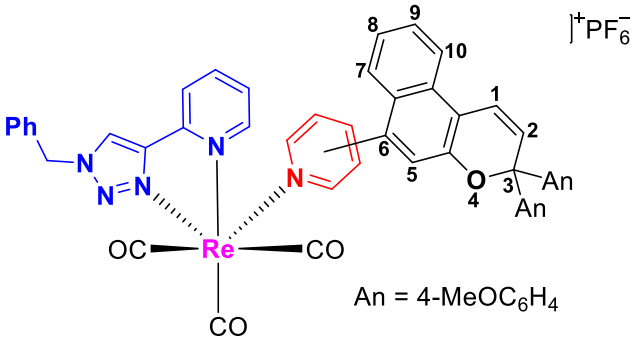

2.242 (4-pyridyl)
2.243 (3-pyridyl)

Very interestingly, the photostationary state from the Re(I) complex **2.242** (**Entry 3**, **Table 2.18**) bleached 28 times faster than the corresponding ligands 6-(4-pyridyl)-3*H*-naphtho[2,1-*b*]pyran **2.214** (**Entry 1**, **Table 2.18**) while the photostationary state from the Re(I) complex **2.243** (**Entry 4**, **Table 2.18**) bleached 15 times faster than the corresponding 6-(3-pyridyl)-3*H*-naphtho[2,1-*b*]pyran **2.215** (**Entry 2**, **Table 2.18**). The fast bleaching kinetics was interpreted in light of the destabilization of the photomerocyanines upon coordination to the rhenium atom. As stated before, if the triplet – triplet energy transfer pathway is efficient, the bleaching of the PSS becomes slower, even considering the destabilization effect of the photomerocyanines. For that case, there is a good overlap between the emission band of the Re(I) complex and the absorbance band of the PSS. However, if the triplet – triplet energy transfer pathway is not effective, the bleaching of the PSS becomes faster, as a result of the destabilization effect. For the rhenium(I) complexes **2.242** and **2.243**, there is only a partial overlap between the emission band of the Re(I) complex and the absorbance band of the PSS. The overlap between the emission band and the absorbance band of the PSS is not as good as other PyTz ligand containing rhenium(I) complexes (**Figures 2.75** and **2.76**). Thus, it was hypothesized that the triplet – triplet energy pathway was not efficient enough to generate thermally stable photostationary states. Interestingly, the emission bands of the rhenium(I) complexes **2.242** and **2.243** were blue shifted when compared to the absorbance band of the PSS. Consequently, the ^{3}MLCT excited state was higher in energy than the ^{3}IL excited state. However, both excited states were quite different in terms of energy. Possibly, the degree of energy transfer from the ^{3}MLCT excited state to the lower-lying ^{3}IL excited state depends on the energy difference between both excited states. If the difference is too large, the energy transfer is less efficient.

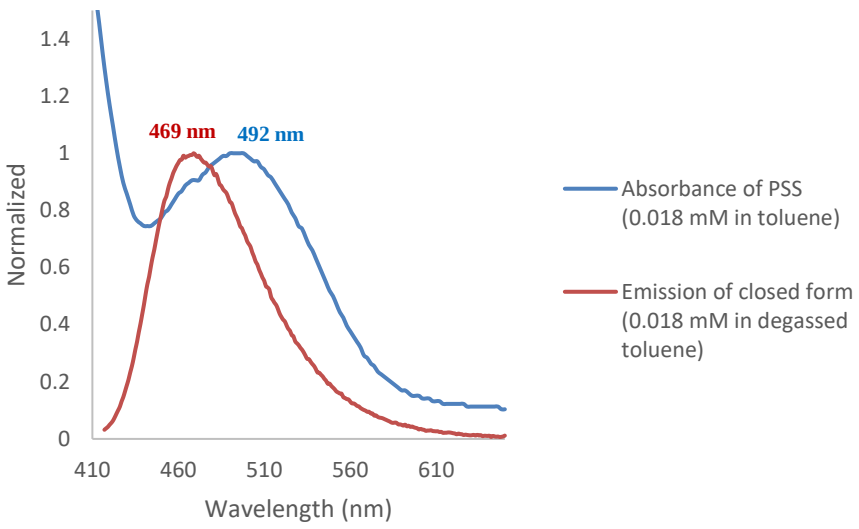

Figure 2.75 Normalized spectra of absorbance of the PSS of **2.242** (0.018 mM in toluene, after UV irradiation, blue) and emission of **2.242** (0.018 mM in degassed toluene, λ_{exc} 402 nm, red).

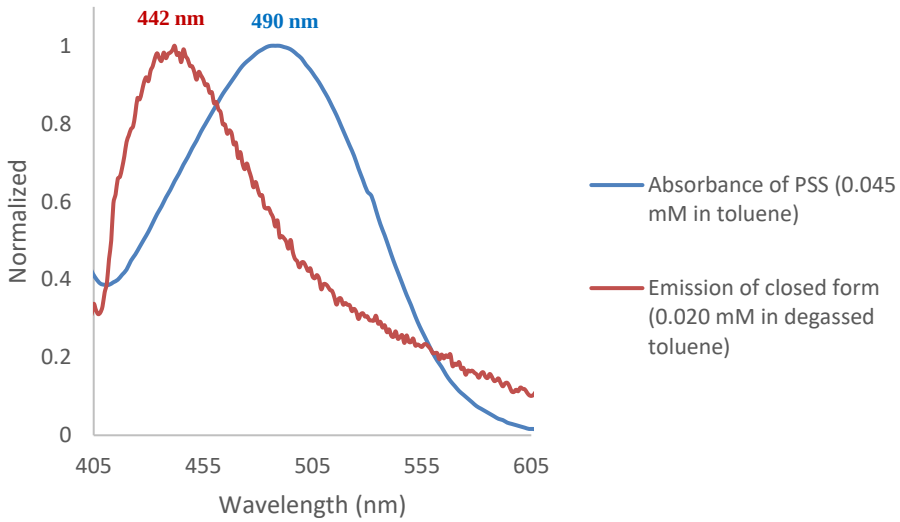

Figure 2.76 Normalized spectra of absorbance of the PSS of **2.243** (0.045 mM in toluene, after UV irradiation, blue) and emission of **2.243** (0.020 mM in degassed toluene, λ_{exc} 358 nm, red).

Another indication of the relatively poor energy transfer from the ^{3}MLCT excited state to the lower-lying ^{3}IL excited state was the comparatively poor photoswitching of the ^{3}MLCT phosphorescence. Thus, upon UV irradiation of toluene solutions of the Re(I) complexes **2.242** and **2.243**, only 33% and 47% of the ^{3}MLCT phosphorescence was quenched, respectively (**Figures 2.77** and **2.78**).

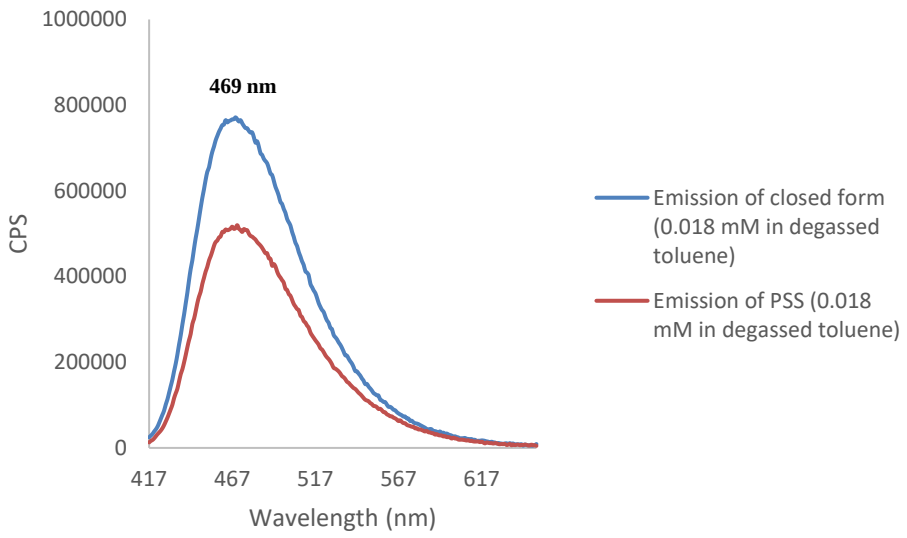

Figure 2.77 Emission spectra of rhenium(I) complex **2.242** with λ_{exc} 402 nm (0.018 mM in degassed toluene) in the closed form (blue) and in the PSS (red).

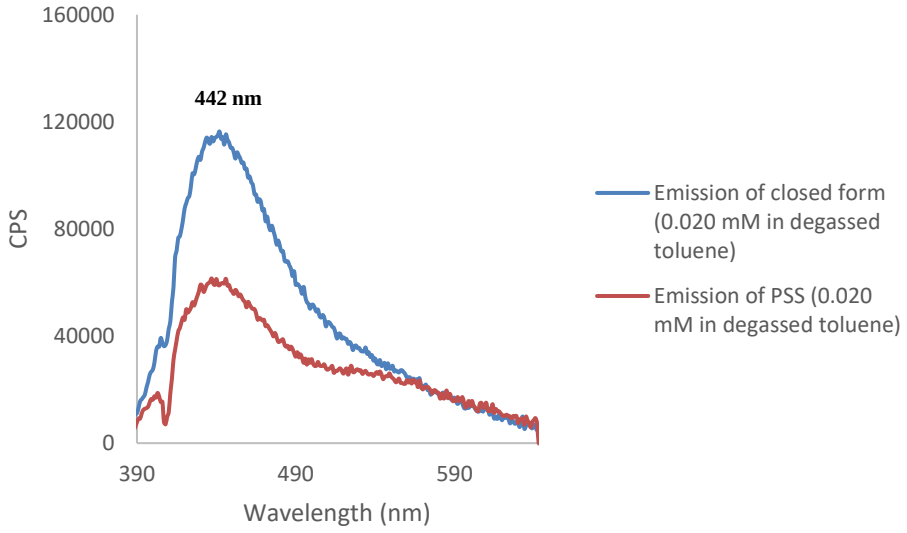

Figure 2.78 Emission spectra of rhenium(I) complex **2.243** with λ_{exc} 358 nm (0.020 mM in degassed toluene) in the closed form (blue) and in the PSS (red).

The ^{3}MLCT phosphorescence of the Re(I) complex **2.242** showed a typical bathochromic shift in the emission energy by increasing the solvent dielectric constant. An improved luminescence quench was obtained when acetonitrile was used as solvent as it allowed a better overlap between the absorbance band of the PSS and the emission band of the rhenium(I) complex **2.242** (**Figure**

2.79). Thus, there was a considerable increase of the luminescence quench from toluene (33%) to acetonitrile (69%).

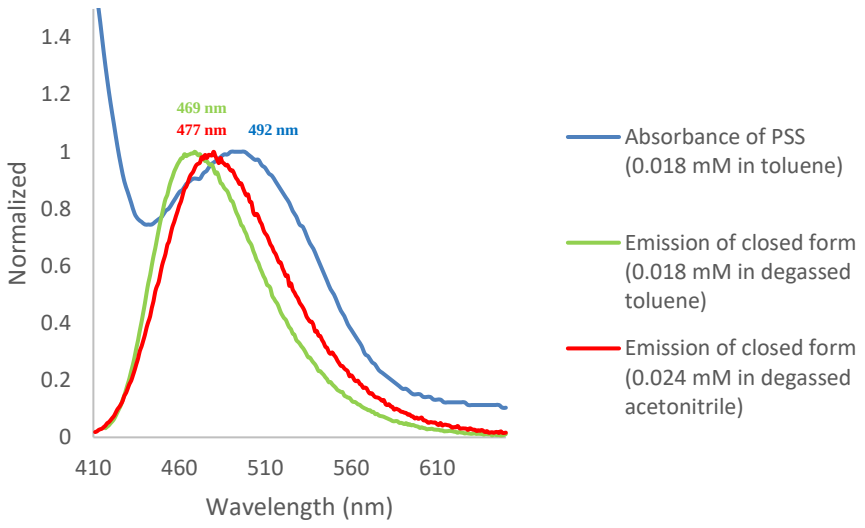

Figure 2.79 Normalized spectra of absorbance of the PSS of **2.242** (0.018 mM in toluene, after UV irradiation, blue), emission of **2.242** (0.018 mM in degassed toluene, λ_{exc} 402 nm, green) and emission of **2.242** (0.024 mM in degassed acetonitrile, λ_{exc} 396 nm, red).

2.3.2.7 Photochromism and Photoswitching of *fac*-[Re(PyTzNP)(CO)$_3$Cl]^0, NP = 3*H*-naphtho[2,1-*b*]pyran

Upon UV irradiation, the rhenium(I) complex **2.247** generated the corresponding photomerocyanines **2.301** in a PhMe:DCM (1:1) solution (**Scheme 2.143**).

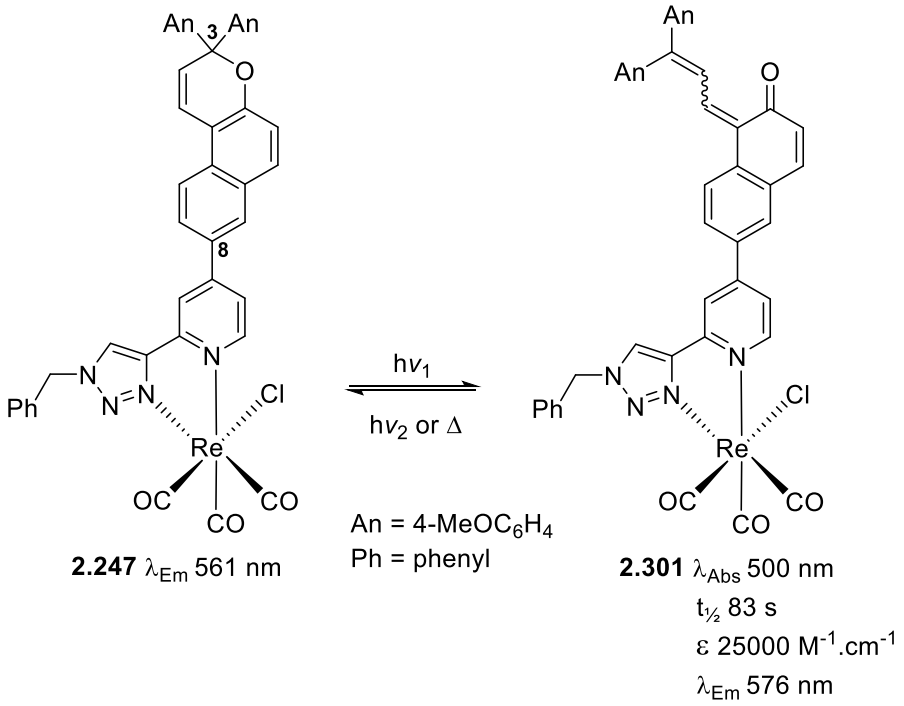

Scheme 2.143 Photoisomerization of Re(I) complex **2.247**.

By comparing the response of the simple 8-(pyridyl-triazole)-3*H*-naphtho[2,1-*b*]pyran **2.110** with the *fac* rhenium(I) complex **2.247**, a photostationary state was generated under UV irradiation that was slightly bathochromic shifted (14 nm) (**Table 2.19**). Furthermore, the colourability increased by a factor of 132 which was a consequence of a triplet photosensitization process. Thus, the red coloured produced in solution persisted for a shorter period of time ($t_{½}$ = 83 s) (**Entry 2**, **Table 19**) when compared to the simple 8-(pyridyl-triazole)-3*H*-naphtho[2,1-*b*]pyran **2.110** ($t_{½}$ = 1204 s) (**Entry 1**, **Table 2.19**). It was rationalized that the faster bleaching kinetics were a consequence of the destabilization of the photomerocyanine upon coordination to the rhenium atom, as it disturbed the electronic conjugation of the delocalized π system.

Table 2.19 Spectroscopic data of *fac*-[Re(PyTzNP)(CO)$_3$Cl]^0 with NP = 3*H*-naphtho[2,1-*b*]pyran in toluene.

Entry	Compounds	λ_{PSS} (nm)	$t_{½}$ (s)	k_{Δ}	ε_{PSS} ($M^{-1}.cm^{-1}$)	λ_{em} (nm)	τ_{em} (ns)	ϕ_{CF} (%)	ϕ_{PSS} (nm)	Quench (%)
1	**2.110**	480 486*	1204*	2.25×10^{-3}* $M^{-1}.s^{-1}$	160 190*	N/A	N/A	N/A	N/A	N/A
2	**2.247**	500*	83*	8.44×10^{-3} s^{-1}*	25000*	514 (Closed form, under air)* 561 (Closed form, degassed)* 574 (PSS, under air)* 576 (PSS, degassed)*	160, 4672 (1.114) [degassed]	0.038 (degassed)*	0.021 (degassed)*	90 (under air)** 45 (degassed)***

* In PhMe:DCM (1:1). ** Quench (%) was calculated by the ratio between the emission intensity of the closed form and PSS at 514 nm. ***Quench (%) was calculated by the ratio between the quantum yield of the emission of the closed form (centered at 561 nm) and the quantum yield of the emission of the PSS (centered at 576 nm).

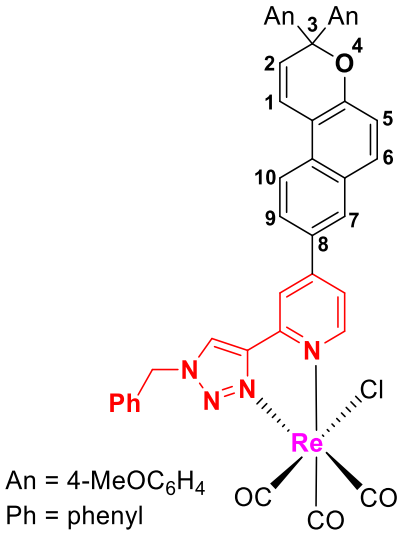

2.247

The rhenium(I) complex **2.247** in an aerated PhMe:DCM (1:1) solution showed an emission band centered at 514 nm, by excitation into the MLCT transition (**Figure 2.80**). Upon UV irradiation to a photostationary state, the emission band at 514 nm disappeared. Interestingly, a small emission band centered at 574 nm was visible in the emission spectrum of the PSS of **2.247**, corresponding to the emission from a different excited state.

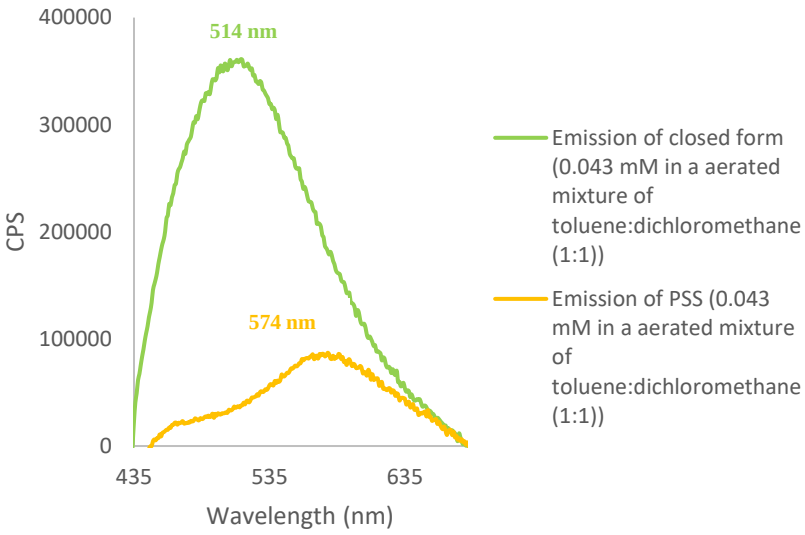

Figure 2.80 Spectra of emission of **2.247** (0.043 mM in a aerated mixture of toluene:dichloromethane (1:1), λ_{exc} 372 nm, green) and emission of the PSS of **2.247** (0.043 mM in a aerated mixture of toluene:dichloromethane (1:1), λ_{exc} 372 nm, yellow).

Curiously, by degassing a PhMe:DCM (1:1) solution of the rhenium(I) complex **2.247**, the emission band centered at 514 nm disappeared, being replaced by a new emission band centered at 561 nm (**Figure 2.81**). Considering the very long lifetime of the emission (τ = 4.7 μs) and the insensitivity of the emission energy to the nature of the bidentate ligand, it was proposed that the emission was originating from a $^3IL_{CF}$ excited state. Furthermore, upon generation of the photostationary state, under UV irradiation, the emission band bathochromic shifted 15 nm with a 45% drop in the quantum yield (ϕ) (**Figure 2.82**). Curiously, the $^3IL_{PSS}$ emission band under degassed conditions (λ_{em} 576 nm) was similar to the emission band of the PSS under aerated conditions (λ_{em} 574 nm), most probably corresponding to emission from the same excited state.

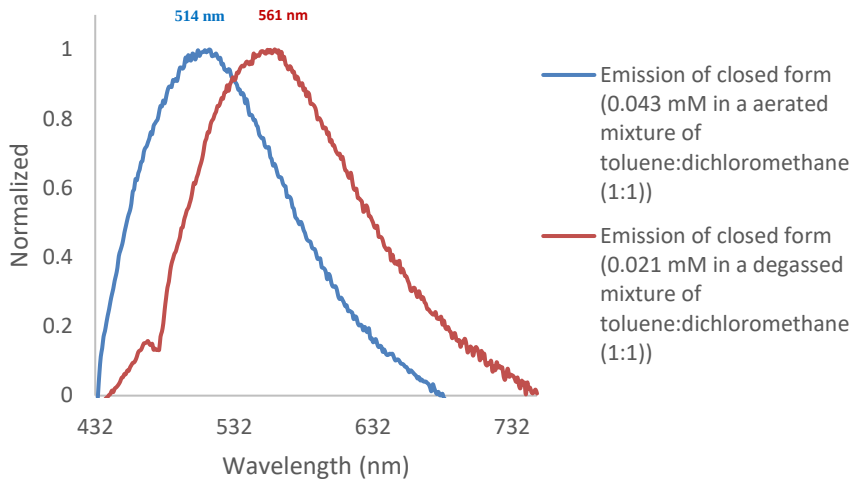

Figure 2.81 Normalized spectra of emission of **2.247** (0.043 mM in a aerated mixture of toluene:dichloromethane (1:1), λ_{exc} 372 nm, blue) and emission of **2.247** (0.021 mM in a degassed mixture of toluene:dichloromethane (1:1), λ_{exc} 411 nm, red).

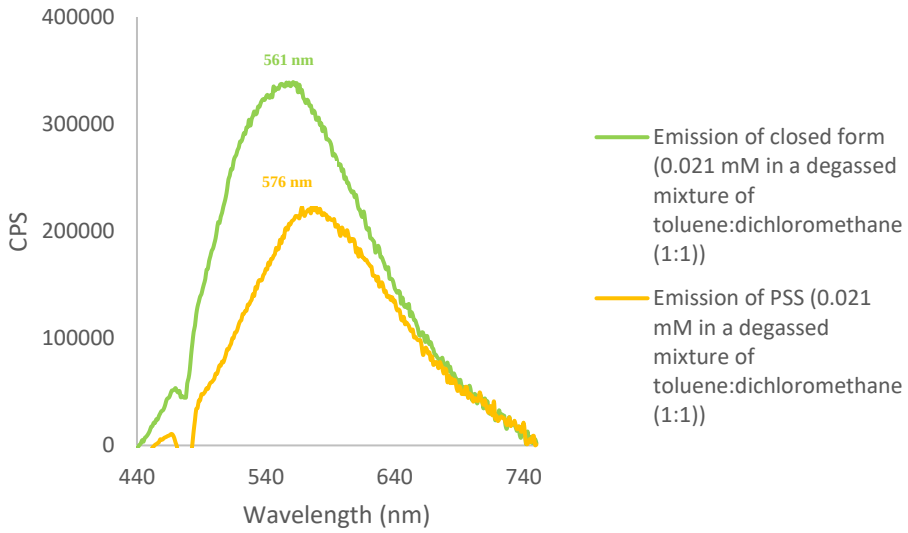

Figure 2.82 Emission of **2.247** (0.021 mM in a degassed mixture of toluene:dichloromethane (1:1), λ_{exc} 411 nm, green) and emission of the PSS of **2.247** (0.021 mM in a degassed mixture of toluene:dichloromethane (1:1), λ_{exc} 411 nm, yellow).

It was rationalized, that under aerated conditions, triplet oxygen ($^3O_2$) quenched to a large degree the $^3IL_{CF}$ excited state. Most probably, energy transfer did occur to a small extent between the ^3MLCT and the $^3IL_{CF}$ excited states, therefore most likely the emission band derived from a ^3MLCT excited state mixed with some ^3IL character. Upon generation of the PSS, the original emission band disappeared with the evolution of a new emission band peaking at 576 nm. The insensitivity of the emission energy to the nature of the bidentate ligand was indicative that the emission derived from a $^3IL_{PSS}$ excited state. Hence, the quenching of the emission (90%) at 514 nm was attributed to intramolecular energy transfer from the $^3MLCT/^3IL$ excited state to the lower-lying $^3IL_{PSS}$ excited state (**Figure 2.83**). Furthermore, considering the improved colourability in solution, it was likely that the drop in the intensity of the emission band (78%) of the $^3IL_{PSS}$ excited state, when compared to the emission band of the $^3MLCT/^3IL$ excited state, was partially due to the depletion of the $^3IL_{PSS}$ excited state by promoting the photochromic reaction.

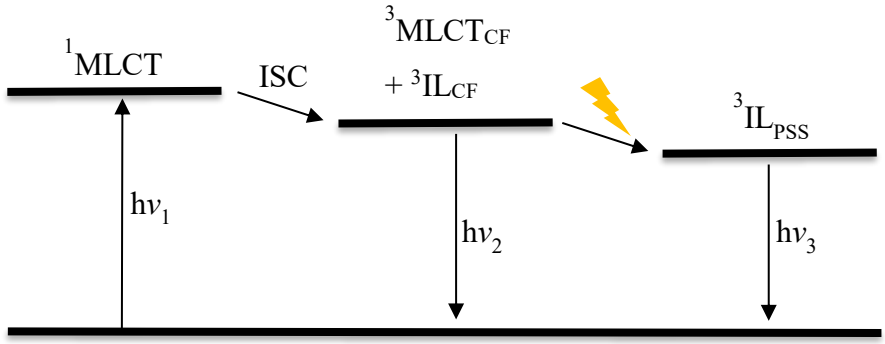

Figure 2.83 Energy-transfer pathway for Re(I) complex **2.247** before and after photoisomerization, under air.

Under degassed conditions, the $^3IL_{CF}$ excited state was not partially quenched any longer. Thus, the ^3MLCT excited state fully populated the $^3IL_{CF}$ excited state, which explained the 47 nm bathochromic shift of the emission band. Upon generation of the PSS, there was energy transfer from the $^3IL_{CF}$ excited state to the lower-lying $^3IL_{PSS}$ which was accompanied by a 15 nm red shift in the emission band (**Figure 2.84**). The improved colourability in solution, suggested that the drop in the quantum yield (ϕ) of the emission band (45%) of the $^3IL_{PSS}$ excited state, when compared to the emission band of the $^3IL_{CF}$ excited state, was partially due to the depletion of the $^3IL_{PSS}$ excited state by promoting the photochromic reaction.

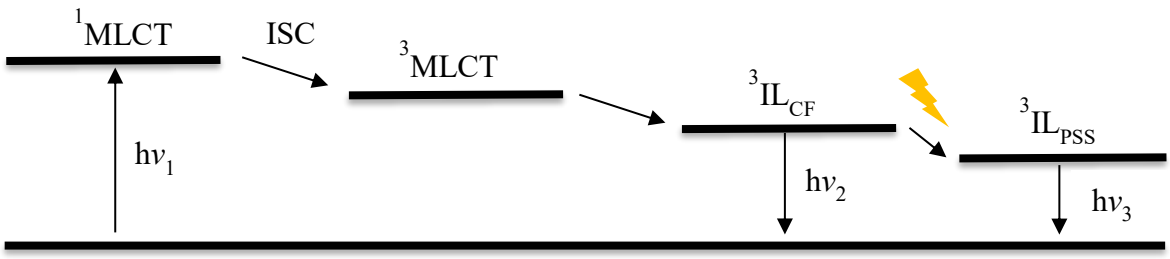

Figure 2.84 Energy-transfer pathway for Re(I) complex **2.247** before and after photoisomerization, under degassed conditions.

2.3.2.6 Photochromism and Photoswitching of *fac*-[Re(N^N)(CO)$_3$NP]PF$_6$, NP = 3-Pyridyl-3*H*-naphtho[2,1-*b*]pyran and N^N = BPy, BTz

Upon UV irradiation, the *fac*-[Re(N^N)(CO)$_3$NP]PF$_6$, NP = 3-Pyridyl-3*H*-naphtho[2,1-*b*]pyran, generated the corresponding photomerocyanines in solution (**Scheme 2.144**).

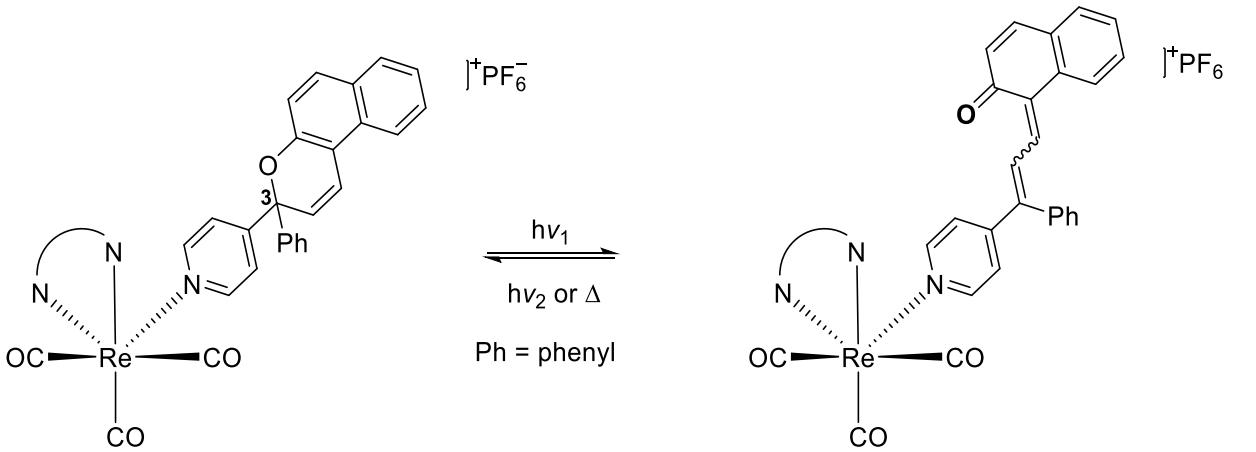

2.236 (N^N = BPy) λ_{Em} 562 nm
2.246 (N^N = BTz)

2.299 (N^N = BPy) λ_{Abs} 410 nm, $t_{½}$ > 60 s, ε 6100 $M^{-1}.cm^{-1}$
2.300 (N^N = BTz) λ_{Abs} 422 nm, $t_{½}$ 117 s, ε 5300 $M^{-1}.cm^{-1}$

Scheme 2.144 Electrocyclic ring-opening of Re(I) complexes **2.236** and **2.246**.

The UV irradiation of the BPy ligand containing Re(I) complex **2.236** (**Entry 2**, **Table 2.20**) generated a slightly hypsochromic shifted (4 nm) photostationary state in toluene when compared to the simple 3-pyridyl-3*H*-naphtho[2,1-*b*]pyran **2.170** (**Entry 1**, **Table 2.20**). In contrast, the BTz ligand containing Re(I) complex **2.246** (**Entry 3**, **Table 2.20**) generated a bathochromic shifted (12 nm) photostationary state in toluene when compared to the 3-pyridyl-3*H*-naphtho[2,1-*b*]pyran **2.170**

(**Entry 1**, **Table 2.20**). Furthermore, the colour produced in toluene was 1.1 – 1.8 times more intense than the 3-pyridyl-3*H*-naphtho[2,1-*b*]pyran **2.170** as a result of the triplet photosensitization mechanism. Thus, the colour produced by the photostationary states from the rhenium(I) complexes **2.236** and **2.246** persisted for comparatively longer periods of time. Note that no $t_{½}$ was presented for the rhenium(I) complex **2.236** due to an unsatisfactory logarithmic fit, however the $t_{½}$ was longer than 60 s ($t_{½}$ > 60 s). The comparatively slower bleaching kinetics of the rhenium(I) complexes **2.236** and **2.246** were attributed to the disruption of the destabilizing electronic withdrawing effect of the pyridyl group upon coordination of the nitrogen to the rhenium atom, which led to relatively more stable and long-lived photomerocyanines. Possibly, population of the ^{3}IL excited state by energy transfer from the ^{3}MLCT excited state might have also contributed to a small degree to the longer $t_{½}$ (s).

Table 2.20 Spectroscopic data of *fac*-[Re(N^N)(CO)$_3$NP]PF$_6$, NP = 3-Pyridyl-3*H*-naphtho[2,1-*b*]pyran in toluene.

Entry	Compounds	N^N	λ_{Abs} (nm)	$t_{½}$ (s)	k_{Δ} (s^{-1})	IOD	ε ($M^{-1}.cm^{-1}$)	λ_{Em} CF (nm)	ϕ_{CF} (%)	ϕ_{PSS} (nm)	Quench (%)**
1	**2.170**	No	414	< 60	3.56×10^{-5}	0.650	3400	N/A	N/A	N/A	N/A
2	**2.236**	BPy	410	> 60	N/A	0.206	6100	562*	0.058*	0.050*	2*
3	**2.246**	BTz	422	117	N/A	0.229	5300	N/A	N/A	N/A	N/A

* In PhMe:DCM (1:1). ** Quench (%) was calculated by the ratio between the emission intensity of the closed form and PSS at the maxima of emission.

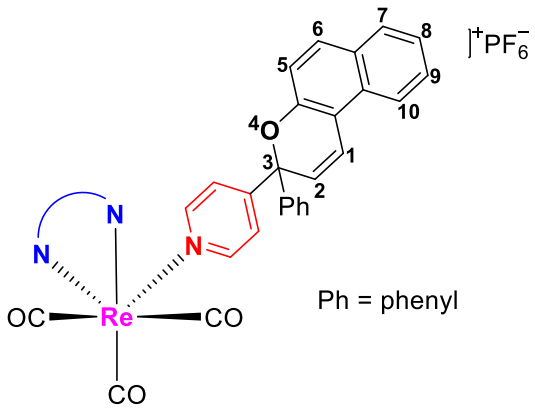

2.236 (N^N = BPy)
2.246 (N^N = BTz)

The BPy ligand containing rhenium(I) complex **2.236** showed a typical ^{3}MLCT phosphorescence band centered at 562 nm in PhMe:DCM (1:1) with a very poor quantum yield (ϕ_{CF} = 0.058) (**Figure 2.85**). The absorbance band of the PSS, centered at 410 nm, and the emission band of the closed form were separated by 152 nm. Consequently, the ^{3}MLCT excited state was too low in energy for a significant energy transfer to the higher-lying ^{3}IL excited state, which was reflected by the very poor phosphorescence quench upon formation of the photostationary state (2%) (**Figure 2.86**).

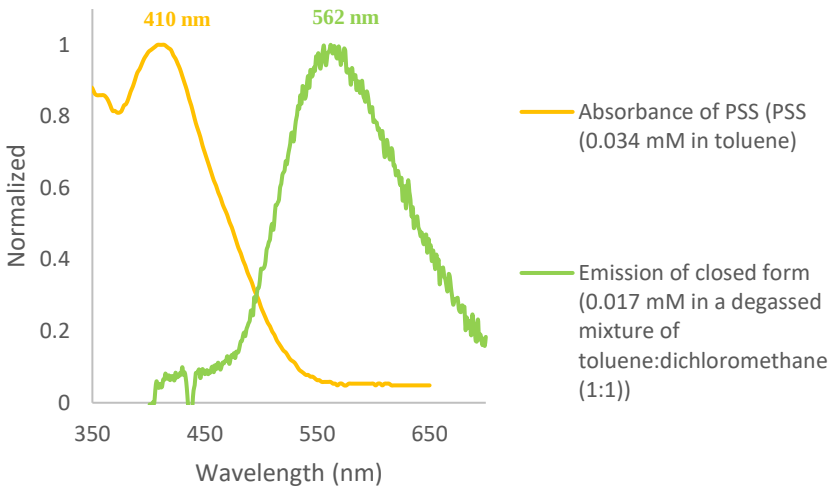

Figure 2.85 Normalized spectra of absorbance of the PSS of **2.236** (0.034 mM in toluene, after UV irradiation, yellow) and emission of **2.236** (0.017 mM in a degassed mixture of toluene:dichloromethane (1:1), λ_{exc} 381 nm, green).

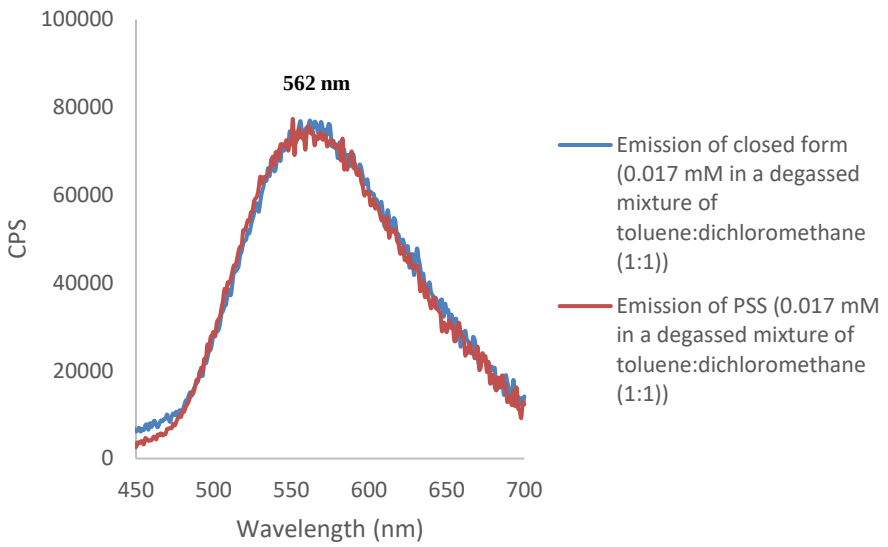

Figure 2.86 Emission spectra of rhenium(I) complex **2.236** with λ_{exc} 381 nm (0.017 mM in a degassed mixture of toluene:dichloromethane (1:1)) in the closed form (blue) and in the PSS (red).

By exciting the BTz ligand containing rhenium(I) complex **2.246** with λ_{exc} 330, 363 and 400 nm in acetonitrile, no typical broad and stuctureless ^{3}MLCT emission band was present in the emission spectra (**Figure 2.87**). Clearly, the observed structured high energy emission bands suggested that they had a singlet excited state origin, probably arising from the organic ligands.

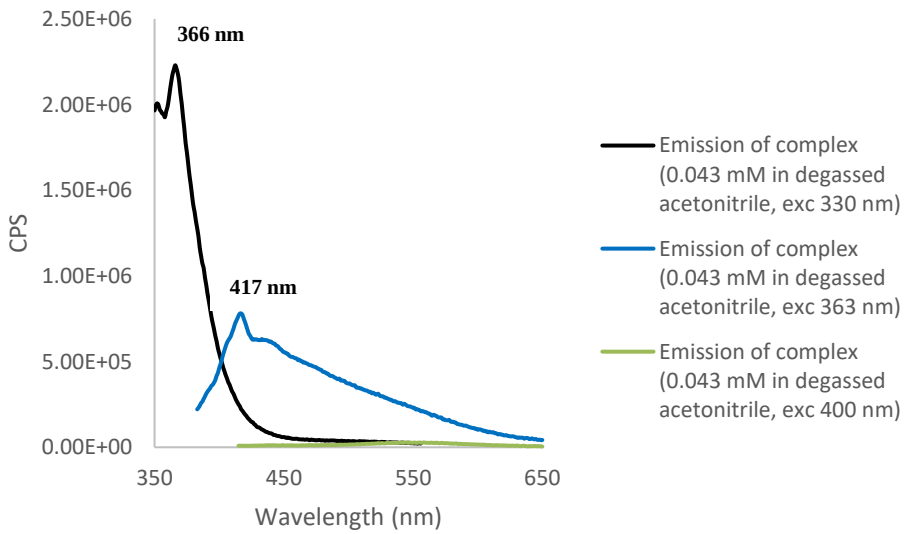

Figure 2.87 Emission spectra of rhenium(I) complex **2.246** with λ_{exc} 330, 363 and 400 nm (0.043 mM in degassed acetonitrile).

2.4 Ring-contraction of Naphthopyrans

2.4.1 Preamble

The ring-contraction of benzopyrans and naphthopyrans has been previously reported in the literature.[225–228] Dmitrieva *et al.*, have reported the oxidative ring-contraction of the 1,2-dihydrospiro[benzo[*f*]chromene-3,9'-xanthene] **2.302** to the 9-(naphtho[2,1-*b*]furan-2-yl)-9*H*-xanthene **2.303** in 34–57% yield (**Scheme 2.145**).[225]

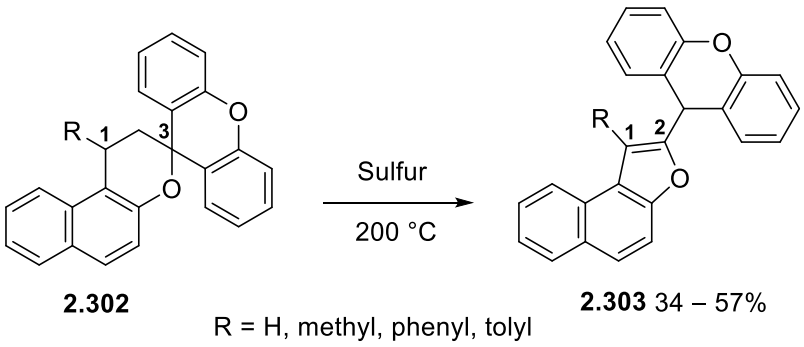

Scheme 2.145 Oxidative ring-contraction of the 1,2-dihydrospiro[benzo[*f*]chromene-3,9'-xanthene] **2.302**.

Sastry *et al.*, have reported the ring-contraction of the 2*H*-naphtho[1,2-*b*]pyran **2.304** to the naphthofuran **2.305** under basic conditions through an addition – dehydrobromination reaction (**Scheme 2.146**).[226]

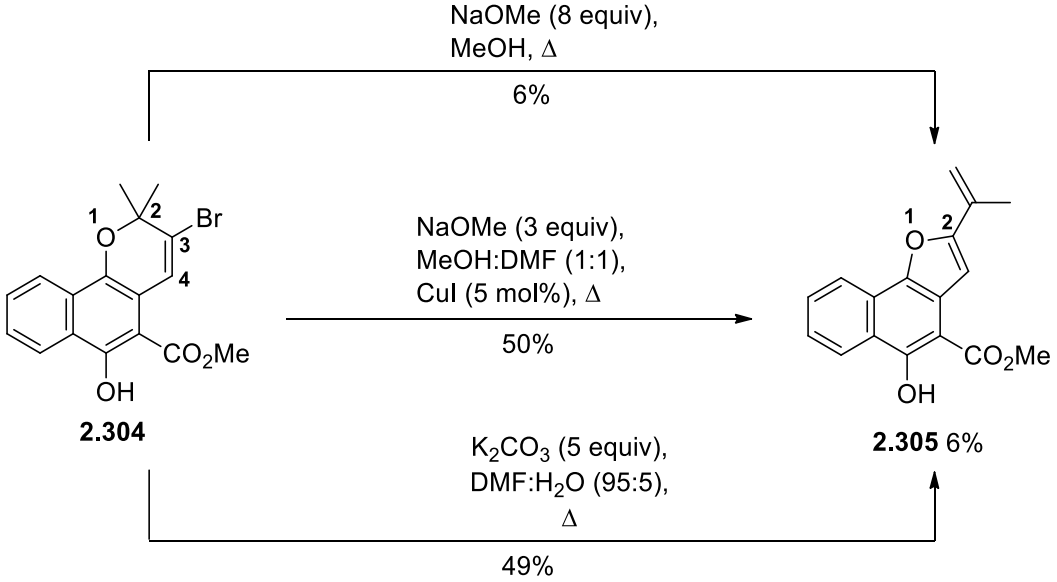

Scheme 2.146 Ring-contraction of the 2*H*-naphtho[1,2-*b*]pyran **2.304**.

According to the authors, the reaction is initiated by a 6π-electrocyclic ring-opening generating the dienone **2.306** (**Scheme 2.147**). Hence, the allylic hydrogen of the dienone **2.306** is abstracted by the base generating the intermediate **2.307**. The phenolate function of **2.307** intramolecularly attacks the double bond which is activated by the electron-withdrawing group. In a final step, the addition – dehydrobromination results in the formation of the naphthofuran **2.305**.

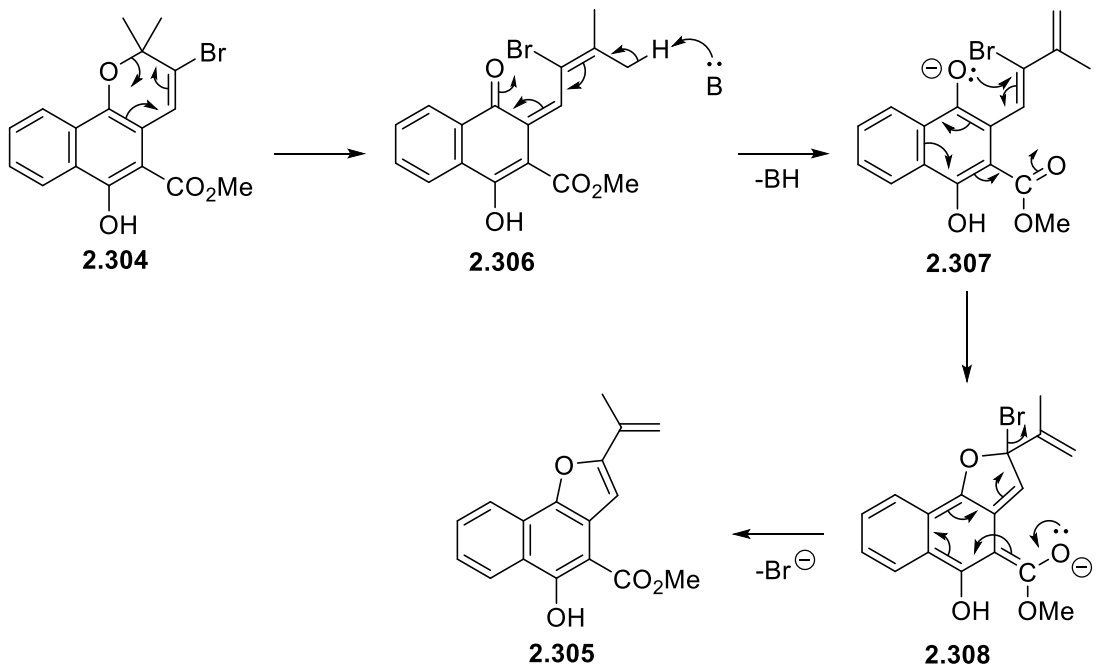

Scheme 2.147 Mechanism of the ring-contraction of the 2*H*-naphtho[1,2-*b*]pyran **2.304**.

According to Gabbutt *et al.*, the presence of very strong electron-withdrawing groups at the saturated carbon of the pyran moiety favours the ring-contraction reaction.[124] The authors have reported the thermal and the photochemical ring-contraction of the spiro(3*H*-naphtho[2,1-*b*]pyran-3,9′-thioxanthene-10,10-dioxide) **2.309** to the 9-(naphtho[2,1-*b*]furan-2-yl)-9*H*-thioxanthene-10,10-dioxide **2.310** (**Scheme 2.148**).

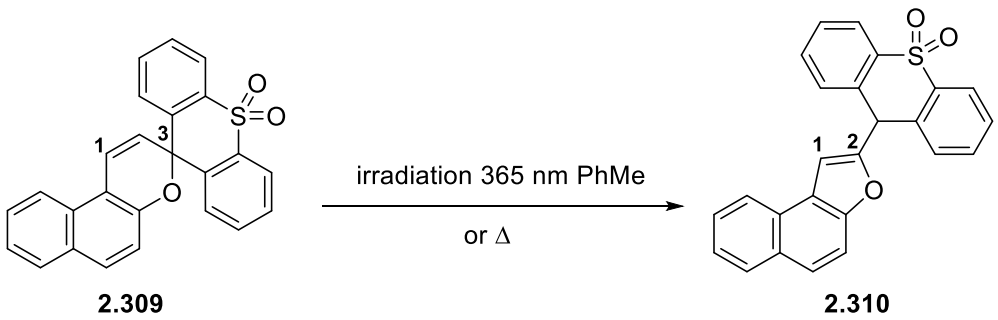

Scheme 2.148 Ring-contraction of the spiro(3*H*-naphtho[2,1-*b*]pyran-3,9′-thioxanthene-10,10-dioxide) **2.309**.

In the same publication, the authors also noted that upon heating a sample of the isomeric spiro(2*H*-naphtho[1,2-*b*]pyran-2,9′-thioxanthene-10,10-dioxide) **2.311** afforded the ring-contracted product **2.312** in 72% yield (**Scheme 2.149**). Furthermore, the reaction could also be driven photochemically under UV irradiation.

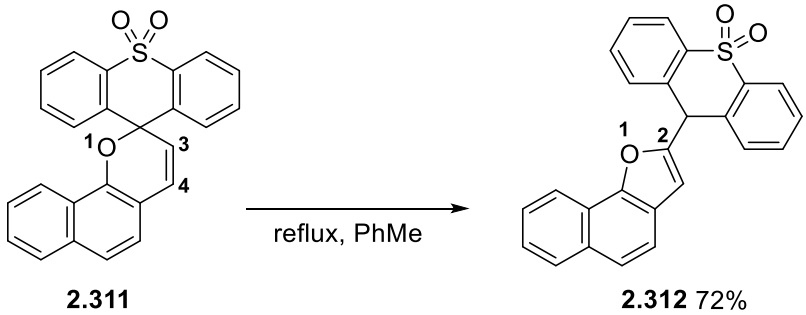

Scheme 2.149 Ring-contraction of the spiro(2*H*-naphtho[1,2-*b*]pyran-2,9′-thioxanthene-10,10-dioxide) **2.311**.

According to the authors, first the thermal or photochemical 6π-electrocyclic ring-opening of the pyran unit generates the dienones **2.313** and **2.314** (**Scheme 2.150**). Hence, the geometry of **2.314** favours the 5-*exo*-*trig* ring closure generating the aromatic thiaanthracene **2.316** and thence the thioxanthene **2.312** upon proton transfer.

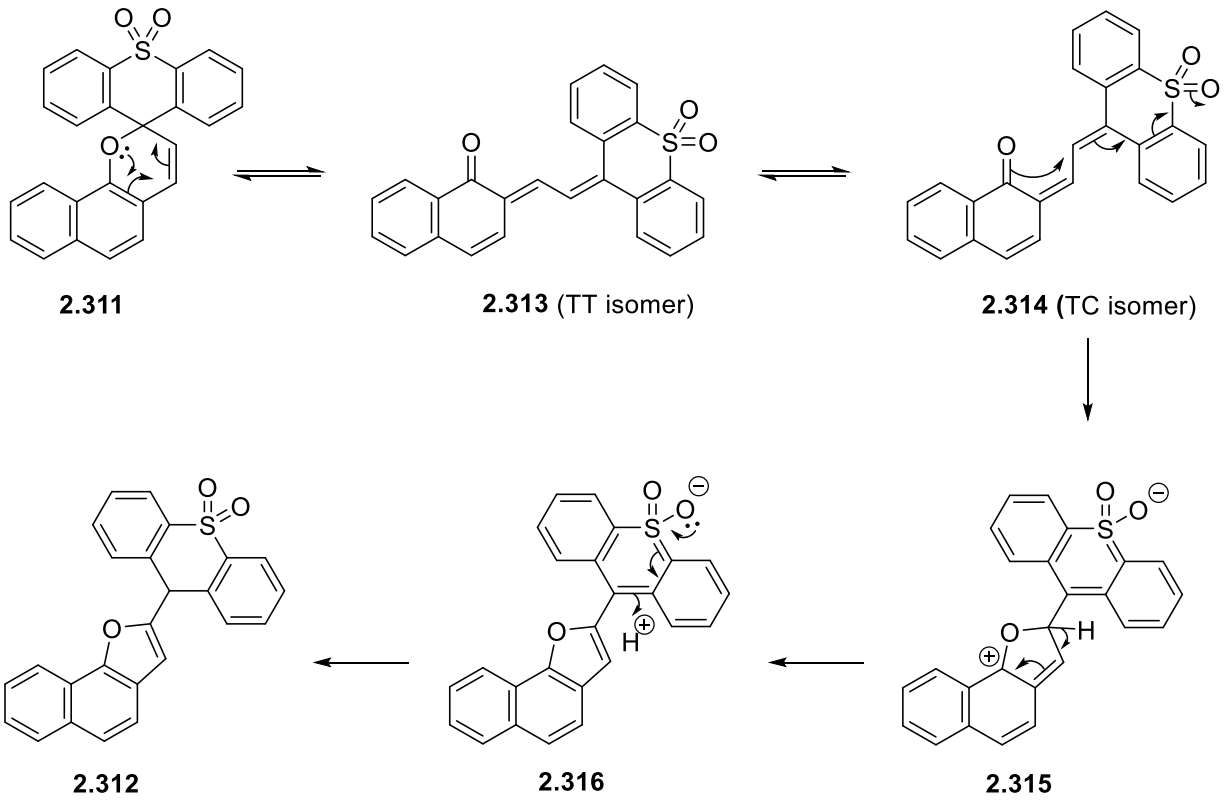

Scheme 2.150 Mechanism of the ring-contraction of the spiro(2*H*-naphtho[1,2-*b*]pyran-2,9′-thioxanthene-10,10-dioxide) **2.311**.

The authors also noted that the bis-sulfone **2.317** ring-contracted to the naphthofuran **2.318** upon UV irradiation in 85% yield, yet the thermal contraction was not observed (**Scheme 2.151**).

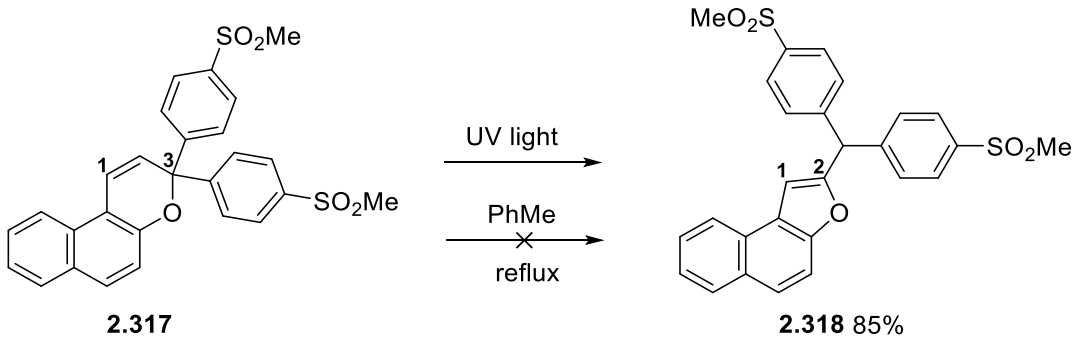

Scheme 2.151 Ring-contraction of the bis-sulfone **2.317**.

Palladium-driven ring contraction of the pyran motif has also been described in the literature. Zinth *et al.*, have reported the ring-contraction of the 3*H*-naphtho[2,1-*b*]pyran **2.319** to the

naphthofuran **2.320** during an attempt to perform a palladium-catalysed cyanation reaction (**Scheme 2.152**).[227]

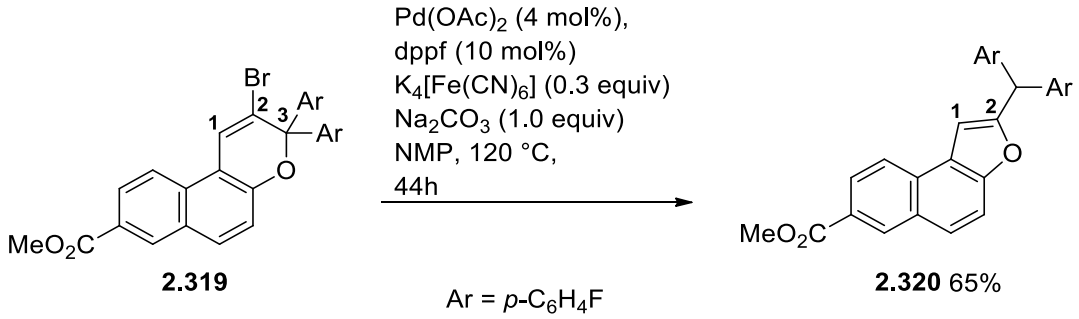

Scheme 2.152 Ring-contraction of the 3*H*-naphtho[2,1-*b*]pyran **2.319**.

Gabbutt *et al.*, have prepared a 2-(diarylmethyl)-5-styrylbenzofuran **2.322** from styrene and a 6-bromo-2,2-diaryl-2*H*-[1]benzopyran **2.321** in 30% yield *via* an unexpected tandem Heck-coupling – ring-contraction reaction (**Scheme 2.153**). [228]

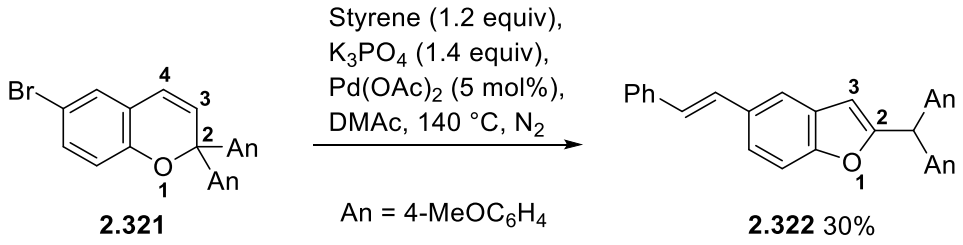

Scheme 2.153 Synthesis of 2-(diarylmethyl)-5-styrylbenzofuran **2.322**.

The authors proposed that in the presence of dimethylacetamide at high temperature, nanoparticulate Pd^0 is generated *in situ* (**Scheme 2.154**). Hence, addition of nucleophilic Pd^0 to C-4 of the benzopyran **2.321**, a process compared to many examples of addition of Pd^0 to allylic acetates with displacement of acetate ion leading to π-allyl Pd species,[229] proceeds with ring-opening and subsequent capture of the palladium to generate the palladacycle **2.325**. Deprotonation by the action of the base, regenerated Pd^0 and forms an allenylphenol **2.326** which undergoes a 5-*exo-dig* cyclization to the benzofuran **2.322**. The ring-contraction sequence operates in tandem with the expected Heck cross-coupling reaction.

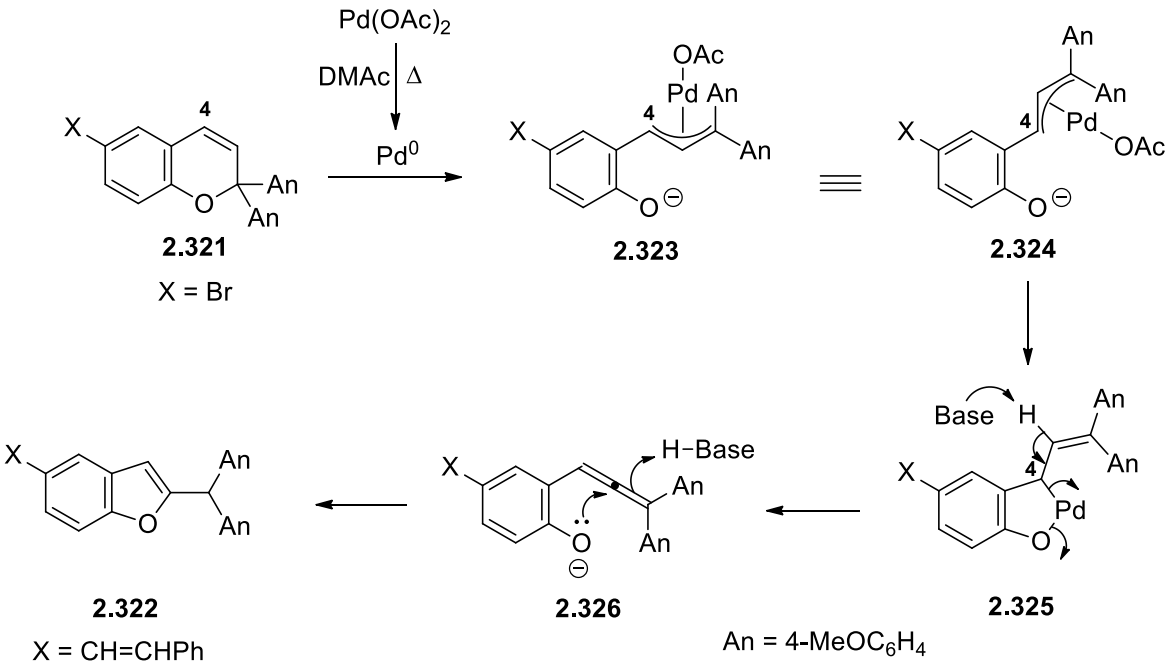

Scheme 2.154 Mechanism of the synthesis of 2-(diarylmethyl)-5-styrylbenzofuran **2.322**.

2.4.2 Discussion

During the Suzuki cross-coupling reactions between the halo or pseudo-halo substituted 3*H*-naphtho[2,1-*b*]pyrans **2.327** and the pyridine boronic acid pinacol esters **2.40**, the ring-contraction of the pyran motif was observed, affording the corresponding weakly fluorescent (on TLC) non-photochromic naphthofurans **2.329** as by-products (**Scheme 2.155**). Their formation implied a very concrete practical problem, as the purification by flash column chromatography was extremely difficult due to the similar R_f of both structural isomers in both a variety of mobile phases and stationary phases. Consequently, a kinetic study was developed in order to gather more information about the ring-contraction process and also to determine the experimental conditions to perform the Suzuki cross-coupling reactions without the competing side-reaction.

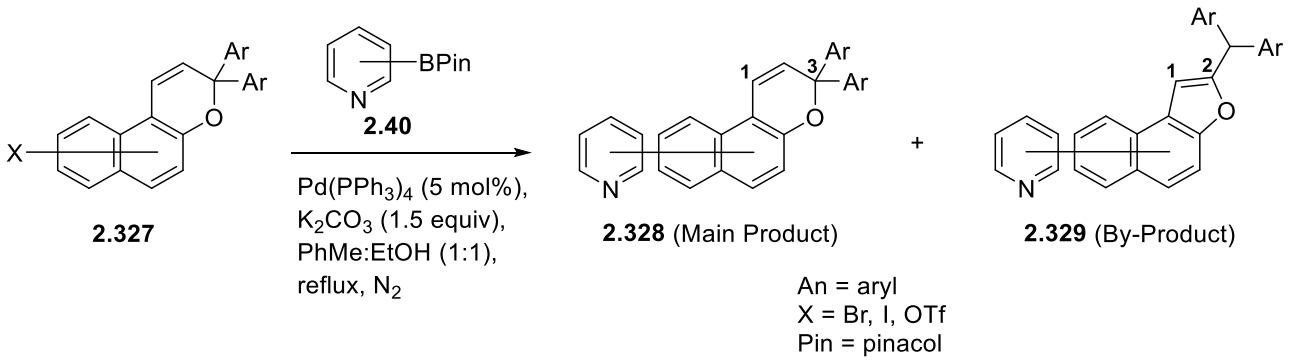

Scheme 2.155 Generic Suzuki cross-coupling reaction between the halo or pseudo-halo substituted 3*H*-naphtho[2,1-*b*]pyran **2.327** and the pyridine boronic acid pinacol ester **2.40**.

The ring-contraction of the 3,3-bis(4-methoxyphenyl) substituted 3*H*-naphtho[2,1-*b*]pyran **2.330** under different experimental conditions was analysed (**Scheme 2.156**). The reactions were monitored by ^{1}H NMR analysis by collecting aliquots from the reaction mixtures over time. The ratio = (∫furan/ (∫pyran + ∫furan))*100 was used to calculate the concentration of 3*H*-naphtho[2,1-*b*]pyran **2.330** over time. An NMR interpulse delay of 2s was enough to acquire experimental data that was sufficiently robust to give statistically reliable experimental fits.

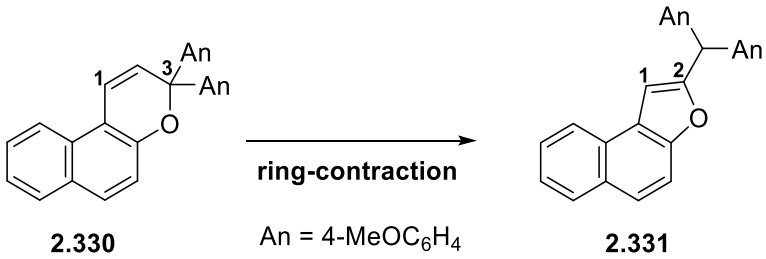

Scheme 2.156 Ring-contraction of 3*H*-naphtho[2,1-*b*]pyran **2.330**.

The first few reactions were performed in order to evaluate the overall stability of the 3*H*-naphtho[2,1-*b*]pyran **2.330**. Thus, there was no ring-contraction after:

1) stirring **2.330** in DCM at room temperature for 18h;
2) stirring **2.330** in DCM with $Pd(PPh_3)_4$ (5 mol%) at room temperature for 23h;
3) stirring **2.330** in toluene at room temperature for 17h.

When using K_2CO_3 (1.5 equiv) and $Pd(PPh_3)_4$ (5 mol%) in PhMe:EtOH (1:1) at reflux, a typical Suzuki cross-coupling reagent combination (**Entry 1**, **Table 2.21**), ring-contraction occurred

at a relatively slow rate – after 80h, 74% of the 3*H*-naphtho[2,1-*b*]pyran **2.330** had ring-contracted to the naphthofuran **2.331** (**Figure 2.88**).

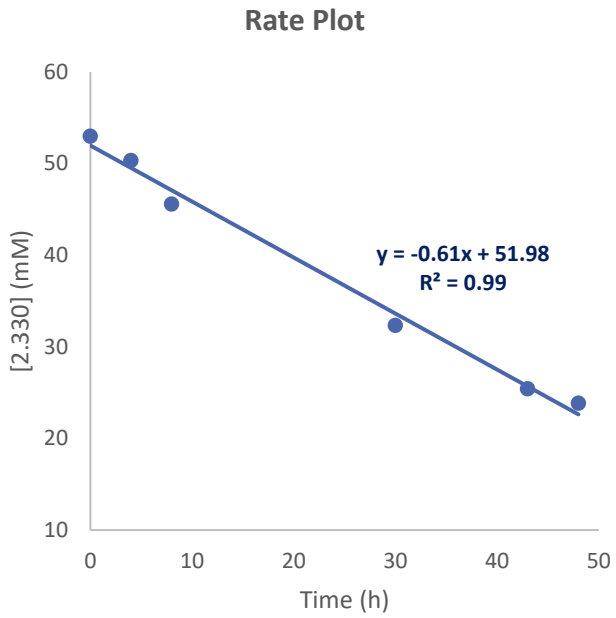

Figure 2.88 Rate plot of the ring-contraction of **2.330** by using K_2CO_3 (1.5 equiv) and $Pd(PPh_3)_4$ (5 mol%) in PhMe:EtOH (1:1) at reflux.

Surprisingly, the ring-contraction of the 3*H*-naphtho[2,1-*b*]pyran **2.330** occurred without the addition of the palladium catalyst. Thus, when using K_2CO_3 (1.5 equiv) in PhMe:EtOH (1:1) at reflux, 67% of the 3*H*-naphtho[2,1-*b*]pyran **2.330** had ring-contracted to the naphthofuran **2.331** after 80h of reaction (**Entry 2**, **Table 2.21**).

Notably, in the absence of K_2CO_3, but employing $Pd(PPh_3)_4$ (5 mol%) in PhMe:EtOH (1:1) at reflux, no ring-contraction of the 3*H*-naphtho[2,1-*b*]pyran **2.330** was observed after 48h of reaction, which strongly indicated that the base played a pivotal role in the ring-contraction process (**Entry 3**, **Table 2.21**).

Additionally, it was determined that the rate of the ring-contraction of the 3*H*-naphtho[2,1-*b*]pyran **2.330** depended on the stoichiometry of K_2CO_3: by doubling the molar quantity of K_2CO_3 (3 equiv), the rate constant of the reaction increased by 23% (**Entry 4**, **Table 2.21**). Thus, the ring-contraction of the 3*H*-naphtho[2,1-*b*]pyran **2.330** was complete after 74h of reaction (**Figure 2.89**).

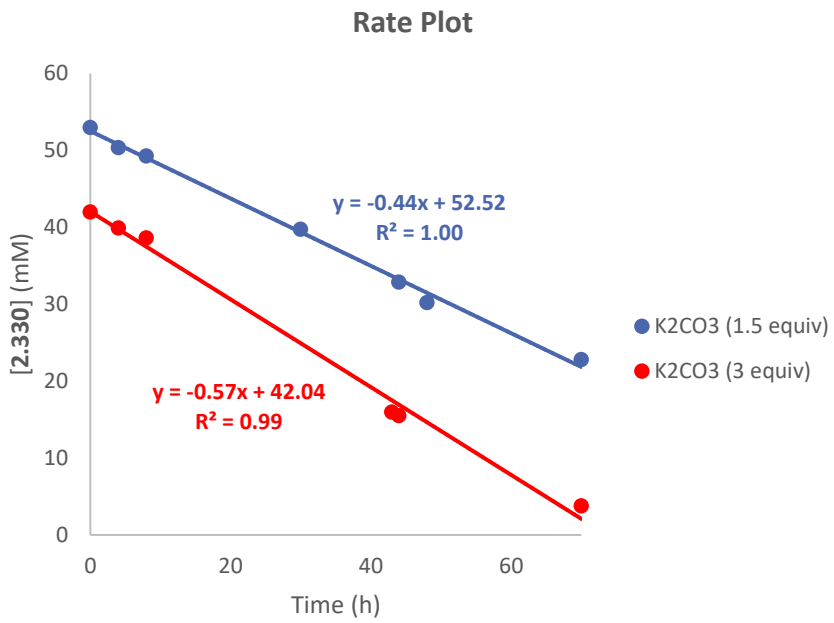

Figure 2.89 Rate plot of the ring-contraction of the 3*H*-naphtho[2,1-*b*]pyran **2.330** by using K_2CO_3 (1.5 and 3 equiv) in PhMe:EtOH (1:1) at reflux.

The kinetics of the ring-contraction of the 3*H*-naphtho[2,1-*b*]pyran **2.330** varied with the nature of the carbonate bases (**Figure 2.90**). A similar rate constant was observed between Cs_2CO_3 and K_2CO_3 (**Entries 2** and **6**, **Table 2.21**). On the other hand, when employing Li_2CO_3, the rate constant was two times smaller when compared to K_2CO_3 (**Entry 4**, **Table 2.21**). Hence, when using Na_2CO_3, the ring-contraction occurred faster than Li_2CO_3 yet slower than K_2CO_3 and Cs_2CO_3 – after 83h only 45% of the 3*H*-naphtho[2,1-*b*]pyran **2.330** had ring-contracted (**Entry 5**, **Table 2.21**). The differences in the kinetics of the ring-contraction of the 3*H*-naphtho[2,1-*b*]pyran **2.330** by employing different carbonate bases could be attributed to differences in solubility in PhMe:EtOH (1:1) – Li_2CO_3 is less soluble in PhMe:EtOH (1:1) when compared to K_2CO_3 and Cs_2CO_3.

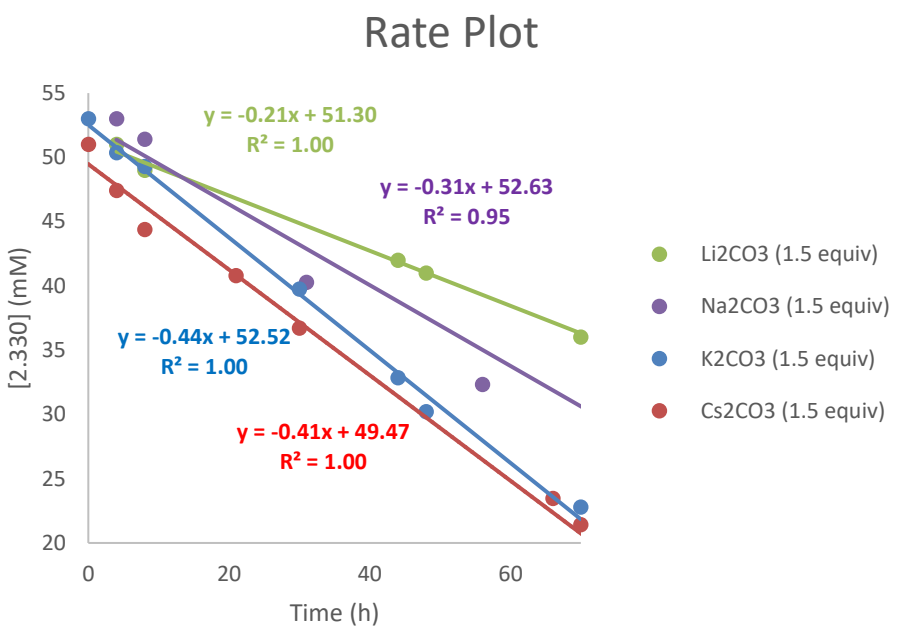

Figure 2.90 Rate plot of the ring-contraction of the 3*H*-naphtho[2,1-*b*]pyran **2.330** by using different carbonate bases (1.5 equiv) in PhMe:EtOH (1:1) at reflux.

Bases with different pKb were also tested: when using K_3PO_4 (1.5 equiv), which is a stronger base than K_2CO_3, in PhMe:EtOH (1:1) at reflux, a mixture of **2.330**:**2.331** (73:27) was formed after 14h of reaction (**Entry 7**, **Table 2.21)**. When employing K_2CO_3 (1.5 equiv), only 13% of the ring-contracted product **2.331** was formed after 14h of reaction. Therefore, the kinetics of the ring-contraction of the 3*H*-naphtho[2,1-*b*]pyran **2.330** when using K_3PO_4 were faster in comparison to K_2CO_3.

Suzuki cross-coupling reactions by employing KF as a base have been reported in the literature.[230] Considering that the strength of the base affected the rate of the ring-contraction and that the rate of the Suzuki cross-coupling reaction was generally much faster than the rate of the ring-contraction, it was envisioned that if a weaker base was used, e.g. KF, it could lead to Suzuki cross-coupling reactions with no ring-contraction. Thus, when using KF (1.5 equiv) and $Pd(PPh_3)_4$ (5 mol%) in PhMe:EtOH (1:1) at reflux, 8-bromo-3*H*-naphtho[2,1-*b*]pyran **2.56** was successfully coupled to 4-pyridineboronic acid pinacol ester **2.35** affording the 8-(4-pyridyl)-3*H*-naphtho[2,1-*b*]pyran **2.57** in 67% yield, without the formation of the corresponding naphthofuran as a by-product (**Scheme 2.157**).

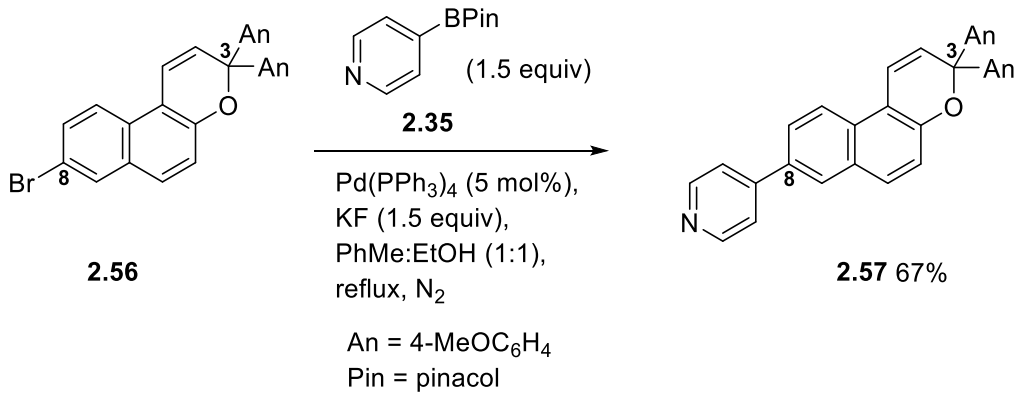

Scheme 2.157 Selective coupling of **2.56** and **2.35** to give 3*H*-naphtho[2,1-*b*]pyran **2.57**.

The same conditions were also employed to the Suzuki cross-coupling reaction between 10-iodo-3*H*-naphtho[2,1-*b*]pyran **2.34** and 4-pyridineboronic acid pinacol ester **2.35** affording the 10-(4-pyridyl)-3*H*-naphtho[2,1-*b*]pyran **2.36** in 66% yield without the formation of the corresponding naphthofuran (**Scheme 2.158**). It is worth mentioning that one implication of the mechanism of the Suzuki cross-coupling reaction is that at least 2 equiv of a monobasic base like KF would be required for a fully successful cycle. However, only 1.5 equiv of KF were used in these reactions which could rationalise the fair yields obtained (66 – 67%). On the other hand, it must be considered that the absence of the formation of the corresponding naphthofurans might have been a consequence of the consumption of the KF in the Suzuki cross-coupling reactions, which would leave no KF available to promote the ring-contraction. Nonetheless, the developed procedure allowed Suzuki cross-coupling reactions to be performed with 3*H*-naphtho[2,1-*b*]pyrans without the ring-contraction side reaction.

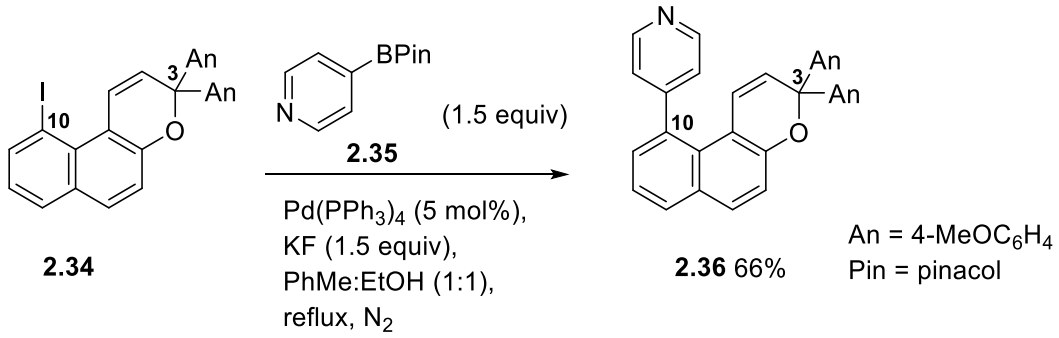

Scheme 2.158 Selective synthesis of 10-(4-pyridyl)-3*H*-naphtho[2,1-*b*]pyran **2.36**.

Table 2.21 Experimental conditions and rate constant for the ring-contraction of the 3*H*-naphtho[2,1-*b*]pyran **2.330**.

Entry	$[2.330]_0$ /mM	Pd Catalyst	Base	pKb in water	Solvent	Temp.	k / $M.h^{-1}$	Conversion after 80h (%)
1	53	$Pd(PPh_3)_4$ (5 mol%)	K_2CO_3 (1.5 equiv)	3.75	PhMe:EtOH (1:1)	reflux	0.61	74
2	53	No	K_2CO_3 (1.5 equiv)	3.75	PhMe:EtOH (1:1)	reflux	0.44	67
4	53	$Pd(PPh_3)_4$ (5 mol%)	No	No	PhMe:EtOH (1:1)	reflux	0	0*
5	42	No	K_2CO_3 (3 equiv)	3.75	PhMe:EtOH (1:1)	reflux	0.57	100
4	51	No	Li_2CO_3 (1.5 equiv)	3.75	PhMe:EtOH (1:1)	reflux	0.21	34
5	51	No	Na_2CO_3 (1.5 equiv)	3.75	PhMe:EtOH (1:1)	reflux	0.31	45**
6	51	No	Cs_2CO_3 (1.5 equiv)	3.75	PhMe:EtOH (1:1)	reflux	0.41	67
7	51	No	K_3PO_4 (1.5 equiv)	1.62	PhMe:EtOH (1:1)	reflux	N/A	27***

*After 48h. **After 83h. ***After 14h.

Moreover, the effect of 18-crown-6 was tested as it could act as a phase-transfer catalyst.[231] Thus, when using 18-crown-6 (3 equiv) and K_2CO_3 (1.5 equiv) in toluene at reflux, the rate constant of the ring-contraction increased by one order of magnitude (**Entry 1**, **Table 2.22**). Consequently, the 3*H*-naphtho[2,1-*b*]pyran **2.330** fully ring-contracted to the naphthofuran **2.331** after only 10h of reaction (**Figure 2.91**).

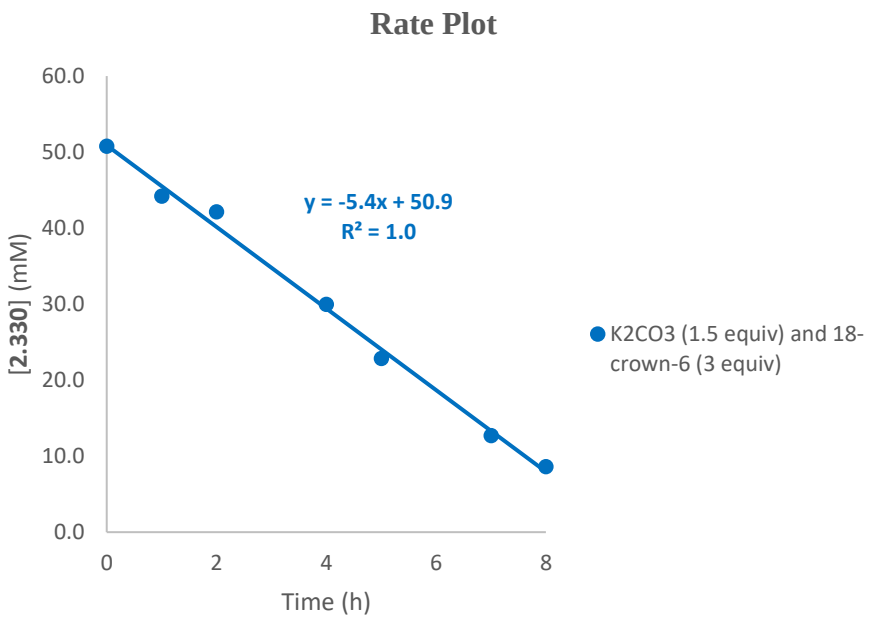

Figure 2.91 Rate plot of the ring-contraction of the 3*H*-naphtho[2,1-*b*]pyran **2.330** by using K_2CO_3 (1.5 equiv) and 18-crown-6 (3 equiv) in toluene at reflux.

Hence, when using K_2CO_3 (1.5 equiv), $Pd(PPh_3)_4$ (5 mol%) and 18-crown-6 (3.1 equiv) in toluene at reflux for 19h, the 8-bromo-3*H*-naphtho[2,1-*b*]pyran **2.56** was successfully coupled to 4-pyridineboronic acid pinacol ester **2.35** affording the 8-(4-pyridyl)-3*H*-naphtho[2,1-*b*]pyran **2.57** that rapidly ring-contracted to the corresponding naphthofuran **2.58**. The latter was isolated as the single product of the reaction and was attained in 47% yield after flash column chromatography (**Scheme 2.159**). The foregoing reaction conditions constitute an effective protocol to selectively prepare naphthofurans *via* a tandem Suzuki-coupling – ring-contraction process.

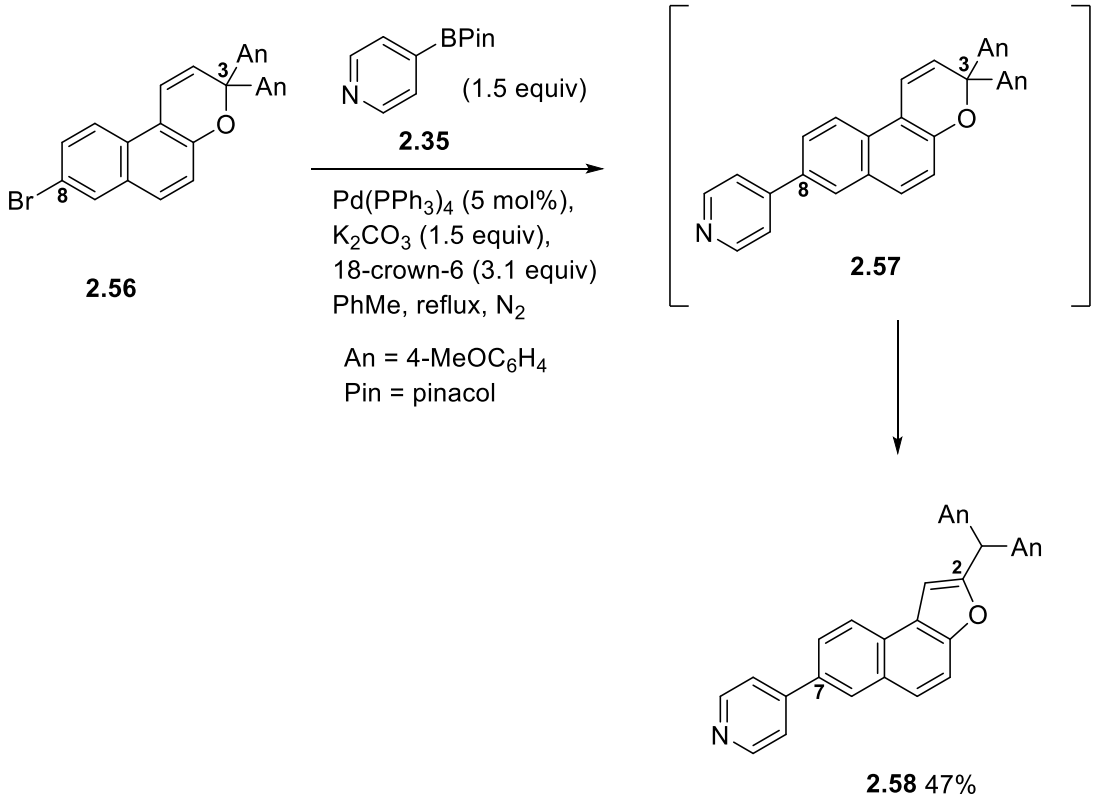

Scheme 2.159 Synthesis of the naphthofuran **2.58**.

Leadbeater *et al.* have reported Pd-free Suzuki cross-coupling reactions,[232] and subsequently the authors reassessed these initial publications by stating that there was palladium contamination in the commercially available carbonate bases, down to a level of 50 ppb – 2.5 ppm, which catalysed the Suzuki reactions.[233] Given this prior work, it was deemed important to establish the palladium content in the bases employed in this work.

By ICP-MS it was determined that the K_2CO_3 (supplied by Alfa Aesar) employed in the ring-contraction reactions contained 24 ppm (per 0.50 g of sample) of amorphous palladium. It was rationalized that there might have been freak contamination with amorphous palladium probably arising from the bases, which catalysed the ring-contraction reactions. In order to determine if palladium was involved in the ring-contraction process, two reactions were performed by using a new bottle of Na_2CO_3 (supplied by Alfa Aesar; 2.20 ppb of amorphous palladium per 0.50 g of sample). When using Na_2CO_3 (1.5 equiv) and 15-crown-5 (3 equiv) in toluene at reflux, no ring-contraction was observed after 8h of reaction (**Entry 2**, **Table 2.22**). However, by adding $Pd(PPh_3)_4$ (5 mol%) the reaction rate increased dramatically (**Entry 3**, **Table 2.22**). Consequently, the 3*H*-naphtho[2,1-*b*]pyran **2.330** fully ring-contracted to the naphthofuran **2.331** after only 12h of

reaction (**Figure 2.92**). This result was a strong indication that the ring-contraction of the 3*H*-naphtho[2,1-*b*]pyran **2.330** was a palladium-driven reaction.

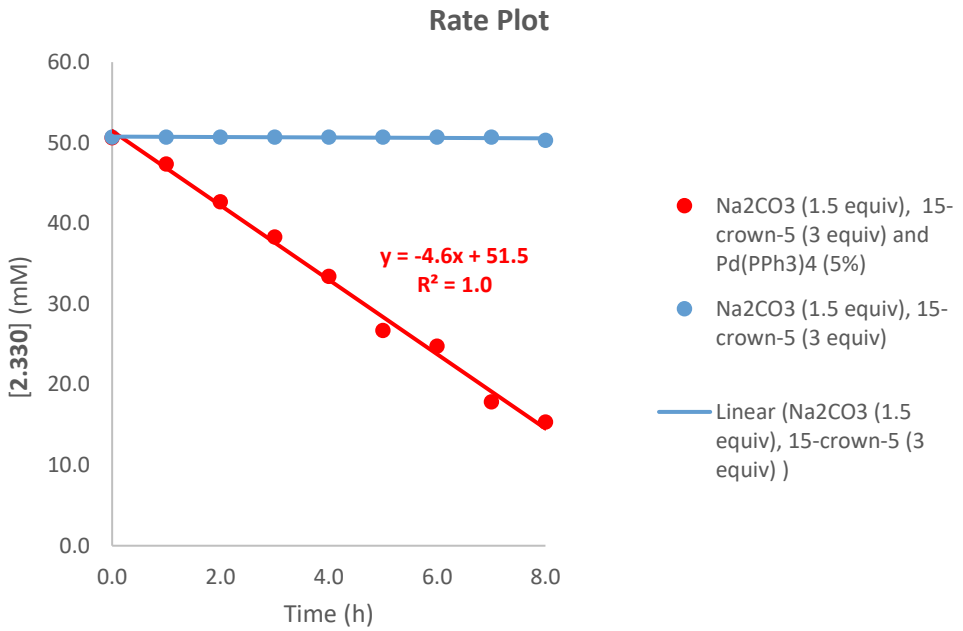

Figure 2.92 Rate plot of the ring-contraction of the 3*H*-naphtho[2,1-*b*]pyran **2.330** by using Na_2CO_3 (1.5 equiv) and 15-crown-5 (3 equiv) in PhMe at reflux, in the presence and in the absence of $Pd(PPh_3)_4$ (5 mol%).

In order to gather further insight on the involvement of the base in the ring-contraction process, a reaction was performed in which 10 mol% of K_2CO_3 [containing 24 ppm of amorphous Pd (per 0.50 g of sample)] and 18-crown-6 (20 mol%) were employed in toluene at reflux (**Entry 4**, **Table 2.22**). Consequently, the ring-contraction of the 3*H*-naphtho[2,1-*b*]pyran **2.330** occurred (**Figure 2.93**), yet at a slower rate when compared to using K_2CO_3 (1.5 equiv) and 18-crown-6 (3 equiv) (**Entry 1**, **Table 2.22**). This result showed that the K_2CO_3 base was not being consumed in the reaction and was instead being regenerated in a catalytic fashion.

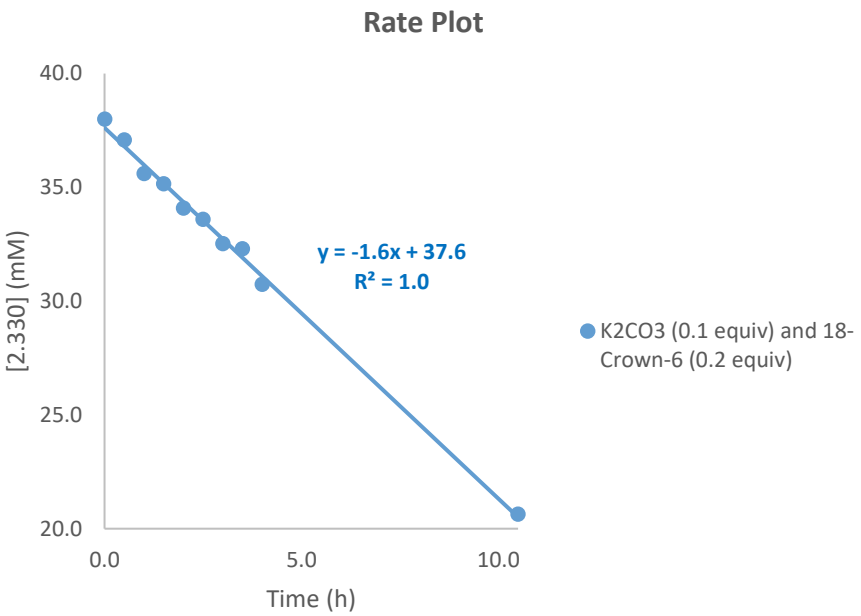

Figure 2.93 Rate plot for the ring-contraction of the 3*H*-naphtho[2,1-*b*]pyran **2.330** by using K_2CO_3 (0.1 equiv) and 18-crown-6 (0.2 equiv).

Table 2.22 Experimental conditions and rate constant of the ring-contraction of the 3*H*-naphtho[2,1-*b*]pyran **2.330** using different crown ethers.

Entry	$[2.330]_0$ /mM	Palladium Source	Crown Ether	Base	Solvent	Temp.	k/ $M.h^{-1}$
1	**51**	-	18-crown-6 (3 equiv)	K_2CO_3* (1.5 equiv)	PhMe	reflux	5.4
2	**51**	-	15-crown-5 (3 equiv)	Na_2CO_3† (1.5 equiv)	PhMe	reflux	0
3	**51**	$Pd(OAc)_2$ (5 mol%)	15-crown-5 (3 equiv)	Na_2CO_3† (1.5 equiv)	PhMe	reflux	4.6
4	**38**	-	18-crown-6 (0.2 equiv)	K_2CO_3* (0.1 equiv)	PhMe	reflux	1.6

*24 ppm of palladium (per 0.50 g of sample); †2.20 ppb of amorphous palladium (per 0.50 g of sample).

Based on the data collected, a mechanism for the ring-contraction of the 3*H*-naphtho[2,1-*b*]pyran **2.330** was proposed: first the thermal 6π-electrocyclic ring-opening of the pyran unit of the 3*H*-naphtho[2,1-*b*]pyran **2.330** led to the formation of the dienone **2.332** – reaction mixture acquired an orange colour once heated (**Scheme 2.160**). Oxidative insertion of amorphous Pd^0 in between C-1 and oxygen led to the formation of the 5-membered ring palladate **2.334**. Hence, the

reductive elimination promoted by the base afforded the allene **2.335** and regenerated the amorphous Pd^0. In a final step, the 5-*exo-dig* cyclization of the allene **2.335** led to the formation of the naphthofuran **2.331** and regeneration of the base.

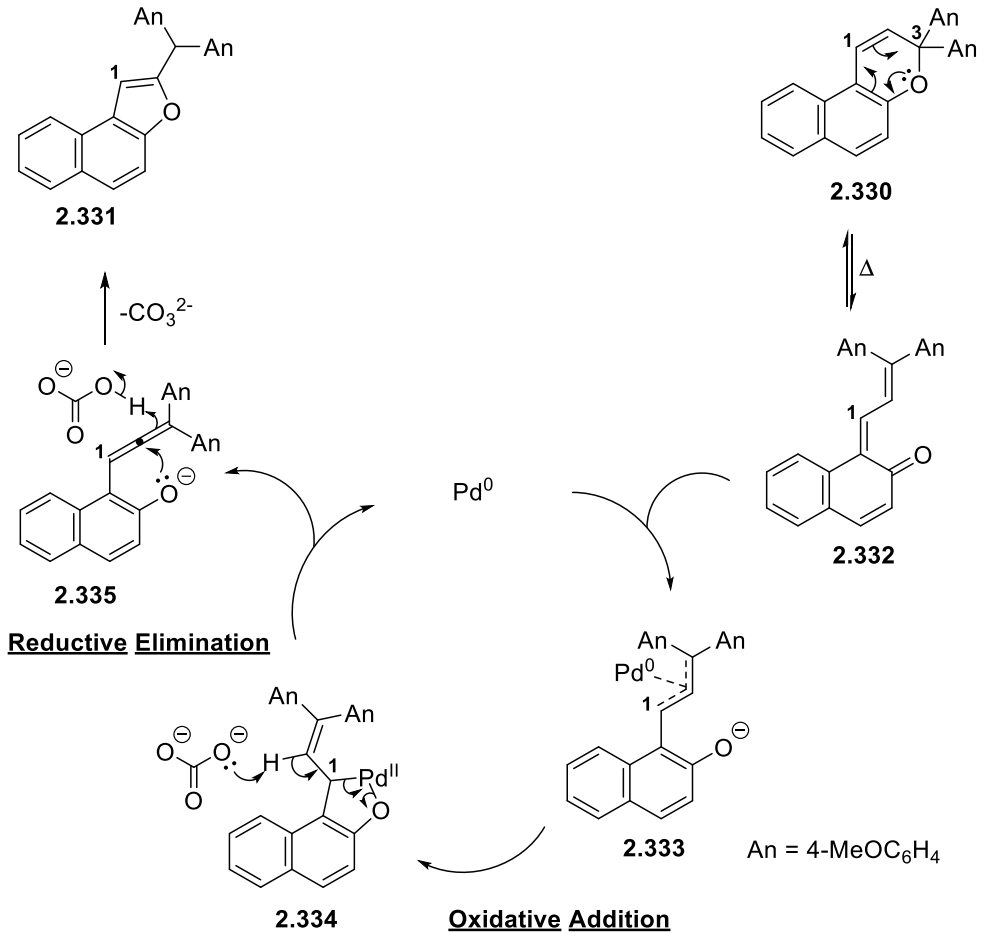

Scheme 2.160 Proposed mechanism for the ring-contraction of the 3*H*-naphtho[2,1-*b*]pyran **2.330**.

In order to extend the scope of the ring-contraction, a variety of pyran containing substrates that were to hand were subjected to the optimized ring-contraction conditions. Thus, by refluxing multiple naphthopyrans and benzoquinolines in toluene in the presence of 1.5 equiv of K_2CO_3 [containing 24 ppm of amorphous Pd (per 0.50 g of sample)] and 18-crown-6 (3 equiv), a series of naphthofurans, naphthodifurans and benzo-fused indoles were prepared in generally good yields, with short reaction times and easy purification procedures (**Table 2.23**). It is noteworthy that, although palladium was not added to the reaction mixture, it was present as a contaminant of the base. Even though the ring-contraction requires ultralow palladium concentrations, for a good reproducibility, the addition of a catalytic amount of palladium would be recommended.

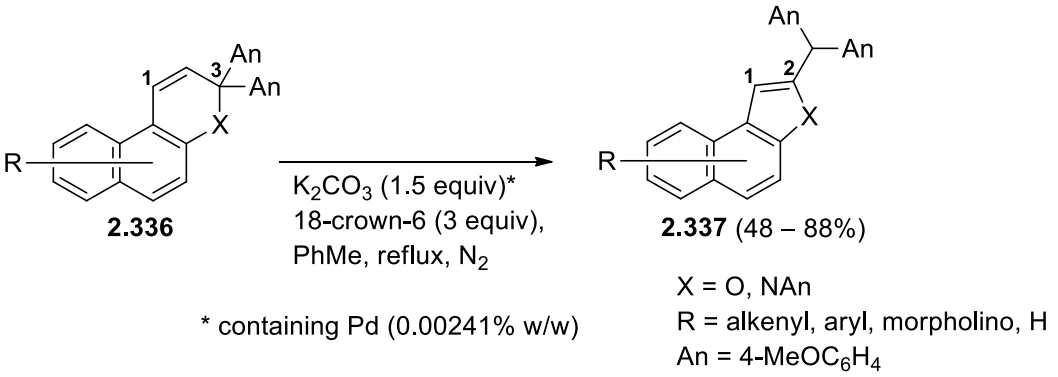

Scheme 2.161 Synthesis of naphthofurans, naphthodifurans and benzo-fused indoles.

Table 2.23 Synthesis of naphthofurans, naphthodifurans and benzo-fused indoles.

Entry	Starting Material	Product	Key NMR (δ)	Yield (%)
1	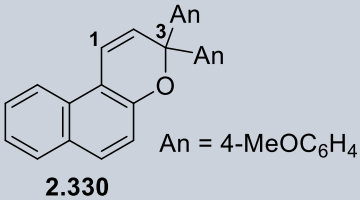	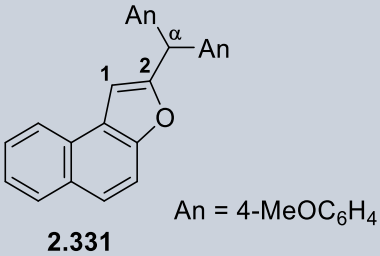	δ_H 5.63 (α-H) δ_C 49.8 (α-H) δ_H 6.76 (1-H)	80
2	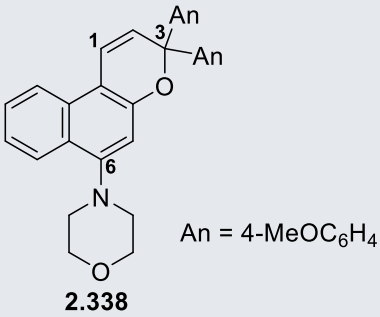	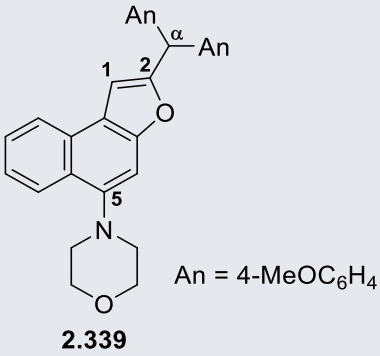	δ_H 5.58 (α-H) δ_C 49.8 (α-H) δ_H 6.68 (1-H)	76
3	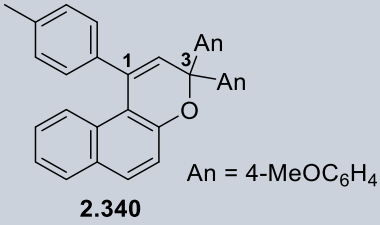	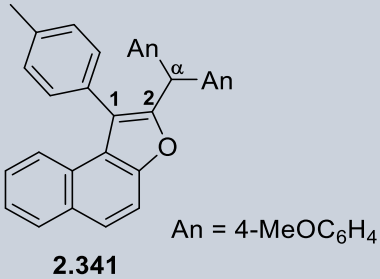	δ_H 5.42 (α-H) δ_C 46.7 (α-H)	49

Table 2.23 Synthesis of naphthofurans, naphthodifurans and benzo-fused indoles (continuation).

Entry	Starting Material	Product	Key NMR (δ)	Yield (%)
4	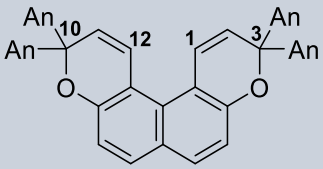 **2.342** An = 4-MeOC$_6$H$_4$	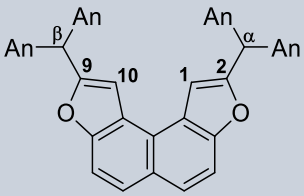 **2.343** An = 4-MeOC$_6$H$_4$	δ_H 5.61 (α, β-H) δ_C 49.8 (α, β-H) δ_H 6.81 (1, 10-H)	88
5	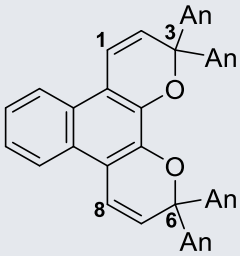 **2.344** An = 4-MeOC$_6$H$_4$	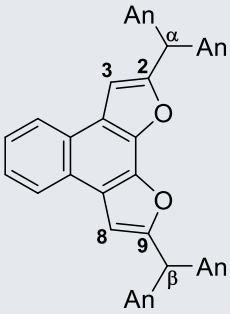 **2.345** An = 4-MeOC$_6$H$_4$	δ_H 5.60 (α, β-H) δ_C 49.8 (α, β-H) δ_H 6.75 (3, 8-H)	48
6	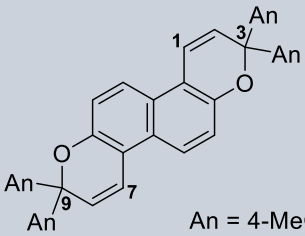 An = 4-MeOC$_6$H$_4$ **2.346**	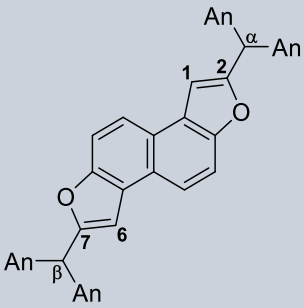 **2.347** An = 4-MeOC$_6$H$_4$	δ_H 5.73 (α, β-H) δ_C 49.2 (α, β-H) δ_H 6.68 (1, 6-H)	74
7	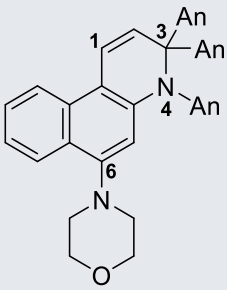 **2.348** An = 4-MeOC$_6$H$_4$	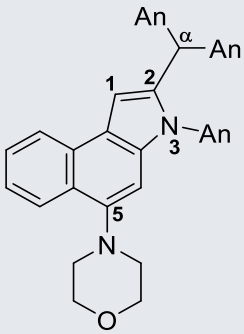 **2.349** An = 4-MeOC$_6$H$_4$	δ_H 5.27 (α-H) δ_C 48.1 (α-H) δ_H 6.56 (1-H)	80

It is noteworthy that the slower rate of reaction (64h) and lower yield (49%) of the ring-contraction of the 3*H*-naphtho[2,1-*b*]pyran **2.340** (**Entry 3**, **Table 2.23**) was possibly due to the increased steric encumberment of the phenyl at C-1.

Furthermore, the developed protocol was successfully applied to both electron-rich naphthopyrans (**Entry 2**, **Table 2.23**) and more electronically neutral naphthopyrans (**Entry 1**, **Table 2.23**).

The developed conditions were also employed in the ring-contraction of the benzo-1,2-dihydroisoquinoline **2.348** which afforded the corresponding benzo-fused indole **2.349** in very good yield (**Entry 7**, **Table 2.23**).

The developed methodology was also applied to the ring-contraction of the 2*H*-naphtho[1,2-*b*]pyrans **2.350** and **2.352**, affording the corresponding naphthofurans in poor yield (19 – 34%) (**Table 2.24**). It is generally established that the 2*H*-naphtho[2,1-*b*]pyrans are more prone to degradation when compared to 3*H*-naphtho[2,1-*b*]pyrans, and this feature might have contributed to the lower yields.[111]

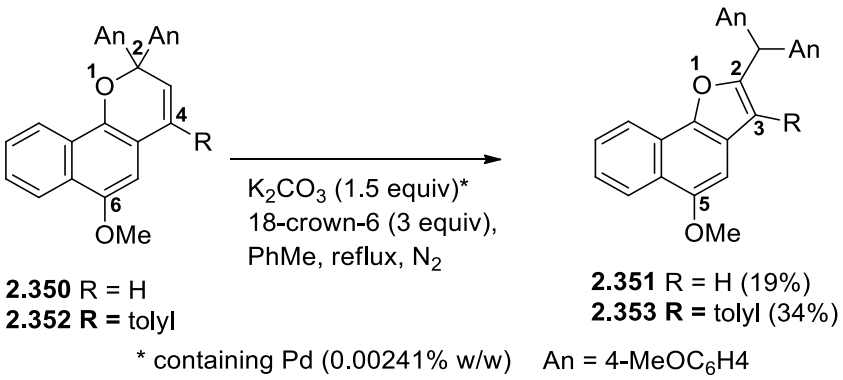

Scheme 2.162 Ring-contraction of the 2*H*-naphtho[1,2-*b*]pyrans **2.350** and **2.352**.

Table 2.24 Ring-contraction of the 2*H*-naphtho[1,2-*b*]pyrans **2.350** and **2.352**.

Entry	Starting Material	Product	Key NMR (δ)	Yield (%)
1	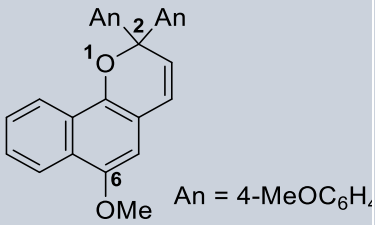 **2.350**	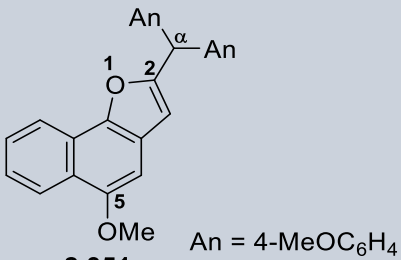 **2.351**	δ_H 5.59 (α-H) δ_C 49.8 (α-H) δ_H 6.31 (3-H)	19
2	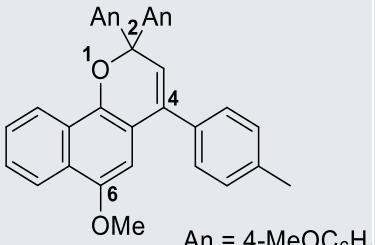 **2.352**	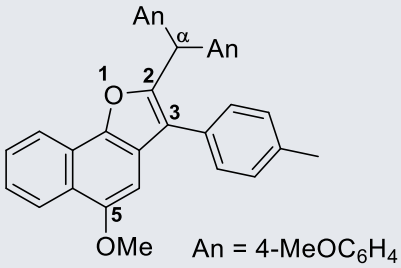 **2.353**	δ_H 5.61 (α-H) δ_C 47.2 (α-H)	34

In summary an efficient methodology has been developed for the transformation of naphthopyrans and dihydroquinolines to naphthofurans and benzo-fused indoles, respectively. The method can be adapted to a tandem process in which heteroarylation can be combined with ring-contraction.

3. EXPERIMENTAL

3.1 Equipment and Reagents

Reagents were purchased from Alfa Aesar, Apollo Chemicals, Fluorochem, Manchester Organics and Sigma Aldrich, and were used as supplied.

Reactions were heated using Heidolph MR3001K and Asynt ADS HP-NT hotplates, with Asynt DrySyn heating blocks.

In all Suzuki-Miyaura coupling reactions solvents were degassed previously under a flow of N_2 for 15–30 min, prior to running the reaction under a N_2 or Ar atmosphere.

Masses were measured on Ohaus Voyager Pro (Max 110 g, d = 0.1 mg) and on an Ohaus Pioneer (Max 2100 g, d = 0.01 g) balances.

TLC was performed on either Merck TLC Aluminium sheets (silica gel 60 Å F254), or on Alugram pre-coated TLC sheets (silica gel 60 Å F254), or on Fluorochem aluminium backed TLC sheets (silica gel 60 Å F254), using a range of eluent systems of differing polarity. Chromatographic separations were performed on either Aldrich silica gel (60 Å, 230-400 mesh, 40-63 μm), or on Aldrich silica gel (60 Å, 70-230 mesh, 63-200 μm), or on Fluorochem silica gel (60 Å, 40-63 μm), or on Merck Silica gel 60 F_{254} plates, or on Acros Organics Al_2O_3 (50-200 μm 60 Å). Al_2O_3 was activated by mixing Al_2O_3 (300 g) with H_2O (9 mL) prior to flash column chromatography separations. For the rhenium(I) complexes, $CDCl_3$ was neutralized by passing it through a plug of basic Al_2O_3.

NMR spectra were recorded on a Bruker Avance 400 instrument (^{1}H 400 MHz, ^{13}C 100 MHz, ^{19}F 376 MHz, ^{31}P 162 MHz). FT-IR spectra were recorded on a Nicolet 380 FT-IR equipped with a diamond probe ATR attachment (neat sample). Accurate mass measurements were obtained from the Innovative Physical Organic Solutions (IPOS) centre at the University of Huddersfield. Melting points were determined in capillary tubes, using a Stuart SMP10 melting point apparatus, and are uncorrected. UV-visible spectra were recorded for PhMe, DCM, PhMe:DCM (1:1) or MeCN solutions of the samples (10 mm path length quartz cuvette, PTFE capped, concentration in the range 10^{-2} – 10^{-6} moldm^{-3}). A bespoke Shimadzu UV-3600 Plus UV-Vis-NIR spectrophotometer was used and equipped with a single cell Peltier temperature controlled (23 °C) stirred fluorescence cell holder attachment. The spectrophotometer sample chamber door was modified to accept activating irradiation delivered from the light source by liquid light guides (Newport 77557, Newport 77569). Irradiation was provided by a xenon ozone free arc lamp (Newport 6255) powered by an Oriel 300-Watt xenon arc lamp source (Newport 66906) (set in Current Mode l_{set} 8.5 A/l_{max} 10.5A, 149–150 W). An in-line destilled water liquid filter (Newport 6177), multiple filter holder (Newport 62020), UG11 filter (Newport FSO-UG11), fibre optic coupler (Newport 77799) completed the irradiation equipment. Spectra (310 – 650 nm) were recorded prior to (ground state)

and immediately after cessation of activating irradiation to a steady state (1 – 10 min irradiation). Activation of the colourless closed forms of the photochromic compounds and rhenium(I) complexes to a photostationary state was achieved by using UV irradiation using different Newport filters (UG11, BG3). Bleaching of the coloured (opened forms) when required was effected by irradiation with visible light using different Newport filters (GG420, GG420, GG455) Concerning the fatigue cycles, activation of the colourless closed forms of the photochromic rhenium(I) complexes to a photostationary state was attained by using UV irradiation (365 nm, 20 s) using a Spectroline UV Lamp ENF-280C/FE (8 watts, 230 volts). Emission spectra were acquired on a Horiba Scientific Fluoromax-4 Spectrophotometer. Emission lifetimes were recorded on an Edinburgh Instruments EPL-405. Photographs were taken using a Sony ILCE-7RM2 A7R ii with a Samyang AF 35mm F1.4 FE lens.

Quantum yields (Φ) were calculated by applying the equation:

$$(\mathbf{1})\quad \Phi = \Phi(\mathrm{R}) \times \frac{\mathbf{Integral}}{\mathbf{Integral\ (R)}} \times \frac{\mathbf{1-10^{-Abs(R)}}}{\mathbf{1-10^{-Abs}}} \times \frac{\boldsymbol{\eta}^{\mathbf{2}}}{\boldsymbol{\eta}^{\mathbf{2}}\mathbf{(R)}}$$

The standard (R) used was $Ru(bpy)_3^{2+}$ (Φ(R) = 1.8% in MeCN under air; excitation window: 380 – 530 nm),[234] η is the refractive index of the solvent.

3.2 Synthesis of Pyridyl Substituted 3*H*-Naphtho[2,1-*b*]pyrans

3.2.1 Strategy A – By a Suzuki cross-coupling reaction after chromenization

3.2.1.1 Preparation of 10-Pyridyl-3*H*-Naphtho[2,1-*b*]pyrans

3.2.1.1.1 Experimental Procedure for the Synthesis of 8-Iodo-2-naphthol (2.29): a stirred mixture of 8-amino-2-naphthol (10.00 g, 62.82 mmol) in water (200 mL) was cooled to 0–5 °C and then a solution of H_2SO_4 (95–98%, 11 mL) in water (20 mL) was added at such a rate that the internal temperature never exceeded 5 ºC. To the resulting mixture was added a solution of $NaNO_2$ (4.34 g, 62.9 mmol) dissolved in water (200 mL) over a period of 30 min at 0–5 °C. The resulting reaction mixture was stirred at 0–5 °C for further 30 min. A solution of KI (10.43 g, 62.83 mmol) dissolved in water (125 mL) was added to the reaction mixture over a period of 30 min at 0–5 °C and stirred for 3 h. After completion, the reaction mixture was allowed to reach room temperature, diluted with water (200 mL) and extracted with EtOAc (3 × 500 mL). The combined organic layers were washed with brine (2 × 500 mL). The organic layer was dried with anhydrous sodium sulfate and evaporated to dryness under reduced pressure, giving the corresponding product that was used without further purification.

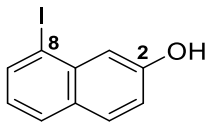

2.29

8-Iodo-2-naphthol (2.29): black powder (12.37 g, 73%); m.p. = 103–106 °C [lit. m.p. = 109 °C[235]]; ν_{max} (neat) 3254 (br), 1621, 1590, 1504, 1440, 1371, 1335, 1222, 1168, 1122, 970, 898, 819, 648 cm^{-1}; ^1H NMR (400 MHz, $CDCl_3$) δ_H 5.19 (s, 1H, OH), 7.04 (t, 1H, *J* = 7.7 Hz, 6-H), 7.13 (dd, 1H, *J* = 8.8, 2.3 Hz, 3-H), 7.44 (d, 1H, *J* = 2.3 Hz, 1-H), 7.70 (d, 1H, *J* = 8.8 Hz, 4-H), 7.76 (d, 1H, *J* = 7.7 Hz, 5-H), 8.03 (d, 1H, *J* = 7.7 Hz, 7-H) ppm; ^{13}C NMR (100 MHz, $CDCl_3$) δ_C 97.3, 114.2, 118.5, 124.7, 128.8, 129.4, 130.9, 135.8, 138.0, 155.1 ppm; HRMS (ESI) found $[M+H]^+$ = 270.9616 $C_{10}H_7IO$ requires $[M+H]^+$ = 270.9614.

3.2.1.1.2 Experimental Procedure for the Synthesis of 10-Iodo-3,3-bis(4-methoxyphenyl)-3*H*-naphtho[2,1-*b*]pyran (2.34): 1,1-bis(4-methoxyphenyl)prop-2-yn-1-ol (1.04 g, 3.88 mmol) and 8-iodo-2-naphthol (1.00 g, 3.70 mmol) in the presence of PPTS (0.05 g, 0.2 mmol) and trimethyl orthoformate (0.80 mL, 7.3 mmol) in 1,2-DCE (21.0 mL) were refluxed for 5 h under N_2. Solvent was removed under reduced pressure, the residue dissolved in EtOAc (100 mL), washed with water (3 × 100 mL), dried with anhydrous sodium sulfate and evaporated to dryness. Flash column chromatography [Aldrich silica gel (60 Å, 40-63 μm), eluent: EtOAc (20%) in hexanes, fraction 2] led to the corresponding product – approximately 83% pure by ^1H NMR analysis – and it was used in the next step without further purification.

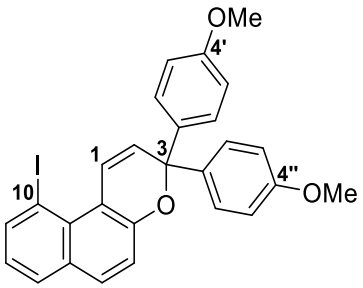

2.34

10-Iodo-3,3-bis(4-methoxyphenyl)-3*H*-naphtho[2,1-*b*]pyran (2.34): brown powder (0.90 g, 39%); m.p. = 50–53 °C; ν_{max} (neat) 2922, 2852, 1606, 1506, 1460, 1246, 1171, 1031, 995, 821, 708 cm^{-1}; ^1H NMR (400 MHz, $CDCl_3$) δ_H 3.76 (6H, s, OMe), 5.97 (1H, d, *J* = 9.7 Hz, 2-H), 6.82–6.85 (4H, m, 3′, 3″, 5′, 5″-H), 6.92 (1H, t, *J* = 7.7 Hz, 8-H), 7.21 (1H, d, *J* = 8.8 Hz, 5-H), 7.42–7.45 (4H, m, 2′, 2″, 6′, 6″-H), 7.55 (1H, d, *J* = 8.8 Hz, 6-H), 7.65–7.67 (1H, m, 7-H), 8.08–8.13 (2H, m, 1, 9-H) ppm; ^{13}C NMR (100 MHz, $CDCl_3$) δ_C 55.2, 81.6, 89.7, 113.3, 116.9, 119.2, 122.6, 124.4, 124.6,

128.6, 129.5, 130.9, 131.0, 131.8, 136.5, 141.5, 152.7, 158.9 ppm; HRMS (ESI) found $[M+H]^+$ = 521.0610 $C_{27}H_{21}IO_3$ requires $[M+H]^+$ = 521.0608.

3.2.1.1.3 Experimental Procedure for the Synthesis of 3,3-Bis(4-methoxyphenyl)-10-(4-pyridyl)-3*H*-naphtho[2,1-*b*]pyran (2.36): a mixture of 10-iodo-3,3-bis(4-methoxyphenyl)-3*H*-naphtho[2,1-*b*]pyran (83%) (200.3 mg, 0.3195 mmol), 4-pyridineboronic acid pinacol ester (98.3 mg, 0.479 mmol), KF (27.8 mg, 0.478 mmol) and $Pd(PPh_3)_4$ (18.6 mg, 0.0161 mmol) in PhMe (5.0 mL) and EtOH (5.0 mL) was heated at reflux under N_2 for 5 days. After this time, the mixture was evaporated to dryness. Afterwards, the residue was dissolved in DCM (50 mL), washed with water (3 × 50 mL), the organic layer dried with anhydrous sodium sulfate and the solvent removed under reduced pressure. Flash column chromatography [Aldrich silica gel (60 Å, 40-63 μm), eluent: EtOAc (50%) in hexanes, fraction 4] led to the corresponding product as a light-yellow powder.

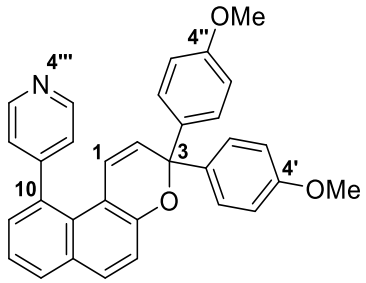

2.36

3,3-Bis(4-methoxyphenyl)-10-(4-pyridyl)-3*H*-naphtho[2,1-*b*]pyran (2.36): light-yellow powder (99.8 mg, 66%); m.p. = 59–63 °C; ν_{max} (neat) 1607, 1593, 1507, 1452, 1245, 1172, 1032, 998, 819, 732 cm^{-1}; Photomerocyanine λ_{max} = 458 nm (PhMe); ^1H NMR (400 MHz, $CDCl_3$) δ_H 3.77 (6H, s, OMe), 5.64 (1H, d, *J* = 9.7 Hz, 2-H), 6.01 (1H, d, *J* = 9.7 Hz, 1-H), 6.84 (4H, app. d, *J* = 8.8 Hz, 3′, 5′, 3″, 5″-H), 7.17 (2H, app. d, *J* = 5.8 Hz, 2‴, 6‴-H), 7.25–7.37 (7H, m, Ar-H), 7.73–7.76 (2H, m, Ar-H), 8.67 (2H, app. d, *J* = 5.8 Hz, 3‴, 5‴-H) ppm; ^{13}C NMR (100 MHz, $CDCl_3$) δ_C 55.3, 81.6, 113.2, 115.3, 119.0, 123.2, 123.9, 124.4, 125.0, 128.4, 129.5, 130.0, 130.5, 130.9, 135.3, 136.7, 149.6, 151.7, 152.9, 159.0 ppm; HRMS (ESI) found $[M+H]^+$ = 472.1906 $C_{32}H_{25}NO_3$ requires $[M+H]^+$ = 472.1907.

3.2.1.2 Preparation of 9-Pyridyl-3*H*-Naphtho[2,1-*b*]pyrans

3.2.1.2.1 Experimental Procedure for the Synthesis of 7-Bromo-2-naphthol (2.38):

Method A – Bromine (1.0 mL, 20 mmol) was added dropwise to a cold (0 ºC) to a suspension of triphenylphosphine (5.00 g, 19.1 mmol) in MeCN (14.0 mL). The reaction mixture was allowed to reach room temperature and 2,7-dihydroxynaphthalene (2.55 g, 15.9 mmol) was added in one portion. The mixture was heated to 70 ºC for 30 min, after which the solvent was removed under reduced pressure. The flask was equipped with a gas trap and the black residue was heated to 250 ºC for 45 min. After cooling to room temperature, the mixture was dissolved in DCM (32 mL) and filtered through a plug of silica. The crude was purified by flash column chromatography [Aldrich silica gel (60 Å, 40-63 μm), eluent: DCM/hexane (1:1)]. Fractions 5 and 6, obtained from the first purification, were purified by flash column chromatography: fraction 5 [Aldrich silica gel (60 Å, 40-63 μm), eluent: EtOAc/hexane (1:4)] and fraction 6 [Aldrich silica gel (60 Å, 40-63 μm), eluent: DCM]. Subsequent recrystallizations from EtOAc/hexane led to the corresponding products.

Method B – Bromine (3.4 mL, 66 mmol) was added slowly over 30 min to a cold (0 ºC) vigorously stirred suspension of triphenylphosphine (17.01 g, 64.85 mmol) in MeCN (3.0 mL). The mixture was warmed to room temperature and 2,7-dihydroxynaphthalene (10.39 g, 64.87 mmol) was added in one portion. Afterwards, the reaction was heated to 85 ºC for 2 h. The resulting brown tar was heated, slowly, to 250 ºC for 6 h. Upon cooling, the mixture was purified by flash column chromatography [Aldrich silica gel (60 Å, 40-63 μm), eluent: EtOAc/hexane (3:7)], with subsequent recrystallization from EtOAc/hexane, affording the corresponding product.

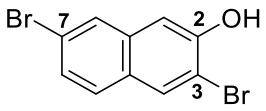

2.44

3,7-Dibromo-2-naphthol (2.44): from method A (fraction 3 from the purification of the crude) provided the title compound as a brown powder (0.63 g, 18%); m.p. = 187–188 °C [lit. m.p. = 185–186 °C[236]]; ν_{max} (neat) 3419, 1615, 1506, 1412, 1355, 1213, 1169, 1061, 923, 878, 796, 550 cm^{-1}; ^{1}H NMR (400 MHz, $CDCl_3$) δ_H 5.74 (s, 1H, OH), 7.29 (s, 1H, 1-H), 7.42 (dd, 1H, *J* = 8.8 Hz, 1.6 Hz 6-H), 7.56 (d, 1H, *J* = 8.8 Hz, 5-H), 7.86 (d, 1H, *J* = 1.6 Hz, 8-H), 8.00 (s, 1H, 4-H) ppm; ^{13}C NMR (100 MHz, $CDCl_3$) δ_C = 109.9, 113.0, 121.2, 127.8, 128.0, 128.4, 128.6, 131.3, 135.1, 150.3 ppm; HRMS (APCI) found $[M-H]^-$ = 298.8697 $C_{10}H_6{}^{79}Br_2O$ requires $[M-H]^-$ = 298.8713.

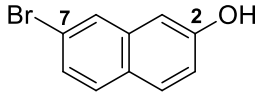

2.38

7-Bromo-2-naphthol (2.38): from method A (fraction 1 from the purification of fraction 5) provided the title compound as a brown powder (0.0180 g, 0.4%); From method B (fraction 2) provided the title compound as a brown powder (7.01 g, 48%); m.p. = 129–131 °C [lit. m.p. = 132–133 °C[237]]; ν_{max} (neat) 3626, 3046 (br), 1649, 1573, 1500, 1435, 1351, 1206, 1062, 919, 855, 827, 736, 596 cm^{-1}; ^{1}H NMR (400 MHz, $CDCl_3$) δ_H 5.35 (s, 1H, OH), 7.06 (app. s, 1H, 1-H), 7.11 (dd, 1H, *J* = 8.8, 2.1 Hz, 3-H), 7.39 (d, 1H, *J* = 8.7 Hz, 6-H), 7.63 (d, 1H, *J* = 8.7 Hz, 5-H), 7.71 (d, 1H, *J* = 8.8 Hz, 4-H), 7.84 (s, 1H, 8-H) ppm; ^{13}C NMR (100 MHz, $CDCl_3$) δ_C 108.7, 118.2, 120.8, 127.0, 127.3, 128.3, 129.4, 129.9, 135.8, 154.1 ppm; HRMS (APCI) found [M-H]$^-$ = 220.9604 $C_{10}H_7{}^{79}BrO$ requires [M-H]$^-$ = 220.9608.

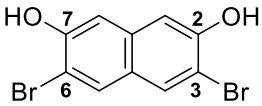

2.45

3,6-Dibromo-2,7-dihydroxynaphthalene (2.45): from method A (fraction 2 from the purification of fraction 6) provided the title compound as a brown powder (0.04 g, 0.6%); m.p. = 154–157 °C [lit. m.p. = 155–159 °C[238], 186–190 °C[239], 188–190 °C[240]]; ν_{max} (neat) 3447, 3161 (br), 1620, 1586, 1514, 1422, 1348, 1166, 1012, 887, 860, 734, 553 cm^{-1}; ^{1}H NMR (400 MHz, $CDCl_3$) δ_H 5.67 (s, 2H, OH), 7.23 (s, 2H, 1, 8-H), 7.86 (s, 2H, 4, 5-H) ppm; ^{13}C NMR (100 MHz, $CDCl_3$) δ_C 109.4, 110.9, 125.6, 130.1, 134.9, 150.4 ppm; HRMS (APCI) found [M-H]$^-$ = 314.8657 $C_{10}H_6{}^{79}Br_2O_2$ requires [M-H]$^-$ = 314.8662.

3.2.1.2.2 Experimental Procedure for the Synthesis of 9-Bromo-3,3-bis(4-methoxyphenyl)-3*H*-naphtho[2,1-*b*]pyran (2.39): 1,1-bis(4-methoxyphenyl)prop-2-yn-1-ol (5.69 g, 21.2 mmol) and 7-bromo-2-naphthol (4.50 g, 20.2 mmol) in the presence of PPTS (0.25 g, 1.0 mmol) and trimethyl orthoformate (4.5 mL, 41 mmol) in 1,2-DCE (41 mL) was refluxed for 3 h under N_2 atmosphere. Solvent was removed under reduced pressure and the residue taken in DCM (150 mL), washed with water (3 × 300 mL) and the organic layer dried with anhydrous sodium sulfate. The residue was crystallized from DCM/hexane giving the title compound as a brick red crystalline solid.

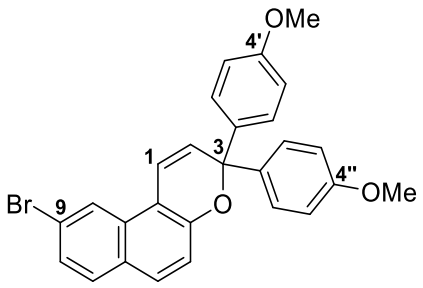

2.39

9-Bromo-3,3-bis(4-methoxyphenyl)-3*H*-naphtho[2,1-*b*]pyran (2.39): brick red crystalline solid (8.24 g, 86%); m.p. = 124–127 °C; ν_{max} (neat) 1606, 1581, 1505, 1441, 1301, 1249, 1172, 1031, 1017, 822, 721, 589 cm^{-1}; Photomerocyanine λ_{max} = 456 nm (PhMe); ^{1}H NMR (400 MHz, $CDCl_3$) δ_H 3.77 (s, 6H, OMe), 6.21 (d, 1H, *J* = 9.9 Hz, 2-H), 6.84 (app. d, 4H, *J* = 8.8 Hz, 3′, 5′, 3″, 5″-H), 7.15–7.20 (m, 2H, 1, 5-H), 7.35–7.38 (m, 5H, 8, 2′, 6′, 2″, 6″-H), 7.56 (d, 1H, *J* = 8.7 Hz, 7-H), 7.60 (d, 1H, *J* = 8.8 Hz, 6-H), 8.09 (s, 1H, 10-H) ppm; ^{13}C NMR (100 MHz, $CDCl_3$) δ_C 55.3, 82.4, 113.3, 113.4, 118.75, 118.84, 121.1, 123.9, 126.8, 127.7, 128.4, 128.6, 129.6, 130.1, 131.0, 136.9, 151.3, 159.0 ppm; HRMS (ESI) found $[M+H]^+$ = 473.0746 $C_{27}H_{21}{}^{79}BrO_3$ requires $[M+H]^+$ = 473.0747.

3.2.1.2.3 Experimental Procedure for the Synthesis of 9-Hydroxy-3,3-bis(4-methoxyphenyl)-3*H*-naphtho[2,1-*b*]pyran (2.42): 1,1-bis(4-methoxyphenyl)prop-2-yn-1-ol (5.04 g, 18.8 mmol) and 2,7-dihydroxynaphthalene (3.01 g, 18.8 mmol) in the presence of PPTS (0.24 g, 0.96 mmol) and trimethyl orthoformate (4.2 mL, 38 mmol) in 1,2-DCE (38.0 mL) was refluxed for 3 h under N_2 atmosphere. Solvent was removed under reduced pressure and the residue purified by flash column chromatography [Aldrich silica gel (60 Å, 40-63 μm), eluent: DCM], to give two pure fractions.

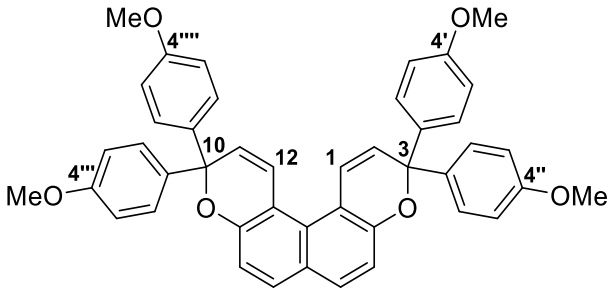

2.52

Fraction 1 – 3,3,10,10-Tetrakis(4-methoxyphenyl)-3,10*H*-naphtho[2,1-*b*]pyran (2.52): off-white powder (2.11 g, 17%); m.p. = 220–223 °C; ν_{max} (neat) 1608, 1509, 1298, 1251, 1172, 1034, 985, 954, 836, 729, 580 cm^{-1}; Photomerocyanine λ_{max} = 448 nm (PhMe); ^{1}H NMR (400 MHz, $CDCl_3$) δ_H 3.77 (s, 12H, OMe), 6.00 (d, 2H, *J* = 9.6 Hz, 2, 11-H), 6.83 (app. d, 8H, *J* = 8.9 Hz, 3′,

5′, 3″, 5″, 3‴, 5‴, 3⁗, 5⁗-H), 7.00 (d, 2H, *J* = 8.7 Hz, 5, 8-H), 7.11 (d, 2H, *J* = 9.6 Hz, 1, 12-H), 7.40 (app. d, 8H, *J* = 8.8 Hz, 2′, 6′, 2″, 6″, 2‴, 6‴, 2⁗, 6⁗-H), 7.49 (d, 2H, *J* = 8.7 Hz, 6, 7-H) ppm; ^{13}C NMR (100 MHz, $CDCl_3$) δ_C 55.2, 81.8, 113.3, 114.7, 115.8, 124.4, 124.7, 125.6, 128.5, 128.5, 130.9, 137.0, 152.8, 158.9 ppm; HRMS (ESI) found $[M+H]^+$ = 661.2585 $C_{44}H_{36}O_6$ requires $[M+H]^+$ = 661.2585.

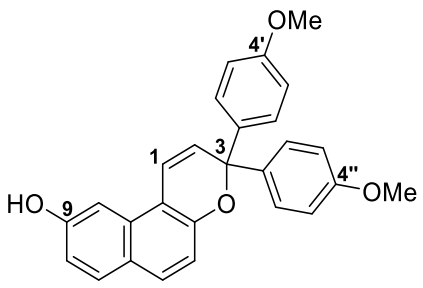

2.42

Fraction 2 – 9-Hydroxy-3,3-bis(4-methoxyphenyl)-3*H*-naphtho[2,1-*b*]pyran (2.42): brown powder (2.16 g, 28%); m.p. = 154–156 °C; ν_{max} (neat) 3390, 1622, 1505, 1452, 1243, 1172, 1082, 1008, 830, 723, 566 cm^{-1}; Photomerocyanine λ_{max} = 444 nm (PhMe); ^{1}H NMR (400 MHz, $CDCl_3$) δ_H 3.77 (s, 6H, OMe), 4.88 (s, 1H, OH), 6.17 (d, 1H, *J* = 9.9 Hz, 2-H), 6.83 (app. d, 4H, *J* = 8.8 Hz, 3′, 5, 3″, 5″-H), 6.90 (dd, 1H, *J* = 8.8, 2.4 Hz, 8-H), 7.01 (d, 1H, *J* = 8.8 Hz, 5-H), 7.14 (d, 1H, *J* = 9.9 Hz, 1-H), 7.24–7.26 (m, 1H, 10-H), 7.37 (app. d, 4H, *J* = 8.8 Hz, 2′, 6′, 2″, 6″-H), 7.56 (d, 1H, *J* = 8.8 Hz, 6-H), 7.61 (d, 1H, *J* = 8.8 Hz, 7-H) ppm; ^{13}C NMR (100 MHz, $CDCl_3$) δ_C 55.3, 82.2, 104.0, 112.8, 113.4, 115.0, 116.0, 119.2, 124.8, 127.6, 128.3, 129.7, 130.5, 131.3, 137.3, 151.3, 154.3, 158.9 ppm; HRMS (ESI) found $[M+H]^+$ = 411.1591 $C_{27}H_{22}O_4$ requires $[M+H]^+$ = 411.1591.

3.2.1.2.4 Experimental Procedure for the Synthesis of 3,3-Bis(4-methoxyphenyl)-9-triflyloxy-3*H*-naphtho[2,1-*b*]pyran (2.43): triflic anhydride (0.64 mL, 3.9 mmol) was added dropwise to a solution of 9-hydroxy-3,3-bis(4-methoxyphenyl)-3*H*-naphtho[2,1-*b*]pyran (1.56 g, 3.80 mmol) and Et_3N (1.2 mL) in DCM (11.5 mL) at 0º C. After 1 h the resulting solution was washed with HCl (1 M) (50 mL), a saturated $NaHCO_3$ solution (50 mL), dried with anhydrous sodium sulfate and evaporated to dryness. Flash column chromatography [Aldrich silica gel (60 Å, 40-63 μm), eluent: EtOAc/hexane (3:7), fraction 1] led to the title compound.

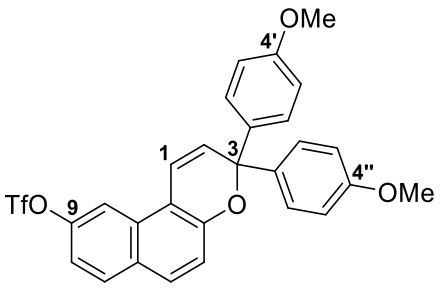

2.43

3,3-Bis(4-methoxyphenyl)-9-triflyloxy-3*H*-naphtho[2,1-*b*]pyran (2.43): canary yellow powder (1.80 g, 87%); m.p. = 90–93 °C; ν_{max} (neat) 1609, 1509, 1401, 1215, 1173, 1122, 1033, 866, 831, 640, 584 cm^{-1}; ^{1}H NMR (400 MHz, $CDCl_3$) δ_H 3.78 (s, 6H, OMe), 6.25 (d, 1H, *J* = 10.0 Hz, 2-H), 6.85 (app. d, 4H, *J* = 8.8 Hz, 3′, 5′, 3″, 5″-H), 7.15 (d, 1H, *J* = 10.0 Hz, 1-H), 7.19 (dd, 1H, *J* = 8.9, 2.4 Hz, 8-H), 7.23 (d, 1H, *J* = 8.9 Hz, 5-H), 7.36 (app. d, 4H, *J* = 8.8 Hz, 2′, 6′, 2″, 6″-H), 7.67 (d, 1H, *J* = 8.9 Hz, 6-H), 7.77–7.80 (m, 2H, 7, 10-H) ppm; ^{13}C NMR (100 MHz, $CDCl_3$) δ_C 55.3, 82.7, 113.3, 113.5, 114.2, 116.9, 117.2, 119.1 (1C, q, *J* = 318.8 Hz, CF_3) 119.8, 128.2, 128.3, 128.9, 129.6, 130.3, 131.1, 136.8, 148.1, 151.9, 159.1 ppm; ^{19}F NMR (376 MHz, $CDCl_3$) δ_F -72.8 ppm; HRMS (ESI) found $[M+H]^+$ = 543.1072 $C_{28}H_{21}F_3O_6S$ requires $[M+H]^+$ = 543.1084.

3.2.1.2.5 Experimental Procedure for the Synthesis of 3,3-Bis(4-methoxyphenyl)-9-pyridyl-3*H*-naphtho[2,1-*b*]pyran:

Method A – A mixture of 9-bromo-3,3-bis(4-methoxyphenyl)-3*H*-naphtho[2,1-*b*]pyran (3.17 mmol), the appropriate pyridineboronic acid pinacol ester (4.8 mmol), K_2CO_3 (4.8 mmol) and $Pd(PPh_3)_4$ (0.16 mmol) in PhMe (37 mL) and EtOH (37 mL) was heated at reflux under N_2 for 16–19 h. After this time, the mixture was cooled and water added (150 mL). Afterwards, the residue was extracted with DCM (3 × 200 mL), washed with water (3 × 200 mL), the organic layer dried with anhydrous sodium sulfate and the solvent removed under reduced pressure to afford the target compounds after purification.

Method B – A mixture of 3,3-bis(4-methoxyphenyl)-9-triflyloxy-3*H*-naphtho[2,1-*b*]pyran (0.3692 mmol), the appropriate pyridineboronic acid pinacol ester (0.5520 mmol), K_2CO_3 (0.559 mmol) and $Pd(PPh_3)_4$ (0.0189 mmol) in PhMe (5 mL) and EtOH (5 mL) was heated at reflux under N_2 for 16 h. After this time, the mixture was cooled and added water (50 mL). The residue was extracted with DCM (3 × 50 mL), washed with water (3 × 50 mL), the organic layer dried with anhydrous sodium sulfate and the solvent removed under reduced pressure to afford the target compounds after purification.

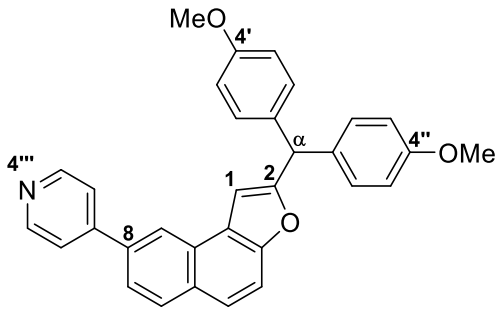

2.49

Fraction 1 – 2-(Bis(4-methoxyphenyl)methyl)-8-(4-pyridyl)naphtho[2,1-*b*]furan (2.49): from 9-bromo-3,3-bis(4-methoxyphenyl)-3*H*-naphtho[2,1-*b*]pyran (Method A: 1.50 g) and 4-pyridineboronic acid pinacol ester after 16 h of reaction; Flash column chromatography [Aldrich silica gel (60 Å, 40-63 μm), eluent: Et_2O/DCM (9:1)] provided the title compound as a brown powder (0.15 g, 10%). From 3,3-bis(4-methoxyphenyl)-9-triflyloxy-3*H*-naphtho[2,1-*b*]pyran (Method B: 200.3 mg) and 4-pyridineboronic acid pinacol ester; Flash column chromatography [Aldrich silica gel (60 Å, 40-63 μm), eluent: Et_2O /DCM (9:1)] provided the title compound as a brown powder (54.8 mg, 31%). m.p. = 156–160 °C; ν_{max} (neat) 1607, 1508, 1462, 1301, 1244, 1173, 1030, 992, 816, 550 cm^{-1}; ^1H NMR (400 MHz, $CDCl_3$) δ_H 3.82 (s, 6H, OMe), 5.62 (s, 1H, α-H), 6.77 (s, 1H, 1-H), 6.90 (app. d, 4H, *J* = 8.7 Hz, 3′, 5′, 3″, 5″-H), 7.18 (app. d, 4H, *J* = 8.7 Hz, 2′, 6′, 2″, 6″-H), 7.63–7.66 (m, 3H, 4, 2‴, 6‴-H), 7.70–7.74 (m, 2H, 5, 7-H), 8.03 (d, 1H, *J* = 8.5 Hz, 6-H), 8.28 (d, 1H, *J* = 1.7 Hz, 9-H), 8.70 (d, 1H, *J* = 6.1 Hz, 3‴, 5‴-H) ppm; ^{13}C NMR (100 MHz, $CDCl_3$) δ_C 49.9, 55.3, 104.4, 113.4, 114.0, 121.9, 122.1, 123.0, 124.0, 124.2, 127.7, 129.7, 129.8, 130.3, 133.5, 135.6, 148.4, 150.3, 152.9, 158.6, 160.7 ppm; HRMS (ESI) found $[M+H]^+$ = 472.1914 $C_{32}H_{25}NO_3$ requires $[M+H]^+$ = 472.1907.

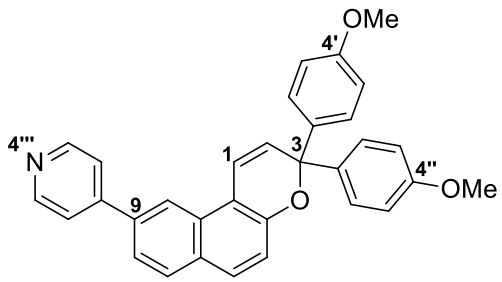

2.48

Fraction 2 – 3,3-Bis(4-methoxyphenyl)-9-(4-pyridyl)-3*H*-naphtho[2,1-*b*]pyran (2.48): from 9-bromo-3,3-bis(4-methoxyphenyl)-3*H*-naphtho[2,1-*b*]pyran (Method A: 1.50 g) and 4-pyridineboronic acid pinacol ester after 16 h of reaction; Flash column chromatography [Aldrich silica gel (60 Å, 40-63 μm), eluent: Et_2O/DCM (9:1)] provided the title compound as a salmon pink

powder (0.85 g, 57%). From 3,3-bis(4-methoxyphenyl)-9-triflyloxy-3*H*-naphtho[2,1-*b*]pyran (Method B: 200.3 mg) and 4-pyridineboronic acid pinacol ester; Flash column chromatography [Aldrich silica gel (60 Å, 40-63 μm), eluent: Et_2O/DCM (9:1)] provided the title compound as a salmon pink powder (36.9 mg, 21%). m.p. = 89–93 °C; ν_{max} (neat) 1597, 1506, 1440, 1302, 1247, 1172, 1088, 1007, 945, 820, 688, 587 cm^{-1}. Photomerocyanine λ_{max} = 472 nm (PhMe); ^{1}H NMR (400 MHz, $CDCl_3$) δ_H 3.77 (s, 6H, OMe), 6.26 (d, 1H, *J* = 10.0 Hz, 2-H), 6.85 (app. d, 4H, *J* = 8.9 Hz, 3′, 5′, 3″, 5″-H), 7.22 (d, 1H, *J* = 8.8 Hz, 5-H), 7.36 (d, 1H, *J* = 10.0 Hz, 1-H), 7.39 (app. d, 4H, *J* = 8.9 Hz, 2′, 6′, 2″, 6″-H), 7.57 (dd, 1H, *J* = 8.4, 1.7 Hz, 8-H), 7.62 (d, 2H, *J* = 6.1 Hz, 2‴, 6‴-H), 7.69 (d, 1H, *J* = 8.8 Hz, 6-H), 7.82 (d, 1H, *J* = 8.4 Hz, 7-H), 8.19 (s, 1H, 10-H), 8.70 (d, 2H, *J* = 6.1 Hz, 3‴, 5‴-H) ppm; ^{13}C NMR (100 MHz, $CDCl_3$) δ_C = 55.3, 82.4, 113.4, 114.5, 118.9, 119.4, 120.1, 122.0, 122.3, 128.4, 128.6, 129.3, 129.50, 129.53, 129.9, 136.2, 137.0, 148.7, 150.3, 151.3, 159.0 ppm; HRMS (ESI) found $[M+H]^+$ = 472.1907 $C_{32}H_{25}NO_3$ requires $[M+H]^+$ = 472.1907.

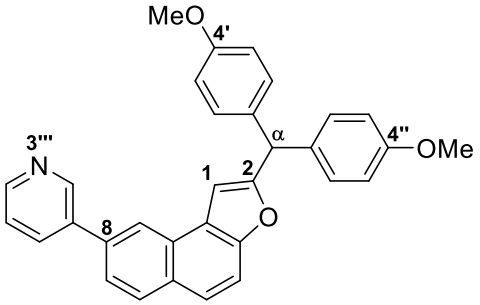

2.51

Fraction 1 – 2-(Bis(4-methoxyphenyl)methyl)-8-(3-pyridyl)naphtho[2,1-*b*]furan (2.51): from 9-bromo-3,3-bis(4-methoxyphenyl)-3*H*-naphtho[2,1-*b*]pyran (Method A: 1.50 g) and 3-pyridineboronic acid pinacol ester after 19 h of reaction; Flash column chromatography [Aldrich silica gel (60 Å, 40-63 μm), eluent: Et_2O/DCM (9:1)] provided the title compound as a brown powder (0.17 g, 11%). From 3,3-bis(4-methoxyphenyl)-9-triflyloxy-3*H*-naphtho[2,1-*b*]pyran (Method B: 204.7 mg) and 3-pyridineboronic acid pinacol ester; Flash column chromatography [Aldrich silica gel (60 Å, 40-63 μm), eluent: Et_2O/DCM (9:1)] provided the title compound as a brown powder (15.7 mg, 9%); m.p. = 126–130 °C; ν_{max} (neat) 1607, 1583, 1507, 1461, 1301, 1244, 1173, 1110, 1030, 994, 804, 710, 554 cm^{-1}; ^{1}H NMR (400 MHz, $CDCl_3$) δ_H 3.81 (s, 6H, OMe), 5.61 (s, 1H, α-H), 6.77 (s, 1H, 1-H), 6.89 (app. d, 4H, *J* = 8.7 Hz, 3′, 5′, 3″, 5″-H), 7.18 (app. d, 4H, *J* = 8.7 Hz, 2′, 6′, 2″, 6″-H), 7.40 (dd, 1H, *J* = 7.8, 4.8 Hz, 5‴-H), 7.62 (d, 1H, *J* = 8.9 Hz, 4-H), 7.67–7.72 (m, 2H, 5, 7-H), 8.00–8.04 (m, 2H, 6, 6‴-H), 8.20 (d, 1H, *J* = 1.6 Hz, 9-H), 8.62 (dd, 1H, *J* = 4.8, 1.6 Hz, 4‴-H), 8.98 (d, 1H, *J* = 1.8 Hz, 2‴-H) ppm; ^{13}C NMR (100 MHz, $CDCl_3$) δ_C 49.9, 55.3, 104.4, 113.0, 114.0, 121.9, 123.5, 123.6, 123.9, 124.2, 127.8, 129.6, 129.7, 129.8, 133.6,

134.7, 135.4, 136.7, 148.5, 148.7, 152.9, 158.6, 160.5 ppm; HRMS (ESI) found $[M+H]^+$ = 472.1909 $C_{32}H_{25}NO_3$ requires $[M+H]^+$ = 472.1907.

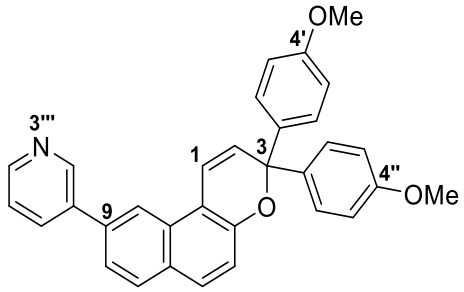

2.50

Fraction 2 – 3,3-Bis(4-methoxyphenyl)-9-(3-pyridyl)-3*H*-naphtho[2,1-*b*]pyran (2.50): from 9-bromo-3,3-bis(4-methoxyphenyl)-3*H*-naphtho[2,1-*b*]pyran (Method A: 1.50 g) and 3-pyridineboronic acid pinacol ester after 19 h of reaction; Flash column chromatography [Aldrich silica gel (60 Å, 40-63 μm), eluent: Et_2O/DCM (9:1)] provided the title compound as a salmon pink powder (1.05 g, 70%). From 3,3-bis(4-methoxyphenyl)-9-triflyloxy-3*H*-naphtho[2,1-*b*]pyran (Method B: 204.7 mg) and 3-pyridineboronic acid pinacol ester; Flash column chromatography [Aldrich silica gel (60 Å, 40-63 μm), eluent: Et_2O/DCM (9:1)] provided the title compound as a salmon pink powder (99.7 mg, 56%); m.p. = 80–83 °C; ν_{max} (neat) 1604, 1505, 1451, 1440, 1378, 1302, 1246, 1172, 1088, 1030, 1003, 945, 824, 711, 588 cm^{-1}; Photomerocyanine λ_{max} = 472 nm (PhMe); ^1H NMR (400 MHz, $CDCl_3$) δ_H 3.77 (s, 6H, OMe), 6.25 (d, 1H, *J* = 10.0 Hz, 2-H), 6.85 (app. d, 4H, *J* = 8.8 Hz, 3′, 5′, 3″, 5″-H), 7.21 (d, 1H, *J* = 8.8 Hz, 5-H), 7.35 (d, 1H, *J* = 10.0 Hz, 1-H), 7.38–7.42 (m, 5H, 2′, 6′, 2″, 6″, 5‴-H), 7.53 (dd, 1H, *J* = 8.4, 1.6 Hz, 8-H), 7.69 (d, 1H, *J* = 8.8 Hz, 6-H), 7.82 (d, 1H, *J* = 8.4 Hz, 7-H), 7.98 (dt, 1H, *J* = 7.9, 2.0 Hz, 6‴-H), 8.12 (s, 1H, 10-H), 8.63 (dd, 1H, *J* = 4.8, 1.8 Hz, 4‴-H), 8.96 (d, 1H, *J* = 2.0 Hz, 2‴-H) ppm; ^{13}C NMR (100 MHz, $CDCl_3$) δ_C 55.3, 82.3, 113.4, 114.3, 118.96, 119.00, 119.9, 122.8, 123.6, 128.4, 128.5, 128.7, 129.5, 129.5, 130.0, 134.7, 135.9, 137.0, 137.1, 148.56, 148.63, 151.2, 158.9 ppm; HRMS (ESI) found $[M+H]^+$ = 472.1906 $C_{32}H_{25}NO_3$ requires $[M+H]^+$ = 472.1907.

3.2.1.3 Preparation of 8-Pyridyl and 8-Aryl Substituted Naphthopyrans

3.2.1.3.1 Experimental Procedure for the Synthesis of 8-Bromo-3,3-bis(4-methoxyphenyl)-3*H*-naphtho[2,1-*b*]pyran (2.56): 1,1-bis(4-methoxyphenyl)prop-2-yn-1-ol (9.47 g, 35.3 mmol) and 6-bromo-2-naphthol (7.50 g, 33.6 mmol) in the presence of PPTS (0.43 g, 1.7 mmol) and triethyl orthoformate (11.2 mL, 67.3 mmol) in 1,2-DCE (67.2 mL) was refluxed for 3 h under N_2 atmosphere. Solvent was removed under reduced pressure, the residue taken in DCM (400 mL),

washed with water (3 × 300 mL) and the organic layer dried with anhydrous sodium sulfate. Subsequently, after solvent evaporation, the residue was recrystallized from DCM/hexane (3:2) giving the corresponding product as a beige crystalline solid in excellent yield.

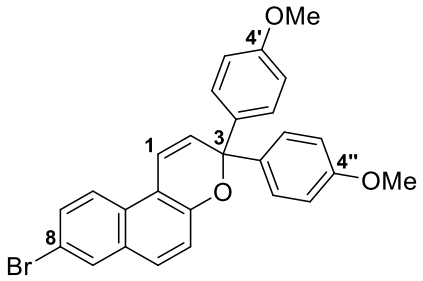

2.56

8-Bromo-3,3-bis(4-methoxyphenyl)-3*H*-naphtho[2,1-*b*]pyran (2.56): beige crystalline solid (15.48 g, 97%); m.p. = 175–177 °C; ν_{max} (neat) 1607, 1578, 1508, 1248, 1175, 1033, 999, 834, 812, 596 cm^{-1}; Photomerocyanine λ_{max} = 474 nm (PhMe); ^{1}H NMR (400 MHz, $CDCl_3$) δ_H 3.77 (s, 6H, OMe), 6.21 (d, 1H, *J* = 10.0 Hz, 2-H), 6.84 (app. d, 4H, *J* = 8.9 Hz, 3′, 5′, 3″, 5″-H), 7.17 (d, 1H, *J* = 8.9 Hz, 5-H), 7.21 (d, 1H, *J* = 10.0 Hz, 1-H), 7.36 (app. d, 4H, *J* = 8.9 Hz, 2′, 6′, 2″, 6″-H), 7.50 (dd, 1H, *J* = 9.0, 2.0 Hz, 9-H), 7.54 (d, 1H, *J* = 8.9 Hz, 6-H), 7.81 (d, 1H, *J* = 9.0 Hz, 10-H), 7.85 (d, 1H, *J* = 2.0 Hz, 7-H); ^{13}C NMR (100 MHz, $CDCl_3$) δ_C 55.3, 82.4, 113.4, 114.1, 117.2, 118.7, 119.5, 123.2, 128.3, 128.6, 128.7, 129.7, 130.37, 130.44, 137.0, 150.8, 159.0 ppm; HRMS (ESI) found $[M+H]^+$ = 473.0745 $C_{27}H_{21}{}^{79}BrO_3$ requires $[M+H]^+$ = 473.0747.

3.2.1.3.2 Experimental Procedure for the Synthesis of 2-(3,3-Bis(4-methoxyphenyl)-3*H*-benzo[*f*]chromen-8-yl)-4,4,5,5-tetramethyl-1,3,2-dioxaborolane (2.62):

a) Method A. Metallation Strategy – *n*-BuLi (6.5 mL, 2.5 M in hexanes) was added dropwise over 10 min to a solution of 8-bromo-3,3-bis(4-methoxyphenyl)-3*H*-naphtho[2,1-*b*]pyran (7.00 g, 14.8 mmol) in anhydrous THF (120 mL) at -58 ºC under N_2 atmosphere. The resulting solution was stirred for 1 h, after which $B(O^iPr)_3$ (4.2 mL, 18 mmol) was added dropwise over 10 min. The resulting solution was stirred for 2 h whilst warming to room temperature. The reaction was stopped by adding water (100 mL) and aq. HCl (2M, 12 mL). The phases were separated, the aqueous layer extracted with EtOAc (3 × 100 mL), the combined organic extracts dried with anhydrous sodium sulfate and then evaporated to dryness under reduced pressure. Afterwards, pinacol (1.90 g, 16.1 mmol) was added in one portion to a mixture of the former residue in PhMe (110 mL) and heated under reflux (Dean-Stark). After 2h, the mixture was allowed to cool to room temperature and the solvent removed under reduced pressure to give the title product after purification.

b) Method B. Pd-Mediated Borylation Strategy – A mixture of 8-bromo-3,3-bis(4-methoxyphenyl)-3*H*-naphtho[2,1-*b*]pyran (1.00 g, 2.11 mmol), bis(pinacolato)diboron (0.81 g, 3.2 mmol), NaOAc (0.70 g, 8.5 mmol) and $Pd(PPh_3)_2Cl_2$ (0.08 , 0.1 mmol) in DMF (50 mL) was stirred at 90 ºC under N_2 atmosphere for 16 h. After this time, the mixture was cooled and the residue evaporated to dryness. The residue was dissolved in DCM (200 mL), washed with water (3 × 100 mL), the organic layer dried with anhydrous sodium sulfate and the solvent removed under reduced pressure to afford pure products after purification.

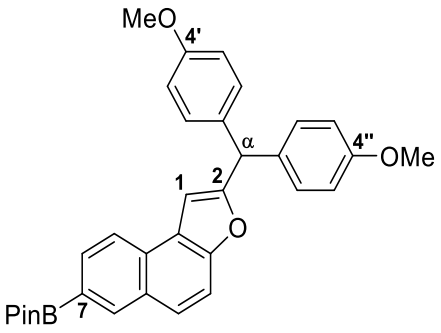

2.63

2-(2-(Bis(4-methoxyphenyl)methyl)naphtho[2,1-b]furan-7-yl)-4,4,5,5-tetramethyl-1,3,2-dioxaborolane (2.63): from method B; Flash column chromatography [Aldrich silica gel (60 Å, 40-63 μm), eluent: hexane/EtOAc (9:1), fraction 3] provided the title compound as a brown powder (0.03 g, 3%); m.p. = 167–168 ºC; ^{1}H NMR (400 MHz, $CDCl_3$) δ_H 1.39 (s, 12H, CH_3), 3.80 (s, 6H, OMe), 5.59 (s, 1H, α-H), 6.72 (s, 1H, 1-H), 6.88 (app. d, 4H, *J* = 8.6 Hz, 3′, 5′, 3″, 5″-H), 7.17 (app. d, 4H, *J* = 8.6 Hz, 2′, 6′, 2″, 6″-H), 7.57 (d, 1H, *J* = 8.9 Hz, 4-H), 7.71 (d, 1H, *J* = 8.9 Hz, 5-H), 7.88 (d, 1H, *J* = 8.2 Hz, 8-H), 7.99 (d, 1H, *J* = 8.2 Hz, 9-H), 8.43 (s, 1H, 6-H); ^{13}C NMR (100 MHz, $CDCl_3$) δ_C 25.0, 49.8, 55.3, 83.9, 104.5, 112.4, 114.0, 122.6, 123.4, 125.3, 129.3, 129.6, 129.8, 130.9, 133.7, 136.9, 153.2, 158.5, 160.0 ppm; HRMS (ESI) found $[M-H_2+H]^+$ = 519.2340 $C_{33}H_{33}BO_5$ requires $[M-H_2+H]^+$ = 519.2457.

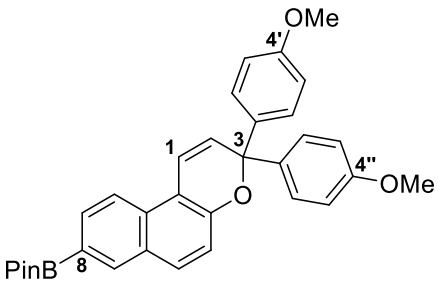

2.62

2-(3,3-Bis(4-methoxyphenyl)-3*H*-benzo[*f*]chromen-8-yl)-4,4,5,5-tetramethyl-1,3,2-dioxaborolane (2.62): from method A; Flash column chromatography [Aldrich silica gel (60 Å, 40-63 μm), eluent: DCM/hexane (1:1), fraction 2] and recrystallization from a mixture of DCM/hexane provided the title compound as a pale white crystalline solid (3.74 g, 49%). From method B; Flash column chromatography [Aldrich silica gel (60 Å, 40-63 μm), eluent: hexane/EtOAc (9:1), fraction 4] and recrystallized from a mixture of DCM/hexane provided the title compound as a pale white crystalline solid (0.02 g, 2%); m.p. = 240–241 ºC; ν_{max} (neat) 1607, 1509, 1464, 1369, 1324, 1298, 1246, 1173, 1138, 1078, 1031, 999, 954, 821, 728, 655, 596 cm^{-1}; Photomerocyanine λ_{max} = 474 nm (PhMe); ^{1}H NMR (400 MHz, $CDCl_3$) δ_H 1.38 (s, 12H, CH_3), 3.77 (s, 6H, OMe), 6.19 (d, 1H, *J* = 10.0 Hz, 2-H), 6.84 (app. d, 4H, *J* = 8.8 Hz, 3′, 5′, 3″, 5″-H), 7.15 (d, 1H, *J* = 8.8 Hz, 5-H), 7.29 (d, 1H, *J* = 10.0 Hz, 1-H), 7.38 (app. d, 4H, *J* = 8.8 Hz, 2′, 6′, 2″, 6″-H), 7.68 (d, 1H, *J* = 8.8 Hz, 6-H), 7.81 (dd, 1H, *J* = 8.5, 1.0 Hz, 9-H), 7.92 (d, 1H, *J* = 8.5 Hz, 10-H), 8.22 (s, 1H, 7-H) ppm; ^{13}C NMR (100 MHz, $CDCl_3$) δ_C 24.9, 55.3, 82.4, 83.8, 113.4, 113.8, 118.3, 119.1, 120.5, 127.9, 128.4, 128.7, 130.7, 131.3, 131.5, 136.9, 137.2, 151.6, 158.9 ppm; HRMS (ESI) found $[M+H]^+$ = 520.2501 $C_{33}H_{33}BO_5$ requires $[M+H]^+$ = 520.2530.

3.2.1.3.3 Experimental Procedure for the Synthesis of 3,3-Bis(4-methoxyphenyl)-8-pyridyl-3*H*-naphtho[2,1-*b*]pyran (2.57):

Method A – A mixture of 8-bromo-3,3-bis(4-methoxyphenyl)-3*H*-naphtho[2,1-*b*]pyran (3.18 mmol), the appropriate pyridineboronic acid pinacol ester (4.8 mmol), K_2CO_3 (4.8 mmol) and $Pd(PPh_3)_4$ (0.16 mmol) in PhMe (37 mL) and EtOH (37 mL) was heated at reflux under N_2 for 16–19 h. After this time, the residue was cooled and added water (200 mL). The residue was extracted with DCM (3 × 200 mL), washed with water (3 × 200 mL), the organic layer dried with anhydrous sodium sulfate and the solvent removed under reduced pressure to afford the target compounds after purification.

Method B – A mixture of 4-bromopyridine hydrochloride (1.4 mmol), 2-(3,3-bis(4-methoxyphenyl)-3*H*-benzo[*f*]chromen-8-yl)-4,4,5,5-tetramethyl-1,3,2-dioxaborolane (0.96 mmol),

K_2CO_3 (2.2 mmol) and $Pd(PPh_3)_4$ (0.05 mmol) in PhMe (8 mL) and EtOH (8 mL) was heated at reflux under N_2 for 16 h. After this time, the mixture was cooled and added water (50 mL). The residue was extracted with DCM (4 × 50 mL), washed with water (3 × 50 mL), the organic layer dried over anhydrous sodium sulfate and the solvent removed under reduced pressure to afford the target compounds after purification.

Method C – A mixture of 2-bromopyridine (1.4 mmol), 2-(3,3-bis(4-methoxyphenyl)-3*H*-benzo[*f*]chromen-8-yl)-4,4,5,5-tetramethyl-1,3,2-dioxaborolane (0.96 mmol), K_2CO_3 (1.4 mmol) and $Pd(PPh_3)_4$ (0.05 mmol) in PhMe (8 mL) and EtOH (8 mL) was heated at reflux under N_2 for 16 h. After this time, the mixture was cooled and added water (50 mL). The residue was extracted with DCM (4 × 50 mL), washed with water (3 × 50 mL), the organic layer dried over anhydrous sodium sulfate and the solvent removed under reduced pressure to afford the target compounds after purification.

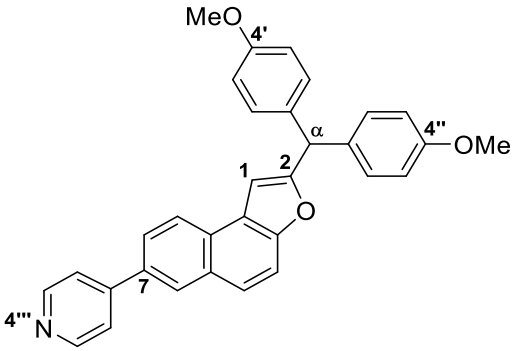

2.58

2-(Bis(4-methoxyphenyl)methyl)-7-(4-pyridyl)naphtho[2,1-*b*]furan (2.58): from 8-bromo-3,3-bis(4-methoxyphenyl)-3*H*-naphtho[2,1-*b*]pyran (Method A: 1.50 g) and 4-pyridineboronic acid pinacol ester after 16 h of reaction; Flash column chromatography [Aldrich silica gel (60 Å, 40-63 μm), eluent: Et_2O/EtOAc (9:1), fraction 1] provided the title compound as a brown powder (0.05 g, 3%). From 2-(3,3-bis(4-methoxyphenyl)-3*H*-benzo[*f*]chromen-8-yl)-4,4,5,5-tetramethyl-1,3,2-dioxaborolane (Method B: 0.50 g); flash column chromatography [Aldrich silica gel (60 Å, 40-63 μm), eluent: Et_2O/DCM (9:1), fraction 1] provided the title compound as a brown powder (0.05 g, 12%); m.p. = 168–172 °C; ν_{max} (neat) 1594, 1507, 1462, 1301, 1244, 1174, 1031, 994, 805, 727, 586 cm^{-1}; ^1H NMR (400 MHz, $CDCl_3$) δ_H 3.81 (s, 6H, OMe), 5.61 (s, 1H, α-H), 6.76 (s, 1H, 1-H), 6.89 (app. d, 4H, *J* = 8.7 Hz, 3′, 5′, 3″, 5″-H), 7.18 (app. d, 4H, *J* = 8.7 Hz, 2′, 6′, 2″, 6″-H), 7.64–7.66 (m, 3H, 4, 2‴, 6‴-H), 7.75 (d, 1H, *J* = 9.0 Hz, 5-H), 7.80 (dd, 1H, *J* = 8.5, 1.7 Hz, 8-H), 8.13 (d, 1H, *J* = 8.5 Hz, 9-H), 8.21 (d, 1H, *J* = 1.7 Hz, 6-H), 8.70 (d, 2H, *J* = 5.9 Hz, 3‴, 5‴-H) ppm; ^{13}C NMR (100 MHz, $CDCl_3$) δ_C 49.9, 55.3, 104.4, 113.3, 114.0, 121.8, 123.6, 124.57, 124.63, 124.9,

127.3, 127.7, 129.8, 130.4, 133.5, 133.8, 148.6, 150.1, 153.0, 158.6, 160.6 ppm; HRMS (ESI) found $[M+H]^+$ = 472.1908 $C_{32}H_{25}NO_3$ requires $[M+H]^+$ = 472.1907.

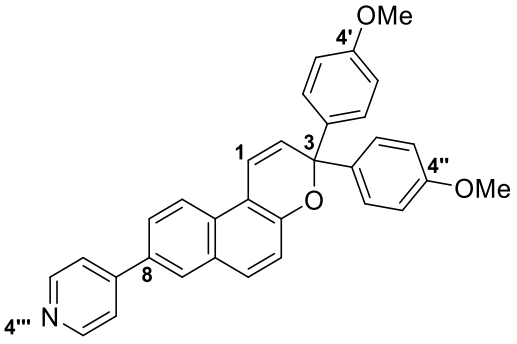

2.57

3,3-Bis(4-methoxyphenyl)-8-(4-pyridyl)-3*H*-naphtho[2,1-*b*]pyran (2.57): from 8-bromo-3,3-bis(4-methoxyphenyl)-3*H*-naphtho[2,1-*b*]pyran (Method A: 1.50 g) and 4-pyridineboronic acid pinacol ester after 16 h of reaction; Flash column chromatography [Aldrich silica gel (60 Å, 40-63 μm), eluent: Et_2O/EtOAc (9:1), fraction 2] followed by recrystallization from DCM/hexane provided the title compound as a pale white crystalline solid (0.92 g, 63%). From 2-(3,3-bis(4-methoxyphenyl)-3*H*-benzo[*f*]chromen-8-yl)-4,4,5,5-tetramethyl-1,3,2-dioxaborolane (Method B: 0.50 g); Flash column chromatography [Aldrich silica gel (60 Å, 40-63 μm), eluent: Et_2O/DCM (9:1)] provided the title compound as a pale yellow powder (0.30 g, 67%); m.p. = 180–184 °C; ν_{max} (neat) 1581, 1505, 1462, 1303, 1250, 1173, 1032, 999, 955, 810, 787, 725, 552 cm^{-1}; Photomerocyanine λ_{max} = 482 nm (PhMe); ^1H NMR (400 MHz, $CDCl_3$) δ_H 3.78 (s, 6H, OMe), 6.25 (d, 1H, *J* = 10.0 Hz, 2-H), 6.85 (app. d, 4H, *J* = 8.8 Hz, 3′, 5′, 3″, 5″-H), 7.23 (d, 1H, *J* = 8.8 Hz, 5-H), 7.30 (d, 1H, *J* = 10.0 Hz, 1-H), 7.39 (app. d, 4H, *J* = 8.8 Hz, 2′, 6′, 2″, 6″-H), 7.60 (d, 2H, *J* = 5.5 Hz, 2‴, 6‴-H), 7.72–7.75 (m, 2H, 6, 9-H), 8.00 (d, 1H, *J* = 1.6 Hz, 7-H), 8.06 (d, 1H, *J* = 8.8 Hz, 10-H), 8.68 (d, 2H, *J* = 5.5 Hz, 3‴, 5‴-H) ppm; ^{13}C NMR (100 MHz, $CDCl_3$) δ_C 55.3, 82.5, 113.4, 114.0, 118.9, 119.3, 121.5, 122.5, 125.1, 127.0, 128.4, 128.5, 129.3, 129.9, 130.3, 133.0, 137.0, 148.1, 150.3, 151.4, 159.0 ppm; HRMS (ESI) found $[M+H]^+$ = 472.1900 $C_{32}H_{25}NO_3$ requires $[M+H]^+$ = 472.1907.

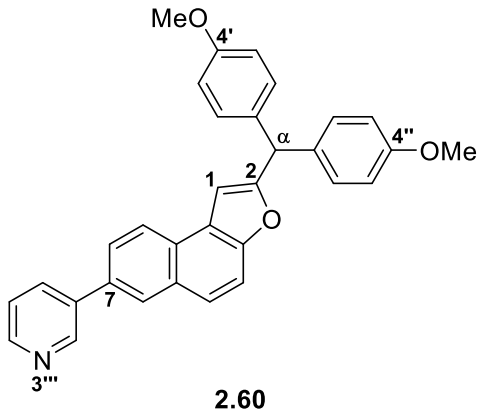

2.60

2-(Bis(4-methoxyphenyl)methyl)-7-(3-pyridyl)naphtho[2,1-*b*]furan (2.60): from 8-bromo-3,3-bis(4-methoxyphenyl)-3*H*-naphtho[2,1-*b*]pyran (Method A: 1.50 g) and 3-pyridineboronic acid pinacol ester after 16 h of reaction; Flash column chromatography [Aldrich silica gel (60 Å, 40-63 μm), eluent: Et_2O/DCM (9:1), fraction 1] provided the title compound as a brown powder (0.09 g, 6%); m.p. = 166–170 °C; ν_{max} (neat) 1606, 1582, 1507, 1462, 1302, 1243, 1173, 1029, 991, 802, 708 cm^{-1}; ^1H NMR (400 MHz, $CDCl_3$) δ_H 3.73 (s, 6H, OMe), 5.53 (s, 1H, α-H), 6.67 (s, 1H, 1-H), 6.81 (app. d, 4H, *J* = 8.7 Hz, 3′, 5′, 3″, 5″-H), 7.10 (app. d, 4H, *J* = 8.7 Hz, 2′, 6′, 2″, 6″-H), 7.32 (dd, 1H, *J* = 7.9, 4.4 Hz, 5‴-H), 7.55 (d, 1H, *J* = 9.0 Hz, 4-H), 7.64–7.68 (m, 2H, 5, 8-H), 7.92 (dt, 1H, *J* = 7.9, 1.9 Hz, 6‴-H), 8.02–8.04 (m, 2H, 6, 9-H), 8.53 (d, 1H, *J* = 4.4 Hz, 4‴-H), 8.90 (s, 1H, 2‴-H) ppm; ^{13}C NMR (100 MHz, $CDCl_3$) δ_C 49.9, 55.3, 104.4, 113.2, 114.0, 123.5, 123.6, 124.5, 124.7, 125.1, 127.0, 129.8, 130.5, 133.6, 133.7, 134.6, 148.3, 148.5, 152.8, 158.6, 160.4 ppm; HRMS (ESI) found $[M+H]^+$ = 472.1921 $C_{32}H_{25}NO_3$ requires $[M+H]^+$ = 472.1907.

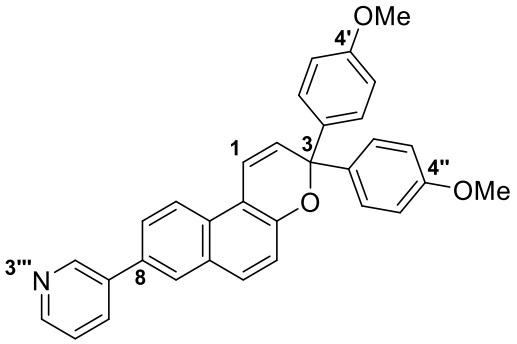

2.59

3,3-Bis(4-methoxyphenyl)-8-(3-pyridyl)-3*H*-naphtho[2,1-*b*]pyran (2.59): from 8-bromo-3,3-bis(4-methoxyphenyl)-3*H*-naphtho[2,1-*b*]pyran (Method A: 1.50 g) and 3-pyridineboronic acid pinacol ester after 16 h of reaction; Flash column chromatography [Aldrich silica gel (60 Å, 40-63 μm), eluent: Et_2O/DCM (9:1)] provided the title compound as a pale yellow powder (1.05 g, 70%); m.p. = 174–176 °C; ν_{max} (neat) 1608, 1582, 1505, 1413, 1307, 1248, 1173, 1030, 999, 810, 787,

709, 551 cm^{-1}; Photomerocyanine λ_{max} = 476 nm (PhMe); ^{1}H NMR (400 MHz, $CDCl_3$) δ_H 3.78 (s, 6H, OMe), 6.25 (d, 1H, *J* = 9.9 Hz, 2-H), 6.85 (app. d, 4H, *J* = 8.9 Hz, 3′, 5′, 3″, 5″-H), 7.22 (d, 1H, *J* = 8.8 Hz, 5-H), 7.30 (d, 1H, *J* = 9.9 Hz, 1-H), 7.38–7.40 (m, 5H, 2′, 6′, 2″, 5″, 6‴-H), 7.69–7.74 (m, 2H, 6, 9-H), 7.92 (d, 1H, *J* = 1.8 Hz, 7-H), 7.96 (dt, 1H, *J* = 7.9, 2.0 Hz, 6‴-H), 8.06 (d, 1H, *J* = 8.8 Hz, 10-H), 8.60 (d, 2H, *J* = 3.9 Hz, 3‴, 5‴-H), 8.94 (s, 1H, 2‴-H) ppm; ^{13}C NMR (100 MHz, $CDCl_3$) δ_C 55.3, 82.4, 113.4, 114.0, 119.0, 119.2, 122.4, 123.6, 125.6, 126.7, 128.4, 128.5, 129.3, 129.5, 130.1, 132.8, 134.3, 136.4, 137.1, 148.3, 148.4, 151.1, 159.0 ppm; HRMS (ESI) found $[M+H]^+$ = 472.1911 $C_{32}H_{25}NO_3$ requires $[M+H]^+$ = 472.1907.

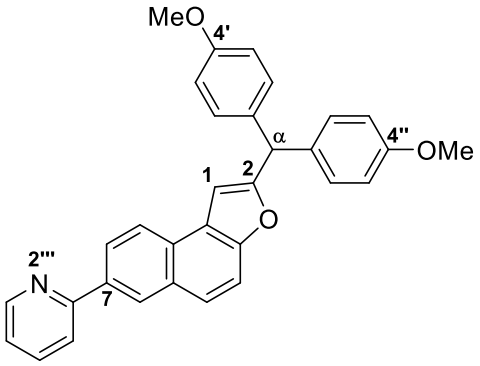

2.66

2-(Bis(4-methoxyphenyl)methyl)-7-(2-pyridyl)naphtho[2,1-*b*]furan (2.66): from 2-(3,3-bis(4-methoxyphenyl)-3*H*-benzo[*f*]chromen-8-yl)-4,4,5,5-tetramethyl-1,3,2-dioxaborolane (Method C: 0.50 g); Flash column chromatography [Aldrich silica gel (60 Å, 40-63 μm), eluent: Et_2O/hexane (3:2), fraction 1] provided the title compound as a brown powder (0.02 g, 4%); m.p. = 149–151°C; ν_{max} (neat) 1608, 1582, 1506, 1462, 1439, 1300, 1240, 1174, 1028, 991, 785, 586 cm^{-1}; ^{1}H NMR (400 MHz, $CDCl_3$) δ_H 3.81 (s, 6H, OMe), 5.61 (s, 1H, α-H), 6.75 (s, 1H, 1-H), 6.89 (app. d, 4H, *J* = 8.7 Hz, 3′, 5′, 3″, 5″-H), 7.19 (app. d, 4H, *J* = 8.7 Hz, 2′, 6′, 2″, 6″-H), 7.24–7.27 (m, 1H, 4‴-H), 7.61 (d, 1 H, *J* = 8.9 Hz, 4-H), 7.77–7.81 (m, 2H, 5, 5‴-H), 7.89 (d, 1H, *J* = 8.0 Hz, 6‴-H), 8.11 (d, 1H, *J* = 8.6 Hz, 9-H), 8.19 (dd, 1H, *J* = 8.6, 1.5 Hz, 8-H), 8.56 (d, 1H, *J* =1.5 Hz, 6-H), 8.75 (d, 1H, *J* = 4.4 Hz, 3‴-H) ppm; ^{13}C NMR (100 MHz, $CDCl_3$) δ_C 49.9, 55.3, 104.5, 112.9, 114.0, 120.8, 122.0, 123.5, 124.1, 124.7, 125.3, 127.2, 127.8, 129.8, 130.4, 133.6, 135.1, 136.9, 149.7, 153.0, 157.4, 158.5, 160.3 ppm; HRMS (ESI) found $[M+H]^+$ = 472.1906 $C_{32}H_{25}NO_3$ requires $[M+H]^+$ = 472.1907.

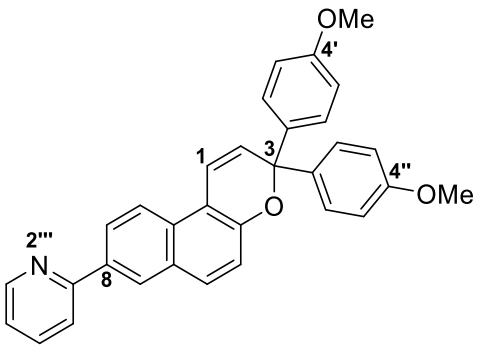

2.65

3,3-Bis(4-methoxyphenyl)-8-(2-pyridyl)-3*H*-naphtho[2,1-*b*]pyran (2.65): from 2-(3,3-bis(4-methoxyphenyl)-3*H*-benzo[*f*]chromen-8-yl)-4,4,5,5-tetramethyl-1,3,2-dioxaborolane (Method C: 0.50 g); Flash column chromatography [Aldrich silica gel (60 Å, 40-63 μm), eluent: Et_2O/hexane (3:2), fraction 2] provided the title compound as a salmon pink powder (0.41 g, 84%); m.p. = 175–178 °C; ν_{max} (neat) 2951, 2833, 1607, 1582, 1506, 1471, 1462, 1304, 1248, 1173, 1088, 1031, 1001, 955, 837, 771, 734, 726, 586 cm^{-1}; ^1H NMR (400 MHz, $CDCl_3$) δ_H 3.77 (s, 6H, OMe), 6.22 (d, 1H, *J* = 10.0 Hz, 2-H), 6.84 (app. d, 4H, *J* = 8.8 Hz, 3′, 5′, 3″, 5″-H), 7.18–7.25 (m, 2H, 5, 4‴-H), 7.30 (d, 1H, *J* = 10.0 Hz, 1-H), 7.39 (app. d, 4H, *J* = 8.8 Hz, 2′, 6′, 2″, 6″-H), 7.73–7.77 (m, 2H, 6, 5‴-H), 7.82 (d, 1H, *J* = 7.9 Hz, 6‴-H), 8.04 (d, 1H, *J* = 8.9 Hz, 10-H), 8.12 (dd, 1H, *J* = 8.9, 1.5 Hz, 9-H), 8.35 (d, 1H, *J* = 1.5 Hz, 7-H), 8.71 (d, 1H, *J* = 4.7 Hz, 3‴-H) ppm; ^{13}C NMR (100 MHz, $CDCl_3$) δ_C 55.3, 82.4, 113.4, 113.8, 118.9, 119.1, 120.5, 121.9, 125.2, 126.9, 128.2, 128.4, 129.4, 130.1, 130.6, 134.4, 136.8, 137.2, 149.7, 151.2, 157.2, 158.9 ppm; HRMS (ESI) found $[M+H]^+$ = 472.1907 $C_{32}H_{25}NO_3$ requires $[M+H]^+$ = 472.1907.

3.2.1.3.4 Experimental Procedure for the Synthesis of (2,4-Dimethoxyphenyl)(4-methoxyphenyl)methanone (2.80): *p*-anisic acid (31.99 g, 0.2103 mmol), 1,3-dimethoxybenzene (26.0 g, 0.200 mmol) and polyphosphoric acid (214 mL) were stirred and heated to 90 °C for 17h. After this time, further 1,3-dimethoxybenzene (13.0 mL, 0.100 mmol) was added and the reaction mixture stirred at 90 °C for 5 h. The mixture was then poured into ice water. The product was extracted into DCM. The combined organic extracts were washed with 2M NaOH (2 × 250 mL), the organic layer dried with anhydrous sodium sulfate and evaporated to dryness giving a red oil. The desired product was obtained by crystallization from Et_2O at -20 °C, followed by recrystallization from hot EtOH, giving the corresponding product as a cream crystalline solid.

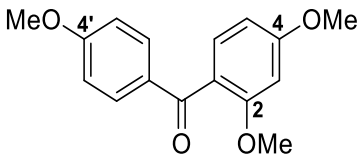

2.80

(2,4-Dimethoxyphenyl)(4-methoxyphenyl)methanone (2.80): cream crystalline solid (32.76 g, 57%); m.p. = 70–71 °C [lit. m.p. = 70–71 °C[241]]; ν_{max} (neat) 1633, 1592, 1249, 1212, 1170, 1102, 1020, 954, 835, 770, 601 cm^{-1}; ^1H NMR (400 MHz, $CDCl_3$) δ_H 3.69 (3H, s, OMe), 3.82–3.83 (6H, m, OMe), 6.51–6.53 (2H, m, 3, 5-H), 6.88 (2H, d, *J* = 8.7 Hz, 3′, 5′-H), 7.32 (1H, d, *J* = 8.2 Hz, 6-H), 7.77 (2H, d, *J* = 8.7 Hz, 2′, 6′-H) ppm; ^{13}C NMR (100 MHz, $CDCl_3$) δ_C 55.4, 55.46, 55.55, 98.8, 104.6, 113.3, 121.9, 131.4, 131.5, 132.1, 159.1, 162.9, 163.2, 194.3 ppm; HRMS (ESI) found $[M+H]^+$ = 273.11209 $C_{16}H_{16}O_4$ requires $[M+H]^+$ = 273.11214.

3.2.1.3.5 Experimental Procedure for the Synthesis of 1-(2,4-Dimethoxyphenyl)-1-(4-methoxyphenyl)prop-2-yn-1-ol (2.79): *n*-BuLi (54.0 mL, 2.5 M in hexanes, 135 mmol) was added dropwise via a syringe to a cold (-5 °C) stirred solution of TMS acetylene (19.0 mL, 137 mmol) in anhydrous THF (500 mL) under N_2. The solution was stirred for 30 min at -5 °C. Afterwards, (2,4-dimethoxyphenyl)(4-methoxyphenyl)methanone (32.01 g, 117.6 mmol) was added in a single portion and the cooling bath was removed and the mixture stirred at room temperature for 4h. The solution was re-cooled to 0 °C and a solution of powdered KOH (85%, 15.5 g) in MeOH (80 mL) was added in a single portion, after which the cooling bath was removed and the mixture stirred for 30 min. Upon completion, the mixture was diluted with water (100 mL) and the layers separated. The aqueous layer was extracted with EtOAc (3 × 150 mL) and the combined organic layers washed with water (2 × 150 mL), dried with anhydrous sodium sulfate and evaporated to dryness, leading to the corresponding product as a yellow oil, which solidified upon standing.

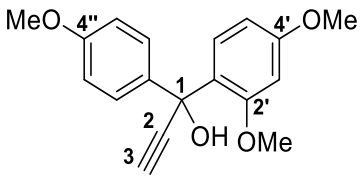

2.79

1-(2,4-Dimethoxyphenyl)-1-(4-methoxyphenyl)prop-2-yn-1-ol (2.79): yellow solid (35.23 g, quant.); m.p. = 80–83 °C; ν_{max} (neat) 3269, 1607, 1582, 1502, 1299, 1250, 1208, 1168, 1127, 1027, 830, 699 cm^{-1}; ^1H NMR (400 MHz, $CDCl_3$) δ_H 2.81 (1H, s, 3-H), 3.80 (3H, s, OMe), 3.82 (3H, s, OMe), 3.83 (3H, s, OMe), 4.79 (1H, s, OH), 6.46 (1H, dd, *J* = 8.6, 2.0 Hz, 5′-H), 6.53 (1H, d, *J* =

2.0 Hz, 3′-H), 6.89 (2H, d, *J* = 8.7 Hz, 3″, 5″-H), 7.23 (1H, d, *J* = 8.6 Hz, 6′-H), 7.49 (2H, d, *J* = 8.7 Hz, 2″, 6″-H) ppm; ^{13}C NMR (100 MHz, $CDCl_3$) δ_C 55.3, 55.4, 55.8, 73.6, 74.4, 86.2 100.1, 104.0, 113.3, 125.1, 127.6, 129.1, 136.4, 157.8, 159.0, 160.8 ppm; HRMS (ESI) found $[M+Na]^+$ = 321.1084 $C_{18}H_{18}O_4$ requires $[M+Na]^+$ = 321.1097.

3.2.1.3.6 Experimental Procedure for the Synthesis of 8-Bromo-3-(2,4-dimethoxyphenyl)-3-(4-methoxyphenyl)-3*H*-naphtho[2,1-*b*]pyran (2.78): 1-(2,4-dimethoxyphenyl)-1-(4-methoxyphenyl)prop-2-yn-1-ol (2.81 g, 9.42 mmol) and 6-bromo-2-naphthol (2.00 g, 8.97 mmol) in the presence of PPTS (0.12 g, 0.48 mmol) and trimethyl orthoformate (2.0 mL, 18 mmol) in 1,2-DCE (50 mL) was refluxed for 4 h under N_2. Solvent was removed under reduced pressure and the residue was taken in DCM (100 mL), washed with water (3 × 200 mL) and the organic layer dried with anhydrous sodium sulfate. Subsequently, the residue was crystallized from a DCM/hexane mixture giving the corresponding product as a brown powder.

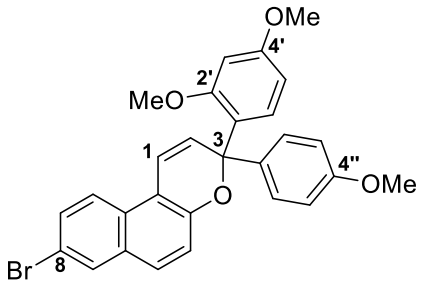

2.78

8-Bromo-3-(2,4-dimethoxyphenyl)-3-(4-methoxyphenyl)-3*H*-naphtho[2,1-*b*]pyran (2.78): brown powder (3.98 g, 88%); m.p. = 121–125 °C; ν_{max} (neat) 1606, 1584, 1505, 1248, 1172, 1028, 1000, 827, 809 cm^{-1}; Photomerocyanine λ_{max} = 486 nm (PhMe); ^{1}H NMR (400 MHz, $CDCl_3$) δ_H 3.57 (3H, s, OMe), 3.75 (3H, s, OMe), 3.76 (3H, s, OMe), 6.45–6.47 (2H, m, 3′, 5′-H), 6.51 (1H, d, *J* = 10.1 Hz, 2-H), 6.78–6.82 (2H, m, 3″, 5″-H), 7.12 (1H, d, *J* = 10.1 Hz, 1-H), 7.18 (1H, d, *J* = 8.9 Hz, 5-H), 7.31–7.35 (2H, m, 2″, 6″-H), 7.48 (1H, dd, *J* = 9.0, 2.1 Hz, 9-H), 7.52 (1H, d, *J* = 8.9 Hz, 6-H), 7.55–7.58 (1H, m, 6′-H), 7.78 (1H, d, *J* = 9.0 Hz, 10-H), 7.84 (1H, d, *J* = 2.1 Hz, 7-H) ppm; ^{13}C NMR (100 MHz, $CDCl_3$) δ_C 55.2, 55.3, 55.5, 81.9, 100.2, 103.7, 113.2, 114.1, 117.1, 117.7, 119.4, 123.3, 124.7, 128.0, 128.1, 128.30, 128.33, 128.4, 129.6, 130.3, 130.4 136.7, 150.6, 156.8, 158.8, 160.6 ppm; HRMS (ESI) found $[M+H]^+$ = 503.0849 $C_{28}H_{23}{}^{79}BrO_4$ requires $[M+H]^+$ = 503.0852.

3.2.1.3.7 Experimental Procedure for the Synthesis of 3-(2,4-Dimethoxyphenyl)-3-(4-methoxyphenyl)-8-(4-pyridyl)-3*H*-naphtho[2,1-*b*]pyran (2.77): a mixture of 8-bromo-3-(2,4-dimethoxyphenyl)-3-(4-methoxyphenyl)-3*H*-naphtho[2,1-*b*]pyran (1.00 g, 1.99 mmol), 4-

pyridineboronic acid pinacol ester (0.61 g, 3.0 mmol), K_2CO_3 (0.41 g, 3.0 mmol) and $Pd(PPh_3)_4$ (0.11 g, 0.095 mmol) in PhMe (23.0 mL) and EtOH (23.0 mL) was heated at reflux under N_2. After 15 h of reaction, the crude was evaporated to dryness. The residue was dissolved in DCM (100 mL), washed with water (3 × 200 mL), the organic layer dried with anhydrous sodium sulfate and the solvent removed under reduced pressure. Afterwards, the residue was purified two times by flash column chromatography [Aldrich silica gel (60 Å, 40-63 μm), eluent: Et_2O] to give two pure fractions.

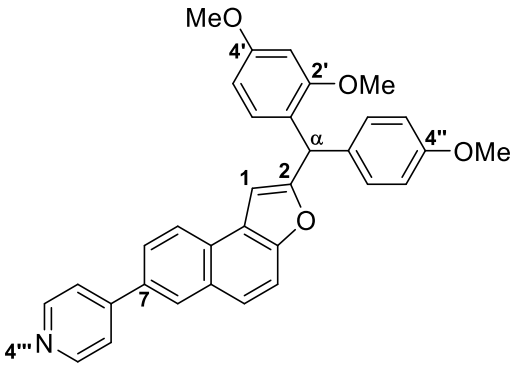

2.89

Fraction 2 – 4-(2-((2,4-Dimethoxyphenyl)(4-methoxyphenyl)methyl)naphtho[2,1-*b*]furan-7-yl)pyridine (2.89): brown powder (0.11 g, 11%); m.p. = 163–167 °C; ν_{max} (neat) 1583, 1508, 1460, 1437, 1417, 1259, 1242, 1207, 1116, 1039, 995, 803 cm^{-1}; ^1H NMR (400 MHz, $CDCl_3$) δ_H 3.69 (3H, s, OMe), 3.72 (6H, s, OMe), 5.90 (1H, s, α-H), 6.37 (1H, app. d, *J* = 8.4 Hz, 5′-H), 6.44 (1H, d, *J* = 1.6 Hz, 3′-H), 6.62 (1H, s, 1-H), 6.79 (2H, d, *J* = 8.4 Hz, 3″, 5″-H), 6.87 (1H, d, *J* = 8.4 Hz, 2′-H), 7.10 (2H, d, *J* = 8.4 Hz, 2″, 6″-H), 7.54–7.72 (5H, m, 4, 5, 8, 3″, 5″-H), 8.03 (1H, d, *J* = 8.5 Hz, 9-H), 8.11 (1H, s, 6-H), 8.61 (2H, d, *J* = 5.0 Hz, 3‴, 5‴-H) ppm; ^{13}C NMR (100 MHz, $CDCl_3$) δ_C 43.0, 55.3, 55.4, 55.7, 98.8, 104.1, 104.2, 113.3, 113.9, 121.8, 122.5, 123.7, 124.5, 124.6, 124.7, 127.2, 127.6, 129.9, 130.0, 130.3, 133.4, 133.7, 148.5, 150.3, 152.9, 157.8, 158.4, 160.0, 160.9 ppm; HRMS (ESI) found $[M+H]^+$ = 502.2013 $C_{33}H_{27}NO_4$ requires $[M+H]^+$ = 502.2013.

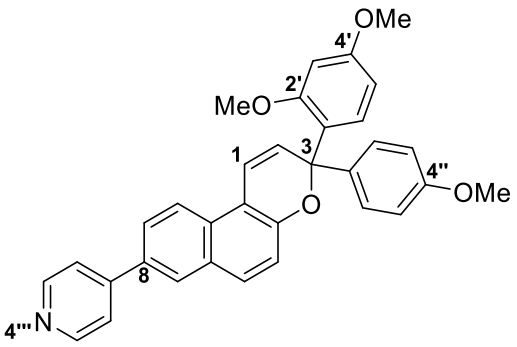

2.77

Fraction 3 – 3-(2,4-Dimethoxyphenyl)-3-(4-methoxyphenyl)-8-(4-pyridyl)-3*H*-naphtho[2,1-*b*]pyran (2.77): trituration with cold Et_2O gave the corresponding product as a off-white powder (0.59 g, 60%); m.p. = 179–181 °C; ν_{max} (neat) 1606, 1584, 1506, 1465, 1286, 1251, 1206, 1175, 1027, 999, 828, 814 cm^{-1}; Photomerocyanine λ_{max} = 490 nm (PhMe); ^1H NMR (400 MHz, $CDCl_3$) δ_H 3.59 (3H, s, OMe), 3.77–3.78 (6H, m, OMe), 6.46–6.49 (2H, m, 3′, 5′-H), 6.54 (1H, d, *J* = 10.1 Hz, 2-H), 6.81 (2H, app. d, *J* = 8.7 Hz, 3″, 5″-H), 7.20–7.25 (2H, m, 1, 5-H), 7.35 (2H, app.d, *J* = 8.7 Hz, 2″, 6″-H), 7.59–7.60 (3H, m, 2‴, 6‴, 6′-H), 7.71–7.74 (2H, m, 6, 9-H), 7.99 (1H, app. s, 7-H), 8.05 (1H, d, *J* = 8.8 Hz, 10-H), 8.67 (2H, d, *J* = 5.8 Hz, 3‴, 5‴-H); ^{13}C NMR (100 MHz, $CDCl_3$) δ_C 55.2, 55.3, 55.5, 82.0, 100.2, 103.8, 113.2, 113.9, 117.8, 119.2, 121.5, 122.5, 124.8, 124.9, 126.9, 127.99, 128.03, 128.3, 129.3, 129.91, 129.92, 132.8, 136.8, 148.1, 150.3, 151.3, 156.9, 158.9, 160.6 ppm; HRMS (ESI) found $[M+H]^+$ = 502.2004 $C_{33}H_{27}NO_4$ requires $[M+H]^+$ = 502.2013.

3.2.1.3.8 General Procedure for the Synthesis of 8-Aryl Substituted Naphthopyrans: a mixture of 8-bromo-3,3-bis(4-methoxyphenyl)-3*H*-naphtho[2,1-*b*]pyran (0.42 mmol), the appropriate boronic acid (0.95 mmol), K_2CO_3 (0.64 mmol) and $Pd(PPh_3)_4$ (0.022 mmol) in PhMe (5 mL) and EtOH (5 mL) was heated at reflux under N_2 for 16 – 17 h. After this time, the mixture was cooled to room temperature and water (100 mL) was added. The residue was extracted with DCM (3 × 100 mL), washed with water (3 × 150 mL), the organic layer dried with anhydrous sodium sulfate and the solvent removed under reduced pressure to afford the target compounds after purification.

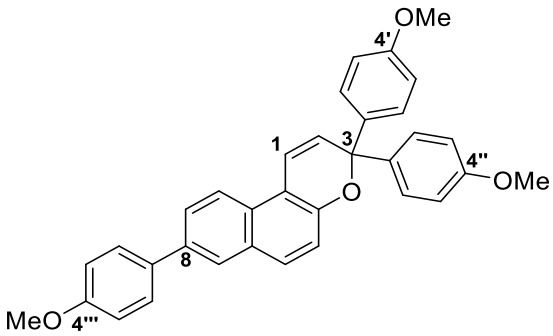

2.70

3,3,8-Tris(4-methoxyphenyl)-3*H*-naphtho[2,1-*b*]pyran (2.70): from 4-methoxyphenylboronic acid (150.8 mg) after 16 h of reaction; Flash column chromatography [Aldrich silica gel (60 Å, 40-63 μm), eluent: EtOAc/hexane (1:9), fraction 2] followed by recrystallization from DCM/hexane provided the title compound as a pale pink crystalline solid (94.5 mg, 44%); m.p. = 223–225 °C; ν_{max} (neat) 1604, 1505, 1451, 1439, 1302, 1245, 1171, 1088, 1023, 1002, 822, 712, 588 cm^{-1}; Photomerocyanine λ_{max} = 486 nm (PhMe); ^{1}H NMR (400 MHz, $CDCl_3$) δ_H 3.77 (s, 6H, 4′, 4″-OMe), 3.86 (s, 3H, 4‴-OMe), 6.22 (d, 1H, *J* = 9.9 Hz, 2-H), 6.84 (app. d, 4H, *J* = 8.8 Hz, 3′, 5′, 3″, 5″-H), 7.00 (d, 2H, *J* = 8.7 Hz, 3‴, 5‴-H), 7.18 (d, 1H, *J* = 8.8 Hz, 5-H), 7.30 (d, 1H, *J* = 9.9 Hz, 1-H), 7.39 (app. d, 4H, *J* = 8.8 Hz, 2′, 6′, 2″, 6″-H), 7.61 (d, 2H, *J* = 8.7 Hz, 2‴, 6‴-H), 7.67–7.71 (m, 2H, 6, 9-H), 7.85 (d, 1H, *J* 1.6 Hz, 7-H), 7.99 (d, 1H, *J* = 8.8 Hz, 10-H); ^{13}C NMR (100 MHz, $CDCl_3$): δ_C 55.3, 55.4, 82.3, 113.4, 113.9, 114.3, 118.8, 119.2, 121.9, 125.7, 126.1, 128.2, 128.3, 128.4, 128.6, 129.6, 129.9, 133.5, 135.9, 137.2, 150.5, 158.9, 159.1 ppm; HRMS (ESI) found $[M+H]^+$ = 501.2053 $C_{34}H_{28}O_4$ requires $[M+H]^+$ = 501.2060.

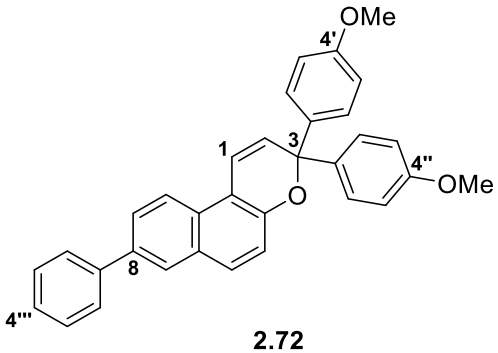

2.72

3,3-Bis(4-methoxyphenyl)-8-phenyl-3*H*-naphtho[2,1-*b*]pyran (2.72): from phenylboronic acid (78.4 mg) after 17 h of reaction; Recrystallization from DCM/hexane provided the title compound as a brown crystalline solid (116.5 mg, 58%); m.p. = 190–195 °C; ν_{max} (neat) 1608, 1583, 1506, 1462, 1303, 1248, 1173, 1087, 1030, 998, 955, 825, 809, 756, 695, 594, 570, 553 cm^{-1}; Photomerocyanine λ_{max} = 480 nm (PhMe); ^{1}H NMR (400 MHz, $CDCl_3$) δ_H 3.77 (s, 6H, OMe), 6.23

(d, 1H, *J* = 9.9 Hz, 2-H), 6.84 (app. d, 4H, *J* = 8.8 Hz, 3′, 5′, 3″, 5″-H), 7.19 (d, 1H, *J* = 8.8 Hz, 5-H), 7.31 (d, 1H, *J* = 9.9 Hz, 1-H), 7.34–7.41 (m, 5H, 2′, 6′, 2″, 6″, 4‴-H), 7.46 (t, 2H, *J* = 7.6 Hz, 3‴, 5‴-H), 7.67–7.75 (m, 4H, 6, 9, 2‴, 6‴-H), 7.91 (d, 1H, *J* = 1.6 Hz, 7-H), 8.02 (d, 1H, *J* = 8.9 Hz, 10-H) ppm; ^{13}C NMR (100 MHz, $CDCl_3$): δ_C 55.3, 82.3, 113.4, 113.9, 118.9, 119.2, 121.9, 126.2, 126.4, 127.1, 127.2, 128.3, 128.4, 128.8, 129.0, 129.5, 130.0, 136.3, 137.2, 141.1, 150.7, 158.9 ppm; HRMS (ESI) found $[M+H]^+$ = 471.1949 $C_{33}H_{26}O_3$ requires $[M+H]^+$ = 471.1955.

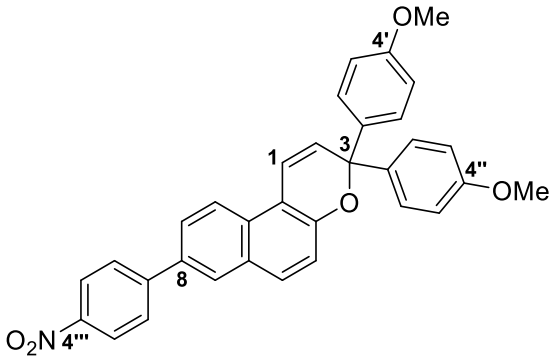

2.74

3,3-Bis(4-methoxyphenyl)-8-(4-nitrophenyl)-3*H*-naphtho[2,1-*b*]pyran (2.74): from 4-nitrophenylboronic acid (158.6 mg) after 16 h of reaction; Flash column chromatography [Aldrich silica gel (60 Å, 40-63 μm), eluent: EtOAc/hexane (1:4), fraction 2] provided the title compound as a yellow powder (145.0 mg, 66%); m.p. = 142–146 °C; ν_{max} (neat) 1593, 1506, 1462, 1338, 1302, 1245, 1173, 1031, 999, 827, 752, 594 cm^{-1}; Photomerocyanine λ_{max} = 488 nm (PhMe); ^{1}H NMR (400 MHz, $CDCl_3$) δ_H 3.77 (s, 6H, OMe), 6.25 (d, 1H, *J* = 9.9 Hz, 2-H), 6.85 (app. d, 4H, *J* = 8.8 Hz, 3′, 5′, 3″, 5″-H), 7.23 (d, 1H, *J* = 8.8 Hz, 5-H), 7.29 (d, 1H, *J* = 9.9 Hz, 1-H), 7.39 (app. d, 4H, *J* = 8.8 Hz, 2′, 6′, 2″, 6″-H), 7.70–7.73 (m, 2H, 6, 9-H), 7.81 (d, 2H, *J* = 8.8 Hz, 2‴, 6‴-H), 7.96 (d, 1H, *J* = 1.7 Hz, 7-H), 8.05 (d, 1H, *J* = 8.8 Hz, 10-H), 8.30 (d, 2H, *J* = 8.8 Hz, 3‴, 5‴-H) ppm; ^{13}C NMR (100 MHz, $CDCl_3$) δ_C 55.3, 82.5, 113.4, 113.9, 118.8, 119.4, 122.5, 124.2, 125.5, 127.4, 127.7, 128.3, 128.6, 129.3, 129.7, 130.3, 133.6, 137.0, 146.9, 147.4, 151.5, 159.0 ppm; HRMS (ESI) found $[M+H]^+$ = 516.1804 $C_{33}H_{25}NO_5$ requires $[M+H]^+$ = 516.1805.

3.2.1.4 Preparation of 7-Pyridyl-3*H*-Naphtho[2,1-*b*]pyrans

3.2.1.4.1 Experimental Procedure for the Synthesis of 5-Bromo-2-naphthol (2.93): 5-amino-2-naphthol (10.00 g, 62.82 mmol) was ground to a fine powder and heated to 55 ºC under a stream of N_2. Sulfuric acid (95%, 13.0 mL, 232 mmol) was added in one portion and mixed rapidly with the solid. Stirring was continued until the mixture became too viscous to stir. The heat was removed, the reaction covered and allowed to stand overnight. The solid was suspended in water (300 mL)

and collected by filtration, washed with acetone and air-dried. The resulting product (13.00 g, 54.34 mmol), NaOH (2.24 g, 56.0 mmol) and $NaNO_2$ (3.75 g, 54.3 mmol) were dissolved in water (93 mL). This solution was added dropwise to a solution of H_2SO_4 (95–98%, 9.6 mL) in water (20.0 mL) at such a rate that the internal temperature never exceeded 5 ºC. The yellow diazonium sulfate precipitate was collected by filtration and washed several times with ice cold water. The moist* filter cake was transfered to a mixture of CuBr (7.80 g, 54.4 mmol), $CuBr_2$ (12.14 g, 54.35 mmol), HBr (6.0 mL) and water (200 mL). The mixture was warmed to 70 ºC for 1 h and then filtered by gravity. The filtrate was saturated with NaCl (105 g) and the solution stirred overnight. The precipitate was collected by filtration. The black solid was air-dried giving the corresponding 5-bromo-2-hydroxynaphthalene-1-sulfonic acid (7.02 g, 37%). Afterwards, the 5-bromo-2-hydroxynaphthalene-1-sulfonic acid (6.80 g, 22.4 mmol) was mixed with 20% aq. H_2SO_4 (153 mL). The slurry was heated to reflux for 20 min. After the reaction cooled, it was extracted with Et_2O (3 × 200 mL). The ether layers were combined, washed with water (3 × 200 mL), dried with anhydrous sodium sulfate and evaporated to dryness, giving the desired product.

*****Hazard - Many diazonium salts are explosive/shock-sensitive when dried. The diazonium salt must be kept damp with water at all times.

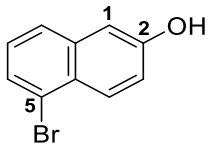

2.93

5-Bromo-2-naphthol (2.93): dark brown powder (3.51 g, 70%); m.p. = 108–110 °C [lit. m.p. = 110–111 °C[242]]; ν_{max} (neat) 3200 (br), 1636, 1561, 1501, 1424, 1343, 1300, 1251, 1229, 1152, 1131, 963, 860, 801, 770, 738, 655, 543 cm^{-1}; ^1H NMR (400 MHz, Methanol-d_4) δ_H 4.90 (s, 1H, OH), 7.13 (d, 1H, *J* = 2.4 Hz, 1-H), 7.18 (dd, 1H, *J* = 9.1, 2.4 Hz, 3-H), 7.23 (dd, 1H, *J* = 8.2, 7.5 Hz, 7-H), 7.54 (dd, 1H, *J* = 7.5, 0.9 Hz, 6-H), 7.64 (d, 1H, *J* = 8.2 Hz, 8-H), 8.05 (d, 1H, *J* = 9.1 Hz, 4-H) ppm; ^{13}C NMR (100 MHz, Methanol-d_4) δ_C 110.9, 121.2, 123.8, 128.0, 128.2, 128.4, 128.5, 130.0, 138.2, 157.9 ppm; HRMS (ESI) found $[M+H]^+$ = 222.9757 $C_{10}H_7{}^{79}BrO$ requires $[M+H]^+$ = 222.9753.

3.2.1.4.2 Experimental Procedure for the Synthesis of 7-Bromo-3,3-bis(4-methoxyphenyl)-3*H*-naphtho[2,1-*b*]pyran (2.94): 1,1-bis(4-methoxyphenyl)prop-2-yn-1-ol (3.78 g, 14.1 mmol) and 5-bromo-2-naphthol (3.00 g, 13.4 mmol) in the presence of PPTS (0.17 g, 0.68 mmol) and trimethyl orthoformate (3.0 mL, 27 mmol) in 1,2-DCE (27 mL) was refluxed for 3 h under N_2 atmosphere. Solvent was removed under reduced pressure, the residue taken in DCM (3 × 200 mL), washed with

water (3 × 200 mL) and the organic layer dried with anhydrous sodium sulfate. Subsequently, after solvent evaporation, the residue was crystallized from DCM/hexane giving the corresponding product as a brown solid.

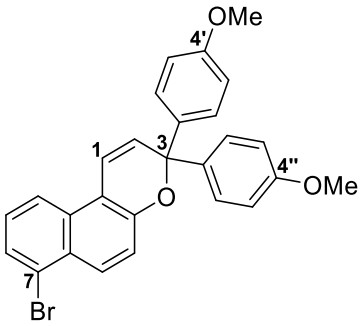

2.94

7-Bromo-3,3-bis(4-methoxyphenyl)-3*H*-naphtho[2,1-*b*]pyran (2.94): brown crystalline solid (3.94 g, 62%); m.p. = 185–189 °C; ν_{max} (neat) 1606, 1506, 1458, 1248, 1170, 1092, 1032, 1021, 963, 841, 756, 572 cm^{-1}; ^{1}H NMR (400 MHz, $CDCl_3$) δ_H 3.77 (s, 6H, OMe), 6.24 (d, 1H, *J* = 10.0 Hz, 2-H), 6.84 (app. d, 4H, *J* = 8.8 Hz, 3′, 5′, 3″, 5″-H), 7.24–7.30 (m, 3H, 1, 5, 9-H), 7.37 (app. d, 4H, *J* = 8.8 Hz, 2′, 6′, 2″, 6″-H), 7.60 (d, 1H, *J* = 7.3 Hz, 8-H), 7.93 (d, 1H, *J* = 8.6 Hz, 10-H), 8.08 (d, 1H, *J* = 9.2 Hz, 6-H) ppm; ^{13}C NMR (100 MHz, $CDCl_3$) δ_C 55.3, 82.4, 113.4, 114.2, 119.0, 119.6, 121.3, 123.6, 126.8, 127.68, 127.71, 128.3, 128.8, 129.0, 131.1, 136.9, 151.2, 159.0 ppm; HRMS (ESI) found $[M+H]^+$ = 473.0749 $C_{27}H_{21}{}^{79}BrO_3$ requires $[M+H]^+$ = 473.0747.

3.2.1.4.3 Experimental Procedure for the Synthesis of 4-Pyridineboronic acid (2.97): *n*-BuLi (30.0 mL, 2.5 M in hexanes) was added dropwise by syringe over 1 h to a stirred solution of 4-bromopyridine (10.04 g, 63.54 mmol) [from 4-bromopyridine hydrochloride (30 g) dissolved in saturated $NaHCO_3$ (300 mL), extracted with Et_2O (4 × 150 mL), the organic layer dried with anhydrous sodium sulfate and the Et_2O evaporated at temperature bellow 30 °C] and $B(O^iPr)_3$ (17.6 mL, 76.3 mmol) in PhMe (92.0 mL) and THF (23.0 mL) at -78 ºC under N_2 atmosphere. The resulting solution was stirred for 30 min, warmed for 20 min, and HCl (2 M, 55 mL) added. The phases were separated and the aqueous phase neutralised with NaOH (5 M) [pH = 7]. The resulting precipitate was filtered and washed with water and air dried to give the corresponding product as a white powder.

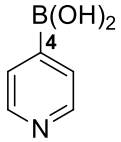

2.97

4-Pyridineboronic acid (2.97): white powder (4.30 g, 55%); m.p. > 300 °C; ν_{max} (neat) 3295 (br), 1621, 1535, 1421, 1270, 1208, 1146, 1067, 949, 766, 740, 656, 567 cm^{-1}; ^{1}H NMR (400 MHz, DMSO-d_6) δ_H 7.66 (d, 2H, *J* = 5.6 Hz, 3, 5-H), 8.49 (s, 2H, $B(OH)_2$), 8.56 (d, 2H, *J* = 5.6 Hz, 2, 6-H) ppm; ^{13}C NMR (100 MHz, DMSO-d_6) δ_C 128.8, 149.3 ppm; HRMS (ESI) found $[M+H]^+$ = 123.0604 $C_5H_6BNO_2$ requires $[M+H]^+$ = 123.0601.

3.2.1.4.4 Experimental Procedure for the Synthesis of 4-Pyridineboronic acid pinacol ester (2.35): a mixture of 4-pyridineboronic acid (4.20 g, 34.2 mmol) and pinacol (4.05 g, 34.3 mmol) in PhMe (36.0 mL) was heated under reflux (Dean-Stark) for 2 h. The mixture was allowed to cool, the solvent reduced and hexane added. The mixture was heated to dissolution and allowed to cool. The resulting precipitate was filtered and washed with cold hexane to give the corresponding product as a white powder (6.46 g, 92%).

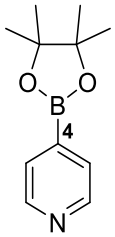

2.35

4-Pyridineboronic acid pinacol ester (2.35): white powder (6.46 g, 92%); m.p. = 150–153 °C [lit. m.p. = 151 °C[243]]; ν_{max} (neat) 1618, 1423, 1383, 1361, 1197, 1151, 1030, 873, 797, 717, 647 cm^{-1}; ^{1}H NMR (400 MHz, $CDCl_3$) δ_H 1.36 (s, 12H, CH_3), 7.63 (d, 2H, *J* = 5.6 Hz, 3, 5-H), 8.64 (d, 2H, *J* = 5.6 Hz, 2, 6-H) ppm; ^{13}C NMR (100 MHz, $CDCl_3$) δ_C 24.9, 84.5, 128.7, 149.2 ppm; HRMS (ESI) found $[M+H]^+$ = 205.1383 $C_{11}H_{16}BNO_2$ requires $[M+H]^+$ = 205.1383.

3.2.1.4.5 Experimental Procedure for the Synthesis of 3,3-Bis(4-methoxyphenyl)-7-(4-pyridyl)-3*H*-naphtho[2,1-*b*]pyran (2.98): a mixture of 7-bromo-3,3-bis(4-methoxyphenyl)-3*H*-naphtho[2,1-*b*]pyran (1.00 g, 2.11 mmol), 4-pyridineboronic acid pinacol ester (0.65 g, 3.2 mmol), K_2CO_3 (0.66 g, 3.2 mmol) and $Pd(PPh_3)_4$ (0.19 g, 0.11 mmol) in PhMe (25 mL) and EtOH (25 mL) was heated at reflux under N_2 for 16 h. After this time, the mixture was cooled and added water (150 mL). Afterwards, the residue was extracted with DCM (3 × 200 mL), washed with water (3 × 200 mL),

the organic layer dried with anhydrous sodium sulfate and the solvent removed under reduced pressure. The residue was then recrystallized from a mixture of DCM/hexane leading to the corresponding product as a grey solid.

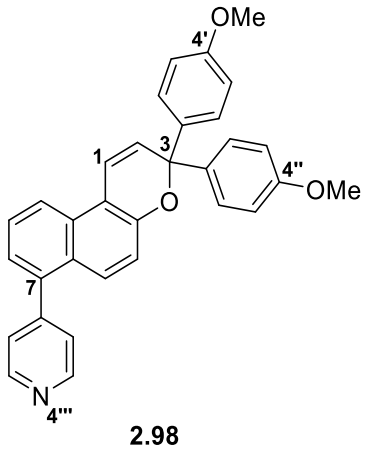

2.98

3,3-Bis(4-methoxyphenyl)-7-(4-pyridyl)-3*H*-naphtho[2,1-*b*]pyran (2.98): grey powder (0.64 g, 66%); m.p. = 229–232 °C; ν_{max} (neat) 1604, 1585, 1509, 1463, 1406, 1298, 1249, 1174, 1082, 1033, 953, 838, 767, 592, 561 cm^{-1}; Photomerocyanine λ_{max} = 470 nm (PhMe); ^{1}H NMR (400 MHz, $CDCl_3$) δ_H 3.78 (s, 6H, OMe), 6.26 (d, 1H, *J* = 10.0 Hz, 2-H), 6.84 (app. d, 4H, *J* = 8.8 Hz, 3′, 5′, 3″, 5″-H), 7.15 (d, 1H, *J* = 9.2 Hz, 5-H), 7.23 (d, 1H, *J* = 7.8 Hz, 8-H), 7.33 (d, 1H, *J* = 10.0 Hz, 1-H), 7.36–7.39 (m, 6H, 2′, 6′, 2″, 6″, 2‴, 6‴-H), 7.52 (t, 1H, *J* = 7.8 Hz, 9-H), 7.62 (d, 1H, *J* = 9.2 Hz, 6-H), 8.04 (d, 1H, *J* = 7.8 Hz, 10-H), 8.70 (d, 2H, *J* = 5.7 Hz, 3‴, 5‴-H) ppm; ^{13}C NMR (100 MHz, $CDCl_3$) δ_C 55.3, 82.3, 113.4, 114.3, 118.9, 119.1, 122.1, 124.6, 125.0, 126.1, 126.6, 127.1, 128.4, 128.6, 130.3, 137.0, 138.0, 148.9, 149.7, 150.7, 159.0 ppm; HRMS (ESI) found $[M+H]^+$ = 472.1907 $C_{32}H_{25}NO_3$ requires $[M+H]^+$ = 472.1907.

3.2.1.5 Preparation of 5-Pyridyl-3*H*-Naphtho[2,1-*b*]pyrans

3.2.1.5.1 Experimental Procedure of the Synthesis of 5-Hydroxy-3-(2,4-dimethoxyphenyl)-3-(4-methoxyphenyl)-3*H*-naphtho[2,1-*b*]pyran (2.101): 1-(2,4-dimethoxyphenyl)-1-(4-methoxyphenyl)prop-2-yn-1-ol (18.65 g, 62.51 mmol) and 2,3-dihydroxynaphthalene (10.00 g, 62.43 mmol) in the presence of PPTS (0.78 g, 3.1 mmol) and trimethyl orthoformate (14.0 mL, 128 mmol) in 1,2-DCE (126 mL) was refluxed for 3 h under N_2 atmosphere. Solvent was removed under reduced pressure and the residue taken in EtOAc (200 mL), washed with water (2 × 150 mL) and the organic layer dried with anhydrous sodium sulfate. Subsequently, the residue (30 g) was purified in 10 g portions by flash column chromatography [Aldrich silica gel (60 Å 230-400 mesh

40-63 μm), eluent: 20% EtOAc in Petroleum Ether] giving the corresponding product as a red powder.

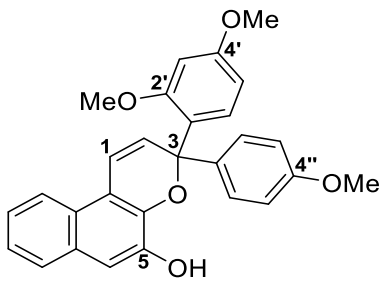

2.101

5-Hydroxy-3-(2,4-dimethoxyphenyl)-3-(4-methoxyphenyl)-3*H*-naphtho[2,1-*b*]pyran (2.101): red powder (9.91 g, 36%); m.p. = 69–73 °C; ν_{max} (neat) 3365 (br), 2930, 2834, 1606, 1508, 1452, 1247, 1206, 1173, 1028, 999, 831, 743 cm^{-1}; ^1H NMR (400 MHz, $CDCl_3$) δ_H 3.59 (3H, s, OMe), 3.77 (3H, s, OMe), 3.79 (3H, s, OMe), 6.14 (1H, bs, OH), 6.34 (1H, d, *J* = 10.1 Hz, 2-H), 6.43 (1H, dd, *J* = 8.5, 2.3 Hz, 5′-H), 6.46 (1H, d, *J* = 2.3 Hz, 3′-H), 6.84 (2H, d, *J* = 8.8 Hz, 3″, 5″-H, 7.18 (1H, s, 6-H), 7.23 (1H, d, *J* = 10.1 Hz, 1-H), 7.29–7.33 (4H, m, 2″, 6″, 8, 9-H), 7.44 (1H, d, *J* = 8.6 Hz, 6′-H), 7.26 (1H, d, *J* = 8.1 Hz, 7-H), 7.88 (1H, d, *J* = 8.1 Hz, 10-H) ppm; ^{13}C NMR (100 MHz, $CDCl_3$) δ_C 55.25, 55.34, 55.6, 82.8, 100.5, 103.6, 110.3, 113.3, 114.7, 118.7, 121.2, 123.4, 124.0, 124.2, 124.7, 127.2, 127.9, 128.37, 128.42, 129.8, 136.6, 140.1, 144.7, 157.7, 158.8, 160.9 ppm; HRMS (ESI) found $[M+H]^+$ = 441.1656 $C_{28}H_{24}O_5$ requires $[M+H]^+$ = 441.1697.

3.2.1.5.2 Experimental Procedure of the Synthesis of 3-(2,4-Dimethoxyphenyl)-3-(4-methoxyphenyl)-5-triflyloxy-3*H*-naphtho[2,1-*b*]pyran (2.104): triflic anhydride (1.1 mL, 6.5 mmol) was added dropwise to an aerated solution of 5-hydroxy-3-(2,4-dimethoxyphenyl)-3-(4-methoxyphenyl)-3*H*-naphtho[2,1-*b*]pyran (2.69 g, 6.11 mmol), Et_3N (1.9 mL, 14 mmol) in DCM at 0 °C. After stirring for 1 h at 0 °C, triflic anhydride (0.4 mL, 2.4 mmol) was added dropwise to force the reaction to completion. After stirring for 30 min at 0 °C, the organic phase was washed with HCl (1M, 50 mL). The phases were separated, the organic phase washed with a saturated solution of $NaHCO_3$ (100 mL), dried with anhydrous sodium sulfate and evaporated to dryness, giving the corresponding product as a red powder that was used in the next step without further purification.

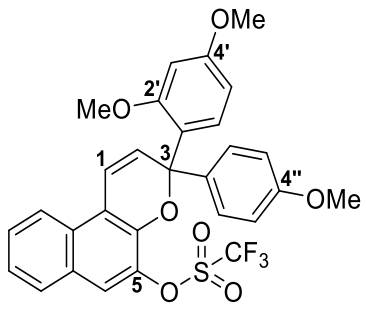

2.104

3-(2,4-Dimethoxyphenyl)-3-(4-methoxyphenyl)-5-triflyloxy-3*H*-naphtho[2,1-*b*]pyran (2.104): m.p. = 64–67 °C (darkened at 57 °C); ν_{max} (neat) 1418, 1245, 1204, 1173, 1135, 1103, 1022, 999, 889, 824, 806, 620 cm^{-1}; ^1H NMR (400 MHz, $CDCl_3$) δ_H 3.55 (3H, s, OMe), 3.75 (3H, s, OMe), 3.80 (3H, s, OMe), 6.44 (1H, d, *J* = 2.4 Hz, 3′-H), 6.53–6.57 (2H, m, 2, 5′-H), 6.78 (2H, d, *J* = 8.8 Hz, 3″, 5″-H), 7.24 (1H, d, *J* = 10.2 Hz, 1-H), 7.35–7.41 (3H, m, 2″, 6″, 8-H), 7.50–7.54 (2H, m, 6, 9-H), 7.71 (2H, app. d., *J* = 8.6 Hz, 7, 6′-H), 7.98 (1H, d, *J* = 8.5 Hz, 10-H) ppm; ^{13}C NMR (100 MHz, $CDCl_3$) δ_C 55.1, 55.3, 55.4, 82.9, 100.2, 103.8, 113.0, 117.4, 117.8, 120.1, 121.6, 124.2, 125.0, 127.5, 127.95, 128.01, 128.2, 128.58, 128.62, 129.2, 135.7, 138.1, 142.3, 156.9, 158.7, 160.7 ppm; ^{19}F NMR (376 MHz, $CDCl_3$) δ_F -73.8 ppm; HRMS (ESI) found $[M+H]^+$ = 573.1189 $C_{29}H_{23}F_3O_7S$ requires $[M+H]^+$ = 573.1163.

3.2.1.5.3 Suzuki cross-coupling reactions between 3-(2,4-dimethoxyphenyl)-3-(4-methoxyphenyl)-5-triflyloxy-3*H*-naphtho[2,1-*b*]pyran (2.104) and different boronic acids under multiple conditions (Table 2.2):

3.2.1.5.3.1 Entry 1 – A degassed mixture of 3-(2,4-dimethoxyphenyl)-3-(4-methoxyphenyl)-5-triflyloxy-3*H*-naphtho[2,1-*b*]pyran (2.50 g, 4.37 mmol), 4-pyridineboronic acid pinacol ester (1.34 g, 6.55 mmol), KF (0.38 g, 6.6 mmol), $Pd(PPh_3)_4$ (0.25 g, 0.22 mmol) in PhMe (52.0 mL) and EtOH (52.0 mL) was refluxed under N_2 for 23 h. ^1H NMR analysis had shown that the reaction afforded a mixture of 5-(4-pyridyl)-3*H*-naphtho[2,1-*b*]pyran **2.106**:naphthofuran **2.107** (90:10).

3.2.1.5.3.2 Entry 2 – 3-(2,4-Dimethoxyphenyl)-3-(4-methoxyphenyl)-5-triflyloxy-3*H*-naphtho[2,1-*b*]pyran (200.5 mg, 0.3502 mmol), 4-pyridineboronic acid pinacol ester (107.9 mg, 0.5262 mmol), KF (66.8 mg, 1.15 mmol) and $Pd(OAc)_2$ (4.2 mg, 0.019 mmol) were added to a dry 25 mL two-neck round-bottom flask. Once the air was evacuated and the flask flushed with N_2, anhydrous THF (6 mL) was added and the mixture degassed for 30 min. PCy_3 (5.8 mg, 0.021 mmol) was added to a dry 10 mL round-bottom flask. Once the air was evacuated and the latter flask flushed with N_2, anhydrous THF (3 mL) was added and the mixture degassed for 30 min. Subsequently, the PCy_3 solution was transferred to the former mixture by cannulation. The resulting mixture was stirred at

room temperature under N_2 in the dark. After 4h, the reaction was stopped. TLC analysis had shown no reaction.

3.2.1.5.3.3 Entry 3 – 3-(2,4-Dimethoxyphenyl)-3-(4-methoxyphenyl)-5-triflyloxy-3*H*-naphtho[2,1-*b*]pyran (199.5 mg, 0.3484 mmol), benzeneboronic acid (65.0 mg, 0.533 mmol), $PdCl_2$ (4.5 mg, 0.025 mmol), KF (66.9 mg, 1.15 mmol) were added to a dry 25 mL two-neck round-bottom flask. The flask was then sealed, the air evacuated and flushed with N_2. Anhydrous DMAc (4.0 mL) was added and the mixture degassed for 30 min. PCy_3 (14.5 mg, 0.0517 mmol) was added to a dried 25 mL round-bottom flask. The latter flask was then sealed, the air evacuated and flushed with N_2. Anhydrous DMAc (4.0 mL) was then added to the latter and the mixture degassed for 30 min. The latter was added to the former by cannulation and the mixture stirred for 5 days at 38 °C in the dark under N_2. After this time, water was added (100 mL), the residue extracted with EtOAc (4 × 75 mL), dried with anhydrous sodium sulfate and evaporated to dryness (0.21 g). The resulting residue was purified by flash column chromatography [Aldrich silica gel (60 Å 230-400 mesh 40-63 μm), eluent: 10% EtOAc in hexanes, fraction 1] giving the corresponding product.

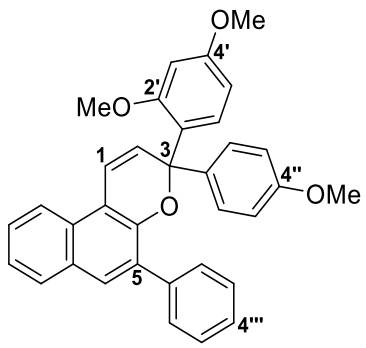

2.108

3-(2,4-Dimethoxyphenyl)-3-(4-methoxyphenyl)-5-phenyl-3*H*-naphtho[2,1-*b*]pyran (2.108): red powder (44.0 mg, 25%); m.p. = 56–60 °C; ν_{max} (neat) 1606, 1504, 1247, 1206, 1172, 1030, 1000, 829, 804, 763, 746, 698 cm^{-1}; ^1H NMR (400 MHz, $CDCl_3$) δ_H 3.46 (3H, s, OMe), 3.718 (3H, s, OMe), 3.724 (3H, s, OMe), 6.35–6.37 (2H, m, 3′, 5′-H), 6.51 (1H, d, *J* = 10.0 Hz, 2-H), 6.70 (2H, app. d, *J* = 8.8 Hz, 3″, 5″-H), 7.23–7.47 (9H, m, 1-H, Ar-H), 7.55–7.57 (2H, m, Ar-H), 7.65 (1H, s, 6-H), 7.72 (1H, d, *J* = 8.0 Hz, 7-H), 7.98 (1H, d, *J* = 8.4 Hz, 9-H) ppm; ^{13}C NMR (100 MHz, $CDCl_3$) δ_C 55.1, 55.27, 55.30, 81.5, 100.0, 103.6, 112.8, 115.0, 119.1, 121.3, 123.8, 125.2, 126.3, 127.1, 127.4, 127.7, 127.8, 128.2, 128.5, 129.0, 129.3, 129.7, 129.9, 131.6, 136.4, 138.1, 147.8, 156.8, 158.4, 160.2 ppm; HRMS (ESI) found $[M+H]^+$ = 501.2025 $C_{34}H_{28}O_4$ requires $[M+H]^+$ = 501.2060.

3.2.1.5.3.4 Entry 4 – 3-(2,4-Dimethoxyphenyl)-3-(4-methoxyphenyl)-5-triflyloxy-3*H*-naphtho[2,1-*b*]pyran (200.6 mg, 0.3504 mmol), 4-pyridineboronic acid pinacol ester (107.8 mg, 0.5257 mmol), KF (69.6 mg, 1.20 mmol) and $PdCl_2$ (4.8 mg, 0.027 mmol) were added to a dry 25 mL two-neck round-bottom flask. Once the air was evacuated and the flask flushed with N_2, anhydrous DMAc (4.0 mL) was added and the mixture degassed for 30 min. PCy_3 (14.5 mg, 0.0517 mmol) was added to a dry 25 mL round-bottom flask. Once the air was evacuated and the latter flask flushed with N_2, anhydrous DMAc (4.0 mL) was added and the mixture degassed for 30 min. Subsequently, the PCy_3 solution was transferred to the former mixture by cannulation. The resulting mixture was stirred at 38 °C under N_2 in the dark. After 16 h, the reaction was stopped. TLC analysis had shown no reaction.

3.2.1.5.3.5 Entry 5 – 3-(2,4-Dimethoxyphenyl)-3-(4-methoxyphenyl)-5-triflyloxy-3*H*-naphtho[2,1-*b*]pyran (199.9 mg, 0.3491 mmol), 4-pyridineboronic acid pinacol ester (65.2 mg, 0.530 mmol), KF (67.0 mg, 1.15 mmol) and $PdCl_2$ (4.2 mg, 0.024 mmol) were added to a dry 25 mL two-neck round-bottom flask. Once the air was evacuated and the flask flushed with N_2, anhydrous DMAc (10.0 mL) was added and the mixture degassed for 30 min. PCy_3 (14.6 mg, 0.0521 mmol) was added to a dry 25 mL round-bottom flask. Once the air was evacuated and the latter flask flushed with N_2, anhydrous DMAc (2.0 mL) was added and the mixture degassed for 15 min. Subsequently, the PCy_3 solution was transferred to the former mixture by cannulation. The resulting mixture was stirred at 38 °C under N_2 in the dark. After 23 h, the reaction was stopped. TLC analysis had shown no reaction.

3.2.1.5.3.6 Entry 6 – 3-(2,4-Dimethoxyphenyl)-3-(4-methoxyphenyl)-5-triflyloxy-3*H*-naphtho[2,1-*b*]pyran (199.4 mg, 0.3483 mmol), 4-pyridineboronic acid pinacol ester (86.5 mg, 0.422 mmol), K_3PO_4 (128.2 mg, 0.6039 mmol), $Pd(PPh_3)_4$ (21.0 mg, 0.0182 mmol) were added to a dry 25 mL two-neck round-bottom flask. Once the air was evacuated and the flask flushed with N_2, anhydrous DMAc (3.0 mL) was added. The mixture was degassed for 15 min and then stirred at 110 °C under N_2. After 3 h, the reaction was stopped. ^{1}H NMR analysis had shown that the reaction afforded a mixture of 5-(4-pyridyl)-3*H*-naphtho[2,1-*b*]pyran **2.106**:naphthofuran **2.107** (9:89).

3.2.1.5.3.7 Entry 7 – 3-(2,4-Dimethoxyphenyl)-3-(4-methoxyphenyl)-5-triflyloxy-3*H*-naphtho[2,1-*b*]pyran (500.0 mg, 0.8733 mmol), 4-pyridineboronic acid pinacol ester (196.9 mg, 0.9602 mmol), K_3PO_4 (213.1 mg, 1.004 mmol), $Pd(PPh_3)_4$ (50.5 mg, 0.0437 mmol) were added to a dry 25 mL two-neck round-bottom flask. Once the air was evacuated and the flask flushed with N_2, anhydrous DMAc (7.5 mL) was added. The mixture was degassed for 15 min and then stirred at 110 °C under N_2. After 20 min of reaction, the crude was poured into water (50 mL) and the residue extracted

with DCM (4 × 50 mL). The organic phase was washed with water (2 × 100 mL), dried with anhydrous sodium sulfate and evaporated to dryness. The resulting red oil was purified by flash column chromatography [Aldrich silica gel (60 Å 230-400 mesh 40-63 μm), eluent: 50% EtOAc in hexanes] giving the corresponding product as a red powder.

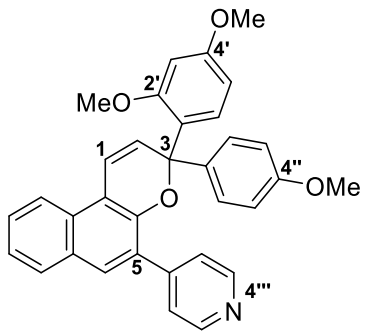

2.106

3-(2,4-Dimethoxyphenyl)-3-(4-methoxyphenyl)-5-(4-pyridyl)-3*H*-naphtho[2,1-*b*]pyran (2.106): red powder (225.2 mg, 51%); m.p. = 74–77 °C; ν_{max} (neat) 1605, 1506, 1461, 1246, 1172, 1030, 1000, 824, 747 cm^{-1}; ^{1}H NMR (400 MHz, $CDCl_3$) δ_H 3.45 (3H, s, OMe), 3.749 (3H, s, OMe), 3.753 (3H, s, OMe), 6.37–6.40 (2H, m, 3′, 5′-H), 6.49 (1H, d, *J* = 10.1 Hz, 2-H), 6.74 (2H, d, *J* = 6.8 Hz, 3″, 5″-H), 7.19–7.26 (2H, m, 2″, 6″-H), 7.31–7.37 (3H, m, 1, 8, 6′-H), 7.49–7.53 (3H, m, 9, 2‴, 6‴-H), 7.68 (1H, s, 7-H), 7.75 (1H, d, *J* = 8.0 Hz, 7-H), 8.01 (1H, d, *J* = 8.5 Hz, 10-H), 8.65 (2H, d, *J* = 6.0 Hz, 3‴, 5‴-H); ^{13}C NMR (100 MHz, $CDCl_3$) δ_C 55.1, 55.2, 55.3, 81.9, 100.1, 103.6, 112.9, 115.2, 118.8, 121.4, 124.1, 124.6, 127.1, 127.8, 128.0, 128.2, 128.6, 128.75, 128.84, 129.1, 129.7, 129.9, 136.1, 146.0, 147.4, 149.4, 156.9, 158.6, 160.4 ppm; HRMS (ESI) found $[M+H]^+$ = 502.1991 $C_{33}H_{27}NO_4$ requires $[M+H]^+$ = 502.2013.

3.2.1.6 Preparation of 8-(Pyridyl-triazole)-3*H*-Naphtho[2,1-*b*]pyran

3.2.1.6.1 Experimental Procedure for the Synthesis of 4-Bromo-2-((trimethylsilyl)ethynyl)pyridine (2.112):

Method A – A degassed solution of TMS-acetylene (0.88 mL, 6.4 mmol), 2,4-dibromopyridine (1.00 g, 4.22 mmol), *i*-Pr_2NH (0.59 mL, 4.2 mmol), $Pd(OAc)_2$ (0.05 g, 0.2 mmol), PPh_3 (0.11 g, 0.42 mmol), CuI (0.04 g, 0.2 mmol) in anhydrous MeCN (21.0 mL) was refluxed under N_2. After 1 day, the solvent was removed under reduced pressure. The reaction mixture was dissolved in DCM (100 mL), washed with water (2 × 100 mL), dried with anhydrous sodium sulfate and evaporated to dryness. The resulting residue was filtered through a plug of silica [Fluorochem silica gel (60 Å, 40-63 μm), eluent: PhMe (100%)] giving the corresponding product that was used in the next step without further purification.

Method B – A degassed mixture of 2,4-dibromopyridine (10.00 g, 42.21 mmol), TMS acetylene (12.0 mL, 86.6 mmol), $Pd(PPh_3)_2Cl_2$ (0.31 g, 0.44 mmol), PPh_3 (1.66 g, 6.33 mmol), CuI (0.60 g, 3.2 mmol) in Et_3N (65.0 mL; freshly distilled from NaH) was heated at reflux for 7 h under N_2. After this time, the crude was filtered and evaporated to dryness. The residue was dissolved in EtOAc (100 mL), washed with water (2 × 100 mL), dried with anhydrous sodium sulfate and evaporated to dryness. Flash column chromatography: 1st – [Aldrich silica gel (60 Å, 40-63 μm), eluent: 50% PhMe in hexanes → PhMe]; 2nd – [Aldrich silica gel (60 Å, 40-63 μm), eluent: 20% Et_2O in hexanes] gave 4-bromo-2-((trimethylsilyl)ethynyl)pyridine as a yellow oil.

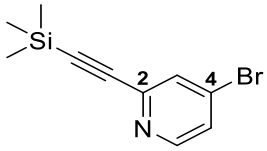

2.112

4-Bromo-2-((trimethylsilyl)ethynyl)pyridine (2.112): yellow oil (0.25 g, 23%) from method A; yellow oil (4.79 g, 45%) from method B; ν_{max} (neat) 1557, 1537, 1452, 1368, 1249, 876, 837, 759, 693, 657 cm^{-1}; ^1H NMR (400 MHz, $CDCl_3$) δ_H 0.27 (9H, s, $Si(CH_3)_3$), 7.42 (1H, dd, J = 1.8, 5.4 Hz, 5-H), 7.65 (1H, d, J = 1.8 Hz, 3-H), 8.38 (1H, d, J = 5.4 Hz, 6-H) ppm; ^{13}C NMR (100 MHz, $CDCl_3$) δ_C -0.0018, 97.1, 102.6, 126.8, 130.8, 133.0, 144.5, 150.8 ppm; HRMS (ESI) found $[M+H]^+$ = 253.9999 $C_{10}H_{12}{}^{79}BrNSi$ requires $[M+H]^+$ = 253.9995.

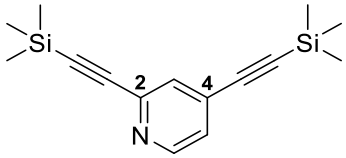

2.115

2,4-Bis((trimethylsilyl)ethynyl)pyridine (2.115): yellow oil (0.67 g, 6%) from method B; ν_{max} (neat) 1583, 1531, 1460, 1379, 1249, 1162, 945, 836, 758, 700, 662, 649 cm^{-1}; ^1H NMR (400 MHz, $CDCl_3$) δ_H 0.25 (9H, s, $Si(CH_3)_3$), 0.26 (9H, s, $Si(CH_3)_3$), 7.22 (1H, d, J = 1.5, 5.1 Hz, 5-H), 7.49 (1H, app. s, 3-H), 8.50 (1H, d, J = 5.1 Hz, 6-H) ppm; ^{13}C NMR (100 MHz, $CDCl_3$) δ_C -0.36, -0.32, 95.6, 100.8, 101.2, 103.0, 124.9, 129.5, 131.6, 143.1, 149.9 ppm; HRMS (ESI) found $[M+H]^+$ = 272.1292 $C_{15}H_{21}NSi_2$ requires $[M+H]^+$ = 272.1285.

3.2.1.6.2 Experimental Procedure for the Synthesis of (Azidomethyl)benzene (2.113): NaN_3 (6.56 g, 101 mmol) was added slowly to a solution of benzyl bromide (8.00 mL, 67.3 mmol) in acetone:water (8.0:20.0 mL) and stirred at 45 °C. After 30 h, the acetone was removed and water (50 mL) was added. The aqueous phase was extracted with Et_2O (3 × 50 mL), washed with brine

(50 mL), dried with anhydrous sodium sulfate and evaporated to dryness. The corresponding product was obtained as a colourless oil and was used in the following step without further purification.

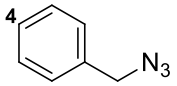

2.113

(Azidomethyl)benzene (2.113): colourless oil (8.08 g, 90%); ν_{max} (neat) 2090, 1496, 1455, 1349, 1252, 1201, 875, 735, 696, 567 cm^{-1}; ^{1}H NMR (400 MHz, $CDCl_3$) δ_H 4.33 (2H, s, CH_2), 7.24–7.41 (5H, m, Ph-H) ppm; ^{13}C NMR (100 MHz, $CDCl_3$) δ_C 54.8, 128.26, 128.35, 128.9, 135.4 ppm.

3.2.1.6.3 Experimental Procedure for the Synthesis of 2-(1-Benzyl-1*H*-1,2,3-triazol-4-yl)-4-bromopyridine (2.111): 4-bromo-2-((trimethylsilyl)ethynyl)pyridine (3.01 g, 11.8 mmol), (azidomethyl)benzene (1.58 g, 11.9 mmol), K_2CO_3 (1.96 g, 14.2 mmol), $CuSO_4.5H_2O$ (1.47 g, 5.89 mmol), ascorbic acid (2.08 g, 11.8 mmol), *t*-BuOH (60.0 mL), pyridine (9.0 mL) in THF (180 mL) and water (180 mL) were stirred for 23 h – reaction mixture colour changed from orange to turquoise. After this time, the organic solvent was evaporated under reduced pressure. Afterwards, $CHCl_3$ (450 mL) and conc. NH_3 (36 mL, 25% w/w) were added, and the mixture stirred rapidly for 1 h. Subsequently, the phases were separated, the yellow organic phase washed with diluted NH_3 (100 mL, 10% w/w), brine (2 × 200 mL), dried with anhydrous sodium sulfate and evaporated to dryness. Crystallization from EtOH at -20 °C gave the corresponding product in very good yield as an off-white crystalline solid.

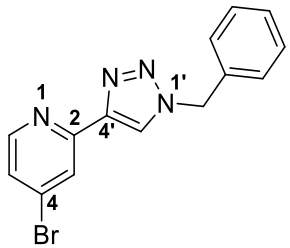

2.111

2-(1-Benzyl-1*H*-1,2,3-triazol-4-yl)-4-bromopyridine (2.111): off-white crystalline solid (3.00 g, 81%); m.p. = 81–83 °C; ν_{max} (neat) 1582, 1456, 1344, 1071, 1039, 817, 753, 698, 678 cm^{-1}; ^{1}H NMR (400 MHz, $CDCl_3$) δ_H 5.59 (2H, s, CH_2), 7.32–7.42 (6H, m, 5, Ph-H), 8.03 (1H, s, 5′-H), 8.34 (1H, d, J = 5.3 Hz, 6-H), 8.38 (1H, d, J = 1.6 Hz, 3-H) ppm; ^{13}C NMR (100 MHz, $CDCl_3$) δ_C 54.5, 122.4, 123.6, 126.1, 128.4, 129.0, 129.3, 133.7, 134.2, 147.5, 150.1, 151.4 ppm; HRMS (ESI) found $[M+H]^+$ = 315.0216 $C_{14}H_{11}{}^{79}BrN_4$ requires $[M+H]^+$ = 315.0240.

3.2.1.6.4 Experimental Procedure for the Synthesis of 2-(1-Benzyl-1*H*-1,2,3-triazol-4-yl)-4-(3,3-bis(4-methoxyphenyl)-3*H*-benzo[*f*]chromen-8-yl)pyridine (2.110): $Pd(PPh_3)_4$ (0.09 g, 0.1 mmol) was added to a degassed mixture of 2-(1-benzyl-1*H*-1,2,3-triazol-4-yl)-4-bromopyridine (0.50 g, 1.6 mmol), 2-(3,3-bis(4-methoxyphenyl)-3*H*-benzo[*f*]chromen-8-yl)-4,4,5,5-tetramethyl-1,3,2-dioxaborolane (0.91 g, 1.7 mmol), K_2CO_3 (0.33 g, 2.4 mmol) in PhMe (19.0 mL) and EtOH (19.0 mL), and refluxed for 13 h under N_2. After this time, the crude was evaporated to dryness, dissolved in EtOAc (100 mL) and filtered through a plug of celite. The organic phase was then reduced to 100 mL, washed with brine (2 × 100 mL), dried with anhydrous sodium sulfate and evaporated to dryness. The resulting brown foam was purified by flash column chromatography [Aldrich silica gel (60 Å 230-400 mesh 40-63 μm), eluent: 20% EtOAc in hexanes → 50% EtOAc in hexanes]. In order to separate the naphthopyran from the naphthofuran, the obtained red residue was purified again by flash column chromatography [Aldrich silica gel (60 Å 230-400 mesh 40-63 μm), eluent: Et_2O (100%); 1 g sample: 150 g SiO_2]. Successive triturations from cold Et_2O:hexane (1:1) – to remove the BHT from the sample – gave the corresponding product.

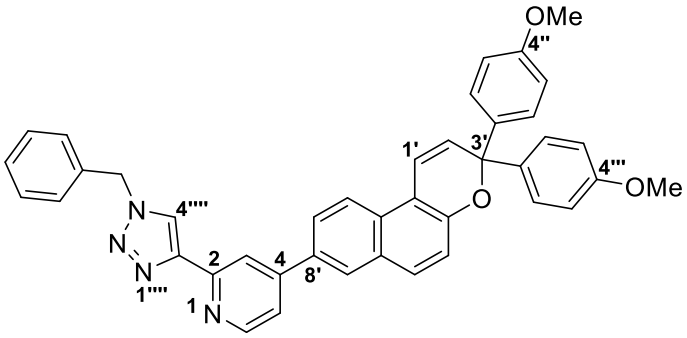

2.110

Fraction 2 – 2-(1-Benzyl-1*H*-1,2,3-triazol-4-yl)-4-(3,3-bis(4-methoxyphenyl)-3*H*-benzo[*f*]chromen-8-yl)pyridine (2.110): pink powder (0.31 g, 31%); m.p. = 107–111 °C; ν_{max} (neat) 1605, 1506, 1246, 1172, 1089, 1031, 1000, 810, 716, 592 cm^{-1}; Photomerocyanine λ_{max} = 480 nm (PhMe); ^1H NMR (400 MHz, $CDCl_3$) δ_H 3.77 (6H, s, OMe), 5.60 (2H, s, CH_2), 6.25 (1H, d, *J* = 9.9 Hz, 2′-H), 6.86 (4H, d, *J* = 8.6 Hz, 3″, 3‴, 5″, 5‴-H), 7.22–7.41 (11H, m, 1′, 5′, 2″, 2‴, 6″, 6‴, Ph-H), 7.53 (1H, d, *J* = 3.9 Hz, 5-H), 7.74 (1H, d, *J* = 8.8 Hz, 6′-H), 7.84 (1H, d, *J* = 8.6 Hz, 9′-H), 8.05–8.12 (3H, m, 3, 7′, 10′-H), 8.55–8.59 (2H, m, 6, 4⁗-H) ppm; ^{13}C NMR (100 MHz, $CDCl_3$) δ_C 54.5, 55.3, 82.5, 113.5, 113.9, 117.9, 118.9, 119.3, 120.6, 122.1, 122.4, 125.1, 127.2, 128.4, 128.5, 128.9, 129.2, 129.3, 130.0, 130.4, 132.7, 134.3, 137.0, 148.8, 149.0, 149.9, 150.7, 151.5, 159.0 ppm; HRMS (ESI) found $[M+H]^+$ = 629.2547 $C_{41}H_{32}N_4O_3$ requires $[M+H]^+$ = 629.2547.

3.2.2 Strategy B – By a Heck cross-coupling reaction protocol

3.2.2.1 Preparation of 3-Pyridyl-3*H*-Naphtho[2,1-*b*]pyrans

3.2.2.1.1 Experimental Procedure for the Synthesis of 1-Phenyl-1-(4-pyridyl)prop-2-en-1-ol (2.126): vinylmagnesium chloride [1.6 M in THF] (56.0 mL, 89.6 mmol) was added to a mixture of phenyl(pyridin-4-yl)methanone (98%) (8.00 g, 42.8 mmol) under N_2 in anhydrous THF (200 mL) at such a rate that the temperature did not rise above 0 °C. The resulting mixture was stirred for 30 min at this temperature and then allowed to reach room temperature. After stirring for 3 h, the reaction was quenched by the addition of a saturated aqueous solution of NH_4Cl (65 mL), after which THF was evaporated under reduced pressure. The aqueous layer was extracted with EtOAc (2 × 200 mL). The organic phase was reduced to 200 mL, washed with water (3 × 200 mL), dried with anhydrous sodium sulfate and evaporated to dryness. The desired product was obtained by crystallization from an EtOAc/hexane mixture.

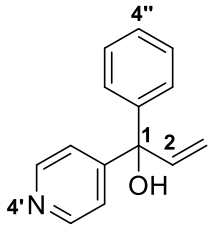

2.126

1-Phenyl-1-(4-pyridyl)prop-2-en-1-ol (2.126): brown microcrystals (7.76 g, 86%); m.p. = 131–133 °C [lit. m.p. = 135–137 °C[244]]; ν_{max} (neat) 3061 (br), 2795 (br), 1597, 1488, 1446, 1223, 1194, 1004, 919, 764, 694 cm^{-1}; ^1H NMR (400 MHz, Acetone-d_6) δ_H 5.26 (1H, s, OH), 5.29–5.35 (2H, m, 3-H_{cis}, 3-H_{trans}), 6.59 (1H, dd, J = 17.0, 10.6 Hz, 2-H), 7.23–7.27 (1H, m, 4″-H), 7.30–7.34 (2H, m, 3″, 5″-H), 7.36–7.42 (4H, m, 2′, 6′, 2″, 6″-H), 8.47–8.49 (2H, m, 3′, 5′-H) ppm; ^{13}C NMR (100 MHz, Acetone-d_6) δ_C 77.9, 113.8, 121.6, 126.9, 127.2, 128.0, 143.1, 145.7, 149.4, 155.3 ppm; HRMS (ESI) found $[M+H]^+$ = 212.1077 $C_{14}H_{13}NO$ requires $[M+H]^+$ = 212.1070.

3.2.2.1.2 Experimental Procedure for the Synthesis of 1,1-Bis(4-methoxyphenyl)prop-2-en-1-ol (2.129): vinylmagnesium chloride [1.6 M in THF] (42.0 mL, 67.2 mmol) was added dropwise to a mixture of bis(4-methoxyphenyl)methanone (8.00 g, 33.0 mmol) in anhydrous THF (160 mL) at 0 °C under N_2. The resulting mixture was stirred for 30 min at this temperature and then allowed to reach room temperature. After stirring for 2 h, the reaction was quenched by the addition of a saturated aqueous solution of NH_4Cl (50 mL), after which THF was evaporated under reduced pressure. The aqueous layer was extracted with EtOAc (2 × 100 mL). The organic phase was

reduced to 100 mL, washed with water (4 × 100 mL), dried with anhydrous sodium sulfate and evaporated to dryness. The resulting crude allyl alcohol was obtained as a pale yellow oil and was used in the next step without further purification.

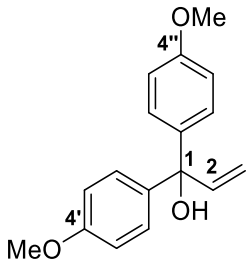

2.129

1,1-Bis(4-methoxyphenyl)prop-2-en-1-ol (2.129): pale yellow oil (8.87 g, 99%); ν_{max} (neat) 3486 (br), 2955, 2835, 1607, 1582, 1506, 1462, 1299, 1242, 1172, 1030, 826 cm^{-1}; ^1H NMR (400 MHz, $CDCl_3$) δ_H 2.24 (s, 1H, OH), 3.79 (6H, s, OMe), 5.25–5.30 (2H, m, 3-H_{cis}, 3-H_{trans}), 6.45 (1H, dd, *J* = 17.0, 10.6 Hz, 2-H), 6.82–6.87 (4H, m, 3′, 3″, 5′, 5″-H), 7.25–7.30 (4H, m, 2′, 2″, 6′, 6″-H) ppm; ^{13}C NMR (100 MHz, $CDCl_3$) δ_C 55.3, 78.9, 113.4, 128.2, 138.2, 143.9, 158.7 ppm; HRMS (ESI) found $[M+Na]^+$ = 293.1142 $C_{17}H_{18}O_3$ requires $[M+Na]^+$ = 293.1148.

3.2.2.1.3 Attempted Heck cross-coupling reactions between 1-bromo-2-naphthol (2.137) and different Heck partners under multiple conditions (Table 2.3):

3.2.2.1.3.1 Entry 1 – 1-bromo-2-naphthol (0.30 g, 1.3 mmol), 1-phenyl-1-(4-pyridyl)prop-2-en-1-ol (0.62 g, 2.9 mmol), TBAB (1.47 g, 4.56 mmol), $NaHCO_3$ (0.38 g, 4.5 mmol), $Pd(OAc)_2$ (0.03 g, 0.1 mmol) were added to a dry 50 mL two-neck round-bottom flask. Once the air was evacuated and the flask flushed with N_2, anhydrous DMF (10.0 ml) was added and the mixture degassed for 30 min. Subsequently, the mixture was stirred at 90 °C under N_2 for 24 h. ^1H NMR analysis had shown no reaction.

3.2.2.1.3.2 Entry 2 – 1-bromo-2-naphthol (200.5 mg, 0.8988 mmol), 1-phenyl-1-(4-pyridyl)prop-2-en-1-ol (246.3 mg, 1.166 mmol), PPh_3 (8.2 mg, 0.031 mmol), $Pd(OAc)_2$ (6.5 mg, 0.027 mmol) were added to a dry 25 mL two-neck round-bottom flask. Once the air was evacuated and the flask flushed with N_2, previously dried Et_3N (0.29 mL, 2.1 mmol) and anhydrous MeCN (2.5 mL) were added and the mixture degassed for 20 min. Subsequently, the mixture was stirred at reflux under N_2 for 21 h. ^1H NMR analysis had shown no reaction.

3.2.2.1.3.3 Entry 3 – 1-bromo-2-naphthol (200.4 mg, 0.8984 mmol), 1-phenyl-1-(4-pyridyl)prop-2-en-1-ol (246.9 mg, 1.169 mmol), Cs_2CO_3 (292.1 mg, 0.8965 mmol) and $Pd(OAc)_2$ (16.3 mg, 0.0726

mmol) were added to a dry 25 mL two-neck round-bottom flask. Once the air was evacuated and the flask flushed with N_2, anhydrous MeCN (2.5 mL) was added and the mixture degassed for 20 min. Subsequently, the mixture was stirred at reflux under N_2 for 16 h. ^{1}H NMR analysis had shown no reaction.

3.2.2.1.3.4 Entry 4 – 1-bromo-2-naphthol (200.7 mg, 0.8997 mmol), 1,1-bis(4-methoxyphenyl)prop-2-en-1-ol (329.0 mg, 1.217 mmol), PPh_3 (8.6 mg, 0.033 mmol), $Pd(OAc)_2$ (6.1 mg, 0.027 mmol) were added to a dry 25 mL two-neck round-bottom flask. Once the air was evacuated and the flask flushed with N_2, previously dried Et_3N (0.29 mL, 2.1 mmol) and anhydrous MeCN (2.5 mL) were added and the mixture degassed for 20 min. Subsequently, the mixture was stirred at reflux under N_2 for 25 h. ^{1}H NMR analysis had shown no reaction.

3.2.2.1.3.5 Entry 5 – 1-bromo-2-naphthol (200.8 mg, 0.9002 mmol), 4-methoxystyrene (157.8 mg, 1.176 mmol), PPh_3 (8.6 mg, 0.033 mmol), $Pd(OAc)_2$ (6.5 mg, 0.029 mmol) were added to a dry 25 mL two-neck round-bottom flask. Once the air was evacuated and the flask flushed with N_2, previously dried Et_3N (0.29 mL, 2.1 mmol) and anhydrous MeCN (2.5 mL) were added and the mixture degassed for 20 min. Subsequently, the mixture was stirred at reflux under N_2 for 16 h. ^{1}H NMR analysis had shown no reaction.

3.2.2.1.4 Experimental Procedure for the Synthesis of 1-Iodo-2-naphthol (2.143): H_2SO_4 (95%, 1.8 mL, 32 mmol) was dissolved in MeOH (108 mL) at 0 °C. 2-Naphthol (3.00 g, 20.8 mmol) and KI (3.45 g, 20.8 mmol) were added and stirred for 5 min. Subsequently, H_2O_2 (35%, 3.6 mL, 42 mmol) was added under N_2 at such a rate the temperature did not rise over 0 °C. The reaction mixture was stirred for 1 h at 0 °C, heated to room temperature and left stirring for 14 h under N_2. After this time, the crude was diluted with DCM (200 mL), washed with 0.1 M $NaHSO_3$ (200 mL) and water (2 × 200 mL). Subsequently, the organic phase was dried with anhydrous sodium sulfate and evaporated to dryness, giving the desired product as a brown powder (5.43 g). The latter was crystallized from a DCM/hexane mixture as brown needles.

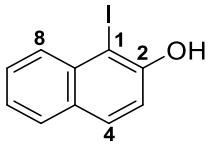

2.143

1-Iodo-2-naphthol (2.143): brown needles (5.19 g, 92%); m.p. = 47–51 °C; ν_{max} (neat) 3230 (br), 1621, 1593, 1495, 1429, 1345, 1207, 1190, 912, 806, 744 cm^{-1}; ^{1}H NMR (400 MHz, $CDCl_3$) δ_H 5.78 (1H, s, OH), 7.25 (1H, d, J = 8.8 Hz, 3-H), 7.36–7.39 (1H, m, 6-H), 7.52–7.56 (1H, m, 7-H),

7.72–7.75 (2H, m, 4, 5-H), 7.92 (1H, d, J = 8.5 Hz, 8-H) ppm; ^{13}C NMR (100 MHz, $CDCl_3$) δ_C 86.3 (C-1), 116.5, 124.2, 128.2, 128.3, 129.7, 130.3, 130.6, 134.8, 153.8 ppm; HRMS (ESI) found $[M+H]^+$ = 268.9458 $C_{10}H_7IO$ requires $[M+H]^+$ = 268.9469.

3.2.2.1.5 Attempted Heck cross-coupling reactions between 1-iodo-2-naphthol (2.143) and different Heck partners under multiple conditions (Table 2.4):

3.2.2.1.5.1 Entry 1 – 1-iodo-2-naphthol (200.0 mg, 0.7405 mmol), 1-phenyl-1-(4-pyridyl)prop-2-en-1-ol (340.5 mg, 0.9634 mmol), Cs_2CO_3 (241.8 mg, 0.7421 mmol) and $Pd(OAc)_2$ (13.7 mg, 0.0610 mmol) were added to a dry 50 mL two-neck round-bottom flask. Once the air was evacuated and the flask flushed with N_2, anhydrous MeCN (10.0 mL) was added and the mixture degassed for 20 min. Subsequently, the mixture was stirred at reflux under N_2 for 15 h. ^{1}H NMR analysis had shown no reaction.

3.2.2.1.5.2 Entry 2 – 1-iodo-2-naphthol (200.3 mg, 0.7417 mmol), 1-phenyl-1-(4-pyridyl)prop-2-en-1-ol (340.5 mg, 0.9634 mmol), Cs_2CO_3 (241.3 mg, 0.7406 mmol), $Pd(OAc)_2$ (13.8 mg, 0.0615 mmol) and TBAB (238.9 mg, 0.7411 mmol) were added to a dry 50 mL two-neck round-bottom flask. Once the air was evacuated and the flask flushed with N_2, anhydrous MeCN (10.0 mL) was added and the mixture degassed for 20 min. Subsequently, the mixture was stirred at reflux under N_2 for 15h. ^{1}H NMR analysis had shown no reaction.

3.2.2.1.5.3 Entry 3 – 1-iodo-2-naphthol (200.1 mg, 0.7409 mmol), 1,1-bis(4-methoxyphenyl)prop-2-en-1-ol (276.6 mg, 1.023 mmol), Cs_2CO_3 (241.3 mg, 0.7406 mmol) and $Pd(OAc)_2$ (13.8 mg, 0.0615 mmol) were added to a dry 50 mL two-neck round-bottom flask. Once the air was evacuated and the flask flushed with N_2, anhydrous MeCN (10.0 mL) was added and the mixture degassed for 20 min. Subsequently, the mixture was stirred at reflux under N_2 for 28 h. Afterwards, the crude was diluted with DCM (100 mL), passed through celite, washed with water (3 × 200 mL), dried with anhydrous Na_2SO_4 and evaporated to dryness. The reaction mixture was purified by flash column chromatography [Fluorochem silica gel (60 Å, 40-63 μm), eluent: 10% EtOAc in hexanes, fraction 3], leading to the corresponding product as a brown powder.

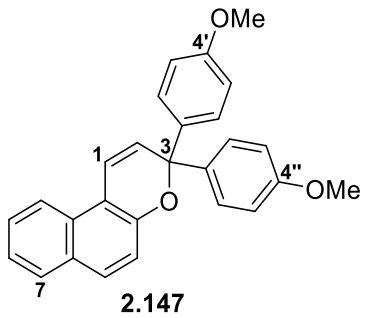

2.147

3,3-Bis(4-methoxyphenyl)-3*H*-naphtho[2,1-*b*]pyran (2.147): from method C as a brown powder (8.3 mg, 3%); m.p. = 174–177 °C; ν_{max} (neat) 1508, 1247, 1174, 1029, 1000, 827, 813, 805, 746, 724, 590 cm^{-1}; ^1H NMR (400 MHz, $CDCl_3$) δ_H 3.77 (6H, s, OMe), 6.20 (1H, d, *J* = 9.9 Hz, 2-H), 6.84 (4H, app. d, *J* = 8.7 Hz, 3′, 3″, 5′, 5″-H), 7.16 (1H, d, *J* = 8.8 Hz, Ar-H), 7.24–7.32 (2H, m, 1-H, Ar-H), 7.38 (4H, app. d, *J* = 8.7 Hz, 2′, 2″, 6′, 6″-H), 7.45 (1H, t, *J* = 7.6 Hz, Ar-H), 7.64 (1H, d, *J* = 8.8 Hz, Ar-H), 7.71 (1H, d, *J* = 8.2 Hz, Ar-H), 7.95 (1H, d, *J* = 8.5 Hz, Ar-H) ppm; HRMS (ESI) found $[M+H]^+$ = 395.1649 $C_{27}H_{22}O_3$ requires $[M+H]^+$ = 395.1642.

3.2.2.1.6 Experimental Procedure for the Synthesis of 2-Acetoxy-1-bromonaphthalene (2.149): acetic anhydride (1.4 mL, 15 mmol) was added dropwise at 0 °C under N_2 to a solution of 1-bromo-2-naphthol (3.00 g, 13.4 mmol) and Et_3N (6.0 mL, 43 mmol) in DCM (74 mL). The reaction mixture was then warmed to room temperature and left stirring for 18 h. After this time, the mixture was diluted with water (13.5 mL) and aq. HCl (4M, 13.5 mL). The resulting mixture was shaken carefully, the organic phase separated and the aqueous phase extracted with DCM (13.5 mL). The combined organic phases were washed first with brine (3 × 75 mL) and then with water (3 × 150 mL). Subsequently, the organic phase was dried with anhydrous sodium sulfate and evaporated to dryness, giving a yellow oil that solidified upon standing (3.42 g). The latter was crystallized from an Et_2O/acetone mixture giving the desired product as pale-yellow rhombic plates.

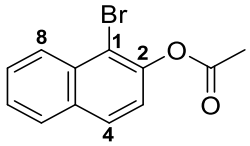

2.149

2-Acetoxy-1-bromonaphthalene (2.149): pale-yellow rhombic plates (2.85 g, 81%); m.p. = 56–58 °C; ν_{max} (neat) 1760, 1371, 1356, 1188, 1152, 1013, 937, 881, 811, 762, 663 cm^{-1}; ^1H NMR (400 MHz, $CDCl_3$) δ_H 2.43 (3H, s, Me), 7.26 (1H, d, *J* = 8.8 Hz, 3-H), 7.51–7.55 (1H, m, 6-H), 7.60–7.64 (1H, m, 7-H), 7.83–7.86 (2H, m, 4, 5-H), 8.26 (1H, app. d, *J* = 8.5 Hz, 8-H) ppm; ^{13}C NMR

(100 MHz, $CDCl_3$) δ_C 20.9, 115.1, 121.9, 126.4, 127.0, 127.9, 128.2, 128.9, 132.5, 132.7, 146.4, 168.8 ppm; HRMS (ESI) found $[M+H]^+$ = 264.9857 $C_{12}H_9{}^{79}BrO_2$ requires $[M+H]^+$ = 264.9859.

3.2.2.1.7 Attempted Heck cross-coupling reactions between 2-acetoxy-1-bromonaphthalene (2.149) and different Heck partners under multiple conditions (Table 2.5):

3.2.2.1.7.1 Entry 1 – 2-acetoxy-1-bromonaphthalene (200.6 mg, 0.7567 mmol), 1-phenyl-1-(4-pyridyl)prop-2-en-1-ol (207.0 mg, 0.9798 mmol), $Pd(PPh_3)_4$ (44.5 mg, 0.0385 mmol) were added to a dry 50 mL two-neck round-bottom flask. Once the air was evacuated and the flask flushed with N_2, previously dried Et_3N (0.25 mL, 1.8 mmol) and anhydrous MeCN (10.0 mL) were added and the mixture degassed for 30 min. Subsequently, the mixture was stirred at reflux under N_2 for 15 h. TLC and ^{1}H NMR analysis had shown no reaction.

3.2.2.1.7.2 Entry 2 – 2-acetoxy-1-bromonaphthalene (199.8 mg, 0.7536 mmol), 1-phenyl-1-(4-pyridyl)prop-2-en-1-ol (207.4 mg, 0.9817 mmol), $PdCl_2$ (7.2 mg, 0.041 mmol) were added to a dry 50 mL two-neck round-bottom flask. Once the air was evacuated and the flask flushed with N_2, previously dried Et_3N (0.25 mL, 1.8 mmol) and anhydrous MeCN (10.0 mL) were added and the mixture degassed for 30 min. Subsequently, the mixture was stirred at reflux under N_2 for 15 h. TLC and ^{1}H NMR analysis had shown no reaction.

3.2.2.1.7.3 Entry 3 – 2-acetoxy-1-bromonaphthalene (200.3 mg, 0.7555 mmol), 4-methoxystyrene (139.3 mg, 1.038 mmol), PPh_3 (8.4 mg, 0.032 mmol), $Pd(OAc)_2$ (5.8 mg, 0.026 mmol) were added to a dry 25 mL two-neck round-bottom flask. Once the air was evacuated and the flask flushed with N_2, previously dried Et_3N (0.25 mL, 1.8 mmol) and anhydrous MeCN (2.5 mL) were added and the mixture degassed for 20 min. Subsequently, the mixture was stirred at reflux under N_2 for 26 h. TLC and ^{1}H NMR analysis had shown no reaction.

3.2.2.1.8 Experimental Procedure for the Synthesis of 1-Iodo-2-trimethylsiloxynaphthalene (2.155): a solution of 1-iodo-2-naphthol (3.00 g, 11.1 mmol) and HMDS (4.2 mL, 20 mmol) in THF (54.0 mL) were refluxed for 90 min under N_2. After the reaction was completed, the crude was poured into water (50 mL), extracted with DCM (50 mL), washed with water (6 × 50 mL), dried with anhydrous sodium sulfate and evaporated to dryness. TLC analysis shown that the residue consisted of a mixture of 1-iodo-2-trimethylsiloxynaphthalene and 1-iodo-2-naphthol formed by the hydrolyses of the silyl ether during the work-up. Purification by flash column chromatography [Fluorochem silica gel (60 Å, 40-63 μm), eluent: 10% DCM in hexanes, fraction 1] led to the corresponding product as an orange oil.

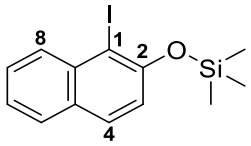

2.155

1-Iodo-2-trimethylsiloxynaphthalene (2.155)*: orange oil (1.19 g, 31%); ν_{max} (neat) 1620, 1593, 1497, 1459, 1352, 1241, 996, 942, 839, 809, 742 cm^{-1}; ^{1}H NMR (400 MHz, $CDCl_3$) δ_H 0.38 (9H, s, Me), 7.08 (1H, d, *J* = 8.7 Hz, 3-H), 7.38 (1H, app. t, *J* = 7.5 Hz, 6-H), 7.51–7.55 (1H, m, 7-H), 7.70–7.74 (2H, m, 4, 5-H), 8.12 (1H, d, *J* = 8.5 Hz, 8-H) ppm; ^{13}C NMR ($CDCl_3$) δ_C -0.0018, 91.8 (C-1), 119.2, 123.7, 127.1, 127.3, 129.1, 129.2, 130.8, 135.1, 153.2 ppm. *****Short half-life at room temperature.

3.2.2.1.9 Experimental Procedure for the Synthesis of 2-(4-Methoxyphenyl)naphtho[2,1-*b*]furan (2.159): a mixture of 1-iodo-2-trimethylsiloxynaphthalene (199.0 mg, 0.5814 mmol), 4-methoxystyrene (119.2 mg, 0.8884 mmol), K_2CO_3 (121.3 mg, 0.8776 mmol), $Pd(OAc)_2$ (10.6 mg, 0.0472 mmol), TBAB (282.4 mg, 0.8760 mmol), KCl (43.6 mg, 0.5848 mmol) in MeCN (10.0 mL) was heated at reflux under N_2 for 17 h. The crude was filtered through celite, diluted with DCM (50 mL), washed with brine (100 mL) and water (150 mL), dried with anhydrous sodium sulfate and evaporated to dryness. The reaction mixture was purified by flash column chromatography [Fluorochem silica gel (60 Å, 40-63 μm), eluent: 10% DCM in hexanes → 20% DCM in hexanes, fraction 2], leading to the corresponding product as a white powder.

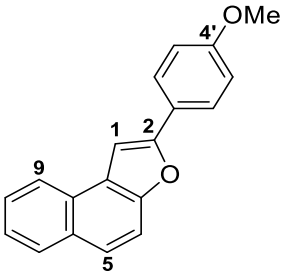

2.159

2-(4-Methoxyphenyl)naphtho[2,1-*b*]furan (2.159): white powder (21.5 mg, 13%); m.p. = 153–157 °C; ν_{max} (neat) 1604, 1495, 1463, 1439, 1249, 1179, 1022, 801, 773 cm^{-1}; ^{1}H NMR (400 MHz, $CDCl_3$) δ_H 3.85 (3H, s, OMe), 6.99 (2H, app. d, *J* = 8.8 Hz, 3′, 5′-H), 7.36 (1H, s, 1-H), 7.45–7.49 (1H, m, Ar-H), 7.55–7.59 (1H, m Ar-H), 7.66 (1H, d, *J* = 9.1 Hz, 5-H), 7.68 (1H, d, *J* = 9.1 Hz, 4-H), 7.84 (2H, app. d, *J* = 8.8 Hz, 2′, 6′-H), 7.93 (1H, d, *J* = 8.1 Hz, Ar-H), 8.14 (1H, app. d, *J* = 8.2 Hz, Ar-H) ppm; ^{13}C NMR (100 MHz, $CDCl_3$) δ_C 55.4, 98.9, 112.2, 114.3, 123.5, 123.6, 124.5,

124.6, 124.8, 126.1, 126.2, 127.5, 128.8, 130.4, 152.1, 155.6, 159.8 ppm; HRMS (ESI) found $[M+H]^+$ = 275.1065 $C_{19}H_{14}O_2$ requires $[M+H]^+$ = 275.1067.

3.2.2.1.10 Experimental Procedure for the Synthesis of 1-Bromo-2-(methoxymethoxy)naphthalene (2.162): MOMCl (3.3 mL, 43 mmol) was added dropwise to a degassed mixture of 1-bromo-2-naphthol (97%, 5.00 g, 21.7 mmol) and K_2CO_3 (9.30 g, 67.3 mmol) in anhydrous MeCN (500 mL) at -15 °C under N_2. The reaction mixture was left stirring for 30 min, after which it was warmed to room temperature and left stirring overnight. After 17 h, the crude was filtered through celite and evaporated to dryness. The resulting red oil was dissolved in EtOAc (50 mL), washed with water (3 × 50 mL), dried with anhydrous sodium sulfate and evaporated to dryness. The residue was then distilled by bulb-to-bulb distillation (impurity distilled at 80 °C at 2.5 x 10^{-2} torr), giving the corresponding product as a brick red oil that was used in the next step without further purification.

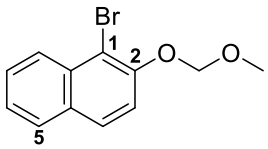

2.162

1-Bromo-2-(methoxymethoxy)naphthalene (2.162): brick red oil (5.72 g, 99%); ν_{max} (neat) 1624, 1595, 1501, 1464, 1352, 1240, 1148, 1082, 1007, 889, 803, 745 cm^{-1}; ^1H NMR (400 MHz, $CDCl_3$) δ_H 3.57 (3H, s, CH_3), 5.35 (2H, s, CH_2), 7.39–7.43 (2H, m, 3, 6-H), 7.54–7.58 (1H, m, 7-H), 7.76–7.78 (2H, m, 4, 5-H), 8.23 (1H, app. d, *J* = 8.6 Hz, 8-H) ppm; ^{13}C NMR (100 MHz, $CDCl_3$) δ_C 56.6, 95.6, 110.5, 117.0, 124.9, 126.4, 127.7, 128.1, 128.9, 130.5, 133.1, 151.8 ppm; HRMS (ESI) found $[M+H]^+$ = 268.9992 $C_{12}H_{11}{}^{81}BrO_2$ requires $[M+H]^+$ = 269.0000.

3.2.2.1.11 Heck cross-coupling reactions between 1-bromo-2-(methoxymethoxy)naphthalene (2.162) and 1,1-bis(4-methoxyphenyl)prop-2-en-1-ol (2.129) under multiple conditions (Table 2.6):

3.2.2.1.11.1 Entry 1 – $Pd(OAc)_2$ (15.9 mg, 0.0708 mmol) was added to a degassed mixture of 1-bromo-2-(methoxymethoxy)naphthalene (199.2 mg, 0.7457 mmol), 1,1-bis(4-methoxyphenyl)prop-2-en-1-ol (245.2 mg, 0.9070 mmol), K_2CO_3 (153.0 mg, 1.107 mmol), TBAB (364.4 mg, 1.130 mmol), KCl (59.7 mg, 0.801 mmol) in anhydrous DMAc [12.0 mL, dried under activated 4Å molecular sieves] and heated at 100 °C under N_2 for 28 h. After this time, brine (50 mL) was added, the residue extracted with EtOAc (3 × 50 mL), washed with brine (50 mL), dried with anhydrous sodium sulfate and evaporated to dryness. The resulting residue was purified by flash column

chromatography [Aldrich silica gel (60 Å 230-400 mesh 40-63 μm), eluent: 20% EtOAc in hexanes, fraction 3] giving the corresponding product.

3.2.2.1.11.2 Entry 2 – $Pd(OAc)_2$ (8.5 mg, 0.038 mmol) was added to a degassed mixture of 1-bromo-2-(methoxymethoxy)naphthalene (199.4 mg, 0.7465 mmol), 1,1-bis(4-methoxyphenyl)prop-2-en-1-ol (248.3 mg, 0.9185 mmol), anhydrous *N*-methyldicyclohexylamine [(0.24 mL, 1.1 mmol), distilled over calcium hydride], TBAC (23.7 mg, 0.0853 mmol), triphenylphosphine (19.7 mg, 0.0751 mmol) in anhydrous DMAc [1.4 mL, dried under activated 4Å molecular sieves] and heated at 80 °C under N_2 for 25 h. After this time, brine (50 mL) was added to the crude, the residue extracted with EtOAc (2 × 50 mL), washed with brine (50 mL), dried with anhydrous sodium sulfate and evaporated to dryness. The resulting residue was purified by flash column chromatography [Aldrich silica gel (60 Å 230-400 mesh 40-63 μm), eluent: 20% EtOAc in hexanes, fraction 3] giving the desired product.

3.2.2.1.11.3 Entry 3 – $Pd(dba)_2$ (8.4 mg, 0.015 mmol) was added to a degassed mixture of 1-bromo-2-(methoxymethoxy)naphthalene (200.4 mg, 0.7502 mmol), 1,1-bis(4-methoxyphenyl)prop-2-en-1-ol (244.5 mg, 0.9045 mmol), anhydrous *N*-methyldicyclohexylamine [(0.24 mL, 1.1 mmol), distilled over calcium hydride], TBAC (20.6 mg, 0.0740 mmol), tri-*tert*-butylphosphonium tetrafluoroborate (8.5 mg, 0.029 mmol) in anhydrous DMAc [1.4 mL, dried under activated 4Å molecular sieves] and heated at 80 °C under N_2 for 20 h. After this time, brine (50 mL) was added to the crude, the residue extracted with EtOAc (2 × 50 mL), washed with brine (50 mL), dried with anhydrous sodium sulfate and evaporated to dryness. Flash column chromatography [Aldrich silica gel (60 Å 230-400 mesh 40-63 μm), eluent: 20% EtOAc in hexanes] gave two pure products.

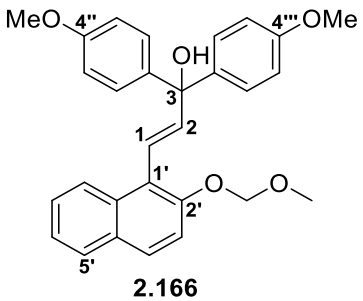

2.166

(*E*)-3-(2-(Methoxymethoxy)naphthalen-1-yl)-1,1-bis(4-methoxyphenyl)prop-2-en-1-ol (2.166): from entry 1 as yellow oil (31.5 mg, 9%); From entry 2 as a yellow oil (25.8 mg, 8%); From entry 3 as a yellow oil that solidified upon standing (120.0 mg, 35%); m.p. = 81–85 °C; ν_{max} (neat) 1606, 1505, 1242, 1172, 1148, 1031, 1014, 996, 929, 811, 746, 580 cm^{-1}; ^1H NMR (400 MHz, $CDCl_3$) δ_H 2.53 (1H, s, OH), 3.43 (3H, s, CH_3), 3.80 (6H, s, OMe), 5.21 (2H, s, CH_2), 6.82–6.89 (5H, m, 2, 3″,

3‴, 5″, 5‴-H), 6.98 (1H, d (AB), *J* = 16.1 Hz, 1-H), 7.33–7.41 (3H, m, Ar-H), 7.44 (4H, app. d, *J* = 8.9 Hz, 2″, 2‴, 6″, 6‴-H), 7.71 (1H, d, *J* = 9.0 Hz, Ar-H), 7.76 (1H, d, *J* = 7.6 Hz, Ar-H), 7.99 (1H, d, *J* = 8.5 Hz, Ar-H) ppm; ^{13}C NMR (100 MHz, $CDCl_3$) δ_C 55.3, 56.3, 79.4, 95.4, 113.5, 116.7, 121.4, 121.9, 124.0, 124.3, 126.4, 128.2, 128.4, 128.6, 129.8, 132.8, 138.7, 142.4, 151.9, 158.7 ppm; HRMS (ESI) found $[M+Na]^+$ = 479.1833 $C_{29}H_{28}O_5$ requires $[M+Na]^+$ = 479.1829.

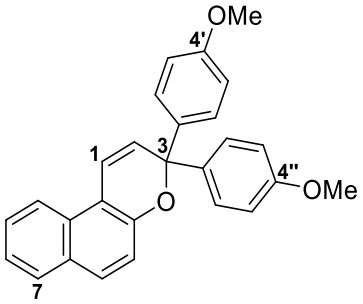

2.147

3,3-Bis(4-methoxyphenyl)-3*H*-naphtho[2,1-*b*]pyran (2.147): from entry 3 as a brown powder (30.3 mg, 10%); m.p. = 174–177 °C; ν_{max} (neat) 1508, 1247, 1174, 1029, 1000, 827, 813, 805, 746, 724, 590 cm^{-1}; ^{1}H NMR (400 MHz, $CDCl_3$) δ_H 3.77 (6H, s, OMe), 6.20 (1H, d, *J* = 9.9 Hz, 2-H), 6.84 (4H, app. d, *J* = 8.7 Hz, 3′, 3″, 5′, 5″-H), 7.16 (1H, d, *J* = 8.8 Hz, Ar-H), 7.24–7.32 (2H, m, 1-H, Ar-H), 7.38 (4H, app. d, *J* = 8.7 Hz, 2′, 2″, 6′, 6″-H), 7.45 (1H, t, *J* = 7.6 Hz, Ar-H), 7.64 (1H, d, *J* = 8.8 Hz, Ar-H), 7.71 (1H, d, *J* = 8.2 Hz, Ar-H), 7.95 (1H, d, *J* = 8.5 Hz, Ar-H) ppm; HRMS (ESI) found $[M+H]^+$ = 395.1649 $C_{27}H_{22}O_3$ requires $[M+H]^+$ = 395.1642.

3.2.2.1.12 Experimental Procedure for the Synthesis of (*E*)-3-(2-(methoxymethoxy)naphthalen-1-yl)-1-phenyl-1-(4-pyridyl)prop-2-en-1-ol (2.165): a mixture of 1-bromo-2-(methoxymethoxy)naphthalene (250.3 mg, 0.9370 mmol), 1-phenyl-1-(4-pyridyl)prop-2-en-1-ol (217.2 mg, 1.028 mmol), K_2CO_3 (193.9 mg, 1.403 mmol), $Pd(OAc)_2$ (17.0 mg, 0.0757 mmol), TBAB (452.7 mg, 1.404 mmol), KCl (69.9 mg, 0.938 mmol) in DMF (16.0 mL) was heated at 100 °C under N_2 for 24 h. After this time, the crude was poured into water (250 mL) and the pH adjusted to 7. The residue was extracted with DCM (3 × 200 mL) and the organic phase reduced to 100 mL. The latter was washed with brine (100 mL), water (2 × 150 mL), dried with anhydrous sodium sulfate and evaporated to dryness. Purification by flash column chromatography [Aldrich silica gel (60 Å, 40-63 μm), eluent: 20% EtOAc in PhMe → 40% EtOAc in PhMe, fraction 3], followed by crystallization from hot PhMe, led to the corresponding product as off-white needles.

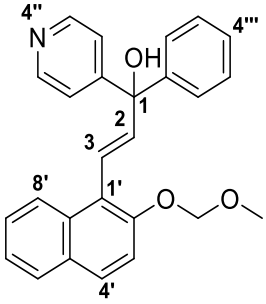

2.165

(*E*)-3-(2-(Methoxymethoxy)naphthalen-1-yl)-1-phenyl-1-(pyridin-4-yl)prop-2-en-1-ol (2.165): off-white needles (150.9 mg, 41%); m.p. = 202–203 °C; ν_{max} (neat) 1595, 1445, 1231, 1192, 1148, 1068, 1000, 991, 752, 698 cm^{-1}; ^{1}H NMR (400 MHz, $CDCl_3$) δ_H 2.92 (1H, s, OH), 3.43 (3H, s, CH_3), 5.24 (2H, s, CH_2), 6.87 (1H, d, *J* = 16.1 Hz, 2-H), 7.07 (1H, d, *J* = 16.1 Hz, 3-H), 7.33–7.42 (6H, m, Ar-H), 7.48 (2H, app. d, *J* = 5.9 Hz, 2″, 6″-H), 7.53 (2H, app. d, *J* = 7.3 Hz, Ar-H), 7.73–7.79 (2H, m, Ar-H), 7.92 (1H, d, *J* = 8.4 Hz, Ar-H), 8.58 (2H, app. d, *J* = 5.9 Hz, 3″, 5″-H) ppm; ^{13}C NMR (100 MHz, $CDCl_3$) δ_C 56.3, 79.2, 95.3, 116.4, 120.9, 121.8, 123.2, 124.0, 124.1, 126.6, 127.1, 128.0, 128.3, 128.6, 129.1, 129.8, 132.6, 140.2, 145.1, 149.7, 152.0, 154.8 ppm; HRMS (ESI) found $[M+H]^+$ = 398.1752 $C_{26}H_{23}NO_3$ requires $[M+H]^+$ = 398.1751.

3.2.2.1.13 Experimental Procedure for the Synthesis of 3-Phenyl-3-(4-pyridyl)-3*H*-naphtho[2,1-*b*]pyran (2.170): TFA (2.1 mL, 27 mmol) was added dropwise to a mixture of (*E*)-3-(2-(methoxymethoxy)naphthalen-1-yl)-1-phenyl-1-(pyridin-4-yl)prop-2-en-1-ol (0.35 g, 0.88 mmol) in DCM (45 mL). After 2 h, the crude was washed with a saturated aqueous solution of $NaHCO_3$ (100 mL). The resulting yellow solution was washed with water (2 × 200 mL), dried with anhydrous sodium sulfate and evaporated to dryness. The residue was triturated with Et_2O, filtered and dried under reduced pressure giving the desired product as an off-white powder (0.16 g, 54%). The resulting filtrate was crystallized from Et_2O/acetone as off-white crystalline plates (0.02 g, 7%).

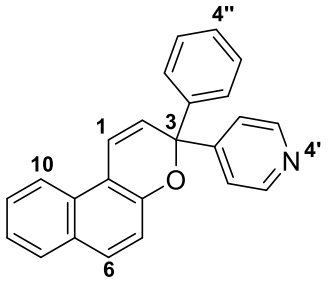

2.170

3-Phenyl-3-(4-pyridyl)-3*H*-naphtho[2,1-*b*]pyran (2.170): off-white solid (0.18 g; 61%); m.p. = 147–148 °C; ν_{max} (neat) 1633, 1588, 1246, 1206, 1192, 1015, 812, 754, 733, 702 cm^{-1};

Photomerocyanine λ_{max} = 414 nm (PhMe); ^{1}H NMR (400 MHz, $CDCl_3$) δ_H 6.21 (1H, d, *J* = 9.9 Hz, 2-H), 7.21 (1H, d, *J* = 8.8 Hz, 5-H), 7.25–7.50 (9H, m, Ar-H, 1-H), 7.67–7.73 (2H, m, 6, 7-H), 7.95 (1H, d, *J* = 8.5 Hz, 10-H), 8.56 (2H, app. d, *J* = 6.1 Hz, 3′, 5′-H) ppm; ^{13}C NMR (100 MHz, $CDCl_3$) δ_C 81.5, 114.0, 118.1, 120.8, 121.3, 121.6, 124.0, 126.2, 126.9, 127.0, 128.1, 128.4, 128.6, 129.5, 129.8, 130.3, 143.3, 149.8, 150.2, 153.6 ppm; HRMS (ESI) found $[M+H]^+$ = 336.1383 $C_{24}H_{17}NO$ requires $[M+H]^+$ = 336.1383.

3.2.3 Strategy C – By a Suzuki cross-coupling reaction before chromenization

3.2.3.1 Preparation of 5-Pyridyl-3*H*-Naphtho[2,1-*b*]pyrans

3.2.3.1.1 Experimental Procedure for the Synthesis of 2-Methoxy-3-(4-pyridyl)naphthalene (2.175):

Method A – A mixture of 3-bromo-2-methoxynaphthalene (2.00 g, 8.44 mmol), 4-pyridineboronic acid pinacol ester (2.60 g, 12.7 mmol), K_2CO_3 (1.75 g, 12.7 mmol), $Pd(PPh_3)_4$ (0.49 g, 0.42 mmol) in PhMe (42 mL) and EtOH (42 mL) was degassed, and heated at reflux under N_2. After 18 h of reaction, the crude was cooled to room temperature, the mixture filtered through celite and the filtrate evaporated to dryness. The resulting residue was dissolved in DCM (100 mL), washed with water (2 × 100 mL), the organic layer dried with anhydrous sodium sulfate and the solvent removed under reduced pressure to afford an oil which was filtered through a plug of silica [Fluorochem silica gel (60 Å, 40-63 μm), EtOAc (25%) in hexanes → EtOAc (100%)]. The resulting yellow oil was purified by flash column chromatography [activated Al_2O_3, eluent: EtOAc (50%) in hexanes, fraction 1]. The resulting yellow oil solidified as an off-white powder upon addition of Et_2O and cooling to -78 °C. Subsequent crystallization from a mixture of DCM/hexane at 3 °C provided the desired product as a white powder.

Method B – $Pd(PPh_3)_4$ (1.95 g, 1.69 mmol) was added to a degassed mixture of 3-bromo-2-methoxynaphthalene (8.00 g, 33.7 mmol), 4-pyridineboronic acid pinacol ester (10.40 g, 50.72 mmol), K_2CO_3 (6.99 g, 50.6 mmol), $Pd(PPh_3)_4$ (1.95 g, 1.69 mmol) in PhMe (167 mL) and EtOH (167 mL), and refluxed under N_2 for 25 h. After cooling to room temperature, the mixture was filtered through celite and the filtrate evaporated to dryness. The resulting residue was dissolved in EtOAc (100 mL), washed with water (3 × 100 mL), the organic layer dried with anhydrous sodium sulfate and the solvent removed under reduced pressure. The resulting yellow oil was filtered through a plug of alumina [activated Al_2O_3, EtOAc (50%) in hexanes, fraction 1] and then recrystallized from an EtOAc/hexane mixture giving the corresponding product as a white powder.

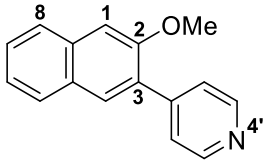

2.175

2-Methoxy-3-(4-pyridyl)naphthalene (2.175): white powder (1.20 g, 60%) from Method A; White powder (5.55 g, 70%) from Method B; m.p. = 108–110 °C; ν_{max} (neat) 1592, 1468, 1410, 1254, 1205, 1176, 1034, 836, 746, 674, 602, 545 cm^{-1}; ^1H NMR (400 MHz, $CDCl_3$) δ_H 3.95 (3H, s, OMe), 7.25 (1H, s, 1-H), 7.39 (1H, app. t, *J* = 7.5 Hz, 6-H), 7.49 (1H, app. t, *J* = 7.5 Hz, 7-H), 7.55 (2H, app. d, *J* = 6.1 Hz, 2′, 6′-H), 7.77–7.82 (3H, m, 4, 5, 8-H), 8.67 (2H, app. d, *J* = 6.1 Hz, 3′, 5′-H) ppm; ^{13}C NMR (100 MHz, $CDCl_3$) δ_C 55.6, 106.1, 124.3, 124.5, 126.5, 127.1, 127.9, 128.6, 129.5, 130.2, 134.6, 146.2, 149.5, 154.8 ppm; HRMS (ESI) found $[M+H]^+$ = 236.1073 $C_{16}H_{13}NO$ requires $[M+H]^+$ = 236.1070.

3.2.3.1.2 Experimental Procedure for the Synthesis of 2-Methoxy-3-(3-pyridyl)naphthalene (2.178): *n*-BuLi [2.5 M in hexanes] (80.0 mL, 200 mmol) was added dropwise to a mixture of 2-methoxynaphthalene (15.00 g, 94.82 mmol) in anhydrous THF (120 mL) at -78 °C under N_2. The resulting mixture was stirred for 30 min at this temperature and then allowed to reach room temperature and further stirred for 1 h. After this time, the reaction was re-cooled to -78 °C and 1,2-dibromoethane (9.0 mL, 1.0 × 10^2 mmol) was added dropwise. The reaction mixture was allowed to reach room temperature and stirred for 20h. Afterwards, the crude was poured into a saturated aqueous solution of NH_4Cl (100 mL) and extracted with EtOAc (2 × 100 mL). The organic phase was washed with water (3 × 100 mL), dried with anhydrous sodium sulfate, evaporated to dryness and used in the next step without further purification. $Pd(PPh_3)_4$ (2.26 g, 1.96 mmol) was added in one portion to a degassed mixture of 3-bromo-2-methoxynaphthalene (aprox. 50% pure) (18.63 g, 39.29 mmol), 3-pyridineboronic acid pinacol ester (12.08 g, 58.91 mmol), K_2CO_3 (8.14 g, 58.9 mmol) in PhMe (198 mL) and EtOH (198 mL), and refluxed under N_2 for 17 h. After cooling to room temperature, the mixture was filtered through celite and the filtrate evaporated to dryness. The resulting residue was dissolved in EtOAc (100 mL), washed with water (3 × 100 mL), the organic layer dried with anhydrous sodium sulfate and the solvent removed under reduced pressure. The resulting oil was filtered through a plug of silica [Fluorochem silica gel (60 Å, 40-63 μm), eluent: EtOAc (25%) in hexanes → EtOAc (100%)] and then purified by bulb-to-bulb distillation giving an amber oil (231 °C at 9.9 × 10^{-2} torr) that solidified upon standing. The resulting residue was

crystallized from benzene/cyclohexane at -20 °C, rinsed with cold IPA, giving the corresponding product as an off-white crystalline solid (5.05 g, 23%). A 2nd and 3rd crop were attained from hot EtOH giving the corresponding product as an off-white crystalline solid (0.93 g, 4%).

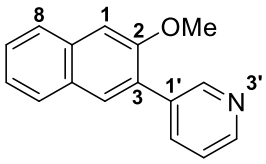

2.178

2-Methoxy-3-(3-pyridyl)naphthalene (2.178): off-white crystalline solid (5.98 g, 27%); m.p. = 112–114 °C; ν_{max} (neat) 1408, 1254, 1174, 1024, 904, 868, 834, 757, 710 cm^{-1}; ^{1}H NMR (400 MHz, $CDCl_3$) δ_H 3.93 (3H, s, OMe), 7.24 (1H, s, 1-H), 7.34–7.40 (2H, m, 6, 5′-H), 7.48 (1H, app. t, *J* = 7.5 Hz, 7-H), 7.76–7.81 (3H, m, 4, 5, 8-H), 7.93 (1H, dt, *J* = 1.9, 7.9 Hz, 6′-H), 8.60 (1H, dd, *J* = 1.6, 4.8 Hz, 4′-H), 8.84 (1H, d, *J* = 1.6 Hz, 2′-H) ppm; ^{13}C NMR (100 MHz, $CDCl_3$) δ_C 55.6, 105.9, 122.9, 124.2, 126.5, 126.8, 127.8, 128.4, 128.8, 130.2, 134.1, 134.4, 137.1, 148.3, 150.4, 155.0 ppm; HRMS (ESI) found $[M+H]^+$ = 236.1070 $C_{16}H_{13}NO$ requires $[M+H]^+$ = 236.1070.

3.2.3.1.3 Experimental Procedure of the Synthesis of 3-(4-Pyridyl)-2-naphthol (2.180): hydrobromic acid (45% w/v solution in AcOH) (34.0 mL) was added dropwise to a solution of 2-methoxy-3-(4-pyridyl)naphthalene (2.60 g, 11.1 mmol), AcOH (33.0 mL) and water (19.0 mL), and refluxed for 28 h. The reaction mixture was then cooled, poured into water (200 mL) and the solution neutralized (pH = 7) with the careful addition of $NaHCO_3$. As a result, a beige precipitate was formed, filtered, rinsed with water (100 mL) and dried under reduced pressure. The latter was triturated with cold Et_2O, filtered, rinsed with cold Et_2O (50 mL) and dried under reduced pressure, providing the corresponding product as a beige powder.

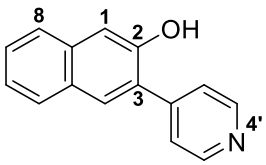

2.180

3-(4-Pyridyl)-2-naphthol (2.180): beige powder (2.21 g, 90%); m.p. = 238–242 °C; ν_{max} (neat) 2546 (br), 1604, 1595, 1411, 1010, 862, 841, 823, 804, 735, 684, 520 cm^{-1}; ^{1}H NMR (400 MHz, DMSO-d_6) δ_H 7.29–7.33 (2H, m, 1, 6-H), 7.44 (1H, app. t, *J* = 7.5 Hz, 7-H), 7.71–7.73 (3H, m, 2′, 6′, 8-H), 7.86 (1H, d, *J* = 8.1 Hz, 5-H), 7.95 (1H, s, 4-H), 8.65 (2H, app. s, 3′, 5′-H), 10.5 (1H, bs, OH) ppm; ^{13}C NMR (100 MHz, DMSO-d_6) δ_C 110.2, 123.6, 124.6, 126.0, 127.3, 128.2, 128.48,

128.51, 130.4, 134.9, 146.3, 149.8, 153.5 ppm; HRMS (ESI) found $[M+H]^+$ = 222.0913 $C_{15}H_{11}NO$ requires $[M+H]^+$ = 222.0913.

3.2.3.1.4 Experimental Procedure of the Synthesis of 3-(3-Pyridyl)-2-naphthol (2.181): hydrobromic acid (45% w/v solution in AcOH) (63.0 mL) was added dropwise to a solution of 2-methoxy-3-(3-pyridyl)naphthalene (4.94 g, 21.0 mmol), AcOH (61.8 mL) and water (30.9 mL), and refluxed for 3 days. The reaction mixture was then cooled, the crude poured into water (200 mL) and the solution neutralized (pH = 7) with the careful addition of $NaHCO_3$. As a result, an off-white precipitate was formed, filtered, rinsed with water (2 × 100 mL) and dried under reduced pressure. Recrystallization from hot EtOH provided the corresponding product as a brown crystalline solid.

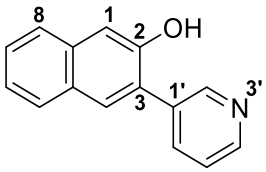

2.181

3-(3-Pyridyl)-2-naphthol (2.181): brown crystalline solid (2.93 g, 63%); m.p. = 204–208 °C; ν_{max} (neat) 3026 (br), 2590 (br), 1629, 1589, 1421, 1176, 1054, 867, 751, 707, 635 cm^{-1}; ^1H NMR (400 MHz, DMSO-d_6) δ_H 7.29–7.33 (2H, m, 1, 6-H), 7.43 (1H, d, *J* = 7.0 Hz, 7-H), 7.48–7.50 (1H, m, 5′-H), 7.73 (1H, d, *J* = 8.2 Hz, 8-H), 7.85 (1H, d, *J* = 8.1 Hz, 5-H), 7.91 (1H, s, 4-H), 8.06 (1H, d, *J* = 7.9 Hz, 6′-H), 8.58 (1H, app. s, 4′-H), 8.85 (1H, app. s, 2′-H), 10.2 (1H, bs, OH) ppm; ^{13}C NMR (100 MHz, DMSO-d_6) δ_C 109.9, 123.6, 126.0, 127.0, 128.0, 128.3, 128.4, 130.3, 134.7, 137.2, 148.4, 150.2, 153.3 ppm; HRMS (ESI) found $[M+H]^+$ = 222.0905 $C_{15}H_{11}NO$ requires $[M+H]^+$ = 221.0913.

3.2.3.1.5 General Method for the Synthesis of 6-(4-Pyridyl)-2-naphthol (2.183):

Method A – A mixture of 6-bromo-2-naphthol (1.00 g, 4.48 mmol), 4-pyridineboronic acid pinacol ester (1.38 g, 6.73 mmol), K_2CO_3 (0.93 g, 6.7 mmol), $Pd(PPh_3)_4$ (0.26 g, 0.22 mmol) in PhMe (20.0 mL) and EtOH (20.0 mL) was heated at reflux under N_2. After 14 h, the crude was evaporated to dryness. Afterwards, MeOH (200 mL) was added and glacial AcOH (120 mL) was slowly added until complete dissolution of the residue. The resulting solution was filtered through celite and evaporated to dryness. The solid was filtered off and rinsed with water. The filtrate was evaporated to dryness, added water and filtered off. The resulting two solids were mixed and crystallized from methylated spirits (200 mL) leading to the corresponding product as a brown powder (0.53 g, 54%). The mother-liquor was purified by flash column chromatography [Fluorochem silica gel (60 Å, 40-

63 μm), eluent: 10% MeOH in EtOAc, fraction 3], with subsequent recrystallization from EtOH, leading to the corresponding product as an off-white crystalline solid (0.07 g, 7%).

Method B – A mixture of 6-bromo-2-naphthol (5.00 g, 22.4 mmol), 4-pyridineboronic acid pinacol ester (6.90 g, 33.6 mmol), K_2CO_3 (4.65 g, 33.6 mmol), $Pd(PPh_3)_4$ (1.29 g, 1.12 mmol) in PhMe (100 mL) and EtOH (100 mL) was heated at reflux under N_2. After 16 h, the crude was evaporated to dryness. Afterwards, MeOH (250 mL) was added and glacial AcOH (300 mL) was slowly added until complete dissolution of the residue. The resulting solution was filtered through celite and evaporated to dryness. Water was then added and the solid filtered off. The resulting two solids were mixed and crystallized from hot methylated spirits (500 mL) with a small quantity of AcOH, filtered, rinsed with water and dried under reduced pressure, leading to the corresponding product as a brown powder (1.81 g, 37%). The mother-liquor was crystallized from hot methylated spirits (300 mL) with AcOH, filtered, rinsed with water and dried under reduced pressure, leading to the corresponding product as a brown powder (0.75 g, 15%).

Method C - $Pd(PPh_3)_4$ (1.29 g, 1.12 mmol) was added to a degassed mixture of 6-bromo-2-naphthol (5.00 g, 22.4 mmol), 4-pyridineboronic acid pinacol ester (6.89 g, 33.6 mmol), K_2CO_3 (4.65 g, 33.6 mmol), $Pd(PPh_3)_4$ (1.29 g, 1.12 mmol) in PhMe (100.0 mL) and EtOH (100.0 mL), and heated at reflux under N_2. After 18 h, the crude was filtered hot and the filtrate evaporated to dryness. The resulting brown residue was triturated with Et_2O (50 mL), collected by filtration, rinsed with water (100 mL) and dried under reduced pressure. Afterwards, the residue was triturated in hot EtOH, cooled to 0 °C, filtered off and rinsed with cold EtOH, giving the corresponding product as a yellow powder (2.88 g, 58%). The filtrate was reduced, cooled to 0 °C, filtered off and the precipitate rinsed with cold EtOH, giving the corresponding product as a yellow powder (0.17 g, 3%).

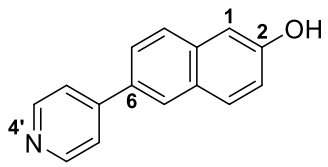

2.183

6-(4-Pyridyl)-2-naphthol (2.183): from method A as a brown powder (0.60 g, 61%); From method B as a brown powder (2.56 g, 52%); From method C a yellow powder (3.05 g, 61%); m.p. = 284–287 °C; ν_{max} (neat) 2513 (br), 1599, 1545, 1494, 1420, 1261, 1156, 902, 864, 822, 796 cm^{-1}; ^1H NMR (400 MHz, DMSO-d_6) δ_H 7.15–7.19 (2H, m, 1, 3-H), 7.79–7.83 (4H, m, 2′, 6′, 7, 8-H), 7.89 (1H, d, *J* = 8.8 Hz, 4-H), 8.28 (1H, s, 5-H), 8.64 (2H, app. d, *J* = 6.0 Hz, 3′, 5′-H), 10.0 (1H, bs,

OH) ppm; ^{13}C NMR (100 MHz, DMSO-d$_6$) δ_C 109.0, 119.8, 121.5, 124.9, 126.5, 127.5, 128.2, 130.7, 131.5, 135.4, 147.5, 150.7, 156.8 ppm; HRMS (ESI) found $[M+H]^+$ = 222.0913 $C_{15}H_{11}NO$ requires $[M+H]^+$ = 222.0913.

3.2.3.1.6 Attempts to Synthesize 3,3-Bis(4-methoxyphenyl)-8-(4-pyridyl)-3*H*-naphtho[2,1-*b*]pyran (2.57) from the acid-catalysed condensation between 6-(4-pyridyl)-2-naphthol (2.183) and 1,1-bis(4-methoxyphenyl)prop-2-yn-1-ol (2.33):

1st Attempt – 1,1-Bis(4-methoxyphenyl)prop-2-yn-1-ol (0.64 g, 2.4 mmol) and 6-(4-pyridyl)-2-naphthol (0.50 g, 2.3 mmol) in the presence of PPTS (0.03 g, 0.1 mmol) and trimethyl orthoformate (1.00 mL, 9.12 mmol) in 1,2-DCE (40.0 mL) was refluxed for 16 h under N_2. TLC analysis had shown no reaction.

2nd Attempt – 1,1-Bis(4-methoxyphenyl)prop-2-yn-1-ol (0.64 g, 2.4 mmol) and 6-(4-pyridyl)-2-naphthol (0.50 g, 2.3 mmol) in the presence of PPTS (0.63 g, 2.5 mmol) and trimethyl orthoformate (0.50 mL, 4.6 mmol) in 1,2-DCE (25.0 mL) was refluxed for 3 days under N_2. TLC analysis had shown no reaction. Solvent was removed under reduced pressure and the crude subjected to flash column chromatography [Aldrich silica gel (60 Å, 40-63 μm), eluent: 10% EtOAc in hexanes] but the desired product was not isolated.

3.2.3.1.7 General Method for the Synthesis of 1-Bromo-6-(4-pyridyl)-2-naphthol (2.186):

Method A – *N*-Bromosuccinimide (0.32 g, 1.8 mmol) was added in a single portion to a solution of 6-(4-pyridyl)-2-naphthol (0.40 g, 1.8 mmol) in DMF (24 mL) and stirred for 100 min at room temperature. After this time, the crude was evaporated to dryness and purified two times by flash column chromatography [Fluorochem silica gel (60 Å, 40-63 μm), eluent: 4% MeOH in DCM] giving the corresponding product.

Method B – *N*-Bromosuccinimide (0.60 g, 3.4 mmol) was added in a single portion to a solution of 6-(4-pyridyl)-2-naphthol (0.75 g, 3.4 mmol) in DMF (25 mL) and stirred for 30 min at room temperature. After this time, the solvent was reduced and the crude poured into water (250 mL). The resulting precipitate was filtered off and rinsed with water (100 mL). The filtrate was evaporated to dryness and water added (200 mL). The resulting precipitate was filtered off, rinsed with water (100 mL) and mixed with the former precipitate. Purification by flash column chromatography [Fluorochem silica gel (60 Å, 40-63 μm), eluent: 4% MeOH in DCM, fraction 4] led to the corresponding product.

Method C – *N*-Bromosuccinimide (1.97 g, 11.1 mmol) was added in a single portion to a solution of 6-(4-pyridyl)-2-naphthol (2.45 g, 11.1 mmol) in DMF (130 mL) and stirred for 28 min at room temperature. After this time, the crude was poured into water (1.3 L). The resulting colloidal solution was filtered through celite and extracted with a solution of DCM and MeOH. The filtrate was evaporated to dryness and crystallized from a boiling solution of EtOH (150 mL) with a small quantity of AcOH, filtered, rinsed with water and Et_2O, and dried under reduced pressure, leading to the corresponding product.

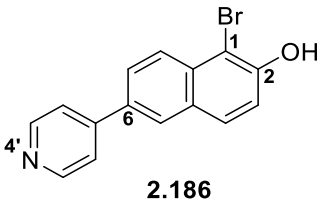

2.186

1-Bromo-6-(4-pyridyl)-2-naphthol (2.186): from method A as a brown powder (0.05 g, 11%); From method B as a tan powder (0.57 g, 56%); From method C as a brown powder (1.76 g, 53%); m.p. = 197–201 °C; ν_{max} (neat) 1619, 1597, 1561, 1417, 1388, 1193, 1174, 1151, 1002, 806, 702 cm^{-1}; ^1H NMR (400 MHz, DMSO-d_6) δ_H 7.35 (1H, d, *J* = 8.8 Hz, 3-H), 7.85 (2H, app. d, *J* = 5.9 Hz, 2′, 6′-H), 7.95 (1H, d, *J* = 8.8 Hz, 4-H), 8.03 (1H, dd, *J* = 8.9, 1.6 Hz, 7-H), 8.13 (1H, d, *J* = 8.9 Hz, 8-H), 8.39 (1H, d, *J* = 1.6 Hz, 5-H), 8.67 (2H, d, *J* = 5.9 Hz, 3′, 5′-H), 10.8 (1H, bs, OH) ppm; ^{13}C NMR (100 MHz, DMSO-d_6) δ_C 104.6, 119.5, 121.6, 126.3, 126.5, 127.1, 129.2, 130.2, 132.3, 133.5, 146.8, 150.8, 153.8 ppm; HRMS (ESI) found $[M+H]^+$ = 300.0019 $C_{15}H_{10}{}^{79}BrNO$ requires $[M+H]^+$ = 300.0019.

Experimental Procedure for the Synthesis of 1,3-Dibromo-6-(4-pyridyl)-2-naphthol (2.185): molecular bromine (0.10 mL, 1.9 mmol) was added in a single portion to a solution of 6-(4-pyridyl)-2-naphthol (0.40 g, 1.8 mmol) in AcOH (8.0 mL) and water (15.0 mL), and stirred at room temperature. After 21 h, the crude was diluted with water, filtered and the filtrand purified by flash column chromatography [Fluorochem silica gel (60 Å, 40-63 μm), eluent: 4% MeOH in DCM, fraction 1] giving the corresponding product as a brown powder (0.12 g, 18%).

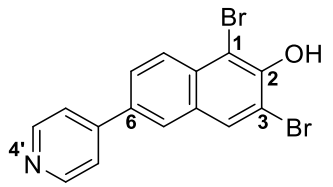

2.185

1,3-Dibromo-6-(4-pyridyl)-2-naphthol (2.185): brown powder (0.12 g, 18%); m.p. = 232–234 °C; ν_{max} (neat) 1604, 1585, 1557, 1420, 1378, 1137, 1067, 1022, 1004, 797, 715 cm^{-1}; ^1H NMR (400 MHz, DMSO-d_6) δ_H 7.82–7.84 (2H, m, 2′, 6′-H), 8.05–8.12 (2H, m, 7, 8-H), 8.40–8.41 (2H, m, 4, 5-H), 8.70 (2H, d, *J* = 5.5 Hz, 3′, 5′-H), 10.4 (1H, bs, OH) ppm; ^{13}C NMR (100 MHz, DMSO-d_6) δ_C 107.9, 114.7, 121.7, 126.3, 126.9, 127.1, 129.9, 132.3, 132.7, 133.7, 146.6, 150.0, 150.7 ppm; HRMS (ESI) found $[M+H]^+$ = 379.9107 $C_{15}H_9{}^{81}Br_2NO$ requires $[M+H]^+$ = 379.9108.

3.2.3.1.8 Experimental Procedure for the Synthesis of 1-Bromo-2-methoxymethoxy-6-(4-pyridyl)naphthalene (2.188): MOMCl (0.03 mL, 0.4 mmol) was added to a degassed misture of 1-bromo-6-(4-pyridyl)-2-naphthol (48.3 mg, 0.161 mmol) and K_2CO_3 (68.9 mg, 0.499 mmol) in anhydrous DMF (4.0 mL) at -15 °C under N_2. The reaction mixture was left stirring for 30 min, after which it was warmed to room temperature and left stirring overnight. After 18 h, the crude was diluted with DCM (100 mL), washed with brine (100 mL) and water (100 mL), dried with anhydrous sodium sulfate and evaporated to dryness. Flash column chromatography [Aldrich silica gel (60 Å, 40-63 μm), eluent: 10% MeOH in DCM, fraction 1] gave the corresponding product.

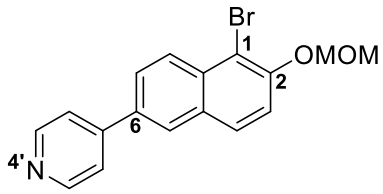

2.188

1-Bromo-2-methoxymethoxy-6-(4-pyridyl)naphthalene (2.188): orange oil (35.2 mg, 63%). ^1H NMR (400 MHz, $CDCl_3$) δ_H 3.59 (3H, s, CH_3), 5.39 (2H, s, CH_2), 7.50 (1H, d, *J* = 9.0 Hz, 3-H), 7.63 (2H, app. d, *J* = 5.7 Hz, 2′, 6′-H), 7.82–7.88 (2H, m, 4, 7-H), 8.07 (1H, d, *J* = 1.7 Hz, 5-H), 8.35 (1H, d, *J* = 8.9 Hz, 8-H), 8.71 (2H, d, *J* = 5.7 Hz, 3′, 5′-H) ppm; ^{13}C NMR (100 MHz, $CDCl_3$) δ_C 56.6, 95.5, 110.3, 117.6, 121.7, 126.2, 126.5, 127.6, 129.4, 130.5, 133.3, 134.3, 147.7, 150.4, 152.5 ppm;

3.2.3.1.9 Experimental Procedure of the Synthesis of 1-Bromo-3-(4-pyridyl)-2-naphthol (2.189): *N*-bromosuccinimide (2.61 g, 14.7 mmol) was added in a single portion to a solution of 3-(4-pyridyl)-2-naphthol (3.25 g, 14.7 mmol) in DMF (39.0 mL) and stirred for 35 min at room

temperature under N_2. After this time, the crude was evaporated to dryness. The resulting reaction mixture was purified by flash column chromatography [Fluorochem silica gel (60 Å, 40-63 μm), eluent: 4% MeOH in DCM, fraction 1], followed by recrystallization from hot ethanol, leading to the corresponding product as a yellow crystalline solid.

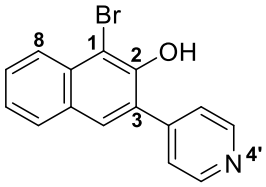

2.189

1-Bromo-3-(4-pyridyl)-2-naphthol (2.189): yellow crystalline solid (3.21 g, 73%); m.p. = 194–195 °C (darkened at 187 °C); ν_{max} (neat) 2615 (br), 1602, 1590, 1356, 1191, 822, 761, 739, 691, 619, 559 cm^{-1}; ^1H NMR (400 MHz, DMSO-d_6) δ_H 7.48 (1H, app. t, J = 7.5 Hz, 6-H), 7.64–7.68 (3H, m, 7, 2′, 6′-H), 7.97 (1H, d, J = 8.0 Hz, 5-H), 8.01 (1H, s, 4-H), 8.05 (1H, d, J = 8.5 Hz, 8-H), 8.68 (2H, app. d, J = 6.0 Hz, 3′, 5′-H), 9.73 (1H, bs, OH) ppm; ^{13}C NMR (100 MHz, DMSO-d_6) δ_C 108.6, 124.8, 125.0, 125.5, 129.0, 129.2, 129.3, 130.2, 130.3, 132.8, 145.9, 149.8, 150.0 ppm; HRMS (ESI) found $[M+H]^+$ = 300.0018 $C_{15}H_{10}{}^{79}BrNO$ requires $[M+H]^+$ = 300.0019.

3.2.3.1.10 Experimental Procedure of the Synthesis of 1-Bromo-3-(3-pyridyl)-2-naphthol (2.190): *N*-bromosuccinimide (2.50 g, 11.3 mmol) was added in a single portion to a solution of 3-(3-pyridyl)-2-naphthol (2.01 g, 11.3 mmol) in DMF (29.0 mL) and stirred for 166 min at room temperature under N_2. After this time, the crude was evaporated to dryness. The reaction mixture was passed through a plug of silica [Fluorochem silica gel (60 Å, 40-63 μm), eluent: 100% EtOAc, fraction 1], followed by recrystallization from hot ethanol, leading to the corresponding product as an orange crystalline solid.

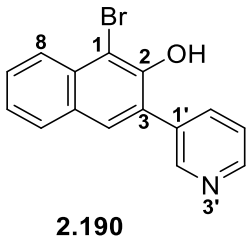

2.190

1-Bromo-3-(3-pyridyl)-2-naphthol (2.190): orange crystalline solid (1.20 g, 35%); m.p. = 178–180 °C (darkened at 175 °C); ν_{max} (neat) 2971 (br), 1159, 1142, 1126, 1099, 1030, 886, 736, 703, 649, 627 cm^{-1}; ^1H NMR (400 MHz, DMSO-d_6) δ_H 7.47 (1H, app. t, J = 7.5 Hz, 6-H), 7.52 (1H, dd, J = 4.8, 7.8 Hz, 5′-H), 7.64 (1H, app. t, J = 7.7 Hz, 7-H), 7.95–7.98 (2H, m, 4, 5-H), 8.02–8.05 (2H,

m, 8, 6′-H), 8.61 (1H, d, *J* = 3.9 Hz, 4′-H), 8.81 (1H, s, 2′-H), 9.66 (1H, bs, OH) ppm; ^{13}C NMR (100 MHz, DMSO-d$_6$) δ_C 108.4, 123.7, 124.9, 125.5, 128.7, 129.0, 129.4, 129.7, 130.2, 132.6, 134.1, 137.4, 148.9, 150.1, 150.2 ppm; HRMS (ESI) found $[M+H]^+$ = 300.0013 $C_{15}H_{10}{}^{79}BrNO$ requires $[M+H]^+$ = 300.0019.

3.2.3.1.11 General Experimental Procedure of the Synthesis of 1-Bromo-2-methoxymethoxy-3-pyridylnaphthalene (2.191): MOMCl (1.7 mmol) was added dropwise to a dried 100 mL two-neck round-bottomed flask containing a degassed mixture of 1-bromo-3-(4-pyridyl)-2-naphthol (1.7 mmol) and K_2CO_3 (3.5 mmol) in anhydrous DMF (38.0 mL) at -10 °C under N_2. The reaction mixture was then warmed to room temperature. After 139 min, the crude was poured into water (100 mL) and the residue extracted with DCM (3 × 100 mL). The organic phase was washed with water (2 × 200 mL), dried with anhydrous sodium sulfate and evaporated to dryness. Flash column chromatography [Aldrich silica gel (60 Å, 40-63 μm), eluent: 3% MeOH in DCM, fraction 1] gave the corresponding products.

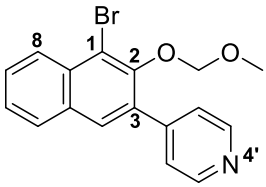

2.191

1-Bromo-2-methoxymethoxy-3-(4-pyridyl)naphthalene (2.191): from 1-bromo-3-(4-pyridyl)-2-naphthol (3.10 g, 10.3 mmol); Yellow oil that solidified upon standing as an off-white powder (1.17 g, 33%); m.p. = 90–92 °C; ν_{max} (neat) 1598, 1409, 1351, 1141, 1132, 1080, 946, 904, 842, 740, 616, 502 cm^{-1}; ^{1}H NMR (400 MHz, $CDCl_3$) δ_H 3.16 (3H, s, CH_3), 4.89 (2H, s, CH_2), 7.53–7.58 (6, 2′, 6′-H), 7.64 (1H, app. t, *J* = 7.7 Hz, 7-H), 7.81 (1H, s, 4-H), 7.85 (1H, d, *J* = 8.1 Hz, 5-H), 8.29 (1H, d, *J* = 8.5 Hz, 8-H), 8.72 (2H, app. s, 3′, 5′-H) ppm; ^{13}C NMR (100 MHz, $CDCl_3$) δ_C 57.8, 100.3, 117.2, 124.5, 126.5, 127.0, 128.3, 128.4, 129.8, 131.4, 133.0, 133.7, 146.3, 149.9, 150.1 ppm; HRMS (ESI) found $[M+H]^+$ = 344.0281 $C_{17}H_{14}{}^{79}BrNO_2$ requires $[M+H]^+$ = 344.0281.

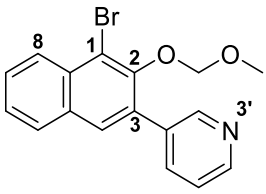

2.192

1-Bromo-2-methoxymethoxy-3-(3-pyridyl)naphthalene (2.192): from 1-bromo-3-(3-pyridyl)-2-naphthol (1.10 g, 3.66 mmol); Yellow oil that solidified upon standing as an off-white powder (0.31

g, 25%); m.p. = 82–84 °C; ν_{max} (neat) 1479, 1430, 1352, 1180, 1148, 1132, 1084, 947, 905, 741, 711 cm^{-1}; ^{1}H NMR (400 MHz, $CDCl_3$) δ_H 3.13 (3H, s, CH_3), 4.89 (2H, s, CH_2), 7.40 (1H, dd, *J* = 4.8, 7.8 Hz, 5′-H), 7.52 (1H, app. t, *J* = 7.5 Hz, 6-H), 7.62 (1H, app. t, *J* = 7.7 Hz, 7-H), 7.79 (1H, s, 4-H), 7.84 (1H, d, *J* = 8.1 Hz, 5-H), 7.96 (1H, dt, *J* = 1.8, 7.9 Hz, 6′-H), 8.28 (1H, d, *J* = 8.5 Hz, 8-H), 8.64 (1H, dd, *J* = 1.3, 4.7 Hz, 4′-H), 8.87 (1H, d, *J* = 1.7 Hz, 2′-H) ppm; ^{13}C NMR (100 MHz, $CDCl_3$) δ_C 57.8, 100.1, 117.1, 123.1, 126.4, 127.0, 128.0, 128.2, 129.8, 131.5, 132.8, 133.0, 134.2, 137.1, 148.7, 150.3, 150.4 ppm; HRMS (ESI) found $[M+H]^+$ = 344.0279 $C_{17}H_{14}{}^{79}BrNO_2$ requires $[M+H]^+$ = 344.0281.

3.2.3.1.12 Attempt to Synthesize 3,3-Bis(4-methoxyphenyl)-5-(4 or 3-pyridyl)-3*H*-naphtho[2,1-*b*]pyran by a Heck Cross–Coupling Reaction: a mixture of 1-bromo-2-(methoxymethoxy)-3-(4 or 3-pyridyl)naphthalene (1 mmol), 3,3-bis(4-methoxyphenyl)prop-2-en-1-ol (1.1 mmol), K_2CO_3 (1.5 mmol), $Pd(OAc)_2$ (7 mmol%), TBAB (1.5 mmol), KCl (1.0 mmol) in DMF (16.0 mL) was heated at 100 °C under N_2. After 24 h of reaction, the crude was poured into water (250 mL) and the pH adjusted to 7. The residue was extracted with DCM (3 × 200 mL) and the organic phase reduced to 100 mL. The latter was washed with brine (100 mL), water (2 × 150 mL), dried with anhydrous Na_2SO_4 and evaporated to dryness. Thus, 3,3-bis(4-methoxyphenyl)-5-(4-pyridyl)-3*H*-naphtho[2,1-*b*]pyran **2.193** was formed but not isolated after flash column chromatography [Aldrich silica gel (60 Å, 40-63 μm), eluent: 50% EtOAc in Petroleum Ether]. On the other hand, 3,3-bis(4-methoxyphenyl)-5-(3-pyridyl)-3*H*-naphtho[2,1-*b*]pyran **2.194** was isolated as a mixture (0.04 g, < 11%) after flash column chromatography [Aldrich silica gel (60 Å, 40-63 μm), eluent: 3% MeOH in DCM, fraction 5].

3.2.3.2 Preparation of 6-Pyridyl-3*H*-Naphtho[2,1-*b*]pyrans

3.2.3.2.1 Experimental Procedure for the Synthesis of Acetyl chloride: freshly distilled thionyl chloride (73.0 mL, 1.01 mol) was added dropwise to glacial AcOH (48.0 mL, 0.839 mol) in a 250 mL three-neck round-bottomed flask, connected to a condenser with an endcap $CaCl_2$ drying tube, and cooled by immersion in a water bath. The temperature of the bath was then raised to 50 °C for 1 h as the evolution of hydrogen chloride slackened and liberation of SO_2 stopped. Acetyl chloride was distilled from the latter flask, as the fraction passing over 52 °C and 56 °C was collected separately, giving a colourless oil which fumed strongly in air, and was used in the next step without further purification.

Acetyl chloride: colourless oil (41.59 g, 63%);

3.2.3.2.2 Experimental Procedure for the Synthesis of 3-Methoxy-1-naphthol (2.197): a solution of methanolic hydrogen chloride was prepared by the dropwise addition of acetyl chloride (18.5 mL) to MeOH (184.0 mL) at 0 °C. Solid 1,3-dihydroxynaphthalene (9.22 g, 57.6 mmol) was added in one portion to the foregoing methanolic HCl solution and the resulting solution stirred for 24 h at room temperature. The mixture was poured into water (300 mL) and extracted with DCM (3 × 100 mL). The extracts were washed with water (3 × 200 mL), the organic layer dried with anhydrous sodium sulfate and the solvent removed under reduced pressure. The resulting mixture was purified by flash column chromatography [Fluorochem silica gel (60 Å, 40-63 μm), eluent: EtOAc/hexane (1:9 → 3:7)] to afford two pure fractions.

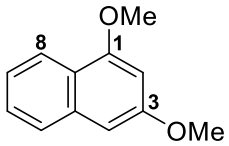

2.197

Fraction 1 – 1,3-Dimethoxynaphthalene (2.197): yellow oil (1.25 g, 14%); ν_{max} (neat) 1628, 1585, 1451, 1406, 1285, 1214, 1153, 1107, 1048, 813, 745 cm^{-1}; ^{1}H NMR (400 MHz, $CDCl_3$) δ_H 3.88 (3H, s, OMe), 3.94 (3H, s, OMe), 6.48 (1H, d, *J* = 1.9 Hz, 2-H), 6.71 (1H, d, *J* = 1.9 Hz, 4-H), 7.30 (1H, app. t, *J* = 7.6 Hz, 6-H), 7.43 (1H, app. t, *J* = 7.5 Hz, 7-H), 7.66 (1H, d, *J* = 8.2 Hz, 8-H), 8.13 (1H, d, *J* = 8.3 Hz, 5-H) ppm; ^{13}C NMR (100 MHz, $CDCl_3$) δ_C 55.4, 55.6, 97.6, 97.9, 121.8, 122.0, 123.0, 126.5, 127.1, 135.1, 156.6, 158.2 ppm; GCMS (EI) found $[M]^+$ = 188.1 $C_{12}H_{12}O_2$ requires $[M]^+$ = 188.1.

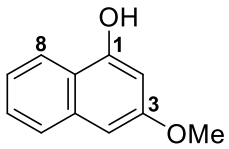

2.196

Fraction 2 – 3-Methoxy-1-naphthol (2.196): pale brown oil that solidified upon standing (8.59 g, 86%); m.p. = 96–98 °C (lit. m.p. = 99–100 °C[245]); ν_{max} (neat) 3383 (br), 1632, 1588, 1408, 1262, 1236, 1137, 1084, 817, 748, 649 cm^{-1}; ^{1}H NMR (400 MHz, $CDCl_3$) δ_H 3.87 (3H, s, OMe), 5.58 (1H, s, OH), 6.51 (1H, d, *J* = 1.9 Hz, 2-H), 6.76 (1H, d, *J* = 1.9 Hz, 4-H), 7.32 (1H, t, *J* = 7.6 Hz, 6-H), 7.44 (1H, t, *J* = 7.5 Hz, 7-H), 7.68 (1H, d, *J* = 8.2 Hz, 8-H), 8.06 (1H, d, *J* = 8.3 Hz, 5-H) ppm; ^{13}C NMR (100 MHz, $CDCl_3$) δ_C 55.4, 98.9, 101.5, 120.6, 121.7, 123.0, 126.7 127.1, 135.5, 152.7, 157.8 ppm; HRMS (ESI) found $[M+H]^+$ = 175.07541 $C_{11}H_{10}O_2$ requires $[M+H]^+$ = 175.07536.

3.2.3.2.3 Experimental Procedure for the Synthesis of 3-Methoxy-1-triflyloxynaphthalene (2.203): triflic anhydride (10.9 mL, 64.9 mmol) was added dropwise to a solution of 3-methoxy-1-naphthol (10.94 g, 62.80 mmol) and Et_3N (22.5 mL, 161 mmol) in DCM (134.0 mL) at 0 ºC under N_2. After 90 min, the resulting solution was washed with HCl (1M) (50 mL), with a saturated $NaHCO_3$ (100 mL), dried with anhydrous sodium sulfate and the solvent removed under reduced pressure. The residue was purified by flash column chromatography [Fluorochem silica gel (60 Å, 40-63 μm), eluent: EtOAc/hexane (1:9), fraction 1] leading to the corresponding product as a pale-yellow oil.

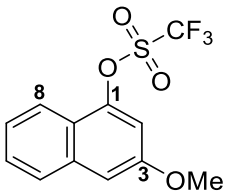

2.203

3-Methoxy-1-triflyloxynaphthalene (2.203): pale-yellow oil (15.55 g, 81%); ν_{max} (neat) 1638, 1605, 1418, 1202, 1129, 1046, 1007, 952, 815, 746, 600 cm^{-1}; ^1H NMR (400 MHz, $CDCl_3$) δ_H 3.94 (3H, s, OMe), 7.168–7.174 (2H, m, 2-H and 4-H), 7.46–7.50 (1H, m, 6-H), 7.52–7.56 (1H, m, 7-H), 7.79 (1H, d, J = 8.2 Hz, 8-H), 7.97 (1H, d, J = 8.3 Hz, 5-H) ppm; ^{13}C NMR (100 MHz, $CDCl_3$) δ_C 55.8, 106.4, 111.3, 120.8, 121.9, 122.1 (1C, q, J = 320.8 Hz, CF_3), 125.3, 127.0, 128.0, 135.3, 146.1, 156.7 ppm; ^{19}F NMR (376 MHz, $CDCl_3$) δ_F -73.3 ppm; HRMS (APCI) found $[M]^+$ = 306.0171 $C_{12}H_9F_3O_4S$ requires $[M]^+$ = 306.0174.

3.2.3.2.4 Experimental Procedure for the Synthesis of 2-Methoxy-4-(4-pyridyl)naphthalene (2.204):

Method A – A mixture of 3-methoxy-1-triflyloxynaphthalene (5.00 g, 16.3 mmol), 4-pyridineboronic acid pinacol ester (5.02 g, 24.5 mmol), K_2CO_3 (3.39 g, 24.5 mmol), $Pd(PPh_3)_4$ (0.94 g, 0.81 mmol) in PhMe (190.0 mL) and EtOH (190.0 mL) were mixed at reflux under N_2. After 14 h of reaction, the mixture was evaporated to dryness, the residue extracted with EtOAc (200 mL), washed with water (3 × 150 mL), the organic layer dried with anhydrous sodium sulfate and the solvent removed under reduced pressure, resulting in the formation of a brown oil which solidified under reduced pressure. The residue was triturated with Et_2O (20 mL), the solid filtered off, rinsed with cold Et_2O (10 mL), cold MeOH (10 mL) and dried under reduced pressure, resulting in the formation of a light grey powder (2.08 g, 54%). The filtrate was crystallized from EtOH, filtered off, rinsed with cold Et_2O (10 mL), cold MeOH (10 mL) and dried under reduced pressure, giving a crystalline light grey solid (0.70, 18%).

Method B – A mixture of 3-methoxy-1-triflyloxynaphthalene (7.21 g, 23.5 mmol), 4-pyridineboronic acid pinacol ester (7.22 g, 35.2 mmol), K_2CO_3 (4.86 g, 35.2 mmol), $Pd(PPh_3)_4$ (1.36 g, 1.18 mmol) in PhMe (274 mL) and EtOH (274 mL) were mixed at reflux under N_2. After 16 h of reaction, the mixture was evaporated to dryness, the residue extracted with EtOAc (100 mL), washed with water (3 × 100 mL), the organic layer dried with anhydrous sodium sulfate and the solvent removed under reduced pressure. The resulting brown oil was filtered through a plug of silica [Fluorochem silica gel (60 Å, 40-63 μm), EtOAc (25%) in hexanes → EtOAc (100%)] and recrystallized from hot EtOH, giving the corresponding product as a beige crystalline solid.

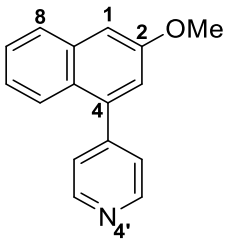

2.204

2-Methoxy-4-(4-pyridyl)naphthalene (2.204): light grey solid (2.78 g, 72%) from Method A; Beige crystalline solid (4.37 g, 79%) from Method B; m.p. = 128–129 °C; ν_{max} (neat) 1619, 1592, 1543, 1398, 1194, 1166, 1038, 1023, 824, 750 cm^{-1}; ^1H NMR (400 MHz, $CDCl_3$) δ_H 3.95 (3H, s, OMe), 7.09 (1H, d, *J* = 1.8 Hz, 3-H), 7.20 (1H, app. s, 1-H), 7.31 (1H, t, *J* = 7.6 Hz, 6-H), 7.41 (2H, app. d, *J* = 4.2 Hz, 2′, 6′-H), 7.47 (1H, t, *J* = 7.4 Hz, 7-H), 7.71 (1H, d, *J* = 8.4 Hz, 5-H), 7.81 (1H, d, *J* = 8.2 Hz, 8-H), 8.72 (2H, d, *J* = 4.2 Hz, 3′, 5′-H) ppm; ^{13}C NMR (100 MHz, $CDCl_3$) δ_C 55.4, 106.6, 119.6, 124.3, 124.9, 125.2, 126.5, 126.7, 127.4, 135.2, 139.0, 148.2, 149.8, 156.9 ppm; HRMS (ESI) found $[M+H]^+$ = 236.1070 $C_{16}H_{13}NO$ requires $[M+H]^+$ = 236.1070.

3.2.3.2.5 Experimental Procedure for the Synthesis of 2-Methoxy-4-(3-pyridyl)naphthalene (2.205): a mixture of 3-methoxy-1-triflyloxynaphthalene (3.50 g, 11.4 mmol), 3-pyridineboronic acid pinacol ester (3.52 g, 17.2 mmol), K_2CO_3 (2.37 g, 17.1 mmol), $Pd(PPh_3)_4$ (0.66 g, 0.57 mmol) in PhMe (130.0 mL) and EtOH (130.0 mL) were mixed at reflux under N_2. After 16 h of reaction, the mixture was evaporated to dryness, the residue dissolved in EtOAc (100 mL), washed with water (3 × 100 mL), the organic layer dried with anhydrous sodium sulfate and the solvent removed under reduced pressure, resulting in the formation of a brown oil that solidified upon standing. The residue was triturated with Et_2O (10 mL), the solid filtered off, rinsed with cold Et_2O (10 mL), cold MeOH (10 mL) and dried under reduced pressure, giving the corresponding product as an off-white powder (1.07 g, 40%). The filtrate was purified by flash column chromatography [Fluorochem

silica gel (60 Å, 40-63 μm), EtOAc (40%) in hexanes, fraction 1] leading to the corresponding product as an off-white powder (1.38 g, 51%).

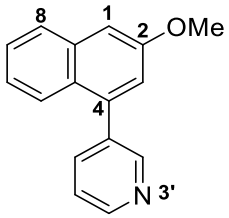

2.205

2-Methoxy-4-(3-pyridyl)naphthalene (2.205): off-white powder (2.45 g, 91%); m.p. = 72–74 °C; ν_{max} (neat) 1622, 1603, 1589, 1565, 1398, 1220, 1167, 1042, 1022, 820, 720 cm^{-1}; ^{1}H NMR (400 MHz, $CDCl_3$) δ_H 3.97 (3H, s, OMe), 7.11 (1H, d, *J* = 2.4 Hz, 3-H), 7.21 (1H, d, *J* = 2.4 Hz, 1-H), 7.30–7.34 (1H, m, 6-H), 7.42–7.50 (2H, m, 7, 5′-H), 7.70 (1H, d, *J* = 8.4 Hz, 5-H), 7.80–7.83 (2H, m, 8, 6′-H), 8.69 (1H, dd, *J* = 4.9, 1.6 Hz, 4′-H), 8.747–8.752 (1H, m, 2′-H) ppm; ^{13}C NMR (100 MHz, $CDCl_3$) δ_C 55.4, 106.3, 120.1, 123.1, 124.2, 125.3, 126.7, 127.2, 127.4, 135.2, 135.9, 137.2, 138.0, 148.8, 150.5, 156.9 ppm; HRMS (ESI) found $[M+H]^+$ = 236.1070 $C_{16}H_{13}NO$ requires $[M+H]^+$ = 236.1070.

3.2.3.2.6 Experimental Procedure for the Synthesis of 4-(4-Pyridyl)-2-naphthol (2.206):

Method A – Hydrobromic acid (45% w/v solution in AcOH) (13.0 mL) was added slowly to a solution of 2-methoxy-4-(4-pyridyl)naphthalene (1.00 g, 4.25 mmol), AcOH (13.0 mL) and water (6.0 mL), and refluxed for 22 h. The reaction mixture was then cooled, added water (200 mL) and the solution neutralized (pH = 7) with the cautious addition of $NaHCO_3$. As a result, an off-white precipitate was formed, filtered, the solid rinsed with water (2 × 10 mL) and DCM (2 × 10 mL) giving the corresponding product (0.69 g, 73%). The filtrate was evaporated to dryness, added water (5 mL), the off-white precipitate filtered, the solid rinsed with water (5 mL) and DCM (2 × 5 mL) affording the corresponding product (0.19 g, 20%).

Method B – Hydrobromic acid (45% w/v solution in AcOH) (51.0 mL) was added slowly to a solution of 2-methoxy-4-(4-pyridyl)naphthalene (4.00 g, 17.0 mmol), AcOH (50.0 mL) and water (25.0 mL), and refluxed for 21 h. The reaction mixture was then cooled, added water (200 mL) and the solution neutralized (pH = 7) with the cautious addition of $NaHCO_3$. As a result, a precipitate was formed, filtered and the solid rinsed with water (2 × 100 mL). Recrystallization from DMF/EtOH provided the corresponding product as an off-white powder.

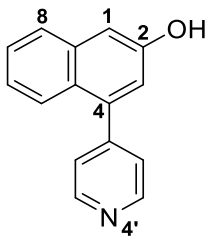

2.206

4-(4-Pyridyl)-2-naphthol (2.206): off-white powder (0.88 g, 93% from Method A; 2.93 g, 78% from Method B); m.p. = 275–279 °C; ν_{max} (neat) 2580 (br), 1592, 1383, 1208, 1178, 1069, 833, 762, 665, 622, 599 cm^{-1}; ^{1}H NMR (400 MHz, DMSO-d_6) δ_H 7.06 (1H, d, *J* = 2.1 Hz, 3-H), 7.26–7.29 (2H, m, 1, 6-H), 7.45 (1H, t, *J* = 7.4 Hz, 7-H), 7.51 (1H, d, *J* = 5.4 Hz, 2′, 6′-H), 7.62 (1H, d, *J* = 8.4 Hz, 5-H), 7.81 (1H, d, *J* = 8.2 Hz, 8-H), 8.72 (2H, d, *J* = 5.4 Hz, 3′, 5′-H), 9.99 (1H, s, OH) ppm; ^{13}C NMR (100 MHz, DMSO-d_6) δ_C 110.1, 119.9, 124.0, 125.1, 125.2, 125.4, 126.9, 127.3, 135.7, 138.9, 147.9, 150.2, 155.0 ppm; HRMS (ESI) found $[M+H]^+$ = 222.0913 $C_{15}H_{11}NO$ requires $[M+H]^+$ = 222.0913.

3.2.3.2.7 Experimental Procedure for the Synthesis of 4-(3-Pyridyl)-2-naphthol (2.207): hydrobromic acid (45% w/v solution in AcOH) (58.0 mL) was added slowly to a solution of 2-methoxy-4-(3-pyridyl)naphthalene (4.50 g, 19.1 mmol), AcOH (58.0 mL) and water (29.0 mL), and refluxed for 21 h. The reaction mixture was then cooled, added water (200 mL) and the solution neutralized (pH = 7) with the cautious addition of $NaHCO_3$. As a result, a precipitate was formed, filtered and rinsed with water (2 × 100 mL). Recrystallization from hot EtOH provided the corresponding product as a grey crystalline solid.

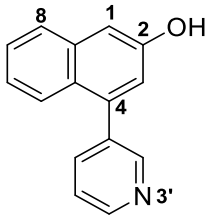

2.207

4-(3-Pyridyl)-2-naphthol (2.207): grey crystalline solid (3.16 g, 75%); m.p. = 193–195 °C; ν_{max} (neat) 3020 (br), 2741 (br), 2579 (br), 1587, 1348, 1294, 1205, 1190, 866, 822, 714 cm^{-1}; ^{1}H NMR (400 MHz, DMSO-d_6) δ_H 7.056–7.062 (1H, m, 3-H), 7.24–7.28 (2H, m, 1, 6-H), 7.44 (1H, app. t, *J* = 7.5 Hz, 7-H), 7.55–7.57 (2H, m, 5, 5′-H), 7.80 (1H, d, *J* = 8.2 Hz, 8-H), 7.91 (1H, dt, *J* = 7.8, 1.8 Hz, 6′-H), 8.67 (2H, app. s, 2′, 4′-H), 9.99 (1H, bs, OH); ^{13}C NMR (100 MHz, DMSO-d_6) δ_C 109.7,

120.3, 123.9, 124.0, 125.2, 126.1, 126.9, 127.3, 135.7, 135.9, 137.6, 138.0, 149.1, 150.2, 155.1 ppm; HRMS (ESI) found $[M+H]^+$ = 222.0918 $C_{15}H_{11}NO$ requires $[M+H]^+$ = 222.0913.

3.2.3.2.8 Experimental Procedure for the Synthesis of 1-Bromo-4-(4-Pyridyl)-2-naphthol (2.208): *N*-bromosuccinimide (2.17 g, 12.2 mmol) was added in a single portion to a solution of 4-(4-pyridyl)-2-naphthol (2.70 g, 12.2 mmol) in DMF (164.0 mL) and stirred for 110 min at 52 °C under N_2. The solvent was reduced to 20 mL and the crude poured into cold water (400 mL). The resulting orange precipitate was filtered off, rinsed with water (100 mL) and dried under reduced pressure. Purification by flash column chromatography [Fluorochem silica gel (60 Å, 40-63 μm), eluent: 4% MeOH in DCM, fraction 3] led to the corresponding product as a yellow powder.

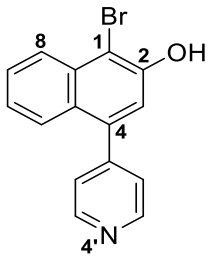

2.208

1-Bromo-4-(4-Pyridyl)-2-naphthol (2.208): yellow powder (1.97 g, 54%); m.p. = 219–222 °C; ν_{max} (neat) 1604, 1541, 1514, 1379, 1224, 1213, 1003, 828, 752, 617 cm^{-1}; ^1H NMR (400 MHz, DMSO-d_6) δ_H 7.23 (1H, s, 3-H), 7.39 (1H, app. t, *J* = 7.56 Hz, Ar-H), 7.51 (2H, app. d, *J* = 5.8 Hz, 2′, 6′-H), 7.62–7.66 (2H, m, Ar-H), 8.16 (1H, d, *J* = 8.6 Hz, 8-H), 8.74 (2H, d, *J* = 5.8 Hz, 3′, 5′-H), 10.8 (1H, s, OH) ppm; ^{13}C NMR (100 MHz, DMSO-d_6) δ_C 105.6, 119.4, 124.8, 125.1, 125.9, 126.0, 126.4, 128.6, 133.5, 138.3, 147.2, 150.3, 152.3 ppm; HRMS (ESI) found $[M+H]^+$ = 300.0026 $C_{15}H_{10}{}^{79}BrNO$ requires $[M+H]^+$ = 300.0019.

3.2.3.2.9 Experimental Procedure for the Synthesis of 1-Bromo-4-(3-Pyridyl)-2-naphthol (2.209): *N*-bromosuccinimide (2.42 g, 13.6 mmol) was added in a single portion to a solution of 4-(3-pyridyl)-2-naphthol (3.00 g, 13.6 mmol) in DMF (35.0 mL) and stirred for 110 min at 52 °C under N_2. After this time, the crude was poured into cold water (400 mL). The resulting beige precipitate was filtered off, rinsed with water (100 mL) and dried under reduced pressure. Purification by flash column chromatography [Fluorochem silica gel (60 Å, 40-63 μm), eluent: 4% MeOH in DCM, fraction 1] led to the corresponding product as an off-white powder.

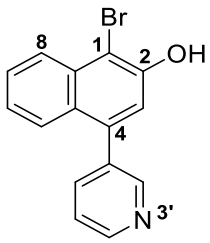

2.209

1-Bromo-4-(3-Pyridyl)-2-naphthol (2.209): off-white powder (2.34 g, 57%); m.p. = 227–228 °C; ν_{max} (neat) 2536 (br), 1440, 1385, 1315, 1230, 945, 867, 808, 753, 708, 646 cm^{-1}; ^1H NMR (400 MHz, DMSO-d_6) δ_H 7.23 (1H, s, 3-H), 7.39 (1H, app. t, *J* = 7.1 Hz, 6-H), 7.57–7.66 (3H, m, 5, 7, 5′-H), 7.92 (1H, dt, *J* = 7.8, 1.9 Hz, 6′-H), 8.16 (1H, d, *J* = 8.4 Hz, 8-H), 8.67 (1H, d, *J* = 1.8 Hz, 2′-H), 8.71 (1H, dd, *J* = 4.8, 1.6 Hz, 4′-H), 10.8 (1H, bs, OH) ppm; ^{13}C NMR (100 MHz, DMSO-d_6): δ_C 105.2, 119.9, 124.0, 124.7, 126.0, 126.1, 127.1, 128.5, 133.5, 135.2, 137.4, 137.6, 149.5, 150.1, 152.3 ppm; HRMS (ESI) found $[M+H]^+$ = 300.0011 $C_{15}H_{10}{}^{79}BrNO$ requires $[M+H]^+$ = 300.0019.

3.2.3.2.10 General Experimental Procedure for the Synthesis of 1-Bromo-2-(methoxymethoxy)-4-pyridyl-2-naphthol (2.210 and 2.211): MOMCl (5.3 mmol) was added dropwise to a dried 250 mL two-neck round-bottom flask containing a degassed mixture of 1-bromo-4-pyridyl-2-naphthol (5.00 mmol) and K_2CO_3 (10.5 mmol) in anhydrous DMF (81.0 mL) at 0 °C under N_2. The reaction mixture was warmed to room temperature. After 4 h, water (100 mL) was added and the residue extracted with DCM (3 × 100 mL). The organic phase was washed with water (2 × 200 mL), dried with anhydrous sodium sulfate and evaporated to dryness. Flash column chromatography [Aldrich silica gel (60 Å, 40-63 μm), eluent: 4% MeOH in DCM, fraction 1] led to the pure products.

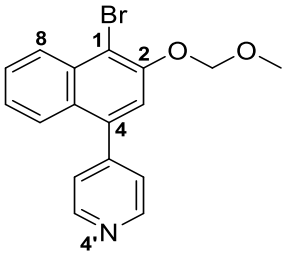

2.210

1-Bromo-2-methoxymethoxy-4-(4-pyridyl)naphthalene (2.210): from 1-bromo-(4-pyridyl)-2-naphthol (1.50 g, 5.00 mmol); brown oil that solidified upon standing (1.34 g, 78%); m.p. = 104–107 °C; ν_{max} (neat) 1159, 1142, 1126, 1099, 886, 736, 703, 649, 627 cm^{-1}; ^1H NMR (400 MHz, $CDCl_3$) δ_H 3.57 (3H, s, CH_3), 5.37 (2H, s, CH_2), 7.36–7.41 (4H, m, 3, 6, 2′, 6′-H), 7.59 (1H, t, *J* = 7.6 Hz, 7-H), 7.72 (1H, d, *J* = 8.4 Hz, 5-H), 8.34 (1H, d, *J* = 8.6 Hz, 8-H), 8.73 (2H, d, *J* = 5.8 Hz,

3′, 5′-H) ppm; ^{13}C NMR (100 MHz, $CDCl_3$) δ_C 56.6, 95.6, 111.3, 117.8, 124.9, 125.5, 125.6, 127.0, 127.9, 133.3, 138.3, 147.6, 149.9, 151.1 ppm; HRMS (ESI) found $[M+H]^+$ = 344.0276 $C_{17}H_{14}{}^{79}BrNO_2$ requires $[M+H]^+$ = 344.0281.

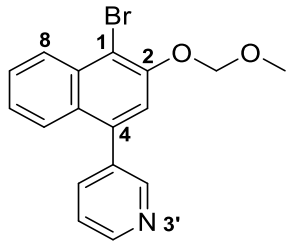

2.211

1-Bromo-2-methoxymethoxy-4-(3-pyridyl)naphthtalene (2.211): from 1-bromo-4-(3-pyridyl)-2-naphthol (1.70 g, 5.66 mmol); brown oil (1.44 g, 74%); ν_{max} (neat) 1344, 1228, 1149, 1086, 1042, 1015, 976, 921, 886, 756, 715 cm^{-1}; ^{1}H NMR (400 MHz, $CDCl_3$) δ_H 3.58 (3H, s, CH_3), 5.38 (2H, s, CH_2), 7.38–7.45 (3H, m, 3, 6, 5′-H), 7.60 (1H, t, *J* = 7.7 Hz, 7-H), 7.70 (1H, d, *J* = 8.4 Hz, 5-H), 7.80 (1H, dt, *J* = 7.8, 1.9 Hz, 6′-H), 8.35 (1H, d, *J* = 8.5 Hz, 8-H), 8.71 (1H, dd, *J* = 4.8, 1.5 Hz, 4′-H), 8.74 (1H, d, *J* = 1.8 Hz, 2′-H) ppm; ^{13}C NMR (100 MHz, $CDCl_3$) δ_C 56.7, 95.7, 111.0, 118.4, 123.2, 125.4, 125.8, 127.0, 127.9, 128.8, 133.4, 135.5, 137.3, 137.5, 149.1, 150.4, 151.2 ppm; HRMS (ESI) found $[M+H]^+$ = 344.0285 $C_{17}H_{14}{}^{79}BrNO_2$ requires $[M+H]^+$ = 344.0281.

3.2.3.2.11 General Experimental Procedure for the Synthesis of (*E*)-3-(2-Methoxymethoxy-4-pyridylnaphthalen-1-yl)-1,1-bis(4-methoxyphenyl)prop-2-en-1-ol (2.212): $Pd(OAc)_2$ (7 mmol%), 1-bromo-2-methoxymethoxy-4-pyridylnaphthalene (1 mmol), 1,1-bis(4-methoxyphenyl)prop-2-en-1-ol (2 mmol), K_2CO_3 (1.5 mmol), TBAB (1.5 mmol), KCl (1 mmol) were degassed in DMF (18.5 mL) and heated at 100 °C under N_2. After 2 days of reaction, the crude was diluted with DCM (100 mL), filtered through celite, washed with water (2 × 200 mL), dried with anhydrous sodium sulfate and evaporated to dryness, leading to the desired products after purification.

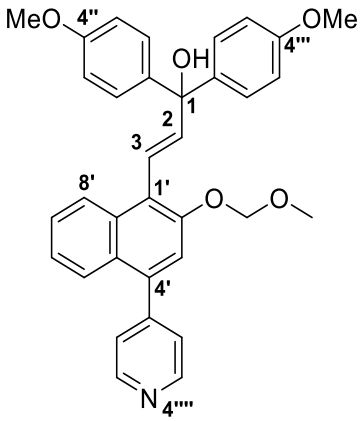

2.212

(*E*)-3-(2-Methoxymethoxy-4-(4-pyridyl)naphthalen-1-yl)-1,1-bis(4-methoxyphenyl)prop-2-en-1-ol (2.212): from 1-bromo-2-methoxymethoxy-4-(4-pyridyl)naphthalene (0.92 g, 2.7 mmol); Flash column chromatography [Aldrich silica gel (60 Å 230-400 mesh 40-63 μm), eluent: 40% EtOAc in PhMe, fraction 4] led the corresponding product as a yellow oil that solidified upon standing (0.36 g, 29%); m.p. = 158–163 °C; ν_{max} (neat) 1584, 1505, 1240, 1185, 1148, 1074, 1041, 1022, 993, 922, 815, 772, 586 cm^{-1}; ^{1}H NMR (400 MHz, $CDCl_3$) δ_H 2.73 (1H, bs, OH), 3.45 (3H, s, CH_3), 3.82 (6H, s, OMe), 5.24 (2H, s, CH_2), 6.85–6.92 (5H, m, 2, 3″, 5″, 3‴, 5‴-H), 7.04 (1H, d, *J* = 16.1 Hz, 3-H), 7.32–7.36 (2H, m, 3′, 6′-H), 7.41–7.47 (7H, m, 7′, 2″, 6″, 2‴, 6‴, 2⁗, 6⁗-H), 7.74 (1H, d, *J* = 8.3 Hz, 5′-H), 8.08 (d, 1H, d, *J* = 8.5 Hz, 8′-H), 8.71 (2H, d, *J* = 5.8 Hz, 3⁗, 5⁗-H) ppm; ^{13}C NMR (100 MHz, $CDCl_3$) δ_C 55.3, 56.4, 79.3, 95.4, 113.5, 117.7, 120.8, 122.8, 124.7, 125.00, 125.05, 125.6, 126.7, 127.2, 128.4, 133.3, 137.9, 138.6, 143.1, 148.4, 149.8, 151.2, 158.8 ppm; HRMS (ESI) found $[M+H]^+$ = 534.2267 $C_{34}H_{31}NO_5$ requires $[M+H]^+$ = 534.2275.

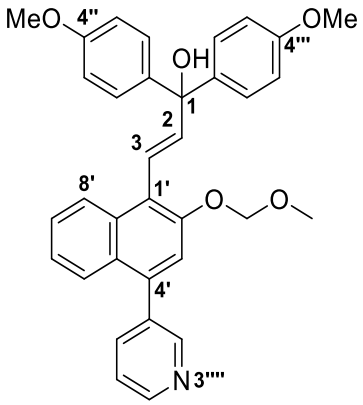

2.213

(*E*)-3-(2-Methoxymethoxy-4-(3-pyridyl)naphthalen-1-yl)-1,1-bis(4-methoxyphenyl)prop-2-en-1-ol (2.213): from 1-bromo-2-methoxymethoxy-4-(3-pyridyl)naphthalene (1.00 g, 2.91 mmol); Flash column chromatography [Aldrich silica gel (60 Å 230-400 mesh 40-63 μm), eluent: 40%

EtOAc in PhMe, fraction 4] giving the corresponding product as a yellow powder (0.87 g, 55%); m.p. = 68–72 °C; ν_{max} (neat) 1606, 1582, 1506, 1244, 1172, 1150, 1001, 919, 828, 757, 714, 580 cm^{-1}; ^1H NMR (400 MHz, $CDCl_3$) δ_H 2.80 (1H, bs, OH), 3.44 (3H, s, CH_3), 3.81 (6H, s, OMe), 5.23 (2H, s, CH_2), 6.86–6.91 (5H, m, 2, 3″, 5″, 3‴, 5‴-H), 7.04 (1H, d, *J* = 16.1 Hz, 3-H), 7.30–7.34 (2H, m, 3′, 6′-H), 7.41–7.48 (6H, m, 7′, 2″, 6″, 2‴, 6‴, 5⁗-H), 7.70 (1H, d, *J* = 8.2 Hz, 5′-H), 7.80 (1H, dt, *J* = 1.9, 7.8 Hz, 6⁗-H), 8.08 (1H, d, *J* = 8.5 Hz, 8′-H), 8.66 (1H, dd, *J* = 1.3, 4.8 Hz, 4⁗-H), 8.71 (1H, d, *J* = 1.6 Hz, 2⁗-H) ppm; ^{13}C NMR (100 MHz, $CDCl_3$) δ_C 55.3, 55.4, 79.3, 95.5, 113.5, 118.3, 120.9, 122.4, 123.2, 124.6, 124.9, 125.7, 126.6, 128.0, 128.4, 133.3, 136.2, 136.9, 137.4, 138.6, 143.0, 148.7, 150.5, 151.2, 158.8 ppm; HRMS (ESI) found $[M+H]^+$ = 534.2261 $C_{34}H_{31}NO_5$ requires $[M+H]^+$ = 534.2275.

3.2.3.2.12 General Experimental Procedure for the Synthesis of 3,3-Bis(4-methoxyphenyl)-6-pyridyl-3*H*-naphtho[2,1-*b*]pyran (2.214): TFA (17 mmol) was added dropwise at 0°C under N_2 to a mixture of (*E*)-3-(2-methoxymethoxy-4-pyridylnaphthalen-1-yl)-1,1-bis(4-methoxyphenyl)prop-2-en-1-ol (0.56 mmol) in DCM (20.0 mL) and glacial AcOH (20.0 mL). The resulting fading blue solution was warmed to room temperature and stirred for 4 h as it acquired a brown colour. Afterwards, the crude was diluted with DCM (100 mL), poured into water (100 mL), neutralized by the addition of $NaHCO_3$ and the phases separated. The resulting yellow organic phase was washed with water (2 × 100 mL), dried with anhydrous sodium sulfate and evaporated to dryness, leading to the corresponding product after purification.

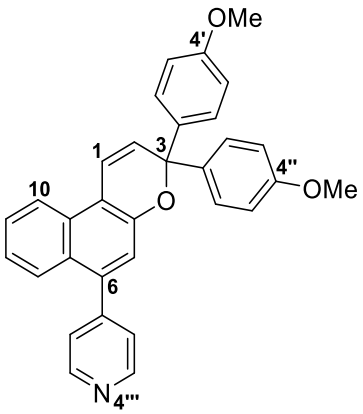

2.214

3,3-Bis(4-methoxyphenyl)-6-(4-pyridyl)-3*H*-naphtho[2,1-*b*]pyran (2.214): from (*E*)-3-(2-methoxymethoxy-4-(4-pyridyl)naphthalen-1-yl)-1,1-bis(4-methoxyphenyl)prop-2-en-1-ol (0.30 g, 0.56 mmol); Flash column chromatography [Aldrich silica gel (60 Å 230-400 mesh 40-63 μm), eluent: 50% EtOAc in hexanes, fraction 1] led to the corresponding product as a pink powder (0.16 g, 61%); m.p. = 141–143 °C; ν_{max} (neat) 1605, 1507, 1246, 1172, 1032, 1002, 825, 716, 586 cm^{-1};

Photomerocyanine λ_{max} = 472 nm (PhMe); ^{1}H NMR (400 MHz, $CDCl_3$) δ_H 3.77 (6H, s, OMe), 6.25 (1H, d, *J* = 10.0 Hz, 2-H), 6.85 (4H, app. d, *J* = 8.9 Hz, 3′, 5′, 3″, 5″-H), 7.13 (1H, s, 5-H), 7.25–7.34 (2H, m, 1, 8-H), 7.37–7.41 (6H, m, 2′, 6′, 2″, 6″, 2‴, 6‴-H), 7.50 (1H, app. t, *J* = 8.2 Hz, 9-H), 7.71 (1H, d, *J* = 8.3 Hz, 7-H), 8.04 (1H, d, *J* = 8.5 Hz, 10-H), 8.70 (2H, app. d, *J* = 6.0 Hz, 3‴, 5‴-H) ppm; ^{13}C NMR (100 MHz, $CDCl_3$) δ_C 55.3, 82.4, 113.5, 114.5, 118.8, 119.3, 121.9, 124.2, 124.9, 125.8, 126.8, 126.9, 128.4, 128.8, 130.3, 137.0, 139.0, 148.2, 149.8, 149.9, 159.0 ppm; HRMS (ESI) found $[M+H]^+$ = 472.1894 $C_{32}H_{25}NO_3$ requires $[M+H]^+$ = 472.1907.

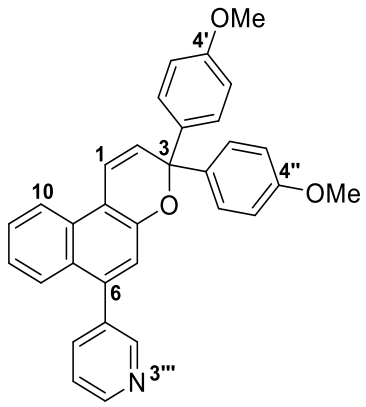

2.215

3,3-Bis(4-methoxyphenyl)-6-(3-pyridyl)-3*H*-naphtho[2,1-*b*]pyran (2.215): from (*E*)-3-(2-methoxymethoxy-4-(3-pyridyl)naphthalen-1-yl)-1,1-bis(4-methoxyphenyl)prop-2-en-1-ol (99.7 mg, 0.187 mmol); Flash column chromatography [Aldrich silica gel (60 Å 230-400 mesh 40-63 μm), eluent: 50% EtOAc in hexanes, fraction 1] led to the corresponding product as a pink powder (60.4 mg, 69%); m.p. = 147–149 °C; ν_{max} (neat) 1606, 1506, 1246, 1172, 1032, 1002, 824, 716, 587 cm^{-1}; Photomerocyanine λ_{max} = 474 nm (PhMe); ^{1}H NMR (400 MHz, $CDCl_3$) δ_H 3.77 (6H, s, OMe), 6.25 (1H, d, *J* = 10.0 Hz, 2-H), 6.85 (4H, app. d, *J* = 8.9 Hz, 3′, 5′, 3″, 5″-H), 7.14 (1H, s, 5-H), 7.28 (1H, app. t, *J* = 7.1 Hz, 8-H), 7.33 (1H, d, *J* = 10.0 Hz, 1-H), 7.37–7.41 (5H, m, 2′, 6′, 2″, 6″, 5‴-H), 7.49 (1H, app. t, *J* = 7.1 Hz, 9-H), 7.68 (1H, d, *J* = 8.3 Hz, 7-H), 7.77 (1H, dt, *J* = 2.0, 7.8 Hz, 6‴-H), 8.04 (1H, d, *J* = 8.5 Hz, 10-H), 8.66 (1H, dd, *J* = 1.6, 8.4 Hz, 4‴-H), 8.71 (1H, d, *J* = 1.7 Hz, 2‴-H) ppm; ^{13}C NMR (100 MHz, $CDCl_3$) δ_C 55.3, 82.4, 113.5, 114.2, 118.9, 119.8, 121.8, 123.1, 124.1, 126.0, 126.8, 127.5, 128.4, 128.6, 130.3, 136.0, 137.1, 137.3, 138.1, 148.7, 149.9, 150.5, 159.0 ppm; HRMS (ESI) found $[M+H]^+$ = 472.1903 $C_{32}H_{25}NO_3$ requires $[M+H]^+$ = 472.1907.

3.3 Synthesis of Photochromic Rhenium(I) Complexes

3.3.1 Synthesis of *fac*-[Re(N^N)(CO)$_3$Cl]^0 Complexes

3.3.1.1 General Experimental Procedure for the Synthesis of *fac*-[Re(N^N)(CO)$_3$Cl]^0 Complexes: rhenium pentacarbonyl chloride (1.00 mmol) and a bidentate ligand (1.00 mmol) were mixed in anhydrous PhMe (24 mL) and heated at reflux under N_2 or Ar in the dark. Upon cooling, the precipitate was collected by filtration, rinsed first with cold PhMe and then with cold Et_2O, and dried under reduced pressure.

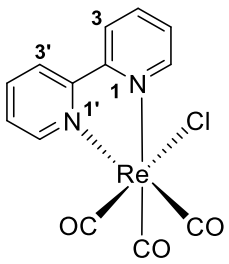

2.218

***fac*-Rhenium(I) tricarbonyl bipyridyl chloride (*fac*-[Re(BPy)(CO)$_3$Cl]^0) (2.218):** 16 h of reaction; Yellow powder (1.22 g, 96%); m.p. > 300 °C; ν_{max} (neat) 2022, 2013, 1870, 1601, 1470, 1444, 765, 732, 647, 631, 536 cm^{-1}; ^{1}H NMR (400 MHz, DMSO-d$_6$) δ_H 7.77 (t, 2H, J = 6.5 Hz, 5, 5′-H), 8.35 (t, 2H, J = 7.8 Hz, 4, 4′-H), 8.77 (d, 2H, J = 8.1 Hz, 3, 3′-H), 9.03 (d, 2H, J = 5.2 Hz, 6, 6′-H) ppm; ^{13}C NMR (100 MHz, DMSO-d$_6$) δ_C 124.8, 128.4, 140.8, 153.4, 155.6, 190.5, 198.3 ppm; HRMS (ESI) found [M-Cl]$^+$ = 427.0089 $C_{13}H_8{}^{35}ClN_2O_3{}^{187}Re$ requires [M-Cl]$^+$ = 427.0093.

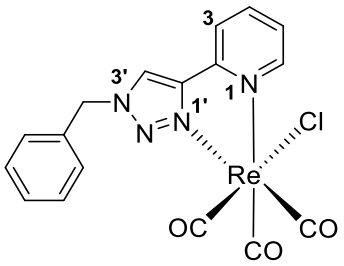

2.220

***fac*-Rhenium(I) tricarbonyl 2-(1-benzyl-1*H*-1,2,3-triazol-4-yl)pyridyl chloride (*fac*-[Re(PyTz)(CO)$_3$Cl]^0) (2.220):** 15 h of reaction; Pale yellow powder (423.9 mg, 94%); m.p. > 300 °C; ν_{max} (neat) 3104, 2023, 1902, 1868, 1616, 1454, 1125, 777, 729 cm^{-1}; ^{1}H NMR (400 MHz, DMSO-d$_6$) δ_H 5.91 (2H, s, CH_2), 7.45–7.48 (5H, m, Ph-H), 7.64 (1H, t, J = 5.9 Hz, 5-H), 8.26–8.33 (2H, m, 3, 4-H), 8.97 (1H, d, J = 4.9 Hz, 6-H), 9.28 (1H, s, 4′-H) ppm; ^{13}C NMR (100 MHz,

DMSO-d_6) δ_C 55.2, 123.3, 126.4, 127.0, 129.1, 129.4, 129.6, 134.6, 141.1, 149.0, 149.1, 153.5, 190.0, 197.2, 198.1 ppm; HRMS (ESI) found $[M+NH_4]^+$ = 560.0475 $C_{17}H_{12}{}^{35}ClN_4O_3{}^{187}Re$ requires $[M+NH_4]^+$ = 560.0499.

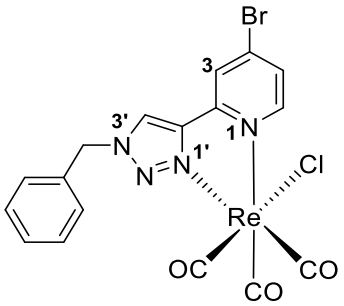

2.222

***fac*-Rhenium(I) tricarbonyl 2-(1-benzyl-1*H*-1,2,3-triazol-4-yl)-4-bromopyridyl chloride (*fac*-[Re(4-BrPyTz)(CO)$_3$Cl]^0) (2.222):** 21 h of reaction; Pale yellow powder (84.7 mg, 62%); m.p. > 300 °C; ν_{max} (neat) 2020, 1921, 1888, 1604, 1574, 1454, 1099, 832, 695 cm^{-1}; ^{1}H NMR (400 MHz, DMSO-d_6) δ_H 5.90 (2H, s, CH_2), 7.42–7.47 (5H, m, Ph-H), 7.86 (1H, dd, *J* = 1.8, 6.0 Hz, 5-H), 8.73 (1H, d, *J* = 1.8 Hz, 3-H), 8.78 (1H, d, *J* = 6.0 Hz, 6-H), 9.20 (1H, s, 4′-H) ppm; ^{13}C NMR (100 MHz, DMSO-d_6) δ_C 55.3, 126.4, 127.0, 129.3, 129.5, 129.6, 129.8, 134.3, 136.7, 148.1, 150.3, 154.1, 189.7, 197.1, 197.8 ppm; HRMS (ESI) found $[M-Cl]^+$ = 582.9548 $C_{17}H_{11}{}^{79}Br^{35}ClN_4O_3{}^{187}Re$ requires $[M-Cl]^+$ = 582.9544.

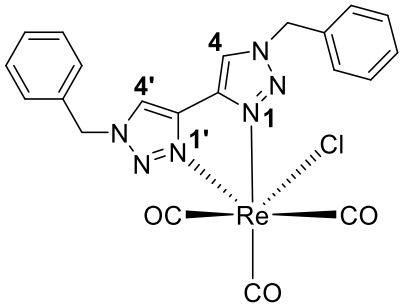

2.224

***fac*-Rhenium(I) tricarbonyl 1,1'-dibenzyl-1*H*,1'*H*-4,4'-bi(1,2,3-triazolyl) chloride (*fac*-[Re(BTz)(CO)$_3$Cl]^0) (2.224):** 15 h of reaction; Pale yellow powder (313.2 mg, 91%); m.p. > 300 °C; ν_{max} (neat) 3134, 2019, 1907, 1871, 1448, 1422, 1292, 1109, 817, 743, 660 cm^{-1}; ^{1}H NMR (400 MHz, DMSO-d_6) δ_H 5.88 (4H, s, CH_2), 7.39–7.47 (10H, m, Ph-H), 8.83 (2H, s, 4, 4′-H) ppm; ^{13}C NMR (100 MHz, DMSO-d_6) δ_C 55.1, 123.9, 129.0, 129.3, 129.6, 134.8, 140.4, 189.8, 197.2 ppm; HRMS (ESI) found $[M+K]^+$ = 661.0137 $C_{21}H_{16}{}^{35}ClN_6O_3{}^{187}Re$ requires $[M+K]^+$ = 661.0167.

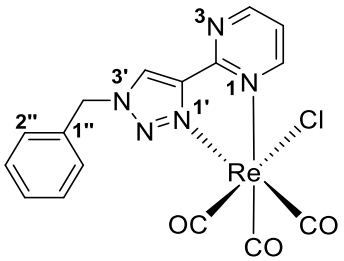

2.226

***fac*-Rhenium(I) tricarbonyl 2-(1-pyrimidyl-1*H*-1,2,3-triazol-4-yl)pyridyl chloride (*fac*-[Re(PymTz)(CO)$_3$Cl]^0) (2.226):** 20 h of reaction; Yellow powder (217.8 mg, 70%); m.p. > 300 °C; ν_{max} (neat) 2021, 1886, 1584, 1411, 1274, 1121, 1024, 796, 704 cm^{-1}; ^{1}H NMR (400 MHz, acetone-d$_6$) δ_H 5.95 (2H, s, CH$_2$), 7.40–7.48 (3H, m, 3″, 4″, 5″-H), 7.56 (2H, d, *J* = 6.6 Hz, 2″, 6″-H), 7.74 (1H, t, *J* = 5.3 Hz, 5-H), 9.10 (1H, s, 4′-H), 9.15 (1H, dd, *J* = 4.9, 2.1 Hz, 6-H), 9.29 (1H, dd, *J* = 5.6, 2.1 Hz, 4-H) ppm; ^{13}C NMR (100 MHz, acetone-d$_6$) δ_C 55.5, 122.0, 127.3, 128.6, 129.1, 129.2, 134.1, 147.3, 159.5, 159.9, 160.2 ppm.

3.3.2 Synthesis of *fac*-[Re(BPy)(CO)$_3$NP]PF$_6$ Complexes

3.3.2.1 General Experimental Procedure for the Synthesis of fac-[Re(BPy)(CO)$_3$NP]PF$_6$ Complexes: *fac*-[Re(BPy)(CO)$_3$Cl]^0 (1.00 mmol), AgPF$_6$ (1.00 mmol) and pyridylnaphthopyran (1.00 mmol) were mixed in DCM (37 mL) and stirred under a N$_2$ or Ar atmosphere in the dark at room temperature. Later, the reaction mixture was filtered through a short pad of celite to remove the Ag salts. Flash column chromatography or crystallization led to the corresponding pure product.

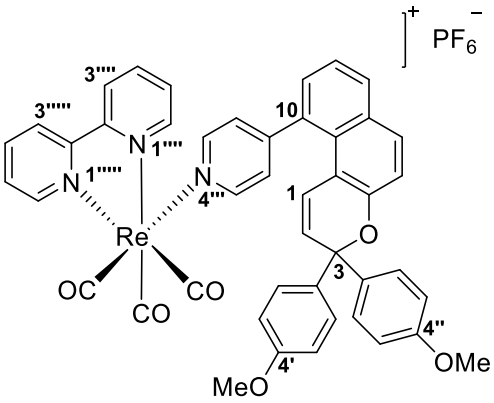

2.229

***fac*-Rhenium(I) tricarbonyl 3,3-bis(4-methoxyphenyl)-10-(4-pyridyl)-3*H*-naphtho[2,1-*b*]pyranyl bipyridine hexafluorophosphate (2.229):** 6 days of reaction; Flash column chromatography [activated Al$_2$O$_3$, eluent: MeOH (0.5%) in DCM → MeOH (1%) in DCM, fraction 4], followed by crystallization from a mixture of DCM/Et$_2$O, afforded the corresponding product as

yellow crystalline needles (57.3 mg, 45%); m.p. > 300 °C; ν_{max} (neat) 2028, 1914, 1606, 1506, 1443, 1245, 1001, 821, 555 cm^{-1}; ^{1}H NMR (400 MHz, acetone-d_6) δ_H 3.78 (6H, s, OMe), 5.40 (1H, d, *J* = 9.6 Hz, 2-H), 5.55 (1H, d, *J* = 9.6 Hz, 1-H), 6.91 (4H, app. d, *J* = 8.8 Hz, 3′, 3″, 5′, 5″-H), 7.17–7.23 (6H, m, 2′, 2″, 2‴, 6′, 6″, 6‴-H), 7.34 (1H, d, *J* = 8.8 Hz, 5-H), 7.40–7.41 (2H, m, 7, 9-H), 7.88–7.92 (2H, m, 6, 8-H), 8.14 (2H, app. t, *J* = 7.0 Hz, 5⁗, 5′′′′′-H), 8.53 (2H, app. t, *J* = 8.0 Hz, 4⁗, 4′′′′′-H), 8.63 (2H, d, *J* = 6.6 Hz, 3‴, 5‴-H), 8.88 (2H, d, *J* = 8.2 Hz, 3⁗, 3′′′′′-H), 9.67 (2H, d, *J* = 5.0 Hz, 6⁗, 6′′′′′-H) ppm; ^{13}C NMR (100 MHz, acetone-d_6) δ_C 54.7, 81.4, 113.4, 114.5, 119.1, 123.5, 124.1, 124.5, 124.9, 126. 9, 127.6, 127.8, 129.3, 130.4, 130.5, 130.7, 131.5, 132.9, 136.4, 141.7, 151.8, 153.3, 154.4, 154.9, 156.1, 159.2 ppm; ^{19}F NMR (376 MHz, acetone-d_6) δ_F -72.6 (d, *J* = 714 Hz) ppm; HRMS (ESI) found $[M\text{-}PF_6]^+$ = 898.1917 $C_{45}H_{33}N_3O_6{}^{187}RePF_6$ requires $[M\text{-}PF_6]^+$ = 898.1921.

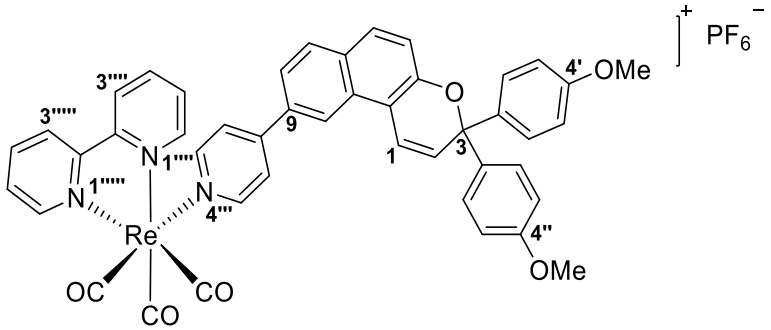

2.230

***fac*-Rhenium(I) tricarbonyl 3,3-bis(4-methoxyphenyl)-9-(4-pyridyl)-3*H*-naphtho[2,1-*b*]pyranyl bipyridine hexafluorophosphate (2.230):** 6 days of reaction; Flash column chromatography [activated Al_2O_3, eluent: MeOH (0.5%) in DCM, fraction 3] gave the corresponding product as an orange powder (0.03 g, 14%); m.p. > 300 °C; ν_{max} (neat) 2030, 1907, 1611, 1506, 1446, 1246, 1173, 1092, 1066, 1025, 826, 763 cm^{-1}; ^{1}H NMR (400 MHz, $CDCl_3$) δ_H 3.73 (6H, s, OMe), 6.19 (1H, d, *J* = 10.0 Hz, 2-H), 6.80 (4H, app. d, *J* = 8.7 Hz, 3′, 3″, 5′, 5″-H), 7.16 (1H, d, *J* = 8.8 Hz, 5-H), 7.26–7.37 (6H, m, Ar-H), 7.54 (1H, d, *J* = 8.8 Hz, 6-H), 7.63–7.68 (5H, m, Ar-H), 8.10–8.15 (5H, m, Ar-H), 8.39 (2H, d, *J* = 8.2 Hz, 3⁗, 3′′′′′-H), 9.05 (2H, d, *J* = 5.3 Hz, 6⁗, 6′′′′′-H) ppm; ^{13}C NMR (100 MHz, $CDCl_3$) δ_C 55.2, 82.4, 113.4, 115.0, 118.7, 120.3, 121.2, 121.3, 124.6, 125.4, 128.3, 128.8, 129.0, 129.2, 129.7, 129.8, 132.2, 132.9, 136.9, 141.5, 151.3, 151.5, 151.9, 152.7, 155.5, 158.9, 191.0, 195.7 ppm; HRMS (ESI) found $[M\text{-}PF_6]^+$ = 898.1913 $C_{45}H_{33}N_3O_6{}^{187}RePF_6$ requires $[M\text{-}PF_6]^+$ = 898.1921.

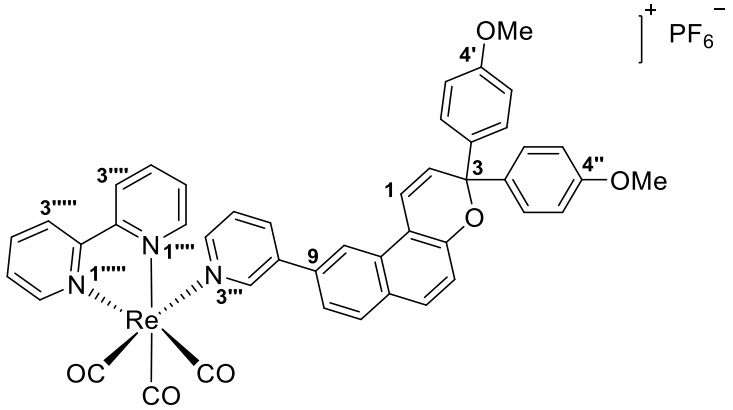

2.231

***fac*-Rhenium(I) tricarbonyl 3,3-bis(4-methoxyphenyl)-9-(3-pyridyl)-3*H*-naphtho[2,1-*b*]pyranyl bipyridine hexafluorophosphate (2.231):** 3 days of reaction; Flash column chromatography [activated Al_2O_3, eluent: MeOH (0.5%) in DCM, fraction 3] gave the corresponding product as an orange powder (0.15 g, 67%); m.p. > 300 °C; ν_{max} (neat) 2029, 1909, 1603, 1506, 1446, 1246, 1173, 831, 764, 556 cm^{-1}; ^1H NMR (400 MHz, DMSO-d_6) δ_H 3.73 (6H, s, OMe), 6.71 (1H, d, *J* = 10.0 Hz, 2-H), 6.92–6.94 (4H, m, 3′, 3″, 5′, 5″-H), 7.31–7.34 (2H, m, 1-H, Ar-H), 7.38–7.42 (5H, m, Ar-H), 7.57 (1H, dd, *J* = 8.0, 5.8 Hz, Ar-H), 7.82–7.84 (2H, m, Ar-H), 7.92–7.99 (3H, m, Ar-H), 8.42–8.55 (5H, m, Ar-H), 8.75 (2H, d, *J* = 8.2 Hz, 3′′′′, 3′′′′′-H), 9.48 (2H, app. d, *J* = 4.9 Hz, 6′′′′, 6′′′′′-H) ppm; ^{13}C NMR (100 MHz, DMSO-d_6) δ_C 55.6, 82.2, 114.0, 114.9, 119.3, 119.8, 121.3, 122.7, 125.5, 127.4, 128.2, 129.1, 129.5, 129.6, 129.7, 130.0, 130.1, 133.2, 137.2, 139.15, 139.24, 142.0, 149.6, 151.1, 151.5, 154.8, 155.7, 159.0, 192.6, 195.8 ppm; HRMS (ESI) found $[M\text{-}PF_6]^+$ = 898.1916 $C_{45}H_{33}N_3O_6{}^{187}RePF_6$ requires $[M\text{-}PF_6]^+$ = 898.1921.

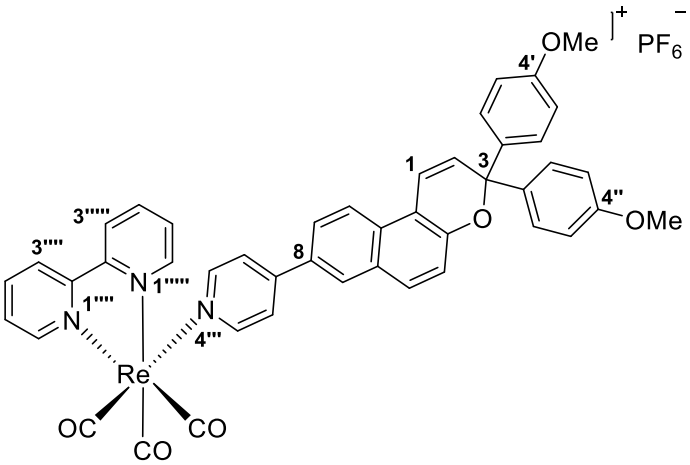

2.232

***fac*-Rhenium(I) tricarbonyl 3,3-bis(4-methoxyphenyl)-8-(4-pyridyl)-3*H*-naphtho[2,1-*b*]pyranyl bipyridine hexafluorophosphate (2.232):** 5 days of reaction; Crystallization from a mixture of DCM/hexane gave the corresponding product as an orange crystalline solid (0.23 g,

69%); m.p. > 300 °C; ν_{max} (neat) 2018, 1927, 1908, 1608, 1506, 1247, 1174, 1025, 1002, 769, 729, 554, 532 cm^{-1}; ^{1}H NMR (400 MHz, DMSO-d_6) δ_H 3.70 (s, 6 H, OMe), 6.52 (d, 1H, *J* = 10.1 Hz, 2-H), 6.89 (app. d, 4H, *J* = 8.8 Hz, 3′, 5′, 3″, 5″-H), 7.31–7.35 (m, 5H, 5, 2′, 6′, 2″, 6″-H), 7.46 (d, 1H, *J* = 10.1 Hz, 1-H), 7.84–7.88 (m, 4H, 6, 9, 2‴, 6‴-H), 7.95 (t, 2H, *J* = 6.5 Hz, 5⁗, 5′′′′′-H), 8.20 (d, 1H, *J* = 9.0 Hz, 10-H), 8.34 (s, 1H, 7-H), 8.40–8.45 (m, 4H, 3‴, 5‴, 4⁗, 4′′′′′-H), 8.75 (d, 2H, *J* = 8.2 Hz, 3⁗, 3′′′′′-H), 9.40 (d, 2H, *J* = 5.2 Hz, 6⁗, 6′′′′′-H) ppm; ^{13}C NMR (100 MHz, DMSO-d_6) δ_C 55.5, 82.3, 113.9, 114.4, 119.1, 119.7, 123.5, 124.0, 125.1, 125.4, 128.2, 128.5, 129.2, 129.59, 129.64, 130.0, 130.5, 131.4, 137.1, 141.9, 150.3, 151.9, 152.5, 154.6, 155.6, 159.0, 192.7, 196.0 ppm; HRMS (ESI) found $[M\text{-}PF_6]^+$ = 898.1927 $C_{45}H_{33}F_6N_3O_6P^{187}Re$ requires $[M\text{-}PF_6]^+$ = 898.1927.

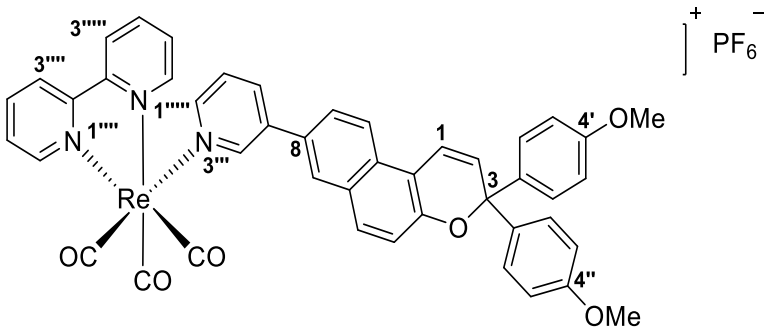

2.233

***fac*-Rhenium(I) tricarbonyl 3,3-bis(4-methoxyphenyl)-8-(3-pyridyl)-3*H*-naphtho[2,1-*b*]pyranyl bipyridine hexafluorophosphate (2.233):** 12 days of reaction; Flash column chromatography [activated Al_2O_3, eluent: MeOH (0.5%) in DCM, fraction 3] gave the corresponding product as an orange powder (0.03 g, 38%); m.p. > 300 °C; ν_{max} (neat) 2030, 1903, 1511, 1472, 1445, 1241, 1171, 1094, 842, 823, 764 cm^{-1}; ^{1}H NMR (400 MHz, $CDCl_3$) δ_H 3.74 (6H, s, OMe), 6.23 (1H, d, *J* = 9.9 Hz, 2-H), 6.82 (4H, app. d, *J* = 8.8 Hz, 3′, 3″, 5′, 5″-H), 7.20–7.28 (3H, m, Ar-H), 7.34–7.41 (5H, m, Ar-H), 7.57 (1H, app. s, 7-H), 7.65–7.72 (3H, m, Ar-H), 7.95 (2H, app. d, *J* = 5.92 Hz, Ar-H), 8.02 (1H, d, *J* = 8.8 Hz, 10-H), 8.19 (2H, app. t, *J* = 7.8 Hz, 4⁗, 4′′′′′-H), 8.36 (1H, s, 2‴-H), 8.47 (2H, d, *J* = 8.1 Hz, 3⁗, 3′′′′′-H), 9.09 (2H, d, *J* = 5.2 Hz, 6⁗, 6′′′′′-H) ppm; ^{13}C NMR (100 MHz, $CDCl_3$) δ_C 55.3, 82.5, 113.5, 114.0, 118.7, 119.7, 123.3, 124.7, 125.5, 127.26, 127.34, 128.3, 128.8, 128.9, 129.2, 129.7, 129.8, 130.3, 136.9, 138.1, 140.0, 141.7, 149.3, 149.6, 151.7, 152.7, 155.6, 159.0, 190.8, 195.6 ppm; HRMS (ESI) found $[M\text{-}PF_6]^+$ = 898.1908 $C_{45}H_{33}N_3O_6{}^{187}RePF_6$ requires $[M\text{-}PF_6]^+$ = 898.1921.

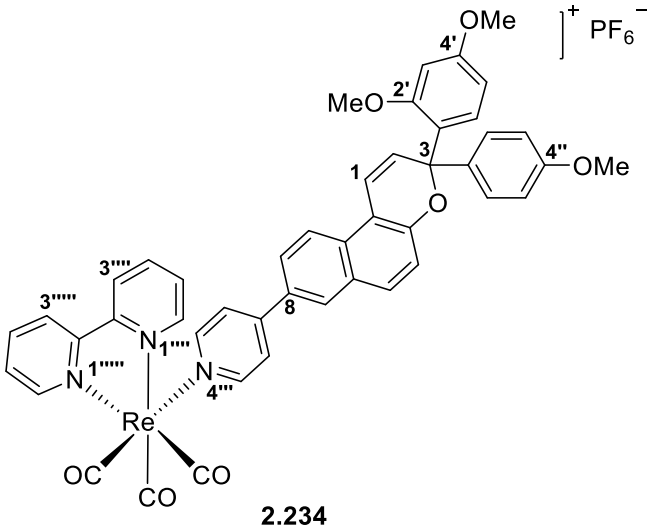

***fac*-Rhenium(I) tricarbonyl 3-(2,4-dimethoxyphenyl)-3-(4-methoxyphenyl)-8-(4-pyridyl)-3*H*-naphtho[2,1-*b*]pyranyl bipyridine hexafluorophosphate (2.234):** 5 days of reaction; Flash column chromatography [activated Al_2O_3, eluent: MeOH (0.5%) in DCM, fraction 4] afforded the corresponding product as a red-brown powder (260.6 mg, 74%); m.p. > 300 °C; ν_{max} (neat) 2030, 1904, 1606, 1499, 1469, 1446, 1246, 1207, 1173, 999, 832, 763, 556 cm^{-1}; ^1H NMR (400 MHz, $CDCl_3$) δ_H 3.56 (3H, s, OMe), 3.73 (6H, s, OMe), 6.43–6.53 (3H, m, 2, 3′, 5′-H), 6.78 (2H, d, J = 7.9 Hz, 3″, 5″-H), 7.02–7.12 (2H, m, 1, 5-H), 7.31 (2H, d, J = 7.9 Hz, 2″, 6″-H), 7.45–7.64 (7H, m, Ar-H), 7.80–7.83 (2H, m, Ar-H), 8.07 (4H, app. s, Ar-H), 8.29 (2H, d, J = 7.6 Hz, 3′′′′, 3′′′′′-H), 9.06 (2H, d, J = 3.8 Hz, 6′′′′, 6′′′′′-H) ppm; ^{13}C NMR (100 MHz, $CDCl_3$) δ_C 55.2, 55.3, 55.5, 82.1, 100.1, 103.8, 113.2, 113.8, 117.5, 119.4, 122.8, 123.9, 124.0, 124.6, 125.0, 127.86, 127.91, 128.2, 128.3, 128.93, 128.95, 129.5, 130.4, 130.5, 136.7, 141.4, 151.1, 151.5, 151.9, 152.8, 155.4, 156.8, 158.9, 160.6, 191.1, 195.5 ppm; HRMS (ESI) found $[M\text{-}PF_6]^+$ = 928.2036 $C_{46}H_{35}N_3O_7{}^{187}RePF_6$ requires $[M\text{-}PF_6]^+$ = 928.2027.

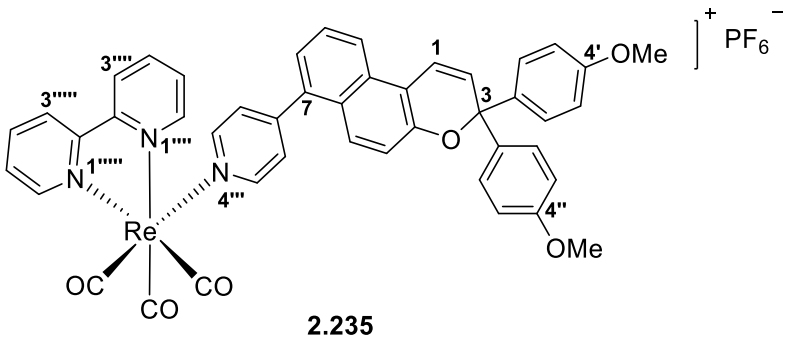

***fac*-Rhenium(I) tricarbonyl 3,3-bis(4-methoxyphenyl)-7-(4-pyridyl)-3*H*-naphtho[2,1-*b*]pyranyl bipyridine hexafluorophosphate (2.235):** 5 days of reaction; Flash column chromatography [activated Al_2O_3, eluent: MeOH (0.5%) in DCM → MeOH (1%) in DCM, fraction

3], followed by trituration with Et_2O, gave the corresponding product as an orange powder (0.12 g, 52%); m.p. > 300 °C; ν_{max} (neat) 2028, 1906, 1604, 1507, 1445, 1247, 1173, 1029, 832, 806, 761, 556 cm^{-1}; ^1H NMR (400 MHz, DMSO-d_6) δ_H 3.70 (6H, s, OMe), 6.52 (1H, d, J = 9.9 Hz, 2-H), 6.88 (4H, app. d, J = 8.4 Hz, 3′, 3″, 5′, 5″-H), 7.22–7.28 (6H, m, Ar-H), 7.45–7.54 (5H, m, Ar-H), 7.95 (2H, t, J = 6.1 Hz, 5′′′′, 5′′′′′-H), 8.23 (1H, d, J = 8.4 Hz, 10-H), 8.44–8.51 (4H, m, Ar-H), 8.80 (2H, d, J = 8.0 Hz, 3′′′′, 3′′′′′-H), 9.38 (2H, d, J = 4.7 Hz, 6′′′′, 6′′′′′-H) ppm; ^{13}C NMR (100 MHz, DMSO-d_6) δ_C 55.5, 82.0, 113.9, 115.0, 119.3, 119.6, 123.9, 125.5, 125.7, 125.9, 126.7, 126.9, 128.1, 128.2, 129.6, 129.9, 130.1, 135.8, 137.1, 142.0, 150.6, 151.9, 152.3, 154.5, 155.7, 159.0, 192.5, 196.0 ppm; HRMS (ESI) found $[M-PF_6]^+$ = 898.1916 $C_{45}H_{33}N_3O_6{}^{187}RePF_6$ requires $[M-PF_6]^+$ = 898.1921.

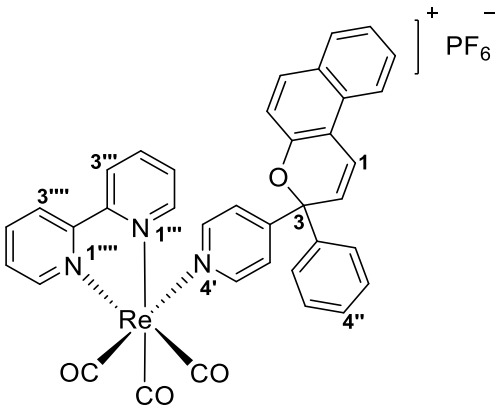

2.236

***fac*-Rhenium(I) tricarbonyl 3-(4-methoxyphenyl)-3-(4-pyridyl)-3*H*-naphtho[2,1-*b*]pyranyl bipyridine hexafluorophosphate (2.236):** 4 days of reaction; Flash column chromatography [activated Al_2O_3, eluent: MeOH (0.5%) in DCM → MeOH (1%) in DCM, fraction 3], followed by trituration with Et_2O, gave the corresponding product as a yellow powder (192.2 mg, 71%); ν_{max} (neat) 2031, 1938, 1904, 1888, 1610, 1444, 1010, 834, 766, 556 cm^{-1}; ^1H NMR (400 MHz, DMSO-d_6) δ_H 6.59 (1H, d, J = 10.0 Hz, 2-H), 7.20–7.38 (5H, m, Ar-H), 7.43–7.56 (7H, m, Ar-H), 7.79–7.88 (4H, m, Ar-H), 8.06 (1H, d, J = 8.5 Hz, 10-H), 8.33–8.39 (3H, m, Ar-H), 8.67 (2H, d, J = 8.2 Hz, 3′, 5′-H), 9.25 (2H, d, J = 5.4 Hz, 6′′′, 6′′′′-H) ppm; ^{13}C NMR (100 MHz, DMSO-d_6) δ_C 80.9, 114.0, 118.3, 121.3, 122.2, 124.0, 124.8, 125.1, 125.4, 126.2, 126.6, 127.7, 128.9, 129.1, 129.5, 129.6, 130.9, 141.9, 142.7, 149.6, 152.7, 154.5, 155.5, 155.6, 157.3, 192.4, 195.9 ppm; ^{19}F NMR (376 MHz, DMSO-d_6) δ_F -70.1 (d, J = 677 Hz) ppm; HRMS (ESI) found $[M-PF_6]^+$ = 760.1366 $C_{37}H_{25}F_6N_3O_4P^{185}Re$ requires $[M-PF_6]^+$ = 760.1369.

3.3.3 Synthesis of *fac*-[Re(PyTz)(CO)$_3$NP]PF$_6$ Complexes

3.3.3.1 General Experimental Procedure for the Synthesis of *fac*-[Re(PyTz)(CO)$_3$NP]PF$_6$ Complexes: fac-$[Re(PyTz)(CO)_3Cl]^0$ (1.00 mmol), $AgPF_6$ (1.00 mmol) and pyridylnaphthopyran

(1.00 mmol) were mixed in DCM (37 mL) and stirred under a N_2 or Ar atmosphere in the dark at room temperature. Later, the reaction mixture was filtered through a short pad of celite to remove the Ag salts. Flash column chromatography led to the corresponding pure product.

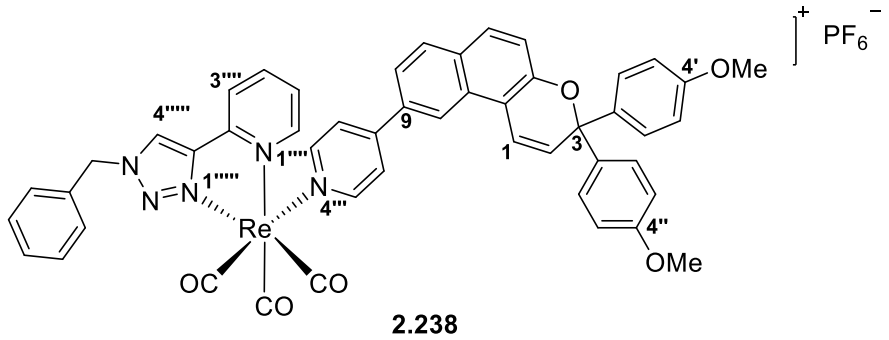

2.238

***fac*-Rhenium(I) tricarbonyl 3,3-bis(4-methoxyphenyl)-9-(4-pyridyl)-3*H*-naphtho[2,1-*b*]pyranyl 2-(1-benzyl-1*H*-1,2,3-triazol-4-yl)pyridine hexafluorophosphate (2.238):** 3 days of reaction; Flash column chromatography [activated Al_2O_3, eluent: MeOH (0.5%) in DCM, fraction 3] gave the corresponding product as an orange powder (26 mg, 17%); m.p. > 300 °C; ν_{max} (neat) 2030, 1915, 1609, 1508, 1028, 837, 778, 734, 557 cm^{-1}; ^1H NMR (400 MHz, CD_2Cl_2) δ_H 3.77 (6H, s, OMe), 5.77 (1H, d (AB), *J* = 14.5 Hz, CH_2), 5.84 (1H, d (AB), *J* = 14.5 Hz, CH_2), 6.33 (1H, d, *J* = 9.9 Hz, 2-H), 6.85 (4H, app. d, *J* = 8.6 Hz, 3′, 5′, 3″, 5″-H), 7.27 (1H, d, *J* = 8.8 Hz, 5-H), 7.32–7.58 (13H, m, 1-H, Ar-H), 7.64 (1H, *t*, *J* = 6.5 Hz, 5′′′′-H), 7.71 (1H, t, *J* = 8.7 Hz, 6-H), 7.84 (1H, d, *J* = 8.6 Hz, Ar-H), 8.06 (1H, d, *J* = 7.8 Hz, Ar-H), 8.16–8.23 (4H, m, Ar-H), 8.71 (1H, s, 4′′′′′-H), 9.13 (1H, d, *J* = 5.2 Hz, 6′′′′-H) ppm; ^{13}C NMR (100 MHz, CD_2Cl_2) δ_C 55.2, 56.6, 82.4, 113.3, 114.9, 118.6, 120.2, 121.0, 121.5, 123.7, 124.5, 125.9, 127.3, 128.2, 129.0, 129.2, 129.4, 129.61, 129.64, 129.8, 129.9, 132.8, 133.3, 136.8, 141.5, 149.45, 149.50, 151.4, 151.7, 152.0, 152.8, 159.1, 196.1 ppm; ^{19}F NMR (376 MHz, acetone-d_6) δ_F -72.4 (d, *J* = 714 Hz) ppm; HRMS (ESI) found $[M-PF_6]^+$ = 978.2291 $C_{49}H_{37}N_5O_6{}^{187}RePF_6$ requires $[M-PF_6]^+$ = 978.2296.

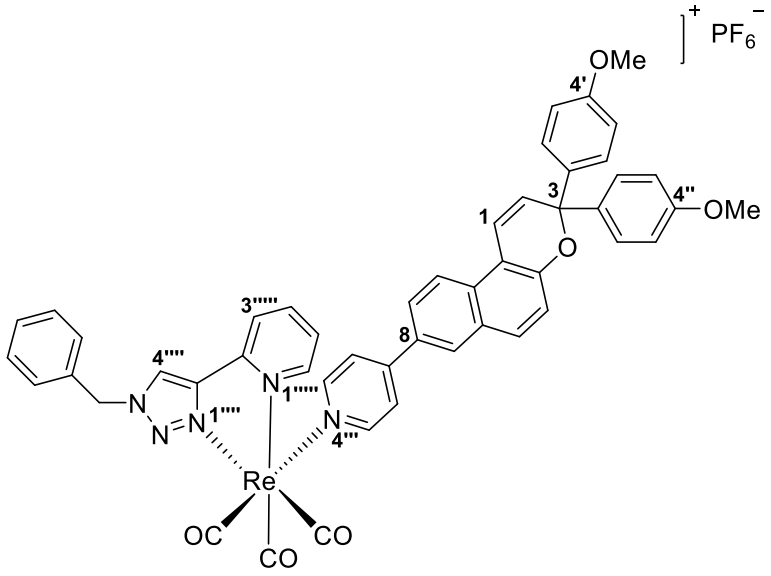

2.239

***fac*-Rhenium(I) tricarbonyl 3,3-bis(4-methoxyphenyl)-8-(4-pyridyl)-3*H*-naphtho[2,1-*b*]pyranyl 2-(1-benzyl-1*H*-1,2,3-triazol-4-yl)pyridine hexafluorophosphate (2.239):** 4 days of reaction; Flash column chromatography [activated Al_2O_3, eluent: MeOH (0.5%) in DCM, fraction 3] afforded the corresponding product as a yellow powder (0.24 g, 75%); m.p. > 300 °C; ν_{max} (neat) 2032, 1910, 1608, 1506, 1456, 1247, 1174, 1091, 1024, 1000, 832, 581 cm^{-1}; ^1H NMR (400 MHz, $CDCl_3$) δ_H 3.71 (6H, s, OMe), 5.96 (1H, d (AB), *J* = 15.1 Hz, CH_2), 6.00 (1H, d (AB), *J* = 15.1 Hz, CH_2), 6.53 (1H, d, *J* = 10.0 Hz, 2-H), 6.90 (4H, app. d, *J* = 8.5 Hz, 3′, 3″, 5′, 5″-H), 7.34–7.36 (5H, m, 5, 2′, 2″, 6′, 6″-H), 7.47–7.50 (6H, m, Ph-H and 1-H), 7.81–7.89 (5H, m, Ar-H), 8.22–8.38 (6H, m, Ar-H), 9.30 (1H, s, 4′′′′-H), 9.36 (1H, d, *J* = 5.2 Hz, 6′′′′′-H) ppm; ^{13}C NMR (100 MHz, $CDCl_3$) δ_C 55.5 55.8, 82.3, 114.0, 114.4, 119.1, 119.8, 123.6, 123.9, 124.0, 125.1, 127.5, 128.2, 128.4, 129.1, 129.2, 129.5, 129.6, 129.7, 130.0, 130.5, 131.4, 134.4, 137.1, 138.3, 142.3, 148.9, 149.6, 150.3, 152.0, 152.5, 154.7, 159.0 ppm; ^{19}F NMR (376 MHz, $CDCl_3$) δ_F -70.1 (d, *J* = 711 Hz) ppm; ^{31}P NMR (162 MHz, $CDCl_3$) δ_P -144.2 (sept, *J* = 711 Hz) ppm; HRMS (ESI) found $[M\text{-}PF_6]^+$ = 978.2287 $C_{49}H_{37}N_5O_6{}^{187}RePF_6$ requires $[M\text{-}PF_6]^+$ = 978.2296.

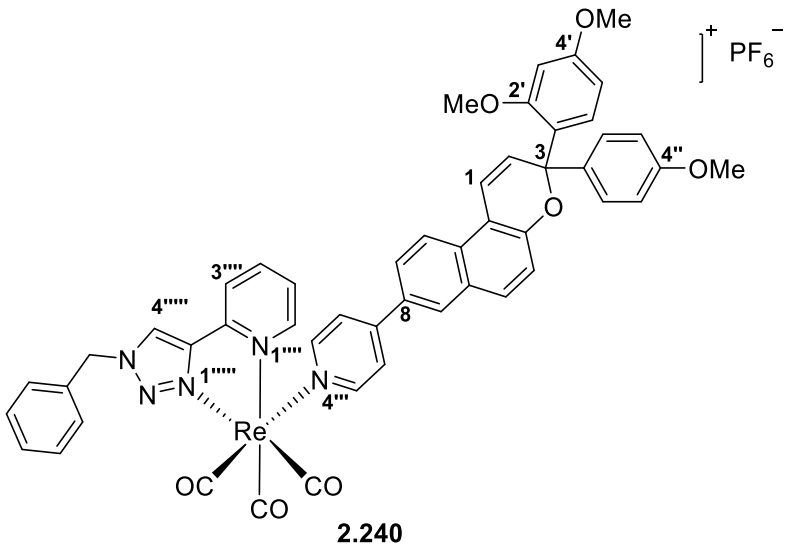

***fac*-Rhenium(I) tricarbonyl 3-(2,4-dimethoxyphenyl)-3-(4-methoxyphenyl)-8-(4-pyridyl)-3*H*-naphtho[2,1-*b*]pyranyl 2-(1-benzyl-1*H*-1,2,3-triazol-4-yl)pyridine hexafluorophosphate (2.240):** 6 days of reaction; Flash column chromatography [activated Al_2O_3, eluent: MeOH (0.5%) in DCM, fraction 3] afforded the corresponding product as a brick-red powder (57.3 mg, 27%); m.p. > 300 °C; ν_{max} (neat) 2033, 1914, 1609, 1505, 1246, 1174, 1026, 830, 776, 556 cm^{-1}; ^1H NMR (400 MHz, acetone-d_6) δ_H 3.61 (3H, s, OMe), 3.73 (3H, s, OMe), 3.76 (3H, s, OMe), 5.99–6.07 (2H, m, CH_2), 6.51 (1H, dd, *J* = 2.3, 6.5 Hz, 5′-H), 6.56 (1H, d, *J* = 2.3 Hz, 3′-H), 6.63 (1H, d, *J* = 10.2 Hz, 2-H), 6.82 (2H, app. d, *J* = 8.9 Hz, 3″, 5″-H), 7.27 (1H, d, *J* = 8.8 Hz, 5-H), 7.33–7.36 (3H, m, Ar-H), 7.44–7.59 (8H, m, Ar-H), 7.79–7.85 (4H, m, Ar-H), 7.89 (1H, t, *J* = 6.0 Hz, 5′′′′-H), 8.18–8.20 (2H, m, 7, 10-H), 8.29 (1H, d, *J* = 7.9 Hz, 3′′′′-H), 8.38 (1H, t, *J* = 7.3 Hz, 4′′′′-H), 8.50 (2H, d, *J* = 6.7 Hz, 3′′′, 5′′′-H), 9.14 (1H, s, 4′′′′′-H), 9.47 (1H, d, *J* = 5.4 Hz, 6′′′′-H) ppm; ^{13}C NMR (100 MHz, acetone-d_6) δ_C 54.5, 54.6, 54.9, 55.9, 81.8, 99.7, 104.0, 112.8, 114.2, 117.6, 119.4, 122.9, 123.4, 123.5, 124.29, 124.34, 126.3, 127.4, 127.6, 127.9, 128.2, 128.5, 128.7, 129.1, 129.20, 129.22, 129.9, 130.4, 130.5, 133.8, 136.4, 141.7, 149.3, 149.8, 150.8, 151.9, 152.3, 154.1, 156.8, 159.0, 160.8 ppm; ^{19}F NMR (376 MHz, acetone-d_6) δ_F -72.4 (d, *J* = 714 Hz) ppm; HRMS (ESI) found $[M-PF_6]^+$ = 1008.2395 $C_{50}H_{39}N_5O_7{}^{187}RePF_6$ requires $[M-PF_6]^+$ = 1008.2402.

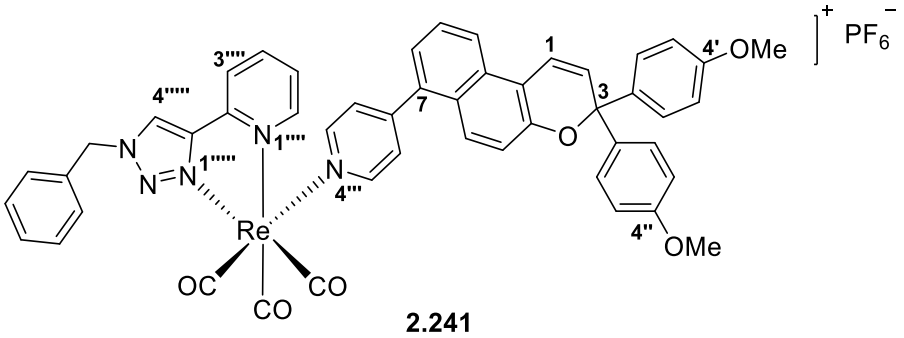

***fac*-Rhenium(I) tricarbonyl 3,3-bis(4-methoxyphenyl)-7-(4-pyridyl)-3*H*-naphtho[2,1-*b*]pyranyl 2-(1-benzyl-1*H*-1,2,3-triazol-4-yl) hexafluorophosphate (2.241):** 3 days of reaction; Flash column chromatography [activated Al_2O_3, eluent: MeOH (0.5%) in DCM → MeOH (1%) in DCM, fraction 3], followed by trituration with Et_2O/hexane, gave the corresponding product as an orange powder (159.7 mg, 79%); m.p. > 300 °C; ν_{max} (neat) 2033, 1908, 1614, 1507, 1247, 1174, 1030, 833, 556 cm^{-1}; ^1H NMR (400 MHz, CD_2Cl_2) δ_H 3.77 (6H, s, OMe), 5.76 (1H, d (AB), *J* = 14.5 Hz, CH_2), 5.82 (1H, d (AB), *J* = 14.5 Hz, CH_2), 6.33 (1H, d, *J* = 10.0 Hz, 2-H), 6.85 (4H, app. d, *J* = 8.6 Hz, 3′, 3″, 5′, 5″-H), 7.14–7.19 (2H, m, 5, 8-H), 7.33–7.55 (14H, m, Ar-H), 7.65 (1H, t, *J* = 6.2 Hz, 5′′′′-H), 8.09–8.13 (2H, m, 10, 2′′′′-H), 8.20 (1H, t, *J* = 7.5 Hz, 4′′′′-H), 8.27 (2H, d, *J* = 6.2 Hz, 3′′′, 5′′′-H), 8.79 (1H, s, 4′′′′′-H), 9.14 (1H, d, *J* = 5.2 Hz, 6′′′′-H) ppm; ^{13}C NMR (100 MHz, CD_2Cl_2) δ_C 55.2, 56.6, 82.2, 113.3, 114.8, 119.0, 119.3, 123.4, 123.7, 125.2, 125.7, 126.0, 126.2, 127.3, 127.8, 128.2, 128.9, 129.2, 129.4, 129.6, 130.2, 132.8, 135.4, 136.8, 141.6, 149.6, 150.8, 151.4, 152.7, 152.8, 159.1, 190.6, 193.9 ppm; ^{19}F NMR (376 MHz, CD_2Cl_2) δ_F -72.2 (d, *J* = 714 Hz) ppm; HRMS (ESI) found $[M\text{-}PF_6]^+$ = 976.2275 $C_{49}H_{37}N_5O_6{}^{185}RePF_6$ requires $[M\text{-}PF_6]^+$ = 976.2268.

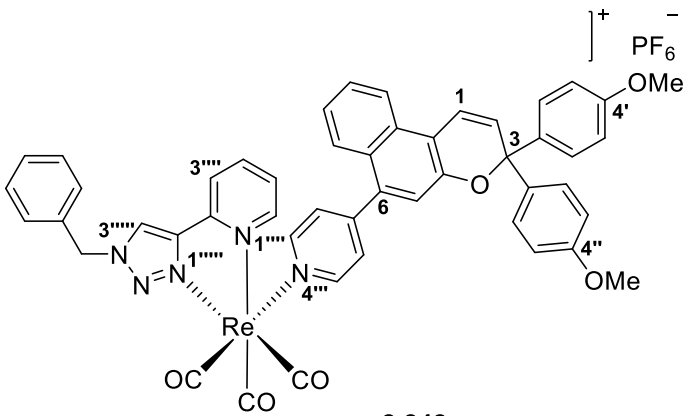

***fac*-Rhenium(I) tricarbonyl 3,3-bis(4-methoxyphenyl)-6-(4-pyridyl)-3*H*-naphtho[2,1-*b*]pyranyl 2-(1-benzyl-1*H*-1,2,3-triazol-4-yl)pyridine hexafluorophosphate (2.242):** 5 days of reaction; Flash column chromatography [activated Al_2O_3, eluent: MeOH (0.5%) in DCM → MeOH

(1%) in DCM, fraction 3], followed by trituration with Et_2O, gave the corresponding product as a yellow powder (206.3 mg, 71%); m.p. > 300 °C; ν_{max} (neat) 2032, 1911, 1613, 1506, 1248, 1174, 1002, 828, 556 cm^{-1}; ^1H NMR (400 MHz, CD_2Cl_2) δ_H 3.77–3.78 (6H, m, OMe), 5.77 (1H, d (AB), *J* = 14.5 Hz, CH_2), 5.81 (1H, d (AB), *J* = 14.5 Hz, CH_2), 6.35 (1H, d, *J* = 10.0 Hz, 2-H), 6.85 (4H, dd, *J* = 2.3, 8.9 Hz, 3′, 5′, 3″, 5″-H), 7.04 (1H, s, 5-H), 7.31–7.56 (15H, m, Ar-H), 7.65 (1H, app. t, *J* = 6.0 Hz, 5′′′′-H), 8.07 (1H, d, *J* = 8.5 Hz, 10-H), 8.12 (1H, d, *J* = 7.9 Hz, 3′′′′-H), 8.19 (1H, app. t, *J* = 7.8 Hz, 4′′′′-H), 8.28 (2H, d, *J* = 6.5 Hz, 3′′′, 5′′′-H), 8.81 (1H, s, 4′′′′′-H), 9.14 (1H, d, *J* = 5.4 Hz, 6′′′′-H) ppm; ^{13}C NMR (100 MHz, CD_2Cl_2) δ_C 55.2, 56.6, 82.4, 113.4, 115.9, 118.7, 119.6, 122.1, 123.8, 124.8, 124.9, 125.9, 126.0, 127.3, 127.4, 127.7, 128.2, 128.9, 129.4, 129.6, 130.0, 130.2, 132.9, 136.1, 136.7, 141.6, 149.6, 149.57, 149.58, 151.5, 151.9, 152.8, 159.14, 194.0, 196.0 ppm; ^{19}F NMR (376 MHz, CD_2Cl_2) δ_F -72.2 (d, *J* = 714 Hz) ppm; HRMS (ESI) found $[M-PF_6]^+$ = 978.2274 $C_{49}H_{37}N_5O_6{}^{187}RePF_6$ requires $[M-PF_6]^+$ = 978.2296.

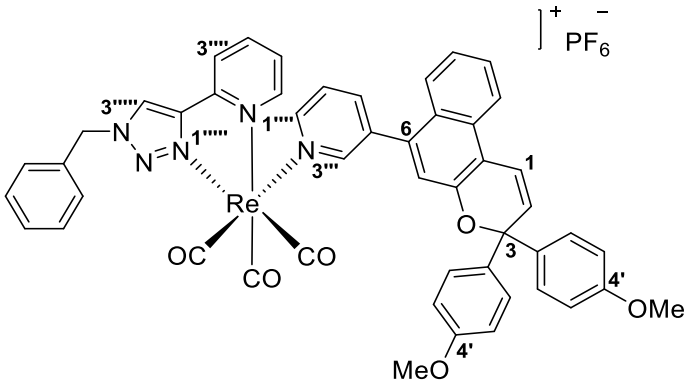

2.243

***fac*-Rhenium(I) tricarbonyl 3,3-bis(4-methoxyphenyl)-6-(3-pyridyl)-3*H*-naphtho[2,1-*b*]pyranyl 2-(1-benzyl-1*H*-1,2,3-triazol-4-yl)pyridine hexafluorophosphate (2.243):** 5 days of reaction; Flash column chromatography [activated Al_2O_3, eluent: MeOH (0.5%) in DCM → MeOH (1%) in DCM, fraction 3], followed by trituration with Et_2O, gave the corresponding product as an off-white powder (251.8 mg, 83%); m.p. > 300 °C; ν_{max} (neat) 2033, 1912, 1607, 1508, 1248, 1174, 1002, 829, 734, 556 cm^{-1}; ^1H NMR (400 MHz, CD_2Cl_2) δ_H 3.76 (3H, s, OMe), 3.78 (3H, s, OMe), 5.64–5.72 (2H, m, CH_2), 6.36 (1H, d, *J* = 10.0 Hz, 2-H), 6.85–6.92 (5H, m, 5, 3′, 5′, 3″, 5″-H), 7.14 (1H, d, *J* = 8.4 Hz, 7-H), 7.26 (1H, t, *J* = 7.6 Hz, 8-H), 7.32–7.42 (11H, m, Ar-H), 7.55–7.69 (2H, m, Ar-H), 7.93 (1H, dt, *J* = 1.5, 8.0 Hz, 6′′′-H), 8.09–8.24 (4H, m, Ar-H), 8.38 (1H, d, *J* = 1.4 Hz, 2′′′-H), 8.78 (1H, s, 4′′′′′-H), 9.06 (1H, d, *J* = 5.4 Hz, 6′′′′-H) ppm; ^{13}C NMR (100 MHz, CD_2Cl_2) δ_C 55.2, 56.5, 82.5, 113.4, 115.4, 118.6, 120.0, 122.2, 123.8, 124.5, 124.9, 126.0, 126.5, 126.7, 127.3, 127.4, 128.21, 128.23, 128.8, 129.3, 129.5, 129.7, 130.2, 132.5, 134.6, 136.7, 136.8, 139.1, 140.9, 141.6, 149.5, 149.6, 149.7, 150.3, 152.4, 152.8, 159.2, 193.9 ppm; ^{19}F NMR (376 MHz, CD_2Cl_2) δ_F

-72.2 (d, J = 714 Hz) ppm; HRMS (ESI) found $[M-PF_6]^+$ = 978.2285 $C_{49}H_{37}N_5O_6{}^{187}RePF_6$ requires $[M-PF_6]^+$ = 978.2296.

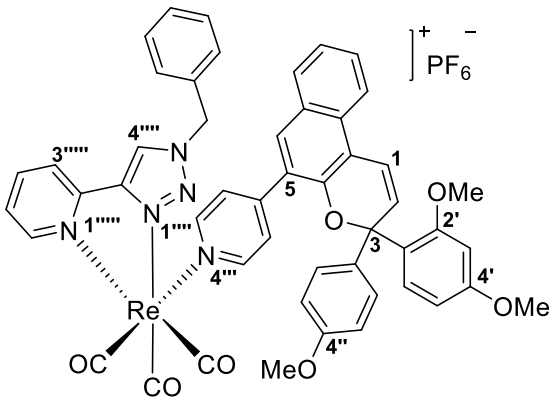

Mixture of diastereomers: *fac*-Rhenium(I) tricarbonyl 3-(2,4-dimethoxyphenyl)-3-(4-methoxyphenyl)-5-(4-pyridyl)-3*H*-naphtho[2,1-*b*]pyranyl 2-(1-benzyl-1*H*-1,2,3-triazol-4-yl)pyridine hexafluorophosphate (2.244): 3 days of reaction; Flash column chromatography [activated Al_2O_3, eluent: MeOH (0.5%) in DCM → MeOH (1%) in DCM, fraction 3], followed by trituration with Et_2O, gave the corresponding product as a red powder (151.7 mg, 72%); m.p. > 300 °C; ν_{max} (neat) 2030, 1911, 1610, 1505, 1208, 1000, 830, 734, 556 cm^{-1}; ^1H NMR both diastereomers (400 MHz, acetone-d_6) δ_H 3.28 (3H, s, OMe), 3.36 (3H, s, OMe), 3.71 (3H, s, OMe), 3.73 (3H, s, OMe), 3.74 (3H, s, OMe), 3.75 (3H, s, OMe), 5.97–6.06 (4H, m, Ar-H), 6.33–6.49 (6H, m, Ar-H), 6.71 (2H, d, J = 8.8 Hz, Ar-H), 6.76 (2H, d, J = 8.8 Hz, Ar-H), 7.13 (2H, d, J = 8.8 Hz, Ar-H), 7.17 (2H, d, J = 8.8 Hz, Ar-H), 7.25 (1H, d, J = 8.6 Hz, Ar-H), 7.32 (1H, d, J = 8.6 Hz, Ar-H), 7.39–7.60 (17H, m, Ar-H), 7.73–7.83 (7H, m, Ar-H), 7.89–7.91 (2H, m, Ar-H), 8.14 (2H, d, J = 8.6 Hz, Ar-H), 8.28–8.38 (4H, m, Ar-H), 8.57 (4H, d, J = 6.3 Hz, Ar-H), 9.14 (1H, s, Ar-H), 9.16 (1H, s, Ar-H), 9.46–9.50 (2H, m, Ar-H) ppm; ^{13}C NMR both diastereomers (100 MHz, acetone-d_6) δ_C 54.4, 54.5, 54.7, 56.0, 82.3, 99.6, 99.7, 103.7, 103.8, 112.9, 113.0, 115.7, 115.8, 118.5, 121.5, 123.4, 123.5, 124.7, 125.8, 125.9, 126.3, 126.4, 127.1, 127.6, 127.76, 127.84, 127.9, 128.1, 128.71, 128.74, 128.8, 128.9, 129.1, 129.3, 130.31, 130.34, 131.8, 133.8, 136.0, 141.77, 141.80, 147.1, 149.3, 149.4, 149.8, 151.6, 154.3, 157.3, 158.77, 158.82, 160.96, 160.99 ppm; ^{19}F NMR (376 MHz, acetone-d_6) δ_F -72.4 (d, J = 714 Hz) ppm; HRMS (ESI) found $[M-PF_6]^+$ = 1023.2452 $C_{51}H_{42}F_6N_5O_7P^{187}Re$ requires $[M-PF_6]^+$ = 1023.2636.

3.3.4 Synthesis of *fac*-[Re(BTz)(CO)$_3$NP]PF$_6$ Complexes

3.3.4.1 Experimental Procedure for the Synthesis of *fac*-Rhenium(I) tricarbonyl 3,3-bis(4-methoxyphenyl)-8-(4-pyridyl)-3*H*-naphtho[2,1-*b*]pyranyl 1,1'-dibenzyl-1*H*,1'*H*-4,4'-bi(1,2,3-triazole) hexafluorophosphate (2.245): *fac*-[Re(BTz)(CO)$_3$Cl]^0 (0.15 g, 0.24 mmol), AgPF$_6$ (0.06 g, 0.24 mmol) and 3,3-bis(4-methoxyphenyl)-8-(4-pyridyl)-3*H*-naphtho[2,1-*b*]pyran (0.11 g, 0.24 mmol) were added to DCM (55 mL) and stirred under an N$_2$ atmosphere in the dark at room temperature for 4 days. Later, the mixture was filtered through a short pad of celite to remove the Ag salts. Flash column chromatography [neutral Al$_2$O$_3$, MeOH (0.5%) in DCM, fraction 3] led to the corresponding product as an orange powder.

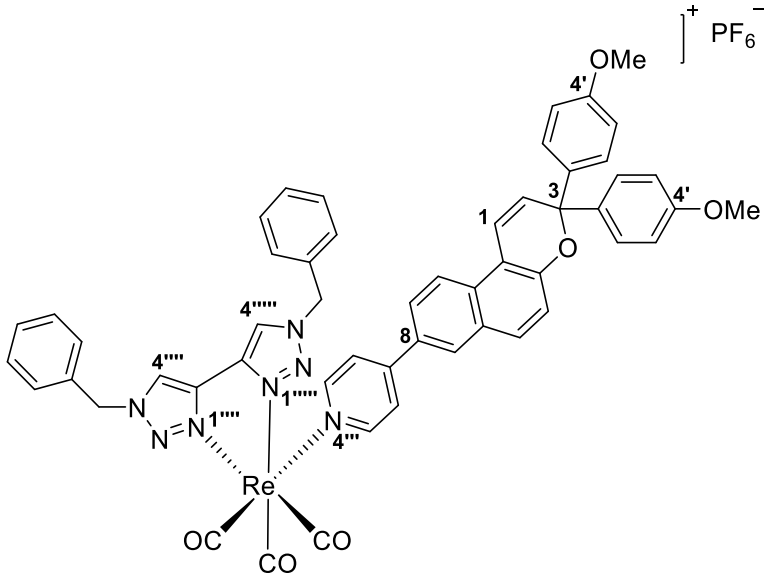

2.245

***fac*-Rhenium(I) tricarbonyl 3,3-bis(4-methoxyphenyl)-8-(4-pyridyl)-3*H*-naphtho[2,1-*b*]pyranyl 1,1'-dibenzyl-1*H*,1'*H*-4,4'-bi(1,2,3-triazole) hexafluorophosphate (2.245):** orange powder (0.10 g, 36%); m.p. > 300 °C; ν_{max} (neat) 2034, 1910, 1608, 1507, 1456, 1247, 1174, 1090, 1026, 1000, 831, 715, 556 cm^{-1}; ^{1}H NMR (400 MHz, CDCl$_3$) δ_H 3.78 (6H, s, OMe), 5.60 (2H, d (AB), *J* = 14.4 Hz, 2 × CH, CH), 5.69 (2H, d (AB), *J* = 14.4 Hz, 2 × CH, CH), 6.25 (1H, d, *J* = 10.0 Hz, 2-H), 6.83–6.86 (4H, m, 3′, 3″, 5′, 5″-H), 7.21–7.25 (2H, m, Ar-H), 7.35–7.43 (16H, m, Ar-H), 7.57 (1H, dd, *J* = 8.9, 1.8 Hz, 9-H), 7.70 (1H, d, *J* = 8.9 Hz, Ar-H), 7.89 (1H, d, *J* = 1.8 Hz, 7-H), 8.02 (1H, d, *J* = 9.0 Hz, Ar-H), 8.14 (2H, app. d, *J* = 6.7 Hz, 3‴, 5‴-H), 8.42 (2H, s, 4⁗, 4′⁗′-H) ppm; ^{13}C NMR (100 MHz, CDCl$_3$) δ_C 55.3, 56.4, 82.7, 113.5, 113.9, 118.5, 119.7, 122.9, 123.7, 123.9, 124.3, 128.0, 128.3, 128.7, 129.1, 129.6, 129.7, 130.2, 130.58, 130.62, 132.3, 136.8, 141.2, 151.5, 151.8, 152.1, 159.0 ppm; HRMS (ESI) found [M-PF$_6$]$^+$ = 1058.2663 $C_{53}H_{41}N_7O_6{}^{187}RePF_6$ requires [M-PF$_6$]$^+$ = 1058.2670.

3.3.4.2 Experimental Procedure for the Synthesis *fac*-Rhenium(I) tricarbonyl 3-(4-methoxyphenyl)-3-(4-pyridyl)-3*H*-naphtho[2,1-*b*]pyranyl 1,1'-dibenzyl-1*H*,1'*H*-4,4'-bi(1,2,3-triazole) hexafluorophosphate (2.246): TFA (0.60 mL, 7.8 mmol) was added dropwise to a mixture of (*E*)-3-(2-(methoxymethoxy)naphthalen-1-yl)-1-phenyl-1-(4-pyridyl)prop-2-en-1-ol (100.3 mg, 0.2523 mmol) in DCM (10.0 mL) at 0 °C. The reaction mixture was then warmed to room temperature and stirred for 4 h. The crude was washed with an aqueous solution of $NaHCO_3$ (50 mL), water (100 mL), dried with anhydrous sodium sulfate and evaporated to dryness. The corresponding product was used in the next step without further purification (85.7 mg). The latter was mixed in DCM (10.0 mL) with (btz)Re(CO)$_3$Cl (157.4 mg, 0.2471 mmol) and $AgPF_6$ (65.2 mg, 0.258 mmol). After stirring under an Ar atmosphere in the dark at room temperature for 4 days, the mixture was filtered through a short pad of celite to remove the Ag salts. Flash column chromatography [activated Al_2O_3, eluent: MeOH (0.5%) in DCM → MeOH (1%) in DCM, fraction 3], followed by trituration from Et_2O/hexane, led to the corresponding product as an off-white powder.

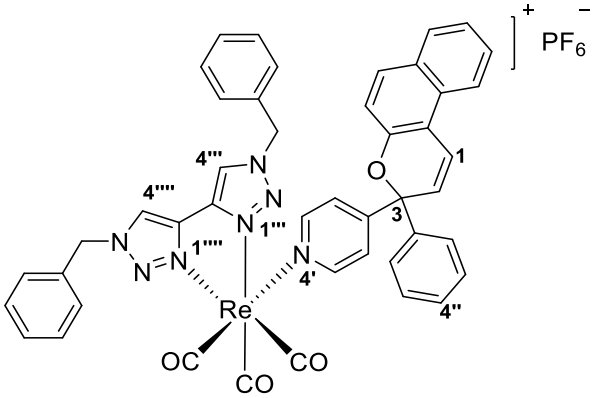

2.246

***fac*-Rhenium(I) tricarbonyl 3-(4-methoxyphenyl)-3-(4-pyridyl)-3*H*-naphtho[2,1-*b*]pyranyl 1,1'-dibenzyl-1*H*,1'*H*-4,4'-bi(1,2,3-triazole) hexafluorophosphate (2.246):** off-white powder (106.5 mg, 39% in two-steps); m.p. > 300 °C; ν_{max} (neat) 2036, 1911, 1615, 1456, 1232, 1112, 1012, 833, 705, 556 cm^{-1}; ^{1}H NMR (400 MHz, acetone-d$_6$) δ_H 5.60–5.74 (4H, m, CH_2), 6.15 (1H, d, *J* = 9.9 Hz, 2-H), 7.21 (1H, d, *J* = 8.8 Hz, 5-H), 7.30–7.46 (21H, m, 1-H, Ar-H), 7.53 (1H, t, *J* = 7.3 Hz, 9-H), 7.74–7.79 (2H, m, 6, 7-H), 7.96–7.98 (1H, m, 10-H), 8.17 (2H, d, *J* = 6.6 Hz, 3′, 5′-H), 8.35–8.37 (2H, m, 4′′′′, 4′′′′′-H) ppm; ^{13}C NMR (100 MHz, acetone-d$_6$) δ_C 56.4, 81.1, 113.9, 117.7, 120.6, 121.3, 121.6, 123.4, 123.5, 124.1, 124.3, 124.7, 126.8, 127.2, 128.1, 128.49, 128.54, 128.60, 128.62, 128.69, 128.73, 129.1, 129.39, 129.42, 129.55, 129.58, 130.6, 132.59, 132.63, 141.3, 141.8, 149.6, 151.8, 157.7, 194.5 ppm; ^{19}F NMR (376 MHz, acetone-d$_6$) δ_F -72.2 (d, *J* = 714 Hz) ppm; HRMS (ESI) found $[M-PF_6]^+$ = 922.2117 $C_{45}H_{33}N_7O_4{}^{187}RePF_6$ requires M = 922.2146.

3.3.5 Synthesis of *fac*-[Re(PyTzNP)(CO)$_3$Cl]^0

3.3.5.1 Experimental Procedure for the Synthesis of *fac*-Rhenium(I) tricarbonyl 2-(1-benzyl-1*H*-1,2,3-triazol-4-yl)-4-(3,3-bis(4-methoxyphenyl)-3*H*-benzo[*f*]chromen-8-yl)pyridinyl chloride (fac-[Re(PyTzNP)(CO)$_3$Cl]^0) (2.247): rhenium pentacarbonyl chloride (102.2 mg, 0.2825 mmol) and 2-(1-benzyl-1*H*-1,2,3-triazol-4-yl)-4-(3,3-bis(4-methoxyphenyl)-3*H*-benzo[*f*]chromen-8-yl)pyridine (177.3 mg, 0.2820 mmol) were mixed in anhydrous PhMe (6.5 mL) and heated at reflux under N_2 for 20 h. After cooling, a yellow precipitate was collected by filtration, rinsed with cold PhMe (10 mL), followed by cold Et_2O (50 mL). The yellow solid was triturated with cold Et_2O (50 mL), filtered and dried under reduced pressure, leading to the corresponding product.

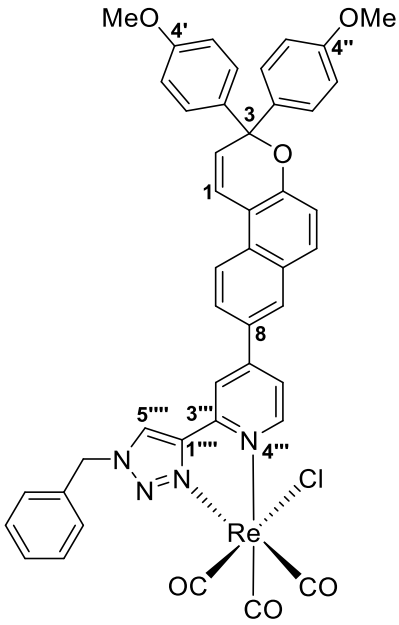

2.247

***fac*-Rhenium(I) tricarbonyl 2-(1-benzyl-1*H*-1,2,3-triazol-4-yl)-4-(3,3-bis(4-methoxyphenyl)-3*H*-benzo[*f*]chromen-8-yl)pyridinyl chloride (*fac*-[Re(PyTzNP)(CO)$_3$Cl]^0) (2.247)**: yellow solid (206.3 mg, 78%); m.p. > 300 °C; ν_{max} (neat) 2021, 1930, 1895, 1614, 1582, 1508, 1246, 1172, 1093, 1000, 817, 720 cm^{-1}; ^{1}H NMR (400 MHz, DMSO-d$_6$) δ_H 3.69 (6H, s, OMe), 5.93 (2H, s, CH_2), 6.52 (1H, d, *J* = 10.0 Hz, 2-H), 6.89 (4H, app. d, *J* = 8.8 Hz, 3′, 5′, 3″, 5″-H), 7.34–7.53 (11H, m, 1-H and Ar-H), 7.91 (1H, d, *J* = 9.0 Hz, 6-H), 8.04–8.06 (2H, m, 9, 6‴-H), 8.30 (1H, d, *J* = 9.1 Hz, 10-H), 8.48 (1H, d, *J* = 1.2 Hz, 7-H), 8.83 (1H, d, *J* = 1.3 Hz, 2‴-H), 8.94 (1H, d, *J* = 6.0 Hz, 5‴-H), 9.28 (1H, s, 5⁗-H) ppm; ^{13}C NMR (100 MHz, DMSO-d$_6$) δ_C 55.3, 55.5, 82.4, 114.0, 114.4, 119.2, 119.8, 120.1, 123.5, 123.6, 125.4, 126.4, 128.2, 128.4, 128.7, 129.2, 129.4, 129.5, 129.7, 130.5, 130.6, 131.3, 134.5, 137.1, 149.3, 149.7, 150.9, 151.9, 153.5, 159.0, 190.1, 197.3 ppm;

HRMS (ESI) found $[M\text{-}Cl+MeCN]^+$ = 940.2135 $C_{44}H_{32}N_4O_6{}^{187}Re^{35}Cl$ requires $[M\text{-}Cl+MeCN]^+$ = 940.2145

3.3.6 Synthesis of *fac*-[Re(N^N)(CO)$_3$naphthalene]PF$_6$

3.3.6.1 Experimental Procedure for the Synthesis of 2-Methoxy-6-(4-pyridyl)naphthalene (2.252): a degassed mixture of 2-bromo-6-methoxynaphthalene (1.50 g, 6.33 mmol), 4-pyridineboronic acid pinacol ester (1.95 g, 9.51 mmol), K_2CO_3 (1.31 g, 9.48 mmol) and $Pd(PPh_3)_4$ (0.37 g, 0.32 mmol) in PhMe (74.0 mL) and EtOH (74.0 mL) was heated at reflux under N_2. After 16 h, the mixture was evaporated to dryness, the residue extracted with EtOAc (100 mL), washed with water (3 × 100 mL), the organic layer dried with anhydrous sodium sulfate and the solvent removed under reduced pressure. Subsequently, after solvent evaporation, the residue was crystallized from a EtOAc/hexane mixture giving the corresponding 2-methoxy-6-(4-pyridyl)naphthalene as a white crystalline solid.

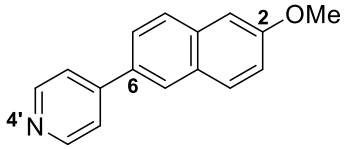

2.252

2-Methoxy-6-(4-pyridyl)naphthalene (2.252): colourless microcrystals (1.01 g, 68%); m.p. = 156–158 °C; ν_{max} (neat) 1622, 1584, 1544, 1494, 1254, 1206, 1021, 822, 799 cm^{-1}; ^{1}H NMR (400 MHz, $CDCl_3$) δ_H 3.95 (3H, s, OMe), 7.17 (1H, d, *J* = 2.4 Hz, 1-H), 7.21 (1H, dd, *J* = 8.6, 2.4 Hz, 3-H), 7.61–7.63 (2H, m, 2′, 6′-H), 7.72 (1H, dd, *J* = 8.6, 1.6 Hz, 4-H), 7.82 (1H, d, *J* = 9.4 Hz, 7-H), 7.85 (1H, d, *J* = 9.4 Hz, 8-H), 8.06 (1H, d, *J* = 1.6 Hz, 5-H), 8.67–8.69 (2H, m, 3′, 5′-H) ppm; ^{13}C NMR (100 MHz, $CDCl_3$) δ_C 55.4, 105.6, 119.7, 121.6, 125.0, 126.2, 127.7, 129.0, 130.0, 133.1, 134.8, 148.3, 150.3, 158.5 ppm; HRMS (ESI) found $[M+H]^+$ = 236.1070 $C_{16}H_{13}NO$ requires $[M+H]^+$ = 236.1070.

3.3.6.2 General Experimental Procedure for the Synthesis of *fac*-Rhenium(I) tricarbonyl 2-methoxy-6-(4-pyridyl)naphthyl diimine hexafluorophosphate (*fac*-[Re(N^N)(CO)$_3$naphthalene]PF$_6$): *fac*-$[Re(N^N)(CO)_3Cl]^0$ (1.00 mmol), $AgPF_6$ (1.00 mmol) and 2-methoxy-6-(4-pyridyl)naphthalene (1.00 mmol) were mixed in DCM (37 mL) and stirred under a N_2 or Ar atmosphere in the dark at room temperature. Afterwards, the reaction mixture was filtered through a short pad of celite to remove the Ag salts. Flash column chromatography [activated Al_2O_3, eluent: MeOH (0.5%) in DCM → MeOH (1%) in DCM, fraction 3] led to the corresponding product.

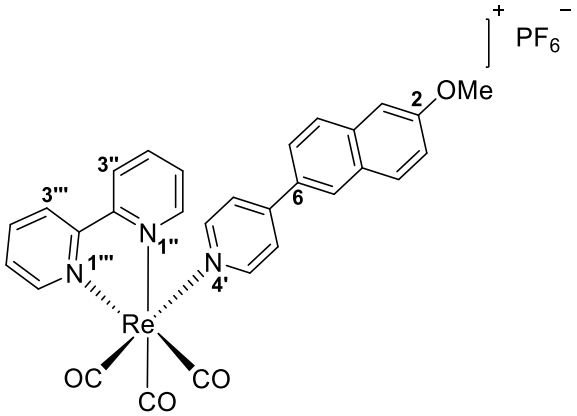

2.248

***fac*-Rhenium(I) tricarbonyl 2-methoxy-6-(4-pyridyl)naphthyl bipyridine hexafluorophosphate (2.248):** 6 days of reaction; Yellow powder (241.4 mg, 92%); m.p. > 300 °C; ν_{max} (neat) 2030, 1900, 1608, 1498, 1472, 1446, 1392, 1260, 1207, 1027, 831, 764, 556 cm^{-1}; ^1H NMR (400 MHz, $CDCl_3$) δ_H 3.89 (3H, s, OMe), 7.07 (1H, app. s, 1-H), 7.10 (1H, dd, *J* = 8.9, 2.2 Hz, 3-H), 7.52–7.54 (1H, m, 7-H), 7.61 (2H, d, *J* = 6.5 Hz, 2′, 6′-H), 7.69–7.74 (4H, m, 4, 8, 5″, 5‴-H), 7.96 (1H, s, 5-H), 8.12 (2H, app. d, *J* = 6.5 Hz, 3′, 5′-H), 8.19 (2H, app. t, *J* = 7.4 Hz, 4″, 4‴-H), 8.42 (2H, d, *J* = 8.1 Hz, 3″, 3‴-H), 9.10 (2H, d, *J* = 5.1 Hz, 6″, 6‴-H) ppm; ^{13}C NMR (100 MHz, $CDCl_3$) δ_C 55.4, 105.6, 120.0, 124.1, 125.3, 127.2, 128.1, 128.6, 128.9, 129.8, 130.4, 135.6, 141.4, 151.5, 151.6, 152.8, 155.5, 159.1, 191.0, 195.6 ppm; HRMS (ESI) found $[M\text{-}PF_6]^+$ = 662.1084 $C_{29}H_{21}N_3O_4{}^{187}RePF_6$ requires $[M\text{-}PF_6]^+$ = 662.1084.

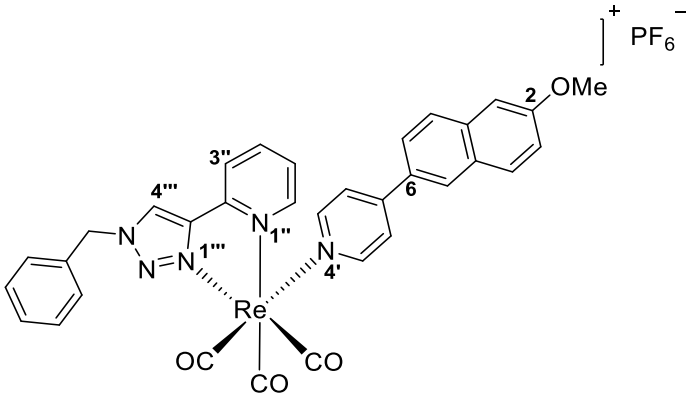

2.249

***fac*-Rhenium(I) tricarbonyl 2-methoxy-6-(4-pyridyl)naphthyl 2-(1-benzyl-1*H*-1,2,3-triazol-4-yl)pyridine hexafluorophosphate (2.249):** 5 days of reaction; Yellow powder (228.8 mg, 92%); m.p. > 300 °C; ν_{max} (neat) 2031, 1907, 1610, 1498, 1457, 1392, 1259, 1207, 1125, 831, 734, 556 cm^{-1}; ^1H NMR (400 MHz, $CDCl_3$) δ_H 3.91 (3H, s, OMe), 5.68 (1H, d (AB), *J* = 14.4 Hz, CH_2), 5.77 (1H, d (AB), *J* = 14.4 Hz, CH_2), 7.10 (1H, app. s, 1-H), 7.15 (1H, app. d, *J* = 9.1 Hz, 3-H), 7.36–7.42 (3H, m, Ar-H), 7.51–7.56 (6H, m, Ar-H), 7.75 (2H, app. d, *J* = 8.7 Hz, 4, 8-H) , 7.97–7.99

(3H, m, Ar-H), 8.12–8.14 (2H, m, Ar-H), 8.75 (1H, s, 4‴-H), 9.03 (1H, d, J = 5.5 Hz, 6″-H) ppm; ^{13}C NMR (100 MHz, $CDCl_3$) δ_C 55.4, 56.5, 105.6, 120.0, 123.8, 124.0, 124.2, 126.3, 127.1, 127.3, 128.2, 128.7, 129.1, 129.5, 129.6, 130.1, 130.4, 132.7, 135.6, 141.3, 149.2, 149.5, 151.6, 151.7, 152.6, 159.2, 190.7, 193.9, 196.0 ppm; HRMS (ESI) found $[M\text{-}PF_6]^+$ = 742.1463 $C_{33}H_{25}N_5O_4{}^{187}RePF_6$ requires $[M\text{-}PF_6]^+$ = 742.1459.

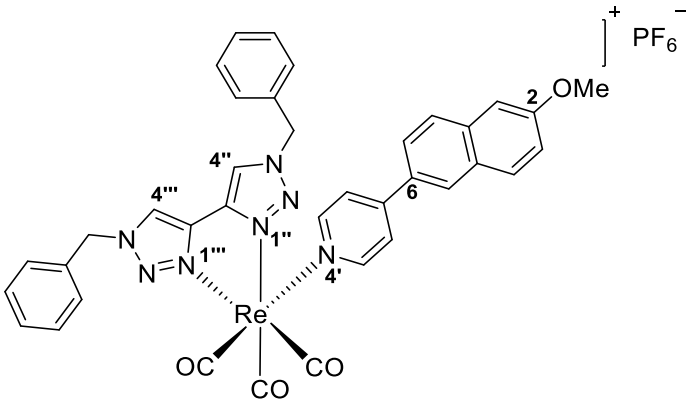

2.250

***fac*-Rhenium(I) tricarbonyl 2-methoxy-6-(4-pyridyl)naphthyl 1,1'-dibenzyl-1*H*,1'*H*-4,4'-bi(1,2,3-triazole) hexafluorophosphate (2.250):** 5 days of reaction; Yellow powder (209.6 mg, 87%); m.p. > 300 °C; ν_{max} (neat) 2031, 1909, 1610, 1498, 1456, 1433, 1261, 1207, 1112, 1028, 834, 715, 556 cm^{-1}; ^{1}H NMR (400 MHz, $CDCl_3$) δ_H 3.93 (3H, s, OMe), 5.58 (2H, d (AB), J = 14.5 Hz, CH, CH), 5.68 (2H, d (AB), J = 14.5 Hz, CH, CH), 7.12 (1H, d, J = 2.0 Hz, 1-H), 7.18 (1H, dd, J = 9.0, 2.2 Hz, 3-H), 7.35–7.39 (10H, m, Ph-H), 7.45 (2H, app. d, J = 6.6 Hz, 2′, 6′-H), 7.56 (1H, dd, J = 8.6, 1.5 Hz, 7-H), 7.77–7.80 (m, 2H, 4, 8-H), 7.97 (1H, app. s, 5-H), 8.15 (2H, app. d, J = 6.6 Hz, 3′, 5′-H), 8.38 (2H, s, 4″, 4‴-H) ppm; ^{13}C NMR (100 MHz, $CDCl_3$) δ_C 55.4, 56.4, 105.7, 120.1, 123.6, 123.9, 124.2, 127.2, 128.2, 128.7, 129.5, 129.6, 130.3, 130.4, 132.5, 135.6, 141.2, 151.6, 151.8, 159.2, 190.6, 194.4 ppm; HRMS (ESI) found $[M\text{-}PF_6]^+$ = 822.1832 $C_{37}H_{29}N_7O_4{}^{187}RePF_6$ requires $[M\text{-}PF_6]^+$ = 822.1833.

3.4 Ring-Contraction of Naphthopyrans

3.4.1 Kinetic Study of the Ring-Contraction of 3,3-Bis(4-methoxyphenyl)-3*H*-naphtho[2,1-*b*]pyran (2.147)

3.4.1.1 Stability in DCM: 3,3-bis(4-methoxyphenyl)-3*H*-naphtho[2,1-*b*]pyran was dissolved in DCM and stirred in a sealed flask at room temperature for 18 h. Samples were obtained over time. TLC analysis had shown no change in the reaction mixture.

3.4.1.2 Stability in DCM with $Pd(PPh_3)_4$: 3,3-bis(4-methoxyphenyl)-3*H*-naphtho[2,1-*b*]pyran was dissolved in DCM and a catalytic amount of $Pd(PPh_3)_4$ was added, and stirred in a sealed flask at room temperature for 23 h. Samples were obtained over time. TLC analysis had shown no change in the reaction mixture.

3.4.1.3 Stability in Toluene: 3,3-bis(4-methoxyphenyl)-3*H*-naphtho[2,1-*b*]pyran was dissolved in PhMe and stirred in a sealed flask at room temperature for 17 h. Samples were obtained over time. TLC analysis had shown no change in the reaction mixture.

3.4.1.4 With K_2CO_3 (1.5 equiv), $Pd(PPh_3)_4$ (5 mol%) in PhMe:EtOH (1:1) at reflux: 3,3-bis(4-methoxyphenyl)-3*H*-naphtho[2,1-*b*]pyran (250.2 mg, 0.6343 mmol), K_2CO_3 (126.2 mg, 0.9131 mmol) and $Pd(PPh_3)_4$ (35.2 mg, 0.0305 mmol) were dissolved in PhMe (6 mL) and EtOH (6 mL), and refluxed under N_2 for 48 h. Several samples were obtained over time and subjected to ^{1}H NMR analysis.

3.4.1.5 With K_2CO_3 (1.5 equiv) in PhMe:EtOH (1:1) at reflux: 3,3-bis(4-methoxyphenyl)-3*H*-naphtho[2,1-*b*]pyran (250.9 mg, 0.6360 mmol) and K_2CO_3 (125.7 mg, 0.9095 mmol) were dissolved in PhMe (6 mL) and EtOH (6 mL), and refluxed under N_2. Several samples were obtained over time and subjected to ^{1}H NMR analysis.

3.4.1.6 With $Pd(PPh_3)_4$ (5 mol%) in PhMe:EtOH (1:1) at reflux: 3,3-bis(4-methoxyphenyl)-3*H*-naphtho[2,1-*b*]pyran (250.2 mg, 0.6343 mmol) and $Pd(PPh_3)_4$ (35.3 mg, 0.0305 mmol) were dissolved in PhMe (6 mL) and EtOH (6 mL), and refluxed under N_2 for 48 h. A sample was collected after 48h and subjected to ^{1}H NMR analysis.

3.4.1.7 With K_2CO_3 (3 equiv) in PhMe:EtOH (1:1) at reflux: 3,3-bis(4-methoxyphenyl)-3*H*-naphtho[2,1-*b*]pyran (100.4 mg, 0.2545 mmol), K_2CO_3 (105.5 mg, 0.7634 mmol) were dissolved in

PhMe (3 mL) and EtOH (3 mL), and refluxed under N_2. Several samples were obtained over time and subjected to ^{1}H NMR analysis.

3.4.1.8 With Li_2CO_3 (1.5 equiv) in PhMe:EtOH (1:1) at reflux: 3,3-bis(4-methoxyphenyl)-3*H*-naphtho[2,1-*b*]pyran (200.9 mg, 0.5093 mmol), Li_2CO_3 (56.7 mg, 0.7674 mmol) were dissolved in PhMe (5 mL) and EtOH (5 mL), and refluxed under N_2. Several samples were obtained over time and subjected to ^{1}H NMR analysis.

3.4.1.9 With Na_2CO_3 (1.5 equiv) in PhMe:EtOH (1:1) at reflux: 3,3-bis(4-methoxyphenyl)-3*H*-naphtho[2,1-*b*]pyran (200.6 mg, 0.5085 mmol), Na_2CO_3 (80.7 mg, 0.7614 mmol) were dissolved in PhMe (5 mL) and EtOH (5 mL), and refluxed under N_2. Several samples were obtained over time and subjected to ^{1}H NMR analysis.

3.4.1.10 With Cs_2CO_3 (1.5 equiv) in PhMe:EtOH (1:1) at reflux: 3,3-bis(4-methoxyphenyl)-3*H*-naphtho[2,1-*b*]pyran (200.9 mg, 0.5093 mmol), Cs_2CO_3 (248.3 mg, 0.7621 mmol) were dissolved in PhMe (5 mL) and EtOH (5 mL), and refluxed under N_2. Several samples were obtained over time and subjected to ^{1}H NMR analysis.

3.4.1.11 With K_3PO_4 (1.5 equiv) in PhMe:EtOH (1:1) at reflux: 3,3-bis(4-methoxyphenyl)-3*H*-naphtho[2,1-*b*]pyran (199.8 mg, 0.5065 mmol), K_3PO_4 (161.4 mg, 0.7604 mmol) were dissolved in PhMe (5 mL) and EtOH (5 mL), and refluxed under N_2. Several samples were obtained over time and subjected to ^{1}H NMR analysis.

3.4.1.12 With K_2CO_3 (1.5 equiv), 18-crown-6 (3 equiv) in PhMe at reflux: 3,3-bis(4-methoxyphenyl)-3*H*-naphtho[2,1-*b*]pyran (199.9 mg, 0.5068 mmol), K_2CO_3 (105.0 mg, 0.7597 mmol) and 18-crown-6 (415.3 mg, 1.571 mmol) were dissolved in PhMe (10 mL), and refluxed under N_2. Several samples were obtained over time and subjected to ^{1}H NMR analysis.

3.4.1.13 Experimental Procedure for the Synthesis of 4-(2-(bis(4-methoxyphenyl)methyl)naphtho[2,1-b]furan-7-yl)pyridine: a mixture of 8-bromo-3,3-bis(4-methoxyphenyl)-3*H*-naphtho[2,1-*b*]pyran (200.1 mg, 0.4227 mmol), 4-pyridineboronic acid pinacol ester (129.9 mg, 0.6335 mmol), K_2CO_3 (87.6 mg, 0.634 mmol), 18-crown-6 (347.0 mg, 1.313 mmol) and $Pd(PPh_3)_4$ (24.8 mg, 0.0215 mmol) in PhMe (10.0 mL) was heated at reflux under N_2 for 19 h. After this time, the mixture was cooled and poured into water (100 mL). Afterwards, the residue was extracted with DCM (3 × 100 mL), washed with water (3 × 150 mL), the organic layer dried over anhydrous sodium sulphate and the solvent removed under reduced pressure. Flash column chromatography [Fluorochem silica gel (60 Å, 40-63 μm), eluent: MeOH (4%) in DCM,

fraction 5], followed by trituration with ethylic ether, led to the corresponding product as a yellow powder (93.8 mg, 47%).

3.4.1.14 With Na_2CO_3 (1.5 equiv), 15-crown-5 (3 equiv) in PhMe at reflux: 3,3-bis(4-methoxyphenyl)-3*H*-naphtho[2,1-*b*]pyran (200.0 mg, 0.5070 mmol), Na_2CO_3 (80.6 mg, 0.7604 mmol) and 15-crown-5 (0.30 mL, 1.5 mmol) were dissolved in PhMe (10 mL), and refluxed under N_2. Several samples were obtained over time and subjected to ^{1}H NMR analysis.

3.4.1.15 With Na_2CO_3 (1.5 equiv), 15-crown-5 (3 equiv), $Pd(OAc)_2$ (5 mol%) in PhMe at reflux: 3,3-bis(4-methoxyphenyl)-3*H*-naphtho[2,1-*b*]pyran (199.6 mg, 0.5060 mmol), Na_2CO_3 (80.6 mg, 0.7604 mmol) and $Pd(OAc)_2$ (6.0 mg, 0.027 mmol) were dissolved in PhMe (10 mL), and refluxed under N_2. Several samples were obtained over time and subjected to ^{1}H NMR analysis.

3.4.1.16 With K_2CO_3 (10 mol%), 18-crown-6 (20 mol%) in PhMe at reflux: 3,3-bis(4-methoxyphenyl)-3*H*-naphtho[2,1-*b*]pyran (427.7 mg, 1.084 mmol), K_2CO_3 (14.9 mg, 0.108 mmol) and 18-crown-6 (57.0 mg, 0.216 mmol) were dissolved in PhMe (28 mL), and refluxed under N_2. Several samples were obtained over time and subjected to ^{1}H NMR analysis.

3.4.2 General Experimental Procedure for the Pyran (Dihydroquinoline) Ring-Contraction

A mixture of naphtho[2,1-b]pyran (1.3 mmol), 18-crown-6 (3.93 mmol), K_2CO_3 (1.9 mmol) in PhMe (25.0 mL) was heated at reflux under N_2. After the completion of the reaction, the crude was evaporated to dryness. The residue was dissolved in DCM (150 mL), washed with water (3 × 150 mL), the organic layer dried with anhydrous sodium sulfate and the solvent removed under reduced pressure, giving the corresponding product after purification if needed.

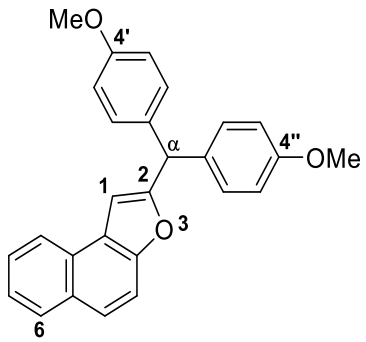

2.331

2-(Bis(4-methoxyphenyl)methyl)naphtho[2,1-*b*]furan (2.331): from 3,3-bis(4-methoxyphenyl)-3*H*-naphtho[2,1-*b*]pyran (0.50 g, 1.3 mmol) after 9 h of reaction; crystallization from a mixture of DCM/hexane gave the corresponding product as a yellow crystalline solid (0.40 g, 80%); m.p. = 172–173 °C; ν_{max} (neat) 1607, 1581, 1505, 1440, 1243, 1176, 1027, 807, 746, 584 cm^{-1}; ^1H NMR (400 MHz, $CDCl_3$) δ_H 3.84 (6H, s, OMe), 5.63 (1H, s, α-H), 6.76 (1H, s, 1-H), 6.91 (4H, app. d, *J* = 8.6 Hz, Ar-H), 7.20 (4H, app. d, *J* = 8.6 Hz, Ar-H), 7.48 (1H, app. t, *J* = 7.5 Hz, 8-H), 7.55 (1H, app. t, *J* = 7.5 Hz, 7-H), 7.61 (1H, d, *J* = 8.9 Hz, 5-H), 7.70 (1H, d, *J* = 8.9 Hz, 4-H), 7.95 (1H, d, *J* = 8.0 Hz, 9-H), 8.05 (1H, d, *J* = 8.1 Hz, 6-H) ppm; ^{13}C NMR (100 MHz, $CDCl_3$) δ_C 49.8, 55.3, 104.4, 112.4, 114.0, 123.4, 123.6, 124.3, 124.5, 126.1, 127.5, 128.7, 129.8, 130.2, 133.7, 152.4, 158.5, 160.0 ppm; HRMS (ESI) found $[M+H]^+$ = 395.1634 $C_{27}H_{22}O_3$ requires $[M+H]^+$ = 395.1642.

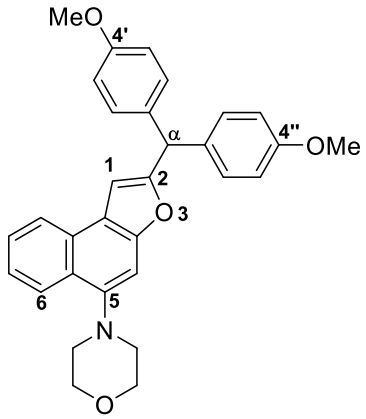

2.339

4-(2-(Bis(4-methoxyphenyl)methyl)naphtho[2,1-*b*]furan-5-yl)morpholine (2.339): from 3,3-bis(4-methoxyphenyl)-6-morpholino-3*H*-naphtho[2,1-*b*]pyran (0.17 g, 0.35 mmol) after 9 h of reaction; Flash column chromatography [Aldrich silica gel (60 Å, 40-63 μm), eluent: EtOAc (25%) in petroleum ether, fraction 1] led to the corresponding product as a white powder (0.13 g, 76%); m.p. = 178–180 °C; ν_{max} (neat) 2963, 1606, 1507, 1301, 1241, 1145, 1129, 1029, 801, 579, 564 cm^{-1}; ^1H NMR (400 MHz, $CDCl_3$) δ_H 3.10 (4H, bs, $N(CH_2)_2$), 3.81 (6H, s, OMe), 4.00 (4H, t, *J* = 4.4 Hz, $O(CH_2)_2$), 5.58 (1H, s, α-H), 6.68 (1H, s, 1-H), 6.89 (4H, app. d, *J* = 8.6 Hz, Ar-H), 7.18 (4H,

app. d, J = 8.6 Hz, Ar-H), 7.30 (1H, s, 4-H), 7.45–7.54 (2H, m, Ar-H), 8.01 (1H, d, J = 7.9 Hz, 9-H), 8.30 (1H, d, J = 8.2 Hz, 6-H) ppm; ^{13}C NMR ($CDCl_3$) δ_C 49.8, 53.9, 55.3, 67.5, 102.6, 104.2, 114.0, 119.8, 124.0, 124.5, 126.1, 126.3, 128.2, 129.8, 133.8, 147.1, 152.6, 158.5, 159.3 ppm; HRMS (ESI) found $[M+H]^+$ = 480.2173 $C_{31}H_{29}NO_4$ requires $[M+H]^+$ = 480.2169.

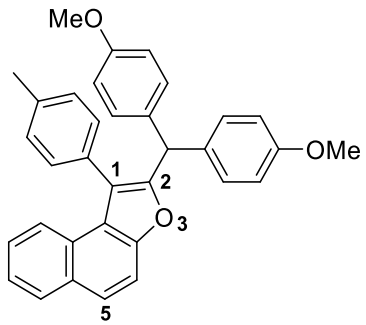

2.341

2-(Bis(4-methoxyphenyl)methyl)-1-(*p*-tolyl)naphtho[2,1-*b*]furan (2.341): from 3,3-bis(4-methoxyphenyl)-1-(*p*-tolyl)-3*H*-naphtho[2,1-b]pyran (75.6 mg, 0.156 mmol) after 64 h of reaction; Purification by preparative TLC [Merck Silica gel 60 F_{254}, EtOAc (10%) in hexanes, fraction 2] led to the corresponding product as an off-white powder (38.6 mg, 49%); m.p.= 164–165 °C; ν_{max} (neat) 2929, 2833, 1608, 1582, 1507, 1461, 1244, 1175, 1033, 1004, 822, 746, 569 cm^{-1}; ^{1}H NMR (400 MHz, $CDCl_3$) δ_H 2.52 (3H, s, Me), 3.80 (6H, s, OMe), 5.42 (1H, s, α-H), 6.85–6.88 (4H, m, Ar-H), 7.18–7.21 (4H, m, Ar-H), 7.29–7.36 (3H, m, Ar-H), 7.38–7.42 (3H, m, Ar-H), 7.67 (1H, d, J = 9.0 Hz, 4-H), 7.72 (1H, d, J = 9.0 Hz, 5-H), 7.79 (1H, d, J = 8.3 Hz, 9-H), 7.92 (1H, d, J = 8.0 Hz, 6-H) ppm; ^{13}C NMR (100 MHz, $CDCl_3$) δ_C 21.5, 46.7, 55.3, 112.6, 113.8, 120.0, 122.2, 123.3, 124.1, 124.9, 125.8, 128.2, 128.8, 129.5, 129.9, 130.5, 130.7, 130.8, 134.3, 137.6, 151.9, 154.5, 158.3 ppm; HRMS (ESI) found $[M+H]^+$ = 485.2105 $C_{34}H_{28}O_3$ requires $[M+H]^+$ = 485.2111.

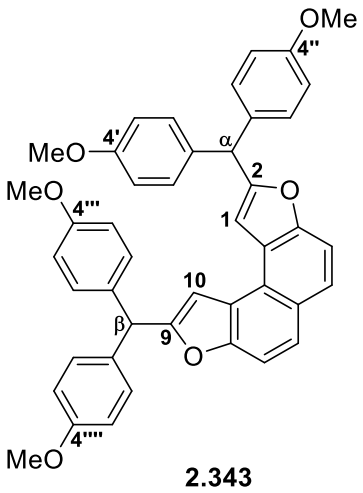

2,9-Bis(bis(4-methoxyphenyl)methyl)naphtho[2,1-*b*:7,8-*b*']difuran (2.343): from 3,3,10,10-tetrakis(4-methoxyphenyl)-3,10-dihydrochromeno[5,6-*f*]chromene (0.50 g, 0.76 mmol) after 9 h of reaction; brown powder (0.44 g, 88%); m.p. = 160–162 ºC; ν_{max} (neat) 2927, 2833, 1609, 1507, 1301, 1248, 1173, 1024, 810, 770, 567 cm^{-1}; ^{1}H NMR (400 MHz, $CDCl_3$) δ_H 3.81 (12H, s, OMe), 5.61 (2H, s, α, β-H), 6.81 (2H, s, 1, 10-H), 6.86–6.89 (8H, m, Ar-H), 7.18–7.20 (8H, m, Ar-H), 7.57 (2H, d, *J* = 8.9 Hz, 5, 6-H), 7.76 (2H, d, *J* = 8.9 Hz, 4, 7-H) ppm; ^{13}C NMR (100 MHz, $CDCl_3$) δ_C 49.8, 55.3, 105.3, 110.5, 113.9, 121.5, 122.0, 125.3, 127.0, 129.8, 133.8, 153.2, 158.5, 159.5 ppm; HRMS (ESI) found $[M+H]^+$ = 661.2553, $C_{44}H_{36}O_6$ requires $[M+H]^+$ = 661.2585.

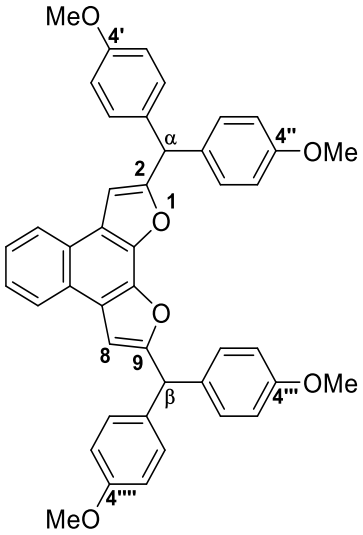

2,9-Bis(bis(4-methoxyphenyl)methyl)naphtho[2,1-*b*:3,4-*b*']difuran (2.345): from 2,2,11,11-tetrakis(4-methoxyphenyl)-2,11-dihydrobenzo[*f*]pyrano[3,2-*h*]chromene (0.50 g, 0.76 mmol) after 9 h of reaction; Crystallization from a mixture of DCM/hexane led to the corresponding product as a brown crystalline powder (0.24 g, 48%); m.p. = 184–188 °C (darkened at 141 °C); ν_{max} (neat) 2930,

2833, 1606, 1582, 1508, 1440, 1238, 1175, 1110, 1028, 815, 760, 556 cm^{-1}; ^{1}H NMR (400 MHz, $CDCl_3$) δ_H 3.80 (12H, s, OMe), 5.60 (2H, s, α, β-H), 6.75 (2H, s, 3, 8-H), 6.86 (8H, app. d, *J* = 8.6 Hz, Ar-H), 7.16 (8H, app. d, *J* = 8.6 Hz, Ar-H), 7.46–7.49 (2H, m, 5, 6-H), 8.03–8.05 (2H, m, 4, 7-H) ppm; ^{13}C NMR (100 MHz, $CDCl_3$) δ_C 49.8, 55.3, 105.3, 114.0, 122.2, 124.1, 124.7, 124.9, 129.8, 133.7, 139.5, 158.5, 159.4 ppm; HRMS (ESI) found $[M+K]^+$ = 699.2135 $C_{44}H_{36}O_6$ requires $[M+K]^+$ = 699.2143.

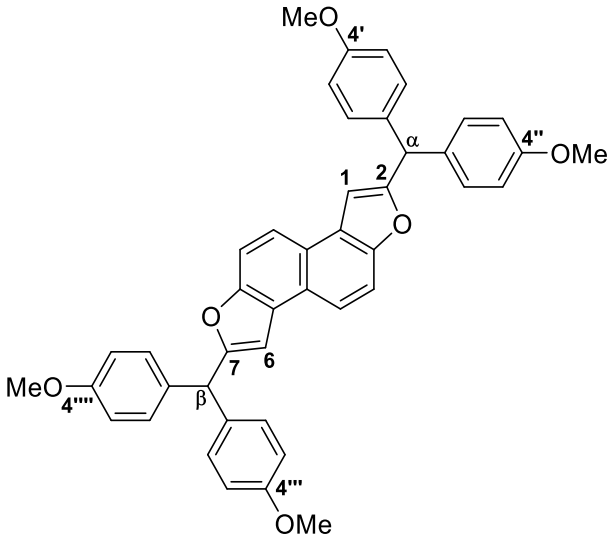

2.347

2,7-Bis(bis(4-methoxyphenyl)methyl)naphtho[2,1-*b*:6,5-*b'*]difuran (2.347): from 2,2,8,8-tetrakis(4-methoxyphenyl)-2,8-dihydrochromeno[6,5-*f*]chromene (0.50 g, 0.76 mmol) after 21 h of reaction; After the reaction was completed, the crude was evaporated to dryness. Afterwards, PhMe (200 mL) was added and the resulting mixture filtered hot. The resulting filtrand was poured into water (50 mL), filtered off, rinsed with water (100 mL), cold PhMe (15 mL) and cold Et_2O (5 mL) giving the corresponding product as an off-white powder (0.16 g, 32%). The former filtrate was reduced and the solid filtered off, rinsed with water (100 mL), cold PhMe (15 mL) and cold Et_2O (5 mL) giving the corresponding product as an off-white powder (0.21 g, 42%); m.p. = 279–282 °C (darkened at 264 °C); ν_{max} (neat) 2834, 1606, 1508, 1239, 1175, 1156, 1033, 816, 571 cm^{-1}; ^{1}H NMR (400 MHz, DMSO-d_6) δ_H 3.74 (12H, s, OMe), 5.73 (2H, s, α, β-H), 6.93 (8H, app. d, *J* = 8.7 Hz, Ar-H), 7.08 (2H, s, 1, 6-H), 7.22 (8H, app. d, *J* = 8.7 Hz, Ar-H), 7.74 (2H, d, *J* = 9.0 Hz, Ar-H), 8.08 (2H, d, *J* = 9.0 Hz, Ar-H) ppm; ^{13}C NMR (100 MHz, DMSO-d_6)* δ_C 49.2, 55.5, 104.5, 112.5, 114.4, 120.6, 124.2, 124.6, 130.0, 134.0, 151.4, 158.4, 160.5 ppm; HRMS (ESI) found $[M+K]^+$ = 699.2144 $C_{44}H_{36}O_6$ requires $[M+K]^+$ = 699.2143.

*Due to the low solubility of the compound, the ^{13}C NMR peaks were inferred from HSQC and HMBC analysis.

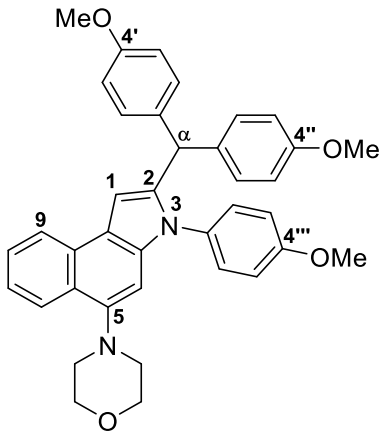

2.349

4-(2-(Bis(4-methoxyphenyl)methyl)-3-phenyl-3*H*-benzo[*e*]indol-5-yl)morpholine (2.349): from 4-(3,3,4-tris(4-methoxyphenyl)-3,4-dihydrobenzo[*f*]quinolin-6-yl)morpholine (0.50 g, 0.86 mmol) after 9 days of reaction; The residue was crystallized from a mixture of DCM/hexane giving the corresponding product as an off-white crystalline solid (0.28 g, 56%). The resulting mother-liquor was purified by flash column chromatography [Aldrich silica gel (60 Å, 40-63 μm), eluent: EtOAc (25%) in hexanes, fraction 2] giving the corresponding product as a beige powder (0.12 g, 24%); m.p. = 215–217 °C; ν_{max} (neat) 2969, 1508, 1457, 1358, 1244, 1174, 1114, 1035, 842, 760 cm^{-1}; ^{1}H NMR (400 MHz, $CDCl_3$) δ_H 2.97 (4H, bs, $N(CH_2)_2$), 3.78 (6H, s, OMe), 3.86 (3H, s, 4′′′-OMe), 3.92 (4H, t, *J* = 4.5 Hz, $O(CH_2)_2$), 5.27 (1H, s, α-H), 6.56 (1H, s, 1-H), 6.76–6.79 (5H, m, Ar-H), 6.88–6.90 (2H, m, Ar-H), 6.99 (6H, app. d, *J* = 8.6 Hz, Ar-H), 7.37–7.41 (1H, m, 7-H), 7.46–7.50 (1H, m, 8-H), 8.13 (1H, app. d, *J* = 7.7 Hz, 9-H), 8.26 (1H, app. d, *J* = 8.3 Hz, 6-H) ppm; ^{13}C NMR (100 MHz, $CDCl_3$) δ_C 48.1, 53.9, 55.3, 55.5, 67.6, 101.7, 101.9, 113.6, 114.4, 119.1, 123.0, 123.6, 124.2, 125.3, 125.8, 128.6, 129.9, 130.0, 130.1, 134.9, 135.1, 142.2, 145.2, 158.1, 159.2 ppm; HRMS (ESI) found $[M+H]^+$ = 585.2748 $C_{38}H_{36}N_2O_4$ requires $[M+H]^+$ = 585.2748.

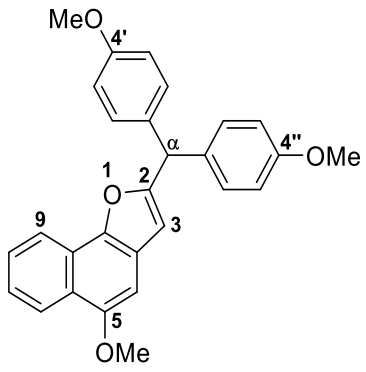

2.351

2-(Bis(4-methoxyphenyl)methyl)-5-methoxynaphtho[1,2-*b*]furan (2.351): from 6-methoxy-2,2-bis(4-methoxyphenyl)-2*H*-naphtho[1,2-*b*]pyran (185.5 mg, 0.4370 mmol) after 9 h of reaction; Purification by preparative TLC [Merck Silica gel 60 F_{254}, eluent: EtOAc (10%) in hexanes, fraction 1] led to the corresponding product as an off-white powder (34.9 mg, 19%); m.p. = 115–118 °C; ν_{max} (neat) 2926, 2834, 1607, 1588, 1508, 1456, 1378, 1240, 1176, 1032, 830, 770, 549 cm^{-1}; ^1H NMR (400 MHz, $CDCl_3$) δ_H 3.79 (6H, s, OMe), 3.98 (3H, s, 5-OMe), 5.59 (1H, s, α-H), 6.31 (1H, d, *J* = 0.9 Hz, 3-H), 6.83–6.87 (5H, m, Ar-H), 7.14–7.17 (4H, m, Ar-H), 7.41–7.45 (1H, m, 7-H), 7.51–7.55 (1H, m, 8-H), 8.13 (1H, app. d, *J* = 7.9 Hz, 9-H), 8.28 (1H, app. d, *J* = 8.3 Hz, 6-H) ppm; ^{13}C NMR (100 MHz, $CDCl_3$) δ_C 49.8, 55.3, 55.9, 96.9, 106.6, 113.9, 119.8, 121.7, 122.9, 123.2, 123.6, 124.2, 126.7, 129.8, 134.1, 145.3, 152.0, 158.4, 159.7 ppm; HRMS (ESI) found $[M+H]^+$ = 425.1749 $C_{28}H_{24}O_4$ requires $[M+H]^+$ = 425.1747.

3.4.3 General Methods for the Synthesis of 2-(Bis(4-methoxyphenyl)methyl)-5-methoxy-3-(*p*-tolyl)naphtho[1,2-*b*]furan (2.353)

Method A – A mixture of 6-methoxy-2,2-bis(4-methoxyphenyl)-4-(*p*-tolyl)-2*H*-naphtho[1,2-*b*]pyran (0.50 g, 0.97 mmol), K_2CO_3 (0.20 g, 1.4 mmol) and 18-crown-6 (0.80 g, 3.0 mmol) in PhMe (25.0 mL) was heated at reflux under N_2. After for 25 h of reaction, the crude was evaporated to dryness. Afterwards, water (100 mL) was added and the aqueous layer extracted with EtOAc (3 × 100 mL). The organic phase was reduced to 100 mL, washed with water (6 × 100 mL), dried with anhydrous sodium sulfate and evaporated to dryness. The residue was crystallized from a mixture of DCM/hexane. The resulting crop and mother-liquor were purified separately by flash column chromatography [Aldrich silica gel (60 Å, 40-63 μm), eluent: EtOAc (10%) in hexanes, fraction 1] giving the corresponding product as an off-white powder.

Method B – A mixture of 6-methoxy-2,2-bis(4-methoxyphenyl)-4-(*p*-tolyl)-2*H*-naphtho[1,2-*b*]pyran (0.50 g, 0.97 mmol), KOAc (0.19 g, 1.9 mmol), TBAB (0.31 g, 0.96 mmol) and $Pd(OAc)_2$

(0.02 g, 0.09 mmol) in DMAc (20.0 mL) was heated at reflux under N_2. After for 22 h of reaction, the crude was evaporated to dryness. Afterwards, water (100 mL) was added and the aqueous layer extracted with EtOAc (2 × 100 mL). The organic phase was washed with water (6 × 200 mL), dried with anhydrous sodium sulfate and evaporated to dryness. The residue was crystallized from a mixture of DCM/hexane. The resulting crop and mother-liquor were purified separately by flash column chromatography [Aldrich silica gel (60 Å, 40-63 μm), eluent: EtOAc (10%) in hexanes, fraction 1] giving the corresponding product as an off-white powder.

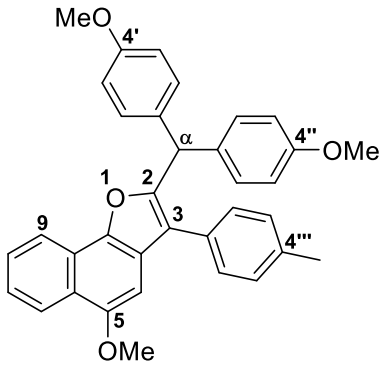

2.353

2-(Bis(4-methoxyphenyl)methyl)-5-methoxy-3-(*p*-tolyl)naphtho[1,2-*b*]furan (2.353): from method A as an off-white powder (0.17 g, 34%); From method B as an off-white powder (0.10 g, 20%); m.p. = 196–200 °C; ν_{max} (neat) 2926, 2832, 1610, 1585, 1507, 1459, 1376, 1247, 1173, 1034, 831, 765, 515 cm^{-1}; ^1H NMR (400 MHz, $CDCl_3$) δ_H 2.45 (3H, s, CH_3), 3.77 (6H, s, OMe), 3.97 (3H, s, OMe), 5.61 (1H, s, α-H), 6.82–6.85 (4H, m, Ar-H), 6.91 (1H, s, 4-H), 7.21–7.24 (4H, m, Ar-H), 7.32 (2H, app. d, *J* = 7.8 Hz, Ar-H), 7.39–7.41 (2H, m, Ar-H), 7.43–7.47 (1H, m, 7-H), 7.54–7.58 (1H, m, 8-H), 8.19 (1H, app. d, *J* = 7.9 Hz, 9-H), 8.29 (1H, app. d, *J* = 8.3 Hz, 6-H) ppm; ^{13}C NMR (100 MHz, $CDCl_3$) δ_C 21.3, 47.2, 55.3, 56.0, 95.9, 113.8, 119.5, 119.9, 121.7, 123.0, 123.2, 123.8, 124.3, 126.7, 129.2, 129.6, 129.8, 129.9, 134.6, 137.1, 144.8, 152.3, 153.4, 158.2 ppm; HRMS (ESI) found $[M+H]^+$ = 515.2207 $C_{35}H_{30}O_4$ requires $[M+H]^+$ = 515.2217.

4. CONCLUSIONS AND FURTHER WORK

The direct synthesis of pyridyl substituted 3*H*-naphtho[2,1-*b*]pyrans could not be accomplished by the classical acid-catalysed reaction between either a pyridyl substituted 2-naphthol and a 1,1-diarylprop-2-yn-1-ol or a 2-naphthol and a 1-aryl-1-pyridylprop-2-yn-1-ol. The foregoing problem was successfully resolved and a series of novel 2-, 3- and 4-pyridyl substituted 3*H*-naphtho[2,1-*b*]pyrans were efficiently synthesised by employing three different strategies:

- Strategy A – By a Suzuki cross-coupling reaction to introduce either a 2-, 3- or 4- pyridyl unit into either a preformed iodo-, bromo- or trifloxy- substituted naphthopyran. This versatile post-chromenization strategy allowed the preparation of several 10-, 9-, 8-, 7- and 5-pyridyl- 3*H*-naphtho[2,1-*b*]pyrans and was also effective for the synthesis of the 8-(pyridyl-triazole)-3*H*-naphtho[2,1-*b*]pyran **2.110** and the 8-aryl-3*H*-naphtho[2,1-*b*]pyrans **2.70**, **2.72** and **2.74**.
- Strategy B – By a Heck cross-coupling reaction between 1-phenyl-1-(4-pyridyl)prop-2-en-1-ol and MOM protected 1-bromo-2-naphthol with subsequent TFA-mediated unmasking of the 2-naphthol function which proceeded with concomitant cyclization to the 3-phenyl-3-(4-pyridyl)-3*H*-naphtho[2,1-*b*]pyran **2.170**.
- Strategy C – By a Suzuki cross-coupling reaction to introduce the pyridyl unit before a chromenization step entailing a Heck cross-coupling reaction – deprotective cyclization protocol – which afforded the 6-(pyridyl)-3*H*-naphtho[2,1-*b*]pyrans **2.214** and **2.215**.

With the exception of the 3-(4-pyridyl)-3*H*-naphtho[2,1-*b*]pyran **2.170** (ε = 3400 $M^{-1}.cm^{-1}$) and the trimethoxy substituted 3*H*-naphtho[2,1-*b*]pyran **2.77** (ε = 18000 $M^{-1}.cm^{-1}$), the pyridyl substituted 3*H*-naphtho[2,1-*b*]pyrans have shown relatively weak colourability in toluene (ε = 29 – 206 $M^{-1}.cm^{-1}$). The λ_{max} and bleaching kinetics of the photomerocyanines varied tremendously depending on the point of connection and orientation of the pyridyl group on the naphthopyran scaffold.

The pyridyl substituted 3*H*-naphtho[2,1-*b*]pyrans were coordinated to pre-prepared *fac*-$[Re(N\wedge N)(CO)_3Cl]^0$ complexes, **2.218**, **2.220** and **2.224**, in high yield by simple dissolution in DCM containing $AgPF_6$. The pyridyl-triazole substituted 3*H*-naphtho[2,1-*b*]pyran **2.110** was efficiently coordinated to rhenium pentacarbonyl chloride upon an overnight reflux in PhMe to afford rhenium(I) complex **2.247**. A total of eighteen photochromic rhenium(I) complexes were obtained for spectroscopic evaluation.

The photochromic rhenium(I) complexes produced photostationary states in solution, by either irradiation with UV or visible light, that were characterized by a 2 – 22 nm bathochromic shift of the λ_{max} (the only exception being the Re(I) complex **2.236**) and an overall increase in the colourability (ε = 4000 – 32000 $M^{-1}.cm^{-1}$) when compared to their pyridyl substituted 3*H*-

naphtho[2,1-*b*]pyran precursors. It was proposed that the increase in the colourability of the novel photochromic rhenium(I) complexes was due to a triplet photosensitization mechanism that involved the intramolecular energy transfer from the ^{3}MLCT excited state to a ^{3}IL excited state localized in the pyridyl substituted 3*H*-naphtho[2,1-*b*]pyran. Thus, the photochromic reaction, besides being triggered from a singlet excited state, would also be triggered from this ^{3}IL excited state. The bleaching kinetics varied with both the nature of the pyridyl substituted 3*H*-naphtho[2,1-*b*]pyran and the bidentate ligand (N^N = BPy, PyTz and BTz).

With the exception of the rhenium(I) complexes **2.229** and **2.246**, all the *fac*-[Re(N^N)(CO)$_3$NP]PF$_6$ complexes exhibited bidentate-ligand sensitive ^{3}MLCT phosphorescence with a lifetime of 50 – 171 ns. Reversible photoswitching (up to 81%) of the ^{3}MLCT phosphorescence occurred with the photochromic reaction. A more significant quench of the luminescence was consistently obtained when there was an extensive overlap between the absorbance band of the photomerocyanine and the ^{3}MLCT emission band. It was rationalized that the closer in energy the ^{3}MLCT excited state and the non-emissive ^{3}IL excited state were, the more efficient the intramolecular energy transfer from the ^{3}MLCT excited state to the ^{3}IL excited state would be and, consequently, a larger luminescence photoswitch would be attained. Furthermore, the highly efficient phosphorescence photoswitches showed no fatigue after 10 irradiation cycles with UV (365 nm) / visible light ($\lambda > 450$ nm).

The *fac*-[Re(PyTzNP)(CO)$_3$Cl]^0 **2.247** was characterized by an air-sensitive long-lived ($\tau = 4.7$ µs) emissive ^{3}IL excited state that bathochromic shifted (15 nm) once the photostationary state was reached. Evidence showed that the emissive ^{3}IL excited state of the *fac*-[Re(PyTzNP)(CO)$_3$Cl]^0 **2.247** was populated by energy transfer from the ^{3}MLCT excited state.

Future work includes the design of novel naphthopyran scaffolds, which may include examination of other fused pyran photochromes such as the alternate 2*H*-naphtho[1,2-*b*]pyran isomer, that would translate in a better colourability of the derived rhenium(I) complexes in solution while ensuring that the ^{3}MLCT and the ^{3}IL excited states would be as close in energy as possible. Theoretically, these future designs would result in even larger ^{3}MLCT phosphorescence photoswitching and would eliminate the residual phosphorescence of the photostationary states. On the other hand, the dramatic increase in colourability brought by the triplet photosensitization mechanism opens a new opportunity of designing super-fast photochromes with good colourability. Theoretically, this could be accomplished by ‘tuning’ the naphthopyran scaffold in such a way so that photostationary states in solution would be generated with very fast $t_{½}$ values that would produce better coloration once coordinated to the metal centre. Such an intense colouring superfast

photochromic system would represent a significant enhancement over the current photochromic systems which have commercial application in the eyewear and glazing sectors.

A protocol to perform Suzuki cross-coupling reactions with naphthopyrans bearing halogens and pseudo-halogens which obviates the complication of the ring-contraction side-reaction was developed. A mechanism to account for the ring-contraction of the naphthopyrans was proposed based on evidence gathered during a kinetic study. An efficient base-mediated protocol to access multiple naphthofurans, naphthodifurans and benzo-fused indoles in generally good yields was developed. Further work includes expanding the developed methodology to more diverse pyran systems, e.g. electron-deficient naphthopyrans, benzopyrans, and to other benzo-1,2-dihydroisoquinoline systems.

5. REFERENCES

[1] Photomechanical Materials, Composites, and Systems: Wireless Transduction of Light into Work Vol. 1, ed. T.J. White, **2017**.

[2] S. Aiken, R.J.L. Edgar, C.D. Gabbutt, B.M. Heron and P.A. Hobson, *Dyes Pigm.*, **2018**, *149*, 92−121.

[3] H. Dürr and H. Bouas-Laurent, *Pure Appl. Chem.*, **2001**, *73*, 639−665.

[4] V.I. Slovetskii, V.P. Balykin, O.G. Strukov, Y.V. Salyn' and A.A. Fainzil'berg, *Bulletin of Academy of Sciences of the USSR, Division of chemical science*, **1975**, *24*, 150−152.

[5] Photochromism, Techniques of Chemistry Vol. 3, ed. G.H. Brown, Wiley Interscience (New York), **1971**.

[6] R. Pardo, M. Zayat and D. Levy, *Chem. Soc. Rev.*, **2011**, *40*, 672–687.

[7] M-S Wang, G. Xu, Z-J Zhang, and G-C Guo, *Chem. Commun.*, **2010**, *46*, 361–376.

[8] A. Perrier, F. Maurel and D. Jacquemin, *Acc. Chem. Res.*, **2012**, *45*, 1173–1182.

[9] A. Mukhopadhyay and J.N. Moorthy, *J. Phys. Chem. C*, **2016**, *29*, 73–106; S. Aiken, C.D. Gabbutt, B.M. Heron and S.B. Kolla, *Dyes Pigm.*, **2015**, *113*, 239−250.

[10] B. Mondal, A.K. Ghosh and P.S. Mukherjee, *J. Org. Chem.*, **2017**, *82*, 7783−7790.

[11] E.I. Balmond, B.K. Tautges, A.L. Faulkner, V.W. Or, B.M. Hodur, J.T. Shaw and A.Y. Louie, *J. Org. Chem.*, **2016**, *81*, 8744−8758; H. Sun, X. Tian, J. Autschbach, Y. Yuan, J. Sun, X. Liu, C. Chen and H. Cao, *J. Mater. Chem. C*, **2013**, *1*, 5779 – 5790.

[12] A. Mukhopadhyay, V.K. Maka and J.N. Moorthy, *Eur. J. Org. Chem.*, **2016**, 274−281; M.-J.R.P. Queiroz, P.M.S. Plasencia, R. Dubest, J. Aubard and R. Guglielmetti, *Tetrahedron*, **2003**, *59*, 2567–2573.

[13] L. Vetráková, V. Ladányi, J.A. Anshori, P. Dvořák, J. Wirz and D. Heger, *Photochem. Photobiol. Sci.*, **2017**, *16*, 1749–1756; C. Zhang, M.-H. Du, H.-P. Cheng, X.-G. Zhang, A.E. Roitberg and J.L. Krause, *Phys. Rev. Lett.*, **2004**, *92*, 158301/1−158301/4.

[14] P. Yang, C. Lee, W. Chen and C. Lin, *Can. J. Chem. Eng.*, **2013**, *91*, 1513–1522.

[15] A. Carletta, F. Spinelli, S. d'Agostino, B. Ventura, M.R. Chierotti, R. Gobetto, J. Wouters and F. Grepioni, *Chem. Eur. J.*, **2017**, *23*, 5317–5329.

[16] C. Chen, J. Sun, Y. Zhang, X. Yang and J. Zhang, *Angew. Chem. Int. Ed.*, **2017**, *56*, 14458–14462; X. Chen, N. Zhang, L. Cai, P. Li, M. Wang and G. Guo, *Chem. Eur. J.*, **2017**, *23*, 7414–7417.

[17] R.K. Weerasekara, H. Uekusa and C.V. Hettiarachchi, *Cryst. Growth Des.*, **2017**, *17*, 3040−3047; J. Harada, M. Taira and K. Ogawa, *Cryst. Growth Des.*, **2017**, *17*, 2682−2687.

[18] S. Gago, M. Pessêgo, C.A.T. Laia and A.J. Parola, *ACS Omega*, **2017**, *2*, 122−126; M. Pessêgo, S. Gago, N. Basílio, C.A.T. Laia and A.J. Parola, J.C. Lima and F. Pina, *Org. Biomol. Chem.*, **2017**, *15*, 338−347.

[19] L. Wang and Q. Li, *Chem. Soc. Rev.*, **2018**, *47*, 1044−1097.

[20] J.D. Hepworth and B.M. Heron, in Functional Dyes, Ed. S-H Kim, Elsevier, (Amsterdam), **2006**, 85–135.

[21] Excited States in Organic Chemistry, J.A Barltrop and J.D. Coyle, John Wiley & Sons (Weinheim), **1975**.

[22] Y. Kobayashi, K. Mutoh and J. Abe, *J. Photochem Photobiol. C*, **2018**, *34*, 2−28.

[23] March's Advanced Organic Chemistry Reactions, Mechanism and Structure (7th Edn), Ed. M.B. Smith, Wiley & Sons (New York), **2013**.

[24] G. Pariani, M. Quintavalla, L. Colella, L. Oggioni, R. Castagna, F. Ortica, C. Bertarelli and A. Bianco, *J. Phys. Chem. C*, **2017**, *121*, 23592−23598.

[25] Molecular Switches (2nd Edn) Vol. 1 and Vol. 2. Ed. B.L. Feringa and W.R. Browne; Wiley–VCH (Weinheim), **2011**.

[26] Photochromic Materials; Preparations, Properties and Applications. Ed. H. Tian and J. Zhang; Wiley–VCH (Weinheim), **2016**.

[27] Molecular Devices and Machines; Concepts and Perspectives for the Nanoworld (2nd Edn.). Ed. V. Balzani, A. Credi and M. Venturi; Wiley–VCH (Weinheim), **2011**.

[28] C. Ko and V.W. Yam, *J. Mater. Chem.*, **2010**, *20*, 2063–2070.

[29] T.H.L. Nguyen, N. Gigant and D. Joseph, *ACS Catal.*, **2018**, *8*, 1546−1579.

[30] E. Merino, *Chem. Soc. Rev.*, **2011**, *40*, 3835–3853.

[31] K. Haghbeen and E.W. Tan, *J. Org. Chem.*, **1998**, *63*, 4503−4505.

[32] H.H. Davey, R.D. Lee and T.J. Marks, *J. Org. Chem.*, **1999**, *64*, 4976−4979.

[33] I. Shimao and S. Oae, *Bull. Chem. Soc. Jpn.*, **1983**, *56*, 643−644.

[34] Q. Yan, D. Han and Y. Zhao, *Polym. Chem.*, **2013**, *4*, 5026–5037.

[35] T. Hugel, N.B. Holland, A. Cattani, L. Moroder, M. Seitz and H.E. Gaub, *Science*, **2002**, *296*, 1103–1106.

[36] D.A. Siriwardane, O. Kulikov, B.L. Batchelor, Z. Liu, J.M. Cue, S.O. Nielsen and B.M. Novak, *Macromolecules*, **2018**, *51*, 3722−3730.

[37] D. Bléger, T. Liebig, R. Thiermann, M. Maskos, J.P. Rabe and S. Hecht, *Angew. Chem.*, **2011**, *50*, 12559–12563.

[38] Y. Wang, B. Li, L. Zhang, H. Song and L. Zhang, *Acs Appl. Mater. Interfaces*, **2013**, *5*, 11–15; H. Yan, C. Teh, S. Sreejith, L. Zhu, A. Kwok, W. Fang, X. Ma, N.K. Truc, V. Korzh, Y. Zhao, *Angew. Chem.*, **2012**, *124*, 8498–8502; N.Ž. Kneževic, B.G. Trewyn and V.S.Y. Lin, *Chem. Commun.*, **2011**, *47*, 2817–2819.

[39] J. Croissant, M. Maynadier, A. Gallud, H.P. N'Dongo, J.L. Nyalosaso, G. Derrien, C. Charnay, J. Durand, L. Raehm, F. Serein-Spirau, N. Cheminet, T. Jarrosson, O. Mongin, M. Blanchard-Desce, M. Gary-Bobo, M. Garcia, J. Lu, F. Tamanoi, D. Tarn, T.M. Guardado-Alvarez and J.I. Zink, *Angew. Chem.*, **2013**, *125*, 14058–14062.

[40] H. Murakami, A. Kawabuchi, R. Matsumoto, T. Ido and N. Nakashima, *J. Am. Chem. Soc.*, **2005**, *127*, 15891–15899; D. Qu, Q. Wang, J. Ren and H. Tian, *Org. Lett.*, **2004**, *6*, 2085–2088.

[41] D. Patra, H. Zhang, S. Sengupta, A. Sen, *ACS Nano*, **2013**, *7*, 7674–7679.

[42] P.J. Coelho, M.C.R. Castro and M.M.M. Raposo, *Dyes Pigm.*, **2015**, *117*, 163–169.

[43] K.B. Jørgensen, *Molecules*, **2010**, *15*, 4334–4358.

[44] Z.A. Khan, A. Iqbal and S.A. Shahzad, *Mol. Divers.*, **2017**, *21*, 483–509.

[45] D.P. Lima, R. Rotta, A. Beatriz, M.R. Marques, R.C. Montenegro, M.C. Vasconcellos, C. Pessoa, M.O. Moraes and L.V. Costa-Lotufo, *Eur. J. Med. Chem.*, **2009**, *44*, 701–707.

[46] S.G. Hahm, S.W. Lee, T.J. Lee, S.A. Cho, B. Chae, Y.M. Jung, S.B. Kim and M. Re, *J. Phys. Chem. B*, **2008**, *112*, 4900–4912.

[47] M. Mahdavi, K. Pedrood, M. Safavi, M. Saeedi, M. Pordeli, S.K. Ardestani, S. Emami, M. Adib, A. Foroumadi and A. Shafiee, *Eur. J. Med. Chem.*, **2015**, *95*, 492–499.

[48] Electron Transfer in Chemistry, Ed. V. Balzani, Wiley–VCH (Weinheim), **2001**.

[49] Y. Zhou, Y. Wu, O. Pokholenko, M. Grimsrud, Y. Sham, V. Papper, R. Marks and T. Steele, *Sensors and Actuators B*, **2018**, *257*, 245–255.

[50] K. Ogawa, M. Hara, S. Nagano, T. Seki and Y. Takeoka, *Chem. Lett.*, **2017**, *46*, 1386–1389.

[51] M. Cao, Z. Cai, X. Chen, K. Yi and D. Wei, *J. Mater. Chem. C*, **2017**, *5*, 9597–9601.

[52] R.M. Kellogg, B. Groen and H. Wynberg, *J. Org. Chem.*, **1967**, *32*, 3093–3100.

[53] M. Irie and K. Uchida, *Bull. Chem. Soc. Jpn.*, **1998**, *71*, 985–996.

[54] M. Irie, *Chem. Rev.*, **2000**, *100*, 1685–1716.

[55] M. Irie, T. Fukaminato, K. Matsuda and S. Kobatake, *Chem. Rev.*, **2014**, *114*, 12174−12277.

[56] M.M. Krayushkin, V.A. Barachevsky and M. Irie, *Heteroatom Chem.*, **2007**, *18*, 557−567.

[57] D. Roke, C. Stuckhardt, W. Danowski, S.J. Wezenberg and B.L. Feringa, *Angew. Chem. Int. Ed.*, **2018**, *57*, 1−6.

[58] D. Kitagawa, K. Kawasaki, R. Tanaka and S. Kobatake, *Chem. Mater.*, **2017**, *29*, 7524−7532.

[59] O. Nevskyi, D. Sysoiev, J. Dreier, S.C. Stein, A. Oppermann, F. Lemken, T. Janke, J. Enderlein, I. Testa, T. Huhn and D. Wöll, *Small*, **2018**, *14*, 1703333.

[60] N. Wang, R. Wang, Y. Tu, S. Pu and G. Liu, *Spectrochim. Acta A*, **2018**, *196*, 303–310.

[61] G. Li, G. Liu, D. Zhang and S. Pu, *Tetrahedron*, **2016**, *72*, 6390−6396.

[62] X.G. Tang, H.L. Liu and S.Z. Pu, *Photochem. Photobiol. Sci.*, **2016**, *15*, 1579−1585.

[63] M. Schulz-Senft, P.J. Gates, F.D. Sönnichsen and A. Staubitz, *Dyes Pigm.*, **2017**, *136*, 292−301.

[64] E. Fischer and H. Hirshberg, *J. Chem. Soc.*, **1952**, *61*, 4522–4524.

[65] Organic Photochromic and Thermochromic Compounds Vol. 1: Main Photochromic Families, Ed. J.C. Crano and R.J. Guglielmetti, Plenum, New York, **1999**.

[66] J. Hobley, V. Malatesta, R. Millini, L. Montanari and W.O. Parker Jr., *Phys. Chem. Chem. Phys.*, **1999**, *1*, 3259–3267.

[67] B.S. Lukyanov and M.B. Lukyanova, *Chem. Heterocycl. Compd.*, **2005**, *41*, 281–311.

[68] M. Querol, B. Bozic, N. Salluce and P. Belser, *Polyhedron*, **2003**, *22*, 655−664.

[69] G. Berkovic, V. Krongauz and V Weiss, *Chem. Rev.*, **2000**, *100*, 1741–1754.

[70] V.A. Lokshin, A. Samata and A.V. Metelitsa, *Russ. Chem. Rev.*, **2002**, *71*, 893–916; E.B. Gaeva, V. Pimienta, J.C. Micheau, E.B. Gaeva, A.V. Metelitsa and N.A. Voloshin, *Mol. Cryst. Liq. Cryst.*, **2005**, *430*, 81–88.

[71] A. Samat, V. Lokshin, K. Chamontin, D. Levi, G. Pepe and R. Guglielmetti, *Tetrahedron*, **2001**, *57*, 7349–7359.

[72] R. Klajn, *Chem. Soc. Rev.*, **2014**, *43*, 148–184.

[73] T. Halbritter, C. Kaiser, J. Wachtveitl and A. Heckel, *J. Org. Chem.*, **2017**, *82*, 8040−8047.

[74] D. Liu, W. Chen, K. Sun, K. Deng, W. Zhang, Z. Wang and X. Jiang, *Angew. Chem. Int. Ed.* **2011**, *50*, 4103−4107.

[75] M.E. Genovese, G. Caputo, G. Nanni, C. Setti, M. Bustreo, G. Perotto, A. Athanassiou and D. Fragouli, *ACS Appl. Mater. Interfaces*, **2017**, *9*, 40707–40715.

[76] L. Yu, C. Schlaich, Y. Hou, J. Zhang, P.M. Noeske and R. Haag, *Chem. Eur. J.*, **2018**, 24, 7742–7748.

[77] J. Fan, W. Wang and D. Yu, *Dyes Pigm.*, **2018**, *151*, 348–355.

[78] F. Nickel, M. Bernien, D. Krüger, J. Miguel, A.J. Britton, L.M. Arruda, L. Kipgen and W. Kuch, *J. Phys. Chem. C*, **2018**, *122*, 8031−8036.

[79] Y. Xiong, A.V. Jentzsch, J.W.M. Osterrieth, E. Sezgin, I.V. Sazanovich, K. Reglinski, S. Galiani, A.W. Parker, C. Eggelingbde and H.L. Anderson, *Chem. Sci.*, **2018**, *9*, 3029−3040.

[80] R. Ji, S. Fu, X. Zhang, X. Han, S. Liu, X. Wang and Y. Liu, *Sci. Rep.*, **2018**, *8*, 1−10.

[81] I. Iwai, J. Ide, *Chem. Pharm. Bull.*, **1962**, *10*, 926−929.

[82] a. J. Cottam and R. Livingstone, *J. Chem. Soc.*, **1964**, 5228–5231; b. J. Cottam and R. Livingstone, *J. Chem. Soc.*, **1965**, 6646−6649.

[83] R.S. Becker and J. Michl, *J. Am. Chem. Soc.*, **1966**, *88*, 5931–5933.

[84] A.A. Hussein, I. Barberena, T.L. Capson, T.A. Kursar, P.D. Coley, P.N. Solis and M.P. Gupta, *J. Nat. Prod.*, **2004**, *67*, 451−453.

[85] D.S. Jang, E.J. Park, M.E. Hawthorne, J.S. Vigo, J.G. Graham, F. Cabieses, B.D. Santarsiero, A.D. Mesecar, H.H.S Fong, R.G. Mehta, J.M. Pezzuto and A.D. Kinghorn, *J. Agric. Food. Chem.*, **2002**, *50*, 6330−6334.

[86] M.D. Braccio, G. Grossi, G. Roma, C. Marzano, F. Baccichetti, M. Simonato and F. Bordin, *Il Farmaco*, **2003**, *58*, 1083−1097; M. Hirao, J. Posakony, M. Nelson, H. Hruby, M. Jung, J.A. Simon and A. Bedalov, *J. Biol. Chem.*, **2003**, *278*, 52773−52782.

[87] S.N. Corns, S.M. Partington and A.D. Towns, *Color. Technol.*, **2009**, *125*, 249−261.

[88] C. Mann, M. Melzig and U. Weigand, *Ger. Pat., Ger. Patent No. WO 03/080595 A1*, **2003**; Y-P. Chan and O. Breyne, *Fr. Pat., Fr. Pat. No. WO 01/36424 A2*, **2001**.

[89] J.D.W. McCallien and M. Bezer, *Br. Pat., GB Patent No. 2344599*, **2000**.

[90] C.J. Ames, D.W. Thomas and D.C. Colgan, *U.S. Patent, U.S. Patent. No. WO 02/03949*, A2, **2002**.

[91] M. McManus and B. Federer, *U.S. Pat., U.S. Patent No. 0,122,780 A1*, **2002**.

[92] J.D. Hepworth, C.D. Gabbutt and B.M. Heron, Colour Science ’98; Volume 1: Dye and Pigment Chemistry, ed. J Griffiths, University of Leeds, UK, **1999**, 161; V. Gemert, Organic Photochromic and Thermochromic Compounds, Volume 1: Main Photochromic Families, Eds. H. Durr and H. Bouas-Laurent, Elsevier (Amsterdam), **2003**, 111.

[93] S. Delbaere, B. Luccioni-Houze, C. Bochu, Y. Teral, M. Campredon and G. Vermeersch, *J. Chem. Soc., Perkin Trans. 2*, **1998**, 1153−1157.

[94] S. Aiken, K. Booth, C.D. Gabbutt, B.M. Heron, C.R. Rice, A. Charaf-Eddinb and D. Jacquemin, *Chem. Commun.*, **2014**, *50*, 7900−7903.

[95] H. Görner and A. K. Chibisov, *J. Photochem. Photobiol. A*, **2002**, *149*, 83–89.

[96] T.T. Herzog, G. Ryseck, E. Ploetza and T. Cordes, *Photochem. Photobiol. Sci.*, **2013**, *12*, 1202–1209.

[97] S. Brazevic, M. Sliwa, Y. Kobayashi, J. Abe and G. Burdzinski, *J. Phys. Chem. Lett.*, **2017**, *8*, 909–914.

[98] Sabina Brazevic, Stanislaw Nizinski, Rafał Szabla, Michał F. Rode and Gotard Burdzinski, *Phys. Chem. Chem. Phys.*, **2019**, *21*, 11861–11870.

[99] G. Ottavi, G. Favaro and V. Malatesta, *J. Photochem. Photobiol. A*, **1998**, *115*, 123; H. Görner and A.K. Chibisov, *J. Photochem Photobiol. A*, **2002**, *149*, 83–89.

[100] A. Jha and P.J. Huang, *J. Heterocyclic Chem.*, **2009**, *46*, 1098–1106.

[101] W.D. Cotterill, R. Livingstone and M.V. Walshaw, *J. Chem. Soc.*, **1970**, 1758–1764.

[102] J.J. Talley, *Synthesis*, **1983**, 845–846.

[103] C.D. Gabbutt, D.J. Hartley, J.D. Hepworth, B.M. Heron, M. Kanjia and M. Rahman, *Tetrahedron*, **1994**, *50*, 2507–2522.

[104] J.-L. Pozzo, V.A. Lokshin and R. Guglielmetti, *J. Chem. Soc. Perkin Trans. 1*, **1994**, 2591–2595.

[105] A. Kickova, J. Donovavolá, P. Kasák and M. Putala, *New J. Chem.*, **2010**, *34*, 1109–1115.

[106] J.-L. Pozzo, A. Samat, R. Guglielmetti, R. Dubest and J. Aubard, *Helv. Chim. Acta*, **1997**, *80*, 725–738; B.V. Gemert, M. Bergomi and D. Knowles, *Mol. Cryst. Liq. Cryst.*, **1994**, *246*, 67–73; H.G. Heller, S.N. Oliver, J. Whittall and I. Tornlinson, *U.S. Pat., U.S. Patent No. 4,826,977*, **1989**.

[107] C. Moustrou, N. Rebière, A. Samat, R. Guglielmetti, A.E. Yassar, R. Dubest and J. Aubard, *Helv. C. Acta*, **1998**, *81*, 1293–1302.

[108] S.V. Paramonov, V. Lokshin and O.A. Fedorova, *Synthesis*, **2014**, *46*, 1659–1666.

[109] C.D. Gabbutt, B.M. Heron, C. Kilner and S.B. Kolla, *Chem. Commun.*, **2010**, *46*, 8481–8483.

[110] C.D. Gabbutt, J.D. Hepworth, B.M. Heron, D.A. Thomas, C. Kilner and S.M. Partington, *Heterocycles*, **2004**, *63*, 567–582.

[111] C.D. Gabbutt, B.M. Heron, A.C. Instone, D.A. Thomas, S.M. Partington, M.B. Hursthouse and T. Gelbrich, *Eur. J. Org. Chem.*, **2003**, 1220–1230.

[112] S. Aiken, C.D. Gabbutt, B.M. Heron and S.B. Kolla, *Dyes Pigm.*, **2015**, *113*, 239–250.

[113] R. Demadrille, C. Moustrou, A. Samat and R. Guglielmetti, *Heterocycl. Commun.*, **1999**, *5*, 123–126.

[114] M. Frigoli, C. Moustrou, A. Samat and R. Guglielmetti, *Eur. J. Org. Chem.*, **2003**, 2799–2812.

[115] S. Aiken, B. Armitage, C.D. Gabbutt and B.M. Heron, *Tetrahedron Lett.*, **2015**, *56*, 4840–4842.

[116] W. Zhao and E.M. Carreira, *Org. Lett.*, **2003**, *5*, 4153–4154.

[117] J.-L. Pozzo, A. Samat and R. Guglielmetti, *Helv. Chim. Acta*, **1997**, *80*, 725–738.

[118] S. Brazevic, M. Sliwa, Y. Kobayashi, J. Abe and G. Burdzinski, *J. Phys. Chem. Lett.*, **2017**, *8*, 909−914; C.M. Sousa, J. Berthet, S. Delbaere and P.J. Coelho, *J. Org. Chem.*, **2012**, *77*, 3959−3968.

[119] K. Arai, Y. Kobayashi and J. Abe, *Chem. Commun.*, **2015**, *51*, 3057–3060.

[120] B. Van Gemert, M. Bergomi and D. Knowles, *Mol. Cryst. Liq. Cryst.*, **1994**, *246*, 61–73.

[121] C.D. Gabbutt, J.D. Hepworth, B.M. Heron, S.M. Partington and D.A. Thomas, *Dyes Pigm.*, **2001**, *49*, 65–74.

[122] C.D. Gabbutt, B.M. Heron and A.C. Instone, *Heterocycles*, **2003**, *60*, 843–855.

[123] B. Van Gemert and M.P. Bergomi, *U.S. Pat., US Patent No.5,066,818*, **1991**.

[124] C.D. Gabbutt, B.M. Heron, S.B. Kolla, C. Kilner, S.J. Coles, P.N. Horton and M.B. Hursthouse, *Org. Biomol. Chem.*, **2008**, *6*, 3096–3104.

[125] A. Alberti, Y. Teral, G. Roubaud, R. Faure and M. Campredon, *Dyes Pigm.*, **2009**, *81*, 85–90.

[126] C.D. Gabbutt, B. M. Heron, A.C. Instone, P.N. Horton and M.B. Hursthouse, *Tetrahedron*, **2005**, *61*, 463–471.

[127] C.D. Gabbutt, B.M. Heron, C. Kilner and S.B. Kolla, *Org. Biomol. Chem.*, **2010**, *8*, 4874–4883.

[128] N. Rebiere, C. Moustrou, M. Meyer, A. Samat, R. Guglielmetti, J.C. Micheau and J. Aubard, *J. Phys. Org. Chem.*, **2000**, *13*, 523–530.

[129] J.C. Crano, T. Flood, A. Kumar and B.V. Gemert, *Pure Appl. Chem.*, **1996,** *68*, 1395–1398.

[130] X. Sallenave, S. Delbaere, G. Vermeersch and J.-L. Pozzo, *J. Phys. Org. Chem.*, **2007**, *20*, 872–877.

[131] M. Frigoli, C. Moustrou, A. Samat, R. Guglielmetti, R. Dubest and J. Aubard, *Mol. Cryst. Liq. Cryt.*, **2000**, *344*, 139–144.

[132] Z. Wang, Q. Meng, Z. Zhang, D. Fu and W. Zhang, *Tetrahedron*, **2011**, *67*, 2246–2250.

[133] M. Rickwood, K.E. Smith, CD. Gabbutt and J.D. Hepworth, *PCT Int. Appl. WO* 22850, **1994**.

[134] S. Aldoshin, I. Chuev, O. Filipenko, V. Lokshin, A. Samat and G. Pèpe, *Z. Kristallogr.*, **1998**, *213*, 568–570.

[135] J. Abe, H. Kato, T. Shimizu and Y. Nakagawa, *Jpn. Kokai Tokkyo Koho JP6071871 (B2)*, **2015**.

[136] A.R. Katritzky, R. Sakhuja, L. Khelashvili and K. Shanab, *J. Org. Chem.*, **2009**, *74*, 3062–3065.

[137] E.A. Shilova, G. Pèpe, A. Samat, C. Moustrou, *Tetrahedron*, **2008**, *64*, 9977–9982.

[138] S. Coen, C. Moustrou, M. Frigoli, M. Julliard, A. Samat and R. Guglielmetti, *J. Photoch. Photobio. A*, **2001**, *139*, 1–4.

[139] R.L. Demeio, A. Kumar, M. He, D.R. Dabideen and S. Mondal, *PCT Int. Appl. WO 2014149852*, **2014**.

[140] S. Matsuoka, J. Momota and T. Hara, *Jpn. Kokai Tokkyo Koho JP08176139*, **1996**.

[141] K. Chamontin, V. Lokshin, V. Rossollin, Andre Samat and R. Guglielmetti, *Tetrahedron* **1999**, *55*, 5821–5830.

[142] J.-L. Pozzo, V. Lokshin, A. Samat, R. Guglielmetti, R. Dubest and J. Aubard, *J. Photochem. Photobiol. A*, **1998**, *114*, 185–191.

[143] M.J.R.P. Queiroz, R. Dubest, J. Aubard, R. Faure and R. Guglielmetti, *Dyes Pigm.*, **2000**, *47*, 219–229.

[144] J. Abe, H. Kato, Y. Nakagawa and H. Iuchi, *Jpn. Kokai Tokkyo Koho JP2017132736*, **2017**; C. Salemi-Delvaux, E. Pottier, R. Guglielmetti, R. Dubest and J. Aubard, *Dyes Pigm.*, **1999**, *40*, 157–162.

[145] A. Mukhopadhyay and J.N. Moorthy, *J. Photoch. Photobio. C*, **2016**, *29*, 73–106.

[146] C.D. Gabbutt, T. Gelbrich, J.D. Hepworth, B.M. Heron, M.B. Hursthouse and S.M. Partington, *Dyes Pigm.*, **2002**, *54*, 79–93.

[147] G. Favaro, D. Levi, F. Ortica, A. Samat, R. Guglielmetti and U. Mazzucato, *J. Photochem. Photobiol. A*, **2002**, *149*, 91–100.

[148] S. Delbaere, G. Vermeersch, M. Frigoli and G.H. Mehl, *Org. Lett.*, **2010**, *12*, 4090–4093.

[149] W. Zhao and E.M. Carreira, *Chem. Eur. J.*, **2007**, 13, 2671–2685.

[150] M. Frigoli and G.H. Mehl, *Angew. Chem. Int. Ed.*, **2005**, *44*, 5048–5052.

[151] D.A. Clarke, B.M. Heron, C.D. Gabbutt, J.D. Hepworth, S.M. Partington and S.N. Corns, *EP1117656*, **2002**; D.A. Clarke, B.M. Heron, C.D. Gabbutt, J.D. Hepworth, S.M. Partington and S.N. Corns, *US6248264*, **2001**.

[152] C.D. Gabbutt, B.M. Heron, C. Kilner and S.B. Kolla, *Dyes Pigm.*, **2012**, *94*, 175–182; Song, Y. Yang, Q. Zhang, H. Tian and W.J. Zhu, *Phys. Chem. B*, **2011**, *115*, 14648–14658.

[153] S. Wang, Y. Si, C. Tong, G. Wang, B. Qi and G. Yang, *Optical Materials*, **2013**, *35*, 1504–1512.

[154] Y. He, G. Wang and M. Wang, *J. Mol. Struct.*, **2016**, *1116*, 109–115.

[155] M. Natali and S. Giordani, *Chem. Soc. Rev.*, **2012**, *41*, 4010–4029; S.V. Paramonov, V. Lokshin and O.A. Fedorova, *J. Photochem. Photobiol. C*, **2011**, *12*, 209–236; V.I. Minkin, A.D. Dubonosov, V.A. Bren and A.V. Tsukanov, *Arkivoc*, **2008**, *iv*, 90–102; M.T. Stauffer, D.B. Knowles, C. Brennan, L. Funderburk, F. Lin and S.G. Weber, *Chem. Commun.*, **1997**, 287–288.

[156] P.R. Sahoo and S. Kumar, *RSC Adv.*, **2016**, *6*, 20145–20154.

[157] O.A. Fedorova, Y.P. Strokach, A.V. Chebunkova, T.M. Valova, S.P. Gromov, M.V. Alfimov, V. Lokshin and A. Samat, *Russ. Chem. Bull.*, **2006**, *55*, 287–294.

[158] E.N. Ushakov, V.B. Nazarov, O.A. Fedorova, S.P. Gromov, A.V. Chebunkova, M.V. Alfimov and F. Barigelletti, *J. Phys. Org. Chem.*, **2003**, 16**,** 306–309.

[159] A. Yassar, H. Jaafari, N. Rebière-Galy, M. Frigoli, C. Moustrou, A. Samat and R. Guglielmetti, *Eur. Phys. J. AP*, **2002**, *18*, 3–8.

[160] A. Yassar, F. Garnier, H. Jaafari, N. Rebière-Galy, M. Frigoli, C. Moustrou, A. Samat, and R. Guglielmetti, *Appl. Phys. Lett.*, **2002**, *80*, 4297–4299.

[161] D. Li, J. Jiang, Q. Huang, G. Wang, M. Zhanga and J. Du, *Polym. Chem.*, **2016**, *7*, 3444–3450.

[162] Y.Y. Chia and M.G. Tay, *Dalton Trans.*, **2014**, *43*, 13159–13168.

[163] M.D. Ward, *J. Solid State Electrochem.*, **2005**, *9*, 778–787.

[164] L.K. Thompson and L.N. Dawe, *Coordin. Chem. Rev.*, **2005**, *289–290*, 13–31.

[165] Comprehensive Inorganic Chemistry II (2nd Edn.). Ed. J. Reedijk and K.R. Poeppelmeier, Elsevier (Amsterdam), **2013**.

[166] V. Sathish, E. Babu, A. Ramdass, Z. Lu, T. Chang, M. Velayudham, P. Thanasekaran, K. Lu, W. Li and S. Rajagopal, *RSC Adv.*, **2013**, *3*, 18557–18566.

[167] P.A. Scattergood, A. Sinopoli and P.I.P. Elliott, *Coordin. Chem. Rev.*, **2017**, *350*, 136–154.

[168] S. Sato and O. Ishitani, *Coordin. Chem. Rev.*, **2015**, *282*, 50–59.

[169] Photochromic Materials – Preparation, Properties and Applications, Ed. H. Tian and J. Zhang, Wiley-VCH (Germany), **2016**.

[170] V.W. Yam, V.C. Lau and L. Wu, *J. Chem. Soc. Dalton Trans.*, **1998**, 1461–1468.

[171] C. Ko and V.W. Yam, *Acc. Chem. Res.*, **2018**, *51*, 149−159.

[172] K.P.M. Frin and N.Y.M. Iha, *Inorg. Chim. Acta*, **2011**, *376*, 531–537; A.S. Polo, M.K. Itokazu and N.Y.M. Iha, *J. Photoch. Photobio. A*, **2006**, *181*, 73–78; K.M. Frin and N.Y.M. Iha, *J. Braz. Chem. Soc.*, **2006**, *17*, 1664−1671; O.S. Wenger, L.M. Henling, M.W. Day, J.R. Winkler and H.B. Gray, *Inorg. Chem.*, **2004**, *43*, 2043−2048.

[173] R.C. Amaral, L.S. Matos, K.P.S. Zanoni and N.Y.M. Iha, *J. Phys. Chem. A*, **2018**, *122*, 6071−6080.

[174] O.S. Wenger, L.M. Henling, M.W. Day, J.R. Winkler and H.B. Gray, *Polyhedron*, **2004**, *23*, 2955–2958.

[175] V.W. Yam, C. Ko, L. Wu, K. M. Wong and K. Cheung, *Organometallics*, **2000**, *19*, 1820−1822.

[176] C. Ko, L. Wu, K.M. Wong, N. Zhu and V.W. Yam, *Chem. Eur. J.*, **2004**, *10*, 766−776.

[177] H. Le Bozec and V. Guerchais, *C. R. Chimie*, **2013**, *16*, 1172−1182.

[178] V.W. Yam, C. Ko and N. Zhu, *JACS*, **2004**, *126*, 12734−12735.

[179] C. Ko, W. Kwok, V.W. Yam and D.L. Phillips, *Chem. Eur. J.*, **2006**, *12*, 5840–5848.

[180] P.H. Lee, C. Ko, N. Zhu and V.W. Yam, *J. Am. Chem. Soc.*, **2007**, *129*, 6058–6059.

[181] B. Kandagatla, V.V.N.K.V.P. Raju, G.M. Reddy, S.C. Rao, J. Iqbal, R. Bandichhor and S. Oruganti., *Tetrahedron Lett.*, **2012**, *53*, 7125−7127.

[182] S. Aiken, J.P Cano, C.D. Gabbutt, B.M. Heron, T. Kosa, L. Su, L. Sukhomlinova and B. Taheri, *PCT Int. Appl. WO 2008030226*, **2008**.

[183] C. Amatore, A. Jutand and G. Le Duc, *Angew. Chem. Int. Ed.*, **2012**, *51*, 1379 –1382.

[184] J.P. Schaefer, J. Higgins and P.K. Shenoy, *Org. Synth.*, **1969**, *49*, 6−8; G. Porzi and C. Concilio, *J. Organomet. Chem.*, **1977**, *128*, 95−98; T. Igaki, K. Horisawa, M. Saito, T. Obitsu and M. Kinoshita, *Jpn Kokai Tokyo Kono JP 63063753 A2; Chem Abstr.*, **1989**, CA, 31502J.

[185] Q. Zhou, X. Li, J. Zhou, K. Bai and H. Ågren, *Dyes Pigm.*, **2014**, *107*, 174–181.

[186] M. Bandin, S. Casolari, P.G. Cozzi, G. Proni, E. Schmohel, G.P. Spada, E. Tagliavini and A. Umani-Ronchi, *Eur. J. Org. Chem.*, **2000**, 491–497.

[187] A.G. Anderson Jr. and F.J. Freenor, *J. Org. Chem.*, **1972**, *37*, 626–630.

[188] W. Sriprom, M. Néel, C.D. Gabbutt, B.M. Heron and S. Perrier, *J. Mater. Chem.*, **2007**, *17*, 1885–1893.

[189] M. Rawat, V. Prutyanov and W.D. Wulf, *J. Am. Chem. Soc.*, **2006**, *128*, 11044–11053.

[190] Y. Liu, L.J. Milo Jr. and J.H. Lai, *Arkivoc*, **2013**, *i*, 135–153.

[191] Pyridines: From Lab to Production (1st Edition), Ed. E.F.V. Scriven, Academic Press (Oxford, U.K.), **2013**.

[192] B. Avitia, E. MacIntosh, S. Muhia and E. Kelson, *Tetrahedron Lett.*, **2011**, *52*, 1631–1634.

[193] J. Lu, Z. Guan, J. Gao and Z. Zhang, *Appl. Organometal. Chem.*, **2011**, *25*, 537–541.

[194] R. Everett, J. Hamilton and C. Abelt, *Molbank*, **2009**, M602.

[195] W. Li, D.P. Nelson, M.S. Jensen, R.S. Hoerrner, D. Cai, R.D. Larsen and P.J. Reider, *J. Org. Chem.*, **2002**, *67*, 5394–5397.

[196] J. Berthet, P.J. Coelho, L.M. Carvalho, G. Vermeersch, S. Delbaere, *J. Photoch. Photobio. A*, **2009**, *208*, 180–185; S. Delbaere and G. Vermeersch, *J. Photoch. Photobio. A*, **2003**, *159*, 227–232.

[197] G.C. Fu, *Acc. Chem. Res.*, **2008**, *41*, 1555 – 1564.

[198] J.W. Tilley and S. Zawoiski, *J. Org. Chem.*, **1988**, *53*, 386–390.

[199] B. Zhang, R. Chen, H. Jiang, Q. Zhou, F. Qiu, D. Han, R. Li, W. Tang, A. Zhong, J. Zhang, X. Yu, *Tetrahedron*, **2016**, *72*, 2813–2817.

[200] K.D. Siebertzab and C.P.R. Hackenberger, *Chem. Commun.*, **2018**, *54*, 763–766.

[201] S. Ladouceur, A.M. Soliman and E. Zysman-Colman, *Synthesis*, **2011**, *22*, 3604–3611.

[202] B.T. Worell, J.A. Malik and V.V. Fokin, *Science*, **2013**, *340*, 457–460.

[203] J-J. Zhang, C-S. Yan, Y. Peng, Z-B. Luo, X-B. Xu and Y-W. Wang, *Org. Biomol. Chem.*, **2013**, *11*, 2498–2513.

[204] J. Iskra, S. Stavber and M. Zupan, *Synthesis*, **2004**, *11*, 1869–1873.

[205] Protecting Groups (3rd Edition), Ed. P.J. Kocieński, Georg Thieme Verlag (Stuttgart, Germany), **2005**.

[206] K. Niimi, H. Mori, E. Miyazaki, I. Osaka, H. Kakizoe, K. Takimiya and C. Adachi, *Chem. Commun.*, **2012**, *48*, 5892–5894.

[207] D. Pena, D. Perez, E. Guitian and L. Castedo, *J. Org. Chem.*, **2000**, *65*, 6944–6950.

[208] F.V. Singh and T. Wirth, *Synthesis*, **2012**, *44*, 1171–1177.

[209] D. Yang, Y. Zhu, N. Yang, Q. Jiang and R. Liu, *Adv. Synth. Catal.*, **2016**, *358*, 1731–1735.

[210] A. Bahr, A.S. Droz, M. Puntener, U. Neidlein, S. Anderson, P. Seiler and F. Diederich, *Helv. Chim. Acta*, **1998**, *81*, 1931–1963.

[211] O.D.C.C. de Azevedo, R.S.G.R. Seixas and A.M.S. Silva, *Synlett*, **2015**, *26*, 1379–1384.

[212] L. He, *Synlett*, **2015**, *26*, 851–852.

[213] P.M. Murray, J.F. Bower, D.K. Cox, E.K. Galbraith, J.S. Parker and J.B. Sweeney, *Org. Process Res. Dev.*, **2013**, *17*, 397–405.

[214] S.D. Zanatta, B. Jarrott and S.J. Williams, *Aust. J. Chem.*, **2010**, *63*, 946–957.

[215] K. Niimi, H. Mori, E. Miyazaki, I. Osaka, H. Kakizoe, K. Takimiya and C. Adachi, *Chem. Commun.*, **2012**, *48*, 5892–5894.

[216] T. Aoyama, T. Okutome, T. Nakayama, T. Yaegashi, R. Matsui, S. Nunomura, M. Kurumi and Y. Sakurai, *Chem. Pharm. Bull.*, **1985**, *33*, 1458–1471.

[217] M.C. Carreno, J.L.G. Ruano, G. Sanz, M.A. Toledo, A. Urbano, *Synlett*, **1997**, *11*, 1241–1242.

[218] K.H. Bell and L.F. McCaffery, *Aust. J. Chem.*, **1993**, *46*, 731–737.

[219] H.D. Stoeffler, N.B. Thornton, S.L. Temkin and K.S. Schanze, *J. Am. Chem. Soc.*, **1995**, *117*, 7119–7128.

[220] E.D. Olmon, P.A. Sontz, A.M. Blanco-Rodríguez, M. Towrie, I.P. Clark, A. Vlček Jr. and J.K. Barton, *J. Am. Chem. Soc.*, **2011**, *133*, 13718–13730.

[221] M. Christl, H.J. Reich and J.D. Roberts, *J. Am. Chem. Soc.*, **1971**, *93*, 3463–3467; A. Puszko and L. Wasylina, *Chem. Pap.*, **1995**, *49*, 176–181.

[222] S.D. Zanatta, B. Jarrott and S.J. Williams, *Aust. J. Chem.*, **2010**, *63*, 946–957.

[223] S. Pingali, J.P. Donahueb and F. Payton-Stewarta, *Acta Cryst.*, **2000**, *C56*, 263–264.

[224] C. Ko, J.W. Siu, A.W. Cheung and S. Yiu, *Organometallics*, **2011**, *30*, 2701–2711.

[225] N.D. Dmitrieva, R.M. Liberzon and Y.S. Ryabokobylko, *Zh. Org. Khim.*, **1985**, *21*, 1340–1345.

[226] M.N.V. Sastry, S. Claessens, P. Habonimana and N. De Kimpe, *J. Org. Chem.*, **2010**, *75*, 2274–2280.

[227] C. Böttcher, G. Zeyat, S.A. Ahmed, E. Irran, T. Cordes and C. Elsner, *Beilstein J. Org. Chem.*, **2009**, *5*, doi: 10.3762/bjoc.5.25, number 25.

[228] C.D. Gabbutt, B.M. Heron, C. Kilner and S.B. Kolla, *Dyes Pigm.*, **2012**, *92*, 825–830.

[229] Palladium reagents and catalysts innovations in organic synthesis, Ed. J. Trust, John Wiley & Sons (Chichester), **1995**, 290–422.

[230] F. Proutiere and F. Schoenebeck, *Angew. Chem. Int. Ed.*, **2011**, *50*, 8192–8195.

[231] R. Schettini, M. Sicignano, F. De Riccardis, I. Izzo and G. Della Sala, *Synthesis*, **2018**, *50*, 4777–4795.

[232] N.E. Leadbeater and M. Marco, *Angew. Chem. Int. Ed.*, **2003**, *42*, 1407–1409; N.E. Leadbeater and M. Marco, *J. Org. Chem.*, **2003**, *68*, 5660–5667.

[233] R.K. Arvela, N.E. Leadbeater, M.S. Sangi, V.A. Williams, P. Granados and R.D. Singer, *J. Org. Chem.*, **2005**, *70*, 161–168.

[234] A.M. Brouwer, *Pure Appl. Chem.*, **2011**, *83*, 2213–2228.

[235] B. Kandagatla, V.V.N.K.V.P. Raju, G.M. Reddy, S.C. Rao, J. Iqbal, R. Bandichhor and S. Oruganti., *Tetrahedron Lett.*, **2012**, *53*, 7125–7127.

[236] M. Jakeš, *Collect. Czech. Chem. Commun.*, **1929**, *1*, 245–246.

[237] M. Jakeš, *Chem. Obzor.*, **1926**, *1*, 285.

[238] I.S. Ioffe, *Zhurnal Obshchei Khimii*, **1936**, *6*, 1079.

[239] L.S. El-Assal and S.A.M. El-Wahhab, *J. Chem. Soc.*, **1960**, 849–852.

[240] D.J. Tate, M. Abdelbasit, C.A. Kilner, H.J. Shepherd, S.L. Warriner and R.J. Bushby, *Tetrahedron*, **2014**, *70*, 67–74.

[241] K. Ziegler and C. Ochs, *Ber. Dtsch. Chem. Ges.*, **1922**, *55B*, 2257–2277.

[242] R. Everett, J. Hamilton and C. Abelt, *Molbank*, **2009**, M602.

[243] C. Coudret, *Synth. Commun.*, **1996**, *26*, 3543–3547.

[244] J.E. Baeckvall, R.E. Nordberg, J.E. Nystroem, T. Hoegberg and B. Ulff, *J. Org. Chem.*, **1981**, *46*, 3479–3483.

[245] K.H. Bell, L.F. McCaffery, *Aust. J. Chem.*, **1993**, *46*, 731–737.